IMMUNOTHERAPY FOR NSCLC WITH ONCOGENIC DRIVER VARIANTS

EDITED BY: Meijuan Huang, Hongbo Hu, Qian Chu, Yanyan Lou and Yong He

PUBLISHED IN: Frontiers in Oncology and Frontiers in Immunology

frontiers Research Topics

frontiers

ISSN 1664-8714
ISBN 978-2-83250-306-5
DOI 10.3389/978-2-83250-306-5

About Frontiers

Frontiers is more than just an open-access publisher of scholarly articles: it is a pioneering approach to the world of academia, radically improving the way scholarly research is managed. The grand vision of Frontiers is a world where all people have an equal opportunity to seek, share and generate knowledge. Frontiers provides immediate and permanent online open access to all its publications, but this alone is not enough to realize our grand goals.

Frontiers Journal Series

The Frontiers Journal Series is a multi-tier and interdisciplinary set of open-access, online journals, promising a paradigm shift from the current review, selection and dissemination processes in academic publishing. All Frontiers journals are driven by researchers for researchers; therefore, they constitute a service to the scholarly community. At the same time, the Frontiers Journal Series operates on a revolutionary invention, the tiered publishing system, initially addressing specific communities of scholars, and gradually climbing up to broader public understanding, thus serving the interests of the lay society, too.

Dedication to Quality

Each Frontiers article is a landmark of the highest quality, thanks to genuinely collaborative interactions between authors and review editors, who include some of the world's best academicians. Research must be certified by peers before entering a stream of knowledge that may eventually reach the public - and shape society; therefore, Frontiers only applies the most rigorous and unbiased reviews.
Frontiers revolutionizes research publishing by freely delivering the most outstanding research, evaluated with no bias from both the academic and social point of view. By applying the most advanced information technologies, Frontiers is catapulting scholarly publishing into a new generation.

What are Frontiers Research Topics?

Frontiers Research Topics are very popular trademarks of the Frontiers Journals Series: they are collections of at least ten articles, all centered on a particular subject. With their unique mix of varied contributions from Original Research to Review Articles, Frontiers Research Topics unify the most influential researchers, the latest key findings and historical advances in a hot research area! Find out more on how to host your own Frontiers Research Topic or contribute to one as an author by contacting the Frontiers Editorial Office: frontiersin.org/about/contact

IMMUNOTHERAPY FOR NSCLC WITH ONCOGENIC DRIVER VARIANTS

Topic Editors:
Meijuan Huang, Sichuan University, China
Hongbo Hu, Sichuan University, China
Qian Chu, Huazhong University of Science and Technology, China
Yanyan Lou, Mayo Clinic, United States
Yong He, Army Medical University, China

Citation: Huang, M., Hu, H., Chu, Q., Lou, Y., He, Y., eds. (2022). Immunotherapy for NSCLC With Oncogenic Driver Variants. Lausanne: Frontiers Media SA.
doi: 10.3389/978-2-83250-306-5

Table of Contents

frontiers | Frontiers in Oncology

TYPE Editorial
PUBLISHED 08 December 2022
DOI 10.3389/fonc.2022.1095947

OPEN ACCESS

EDITED AND REVIEWED BY
Paul Zarogoulidis,
Euromedica General Clinic, Greece

*CORRESPONDENCE
Meijuan Huang
hmj107@163.com

SPECIALTY SECTION
This article was submitted to Cancer Immunity and Immunotherapy, a section of the journal Frontiers in Oncology

RECEIVED 11 November 2022
ACCEPTED 28 November 2022
PUBLISHED 08 December 2022

CITATION
Du Y, Chu Q, Lou Y, He Y, Hu H, Hu Q and Huang M (2022) Editorial: Immunotherapy for NSCLC with oncogenic driver variants. *Front. Oncol.* 12:1095947. doi: 10.3389/fonc.2022.1095947

Editorial: Immunotherapy for NSCLC with oncogenic driver variants

Yijia Du[1], Qian Chu[2], Yanyan Lou[3], Yong He[4], Hongbo Hu[5], Qipeng Hu[6] and Meijuan Huang[1]*

[1]Thoracic Oncology Ward, Cancer Center, West China Hospital of Sichuan University, Chengdu, Sichuan, China, [2]Department of Oncology, Tongji Hospital, Tongji Medical College, Huazhong University of Science and Technology, Wuhan, China, [3]Division of Hematology and Medical Oncology, Mayo Clinic, Jacksonville, FL, United States, [4]Department of Respiratory Medicine, Daping Hospital, Army Medical University, Chongqing, China, [5]Department of Rheumatology and Immunology, State Key Laboratory of Biotherapy and Collaborative Innovation Center for Biotherapy, West China Hospital, Sichuan University, Chengdu, China, [6]Division of Pathogenesis of Virus Associated Tumors, German Cancer Research Centre Deutsches Krebsforschungszentrum (DKFZ), Heidelberg University, Heidelberg, Germany

KEYWORDS

oncogenic driver variants, tumor immune microenvironment, lung cancer, targeted therapy resistance, immune checkpoint inhibitors

Editorial on the Research Topic
Immunotherapy for NSCLC with Oncogenic driver variants

Immune checkpoint inhibitor (ICI) has been recognized as a gold standard treatment for advanced non-small cancer (NSCLC) without driver variants (1). However, the activity of ICIs across NSCLC harboring oncogenic alterations (such as EGFR, ALK, ROS1, or BRAF) is poorly characterized (2). Herein, we set this Research Topic to broadly collect research regarding immunotherapy for advanced NSCLC with oncogenic mutations, expecting to explore the role of immunotherapy (such as ICIs or in combination with other therapies) in these patient populations.

We would like to thank all authors for their contribution to providing further evidence regarding the treatment timing and treatment option with ICIs in the mutation population. Considering the high toxicity and low therapy efficacy of administrating ICIs as the first-line treatment of driver gene-positive NSCLC, the research reported on the Topic mostly focused on the application of ICIs in the ≥ second-line treatment setting (3, 4). What is more, Tian et al. reported that patients who received subsequent ICIs after progression on tyrosine kinase inhibitors (TKIs) achieved a higher quality of survival benefits compared with those who received ICI as later lines treatment. Moreover, Zhai et al. reported the re-sensitization to TKIs after pembrolizumab resistance in a non-smoker patient carrying EGFR 19 deletions (19del) who received previous targeted therapy. In terms of treatment options, the investigators also revealed the encouraging efficacy of ICI-based combination therapy especially in combination with chemotherapy, which was consistent with other studies. The platinum-based chemo-immunotherapy

combination provides a greater survival advantage compared with single-agent therapy for patients with EGFR mutation (Tian et al.). In addition to the classical platinum-based chemotherapy, platinum-free chemotherapy combined with ICI is associated with favorable progression-free survival in patients with EGFR-TKI-resistant advanced NSCLC from the retrospective study by Deng et al.

The authors move on to discuss the potential beneficiaries of ICIs therapy and found that the genetic and immunological diversity of the various mutational subtypes may possess different prognostic. Lei et al. indicated that several uncommon EGFR mutation subtypes (such as S768I, T790M, G718A, LL861Q, G719C, and 20ins) had a higher proportion of tumor mutational burden (TMB)-high or strong positive programmed death-ligand 1 (PD-L1) expression than the total EGFR mutation group (Leu858Arg [L858R] and 19del) by analysis of 9649 Chinese patients with primary NSCLC. Besides, a case report from Peng et al. demonstrated that ICIs may be more effective for *EGFR* L858R mutation than for other *EGFR* mutant subtypes, which is related to some potential predictors, such as TMB and concurrent PD-L1 plus $CD8^+$tumour-infiltrating lymphocyte (TIL) expression. Meanwhile, patients with *EGFR* mutations and higher PD-L1 expression are more likely to obtain potential benefits from immunotherapy after TKIs resistance (Zhai et al.). However, an EGFR mutant NSCLC case with high PD-L1 expression showed resistance to chemo-immunotherapy in an "immune-cold" microenvironment (Zhao et al.). Moreover, Dong et al. showed that an *ALK*-positive NSCLC patient with multiple driving mutations (*BRAF, KRAS, PIK3CA*), high TMB, PD-L1 overexpression, and $CD8^+$TIL may benefit from nivolumab.

To our knowledge, there are extremely limited data on the use of immunotherapy in populations of other gene aberation compared to EGFR. Therefore, collecting more evidence is necessary to confirm the efficacy of immunotherapy in these populations. The authors published in this "Research Topic" presented some populations containing oncogenic driver variants that benefit and lack of benefit from ICIs or high risk of toxicities or hyper-progression of anti-PD-1/anti-PD-L1 therapy. Zhou et al. performed whole exome sequencing in a cohort of 33 Chinese patients with NSCLC and identified that NSCLC tumors harboring mutated mucin 19 mutation exhibited good responses to anti-PD-1 inhibitors. Besides, Yang et al. demonstrate that endoplasmic reticulum aminopeptidase 2 (ERAP2) was lowly expressed in squamous cell lung carcinoma (SqCLC) and was significantly associated with longer survival. In addition, patients with higher oxidized low density lipoprotein receptor 1(OLR1) expression were predicted to have better immunotherapy outcomes based on Gene Expression Omnibus (GEO) data mining in the study by Liu et al. Moreover, a 5-genomic mutation signature could predict the survival of patients with NSCLC receiving atezolizumab (Lin et al.) and co-occurring alteration of NOTCH and DDR pathways served as a novel predictor to efficacious immunotherapy in NSCLC (Zhang et al.). In contrast to the above-mentioned studies, another study found that high expression of nsulin-like growth factor-I (IGF-1) was closely bound up with the unfavorable overall survival for patients with bladder urothelial carcinoma (BLCA), cholangiocarcinoma (CHOL), and acute myeloid leukemia (LAML) based on Cox regression analysis and Kaplan-Meier survival analysis (Zhang et al.). Besides, Zheng et al. found secretory phosphoprotein 1 (SPP1) expression was higher in patients with EGFR mutation and its high expression was associated with poor prognosis.

In conclusion, setting the "Research Topic" of "*Immunotherapy for NSCLC with Oncogenic Driver Variants*" to publish relevant research is an extraordinary and timely effort. We have tried to uncover more treatment details on the application of immunotherapy for EGFR-mutant, as well as to report more novel efficacy-related gene aberration that benefit from ICIs or lack of benefit of anti-PD-1/anti-PD-L1 therapy. We truly believe that these efforts will be beneficial for us to build a clearer picture of the role of ICIs for NSCLC with oncogenic driver variants and greatly enhance existing treatment strategies to maximize patient benefit.

Author contributions

All authors listed have made a substantial, direct, and intellectual contribution to the work and approved it for publication.

Acknowledgments

We will also like to thank all the authors in the collection for their valuable contribution.

Conflict of interest

The authors declare that the research was conducted in the absence of any commercial or financial relationships that could be construed as a potential conflict of interest.

Publisher's note

References

1. Reck M, Remon J, Hellmann MD. First-line immunotherapy for non-Small-Cell lung cancer. *J Clin Oncol* (2022) 40(6):586–97. doi: 10.1200/JCO.21.01497

2. Mazieres J, Drilon A, Lusque A, Mhanna L, Cortot AB, Mezquita L, et al. Immune checkpoint inhibitors for patients with advanced lung cancer and oncogenic driver alterations: results from the IMMUNOTARGET registry. *Ann Oncol* (2019) 30(8):1321–8. doi: 10.1093/annonc/mdz167

3. Oshima Y, Tanimoto T, Yuji K, Tojo A. EGFR-TKI-Associated interstitial pneumonitis in nivolumab-treated patients with non-small cell lung cancer. *JAMA Oncol* (2018) 4(8):1112–5. doi: 10.1001/jamaoncol.2017.4526

4. Gettinger S, Rizvi NA, Chow LQ, Borghaei H, Brahmer J, Ready N, et al. Nivolumab monotherapy for first-line treatment of advanced non-Small-Cell lung cancer. *J Clin Oncol* (2016) 34(25):2980–7. doi: 10.1200/JCO.2016.66.9929

frontiers in Oncology

ORIGINAL RESEARCH
published: 22 March 2021
doi: 10.3389/fonc.2021.596542

Association of *MUC19* Mutation With Clinical Benefits of Anti-PD-1 Inhibitors in Non-small Cell Lung Cancer

Li Zhou[1†], Litang Huang[2†], Qiuli Xu[1†], Yanling Lv[3], Zimu Wang[1], Ping Zhan[1], Hedong Han[1], Yang Shao[4], Dang Lin[5], Tangfeng Lv[1*] and Yong Song[1*]*

[1] Department of Respiratory and Critical Care Medicine, Affiliated Jinling Hospital, Medical School of Nanjing University, Nanjing, China, [2] Department of Respiratory and Critical Care Medicine, Affiliated Jinling Hospital, School of Medicine, Southeast University, Nanjing, China, [3] Department of Respiratory and Critical Care Medicine, The Second Hospital of Nanjing, Nanjing University of Chinese Medicine, Nanjing, China, [4] Geneseeq Technology Inc., Nanjing, China, [5] Department of Respiratory and Critical Care Medicine, The Affiliated Suzhou Hospital of Nanjing Medical University, Suzhou, China

Although anti-PD-1 inhibitors exhibit impressive clinical results in non-small cell lung cancer (NSCLC) cases, a substantial percentage of patients do not respond to this treatment. Moreover, the current recommended biomarkers are not perfect. Therefore, it is essential to discover novel molecular determinants of responses to anti-PD-1 inhibitors. We performed Whole Exome Sequencing (WES) in a cohort of 33 Chinese NSCLC patients. Patients were classified into the durable clinical benefit (DCB) and no durable benefit (NDB) groups. Infiltrating $CD8^+$ cells in the tumor microenvironment (TME) were investigated by immunohistochemistry. We also used public datasets to validate our results. In our cohort, good clinical responses to anti-PD-1 inhibitors were more pronounced in younger patients with lower Eastern Cooperative Oncology Group (ECOG) scores and only extra-pulmonary metastasis. More importantly, we identified a novel *MUC19* mutation, which was significantly enriched in DCB patients ($P = 0.015$), and *MUC19*-mutated patients had a longer progression-free survival (PFS) (hazard ratio = 0.3, 95% CI 0.1–0.9; $P = 0.026$). Immunohistochemistry results indicated that the *MUC19* mutation was associated with increased infiltration by $CD8^+$ T cells in the TME ($P = 0.0313$). When combining *MUC19* mutation with ECOG scores and intra-pulmonary metastasis status, patients with more positive predictors had longer PFS ($P = 0.003$). Furthermore, *MUC19* mutation was involved in immune responses and associated with a longer PFS in the Memorial Sloan-Kettering Cancer Center (MSKCC) cohort. Collectively, we identified that *MUC19* mutations were involved in immune responses, and NSCLC tumors harboring mutated *MUC19* exhibited good responses to anti-PD-1 inhibitors.

Keywords: *MUC19* mutation, predictive biomarker, whole exome sequencing, immunotherapy, lung cancer

OPEN ACCESS

Edited by:
Yong He,
Army Medical University, China

Reviewed by:
Rafael Rosell,
Catalan Institute of Oncology, Spain
Robert J. Canter,
University of California, Davis, United States

***Correspondence:**
Dang Lin
danglin4067@163.com
Tangfeng Lv
bairoushui@163.com
Yong Song
yong.song@nju.edu.cn

†These authors have contributed equally to this work

Specialty section:
This article was submitted to Cancer Immunity and Immunotherapy, a section of the journal Frontiers in Oncology

Received: *19 August 2020*
Accepted: *18 February 2021*
Published: *22 March 2021*

Citation:
Zhou L, Huang L, Xu Q, Lv Y, Wang Z, Zhan P, Han H, Shao Y, Lin D, Lv T and Song Y (2021) Association of MUC19 Mutation With Clinical Benefits of Anti-PD-1 Inhibitors in Non-small Cell Lung Cancer. Front. Oncol. 11:596542. doi: 10.3389/fonc.2021.596542

INTRODUCTION

The PD-1/PD-L1 blockade, which reactivates the anti-tumor activity of $CD8^+$ T cells by blocking T cell signals, has dramatically revolutionized the management of non-small cell lung cancer (NSCLC) over the past decade (1). Although treatment with anti-PD-1 inhibitors has demonstrated impressive response rates and durable disease remission (2), only a small subset of patients can benefit from them (3). Currently, anti-PD-1 inhibitors that have been approved or are in clinical research include pembrolizumab, nivolumab, atezolizumab, toripalimab, and sintilimab. Apart from their high efficacy, these drugs also display significant immunotoxicity in clinical practice (4), and the cost is high. Therefore, identifying which patients might most likely derive clinical benefit from PD-1/PD-L1 blockade is an essential challenge to be resolved (5). Thus, effective biomarkers for predicting PD-1/PD-L1 inhibitor efficacy are urgently needed in clinical practice.

PD-L1 expression is the earliest and most widely used predictive biomarker for PD-1/PD-L1 inhibitors (6), but it is limited by the detection technology employed (multiple detection antibodies, instrument platforms, different thresholds for positivity) and histological sources of PD-L1 (immune and tumor cells, primary and metastatic tumor sites, and dynamic changes in PD-L1 after treatment) (7). Consequently, additional biomarkers, including microsatellite instability (8) and tumor mutational burden (TMB) (3), have been evaluated. Recently, TMB has also been approved by the Food and Drug Administration as a new predictive biomarker for patients with unresectable or metastatic solid tumors receiving pembrolizumab (9). Nevertheless, similar to PD-L1 expression, TMB is not perfectly correlated with immunotherapy responses, with only a 30–50% objective response rate for TMB-high patients (10). An increasing number of studies have suggested other potential biomarkers, including somatic mutations in specific genes (11, 12), copy number alterations affecting immune-related genes (13), tumor infiltrating lymphocytes (14), and inflamed gene expression profiles (15, 16). Therefore, identification of additional novel biomarkers or combining different biomarkers with greater predictive values is crucial for stratifying populations potentially benefiting from immunotherapy (17).

In this context, we performed Whole Exome Sequencing (WES) to explore and uncover novel molecular determinants of anti-PD-1 inhibitors. In order to explore the underlying mechanisms, we detected $CD8^+$ T cells by immunohistochemistry. *MUC19* mutation was associated with good responses to anti-PD-1 inhibitors. These results were further validated in public datasets, encompassing lung cancer patients receiving immunotherapy with *MUC19* mutation data, which further confirmed the association of *MUC19* mutation with good efficacy of anti-PD-1 inhibitors.

Abbreviations: BMI, body mass index; DCB, durable clinical benefit; ECOG, Eastern Cooperative Oncology Group; GO, Gene Ontology; MSKCC, Memorial Sloan-Kettering Cancer Center; NDB, no durable benefit; NSCLC, non-small cell lung cancer; OS, overall survival; PFS, progression-free survival; TMB, tumor mutational burden; TME, tumor microenvironment; WES, whole exome sequencing.

MATERIALS AND METHODS

Patient Recruitment and Sample Collection

A total of 99 NSCLC patients receiving anti-PD-1 inhibitors at the Department of Respiratory and Critical Care Medicine of the Affiliated Jinling Hospital, Medical School of Nanjing University, between May 19, 2017, and April 26, 2019, were enrolled. Among them, we were able to assess efficacy in 65 patients using Response Evaluation Criteria In Solid Tumors (version.1.1). The clinical benefits of anti-PD-1 inhibitors were defined as durable clinical benefit (DCB: complete response, partial response, or stable disease lasting $>$ 6 months) and no durable clinical benefit (NDB: progression disease or stable disease that lasted $\leq$ 6 months). Body mass index (BMI) was calculated as weight in kilograms divided by height in meters squared. WES was performed in 33 patients who could be defined as DCB and NDB and had tumor tissue/matched control samples prior to immunotherapy (**Figure 1A**). The time from the beginning of immunotherapy to the date of disease progression was defined as progression-free survival (PFS). The study was approved by the Ethical Review Committee of the Affiliated Jinling Hospital and all patients had signed informed consent. The clinical characteristics of the 33 patients were presented in **Table 1**.

In addition, we also used public datasets (cBioPortal: https://www.cbioportal.org/, and International Cancer Genome Consortium Data Portal: https://dcc.icgc.org/) to validate our results (**Figure 1B**). Among them, the Memorial Sloan-Kettering Cancer Center (MSKCC) cohort was used to verify the relationship between *MUC19* mutation and response to immune checkpoint inhibitors. Data from the MSKCC cohort (18) were downloaded from the cBioPortal website, which contained WES results of 75 NSCLC patients treated with nivolumab plus ipilimumab.

WES

Tumor tissues/matched control samples were sent to Geneseeq Inc. (Nanjing, China) for WES. The mean target coverage was 150 $\times$ for tumor tissue and 60 $\times$ for normal controls.

CD8 Immunohistochemistry

Four micrometer-thick paraffin-embedded tissue sections were used for CD8 immunohistochemistry. Tissue sections were stained with monoclonal anti-CD8 antibody (clone C8/144B, 70306S) from Cell Signaling Technology. Lymphocytes with membranous staining were regarded as positive for CD8. All immunohistochemical sections were independently evaluated by two pathologists, and all evaluation scores were recorded. Two pathologists independently counted $CD8^+$ cells and randomly selected 4–6 fields (200 $\times$) for each immunohistochemical section.

Statistical Analysis

Fisher's exact test or Chi-squared test was used to compare clinical parameters and gene mutation status between DCB and NDB patients. Differences in $CD8^+$ T cells and TMB were examined using the non-parametric Mann-Whitney U test. The Kaplan-Meier method was used to analyze survival [PFS/overall survival (OS)]. Univariate Cox regression analysis was used

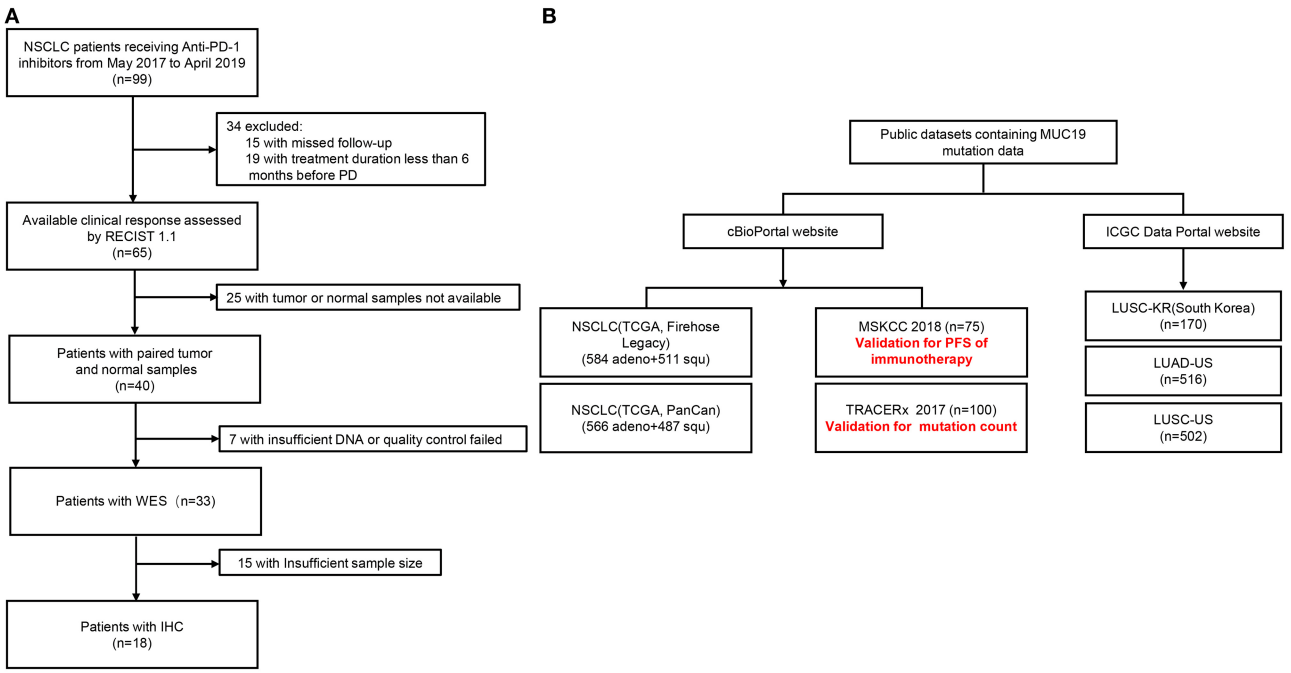

FIGURE 1 | Patient flow of our cohort and public datasets. **(A)** Patient flow of our cohort. **(B)** Patient flow of public datasets.

to define hazard ratios. SPSS v.23.0 and GraphPad Prism v.6 were used for analysis, and P values < 0.05 were considered statistically significant.

RESULTS

Clinical Characteristics of Patients in Our Cohort and MSKCC Cohort

In our cohort, we performed WES in 33 patients who could be defined as DCB and NDB groups and who had tumor tissues/matched control samples prior to immunotherapy. Their clinical characteristics were presented in **Table 1**. Among them, 18 patients (54.5%) were younger than 65 years, and 25 patients (75.8%) were male. Adenocarcinoma was the most common histology, found in 48.5% of cases, followed by squamous cell carcinoma, found in 45.5% of cases. 42.4% patients had previously received platinum-based chemotherapy, 24.2% patients had previously received TKIs and anti-angiogenesis therapy, and the remaining 33.3% patients had no prior therapy before immunotherapy. The immunotherapy regimens included combination of PD-1 inhibitors and chemotherapy (75.8%), and monotherapy (PD-1 inhibitors, 24.2%). **Table 2** showed that good responses were more pronounced in younger patients and those with lower Eastern Cooperative Oncology Group (ECOG) scores, and only extra-pulmonary metastasis. In addition, patients with lower ECOG scores ($P = 0.023$) (**Figure 2A**) and only extra-pulmonary metastasis exhibited more prolonged PFS ($P = 0.029$) (**Figure 2B**).

In MSKCC cohort, we chose 75 patients who received immunotherapy and who had *MUC19* mutation data. Their clinical characteristics are presented in **Supplementary Table 1**. Among them, 39 (52.0%) patients were younger than 65 years, 37 patients (49.3%) were male, and 16 (21.3%) had squamous cell carcinoma. We also found that a lower ECOG score was significantly correlated with better clinical benefits of anti-PD-1 inhibitor treatment ($P = 0.0139$).

Association of *MUC19* Mutation With Clinical Benefits of Anti-PD-1 Inhibitors and Infiltration of $CD8^+$ T Cells in Our Cohort

To investigate whether individual gene mutations were associated with response or resistance to anti-PD-1 inhibitor treatment, we first focused our analysis on total gene mutations. The top gene mutations in our cohort were shown in **Figure 3A**; approximately half of the patients harbored a *TP53* mutation (57.6%). In addition to *TP53* mutations, we also found that the mutation rates of *TTN* (45.5%) and *MUC19* (42.4%) were both > 40%. Other common mutations, involving genes such as *EGFR, ERBB2, KRAS, PTEN*, and *BRAF*, were identified in 15.2, 9.1, 9.1, 9.1, and 3% of patients, respectively, and the related percentage was similar to a prior WES study performed in Chinese NSCLC patients (3). We further compared the gene mutations between DCB and NDB patients. Interestingly, we found that there were large differences in high-frequency mutations between the DCB and NDB groups (**Figure 3B**). Of these, mutations involving *MUC19* ($P = 0.015$) and *PKD1L2* ($P = 0.017$) were significantly enriched in the DCB and NDB groups, respectively. We also found that the mutation rate of *PTEN* (DCB vs. NDB, 5 vs.

TABLE 1 | Baseline clinical characteristics of NSCLC patients in our cohort.

Characteristics	Total (*N* = 33)	%
Age (years), median range	64	(36–83)
< 65	18	54.5
≥ 65	15	45.5
Sex		
Male	25	75.8
Female	8	24.2
Performance status		
0–1	25	75.8
≥ 2	8	24.2
Smoking status		
Former/Current	19	57.6
Never	14	42.4
Histology		
Adenocarcinoma	16	48.5
Squamous cell carcinoma	15	45.5
Other	2	6.1
Clinical benefit		
DCB	20	60.6
NDB	13	39.4
Actionable drivers		
Yes	8	24.2
- *EGFR* mutation	4	
- *ALK* rearrangement	1	
No	25	75.8
Stage		
III	10	30.3
IV	23	69.7
Metastasis site		
Lymph node (yes/no)	25/8	75.8/24.2
Lung (yes/no)	14/19	42.4/57.6
Bone (yes/no)	9/24	27.3/72.7
Liver (yes/no)	2/31	6.1/93.9
Brain (yes/no)	6/27	18.2/81.8
Adrenal (yes/no)	4/29	12.1/87.9
Previous treatment		
No prior therapy	11	33.3
Platinum-based chemotherapy	14	42.4
Others	8	24.2
Immunotherapy regimen		
PD-1 inhibitors	8	24.2
PD-1 inhibitors + Chemotherapy	25	75.8
Therapy Line		
1st	11	33.3
2nd	7	21.2
≥ 3rd	15	45.5

TABLE 2 | Associations of anti-PD-1 inhibitor efficacy with clinical characters in our cohort.

Parameter	DCB	NDB	*P* value
Age			0.038
<65	14	4	
≥ 65	6	9	
Sex			0.681
Male	16	9	
Female	4	4	
Performance status			0.035
0–1	18	7	
≥ 2	2	6	
Smoking status			1.000
Former/Current	12	7	
Never	8	6	
Histology			0.393
Adenocarcinoma	8	8	
Squamous cell carcinoma	11	4	
Other	1	1	
Stage			1.000
III	6	4	
IV	14	9	
Metastasis site			
Lymph node (yes/no)	14/6	11/2	0.432
Lung (yes/no)	5/15	9/4	0.012
Bone (yes/no)	6/14	3/10	1.000
Liver (yes/no)	1/19	1/12	1.000
Brain (yes/no)	5/15	1/12	0.364
Adrenal (yes/no)	3/17	1/12	1.000
Therapy Line			0.698
1st	7	4	
2nd	5	2	
≥3rd	8	7	
Treatment			0.681
Monotherapy	4	4	
Combination therapy	16	9	

15.3%) and *BRAF* (DCB vs. NDB, 0 vs. 7.7%) were higher in the NDB group, while *KRAS* was higher in the DCB group (DCB vs. NDB, 10 vs. 7.7%), which was consistent with previous reports (19)', although it did not reach statistical significance, likely owing to small numbers. In addition, we calculated TMB results. Although TMB is a predictive biomarker for the efficacy of immunotherapy recommended by guidelines (9), there were no significant differences involving TMB in our cohort (**Supplementary Figure 1**).

We next evaluated the association between gene mutations and patient survival. Of all the patients included, 16 died at the time of data collection. The median PFS for all 33 patients was 9.5 months (95% CI 4.5–14.4) and median OS was 26.2 months (95% CI 11.6–40.7). We examined PFS and gene mutations and found that compared with wild-type patients, *MUC19*-mutated patients had significantly longer PFS ($P = 0.024$) (**Figure 2C**), while *PKD1L2*-mutated patients had a shorter PFS ($P = 0.006$) (**Figure 2D**). In addition, we also discovered that *FNDC1, FSIP2, GSE1, KIAA1217, LRRK2, OTOGL, SCN5A, SRRT*, and *TOPAZ1* gene mutations were potentially poor prognostic factors for immunotherapy (**Supplementary Table 2**).

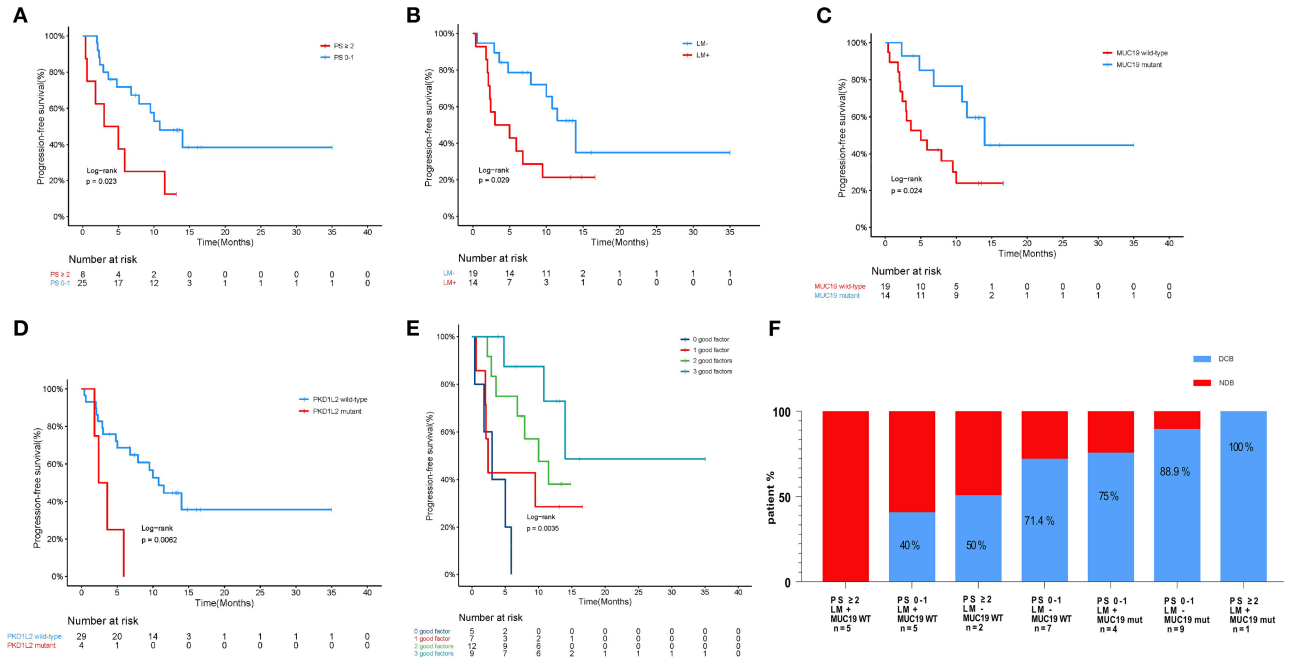

FIGURE 2 | Association of clinicopathological characteristics and gene mutation with anti-PD-1 inhibitor responses in our cohort. **(A)** Kaplan-Meier curves of PFS comparing patients with low performance (PS 0–1) and high performance (PS ≥ 2). **(B)** Kaplan-Meier curves of PFS comparing patients with or without intra-pulmonary metastasis. LM+, intra-pulmonary metastasis in the presence or absence of other extra-pulmonary metastases; LM-, only extra-pulmonary metastasis. **(C)** Kaplan-Meier curves of PFS comparing patients with mutant and wild-type *MUC19*. **(D)** Kaplan-Meier curves of PFS comparing patients with mutant and wild-type *PKD1L2*. **(E)** Effect of *MUC19* mutation status combined with performance and intra-pulmonary metastasis status on PFS in our cohort. **(F)** Histograms depicting proportions of patients who experienced DCB or NDB in different groups, defined by performance status (PS 0–1 or PS ≥ 2), intra-pulmonary metastasis (yes or no), and *MUC19* mutation status (mutant or wild-type), as indicated.

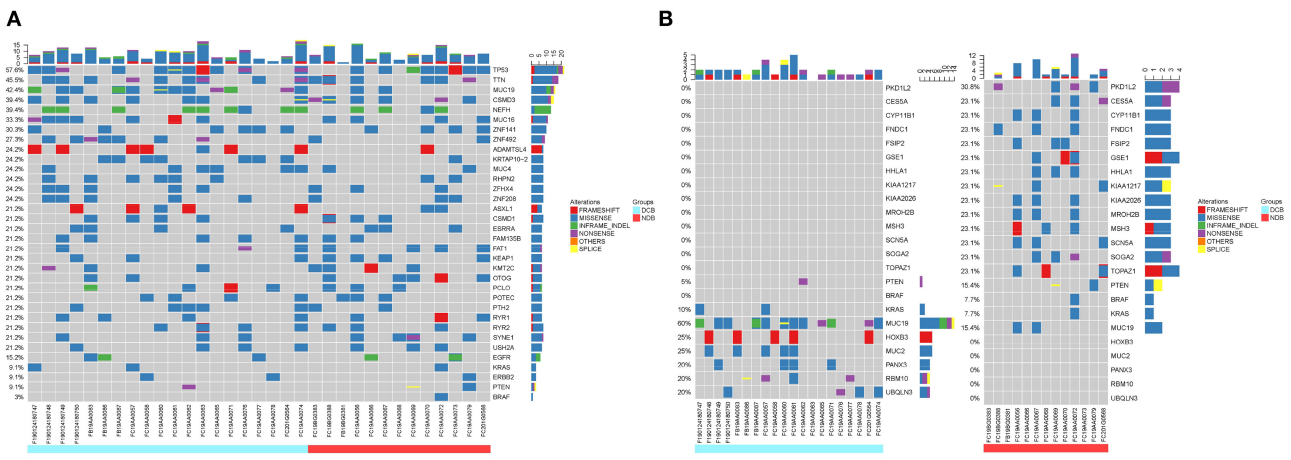

FIGURE 3 | Summary of molecular features associated with anti-PD-1 inhibitor responses. **(A)** The top mutation genes revealed by WES are listed. Sample IDs are shown at the bottom. Mutation frequencies are displayed on the left, and gene abbreviations are listed on the right. Icons representing mutation types are listed in different colors (red = frameshift, blue = missense, green = inframe-indel, purple = nonsense, yellow = splice, and orange = others). The top three mutation genes are *TP53*, *TTN,* and *MUC19* [71.4% (10/14) missense, 21.4% (3/14) inframe-indel, 14.2% (2/14) nonsense, and 7.14% (1/14) splice]. **(B)** Different high-frequency mutations in patients with DCB (left, blue) and NDB patients (right, red).

According to the above results, PFS was significantly prolonged in patients with lower ECOG scores, only extra-pulmonary metastasis, and *MUC19* mutation. Each of these variables is important for predicting sensitivity or resistance to immunotherapy; however, each also has limitations in its ability to explain immune checkpoint inhibitor responses. Combining

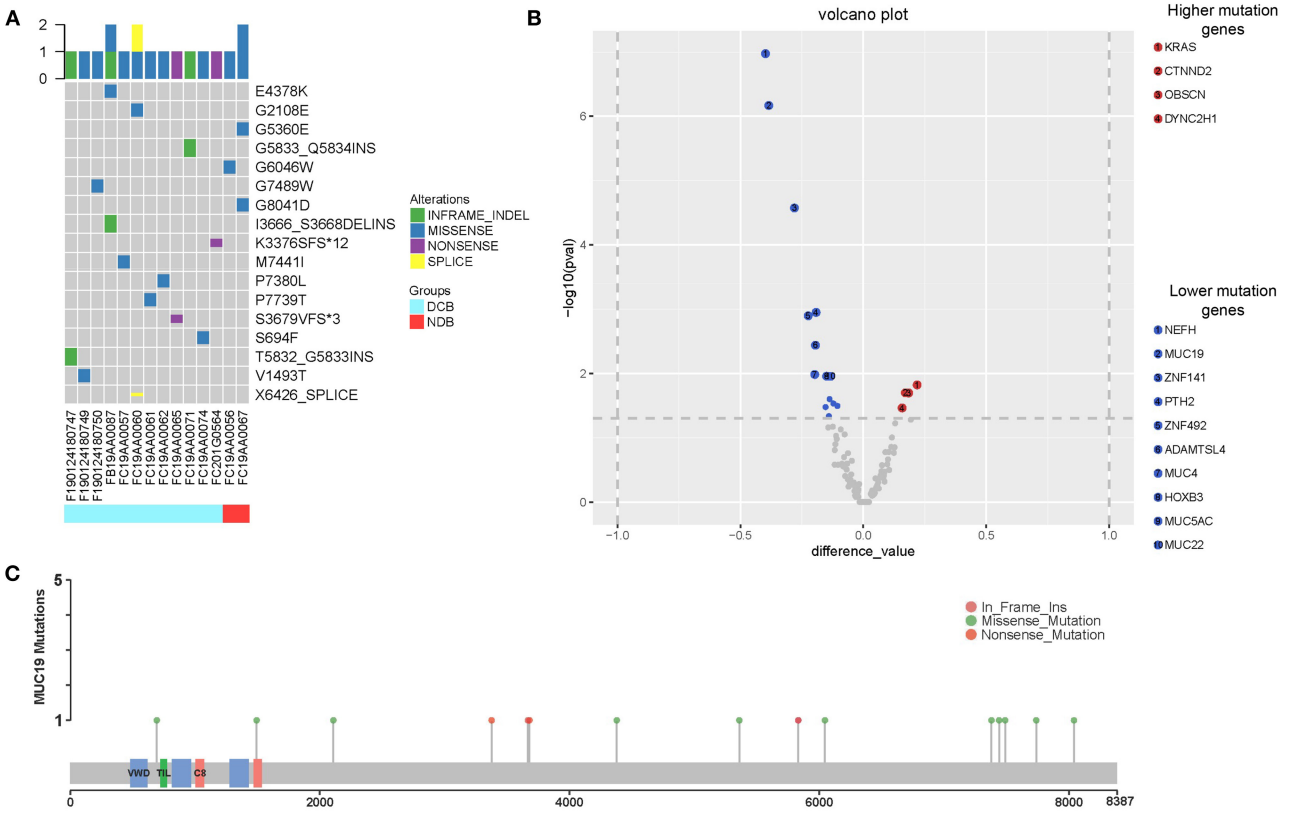

FIGURE 4 | Summary of MUC19 mutation and differential mutated genes between our cohort and MSKCC cohort. **(A)** *MUC19* mutation map of 14 patients including 12 DCB and 2 NDB patients. Sample IDs are shown at the bottom, mutation types on the top and mutants on the right. Icons representing mutation types are listed in different colors (blue = missense, green = inframe-indel, purple = nonsense, yellow = splice). **(B)** Volcano plot displaying differential mutated genes between our cohort and MSKCC cohort. X axis: difference value between gene mutation frequency of our cohort and MSKCC cohort. Y axis: -log10 (pval). Significant events refer to (|difference value| > 0.1 and $p < 0.05$); compared to our cohort, significantly higher mutation genes in MSKCC cohort are in red, significantly lower in blue, others in gray. **(C)** Lolliplot of *MUC19* mutations.

different biomarkers is crucial in stratifying populations benefiting from immunotherapy (17). Therefore, we combined the above variables to test whether this could lead to improved PFS. Intriguingly, when we combined these variables, patients with more positive predictors had longer PFS (**Figure 2E**). The combination of the three factors together was best in predicting clinical outcomes (**Figure 2F**).

In our study, there were 14 patients with *MUC19* mutation (**Figures 4A,C**). Among them, 71.4% (10/14) were missense, 21.4% (3/14) were inframe-indel, 14.2% (2/14) were nonsense, and 7.14% (1/14) were splice; 2 patients had two types of *MUC19* mutation. In DCB patients (12 patients), the mutation types were missense, inframe-indel, nonsense and splice; in NDB patients (2 patients), the mutation type was missense. In addition, the *MUC19* mutants (E4378K, G2108E, G5360E, G5833_Q5834INS, G6046W, G7489W, G8041D, I3666_S3668DELINS, K3376SFS*12, M7441I, P7380L, P77380L, P7739T, S3679VFS*3, S694F, T5832_G5833INS, V1493T, X6426_SPLICE) had the same mutant frequency. To uncover the underlying reason for *MUC19* mutation being associated with clinical benefits of anti-PD-1 inhibitor treatment, we performed CD8 immunohistochemical staining. Compared to *MUC19* wild-type patients, *MUC19*-mutated patients exhibited more infiltration of $CD8^+$ T cells ($P = 0.0313$) (**Figures 5A,B**). And patients with higher $CD8^+$ T cells showed a significantly longer PFS ($P = 0.00021$) (**Figure 5C**).

Association of *MUC19* Mutation With Immune Responses and Clinical Benefits of Anti-PD-1 Inhibitors in Public Datasets

MUC19 is located on the long arm of chromosome 12 and encodes a member of the gel-forming mucin protein family which constitute the physical barrier, and protect epithelial cells from stress-induced damage (20, 21). *MUC19* is highly expressed in the corneal conjunctiva, lacrimal glands, and gastrointestinal glands, and is also expressed in the subtracheal glands (22). From the GeneCards website (https://www.genecards.org/), we identified that *MUC19* was similarly expressed in the lung, bone marrow, lymph node, thymus, and other immune system organs (**Supplementary Figure 2A**). It has been reported that MUC19 expression is involved in the pathogenesis of Sjogren

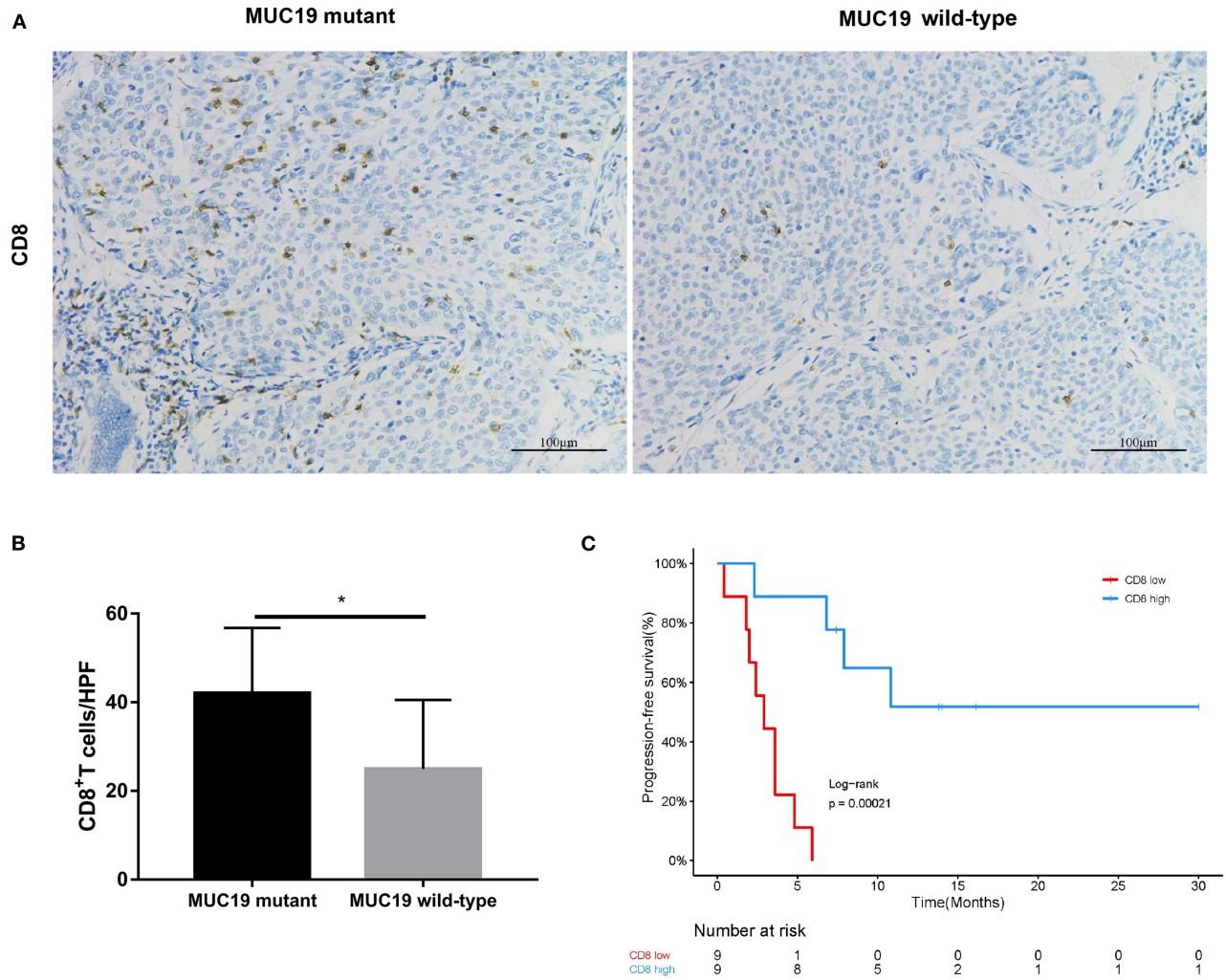

FIGURE 5 | Association of *MUC19* mutation with CD8$^+$ T cell infiltration. **(A)** Representative images of CD8 staining in *MUC19*-mutant (left) and wild-type (right) patients. Acquired at × 200 magnification. Scar bar = 100 μm. **(B)** Manually-counted average CD8$^+$ cells/HPF are shown in the bar. HPF: high-power field. **(C)** Kaplan-Meier curves of PFS comparing patients with high and low CD8. *$P < 0.05$.

syndrome and breast cancer; and breast cancer patients with higher MUC19 expression exhibited worse prognosis (23). In addition, *MUC19* mutation was found in inflammatory bowel disease, melanoma, colorectal adenocarcinoma, and esophageal squamous cell carcinoma (24–27). At present, what we understand regarding *MUC19* is limited, and the role of *MUC19* in lung cancer also remains unclear. This is the first study to explore and uncover the role of *MUC19* in lung cancer.

Using the cBioPortal website, we downloaded all lung cancer datasets containing *MUC19* mutations (**Figure 1B**). These six studies included a total of 2,323 patients/2,672 samples, which included 1.5% Asian and 98.5% non-Asian populations. The mutation rate of *MUC19* was between 2 and 7% (**Figure 6A**). Surprisingly, from the International Cancer Genome Consortium Data Portal website, we found that the mutation rate of *MUC19* was 63.53% in a Korean cohort (LUSC-KR), which was very close to that of our study. However, the *MUC19* mutation rate in the LUSC-US and LUAD-US cohorts was < 6% (**Figure 6A**). The differential mutated genes between eastern (our cohort) and western (MSKCC cohort) people were shown in **Figure 4B**; compared to our cohort, the significantly higher mutation genes in MSKCC cohort were *KRAS, CTNND2, OBSCN,* and *DYNC2H1*, the significantly lower mutation genes were *NEFH, MUC19, ZNF141, PTH2, ZNF492, ADAMTSL4, MUC4, HOXB3, MUC5AC* and *MUC22.* Furthermore, we compared the difference of clinical characteristics between *MUC19* mutants versus *MUC19* wide-type patients in our cohort (**Table 3**), there were no statistical differences between them. As for the role of *MUC19* mutation on OS, we found that wild-type patients presented significantly lower OS compared to *MUC19*-mutated patients ($P = 0.002$) (**Supplementary Figure 2B**).

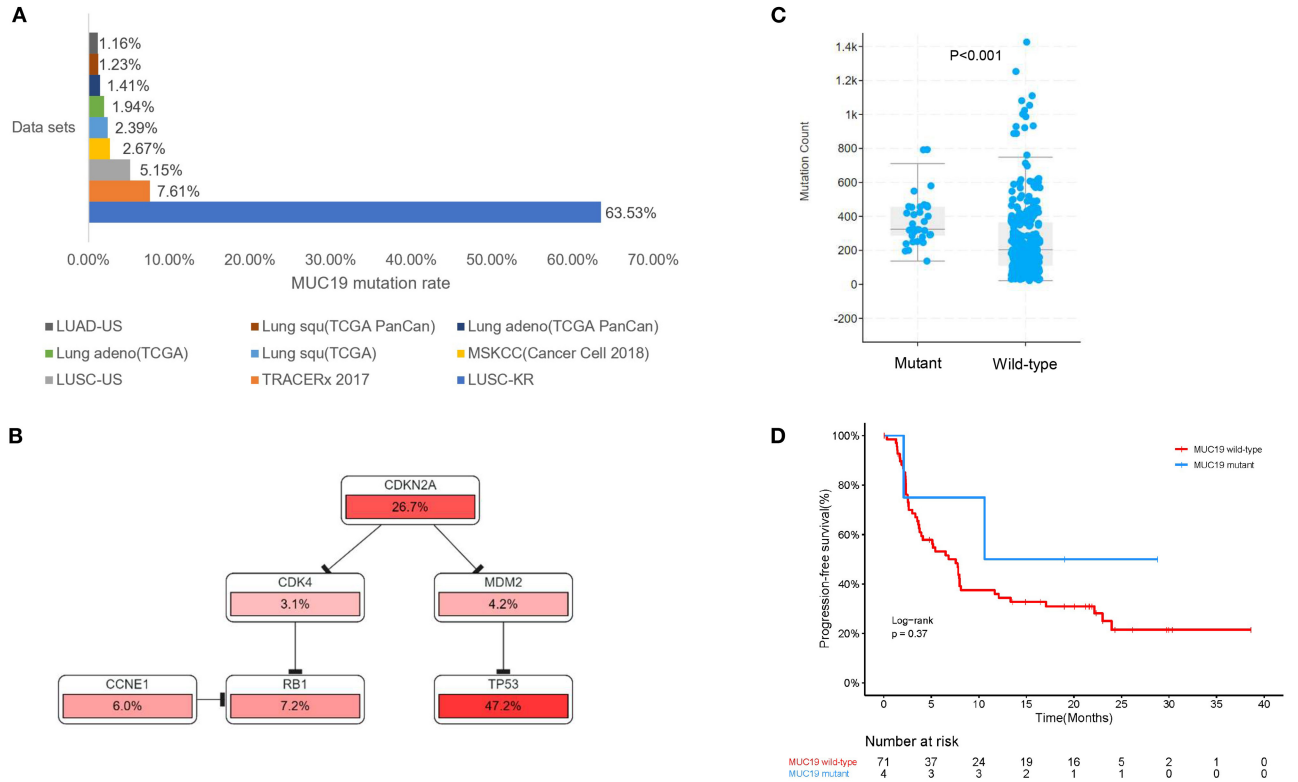

FIGURE 6 | Association of *MUC19* mutation with immune responses and clinical benefits of anti-PD-1 inhibitors in public datasets. **(A)** Mutation rates identified using different public datasets. The LUSC-KR, LUSC-US, and LUAD-US data sets were downloaded from the International Cancer Genome Consortium website. The TRACERx 2017, MSKCC, Lung squ (TCGA), Lung adeno (TCGA), Lung adeno (TCGA PanCan), Lung squ (TCGA PanCan) were downloaded from the cBioPortal website. **(B)** Pathway mapper analysis of patients with or without *MUC19* mutation using the cBioPortal website. TP53-RB1 signaling pathway was the most frequently altered pathway. **(C)** Comparison of mutation count between patients with or without *MUC19* mutation in TRACERx 2017. **(D)** Kaplan-Meier curves of PFS comparing patients with mutated and wild-type *MUC19* in the MSKCC cohort.

We further explored the role of *MUC19* mutations in immune responses. Gene Ontology (GO) annotation revealed that the *MUC19* gene is involved in innate immune response activating cell surface receptor signaling pathway (GO: 0002220). When using pathway mapper analysis on the cBioPortal website, the TP53-RB1 signaling pathway was the most frequently altered in the *MUC19* mutation group compared to the non-mutated group (**Figure 6B**). According to recent studies, *TP53* mutations could have a major impact on the lung tumor microenvironment (TME) and increase sensitivity to anti-PD-1 inhibitors in lung cancer (8). We also analyzed the mutation count in 100 patients/327 samples from another public dataset (TRACERx) through the cBioPortal website (28). *MUC19*-mutated patients had higher mutation counts than the non-mutated group ($P < 0.001$) (**Figure 6C**). It has been suggested that mutation count could reflect the whole exome mutational burden and that the mutation count of certain genes could be used as a new predictive marker to guide immunotherapy for NSCLC patients (29, 30).

More importantly, we validated our results in the MSKCC cohort containing 75 American lung cancer patients receiving immunotherapy and with *MUC19* mutation information. Although there was no significant difference, PFS of the *MUC19* mutation group was longer than that of the non-mutated patients (19.7 vs. 7.6 months, $P = 0.413$) (**Figure 6D**), which was consistent with our results.

DISCUSSION

Although the emergence of immunotherapy has dramatically changed treatment paradigms in NSCLC, only 20% of patients are able to benefit from immunotherapy (3). It is worth noting that some patients might suffer from significant immunotoxicity (4), and a large proportion of patients in China cannot afford them. Considering the low efficacy rate, immunotoxicity, and the drug cost, stratifying patients by specific biomarkers is essential. However, currently recommended biomarkers by National Comprehensive Cancer Network guidelines, such as PD-L1 and TMB, are not perfect biomarkers (31). Therefore, it is essential to discover novel biomarkers that are predictors of immunotherapy responses.

WES is a new method for identifying abnormalities in any gene. Compared to targeted gene panel sequencing, WES can

TABLE 3 | Associations of *MUC19* mutation status with clinical characters in our cohort.

Parameter	*MUC19 wild-type*	*MUC19 mutant*	*P* value
Age			1.000
<65	10	8	
≥ 65	9	6	
Sex			0.416
Male	13	12	
Female	6	2	
BMI			0.455
<24	12	11	
≥ 24	7	3	
Performance status			0.416
0–1	13	12	
≥2	6	2	
Smoking status			0.286
Former/Current	9	10	
Never	10	4	
Histology			0.854
Adenocarcinoma	10	6	
Squamous cell carcinoma	8	7	
Other	1	1	
Stage			0.257
III	4	6	
IV	15	8	
Metastasis site			
Lymph node (yes/no)	16/3	9/5	0.238
Lung (yes/no)	10/9	4/10	0.286
Bone (yes/no)	5/14	4/10	1.000
Liver (yes/no)	1/18	1/13	1.000
Brain (yes/no)	3/16	3/11	1.000
Adrenal (yes/no)	3/16	1/13	0.62
PD-L1			
<1%	4	4	0.716
≥1%	7	6	
Unknown	8	4	
TMB			0.363
<10 mut/Mb	17	10	
≥10 mut/Mb	2	4	

discover abnormalities that have not been previously associated with any disease (32). Therefore, we chose WES to uncover novel gene mutations to identify immune checkpoint inhibitor responders in NSCLC. We identified a novel *MUC19* gene mutation from our data. In our study, both tumor tissue samples and matched control samples were tested, and patient matched control samples were used as negative controls. And none of these mutations detected in negative controls are included in our analysis, therefore, *MUC19* mutations found in our study are somatic mutations.

To our knowledge, this is the first study characterizing *MUC19* in lung cancer. We found that the mutation rate of *MUC19* in lung cancer was higher in Asian patients than in non-Asian patients (LUSC-KR 63.53% vs. LUSC-US 5.15%; LUSC-US 5.15% vs. LUAD-US 1.16%). Consistent with other studies (33, 34), we also found the different mutation rate of KRAS influenced by ethnicity in our study (**Figure 4B**). In addition, environmental factors could also affect gene mutations. Bacterial infection (*F. nucleatum* and *B. fragilis*) led to gene mutations (35), tobacco exposure had an effect on intestinal microbiome and could also produce new gene mutations (36, 37). More interestingly, bacterial infection (*Streptococcus pneumoniae*, nontypeable *Haemophilus influenzae*) upregulated MUC19 expression (38). Hence, the effect of microbiome and tobacco exposure on *MUC19* mutation needs further research.

Remarkably, for the first time, we uncovered a predictive role of *MUC19* mutation in NSCLC patients receiving anti-PD-1 inhibitors. We aimed to understand the underlying mechanism behind this phenomenon. First, we detected infiltration of $CD8^+$ T cells in the TME. We found an association of *MUC19* mutation with more $CD8^+$ T cells (**Figure 7**), which suggests a "hot" TME (39). Second, we searched public datasets to uncover the inner connections and causality of *MUC19* mutations with immune responses. Both GO annotation and cBioPortal pathway mapper analysis indicated the involvement of *MUC19* mutation in immune responses. Lastly, but most importantly, we validated our results in the MSKCC cohort. Compared to wild-type patients, *MUC19*-mutated patients showed a trend for increased PFS, although this was not statistically significant, likely owing to the small number of patients studied. The MSKCC group is an American cohort, so the mutation rate was relatively low in this cohort. Therefore, it was difficult to observe a predictive role for *MUC19* mutations in this cohort. In the future, larger studies are needed to validate our results, especially in Asian patients. In addition to *MUC19* mutation, we also found that gene mutations such as those involving *PKD1L2* and *OTOGL* were poor prognostic factors for immunotherapy. Considering the low numbers of mutation-positive patients, we did not analyze the related information in public datasets. Additional studies are needed to confirm these results.

Although TMB is recommended by the Food and Drug Administration as a new predictive biomarker for patients with unresectable or metastatic solid tumors receiving pembrolizumab, new KETNOTE021 data showed no association of TMB with the efficacy of pembrolizumab plus carboplatin and pemetrexed (40). In our cohort, 75.8% of patients received a combination of immunotherapy and chemotherapy. Therefore, it is not difficult to understand that there were no differences between the two groups.

Taken together, the originality of our work relies on the fact that we uncovered a novel role of *MUC19* mutation in predicting the efficacy of anti-PD-1 inhibitors. Furthermore, we analyzed the association of *MUC19* status with infiltration by $CD8^+$ T cells in the TME. As the sample size in our study was small and represented only a single center investigation, we validated our results using public datasets. Although not perfect, we have discovered potential influencing factors surrounding the clinical benefits of anti-PD-1 inhibitors. Future studies should aim to

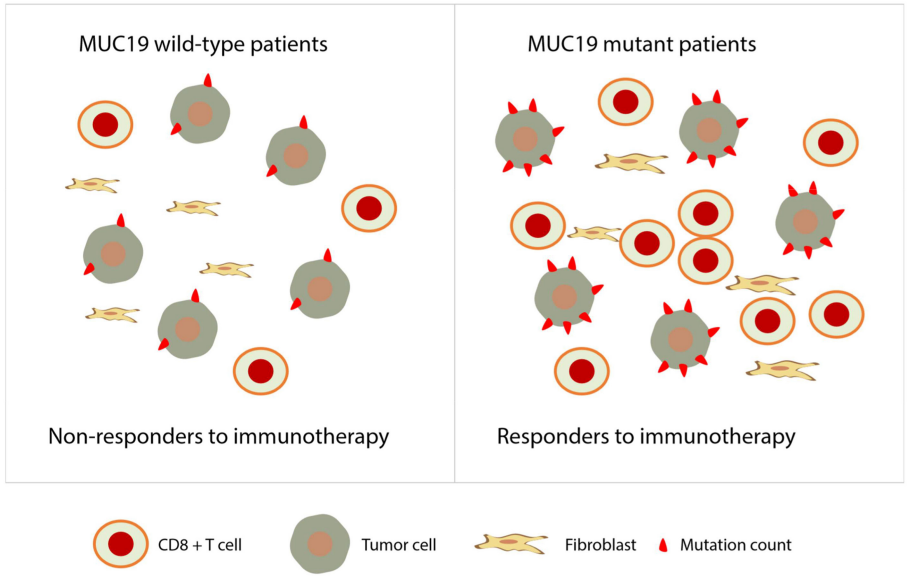

FIGURE 7 | Proposed role of *MUC19* mutation in predicting clinical benefits of immunotherapy. *MUC19*-mutated NSCLC patients are associated with more infiltration of $CD8^+$ T cells and higher mutation count, therefore, they are more likely to be responders to immunotherapy.

characterize the role of *MUC19* mutation in mediating cancer immune responses, and large-scale prospective studies will be required to validate our results.

DATA AVAILABILITY STATEMENT

The whole exome sequencing data has been deposited into a publicly accessible repository: http://db.cngb.org/cnsa/project/CNP0001349/reviewlink/.

ETHICS STATEMENT

The studies involving human participants were reviewed and approved by Medical Ethics Committee of Jinling Hospital. The patients/participants provided their written informed consent to participate in this study. Written informed consent was obtained from the individual(s) for the publication of any potentially identifiable images or data included in this article.

AUTHOR CONTRIBUTIONS

YSo, TL, and DL conceived and designed the experiments. LZ, LH, and QX drafted the manuscript and produced the figures. LZ, YL, ZW, and HH were responsible for data collection and analysis. LH, QX, YSh, and PZ performed statistical analyses and edited references. YSo, TL, and DL revised the manuscript. All authors have approved the final version of the manuscript.

FUNDING

This work was supported by the National Natural Science Foundation of China [Grant Number 81772500], Jiangsu Provincial Social Development—Key Projects—Clinical Frontier Technologies [Grant Number BE2019719], Suzhou technology project [Grant Number SS201653], Jiangsu Provincial Social Development—General Program [Grant Number BE20197180]. 81772500 is used for WES detection, SS201653 is use for publication fees and BE20197180 is used for buying antibody and CD8 detection.

ACKNOWLEDGMENTS

We are grateful to all study participants who made this research possible.

SUPPLEMENTARY MATERIAL

The Supplementary Material for this article can be found online at: https://www.frontiersin.org/articles/10.3389/fonc.2021.596542/full#supplementary-material

REFERENCES

1. Herbst RS, Morgensztern D, Boshoff CJN. The biology and management of non-small cell lung cancer. *Nature.* (2018) 553:446. doi: 10.1038/nature25183
2. Pardoll DM. The blockade of immune checkpoints in cancer immunotherapy. *Nat Rev Cancer.* (2012) 12:252–64. doi: 10.1038/nrc3239
3. Fang W, Ma Y, Yin JC, Hong S, Zhou H, Wang A, et al. Comprehensive genomic profiling identifies novel genetic predictors of response to

anti-PD-(L)1 therapies in non-small cell lung cancer. *Clin Cancer Res.* (2019) 25:5015–26. doi: 10.1158/1078-0432.CCR-19-0585
4. Topalian SL, Hodi FS, Brahmer JR, Gettinger SN, Smith DC, McDermott DF, et al. Safety, activity, and immune correlates of anti-PD-1 antibody in cancer. *N Engl J Med.* (2012) 366:2443–54. doi: 10.1056/NEJMoa1200690
5. Rizvi H, Sanchez-Vega F, La K, Chatila W, Jonsson P, Halpenny D, et al. Molecular determinants of response to anti-programmed cell death (PD)-1 and Anti-Programmed Death-Ligand 1 (PD-L1) blockade in patients with non-small-cell lung cancer profiled with targeted next-generation sequencing. *J Clin Oncol.* (2018) 36:633–41. doi: 10.1200/JCO.2017.75.3384
6. Bodor JN, Boumber Y, Borghaei H. Biomarkers for immune checkpoint inhibition in non-small cell lung cancer (NSCLC). *Cancer.* (2020) 126:260–70. doi: 10.1002/cncr.32468
7. Sacher AG, Gandhi L. Biomarkers for the Clinical Use of PD-1/PD-L1 inhibitors in non-small-cell lung cancer: a review. *JAMA Oncol.* (2016) 2:1217–22. doi: 10.1001/jamaoncol.2016.0639
8. Dong ZY, Zhong WZ, Zhang XC, Su J, Xie Z, Liu SY, et al. Potential predictive value of TP53 and KRAS mutation status for response to PD-1 blockade immunotherapy in lung adenocarcinoma. *Clin Cancer Res.* (2017) 23:3012–24. doi: 10.1016/j.jtho.2016.11.504
9. Samstein RM, Lee CH, Shoushtari AN, Hellmann MD, Shen R, Janjigian YY, et al. Tumor mutational load predicts survival after immunotherapy across multiple cancer types. *Nat Genet.* (2019) 51:202–6. doi: 10.1038/s41588-018-0312-8
10. Marabelle A, Fakih MG, Lopez J, Shah M, Shapira-Frommer R, Nakagawa K, et al. 1192O - Association of tumour mutational burden with outcomes in patients with select advanced solid tumours treated with pembrolizumab in KEYNOTE-158. *Ann Oncol.* (2019) 30:v477–v8. doi: 10.1093/annonc/mdz253.018
11. Chan TA, Yarchoan M, Jaffee E, Swanton C, Quezada SA, Stenzinger A, et al. Development of tumor mutation burden as an immunotherapy biomarker: utility for the oncology clinic. *Ann Oncol.* (2019) 30:44–56. doi: 10.1093/annonc/mdy495
12. Skoulidis F, Goldberg ME, Greenawalt DM, Hellmann MD, Awad MM, Gainor JF, et al. STK11/LKB1 mutations and PD-1 inhibitor resistance in KRAS-mutant lung adenocarcinoma. *Cancer Discov.* (2018) 8:822–35. doi: 10.1158/2159-8290.CD-18-0099
13. Horn S, Leonardelli S, Sucker A, Schadendorf D, Griewank KG, Paschen A. Tumor CDKN2A-associated JAK2 loss and susceptibility to immunotherapy resistance. *J Nat Cancer Inst.* (2018) 110:677–81. doi: 10.1093/jnci/djx271
14. Gao J, Shi LZ, Zhao H, Chen J, Xiong L, He Q, et al. Loss of IFN-γ pathway genes in tumor cells as a mechanism of resistance to anti-CTLA-4 therapy. *Cell.* (2016) 167:397–404.e9. doi: 10.1016/j.cell.2016.08.069
15. Ott PA, Bang YJ, Piha-Paul SA, Razak ARA, Bennouna J, Soria JC, et al. T-Cell-inflamed gene-expression profile, programmed death ligand 1 expression, and tumor mutational burden predict efficacy in patients treated with pembrolizumab across 20 cancers: KEYNOTE-028. *J Clin Oncol.* (2019) 37:318–27. doi: 10.1200/JCO.2018.78.2276
16. Cristescu R, Mogg R, Ayers M, Albright A, Murphy E, Yearley J, et al. Pan-tumor genomic biomarkers for PD-1 checkpoint blockade-based immunotherapy. *Science.* (2018) 362:6411. doi: 10.1126/science.aar3593
17. Camidge DR, Doebele RC, Kerr KM. Comparing and contrasting predictive biomarkers for immunotherapy and targeted therapy of NSCLC. *Nat Rev Clin Oncol.* (2019) 16:341–55. doi: 10.1038/s41571-019-0173-9
18. Hellmann MD, Nathanson T, Rizvi H, Creelan BC, Sanchez-Vega F, Ahuja A, et al. Genomic features of response to combination immunotherapy in patients with advanced non-small-cell lung cancer. *Cancer Cell.* (2018) 33:843–52.e4. doi: 10.1016/j.ccell.2018.03.018
19. Saigi M, Alburquerque-Bejar JJ, Sanchez-Cespedes M. Determinants of immunological evasion and immunocheckpoint inhibition response in non-small cell lung cancer: the genetic front. *Oncogene.* (2019) 38:5921–32. doi: 10.1038/s41388-019-0855-x
20. Chen Y, Zhao YH, Kalaslavadi TB, Hamati E, Nehrke K, Le AD, et al. Genome-wide search and identification of a novel gel-forming mucin MUC19/Muc19 in glandular tissues. *Am J Respir Cell Mol Biol.* (2004) 30:155–65. doi: 10.1165/rcmb.2003-0103OC
21. Kufe DW. Mucins in cancer: function, prognosis and therapy. *Nat Rev Cancer.* (2009) 9:874–85. doi: 10.1038/nrc2761
22. Yu DF, Chen Y, Han JM, Zhang H, Chen XP, Zou WJ, et al. MUC19 expression in human ocular surface and lacrimal gland and its alteration in Sjögren syndrome patients. *Exp Eye Res.* (2008) 86:403–11. doi: 10.1016/j.exer.2007.11.013
23. Song L, Xiao Y. Downregulation of hsa_circ_0007534 suppresses breast cancer cell proliferation and invasion by targeting miR-593/MUC19 signal pathway. *Biochem Biophys Res Commun.* (2018) 503:2603–10. doi: 10.1016/j.bbrc.2018.08.007
24. Rivas MA, Beaudoin M, Gardet A, Stevens C, Sharma Y, Zhang CK. Deep resequencing of GWAS loci identifies independent rare variants associated with inflammatory bowel disease. *Nat Genet.* (2011) 43:1066–73. doi: 10.1038/ng.952
25. Cifola I, Pietrelli A, Consolandi C, Severgnini M, Mangano E, Russo V, et al. Comprehensive genomic characterization of cutaneous malignant melanoma cell lines derived from metastatic lesions by whole-exome sequencing and SNP array profiling. *PLoS ONE.* (2013) 8:e63597. doi: 10.1371/journal.pone.0063597
26. Chu X, Xue Y, Huo X, Wei J, Chen Y, Han R, et al. Establishment and characterization of a novel cell line (cc 006cpm8) of moderately/poorly differentiated colorectal adenocarcinoma derived from a primary tumor of a patient. *Int J Oncol.* (2019) 55:243–56. doi: 10.3892/ijo.2019.4806
27. Chen Z, Yao N, Zhang S, Song Y, Shao Q, Gu H, et al. Identification of critical radioresistance genes in esophageal squamous cell carcinoma by whole-exome sequencing. *Ann Transl Med.* (2020) 8:998. doi: 10.21037/atm-20-5196
28. Jamal-Hanjani M, Wilson GA, McGranahan N, Birkbak NJ, Watkins TBK, Veeriah S, et al. Tracking the Evolution of non-small-cell lung cancer. *N Engl J Med.* (2017) 376:2109–21. doi: 10.1056/NEJMoa1616288
29. Lee DW, Han SW, Bae JM, Jang H, Han H, Kim H, et al. Tumor mutation burden and prognosis in patients with colorectal cancer treated with adjuvant fluoropyrimidine and oxaliplatin. *Clin Cancer Res.* (2019) 25:6141–7. doi: 10.1158/1078-0432.CCR-19-1105
30. Wang S, Jia M, He Z, Liu XS. APOBEC3B and APOBEC mutational signature as potential predictive markers for immunotherapy response in non-small cell lung cancer. *Oncogene.* (2018) 37:3924–36. doi: 10.1038/s41388-018-0245-9
31. Duffy MJ, Crown J. Biomarkers for predicting response to immunotherapy with immune checkpoint inhibitors in cancer patients. *Clin Chem.* (2019) 65:1228–38. doi: 10.1373/clinchem.2019.303644
32. Gray SW, Park ER, Najita J, Martins Y, Traeger L, Bair E, et al. Oncologists' and cancer patients' views on whole-exome sequencing and incidental findings: results from the CanSeq study. *Gen Med.* (2016) 18:1011–9. doi: 10.1038/gim.2015.207
33. Nassar AH, Adib E, Kwiatkowski DJ. Distribution of KRASG12C somatic mutations across race, sex, and cancer type. *N Engl J Med.* (2021) 384:2 doi: 10.1056/NEJMc2030638
34. Dearden S, Stevens J, Wu YL, Blowers D. Mutation incidence and coincidence in non small-cell lung cancer: meta-analyses by ethnicity and histology (mutMap). *Ann Oncol.* (2013) 24:2371–6. doi: 10.1093/annonc/mdt205
35. Greathouse KL, White JR, Vargas AJ, Bliskovsky VV, Beck JA, von Muhlinen N, et al. Interaction between the microbiome and TP53 in human lung cancer. *Genome Biol.* (2018) 19:123. doi: 10.1186/s13059-018-1501-6
36. Gibbons DL, Byers LA, Kurie JM. Smoking, p53 mutation, and lung cancer. *Mol Cancer Res.* (2014) 12:3–13. doi: 10.1158/1541-7786.MCR-13-0539
37. Savin Z, Kivity S, Yonath H, Yehuda S. Smoking and the intestinal microbiome. *Arch Microbiol.* (2018) 200:677–84. doi: 10.1007/s00203-018-1506-2

38. Hong W, Khampang P, Kerschner AR, Mackinnon AC, Yan K, Simpson PM, et al. Antibiotic modulation of mucins in otitis media; should this change our approach to watchful waiting? *Int J Pediatr Otorhinolaryngol.* (2019) 125:134–40. doi: 10.1016/j.ijporl.2019.07.002
39. Langer CJ, Gadgeel S, Borghaei H, Patnaik A, Powell S, Gentzler R, et al. OA04.05 KEYNOTE-021: TMB and outcomes for carboplatin and pemetrexed with or without pembrolizumab for non-squamous NSCLC. *J Thor Oncol.* (2019) 14:S216. doi: 10.1016/j.jtho.2019.08.426
40. Galon J, Bruni D. Approaches to treat immune hot, altered and cold tumours with combination immunotherapies. *Nature reviews Drug discovery.* (2019) 18:197–218. doi: 10.1038/s41573-018-0007-y

Conflict of Interest: YSh was employed by the company Geneseeq Technology Inc.

The remaining authors declare that the research was conducted in the absence of any commercial or financial relationships that could be construed as a potential conflict of interest.

frontiers in Oncology

ORIGINAL RESEARCH
published: 20 April 2021
doi: 10.3389/fonc.2021.629333

GEO Data Mining Identifies OLR1 as a Potential Biomarker in NSCLC Immunotherapy

Bin Liu[1], Ziyu Wang[1], Meng Gu[1], Cong Zhao[1], Teng Ma[1] and Jinghui Wang[1,2]**

[1] Department of Cellular and Molecular Biology, Beijing Chest Hospital, Capital Medical University, Beijing Tuberculosis and Thoracic Tumor Research Institute, Beijing, China, [2] Department of Medical Oncology, Beijing Chest Hospital, Capital Medical University, Beijing Tuberculosis and Thoracic Tumor Research Institute, Beijing, China

OPEN ACCESS

Edited by:
Qian Chu,
Huazhong University of Science and Technology, China

Reviewed by:
Chengrong Xie,
Xiamen University, China
Xiaomin Wang,
Xiamen University, China

***Correspondence:**
Teng Ma
mateng82913@163.com
Jinghui Wang
jinghuiwang2006@163.com

Specialty section:
This article was submitted to Cancer Immunity and Immunotherapy, a section of the journal Frontiers in Oncology

Received: *14 November 2020*
Accepted: *18 March 2021*
Published: *20 April 2021*

Citation:
Liu B, Wang Z, Gu M, Zhao C, Ma T and Wang J (2021) GEO Data Mining Identifies OLR1 as a Potential Biomarker in NSCLC Immunotherapy. Front. Oncol. 11:629333. doi: 10.3389/fonc.2021.629333

Non-small cell lung cancer (NSCLC) is the most common type of lung cancer. The tumor immune microenvironment (TME) in NSCLC is closely correlated to tumor initiation, progression, and prognosis. TME failure impedes the generation of an effective antitumor immune response. In this study, we attempted to explore TME and identify a potential biomarker for NSCLC immunotherapy. 48 potential immune-related genes were identified from 11 eligible Gene Expression Omnibus (GEO) data sets. We applied the CIBERSORT computational approach to quantify bulk gene expression profiles and thereby infer the proportions of 22 subsets of tumor-infiltrating immune cells (TICs); 16 kinds of TICs showed differential distributions between the tumor and control tissue samples. Multiple linear regression analysis was used to determine the correlation between TICs and 48 potential immune-related genes. Nine differential immune-related genes showed statistical significance. We analyzed the influence of nine differential immune-related genes on NSCLC immunotherapy, and OLR1 exhibited the strongest correlation with four well-recognized biomarkers (PD-L1, CD8A, GZMB, and NOS2) of immunotherapy. Differential expression of OLR1 showed its considerable potential to divide TICs distribution, as determined by non-linear dimensionality reduction analysis. In immunotherapy prediction analysis with the comparatively reliable tool TIDE, patients with higher OLR1 expression were predicted to have better immunotherapy outcomes, and OLR1 expression was potentially highly correlated with PD-L1 expression, the average of CD8A and CD8B, IFNG, and Merck18 expression, T cell dysfunction and exclusion potential, and other significant immunotherapy predictors. These findings contribute to the current understanding of TME with immunotherapy. OLR1 also shows potential as a predictor or a regulator in NSCLC immunotherapy.

Keywords: non-small cell lung cancer, immunotherapy, tumor microenvironment, PD-L1, immune checkpoint

INTRODUCTION

Lung cancer is one of the most commonly occurring malignancies and is identified as leading cause of cancer-related deaths worldwide. Statistics on cancer reveal that in 2018, more than 2 million patients suffered from lung cancer worldwide, and lung cancer ranked first among all cancer types (1). In China, lung cancer has shown the highest incidence and mortality over the last decade and posed a significant threat to human health (2). Lung cancer comprises nearly 20% of all cancer deaths and its mortality may increase by approximately 40% by 2030 (3). Lung cancer has been subdivided based on pathological classification into two groups: small-cell lung cancer (SCLC) and Non-small cell lung cancer (NSCLC). NSCLC is further stratified into three subsets: adenocarcinoma (the most common type, which comprises 40% of all lung cancer types), squamous cell carcinoma (25%) and large cell carcinoma (about 10%) (4). 75% of NSCLC is diagnosed at the advanced stage, resulting in a five-year survival rate of less than 15% (5). In addition to surgery and chemoradiotherapy, immunotherapy shows promising potential in treatment of NSCLC.

Programmed death-1 (PD-1) and its ligand (PD-L1) antibody based Immunotherapies have recently shown significant advances in the treatment of NSCLC through enhancing the attack of the host immune system on malignant cells (6). However, a number of patients still fail to benefit from these immunotherapies possibly because of tumor immune microenvironment (TME) alterations (7). The tumor microenvironment includes cross-talks among cancer cells, endothelial cells, fibroblasts and immune cells. Previous studies have shown the potential associations between the microenvironment and the effects of immunotherapy (8). The tumor microenvironment presents physical, immunologic, and metabolic barriers to enduring immunotherapy responses, and the suppressive microenvironment of tumors remains one of the limiting factors for immunotherapies. In this study, we screened those genes that enriched in tumor tissue and closely related to the immune microenvironment in NSCLC. Targeting PD-L1, one of the most representative immunotherapy strategies, was studied in relation to the screened microenvironment genes. The response prediction markers of PD-L1 were used as standard and to study the predictive value of each gene as biomarker for host tumor immunity in NSCLC. We aimed to find a highly predictive PD-L1 blockade therapy biomarker for clinical use, or the potential targeting genes, to change the tumor microenvironment for enhanced immunotherapy effects.

MATERIALS AND METHODS

Raw Data

Eligible data sets in GEO were selected according to the following criteria and 11 data sets were obtained as of May 2020 (including 268 cases of control samples, 601 cases of lung tumor samples) (9–18). Data sets details are listed in **Table 1**. The selection criteria are as follows: definite diagnosis with NSCLC; inclusion of control samples in the same data set; samples without any treatment before sequencing; gene expression data based on the Affymetrix platform. After normalization of mRNA data with the limma algorithm in R language, all data sets were merged into a new data set for downstream analysis.

Identification and Analysis of DEGs

Data were analyzed using the limma package in the R language. Details on cutoffs were as follows: Fold change>1 or <−1, and adj. P <0.05. Heatmaps and volcano plots were generated using the limma package and pheatmap respectively. Gene ontology (Go) and Kyoto Encyclopedia of Genes and Genomes (KEGG) analyses with "clusterProfiler" and "org.Hs.eg.db" (the same as below) were performed in R.

Identification of Potential Immune-Related Genes and Analysis

In this study, the algorithm ESTIMATE outputs stromal, immune, and ESTIMATE scores by performing "limma" and "estimate" with merged data sets after normalization (19). The cutoffs for high or low scores were 50% higher or lower. The Venn diagram was drawn with the package "VennDiagram" and an online tool from the Bioinformatics & Systems Biology website. The intersection set of the results of the ESTIMATE

TABLE 1 | The detail of datasets using in this study.

Data Set	Country	Platforms	Diagnosis	Paired	Control	Tumor	Control after filter	Tumor after filter
GSE18842	Spain	GPL570	NSCLC	Part	45	46	45	45
GSE101929	USA	GPL570	NSCLC	Part	34	32	32	30
GSE103888	UK	GPL570	NSCLC	No	6	13	6	13
GSE104636	Switzerland	GPL6244	lung tumor	Yes	9	9	5	0
GSE118370	China	GPL570	LUAD	Yes	6	6	0	1
GSE134381	UK	GPL11532	LUSC/LUAD	Yes	37	37	22	22
GSE19804	China	GPL570	lung tumor	Yes	60	60	60	58
GSE23361	USA	GPL5188	NSCLC	part	7	5	0	1
GSE30219	France	GPL570	lung tumor	No	14	293	14	254
GSE33532	Germany	GPL570	NSCLC	Yes	20	20	20	19
GSE43458	USA	GPL6244	LUAD	part	30	80	18	49

NSCLC, there was clear statement that cancer tissues from NSCLC patients, but pathological classification not included in original article; Lung tumor, there was no clear statement about lung cancer subtype, but small cell lung cancer was excluded; LUAD, articles had a clear statement of lung adenocarcinoma. LUSC, articles had a clear statement of lung squamous cell carcinoma.

scores were considered as control intersection genes and tumor intersect genes off the up-regulated and down-regulated genes respectively. In the subsequent step, the consistently intersecting set was excluded from those tumor intersect genes, and the remaining genes were considered as tumor specific intersect genes. The intersection set of the tumor specific intersect genes and DEGs were identified as potential immune-related genes and used for further analysis.

Identification of Statistically TICs

The normalized data set was employed to estimate the TICs abundance profile by using the CIBERSORT computational method on all control and tumor samples (20). The resulting data set was filtered with a self-compiled script in Perl to exclude invalid data (detail of filtered data set is listed in **Table 1**). The landscape of TICs is shown in a barplot. A heatmap was generated with "pheatmap," and a correlation heatmap was generated using "corrplot." As the filtered data were subjected to a normality test based on skewness and kurtosis rather than its fit in a normal distribution, non-parametric tests were used. For the number of TICs in the control and tumor samples, the differential distributions were analyzed using the Wilcoxon rank-sum test.

Multiple Linear Regression Analysis for Identifying Differential Immune-Related Genes From Potential Immune-Related Genes

The filtered data were used to analyze the effect of gene expression on the TICs distribution. A total of 16 TICs with different distributions were entered as dependent variable and potential immune-related genes entered as independent variables. Predictive factor analysis for TICs distribution was conducted *via* least-squares regression. With both accuracy and computational efficiency considered, adjusted $P < 0.1$ was considered significant in this part. We selected the significantly ones from 48 potential immune-related genes and identified those exhibiting the opposite regression trend in different tissue samples. Those selected genes would be labeled as differential immune-related genes.

Gene Set Enrichment Analysis With Differential Immune-Related Genes

Gene set enrichment analysis (GSEA) was conducted on all differential immune-related genes on the GSEA portal (http://www.broad.mit.edu/GSEA/) with the following parameter settings: probe set collapse = false; phenotype = high vs. low; permutation: sample, permutations = 1000. The gene set size was $15 < n < 500$. We manually discriminated pathways of interest in immune related pathways, microenvironment and metabolic pathways, and classic cancer pathways. The GSEA results were separately shown based on the pathway function.

Non-Linear Dimensionality Reduction

In this study, we selected one differential immune-related gene that is most stable and highly correlated with other well-recognized immunotherapy signatures to perform downstream analysis, which was OLR1 (oxidized low density lipoprotein receptor 1). We determined whether OLR1 was a key gene for the microenvironment and could be a biomarker for immunotherapy. We first analyzed the influence of OLR1 expression to divide the differential immune microenvironment with non-linear dimensionality reduction. We used t-distributed stochastic neighbor embedding (t-SNE) to complete the dimensionality reduction. T-SNE, a non-linear dimensionality reduction technique, is particularly suitable for visualizing high-dimensional data sets. We reduced the dimensionality to two dimensions to reveal the significant difference between the 50% higher OLR1 expression tissue samples and the 50% lower OLR expression tissue samples. The T-SNE plot was completed using the R package "t-SNE."

Prediction of Benefits to Immune Checkpoint Blockade Therapy

We used TIDE, an online prediction tool to predict the responder rate in the samples with higher or lower OLR1 expression under immune checkpoint blockade therapy. TIDE is a novel computational framework that evaluates the potential of tumor immune escape, particularly for melanoma and NSCLC, on the basis of gene expression data (21). Owing to tool limitations, only the top or bottom 50 cases of OLR expression data were selected from the 284 samples. The result was reorganized into a figure with improved readability. We collected predictive indicators and calculated them to explore the details of the predicated therapeutic effect.

Cell Culture

We used BEAS-2B (human normal lung epithelial cell, Cat. 3131C0001000200027), NCI-H460 (human large cell lung cancer cell, Cat. 3111C0001CCC000355), PLA-801D (lung giant cell carcinoma cell, Cat. 3142C0001000000356), A549 (human non-small cell lung cancer cell, Cat. 3111C0001CCC000002), HCC827 (human non-small cell lung cancer cell, Cat. 3111C0001CCC000478), NCI-H1299 (human non-small cell lung cancer cell, Cat. 3111C0001CCC000469), and NCI-H661 (human large cell lung cancer cell, Cat. 3111C0001CCC000357) to detect the basic expression of OLR1 in lung normal and tumor cell lines for verification of data mining results. They were purchased from Chinese National Infrastructure of Cell Line Resource and cultured in PRMI-1640 medium with 10% FBS.

qPCR

RNA was isolated with TRIzol® reagent (Cat.15596018, Thermo Fisher). Reverse-transcription of the RNA was performed with EasyScript First-Strand cDNA Synthesis SuperMix Kit (Cat. AE301-03, TransGen Biotech). The qPCR assay was performed in triplicate with PowerUp SYBE Green Master Mix Kit (Cat.A25741, Applied Biosystems) on an ABI StepOnePlus Real-time PCR system (ABI-7500, Applied Biosystems). The qPCR primer was following: OLR1-F:5′-ACTCTCCATGG TGGTGCCTGG-3′; OLR1-R:5′-GCTTGTTGCCGGGCTGA GATCT-3′; GAPDH-F:5′-GGACTCATGACCACAGTCCA

TGCC-3′; GAPDH-R:5′-TCAGGGATGACCTTGCCC ACAG-3′.

Statistical Methods

Microarray data analysis was performed using the R programming language. The normality of data distributions was assessed using the Shapiro-Wilk test. Data that were nor normally distributed were compared using the Wilcoxon rank-sum test run with GraphPad Prism. Multivariate analysis was performed using multiple linear regression in Eviews. P value < 0.05 was considered significant.

RESULTS

613 Differentially Expressed Genes Were Identified in 11 Data Sets

For this study, 11 data sets were selected based on our screening criteria (**Table 1**). After the data sets were merged and normalized, 601 NSCLC samples and 268 control samples were included. We defined statistical differential significance as P < 0.05 and fold change >10 between the tumor and control samples. A total of 613 differentially expressed genes (DEGs) were identified from 869 samples with 12596 gene expression data. Their gene symbols are listed based on their respective logFC (base 2 logarithm of fold change) values (**Supplementary Table 1**). The results revealed that 200 of the DEGs were highly expressed, whereas the remaining 413 DEGs were down-regulated in tumor tissues (**Figures 1A, B**). GO and KEGG pathway enrichment analyses of up-regulated or down-regulated DEGs were implemented separately. The up-regulated DEGs were enriched in the extracellular matrix structural constituent, glycosaminoglycan binding and growth factor binding (**Supplementary Table 2** and **Figure 1C**). The corresponding signaling pathways were the most enriched (**Supplementary Table 3** and **Figure 1D**). The down-regulated DEGs mainly involved the cytokine-cytokine receptor interaction, transcriptional miss-regulation in cancer, and cell cycle, as well as corresponding gene functions (**Figures 1E, F**).

166 Tumor-Specific Intersect Genes Were Identified Using ESTIMATE Scores, With 48 of Them Identified as Potential Immune-Related Genes by the Intersection With DEGs

ESTIMATE scores were calculated based on immune and stromal scores. We calculated the immune and stromal scores in the tumor and control samples, respectively. The samples were divided into the high-score and low-score groups by the median value of the immune score (or stromal score). For the immune score, 1,457 (1,276) and 359 (31) up-regulated (down-regulated) immune scores genes were identified in the control and tumor samples, respectively. For the stromal score, 461 (203) and 351

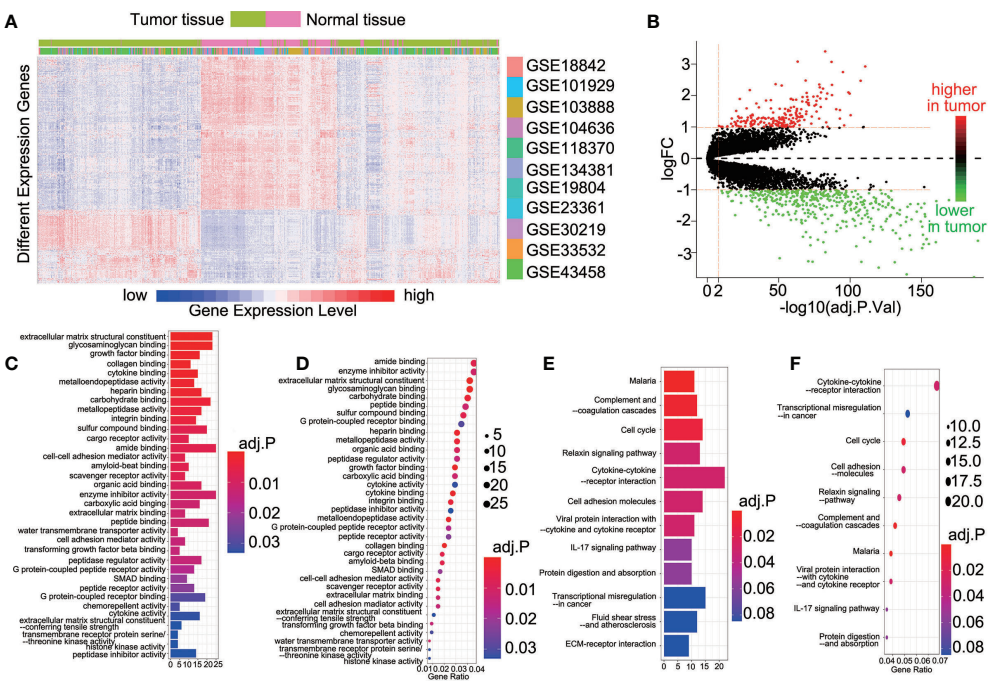

FIGURE 1 | 613 DEGs were identified in 11 datasets. **(A)** Heatmap showed the expression of genes between the tumor and control tissue samples; **(B)** Scatterplot showed the higher or lower DEGs between the tumor and control tissue samples; **(C)** The Go analyses of higher DEGs; **(D)** The KEGG analyses of higher DEGs; **(E)** The Go analyses of lower DEGs; **(F)** The KEGG analyses of lower DEGs.

(30) up-regulated (down-regulated) genes were identified in the control and tumor samples, respectively (**Figure 2A**). The intersection represented the genes with the same trends of up-regulation or down-regulation of immune or stromal score genes in the tumor and control samples. In the control samples, we identified 342 up-regulated immune score genes and 197 down-regulated stromal score genes. Meanwhile, 211 up-regulation immune score genes and 17 down-regulated stromal score genes were found in the tumor samples (**Figure 2A**). A total of 553 up-regulated genes and 214 down-regulated genes were identified in the tumor and control samples (**Figure 2B**). They were regarded as important factors for ESTIMATE scores. Subsequently, 60 up-regulated and two down-regulated genes were duplicates, exhibiting a similar trend of immune or stromal score genes were similar in the tumor and control samples (**Figure 2B**). A concerning finding of this study is that 151 up-regulated and 15 down-regulated ESTIMATE score genes were specifically expressed in the tumor samples (**Supplementary Table 4** and **Figure 2B** with *). Thus, the 166 tumor specific intersect genes were selected for GO enrichment and KEGG pathway analysis. They were enriched in pathways including, immune receptor activity, chemokine activity and receptor binding, receptor ligand activity, glycosaminoglycan binding, phagosome, and IgA immune network (**Supplementary Tables 5** and **6**, **Figures 2C–F**). We then found the intersection of 166 tumor specific intersect genes and 613 DEGs and identified 48 intersected genes (**Supplementary Table 7** and **Figure 2G**).The 48 genes were identified as potential immune-related genes. Potential immune-related genes have significant differences in expression and specific immune effects in the tumor samples.

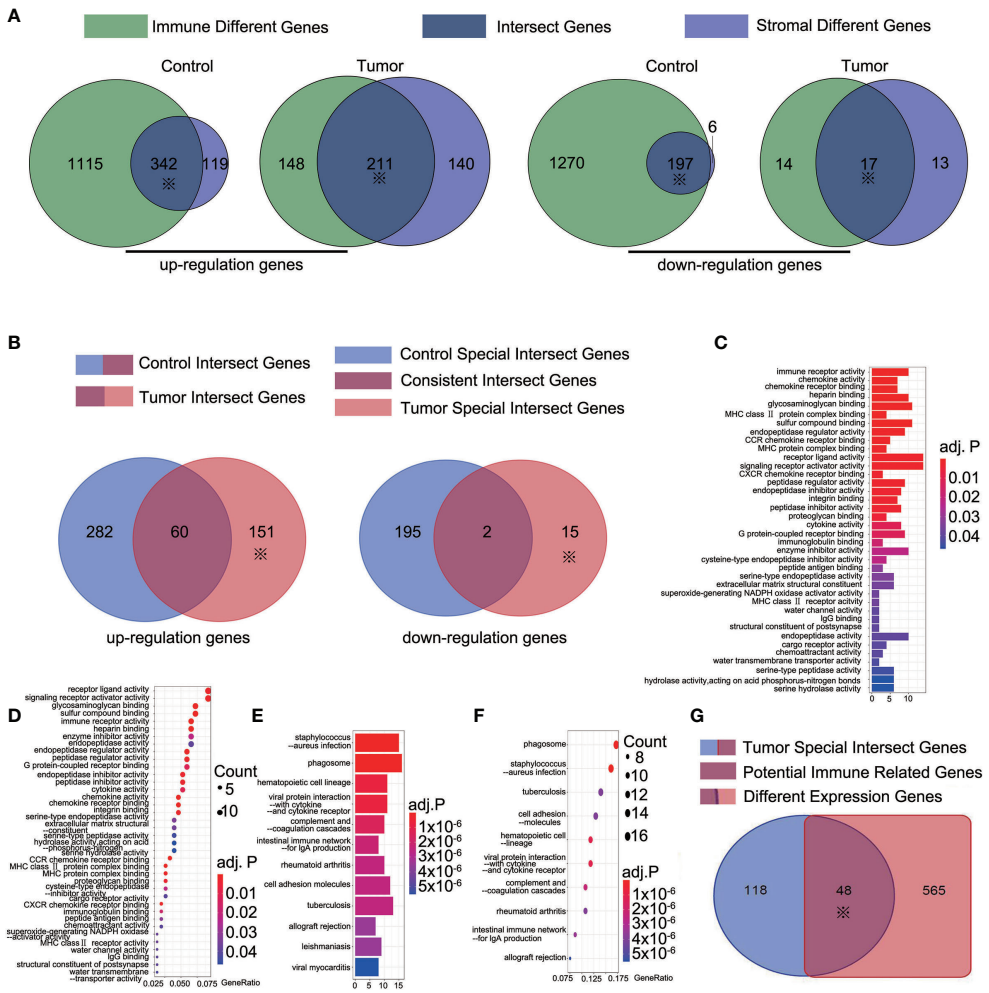

FIGURE 2 | 166 tumor-special intersect genes were identified and 48 of them identified as potential immune-related genes. **(A)** 461 (203) and 351 (30) up-regulated (down-regulated) genes were identified using ESTIMATE in the control and tumor samples. ※ mean this part would be used in following step; **(B)** 151 up-regulated and 15 down-regulated ESTIMATE score genes (total 166 tumor-special intersect genes) were specifically expressed in the tumor samples; **(C)** The Go analyses of 151 up-regulated tumor-special intersect genes; **(D)** The KEGG analyses of 151 up-regulated tumor-special intersect genes; **(E)**. The Go analyses of 15 down-regulated tumor-special intersect genes; **(F)** The KEGG analyses of 15 down-regulated tumor-special intersect genes; **(G)** 48 intersected genes, referred to potential immune-related genes, were identified between 613 DEGs and 166 tumor-special intersect genes.

16 Kinds of TICs Showed Differences in Distribution Between the Tumor and Control Samples

The proportion of tumor-infiltrating immune subsets was analyzed using CIBERSORT in R. A total of 22 TICs profile types in the tumor and control samples were to be constructed. A landscape is presented for preliminary subjective judgment of TICs distributions (**Supplementary Figure 1**). We found that TICs distribution varied based on the kind of TICs. Some of TICs had more immune cells in tumor tissues, whereas others showed the opposite (**Figure 3A**). No significant correlation was found between them with regard to numerical values in both the tumor samples and the control samples (**Figure 3B**). The Mann-Whitney rank-sum test was used to calculate differences in TICs distribution. A significant difference in the distribution of 16 kinds of TICs was found between the tumor and control samples (**Supplementary Table 8** and **Figures 3C–R**).

9 Differentially Expressed Immune-Related Genes Showed Opposite Statistically Significant Regression Trends of TICs Distribution Between the Tumor and Control Samples

We used multiple linear regression with the least square method to calculate the most important genes from 48 potential immune-related genes for differential the distribution of TICs. The control and tumor samples were separated as independent data sets. For an enhanced screen effect, $P<0.1$ was the level of significance selected. A total of 24 intersected genes were statistically significant both in the tumor and control samples; 16 of these genes showed similar regression trends for some kinds of TICs in both samples (**Supplementary Table 9**), and 9 other genes exhibited the opposite regression trend in different tissue samples (**Supplementary Table 10**). OLR1 showed the same regression trend for resting natural killer (NK) cells and eosinophils; however, it exhibited the opposite regression trend for resting mast cell. Thus, OLR1 was counted separately. The genes showing opposite regression trends between the tumor and control samples were referred to as differential immune-related genes in accordance with the purpose of the study. Subsequently, 9 differential immune-related genes were identified: ADH1B, CHRDL1, DMBT1, MMP, OLR1, PBK, PLA2G1B, SCGB3A1, and TREM1. The potential functions of these genes were analyzed by GSEA. We classified some important pathways into three categories, based on their function for clarity. Some pathways could be activated/repressed by each of the 9 differential immune-related genes (**Figure 4**).

OLR1, One of the Differential Immune-Related Genes, Showed Significant Correlations With Four Known Immunotherapy Biomarkers

Since the data were from 11 data sets merged with different platforms, and some data were lost during merging, we selected only 4 well-recognized biomarkers in the data set with gene expression data: PD-L1, CD8A, GZMB, and NOS2. To reduce potential bias and achieve improved effectiveness, we used only part of the data for downstream analysis. The 284 tumor samples in GSE101929 and GSE30219 with clinical data were used to calculate separately the correlation between 9 differential immune-related genes and 4 known biomarkers. Consequently, OLR1 exhibited the highest correlation with PD-L1, CD8A, GZMB, and NOS2 (**Supplementary Table 11** and **Figures 5A–D**), and each correlation was significant ($r>0.4$, $P<0.0001$, moderate intensity). Chi-square test was used to detect whether different expression level of known biomarker was followed by changing of OLR1 expression level. We can found more positive expression for immunotherapy in higher OLR1 group patients (**Supplementary Table 12**). This result suggests the important role of OLR1 in the TME with a changing TICs distribution for immunotherapy prediction.

OLR1 Expression Marked the TICs Distribution

We ran t-SNE to determine the overall distribution of TICs with different levels of OLR1 expression. The OLR1 expression could effectively distinguish the distribution of immune cells (**Figure 5E**). A violin plot of 22 immune cell types shows 14 kinds of immune cells with significantly different distributions between the higher and lower OLR1 expression samples (**Figure 5F**).

OLR1 Affected the Prediction of Clinical Benefits to Immunotherapy in NSCLC Patients

We selected the 50 samples with the highest or lowest OLR1 expression levels from the 284 tumor samples and predicted the responder rate of the immune checkpoint blockade therapy in each group. Among the 50 samples with the lowest OLR1 expression levels, 16 cases were predicted to respond to immune checkpoint blockade therapy. They were also predicted to benefit from immunotherapy. The responder number was 27 in the top 50 OLR1 expression samples. The responder rate was significantly higher in the high OLR1 expression group (**Figure 6A**). We also calculated all indicators of TIDE prediction. OLR1 expression and MSI score exhibited a significant positive correlation. The T cell exclusion potential of the tumor was predicted to be negatively correlated with OLR1 expression. Specifically, a strong positive correlation ($r>0.7$) was observed between OLR1 expression and the T cell-inflamed signature (Merck18), the average of CD8A and CD8B, both of which were important indicators of immunotherapy (**Supplementary Table 13** and **Figures 6B–E**).

Verification of OLR1 Expression in Lung Normal and Tumor Cell Lines

BEAS-2B was human normal lung epithelial cell. It was used as control cell line comparison with other NSCLC cell lines. The result of qPCR analysis showed a significant reduction in the expression of OLR1 in the most NSCLC cell lines (**Figure 7**). The validation result of cell lines had the same trend as data mining in OLR1 expression.

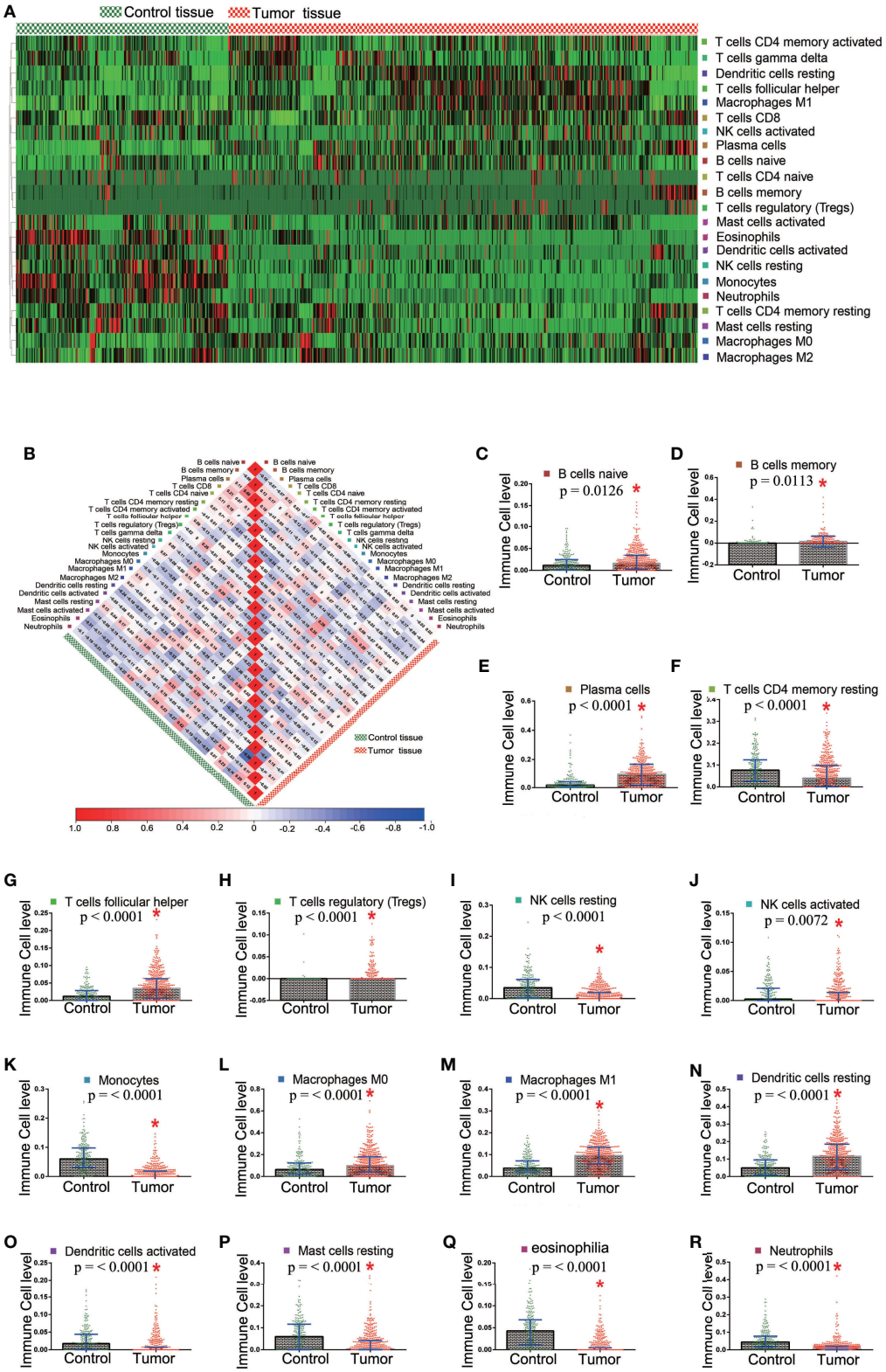

FIGURE 3 | Different distribution of TICs between the tumor and control tissue samples. **(A)** Heatmap showed the distribution state in tumor and control tissue samples; **(B)** The correlation among TICs in the tumor and control tissue samples; **(C–R)** 16 TICs which showed significant difference in the distribution between the tumor and control tissue samples.

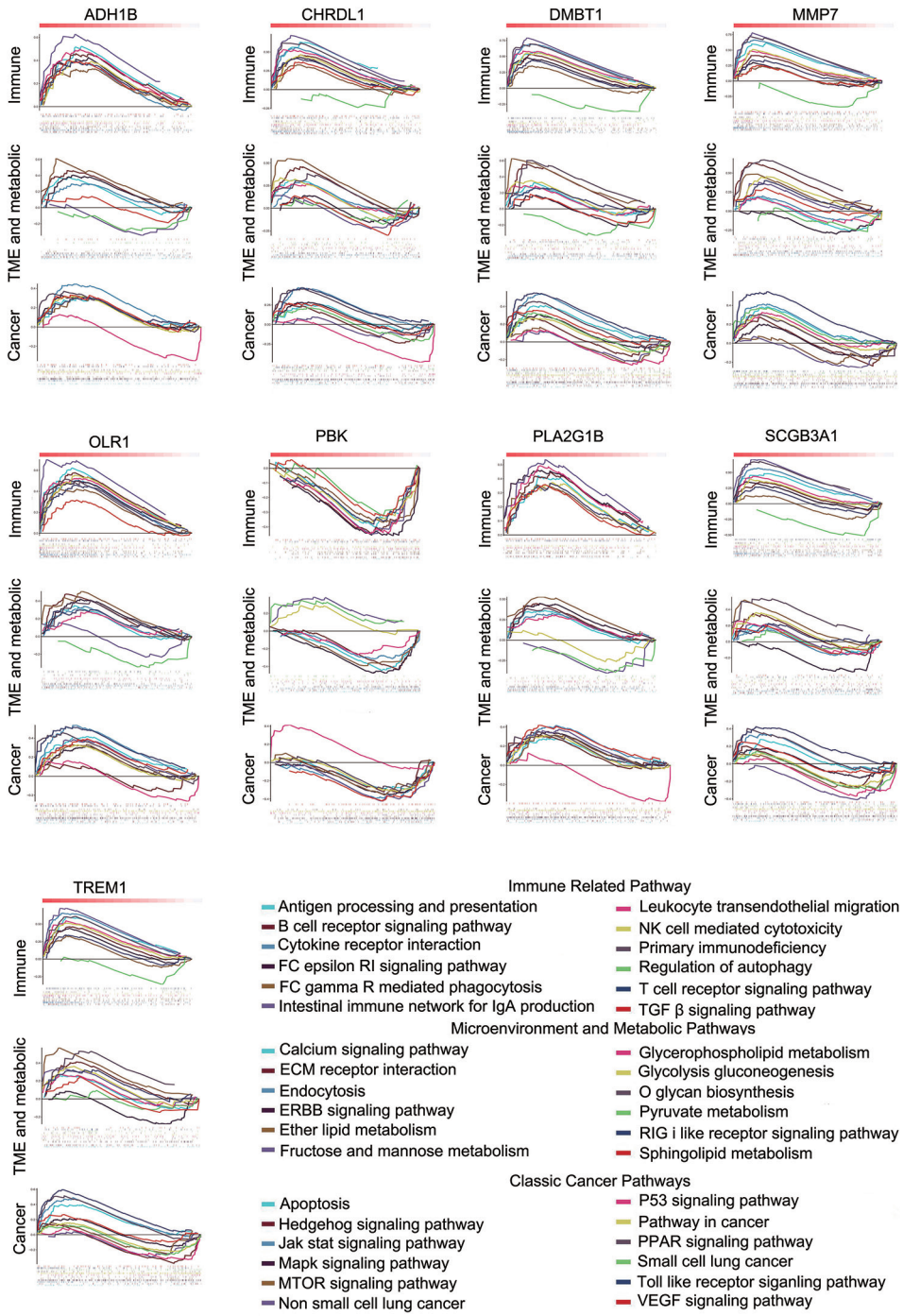

FIGURE 4 | Some pathways could be activated or repressed by each of the 9 differential immune-related genes.

DISCUSSION

In the current study based on GEO data mining, we identified NSCLC microenvironment-related key genes, which show potential as biomarkers for immunotherapy. During the analysis, significant expressions of DEGs were identified between the control and tumor tissue samples; meanwhile, tumor-specific intersect genes also showed significant difference between the immune and stromal components of the tumor samples; further intersection of DEGs and tumor-

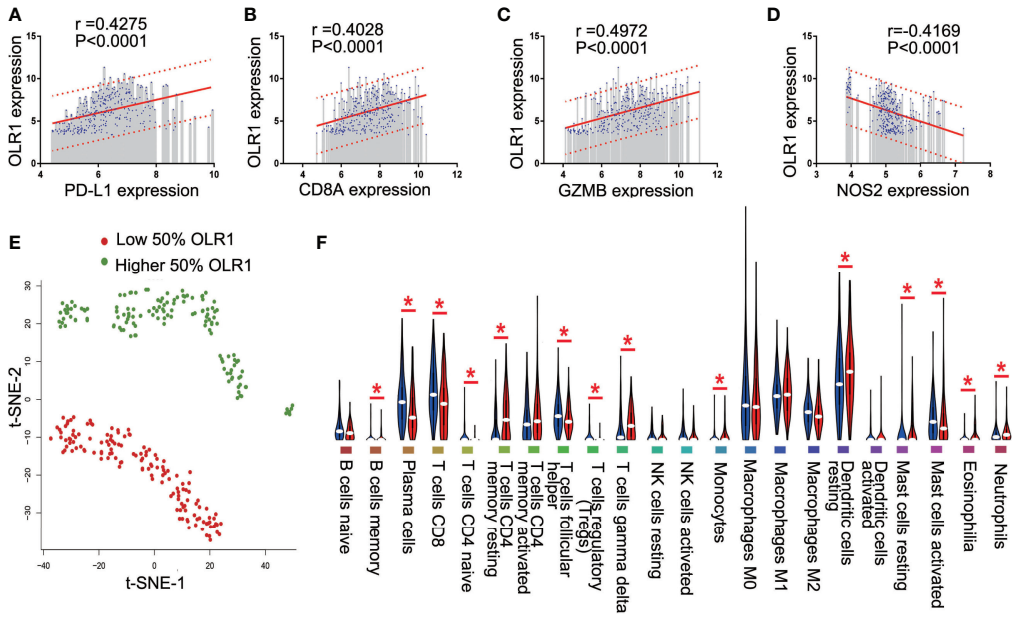

FIGURE 5 | OLR1 showed moderately strong correlations with 4 known immunotherapy biomarkers and its expression marked the TICs distribution. **(A–D)** OLR1 exhibited the highest correlation with PD-L1, CD8A, GZMB, and NOS2; **(E)** OLR1 expression could divide overall status of TICs distribution; **(F)** Violin plot showed the ratio differentiation of 22 kinds of TICs between higher 50% OLR1 expression tumor samples and lower 50% OLR1 expression tumor samples.

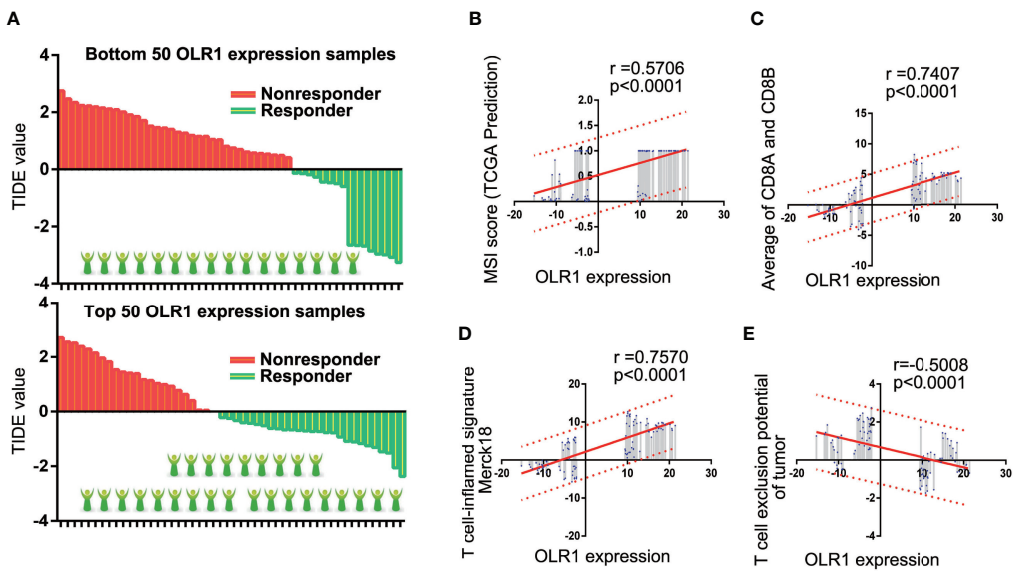

FIGURE 6 | OLR1 may affect the clinical benefits to immunotherapy in NSCLC patients. **(A)** The comparison of responder number in top or bottom OLR1 expression samples. **(B–E)** OLR1 has strong positive correlation with some indicators of TIDE prediction.

specific intersect genes identified potential immune-related genes, both of which were considered different gene expression and significantly affected the ESTIMATE TME scores; finally differential immune-related genes exhibited a significant and opposite correlation with the differential distribution of TICs between the tumor and control samples. OLR1 was considered as a novel potential predictor to immunotherapy of NSCLC.

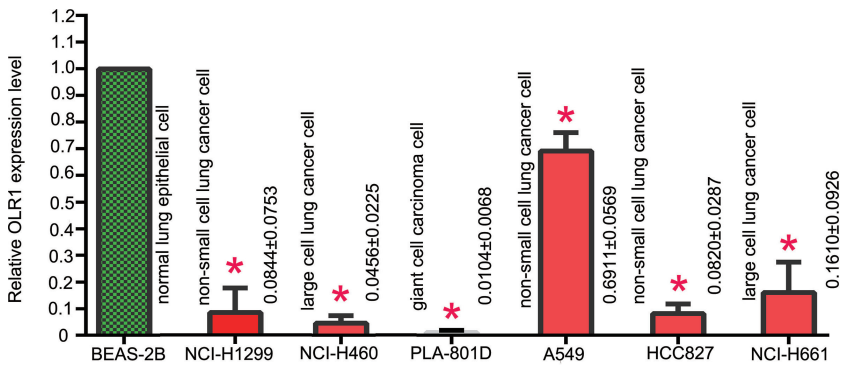

FIGURE 7 | The basic expression level of OLR1 in normal and part NSCLC cell lines.

DEG analysis has been demonstrated as a canonical way to identify novel biomarker genes or novel therapeutic target genes between the normal and tumor samples. In this study, DEG acted as a signature of potential immune-related factors. The screening accuracy of DEGs may be improved using two methods (22). A large sample is expected to improve the screening yield, and analysis with perspective-taking may help improve accuracy based on multiple bioinformatics methods. Other studies randomly chose data sets; in this study, we filtered all GEO data sets by using the selection criteria (see Methods), ultimately including 11 data sets in our analysis cohort. There were 601 tumor samples and 268 control samples across 7 countries and 11 research groups. As our selection criteria, all the 11 data sets should include tumor and normal tissue data for better comparability and higher quality of homogenization data. All data sets were also based on the Affymetrix platform for less data loss in the normalization process. A total of 613 DEGs were identified based on the mRNA array data. These results may be representative and provide an insight in the differences in gene expression in NSCLC. The 613 DEGs were the limited scope for screening in downstream analysis.

The TME is rather complex and largely varies from the microenvironment of normal tissue (7). The TME has been implicated in cancer initiation, development, and treatment resistance. Except for cancer cells, the stromal tumor microenvironment consists of stromal cells and immune cells. The immune cells include T cells, B cells, NK cells, and so on. Stromal cells are the main non-tumor components of the tumor microenvironment (23). Thus, the ESTIMATE algorithm consists of a non-immune "stromal score" parameter and an "immune score" parameter. In this study, the immune and stromal scores, which were determined using ESTIMATE, were used to analyze the infiltration levels of the immune and stromal cells in the tumor and control samples. We focused on genes that specifically regulated the stromal and immune cells in the tumor samples, referred to as the tumor specific intersect gene. We found 166 tumor specific intersect genes in our cohort. They may exhibit cancer-specific effects and show potential to highly regulate the development of the TME in the tumor tissue samples. To determine the type of tumor specific intersect genes with the potential to regulate and control expression; thus the intersecting of the tumor specific intersect genes and DEGs was identified as potential immune-related genes.

Immune cells in TME are the most important defense to eliminate damaged or cancerous cells (23). An established view is that the spatial distribution and the location of immune cells are critical in the immune-oncology field (24). In this study, we tried to identify the differential distributions of immune cells, particularly for TICs. CIBERSORT estimate the abundances of cell types in a mixed cell population based on gene expression data. The CIBERSORT method identified 16 kinds of TICs in our cohort, which were significantly different between the tumor and control samples and not correlated among them. They may each play an independent role in the tumor environment. We explored the correlation between the TICs and 48 potential immune-related genes; the results of multiple non-linear regression analysis indicated that 9 potential immune-related genes with opposite significant correlation between the control and tumor tissue samples. Referred to as differential immune-related genes, those 9 potential immune-related genes, may have tumor tissue-specific functions in the regulation of the immune environment. We evaluated their potential influence on the biological function by using GSEA, and the results showed their potential to activate or inactivate multiple types of signaling pathways, including the immune pathway, microenvironment, and metabolic pathway, and some canonical cancer pathways. The pathways are widely recognized as cancer regulatory mechanisms.

Though much effort has been on identifying genes as biomarkers for immunotherapy, little progress has been made. We thus determined the predicted values for differential immune-related genes in NSCLC. We selected well-recognized biomarkers with gene expression data in our data set (25). PD-L1, also named as B7-H1 or CD274, is the first ligand of PD-1 discovered and widely expressed. It is the main factor responsible for promoting tumor immune evasion (26), and has been a major

clinical target for immunotherapy in NSCLC. CD8A is one of the hallmarks of CD8+ T-cell activation signature genes, as well as GZMB (27). NOS2 is the classically activated macrophage transcript (28). They are widely used in multiple studies to predict the efficacy of immunotherapy. In this study, we calculate the relationship between differential immune-related genes and 4 well-recognized immunotherapy biomarkers. OLR1 showed the best correlation with those existing biomarkers and thus was selected to explore its specific relationship with TME. PD-L1 is the most important clinical predictors of immunotherapy and its expression level in tumor tissue determines whether to apply immunotherapy. The NSCLC patient with higher PD-L1 would be believed get better clinical benefit from PD-1/PD-L1 antibody therapy. In this study, there were numerically positive correlations between PD-L1 and OLR1. It may imply that OLR1 could be used as an auxiliary diagnostic marker for immunotherapy. CD8+ activation is the signature event of anti-cancer effect for immune-checkpoint inhibitors. The positive numerically correlation between OLR1 and CD8+ could provide further support for OLR1 plays as a biomarker of immunotherapy. Notably, all analyses were based on gene expression data and all positive or negative correlations just showed statistically significant. However, they have not been assessed in either clinical or experimental models.

Moreover, t-SNE analysis showed a significant difference in the distribution of immune cells with 50% high or low OLR1 expression tumor samples. This finding suggests that OLR1 can distinguish the state of TME by influencing the distribution of immune cells. Fourteen kinds of immune cells changed in OLR1 expression level, and the ratios (low or high) of four well-recognized immunotherapy biomarkers were significantly different between the low and high OLR1 expression groups. Furthermore, we found an interesting result when we compared TILs distribution between "normal vs. tumor" and "lower OLR1 expression vs. higher OLR1 expression" (**Figures 3C–R**, and **Figure 5F**). There were 16 kinds of TILs with different distribution between normal tissue and tumor tissue and 14 kinds of different distribution TILs between lower OLR1 expression tissue and higher OLR1 expression tissue. Ten kinds of TILs were identical in both comparisons. A term TILs (B cells memory, plasma cells, T cells follicular helper and T cells regulatory) have more distribution in tumor tissue (compared with normal tissue) and lower OLR1 expression tissue (compared with higher OLR1 expression tissue), and another term (T cells CD4 memory resting, monocytes, eosinophilia and neutrophils) showed the opposite distribution. It indicates that lower OLR1 expression has close relationship with tumor microenvironment. OLR1 also named LOX1. It was first identified as a scavenger receptor for oxLDL in bovine aortic endothelias cells (29). It is also expressed in macrophages, vascular smooth muscle cells, platelets and tumor cells (30). Its overexpression enhances the migration in breast *via* NF-κB (31). The transcription of OLR1 could be regulated by multiple transcriptional factors, and its activation depended on a wide range of stimuli indicative of dyslipidemia, inflammation and damage initiates several signaling cascades including MAPKs, other protein kinases as well as transcription factors NF-κB and AP-1 (32).

The predictive values of biomarkers should support clinical values. We used TIDE to detect the predictive effect of OLR1 on NSCLC immunotherapy. TIDE is a gene expression biomarker for predicting clinical response to immune checkpoint blockade. Melanoma and NSCLC data are included in the data sets. Given the limitation of the website, we chose 100 tumor samples (top 50 and bottom 50 samples of OLR1 expression in the last cohort) to run the TIDE prediction process. Results showed that the prediction response rate in the top 50 OLR1 expression group was 54% (27/50), which was significantly higher than that in the bottom 50 OLR1 expression group (16/50). In the comparison of other predictive indicators of TIDE, OLR1 expression showed statistical relevance. The results suggested that OLR1 could be used as a biomarker for immunotherapy in NSCLC. As the main disadvantage of data mining study, there are number of limitations of the work. In this study, all analyses used the same data set and all data was from gene expression micro-assay. The single source of data might affect the reliability of the results. Meanwhile, data are derived from multiple countries in this study. Though we set explicit criteria before normalization of data sets, it is inevitable that data missing happens, or some data from different sources may interfere and cancel each other. Therefore, the results might have been biased to a certain degree. In addition, the algorithms are also immature, though we used the well-accepted ones, such as limma, ESTIMATE or CIBERSORT. At last, TIDE, a novel online tool to predict immunotherapy outcome with gene expression data, is used as the last analyses of OLR1 in this research. It is likely that there is no enough evidence for authenticity and reliability of the TIDE prediction results. Those data mining results may change with different data processing or novel algorithm. However, it also provided some clues now for our study and we are trying to validated it experimentally for more evidence. In verification the basic gene expression of OLR1 in multiple NSCLC cell lines, the result showed the significant reduction of OLR1 level in most NSCLC cells than normal lung cell line.

This study explores TME with bioinformatics analysis of public gene expression data sets in NSCLC. Multi-omics data mining shows its reliability in screening meaningful genes in NSCLC with public data sets. The principal findings of this research are that OLR1 played a key role in TME and could predict or potentially be regulated for NSCLC immunotherapy. OLR1 expression was correlated with some well-recognized biomarkers of immunotherapy, including PD-L1, CD8A, GZMB, NOS2, and other predictors. OLR1 expression could divide the differential TICs distribution, and those patients with higher OLR1 expression were predicted to obtain more benefits from immunotherapy in NSCLC. Given the limitations in time and technology, the regulatory role and molecular mechanism of OLR1 were not investigated in depth; regardless, the properties of OLR1 indicate its potential value in NSCLC immunotherapy. We intend to continue this study in future research and explore more clinical data.

DATA AVAILABILITY STATEMENT

The original contributions presented in the study are included in the article/**Supplementary Material**. Further inquiries can be directed to the corresponding authors.

AUTHOR CONTRIBUTIONS

Concept and design: TM and JW. Administrative support: MG and ZW. Collection and assembly of data: BL and CZ. Data analysis and interpretation: BL, TM, and JW. Manuscript writing: all authors. Final approval of manuscript: all authors. All authors contributed to the article and approved the submitted version.

SUPPLEMENTARY MATERIAL

The Supplementary Material for this article can be found online at: https://www.frontiersin.org/articles/10.3389/fonc.2021.629333/full#supplementary-material

REFERENCES

1. Siegel RL, Miller KD, Jemal A. Cancer statistics, 2020. *CA: Cancer J Clin* (2020) 70(1):7–30. doi: 10.3322/caac.21590
2. Chen W, Zheng R, Baade PD, Zhang S, Zeng H, Bray F, et al. Cancer statistics in China, 2015. *CA: Cancer J Clin* (2016) 66(2):115–32. doi: 10.3322/caac.21338
3. Alberg AJ, Brock MV, Samet JM. Epidemiology of lung cancer: looking to the future. *J Clin Oncol Off J Am Soc Clin Oncol* (2005) 23(14):3175–85. doi: 10.1200/JCO.2005.10.462
4. Duruisseaux M, Esteller M. Lung cancer epigenetics: From knowledge to applications. *Semin Cancer Biol* (2018) 51:116–28. doi: 10.1016/j.semcancer.2017.09.005
5. Duma N, Santana-Davila R, Molina JR. Non-Small Cell Lung Cancer: Epidemiology, Screening, Diagnosis, and Treatment. *Mayo Clin Proc* (2019) 94(8):1623–40. doi: 10.1016/j.mayocp.2019.01.013
6. Osmani L, Askin F, Gabrielson E, Li QK. Current WHO guidelines and the critical role of immunohistochemical markers in the subclassification of non-small cell lung carcinoma (NSCLC): Moving from targeted therapy to immunotherapy. *Semin Cancer Biol* (2018) 52(Pt 1):103–9. doi: 10.1016/j.semcancer.2017.11.019
7. Osipov A, Saung MT, Zheng L, Murphy AG. Small molecule immunomodulation: the tumor microenvironment and overcoming immune escape. *J Immunother Cancer* (2019) 7(1):224. doi: 10.1186/s40425-019-0667-0
8. Musetti S, Huang L. Nanoparticle-Mediated Remodeling of the Tumor Microenvironment to Enhance Immunotherapy. *ACS Nano* (2018) 12 (12):11740–55. doi: 10.1021/acsnano.8b05893
9. Calverley DC, Phang TL, Choudhury QG, Gao B, Oton AB, Weyant MJ, et al. Significant downregulation of platelet gene expression in metastatic lung cancer. *Clin Trans Sci* (2010) 3(5):227–32. doi: 10.1111/j.1752-8062.2010.00226.x
10. Fregni G, Quinodoz M, Moller E, Vuille J, Galland S, Fusco C, et al. Reciprocal modulation of mesenchymal stem cells and tumor cells promotes lung cancer metastasis. *EBioMedicine* (2018) 29:128–45. doi: 10.1016/j.ebiom.2018.02.017
11. Hoang LT, Domingo-Sabugo C, Starren ES, Willis-Owen SAG, Morris-Rosendahl DJ, Nicholson AG, et al. Metabolomic, transcriptomic and genetic integrative analysis reveals important roles of adenosine diphosphate in haemostasis and platelet activation in non-small-cell lung cancer. *Mol Oncol* (2019) 13(11):2406–21. doi: 10.1002/1878-0261.12568
12. Kabbout M, Garcia MM, Fujimoto J, Liu DD, Woods D, Chow CW, et al. ETS2 mediated tumor suppressive function and MET oncogene inhibition in human non-small cell lung cancer. *Clin Cancer Res Off J Am Assoc Cancer Res* (2013) 19(13):3383–95. doi: 10.1158/1078-0432.CCR-13-0341
13. Kuo CS, Liu CY, Pavlidis S, Lo YL, Wang YW, Chen CH, et al. Unique Immune Gene Expression Patterns in Bronchoalveolar Lavage and Tumor Adjacent Non-Neoplastic Lung Tissue in Non-Small Cell Lung Cancer. *Front Immunol* (2018) 9:232. doi: 10.3389/fimmu.2018.00232
14. Lu TP, Hsiao CK, Lai LC, Tsai MH, Hsu CP, Lee JM, et al. Identification of regulatory SNPs associated with genetic modifications in lung adenocarcinoma. *BMC Res Notes* (2015) 8:92. doi: 10.1186/s13104-015-1053-8
15. Mitchell KA, Zingone A, Toulabi L, Boeckelman J, Ryan BM. Comparative Transcriptome Profiling Reveals Coding and Noncoding RNA Differences in NSCLC from African Americans and European Americans. *Clin Cancer Res Off J Am Assoc Cancer Res* (2017) 23(23):7412–25. doi: 10.1158/1078-0432.CCR-17-0527
16. Rousseaux S, Debernardi A, Jacquiau B, Vitte AL, Vesin A, Nagy-Mignotte H, et al. Ectopic activation of germline and placental genes identifies aggressive metastasis-prone lung cancers. *Sci Trans Med* (2013) 5(186):186ra66. doi: 10.1126/scitranslmed.3005723
17. Sanchez-Palencia A, Gomez-Morales M, Gomez-Capilla JA, Pedraza V, Boyero L, Rosell R, et al. Gene expression profiling reveals novel biomarkers in nonsmall cell lung cancer. *Int J Cancer* (2011) 129(2):355–64. doi: 10.1002/ijc.25704
18. Xu L, Lu C, Huang Y, Zhou J, Wang X, Liu C, et al. SPINK1 promotes cell growth and metastasis of lung adenocarcinoma and acts as a novel prognostic biomarker. *BMB Rep* (2018) 51(12):648–53. doi: 10.5483/BMBRep.2018.51.12.205
19. Yoshihara K, Shahmoradgoli M, Martinez E, Vegesna R, Kim H, Torres-Garcia W, et al. Inferring tumour purity and stromal and immune cell admixture from expression data. *Nat Commun* (2013) 4:2612. doi: 10.1038/ncomms3612
20. Newman AM, Steen CB, Liu CL, Gentles AJ, Chaudhuri AA, Scherer F, et al. Determining cell type abundance and expression from bulk tissues with digital cytometry. *Nat Biotechnol* (2019) 37(7):773–82. doi: 10.1038/s41587-019-0114-2
21. Jiang P, Gu S, Pan D, Fu J, Sahu A, Hu X, et al. Signatures of T cell dysfunction and exclusion predict cancer immunotherapy response. *Nat Med* (2018) 24 (10):1550–8. doi: 10.1038/s41591-018-0136-1
22. Vougas K, Sakellaropoulos T, Kotsinas A, Foukas GP, Ntargaras A, Koinis F, et al. Machine learning and data mining frameworks for predicting drug response in cancer: An overview and a novel in silico screening process based on association rule mining. *Pharmacol Ther* (2019) 203:107395. doi: 10.1016/j.pharmthera.2019.107395
23. Quail DF, Joyce JA. Microenvironmental regulation of tumor progression and metastasis. *Nat Med* (2013) 19(11):1423–37. doi: 10.1038/nm.3394
24. Holmgaard RB, Schaer DA, Li Y, Castaneda SP, Murphy MY, Xu X, et al. Targeting the TGFbeta pathway with galunisertib, a TGFbetaRI small molecule inhibitor, promotes anti-tumor immunity leading to durable, complete responses, as monotherapy and in combination with checkpoint blockade. *J Immunother Cancer* (2018) 6(1):47. doi: 10.1186/s40425-018-0356-4
25. Camidge DR, Doebele RC, Kerr KM. Comparing and contrasting predictive biomarkers for immunotherapy and targeted therapy of NSCLC. *Nat Rev Clin Oncol* (2019) 16(6):341–55. doi: 10.1038/s41571-019-0173-9
26. Jiang Y, Zhan H. Communication between EMT and PD-L1 signaling: New insights into tumor immune evasion. *Cancer Lett* (2020) 468:72–81. doi: 10.1016/j.canlet.2019.10.013
27. Oja AE, Piet B, van der Zwan D, Blaauwgeers H, Mensink M, de Kivit S, et al. Functional Heterogeneity of CD4(+) Tumor-Infiltrating Lymphocytes With a Resident Memory Phenotype in NSCLC. *Front Immunol* (2018) 9:2654. doi: 10.3389/fimmu.2018.02654
28. Kahn DA, Archer DC, Gold DP, Kelly CJ. Adjuvant immunotherapy is dependent on inducible nitric oxide synthase. *J Exp Med* (2001) 193(11):1261–8. doi: 10.1084/jem.193.11.1261
29. Sawamura T, Kume N, Aoyama T, Moriwaki H, Hoshikawa H, Aiba Y, et al. An endothelial receptor for oxidized low-density lipoprotein. *Nature* (1997) 386(6620):73–7. doi: 10.1038/386073a0
30. Hirsch HA, Iliopoulos D, Joshi A, Zhang Y, Jaeger SA, Bulyk M, et al. A transcriptional signature and common gene networks link cancer with lipid

metabolism and diverse human diseases. *Cancer Cell* (2010) 17(4):348–61. doi: 10.1016/j.ccr.2010.01.022

31. Khaidakov M, Mitra S, Kang BY, Wang X, Kadlubar S, Novelli G, et al. Oxidized LDL receptor 1 (OLR1) as a possible link between obesity, dyslipidemia and cancer. *PloS One* (2011) 6(5):e20277. doi: 10.1371/journal.pone.0020277
32. Li D, Saldeen T, Romeo F, Mehta JL. Oxidized LDL upregulates angiotensin II type 1 receptor expression in cultured human coronary artery endothelial cells: the potential role of transcription factor NF-kappaB. *Circulation* (2000) 102(16):1970–6. doi: 10.1161/01.CIR.102.16.1970

Conflict of Interest: The authors declare that the research was conducted in the absence of any commercial or financial relationships that could be construed as a potential conflict of interest.

frontiers in Oncology

ORIGINAL RESEARCH
published: 22 April 2021
doi: 10.3389/fonc.2021.659321

Co-Occurring Alteration of NOTCH and DDR Pathways Serves as Novel Predictor to Efficacious Immunotherapy in NSCLC

Zhimin Zhang[1†], Yanyan Gu[2†], Xiaona Su[3†], Jing Bai[4†], Wei Guan[3], Jungang Ma[3], Jia Luo[3], Juan He[3], Bicheng Zhang[1], Mingying Geng[3], Xuefeng Xia[4], Yanfang Guan[4], Cheng Shen[5] and Chuan Chen[3*]*

[1] Cancer Center, Renmin Hospital of Wuhan University, Wuhan, China, [2] Department of Nutrition, Changzheng Hospital, Second Military Medical University, Shanghai, China, [3] Cancer Center, Daping Hospital, Army Medical University (Third Military Medical University), Chongqing, China, [4] Geneplus-Beijing Institute, Beijing, China, [5] Department of Thoracic Surgery, Daping Hospital, Army Medical University (Third Military Medical University), Chongqing, China

OPEN ACCESS

Edited by:
Meijuan Huang,
Sichuan University, China

Reviewed by:
Damini Chand,
Canada's Michael Smith Genome Sciences Centre, Canada
Jianchun Duan,
Chinese Academy of Medical Sciences and Peking Union Medical College, China

***Correspondence:**
Cheng Shen
sc941@sina.com
Chuan Chen
sinkriver@126.com

†These authors have contributed equally to this work

Specialty section:
This article was submitted to Cancer Immunity and Immunotherapy, a section of the journal Frontiers in Oncology

Received: 27 January 2021
Accepted: 29 March 2021
Published: 22 April 2021

Citation:
Zhang Z, Gu Y, Su X, Bai J, Guan W, Ma J, Luo J, He J, Zhang B, Geng M, Xia X, Guan Y, Shen C and Chen C (2021) Co-Occurring Alteration of NOTCH and DDR Pathways Serves as Novel Predictor to Efficacious Immunotherapy in NSCLC. Front. Oncol. 11:659321. doi: 10.3389/fonc.2021.659321

Although immune checkpoint inhibitors (ICIs) have shown remarkable benefit for treatment of advanced non-small lung cancer (NSCLC), only a minority of patients can achieve durable responses and the most patients produce an ultra-rapid progressive disease. Here, we collected the availably published datasets and mined the determinants of response to immunotherapy on pathway levels. One hundred six NSCLC patients treated with immunotherapy were combined from Rizvi et al. and Hellman et al. studies (whole exon sequencing). Two independent validation datasets consisted of the MSKCC cohort (targeted sequencing) and data by Anagnostou and colleagues (whole exon sequencing). The Cancer Genome Atlas (TCGA) somatic mutation and gene expression data were applied to explore the immunobiology features. In the first combined cohort, we detected NOTCH pathway altered in 71% patients with durable clinical benefit (DCB) while only 36% among no durable benefit (NDB) ($p = 0.005$). Compared to NDB group, co-occurrence of NOTCH and at least two DDR (co-DDR) pathway was discovered in DCB group and contributed to a prolonged progression-free survival (PFS) [22.1 *vs* 3.6 months, $p < 0.0001$, HR, 0.34, 95% confidence interval (CI), 0.2–0.59]. In two independent datasets, co-occurrence of NOTCH+/co-DDR+ was also validated to be a better immunotherapy efficacy [Cohort 2: 13 *vs* 6 months, $p = 0.034$, HR, 0.55, 95% CI, 0.31–0.96; Cohort 3: 21 *vs* 11 months, $p = 0.067$, HR, 0.45, 95% CI, 0.18–1.1]. By analyzing TCGA cohort, we found patients with coexisting NOTCH+/co-DDR+ pathway had a higher TMB, more infiltration of CD4+T cells. Overall, co-occurrence of NOTCH and co-DDR pathway reflect a better immunotherapy efficacy in advanced NSCLC. This genomic predictor show promise in stratifying patients that suit for immunotherapy for future clinical practice.

Keywords: NOTCH pathway, DDR pathway, co-occurring mutations, immunotherapy, predictive biomarker, non-small cell lung cancer

INTRODUCTION

Immune checkpoint inhibitors (ICIs) has shown remarkable benefit for treatment of advanced non-small lung cancer (NSCLC) (1, 2). Nevertheless, only a limited patient population can generate durable responses after immunotherapy, while the majority of patients undergo inferior survival (3, 4). Therefore, there is an urgent need to stratify the patients who will benefit from ICIs.

A plethora of studies have shown biomarkers for predicting response to immunotherapy. The most heavily studied biomarker was programmed death-ligand 1 (PD-L1) expression correlated to efficacious immunotherapy (5–8), but subsequent trials proven a sizeable proportion of patients still achieve durable responses with PD-L1 negative (2, 9). Furthermore, some genomic markers have been reported for predicting the response to ICI, including tumor mutation burden (TMB) (10, 11), tumor neoantigen burden (TNB) (12, 13), and DNA repair alterations (14–16). Meanwhile, several studies explored the alterations on pathway level that correlates to ICI. Zhang et al. found NOTCH signaling related to better ICI efficacy (17). Wang et al. revealed co-mutations in DNA damage response (DDR) pathways could serve as predictors of response to ICB (18).

Due to the interactions and dependencies among different pathways, we supposed single pathway was not high enough to reflect the response of ICI. Therefore, we focused on the co-occurrent pathways to predict the superior survival outcomes after immunotherapy. Availably published datasets were collected from four studies. The first cohort was combined by data from Rizvi et al. and Hellman et al., which was used to identify the co-occurrent pathways correlated to ICI (15, 19). We further validated the co-occurrent pathways correlated to better efficacy after immunotherapy in two independent datasets (data from Anagnostou et al. and the MSKCC cohort) (20, 21). Using the somatic mutation and gene expression data from TCGA, we explored the immunobiology features about the co-occurrent pathway.

MATERIALS AND METHODS

Datasets Used

We collected four publicly available datasets treated with immunotherapy (**Supplementary Table 1**). Thirty-four NSCLC patients sequenced by WES were downloaded from Rizvi et al. Another 75 patients with WES data were derived from Hellman et al. studies. Data from the two studies were merged as the first combined cohort. After excluding three patients lack of efficacy information, data from 106 patients was obtained. The second cohort was from Anagnostou et al., including 89 NSCLC patients treated with ICIs. Two patients were excluded because of lacking definitive response evaluation. For the third cohort, MSKCC cohort was downloaded from cBioPortal (http://www.cbioportal.org/study/summary?id=tmb_mskcc_2018). We also acquired the genome mutation from 1026 NSCLC patients and transcriptome expression data from 59 advanced NSCLC patients in TCGA.

Pathway Alterations

Genes involved in 10 oncogenic signaling pathways and eight DDR pathways were listed in **Supplementary Table 2**. The 10 canonical oncogenic signaling pathways were downloaded from (22) and included: cell cycle, Hippo signaling, Myc signaling, Notch signaling, oxidative stress response/Nrf2, PI-3-Kinase signaling, receptor-tyrosine kinase (RTK)/RAS/MAP-Kinase signaling, TGFb signaling, p53 and b-catenin/Wnt signaling. Eight DDR pathways analyzed were: mismatch repair (MMR); base excision repair (BER); check point factors (CPF); Fanconi anemia (FA); homologous recombination repair (HRR); nucleotide excision repair (NER); non-homologous end-joining (NHEJ); and DNA translesion synthesis (TLS) (23). We defined pathway alteration as at least one gene in this pathway mutated. Co-DDR was defined as two or more DDR pathway altered. Co-occurring alteration of NOTCH and DDR pathway was referred as NOTCH+/co-DDR+.

Immune Infiltration Analysis

SsGSEA was utilized to calculate the enrichment scores (ES) of immune cell types in the tumor microenvironment (24). Gene signatures of 28 immune cell types were downloaded from previous study (25). Tumors were further subclassified into different immune groups using the Euclidean distance and "ward.D" clustering. The expression levels of genes were first z-score normalized across all patients. Then we calculated the mean z-scores for each group and ranked in descending order. Based on the pre-ranked GSEA method, for each immune cell signature, we defined the q-value <10% and NES >0 as the enrichment, while the q-value <10% and NES <0 as the depletion.

Statistical Analyses

We performed univariable and multivariable Cox regression analyses to identify potential predictors of survival. Survival curves were estimated with the Kaplan-Meier product-limit method and compared by log-rank test. Comparisons of TMB, TNB, and expression levels between different groups were used with the Wilcoxon rank-sum test or t test. Enrichment analysis of gene function was calculated by GSEA with Benjamini-Hochberg correction for multiple hypothesis testing ($q < 0.05$). All statistical analyses were performed in the R statistical environment version 3.6.2.

RESULTS

Pathway Alterations in NSCLC Treated With Immunotherapy

We collected WES data from 106 NSCLC patients treated with immunotherapy derived from published data as the discovery cohort (15, 19). Of these patients, 51 (48.1%) achieved durable clinical benefit and 55 (51.9%) had no response to the

immunotherapy. The clinical features and efficacy outcomes were summarized in **Table 1**. To unravel the determinants of response to immunotherapy on pathway levels, we mapped all mutated genes to 10 oncogenic signaling pathways and eight DDR pathways (**Supplementary Table 2**, **Figure 1**). A tumor sample was considered as altered in a given pathway if one or more genes in this pathway contained non-synonymous mutations. Data from 99 patients succeeded to map to pathways that were further analyzed. The most frequently altered pathway was RTK/RAS in both DCB and NDB group (80 *vs* 82%), followed by HIPPO pathway (65% in DCB *vs* 52% in NDB). Notably, 71% patients with DCB had alteration in NOTCH pathway while only 36% in NDB group (p = 0.005). This was consistent with previous study that NOTCH signaling correlated with better ICI efficacy (17). More DDR-related pathways were altered in DCB. Co-mutations in DDR

TABLE 1 | Clinical characteristics of discovery cohort.

	Total	DCB	NDB	P-value
Histology				
Squamous	87 (82.1%)	44 (86.3%)	43 (78.2%)	0.32
Non-squamous	19 (17.9%)	7 (13.7%)	12 (21.8%)	
Sex				
Female	54 (50.9%)	26 (51.0%)	28 (50.9%)	1
Male	52 (49.1%)	25 (49.0%)	27 (49.1%)	
Smoking Status				
Current/Former	85 (80.2%)	43 (84.3%)	42 (76.4%)	0.34
Never	21 (19.8%)	8 (15.7%)	13 (23.6%)	
PD L1 expression				
Strong	18 (17.0%)	14 (27.5%)	4 (7.3%)	0.045
Weak	48 (45.3%)	21 (41.2%)	27 (49.1%)	
Negative	31 (29.2%)	12 (23.5%)	19 (34.5%)	
Unknown	9 (8.5%)	4 (7.84%)	5 (9.1%)	
Best Overall Response				
CR/PR	34 (32.1%)	34 (66.7%)	0 (0.0%)	<0.001
PD/NE	36 (34.0%)	0 (0.0%)	36 (65.5%)	
SD	36 (34.0%)	17 (33.3%)	19 (34.5%)	
Treatment				
PD-1 blockade	31 (29.2%)	14 (27.5s%)	17 (30.9%)	0.83
PD-1 plus CTLA-4 blockade	75 (70.8%)	37 (72.5%)	38 (69.1%)	

CR, complete response; CTLA-4, cytotoxic T-cell lymphocyte-4; DCB, durable clinical benefit; NDB, no durable benefit; NE, not evaluable; PD, progressive disease; PD-1, programmed cell death-1; PR, partial response; SD, stable disease.

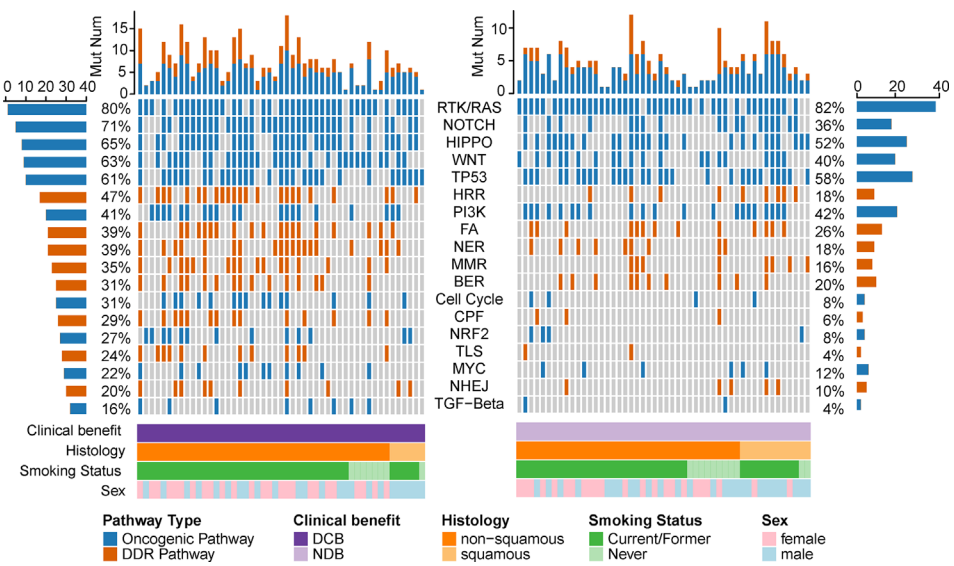

FIGURE 1 | Pathway alterations in NSCLC with or without efficacious immunotherapy. Stacked plot showed the number of mutated pathway (histogram, top). Clinical characters are listed at the bottom of the figure. The prevalence of mutated pathways was calculated at left (in DCB group) and right (in NDB group). Orange represents the oncogenic pathway and blue stands for the DDR pathway.

pathways (hereafter referred as co-DDR) have been reported to a better clinical benefit to ICI by Wang et al. (18), we also detected a higher prevalence of co-DDR pathway alteration in DCB group (69.3 *vs* 30%, p = 0.0002). Taken together, alterations on pathway level can reflect the divergent response in immunotherapy.

Identification of NOTCH Co-occurring Pathways to Distinguish ICI Efficacy

Given that single pathway fails to adequately reveal the response of ICI, we applied a co-occurrence strategy to investigate how the NOTCH co-occurring pathways impacted the ICI efficacy. Comparing to NDB group, we identified the HIPPO and/or co-DDR pathway co-occurring with NOTCH pathway, which displayed a better clinical benefit (**Figure 2A**). After testing in univariate and multivariate cox regression for progressive free survival (PFS), only co-occurrence of NOTCH and co-DDR pathway proved to be an independently protective factor for PFS (**Figure 2B**, **Supplementary Figure 1**). Thus, 99 patients were further stratified into two groups according to the co-occurrent alteration of NOTCH and co-DDR pathways (hereafter referred as NOTCH+/co-DDR+). Altered genes for each pathway of NOCTH+/co-DDR+ were shown in **Supplementary Figure 2**. We defined the patients with NOTCH+/co-DDR+ as "GoodBenefit" (37 patients) and others were "BadBenefit" (62 patients). Patients grouped as "GoodBenefit" showed a longer PFS (22.1 *vs* 3.6 months, p < 0.0001, **Figure 2C**). Notably, co-occurrence of NOTCH+/co-DDR+ showed more prolonged PFS than single pathway (alteration either in NOTCH or co-DDR pathway) (**Supplementary Figure 3A**). In the NOTCH+/co-DDR+ group, we also detected higher tumor mutation burden (TMB, **Figure 2D**), higher tumor neoantigen burden (TNB, **Figure 2E**), more durable clinical benefit (p < 0.001, **Figure 2F**), and more improved objective response (p < 0.001, **Figure 2G**). These

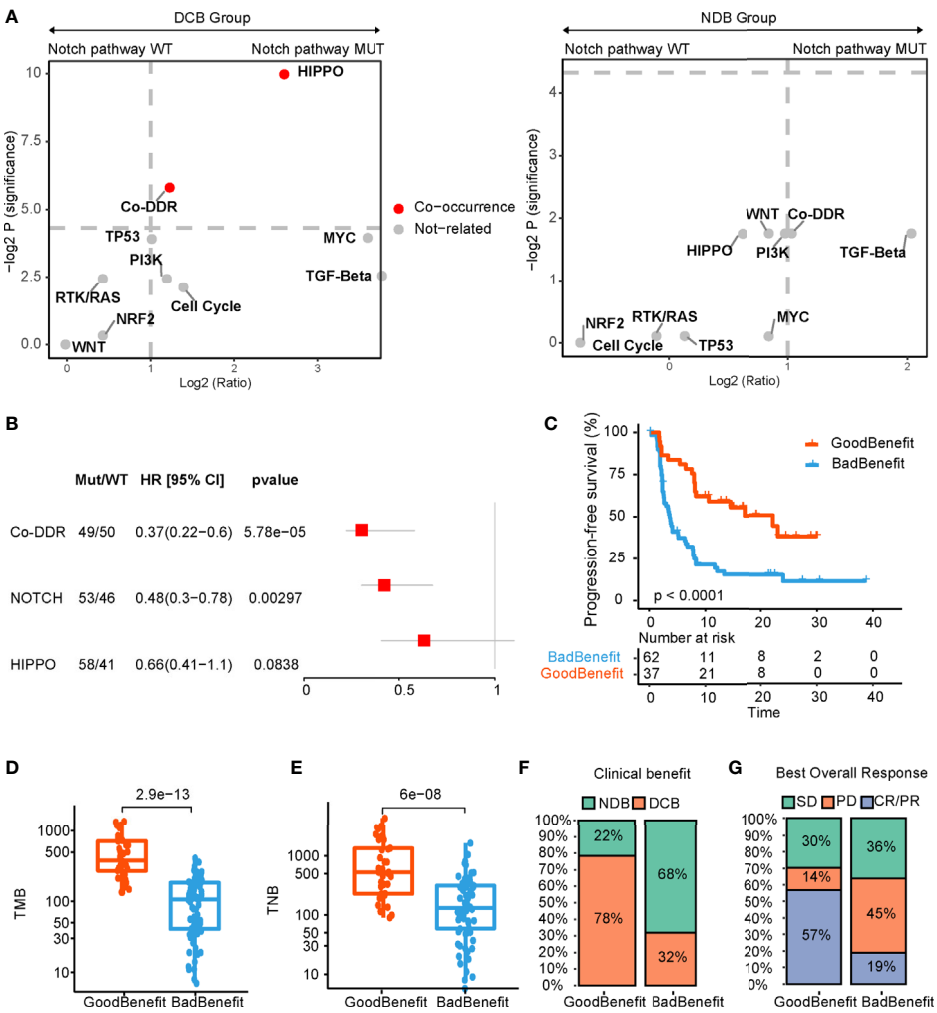

FIGURE 2 | NOTCH co-occurring pathways that contributed to ICI efficacy. **(A)** log2 (odds ratio) and -log2 (p value) for enrichment of altered pathways co-occurred with and without NOTCH pathway. **(B)** Forest plot displaying univariate cox regression analyses for PFS of individually considered pathway. **(C)** Kaplan-Meier survival curves for PFS comparing "GoodBenefit" *versus* "BadBenefit." **(D, E)** Boxplot of TMB **(D)** and TNB **(E)** in "GoodBenefit" *versus* "BadBenefit." **(F, G)** Percentage of patients with clinical benefit evaluation **(F)** and objective response **(G)**.

results were also observed when we stratified patients into the following three groups: CoPath (NOTCH+/co-DDR+) *versus* SinglePath (alterations in NOTCH or at least two DDR pathway) *versus* wild type (**Supplementary Figures 3B–E**). In summary, we identified NOTCH co-occurring with co-DDR pathways reflecting a better immunotherapy efficacy.

Independent Validation of the Model in Two Cohorts

To evaluate whether the co-occurrence of NOTCH+/co-DDR+ could serve as a potential predictor of immunotherapy efficacy, we crossed-validated our findings using two independent cohorts who received ICI therapies.

One validated dataset was from Anagnostou and colleagues (20), 87 NSCLC patients with definitive response evaluation were obtained. Using our stratification criteria, 26 patients were grouped into "GoodBenefit," where 61 were classified as "BadBenefit." Utilizing the univariate cox regression for PFS, "GoodBenefit" group showed a decreased risk of PFS (**Figure 3A**). Comparing to the group of "BadBenefit," patients with co-existing pathways had longer PFS (13 *vs* 6 months, p = 0.034, HR, 0.55, 95% CI, 0.31–0.96) (**Figure 3B**). As expected, the TMB was

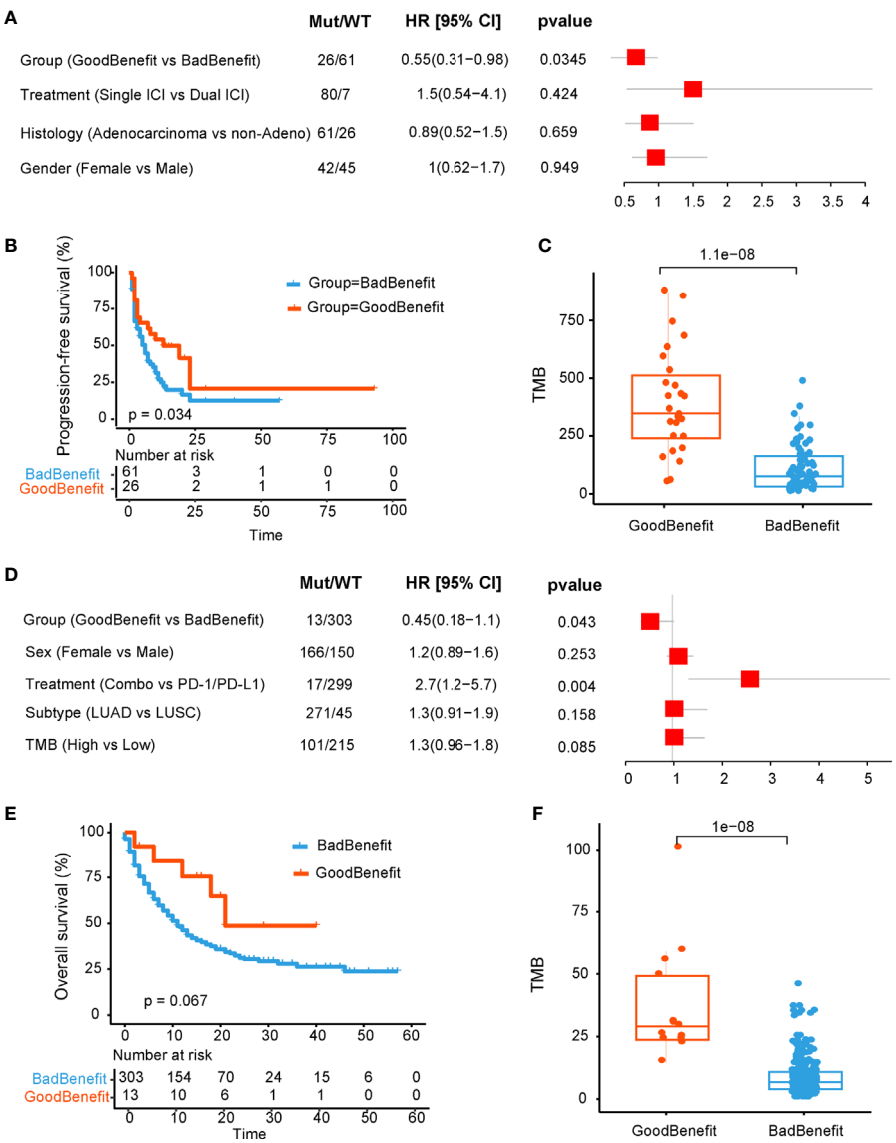

FIGURE 3 | Validation of NOTCH/co-DDR co-occurring pathways to ICI efficacy in Anagnostou et al. cohort **(A–C)** and MSKCC cohort **(D–F)**. **(A)** Forest plot displaying univariate cox regression analyses for PFS of individually considered pathway for Anagnostou et al. dataset. **(B)** Kaplan-Meier survival curves for PFS comparing "GoodBenefit" *versus* "BadBenefit." **(C)** Boxplot of TMB in "GoodBenefit" *versus* "BadBenefit." **(D)** Forest plot displaying univariate cox regression analyses for OS of individually considered pathway for MSKCC data. **(E)** Kaplan-Meier survival curves for OS comparing "GoodBenefit" *versus* "BadBenefit." **(F)** Boxplot of TMB in "GoodBenefit" *versus* "BadBenefit."

significantly higher in "GoodBenefit" group than "BadBenefit" group (**Figure 3C**). When Comparing among the three groups (NOTCH+/co-DDR+ *versus* NOTCH or co-DDR occurrence *versus* Wildtype), co-occurrence of NOTCH/co-DDR also exhibited superior survival outcomes and the highest TMB (**Supplementary Figures 4A, B**).

For another independent cohort from MSKCC, 1,661 patients received immunotherapy by targeted sequencing, we retained the 316 NSCLC tissue [271 lung adenocarcinoma (LUAD) and 45 Lung squamous cell carcinoma (LUSC)] for further analyses (21). Co-occurrence of NOTCH+/co-DDR+ was found act as a protective factor (**Figure 3D**). Overall survival in co-occurrence group was prolonged, although did not reached the statistical significance (21 *vs* 11 months, p = 0.067, HR, 0.45, 95% CI, 0.181.1, **Figure 3E**). We speculated the limited genes from panel may underestimate the pathway alteration. In this cohort, targeted capture panel comprised of 341 and 410 genes, respectively, covering 10 oncogenic pathways and seven DDR pathways without TLS pathway. In addition, the TMB was significantly higher in "GoodBenefit" group (**Figure 3F**). When compared among the three groups, the co-occurrent group still performed improved OS prognostication and higher TMB (**Supplementary Figures 4C, D**).

Genomic Characteristics of NOTCH/co-DDR Co-occurrence in TCGA Cohort

We next explored the genomic characteristics in TCGA cohort according to our stratification criterion. One thousand twenty-six NSCLC WES data and clinical features were downloaded. All mutated genes were mapped to 18 canonical pathways. TMB in "GoodBenefit" group was significantly higher than "BadBenefit" group regardless of stage (**Supplementary Figure 5A**). Considering the predictor of NOTCH+/co-DDR+ was trained based on advanced NSCLC and without EGFR mutation. We filtered out the patients with early stage and EGFR alteration. Ultimately, 120 advanced NSCLC patients retained; 39.2% (47) patients were classified as "GoodBenefit" group while 60.8% (73) as "BadBenefit" group. This ratio of potential efficiency coincided with previous reports on NSCLC patients beneficial of ICIs delivery (26–29). In order to exclude NOTCH+/co-DDR+ as a potential prognostic factor, we performed the survival analyses in TCGA cohort treated with standard treatment. No significant difference of overall survival was detected between GoodBenefit *versus* BadBenefit group or among three groups (**Figure 4A**, **Supplementary Figure 5B**). This result demonstrated co-occurrent NOTCH+/co-DDR+ was not a prognostic factor *per se*, but can serve as predictor in condition of immunotherapy. Recent studies have shown the TMB was a predictor of the pathological response to immune checkpoint inhibitors treatment in advanced lung cancer patients, we next checked the TMB distribution in our groups. Comparing to wildtype, higher TMB was observed in "GoodBenefit" group (**Figure 4B**). In details, the TMB was significantly higher in co-occurrence group than those harbored single pathway (either NOCTH or co-DDR alteration) and wildtype (neither NOTCH nor co-DDR alteration) (**Supplementary Figure 5C**).

Immunobiology Features of NOTCH/co-DDR Co-occurrence

To further explore the immunobiology features of NOTCH+/co-DDR+ co-occurrence, we obtained 59 of 120 patients from TCGA whose RNA-seq data were available. The single sample gene set enrichment analysis (ssGSEA) method was employed to deconvolute the relative abundance of each immune cell type. By unsupervised clustering, we classified the 59 NSCLC into three clusters [immune-high (n = 27), immune-intermediate (n = 15), and immune-low (n = 17), **Figure 5A**]. Patients with NOTCH+/co-DDR+ co-occurrence had no preference to specific immune group (immune-high 14/27 *vs* immune-intermediate 3/15 *vs* immune-low 6/17, p = 0.12). Of note, CD4+ T cell were enriched in NOTCH+/co-DDR+ group (**Figure 5B**). We also found Interleukin 4 (IL-4), a quintessential T helper type 2 (Th2) cytokine produced by CD4+ T cells, expressed lower in "GoodBenefit" group (**Figure 5C**). TNFRSF18 was up-regulated in "GoodBenefit" group (**Figure 5C**), playing a role in promoting T effector cell activity by inducing proliferation and supporting survival in T cells, while also suppressing Treg activity (30). Another Tumor necrosis factor superfamily, TNFSF15 was downregulated in "GoodBenefit" group. TNFSF15 has been reported being an inhibitor of endothelial cell growth (31). Functional enrichment analyses revealed "GoodBenefit" group up-

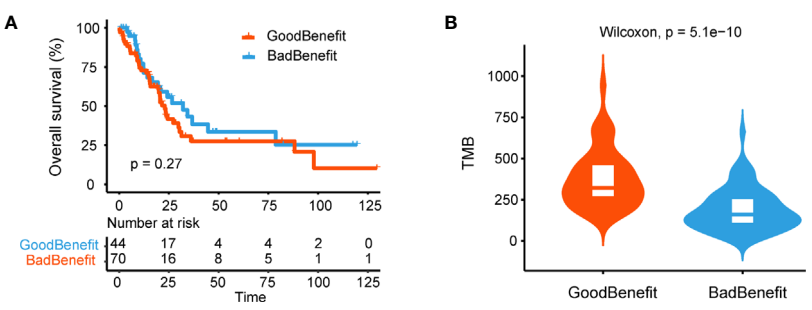

FIGURE 4 | Genomic characteristics of NOTCH/co-DDR co-occurring pathways in TCGA cohort. **(A)** Kaplan-Meier survival curves for OS comparing "GoodBenefit" *versus* "BadBenefit." **(B)** Violin plot of TMB between "GoodBenefit" *versus* "BadBenefit."

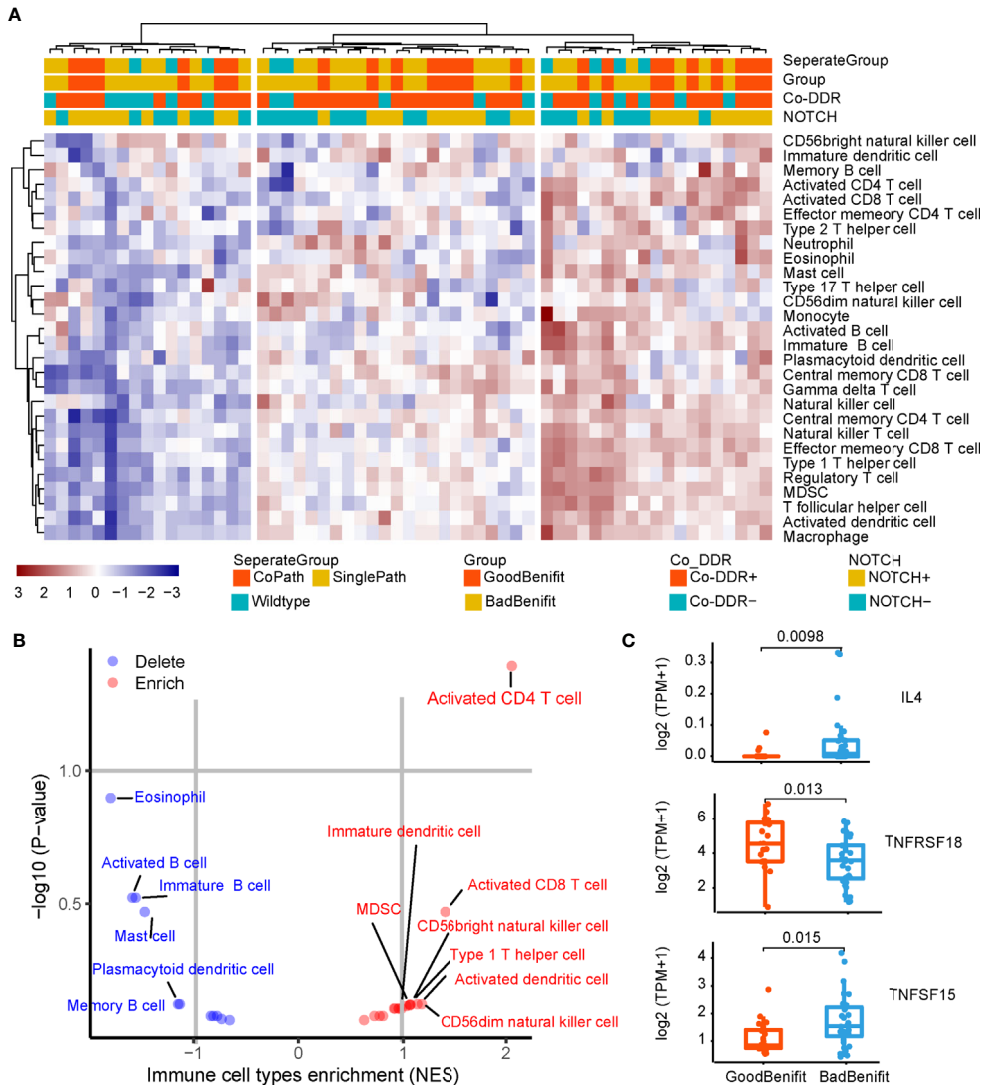

FIGURE 5 | Immunobiology features of NOTCH/co-DDR co-occurrence. **(A)** Heatmap of immune infiltration in each patient. **(B)** Volcano plots for the enrichment (red) and depletion (blue) of immune cell types for GoodBenefit and BadBenefit. The expression levels of genes were first z-score normalized across all patients. Then we calculated the mean z-scores for each group and ranked in descending order. Based on the pre-ranked GSEA method, for each immune cell signature, we defined the q-value <10% and NES >0 as the enrichment, while the q-value <10% and NES <0 as the depletion. Immune cells with absolute NES greater than 1 were shown. **(C)** Normalized express of immune-related genes between Goodbenefit *versus* Badbenefit.

regulated growth factor receptor pathway, down-regulated DNA repair pathways and immune response pathways, this tumor context may contribute to the clinical benefit of ICI (**Supplementary Figure 6**).

DISCUSSION

In this study, we demonstrated the co-occurrence of NOTCH and co-DDR pathways can predict the superior survival outcomes after immunotherapy in advanced NSCLC. This phenomenon was first identified in one combined cohort and validated across another two independent cohorts. All the data we analyzed was performed WES, except one validated cohort from MSKCC (targeted sequencing). Using WES data was an advantage because it can cover enough genes of the pathway, overcoming the deficiency of targeted sequencing. To the best of our knowledge, this is the first report focusing on co-occurrence event on pathway level to explore the determinants of response to ICIs.

To explore whether there were dominant gene mutations in the co-occurring pathway, we depicted the co-occurring event on gene level involved in NOTCH and DDR pathways (**Supplementary Figure 1**). It can be observed that more alterations occurred in DCB group than NDB group. However, the overall mutation incidence on gene level was quite low. The most frequently mutated genes in

NOTCH pathway were NOTCH1 (7%), NOTCH2 (7%), and JAG2 (7%). Meanwhile, low mutation rates of genes were observed in DDR pathway. Taken together, our data suggested that different genes converging to the co-occurring pathways effect the immunotherapy effect, rather than the specific gene of co-occurrence drives.

Although a single pathway of NOTCH or co-DDR has been reported as a predictor to ICI, we revealed co-occurrent NOTCH+/co-DDR+ pathway preferred in DCB and was more predictive to patients beneficial of ICIs delivery. In the first combined cohort, patients carrying co-mutations in NOTCH and co-DDR pathways had significantly longer PFS as compared to the SinglePath (alterations in NOTCH or at least two DDR pathway) or wild type, and the TMB was gradually decreasing. As for the validation dataset of cohort 2, we also observed the longer PFS in CoPath group than SinglePath, but there was no significant different in SinglePath *versus* Wild type. Thus, we speculated alteration in single pathway of NOTCH or co-DDR was incomplete correlate of immunotherapy.

Patients carrying alterations of NOTCH+/co-DDR+ pathway associated with increased TMB, TNB, and more infiltration of CD4+ T cell. Previous study has revealed that alterations in co-DDR pathway appeared to higher TMB and TNB (18). Since a higher mutation and neoantigen load could induce T cell-mediated antitumor response (32), we speculated that alterations in co-DDR contributed to more mutation and neoepitope, and further increased the likelihood of recognition by T cell. NOTCH signaling pathway has been reported as a pivotal role in regulating T cell modulation, differentiation, and activation (33, 34). In addition, previous study also reported NOTCH can control the fate of various T cell types, including Th1, Th2, and the regulatory T cells (35). In our result, we found co-occurrence of NOTCH/co-DDR tended to infiltrate more CD4+ T cell, but down-regulated the cytokine of Th2, suggesting more CD4 T cell that not secrete Th2 exist in NOTCH/co-DDR group. Moreover, recent studies have shown that NOTCH signaling is required for optimal T-cell-mediated anti-tumor immunity (36). Collectively, one potential explanation may be alteration of co-DDR pathway cause more mutations producing immunogenic neoantigens that are recognized and targeted by T cells and NOTCH pathway mediate more infiltration of CD4+ T cells and enhance effector T-cell activity. However, the underlying mechanism of co-ordination between NOTCH and co-DDR pathways and how these pathways shape together the microenvironment suit for immunotherapy should be further investigated in the future. Expanded data and more experiments are warranted to reveal the mechanism on how these pathways cross-talk to determine a better response to immunotherapy.

In conclusion, preliminary data from three cohorts showed evidence that co-mutations in NOTCH and co-DDR pathways indicated better immunotherapy efficacy. This genomic marker provided a new dimension to predict the superior survival outcomes in response to immunotherapy.

DATA AVAILABILITY STATEMENT

The original contributions presented in the study are included in the article/**Supplementary Material**. Further inquiries can be directed to the corresponding authors.

AUTHOR CONTRIBUTIONS

CC, CS, and ZZ conceived and designed the present study. ZZ, YYG, XS, and JB contributed equally to this work. ZZ and CC wrote the manuscript. ZZ, YYG, and XS collected and interpreted data. JB and WG performed the data analysis. JM, JL, and XX gave material support. JH, BZ, and YFG helped in improving the language and correcting grammar mistakes. All authors contributed to the article and approved the submitted version.

FUNDING

China Postdoctoral Science Foundation funded project (Grant #2014T70977). Hubei Province National Natural Science Foundation of China (Grant #2018CFB733).

SUPPLEMENTARY MATERIAL

The Supplementary Material for this article can be found online at: https://www.frontiersin.org/articles/10.3389/fonc.2021.659321/full#supplementary-material

REFERENCES

1. Reck M, Rodríguez-Abreu D, Robinson AG, Hui R, Csőszi T, Fülöp A, et al. Pembrolizumab Versus Chemotherapy for Pd-L1–Positive Non–Small-Cell Lung Cancer. *N Engl J Med* (2016) 375:1823–33. doi: 10.1056/NEJMoa1606774
2. Socinski MA, Jotte RM, Federico C, Francisco O, Daniil S, Naoyuki N, et al. Atezolizumab for First-Line Treatment of Metastatic Nonsquamous Nsclc. *N Engl J Med* (2018) 378:Nejmoa1716948–1716948. doi: 10.1056/NEJMoa1716948
3. Camidge DR, Doebele RC, Kerr KM. Comparing and Contrasting Predictive Biomarkers for Immunotherapy and Targeted Therapy of Nsclc. *Nat Rev Clin Oncol* (2019) 16:341–55. doi: 10.1038/s41571-019-0173-9
4. Gibney GT, Weiner LM, Atkins MB. Predictive Biomarkers for Checkpoint Inhibitor-Based Immunotherapy. *Lancet Oncol* (2016) 17:E542–542e551. doi: 10.1016/S1470-2045(16)30406-5
5. Garon EB, Rizvi NA, Hui R, Leighl N, Gandhi L. Pembrolizumab for the Treatment of Non–Small-Cell Lung Cancer. *N Engl J Med* (2015) 372:2018–28. doi: 10.1056/NEJMoa1501824
6. Chae YK, Pan A, Davis AA, Raparia K, Mohindra NA, Matsangou M, et al. Biomarkers for Pd-1/Pd-L1 Blockade Therapy In Non-Small-Cell Lung Cancer: Is Pd-L1 Expression a Good Marker for Patient Selection. *Clin Lung Cancer* (2016) 17:350–61. doi: 10.1016/J.Cllc.2016.03.011
7. Tumeh PC, Harview CL, Yearley JH, Shintaku IP, Taylor EJ, Robert L, et al. Pd-1 Blockade Induces Responses by Inhibiting Adaptive Immune Resistance. *Nature* (2014) 515:568–71. doi: 10.1038/Nature13954

8. Anagnostou V, Forde PM, White JR, Niknafs N, Hruban C, Naidoo J, et al. Dynamics of Tumor and Immune Responses During Immune Checkpoint Blockade in Non-Small Cell Lung Cancer. *Cancer Res* (2019) 79:1214–25. doi: 10.1158/0008-5472.Can-18-1127
9. Motzer RJ, Rini BI, Mcdermott DF, Redman BG, Kuzel TM, Harrison MR, et al. Nivolumab for Metastatic Renal Cell Carcinoma: Results of a Randomized Phase Ii Trial. *J Clin Oncol* (2014) 33:1430–7. doi: 10.1200/JCO.2014.59.0703
10. Hellmann MD, Callahan MK, Awad MM, Calvo E, Ascierto PA, Atmaca A, et al. Tumor Mutational Burden and Efficacy of Nivolumab Monotherapy and in Combination With Ipilimumab in Small-Cell Lung Cancer. *Cancer Cell* (2018) 33:853–61.e4. doi: 10.1016/j.ccell.2019.01.011
11. Carbone DP, Reck M, Paz-Ares L, Creelan B, Horn L, Steins M, et al. First-Line Nivolumab in Stage Iv or Recurrent Non-Small-Cell Lung Cancer. *N Engl J Med* (2017) 376:2415–26. doi: 10.1056/Nejmoa1613493
12. Van Allen EM, Miao D, Schilling B, Shukla SA, Blank C, Zimmer L, et al. Genomic Correlates of Response to Ctla-4 Blockade in Metastatic Melanoma. *Science* (2015) 350:207–11. doi: 10.1126/science.aad0095
13. Gubin MM, Zhang X, Schuster H, Caron E, Ward JP, Noguchi T, et al. Checkpoint Blockade Cancer Immunotherapy Targets Tumour-Specific Mutant Antigens. *Nature* (2014) 515:577–81. doi: 10.1038/Nature13988
14. Finn OJ. Cancer immunology. *Cancer Immunol* (2008) 358:2704–15. doi: 10.1056/NEJMra072739
15. Rizvi NA, Hellmann MD, Snyder A, Kvistborg P, Makarov V, Havel JJ, et al. Mutational Landscape Determines Sensitivity to Pd-1 Blockade in Non–Small Cell Lung Cancer. *Science* (2015) 348:124–8. doi: 10.1126/science.aaa1348
16. Bhangoo MS, Boasberg P, Mehta P, Elvin JA, Ali SM, Wu W, et al. Tumor Mutational Burden Guides Therapy in a Treatment Refractory Pole-Mutant Uterine Carcinosarcoma. *Oncologist* (2018) 23:518. doi: 10.1634/theoncologist.2017-0342
17. Zhang K, Hong X, Song Z, Xu Y, Liu L. IIdentification of Deleterious NOTCH Mutation as Novel Predictor to Efficacious Immunotherapy in NSCLC. *Clin Cancer Res* (2020) 26:3649–661. doi: 10.1158/1078-0432.CCR-19-3976
18. Wang Z, Zhao J, Wang G, Zhang F, Zhang Z, Zhang F, et al. Comutations in Dna Damage Response Pathways Serve as Potential Biomarkers for Immune Checkpoint Blockade. *Cancer Res* (2018) 78:6486–96. doi: 10.1158/0008-5472.Can-18-1814
19. Hellmann MD, Nathanson T, Rizvi H, Creelan BC, Sanchez-Vega F, Ahuja A, et al. Genomic Features of Response to Combination Immunotherapy in Patients With Advanced Non-Small-Cell Lung Cancer. *Cancer Cell* (2018) 33:843–52.e4. doi: 10.1016/j.ccell.2018.03.018
20. Anagnostou V, Niknafs N, Marrone K, Bruhm DC, White JR, Naidoo J, et al. Multimodal Genomic Features Predict Outcome of Immune Checkpoint Blockade in Non-Small-Cell Lung Cancer. *Nat Cancer* (2020) 1:99–111. doi: 10.1038/s43018-019-0008-8
21. Samstein RM, Lee C, Shoushtari AN, Hellmann MD, Shen R, Janjigian YY, et al. Tumor Mutational Load Predicts Survival After Immunotherapy Across Multiple Cancer Types. *Nat Genet* (2019) 51:202–6. doi: 10.1038/s41588-018-0312-8
22. Sanchez-Vega F, Mina M, Armenia J, Chatila WK, Luna A, La KC, et al. Oncogenic Signaling Pathways in the Cancer Genome Atlas. *Cell* (2018) 173:321–37.E10. doi: 10.1016/J.Cell.2018.03.035
23. Scarbrough PM, Weber RP, Iversen ES, Brhane Y, Amos CI, Kraft P, et al. a Cross-Cancer Genetic Association Analysis of the Dna Repair and Dna Damage Signaling Pathways for Lung, Ovary, Prostate, Breast, and Colorectal Cancer. *Cancer Epidemiol Biomarkers Prev* (2016) 25:193–200. doi: 10.1158/1055-9965.EPI-15-0649
24. Hnzelmann S, Castelo R, Guinney J. Gsva: Gene Set Variation Analysis for Microarray and Rna-Seq Data. *BMC Bioinformatics* (2013) 14:7–7. doi: 10.1186/1471-2105-14-7
25. Charoentong P, Finotello F, Angelova M, Mayer C, Efremova M, Rieder D, et al. Pan-Cancer Immunogenomic Analyses Reveal Genotype-Immunophenotype Relationships and Predictors of Response to Checkpoint Blockade. *Cell Rep* (2017) 18:248–62. doi: 10.1016/j.celrep.2016.12.019
26. Barlesi F, Vansteenkiste J, Spigel D, Ishii H, Garassino M, De Marinis F, et al. Avelumab versus docetaxel in patients with platinum-treated advanced non-small-cell lung cancer (JAVELIN Lung 200): An open-label, randomised, phase 3 study. *Lancet Oncol* (2018) 19:1468–79. doi: 10.1016/S1470-2045(18)30673-9
27. Borghaei H, Paz-Ares L, Horn L, Spigel DR, Steins M, Ready NE, et al. Nivolumab Versus Docetaxel in Advanced Nonsquamous Non–Small-Cell Lung Cancer. *N Engl J Med* (2015) 373:1627–39. doi: 10.1056/NEJMoa1507643
28. Garassino MC, Cho B, Kim J, Mazières J, Vansteenkiste J, Lena H, et al. Durvalumab as Third-Line or Later Treatment for Advanced Non-Small-Cell Lung Cancer (Atlantic): an Open-Label, Single-Arm, Phase 2 Study. *Lancet Oncol* (2018) 19:521–36. doi: 10.1016/S1470-2045(18)30144-X
29. Herbst RS, Baas P, Kim D, Felip E, Pérez-Gracia JL, Han J, et al. Pembrolizumab Versus Docetaxel for Previously Treated, Pd-L1-Positive, Advanced Non-Small-Cell Lung Cancer (Keynote-010): a Randomised Controlled Trial. *Lancet* (2016) 387:1540–50. doi: 10.1016/S0140-6736(15)01281-7
30. Mahoney KM, Rennert PD, Freeman GJ. Combination Cancer Immunotherapy and New Immunomodulatory Targets. *Nat Rev Drug Discov* (2015) 14:561–84. doi: 10.1038/nrd4591
31. Yu J, Tian S, Metheny-Barlow L, Chew LJ, Hayes AJ, Pan H, et al. Modulation of Endothelial Cell Growth Arrest and Apoptosis by Vascular Endothelial Growth Inhibitor. *Circ Res* (2001) 89:1161–7. doi: 10.1161/hh2401.101909
32. Keenan TE, Burke KP, Van Allen EM. Genomic Correlates of Response to Immune Checkpoint Blockade. *Nat Med* (2019) 25:1. doi: 10.1038/s41591-019-0382-x
33. Laky K, Fowlkes BJ. Notch Signaling in Cd4 and Cd8 T Cell Development. *Curr Opin Immunol* (2008) 20:197–202. doi: 10.1016/J.Coi.2008.03.004
34. Janghorban M, Xin L, Rosen JM, Zhang XH. Notch Signaling as a Regulator of the Tumor Immune Response: to Target or Not to Target. *Front Immunol* (2018) 9:1649:1649. doi: 10.3389/Fimmu.2018.01649
35. Luo X, Xu L, Li Y, Tan H. Notch Pathway Plays a Novel and Critical Role in Regulating Responses of T and Antigen-Presenting Cells in Agvhd. *Front Immunol* (2017) 33:169–81. doi: 10.1007/s10565-016-9364-7
36. Kelliher MA, Roderick JE. NOTCH Signaling in T-Cell-Mediated Anti-Tumor Immunity and T-Cell-Based Immunotherapies. *Front Immunol* (2018) 9:1718 doi: 10.3389/fimmu.2018.01718

Conflict of Interest: The authors declare that the research was conducted in the absence of any commercial or financial relationships that could be construed as a potential conflict of interest.

frontiers in Oncology

ORIGINAL RESEARCH
published: 31 May 2021
doi: 10.3389/fonc.2021.591922

Exploration of the Tumor-Suppressive Immune Microenvironment by Integrated Analysis in *EGFR*-Mutant Lung Adenocarcinoma

Teng Li[1], Xiaocong Pang[2], Junyun Wang[3,4], Shouzheng Wang[1], Yiying Guo[1], Ning He[4], Puyuan Xing[1] and Junling Li[1]**

[1] Department of Medical Oncology, National Cancer Center/National Clinical Research Center for Cancer/Cancer Hospital, Chinese Academy of Medical Sciences and Peking Union Medical College, Beijing, China, [2] Department of Pharmacy, Peking University First Hospital, Beijing, China, [3] CAS Key Laboratory of Genome Sciences and Information, Beijing Institute of Genomics, Chinese Academy of Sciences/China National Center for Bioinformation, Beijing, China, [4] Research Institute, GloriousMed Clinical Laboratory (Shanghai) Co., Ltd., Shanghai, China

OPEN ACCESS

Edited by:
Qian Chu,
Huazhong University of Science and Technology, China

Reviewed by:
Jing Zhang,
Beihang University, China
Lin Li,
Beijing Hospital, China

***Correspondence:**
Junling Li
lijunling@cicams.ac.cn
Puyuan Xing
xingpuyuan@cicams.ac.cn

Specialty section:
This article was submitted to Cancer Immunity and Immunotherapy, a section of the journal Frontiers in Oncology

Received: 05 August 2020
Accepted: 29 March 2021
Published: 31 May 2021

Citation:
Li T, Pang X, Wang J, Wang S, Guo Y, He N, Xing P and Li J (2021) Exploration of the Tumor-Suppressive Immune Microenvironment by Integrated Analysis in EGFR-Mutant Lung Adenocarcinoma. Front. Oncol. 11:591922. doi: 10.3389/fonc.2021.591922

Background: Clinical evidence has shown that few non-small cell lung cancer (NSCLC) patients with epidermal growth factor receptor (*EGFR*) mutations can benefit from immunotherapy. The tumor immune microenvironment (TIME) is a significant factor affecting the efficacy of immunotherapy. However, the TIME transformational process in *EGFR*-mutation patients is unknown.

Methods: The mRNA expression and mutation data and lung adenocarcinoma (LUAD) clinical data were obtained from The Cancer Genome Atlas (TCGA) database. Profiles describing the immune landscape of patients with *EGFR* mutations were characterized by differences in tumor mutation burden (TMB), ESTIMATE, CIBERSORT, and microenvironment cell populations-counter (MCP-counter).

Results: In total, the TCGA data for 585 patients were analyzed. Among these patients, 98 had *EGFR* mutations. The TMB was lower in the *EGFR* group (3.94 mut/Mb) than in the *KRAS* mutation group (6.09 mut/Mb, $P < 0.001$) and the entire LUAD (6.58 mut/Mb, $P < 0.001$). The *EGFR* group had a lower population of activated immune cells and an even higher score of immunosuppressive cells. A further inter-group comparison showed that differences in the TMB and tumor-infiltrating lymphocytes were only found between patients with oncogenic mutations and unknown mutation. Meanwhile, there were more myeloid dendritic cells (DCs) in *EGFR* 19del than in L858R-mutation patients and in common mutation patents than in uncommon mutation patients ($P < 0.05$). Additionally, we established a D score, where D = MCP-counter score for cytotoxic T lymphocytes (CTLs)/MCP-counter score for myeloid DCs. Further analysis revealed that lower D scores indicated immune suppression and were negatively related to several immunotherapy biomarkers.

Conclusions: The TIME of *EGFR* mutant NSCLC was immunosuppressive. Myeloid DCs gradually increased in *EGFR* 19del, L858R, and uncommon mutations. The potential role of CTLs and DCs in the TIME of patients requires further investigation.

Keywords: immune microenvironment, lung adenocarcinoma, epidermal growth factor receptor (EGFR) mutation, Bioinformatics & Computational Biology, myeloid dendritic cells (mDCs), cytotoxic T lymphocyte (CTL)

INTRODUCTION

Lung cancer is one of the leading causes of cancer mortality worldwide (1). Nearly 85% of patients with lung cancer are diagnosed with non-small-cell lung cancer (NSCLC). The two main histological subtypes of NSCLC are adenocarcinoma (ADC) and squamous cell carcinoma (SCC). However, ADC and SCC show different characteristic according to the mutation landscape at the molecular level. As reported, the epidermal growth factor receptor (*EGFR*) mutation is one of the most common mutated genes detected in adenocarcinoma. Previous studies have shown that *EGFR* mutations occurred more frequently in females, non-smokers, and Asian patients, and the majority of *EGFR* mutations were deletions in exon 19 or the L858R substitution in exon 21. Other mutations located in exons 18 and 20 are rare but can also cause *EGFR* gene activation (2).

For NSCLC patients harboring a sensitizing *EGFR*-mutation, treatment with *EGFR* tyrosine kinase inhibitors (TKIs) leads to longer progression-free survival (PFS) and has already become the first-line treatment. At present, three generations of *EGFR* TKIs are globally available for the treatment of NSCLC and have significantly improved the prognosis of patients (3–5). However, a significant portion of patients with co-mutations or rare mutations of *EGFR* gain little benefit from TKIs treatment (6). Additionally, almost all patients treated with TKIs eventually experience tumor relapse and acquire resistance. For such patients, the use of TKIs combined with chemotherapy or a monoclonal anti-vascular endothelial growth factor antibody has become the treatment of choice (7). However, the efficacy remains unsatisfactory, and there is still a great need for new treatment strategies.

In recent years, clinical trials have provided unequivocal evidence of the efficacy of immune checkpoint inhibitors (ICIs), so they have become a standard therapy in advanced NSCLC. Still, a major limitation was that patients with sensitizing *EGFR* mutations were excluded from most clinical trials. A meta-analysis demonstrated that ICIs prolonged overall survival in the EGFR wild-type subgroup [hazard ratio, (HR), 0.67], but not in the *EGFR* mutant subgroup (HR, 1.11), and prolonged overall survival in the *KRAS*-mutant subgroup (HR, 0.65), but not in the *KRAS* wild-type subgroup (HR, 0.86) (8). Currently available clinical trial data have shown that single-agent immunotherapy and in combination with TKIs are inappropriate for *EGFR* mutant patients (9). Thus, it is challenging to identify potential patients who could benefit from ICIs and to help patients with specific mutations benefit from immunotherapy.

Recent studies on the tumor immune microenvironment (TIME) suggest that the abundance and location of tumor-infiltrating lymphocytes (TILs) can be a potential predictor of response to ICIs (10). Clinical studies also have confirmed that reversing the TIME might reduce tumor-induced immunosuppression in patients with a mutated *EGFR* (11). All of these studies suggest that we should pay attention to the TIME of mutant lung cancer and seek a breakthrough in treatment. Till now, the immune landscape remains unclear in *EGFR* mutant patients, especially for different mutant subtypes. Therefore, this study aims to explore the TIME in $EGFR^{-mt}$ adenocarcinoma and investigate the specific TIME features within different subgroups. The flow chart of this study is shown in **Figure 1**.

METHODS

Patient Cohort and Genomic Data Processing

The Cancer Genome Atlas (TCGA) lung adenocarcinoma (LUAD) mRNA expression data, mutation data, and clinical information were downloaded from TCGA (http://cancergenome.nih.gov/) and the University of California at Santa Cruz Xena (UCSC Xena; http://xena.ucsc.edu/). For transcriptome data, raw counts and Fragments Per Kilobase of transcripts per Million mapped reads [FPKM] were acquired. The FPKM was then transformed to TPM for further calculation. Genomic alteration was downloaded from the cBioPortal for Cancer Genomics (cBioPortal; http://cbioportal.org).

Common *EGFR* mutations were defined as exon 19 deletion and exon 21 L858R without exon 20 T790M. Uncommon *EGFR* mutations were defined as other oncogenic mutations, such as G719X, S768I, and L861Q in exons 18, 20, and 21, respectively. Except as noted above, others that cannot lead to *EGFR* activation were defined as unknown mutations. Patients with co-mutations of different *EGFR*-mutation status were excluded from all groups.

Analysis of Immune Landscape

Tumor mutational burden (TMB): The TMB was defined as the total number of somatic mutations per megabase (Mb) of the genome examined. The normalized TMB = (whole exome non-synonymous mutations)/(38 Mb).

Estimation of STromal and Immune cells in MAlignant Tumor tissues using Expression data (ESTIMATE): ESTIMATE (12) was used to assess the immune infiltration (ImmuneScore), stromal content (StromalScore), and combined (ESTIMATEScore) of the samples. This kind of scoring can be used to estimate tumor purity. ESTIMATE was downloaded from the MD Anderson Cancer Center database (https://bioinformatics.mdanderson.org).

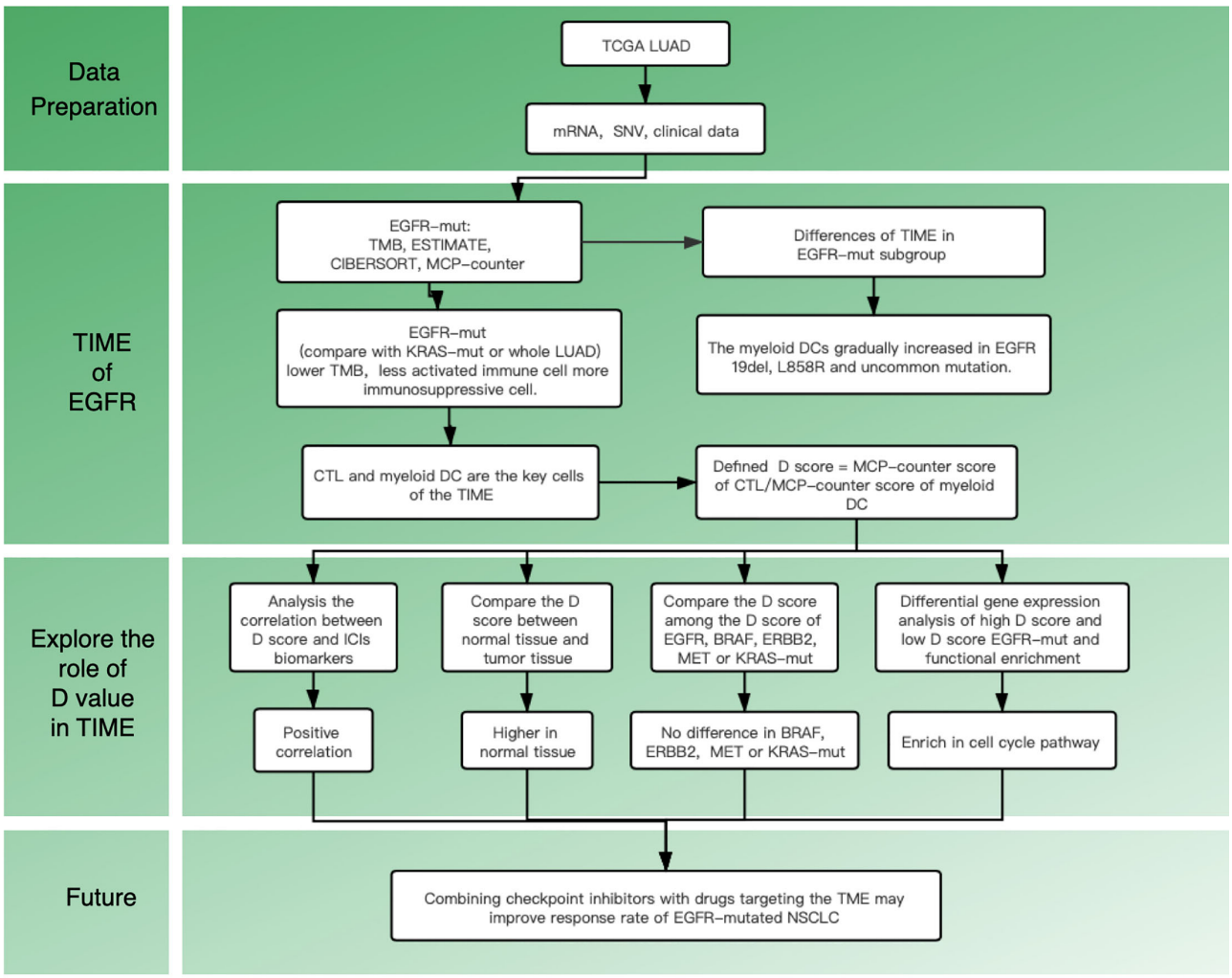

FIGURE 1 | Flowchart of the study design.

CIBERSORT: CIBERSORT (13) is an analytical tool that applies a deconvolution algorithm to estimate the proportions of 22 leucocyte subtypes based on RNA-seq data. Results with a CIBERSORT *P*-value of <0.05 were used for subsequent calculation. The package 'CIBERSORT' was used to calculate the percentage.

Microenvironment cell populations-counter (MCP-counter): MCP-counter (14) is a computational Method based on the mean marker gene expression that is specifically expressed in the cell type. The eight immune-cell lineage scores were estimated by using the R package MCP-counter algorithm.

Differentially Expressed Genes and Functional Pathways Analysis

Differential gene expression was determined by using the EdgeR software package. Gene Ontology (GO) and Kyoto Encyclopedia of Genes and Genomes (KEGG) enrichment (false discovery rate < 0.05, Foldchange > 1) analysis of differentially expressed genes (DEGs) were performed to search for biological functions and pathways.

Statistical Analysis

The statistical analysis of tumor purity and of the presence of infiltrating stromal/immune cells in tumor tissues was performed by using R packages: MCP-counter and CIBERSORT. Statistical comparisons were evaluated by using the Wilcoxon rank-sum test and Kruskal–Wallis tests. The clinicopathological characteristics were compared by using chi-square test. Correlations were assessed by using Pearson correlational distances. A two-sided *P*-value of <0.05 was considered to be indicative of statistical significance.

RESULTS

Clinical Characteristics of the Patients

In total, 585 patients data were downloaded from the TCGA data set. Among these, 98 cases involved *EGFR*-mutation. Then, the patients were divided into four groups according to their *EGFR*-mutation type (19del, L858R, uncommon mutation, unknown mutation group). Clinical data were available for 68 of the 98 patients. Baseline characteristics are presented in **Table 1**.

TIME of the Patients With *EGFR* Mutations

Supplementary Figure 1 shows the immune landscape of the *EGFR* mutant group. For further evaluation, we compared the TIME in the *EGFR* group with that in the *KRAS* group, and the whole LUAD. The results showed that the TMB was lower in the *EGFR* group (3.94 mut/Mb) than in the *KRAS* group (6.09 mut/Mb, $P < 0.001$) and in the whole LUAD (6.58 mut/Mb, $P < 0.001$) (**Figure 2A**). For tumor purity, which was inferred from the ESTIMATE purity score, there were no significant differences between the three groups ($P > 0.05$) (**Figure 2B**). For TILs, the *EGFR* group had a lower score of activated immune cells (CD8 T cells, cytotoxic lymphocytes (CTLs), NK cells) and an even higher score of immunosuppressive cells [myeloid dendritic cells (DCs)] according to the MCP-counter results than *KRAS* group and the whole LUAD (**Figure 2D**, $P < 0.05$). The same trend was observed through analysis of the immune-cell proportion by using the CIBERSORT deconvolution Method (**Figure 2C**. $P < 0.05$).

Further Analysis of the TIME in the *EGFR* Mutations Subgroup

Previous studies have suggested that the efficacy of immunotherapy was different among different mutant subtypes. We hypothesized that this may be related to TIME. We then conducted a subgroup analysis to further explore the differences in TIME among different *EGFR* subgroups. Analysis showed that there were significant differences among the four subgroups (19del, L858R, uncommon mutations, unknown mutations) in the TMB, CD8 T cells, and DCs (**Figure 3**). However, there were no differences in the purity scores among the four groups (by ESTIMATE).

To determine the source of the differences, we first classified the *EGFR*-mutation patients into oncogenic and unknown mutation groups according to whether EGFR was activated. The oncogenic group showed a lower TMB, a lower fractions of activated immune subpopulations (by CIBERSORT), and a high abundance of myeloid DCs (by MCP-counter) (**Supplementary Figure 2**, $P < 0.05$). Second, oncogenic *EGFR* mutations can be divided into common and uncommon mutations. There were more myeloid DCs in the common mutations group than in the uncommon mutations group (by MCP-counter). No statistical differences in TMB, tumor purity or fractions of the most immune subgroup were observed between this two groups (**Supplementary Figure 3**, $P < 0.05$). Thirdly, as mentioned above, common *EGFR* mutations include exon 19 deletion and exon 21 L858R. The analysis results showed that there were also no differences in the TMB and ESTIMATE scores between this two subgroups. But a trend toward an immunosuppressive environment was observed in the 19del group. The proportion of resting DCs in the 19del group showed a significant decrease than that in the L858R group (by CIBERSORT, $P < 0.05$) (**Supplementary Figure 4**).

Define a Score (D) Based on the MCP-Counter

Subgroup analysis of clinical trials showed that the efficacy of tumor immunotherapy was better in the KRAS group than in the EGFR group. To further characterize which types of infiltrating cells have important roles in immunotherapy, the compositions of TILs were compared between the *KRAS* and *EGFR* groups. Analysis by MCP-counter (as well as the CIBERSORT results) showed that more abundant CTLs and a lower population of myeloid DCs were observed in the $KRAS^{-mt}$ group than in the $EGFR^{-mt}$ group (**Supplementary Figure 5**). The results above suggest that CTLs and myeloid DC have an essential role in TIME. According to this result, we built a simplified model (D score) to quantify the generalized TIME state and defined a D score as D = MCP-counter score of CTLs/

TABLE 1 | Demographic characteristics of the patients at baseline.

Characteristics	Type	Total	19del	L858R	Uncommon mutation	Unknown mutation
Age	<=65	33 (48.53%)	11 (42.31%)	9 (50%)	7 (58.33%)	6 (50%)
	>65	32 (47.06%)	12 (46.15%)	9 (50%)	5 (41.67%)	6 (50%)
	Unknown	3 (4.41%)	3 (11.54%)	0 (0%)	0 (0%)	0 (0%)
Gender	FEMALE	49 (72.06%)	22 (84.62%)	15 (83.33%)	9 (75%)	3 (25%)
	MALE	19 (27.94%)	4 (15.38%)	3 (16.67%)	3 (25%)	9 (75%)
Stage	Stage I–II	52 (76.47%)	19 (73.08%)	15 (83.33%)	9 (75%)	9 (75%)
	Stage III–IV	15 (22.06%)	7 (26.92%)	3 (16.67%)	3 (25%)	2 (16.67%)
	Unknown	1 (1.47%)	0 (0%)	0 (0%)	0 (0%)	1 (8.33%)
T	T1–2	58 (85.29%)	26 (100%)	15 (83.33%)	9 (75%)	8 (66.67%)
	T3–4	9 (13.24%)	0 (0%)	3 (16.67%)	2 (16.67%)	4 (33.33%)
	TX	1 (1.47%)	0 (0%)	0 (0%)	1 (8.33%)	0 (0%)
M	M0	47 (69.12%)	17 (65.38%)	15 (83.33%)	7 (58.33%)	8 (66.67%)
	M1	3 (4.41%)	1 (3.85%)	0 (0%)	1 (8.33%)	1 (8.33%)
	Unknown	18 (26.47%)	8 (30.77%)	3 (16.67%)	4 (33.33%)	3 (25%)
N	N0	42 (61.76%)	12 (46.15%)	12 (66.67%)	7 (58.33%)	11 (91.67%)
	N1-3	23 (33.82%)	13 (50%)	6 (33.33%)	3 (25%)	1 (8.33%)
	Unknown	3 (4.41%)	1 (3.85%)	0 (0%)	2 (16.67%)	0 (0%)

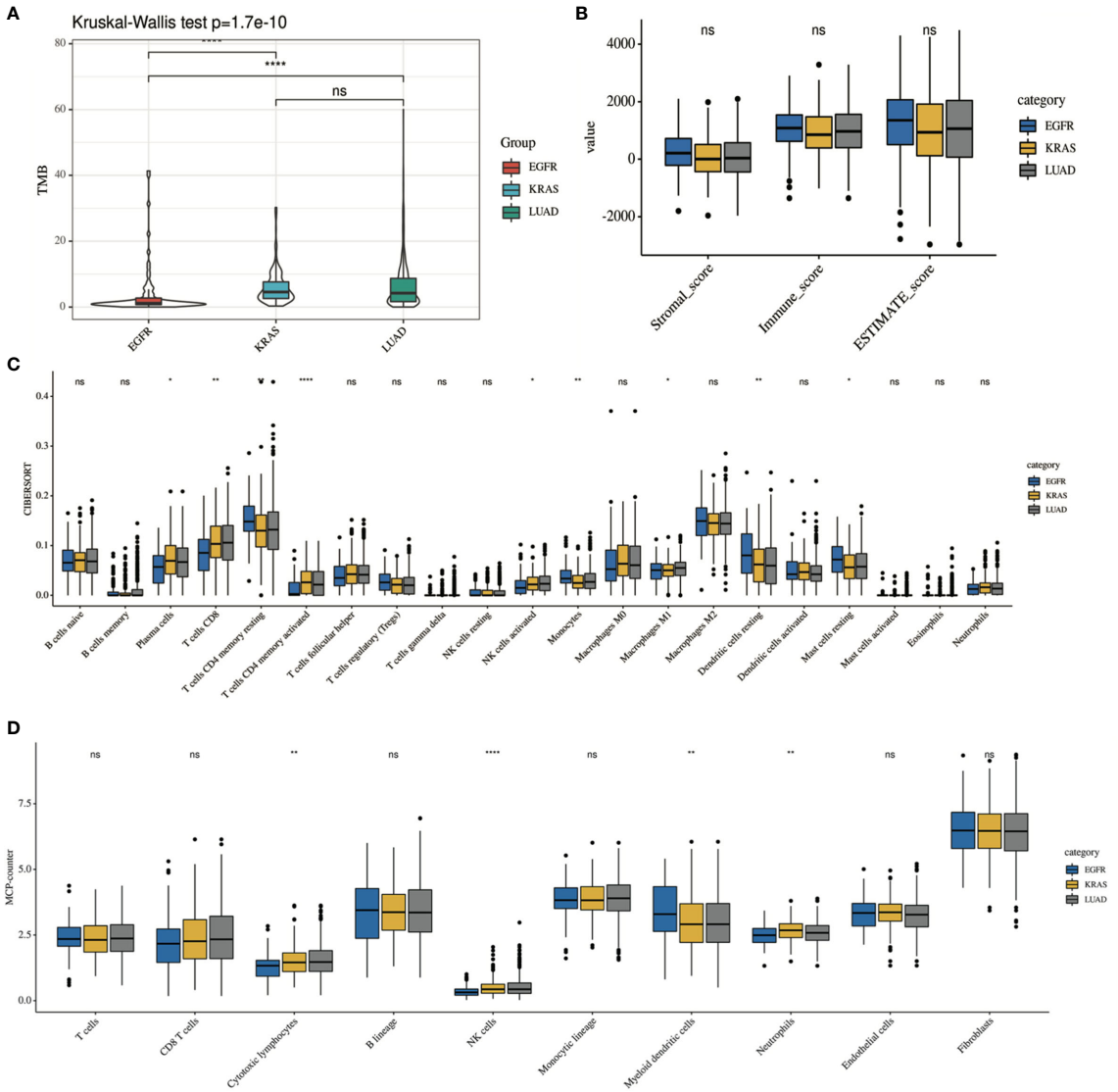

FIGURE 2 | Comparison of the immune landscape of EGFR-mutated group, KRAS-mutated group and the whole lung adenocarcinoma. The TIME of EGFR-mutated NSCLC show an immunosuppressive status with lower **(A)** TMB, a lower score of activated immune cell and an even higher score of immunosuppressive cell, estimated by **(C)** CIBERSORT and **(D)** MCP-counter. No difference was found in tumor purity among three group **(B)**. *P < 0.05, **P < 0.01, and ***P < 0.0001, respectively. ns, not significant.

MCP-counter score of myeloid DCs. The lower the D score, the greater degree of immunosuppression in the TIME. To test the performance of D score, we performed the following analysis.

Functional Enrichment Analysis in Different *EGFR* Mutant Groups Defined by the D Score

To further study the differences in gene expression between different D values, *EGFR*-mutation patients were grouped by D value quartiles, with quartile 1 having the lowest and quartile 3 the highest D level (n = 16 in each group). Differentially expressed genes between the two groups were identified by performing an EdgeR analysis. Among the DEGs identified, 890 were upregulated, and 1373 were downregulated. The DEGs are shown as a volcano plot in **Figure 4A**. The candidate DEG functions and signaling pathway enrichment were analyzed by using GO terms and the KEGG pathway. Overall, 18 KEGG pathways were significantly enriched. The top five KEGG pathways were the cell cycle, viral protein interaction with cytokine and cytokine receptors, cytokine–cytokine receptor interaction, neuroactive ligand–receptor interaction, and hematopoietic cell lineage (**Figure 4B**). The organelle fission GO term was the top GO term, followed by nuclear division, receptor ligand activity chromosome segregation, and chromosomal region (**Figure 4C**).

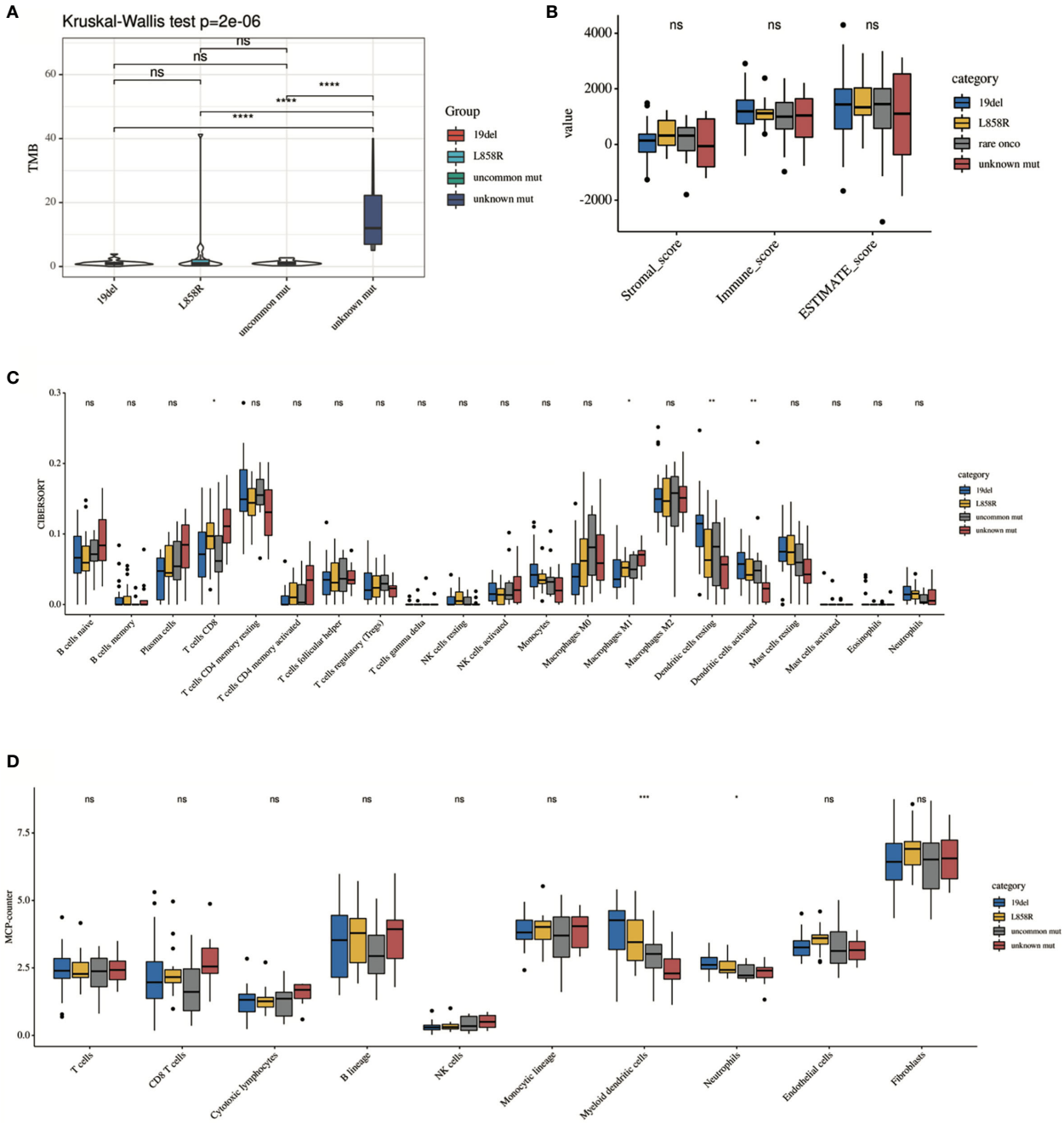

FIGURE 3 | Comparison of the immune landscape among 19del, L858R, uncommon mutation and unknown mutation group. **(A)** TMB, **(B)** ESTIMATE, **(C)** CIBERSORT, **(D)** MCP-counter. Only significant difference in myeloid DC cells was presented among different groups estimated by **(C)** CIBERSORT and **(D)** MCP-counter. *P < 0.05, **P < 0.01, ***P < 0.001 and ****P < 0.0001, respectively. ns, not significant.

Exploration of D Score Among Patients With Different Driver Mutation

Since it remained uncertain whether NSCLC with targetable drivers will benefit from immunotherapy, we further calculated the D value of different mutation subgroups, including *EGFR*, *BRAF*, *ERBB2*, *KRAS*, and *MET* mutations. The results showed that the average D values were 0.37, 0.47, 0.56, 0.57, and 0.51 in patients with EGFR, *BRAF*, *ERBB2*, *KRAS*, and *MET* mutations. Inter-group analysis showed that the D value was lower in the *EGFR* group than in the other rare mutation groups ($P < 0.05$) except for the *MET* mutation. However, there were no significant differences in the D values among the *BRAF*, *ERBB2*, *KRAS*, and *MET* mutations (**Figure 5**).

Clinical Characteristics and Immune-Cell Infiltration of Different D score Groups in LUAD

To examine the significance of the D score, we further studied its role among all TCGA–LUAD patients. We first compared the D score between tumors and normal tissues from TCGA. The results showed that the D value was higher in normal tissue than in tumor tissue, which was consistent with expectations (**Figure 6A**, $P < 0.001$). We then compared the clinicopathological features and immune landscape characteristics of different LUAD patients by their D scores. For further analysis, the median D score was selected as the cutoff value. The patients were divided into two groups: the high (D > 0.51, n = 252) group and low (D ≤ 0.51, n = 251) D group. We found there were no significant differences in the D scores of the samples among the clinicopathological features groups, including T, N, M, Stage, Grade, and Age ($P > 0.05$) (**Supplementary Table 1**). We also observed that the tumor purity difference between the patients in the high- and low-D groups was not significant (median ESTIMATE score, $P > 0.05$). However, the immunescore was higher for the high-D group, as expected ($P < 0.05$) (**Figure 6B**).

Because the D score reflected the immunosuppressive environment based on T cells and DCs, we decided to explore whether the levels of other immune cells in different D groups were consistent with expectations. The different immune cell distribution between the high- and low-D groups is shown in **Figures 6C, D**. In addition to CD8+T cells and DCs, we observed that the high-D group had higher infiltration of activated T cells CD4 memory activated, T- cells follicular helper, NK cells activated, and macrophages M1 according to CIBERSORT ($P < 0.05$). In contrast, the low-D group had higher infiltration of Ts cells CD4 memory resting, T cells regulatory (Tregs), and monocytes and mast cells resting ($P < 0.05$) (**Figure 6C**). Similar to this result, we found that a variety of T-cell MCP-counter scores decreased in the low-D group ($P < 0.05$) (**Figure 6D**).

Relationship Between the D Score and Predictive Biomarkers for Immunotherapy

Immunotherapy is currently a first-line treatment for lung adenocarcinoma. However, it remains challenging to identify immune resistance and the beneficiary groups. To explore the predictive role of the D value in immunotherapy, we further explored the relationship between the D score and predictive biomarkers for ICIs. First, we found a positive correlation between D scores and TMB ($r = 0.30$, $P < 0.001$), which suggests that the lower the D value, the lower the TMB, and the less likely it is to benefit from immunotherapy. In addition, we further explored the association between different patient groups defined by the D score and immune checkpoints. We found that lower mRNA expression levels of PDCD1, CD274, PDCD1LG2, LAG3, TIGIT, and IDO1 were observed in the low-D score patients (**Figures 7A–F**, $P < 0.05$). The results also suggest that a lower D value is a good indicator of immunosuppression and a potentially negative biomarker for immunotherapy.

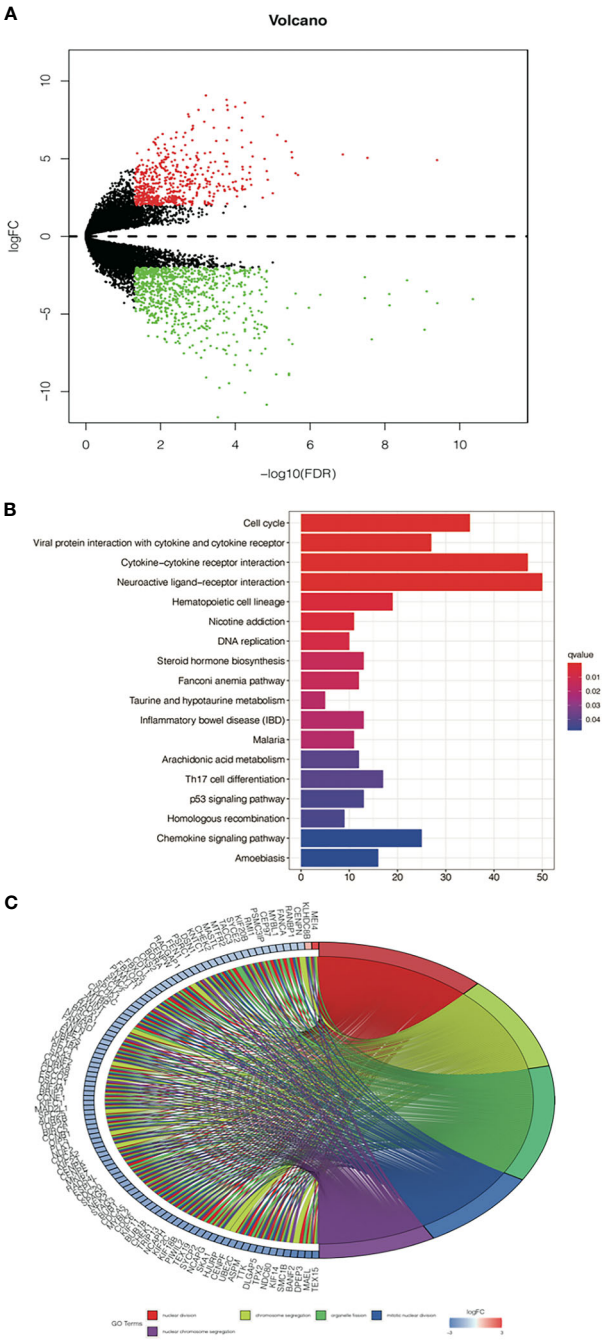

FIGURE 4 | Analysis of differentially expressed genes (DEGs) from the D value of EGFR-mut group quartile 1 compared with quartile 3. **(A)** Volcano plot showing DEGs between higher D score group and lower D score group. **(B)** Top 10 enrichments of up-regulated DEGs by KEGG analyses. **(C)** Gene Ontology analyses of DEGs according to their biological process.

DISCUSSION

Although ICIs have demonstrated clinical activity in a variety of tumors, resistance of cancer to ICI therapy remains a major

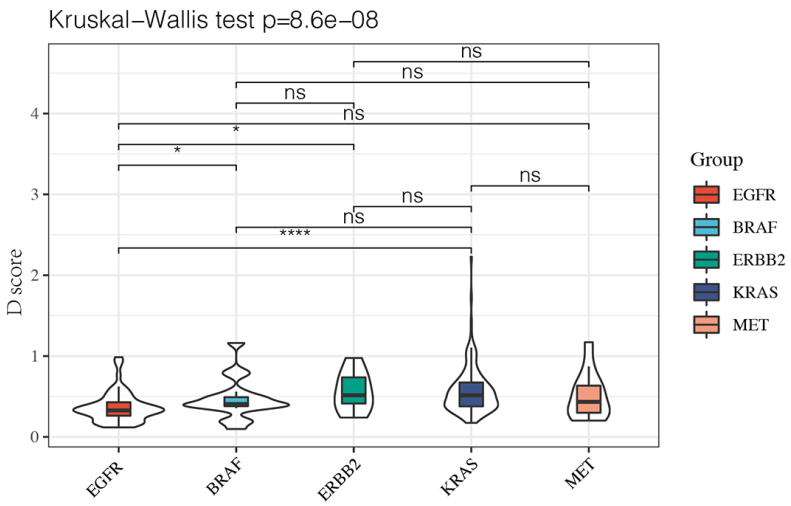

FIGURE 5 | The D value of EGFR group was lower than rare mutation group except MET mutation and there was no significant difference among BRAF, ERBB2, KRAS and MET mutation. *P < 0.05 and ****P < 0.0001, respectively. ns, not significant.

clinical problem (15). From a clinical perspective, resistance to PD-(L)1 inhibitors can be classified into three distinct scenarios: primary resistance, secondary resistance, and progression after treatment discontinuation (16). The mechanisms of primary resistance to immunotherapy include tumor-cell intrinsic (for example, absence of antigenic proteins) and tumor-cell extrinsic (for example, absence of T cells and infiltration of immunosuppressive cells) (17), which can interact with each other. Increasing evidence has suggested that identifying immunophenotyping will help predict outcomes of immunotherapy and provide a novel direction for overcoming resistance (18, 19). On the basis of the above, we conducted the present study. **Figure 8** is a schematic representation of the findings presented in this article.

In this study, we characterized four aspects to describe the immune landscape of patients with *EGFR* mutations. The first aspect is the TMB. Previous studies have shown that the TMB is an important criterion for successful immunotherapy. Our findings suggest that the TMB was lower for the *EGFR* group than for the *KRAS* group and the whole LUAD. In an open-label, randomized, phase 3 trial (CheckMate 227), the researchers demonstrated longer PFS time in NSCLC patients with a high TMB (defined as ≥10 mut/Mb), regardless of PD-L1 expression or tumor type (HR, 0.58; 95% CI, 0.41–0.81) (20). However, in our study, only 12.5% of the *EGFR* patients had TMB of >10mut/Mb. Seventy-eight percent of patients in the *EGFR* group had TMB of <5mut/Mb. This finding partly explains the reason for the poor curative effect in the $EGFR^{-mt}$ group. The second aspect is the ESTIMATE score. The higher the ESTIMATE score, the lower the tumor purity. Our study showed that there were no significant differences in tumor purity among the three groups, which was inferred by using the ESTIMATE purity score. The third and fourth aspects were CIBERSORT and MCP-counter. Both of these tools are mathematical Methods to estimate TILs. A previous study suggested that immune-cell infiltration was associated with antitumor activity. It has been reported that high stromal infiltration of CD8+ ICs and CD4+ ICs was associated with better overall survival by analyzing 139 nivolumab-treated NSCLC simple tumor tissue specimens (21). In our study, compared with KRAS and the whole LUAD group, the TIME in the *EGFR* mutant patients showed a trend of diminishing activated TILs and increasing numbers of immunosuppressive cells. Some previous experimental studies have reported similar results. Although there are artificial intelligence approaches to calculate the absolute count of immune cells, these Methods and tools are still evolving. At present, the most commonly used Method to quantify the number and type of immune cells is by immunohistochemistry (IHC). A study based on 245 Chinese NSCLC patients showed that lower immune infiltration was associated with *EGFR* mutations in adenocarcinoma samples through IHC staining of CD8 (22). Similarly, a French study also confirmed this conclusion; the researchers found that the expression of PD-L1 was decreased, and the density of CD8+T lymphocytes was lower in patients with *EGFR* mutations in lung cancer through IHC. In addition, with the development of technology in recent years, some new technologies, such as Digital Spatial Profiling, have also gradually shown the advantages of quantifying the tumor microenvironment, but it has not been widely used (23). Clinically, our results are also consistent with clinical evidence showing that compared with *KRAS*-mutant patients, patients with *EGFR* mutations-mutant are difficult to rarely benefit from immunotherapy (8).

In the era of molecular targeted therapy, different subtypes of *EGFR* mutations may cause different TKIs sensitivity. However, it remains undetermined if there are differences in the TIMEs and ICI efficacies among different *EGFR*-mutation subtypes. In a registration study, a total of 125 *EGFR*-mutation patients treated

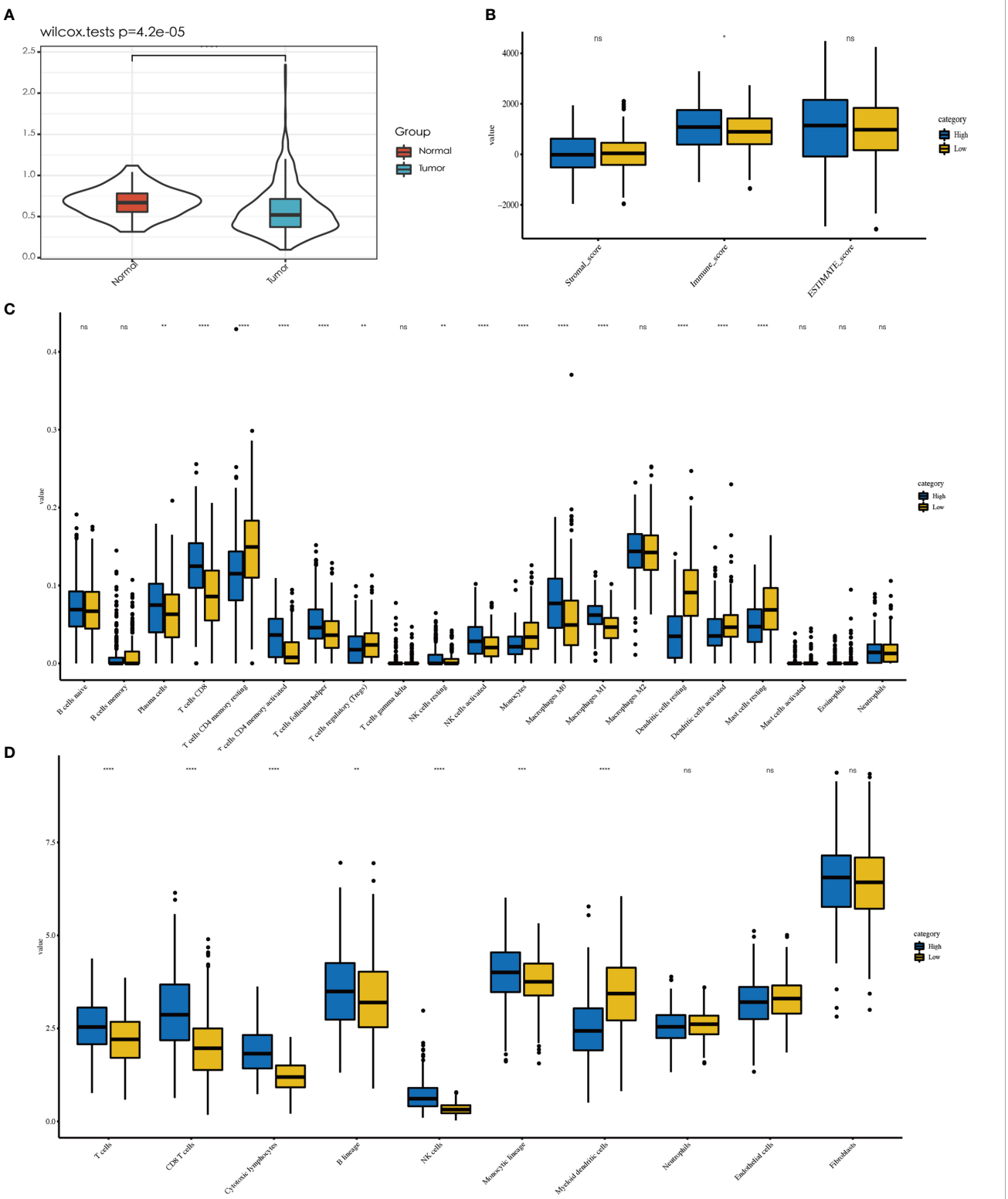

FIGURE 6 | Explore the role of D value in LUAD. Tumor tissue showed a lower D value than normal tissue **(A)**. No difference in tumor purity was observed between high-D and low-D group **(B)**. Less abundant of activated immune cell were observed in low-D group by CIBERSORT **(C)** as well as the result MCP-counter **(D)**. *P < 0.05, **P < 0.01, ***P < 0.001 and ****P < 0.0001, respectively. ns, not significant.

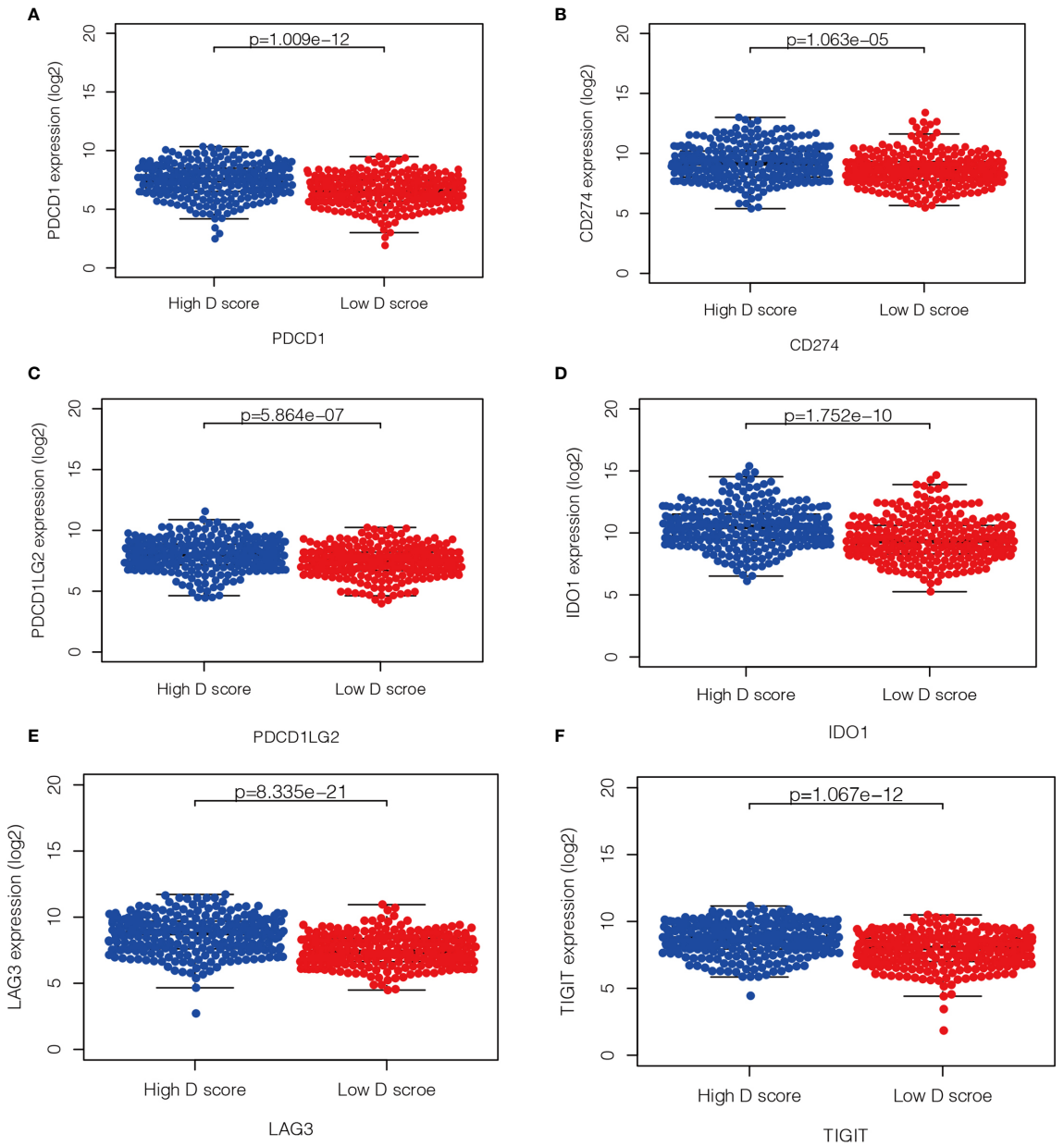

FIGURE 7 | Relationship between the D score and the expression of immune checkpoint. **(A–F)** the distribution of mRNA level of PDCD1, CD274, PDCD1LG2, LAG3, TIGIT and IDO1 in high- and low-D score groups.

with ICIs were included. That study showed that different *EGFR*-patient subgroups had different PFS and OS durations. The median PFS was 1.4 months for patients with T790 single or multiple mutations, 1.8 months for patients with the exon 19del mutation, 2.5 months for patients with the exon21 L858R mutation, and 2.8 months for patients with other mutations ($P < 0.001$) (24). In the present study, we also observed differences in the immune landscapes among the 19del, 21L85R, uncommon-mutant, and unknown-mutant groups. Through a further inter-group comparison, we found that differences in the TMB and TILs were only found between patients with oncogenic mutations and unknown mutations. No significant differences were observed in the activated immune cells between 19del patients and L858R-mutation patients or between common mutation and uncommon mutation patients. However, the myeloid DCs increased in the 19del group relative to those in the L858R group and in the common mutation group relative to those in the uncommon group. These findings indicated that, from an immunological perspective, oncogenic mutation might be an important factor

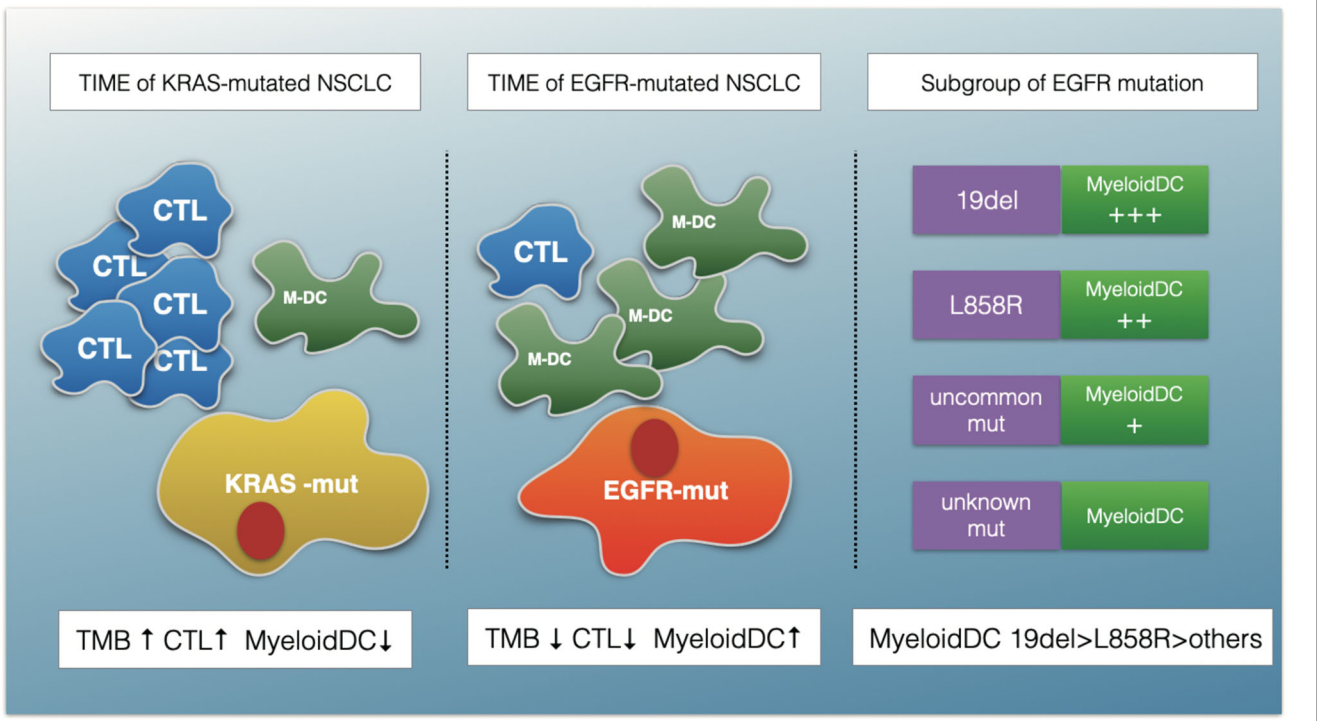

FIGURE 8 | A schematic summarizing the major findings of this study. The TIME of EGFR-mutated NSCLC show an immunosuppressive status with lower TMB, fewer cytotoxic T cells (CTLs) and more myeloid DC (M-DC) cells compared with KRAS-mutated NSCLC. The myeloid DCs increased in EGFR 19del compared with L858R mutation patients, and in common mutation patents compared with uncommon mutations.

for cellular immune suppression. Targeting DC therapy may be an interesting future direction for *EGFR*-mutation patients.

As is known, the tumor microenvironment is a complex and dynamic system formed by stromal, immune, and inflammatory cells and the extracellular matrix (ECM) (18). In our research, to further identify the key immune cells in the TIME, we analyzed the TILs in the KRAS and *EGFR* groups, including CIBERSORT and MCP-counter results, and we finally determined through inter-group comparisons that activated T cells and resting DCs were the key analysis factors. Various studies have proven the significant functions of T cells in the antitumor process. The role of DCs has been gradually recognized in recent years. Previous studies have shown that DCs are central to the initiation of antigen-specific immunity and tolerance. In the TIME, DCs acquire, process, and present tumor-associated antigens on major histocompatibility complex molecules and provide co-stimulation and soluble factors to shape T-cell responses (25). For the above reasons, we defined D = MCP-counter score of CTLs/MCP-counter score of myeloid DCs. Considering that the MCP-counter score presents as the geoMETric mean of marker gene expression (26), the D value, as a further calculation of the MCP-counter score, might have good clinical application and promotional value by validation through multiple IHC analyses with tyramide signal amplification or DSP technology in the future.

An interesting result of D value analysis was that the differential genes were mainly enriched in the cell cycle pathway when the low-D-score group was compared with the high-D-score group for *EGFR*-mutation patients. Although previous clinical trials have shown that necitumumab, an anti-EGFR antibody combined with abemaciclib (a CDK4/6 inhibitor), did not produce an additive effect over single-agent activity in patients with stage IV NSCLC, no clinical studies have been conducted to explore the effectiveness of immunotherapy combined with a CDK4/6 inhibitor (22). Some basic studies have established that CDK4/6 inhibitors could enhance T-cell activation and induce a T-cell inflamed TME (23, 24). Based on our analysis results, the combination of ICIs with a cell cycle-related drug may be a potential therapeutic option for *EGFR*-mutation patients. However, this hypothesis needs to be confirmed.

Mutation features comprise an important signature of LUAD. In addition to classical mutations, some other mutations have gained increasing attention from researchers. Although ICIs have shown promising benefit in NSCLC, the efficacy of ICIs in NSCLC patients with rare mutations remains largely unknown. Previous reports have shown how different mutations affect the microenvironmental phenotype of tumors, which in turn affects the sensitivity of tumors to immunotherapy. For example, the TIME has been shown to have less immune-cell infiltration in *STK11*-mutation patients who have a worse prognosis after immunotherapy (27). A similar phenomenon was also observed in patients with *KEAP1* mutations, despite a high

TMB level (28). Our data shows that the D scores of *BRAF*, *ERBB2*, *MET*, or *KRAS* were very similar, suggesting that they may have similar TIMEs in some ways. On the one hand, this result is consistent with previous real-world study data showing that ICI efficacies against *BRAF*-, *HER2*-, *MET*-, or *RET*-NSCLC patients were close to the efficacy observed in unselected NSCLC patients (29). On the other hand, our results support the application of ICIs from a TIME viewpoint.

Although immunotherapy has greatly improved the prognosis of patients with lung cancer, screening patients who are potentially effective or resistant to treatment remains challenging (30). Through early detection of potential biomarkers, we can choose individualized strategies for patients who may be resistant to immunotherapy, which may help to prolong the survival time (31). In our study, a lower D score was shown to be a new indicator of immunosuppression. This result was further verified by analyzing the TMEs of the high- and low-D groups in the whole LUAD population. Just as we expected, we observed less activated and more resting immune cells in the low-D group through analysis of immune cells. To further clarify the role of the D value in clinical practice, we further investigated the relationship between the D score and the well-studied immunotherapy predictive biomarkers. We found that low-D score patients had significantly lower levels of immune checkpoint gene expression and TMB. These novel findings suggest that the D score may be a predictive biomarker for immunotherapy response. This possibility needs to be confirmed in future prospective clinical studies.

In conclusion, the TIME of *EGFR*$^{-mt}$ NSCLC was found to be immunosuppressive. Myeloid DCs were higher in *EGFR* 19del patients than in L858R mutation patients and in common mutation patients than in uncommon mutations. CTLs and DCs have key roles in the TIME and may be potential predictors of immunotherapy efficacy. Certain aspects of the findings require further validation and qualification in a large longitudinal population study in the future.

DATA AVAILABILITY STATEMENT

Publicly available data sets were analyzed in this study. These data can be found here: portal.gdc.cancer.gov/.

AUTHOR CONTRIBUTIONS

Conception and design: TL and XP. Development of methodology: JW and YG. Analysis and interpretation of data (e.g., statistical analysis, biostatistics, computational analysis): NH and SW. Writing, review, and/or revision of the manuscript: TL and JW. Administrative, technical, or material support (i.e., reporting or organizing data, constructing databases): XP. Study supervision: PX and JL. All authors contributed to the article and approved the submitted version.

SUPPLEMENTARY MATERIAL

The Supplementary Material for this article can be found online at: https://www.frontiersin.org/articles/10.3389/fonc.2021.591922/full#supplementary-material

REFERENCES

1. Sung H, Ferlay J, Siegel RL, Laversanne M, Soerjomataram I, Jemal A, et al. Global Cancer Statistics 2020: GLOBOCAN Estimates of Incidence and Mortality Worldwide for 36 Cancers in 185 Countries. *CA Cancer J Clin* (2021) 71:209–49. doi: 10.3322/caac.21660
2. Sharma SV, Bell DW, Settleman J, Haber DA. Epidermal Growth Factor Receptor Mutations in Lung Cancer. *Nat Rev Cancer* (2007) 7:169–81. doi: 10.1038/nrc2088
3. Lee CK, Davies L, Wu YL, Mitsudomi T, Inoue A, Rosell R, et al. Gefitinib or Erlotinib vs Chemotherapy for EGFR Mutation-Positive Lung Cancer: Individual Patient Data Meta-Analysis of Overall Survival. *J Natl Cancer Inst* (2017) 109:djw279. doi: 10.1093/jnci/djw279
4. Sequist LV, Yang JC, Yamamoto N, O'Byrne K, Hirsh V, Mok T, et al. Phase III Study of Afatinib or Cisplatin Plus Pemetrexed in Patients With Metastatic Lung Adenocarcinoma With EGFR Mutations. *J Clin Oncol* (2013) 31:3327–34. doi: 10.1200/JCO.2012.44.2806
5. Gregorc V, Lazzari C, Karachaliou N, Rosell R, Santarpia M. Osimertinib in Untreated Epidermal Growth Factor Receptor (EGFR)-Mutated Advanced Non-Small Cell Lung Cancer. *Transl Lung Cancer Res* (2018) 7:S165–70. doi: 10.21037/tlcr.2018.03.19
6. Yang JC, Schuler M, Popat S, Miura S, Heeke S, Park K, et al. Afatinib for the Treatment of NSCLC Harboring Uncommon EGFR Mutations: A Database of 693 Cases. *J Thorac Oncol* (2020) 15:803–15. doi: 10.1016/j.jtho.2019.12.126
7. Saito H, Fukuhara T, Furuya N, Watanabe K, Sugawara S, Iwasawa S, et al. Erlotinib Plus Bevacizumab Versus Erlotinib Alone in Patients With EGFR-Positive Advanced Non-Squamous Non-Small-Cell Lung Cancer (NEJ026): Interim Analysis of an Open-Label, Randomised, Multicentre, Phase 3 Trial. *Lancet Oncol* (2019) 20:625–35. doi: 10.1016/S1470-2045(19)30035-X
8. Lee CK, Man J, Lord S, Cooper W, Links M, Gebski V, et al. Clinical and Molecular Characteristics Associated With Survival Among Patients Treated With Checkpoint Inhibitors for Advanced Non-Small Cell Lung Carcinoma: A Systematic Review and Meta-Analysis. *JAMA Oncol* (2018) 4:210–6. doi: 10.1001/jamaoncol.2017.4427
9. Yang JC, Shepherd FA, Kim DW, Lee GW, Lee JS, Chang GC, et al. Osimertinib Plus Durvalumab Versus Osimertinib Monotherapy in EGFR T790M-Positive NSCLC following Previous EGFR TKI Therapy: CAURAL Brief Report. *J Thorac Oncol* (2019) 14:933–9. doi: 10.1016/j.jtho.2019.02.001
10. Mazzaschi G, Madeddu D, Falco A, Bocchialini G, Goldoni M, Sogni F, et al. Low PD-1 Expression in Cytotoxic CD8(+) Tumor-Infiltrating Lymphocytes Confers an Immune-Privileged Tissue Microenvironment in NSCLC with a Prognostic and Predictive Value. *Clin Cancer Res* (2018) 24:407–19. doi: 10.1158/1078-0432.CCR-17-2156
11. Socinski MA, Jotte RM, Cappuzzo F, Orlandi F, Stroyakovskiy D, Nogami N, et al. Atezolizumab for First-Line Treatment of Metastatic Nonsquamous NSCLC. *N Engl J Med* (2018) 378:2288–301. doi: 10.1056/NEJMoa1716948
12. Yoshihara K, Shahmoradgoli M, Martinez E, Vegesna R, Kim H, Torres-Garcia W, et al. Inferring Tumour Purity and Stromal and Immune Cell Admixture From Expression Data. *Nat Commun* (2013) 4:2612. doi: 10.1038/ncomms3612
13. Chen B, Khodadoust MS, Liu CL, Newman AM, Alizadeh AA. Profiling Tumor Infiltrating Immune Cells with CIBERSORT. *Methods Mol Biol* (2018) 1711:243–59. doi: 10.1007/978-1-4939-7493-1_12
14. Becht E, Giraldo NA, Lacroix L, Buttard B, Elarouci N, Petitprez F, et al. Estimating the Population Abundance of Tissue-Infiltrating Immune and Stromal Cell Populations Using Gene Expression. *Genome Biol* (2016) 17:218. doi: 10.1186/s13059-016-1070-5

15. Kalbasi A, Ribas A. Tumour-Intrinsic Resistance to Immune Checkpoint Blockade. *Nat Rev Immunol* (2020) 20:25–39. doi: 10.1038/s41577-019-0218-4
16. Kluger HM, Tawbi HA, Ascierto ML, Bowden M, Callahan MK, Cha E, et al. Defining Tumor Resistance to PD-1 Pathway Blockade: Recommendations From The First Meeting of The SITC Immunotherapy Resistance Taskforce. *J Immunother Cancer* (2020) 8:e000398. doi: 10.1136/jitc-2019-000398
17. Sharma P, Hu-Lieskovan S, Wargo JA, Ribas A. Primary, Adaptive, and Acquired Resistance to Cancer Immunotherapy. *Cell* (2017) 168:707–23. doi: 10.1016/j.cell.2017.01.017
18. Ladanyi A, Timar J. Immunologic and Immunogenomic Aspects of Tumor Progression. *Semin Cancer Biol* (2020) 60:249–61. doi: 10.1016/j.semcancer.2019.08.011
19. Thorsson V, Gibbs DL, Brown SD, Wolf D, Bortone DS, Ou Yang TH, et al. The Immune Landscape of Cancer. *Immunity* (2018) 48:812–30.e814.
20. Hellmann MD, Ciuleanu TE, Pluzanski A, Lee JS, Otterson GA, Audigier-Valette C, et al. Nivolumab Plus Ipilimumab in Lung Cancer with a High Tumor Mutational Burden. *N Engl J Med* (2018) 378:2093–104. doi: 10.1056/NEJMoa1801946
21. Niemeijer AN, Sahba S, Smit EF, Lissenberg-Witte BI, de Langen AJ, Thunnissen E. Association of Tumour and Stroma PD-1, PD-L1, CD3, CD4 and CD8 Expression With DCB and OS to Nivolumab Treatment in NSCLC Patients Pre-Treated With Chemotherapy. *Br J Cancer* (2020) 123:392–40. doi: 10.1038/s41416-020-0888-5
22. Zhang XC, Wang J, Shao GG, Wang Q, Qu X, Wang B, et al. Comprehensive Genomic and Immunological Characterization of Chinese Non-Small Cell Lung Cancer Patients. *Nat Commun* (2019) 10:1772. doi: 10.1038/s41467-019-09762-1
23. Kulasinghe A, Taheri T, O'Byrne K, Hughes BGM, Kenny L, Punyadeera C. Highly Multiplexed Digital Spatial Profiling of the Tumor Microenvironment of Head and Neck Squamous Cell Carcinoma Patients. *Front Oncol* (2020) 10:607349. doi: 10.3389/fonc.2020.607349
24. Mazieres J, Drilon A, Lusque A, Mhanna L, Cortot AB, Mezquita L, et al. Immune Checkpoint Inhibitors for Patients With Advanced Lung Cancer and Oncogenic Driver Alterations: Results From The IMMUNOTARGET Registry. *Ann Oncol* (2019) 30:1321-8. doi: 10.1093/annonc/mdz167
25. Wculek SK, Cueto FJ, Mujal AM, Melero I, Krummel MF, Sancho D. Dendritic Cells in Cancer Immunology and Immunotherapy. *Nat Rev Immunol* (2020) 20:7–24. doi: 10.1038/s41577-019-0210-z
26. Sturm G, Finotello F, Petitprez F, Zhang JD, Baumbach J, Fridman WH, et al. Comprehensive Evaluation of Transcriptome-Based Cell-Type Quantification Methods for Immuno-Oncology. *Bioinformatics* (2019) 35:i436–45. doi: 10.1093/bioinformatics/btz363
27. Wang H, Guo J, Shang X, Wang Z. Less Immune Cell Infiltration and Worse Prognosis After Immunotherapy for Patients With Lung Adenocarcinoma Who Harbored STK11 Mutation. *Int Immunopharmacol* (2020) 84:106574. doi: 10.1016/j.intimp.2020.106574
28. Marinelli D, Mazzotta M, Scalera S, Terrenato I, Sperati F, D'Ambrosio L, et al. KEAP1-Driven Co-Mutations in Lung Adenocarcinoma Unresponsive to Immunotherapy Despite High Tumor Mutational Burden. *Ann Oncol* (2020) 31:1746–54. doi: 10.1016/j.annonc.2020.08.2105
29. Guisier F, Dubos-Arvis C, Vinas F, Doubre H, Ricordel C, Ropert S, et al. Efficacy and Safety of Anti-PD-1 Immunotherapy in Patients With Advanced Non Small Cell Lung Cancer With BRAF, HER2 or MET Mutation or RET-Translocation. GFPC 01-2018. *J Thorac Oncol* (2020) 15:628–36. doi: 10.1016/j.jtho.2019.12.129
30. Litchfield K, Reading JL, Puttick C, Thakkar K, Abbosh C, Bentham R, et al. Meta-Analysis of Tumor- and T Cell-Intrinsic Mechanisms of Sensitization to Checkpoint Inhibition. *Cell* (2021) 184:596–614.e514. doi: 10.1016/j.cell.2021.01.002
31. Camidge DR, Doebele RC, Kerr KM. Comparing and Contrasting Predictive Biomarkers for Immunotherapy and Targeted Therapy of NSCLC. *Nat Rev Clin Oncol* (2019) 16:341–55. doi: 10.1038/s41571-019-0173-9

Conflict of Interest: NH and JW were employed by the company GloriousMed Clinical Laboratory (Shanghai) Co., Ltd.

The remaining authors declare that the research was conducted in the absence of any commercial or financial relationships that could be construed as a potential conflict of interest.

frontiers in Oncology

ORIGINAL RESEARCH
published: 10 June 2021
doi: 10.3389/fonc.2021.592854

The Correlation Between SPP1 and Immune Escape of EGFR Mutant Lung Adenocarcinoma Was Explored by Bioinformatics Analysis

*Yi Zheng[1], Shiying Hao[2], Cheng Xiang[1], Yaguang Han[1], Yanhong Shang[3], Qiang Zhen[1], Yiyi Zhao[1], Miao Zhang[1] and Yan Zhang[1]**

[1] Department of Oncology, Shijiazhuang People's Hospital, Shijiazhuang, China, [2] Department of Cardiothoracic Surgery, Standford University, Stanford, CA, United States, [3] Department of Oncology, Affiliated Hospital of Hebei University, Baoding, China

OPEN ACCESS

Edited by:
Qian Chu,
Huazhong University of Science and Technology, China

Reviewed by:
Yuanning Guo,
Clinical Research Institute, Israel
Mingwei Zhang,
First Affiliated Hospital of Fujian Medical University, China

***Correspondence:**
Yan Zhang
zhangyan201810@163.com

Specialty section:
This article was submitted to Cancer Immunity and Immunotherapy, a section of the journal Frontiers in Oncology

Received: 08 August 2020
Accepted: 17 May 2021
Published: 10 June 2021

Citation:
Zheng Y, Hao S, Xiang C, Han Y, Shang Y, Zhen Q, Zhao Y, Zhang M and Zhang Y (2021) The Correlation Between SPP1 and Immune Escape of EGFR Mutant Lung Adenocarcinoma Was Explored by Bioinformatics Analysis. Front. Oncol. 11:592854. doi: 10.3389/fonc.2021.592854

Background: Immune checkpoint inhibitors have achieved breakthrough efficacy in treating lung adenocarcinoma (LUAD) with wild-type epidermal growth factor receptor (EGFR), leading to the revision of the treatment guidelines. However, most patients with EGFR mutation are resistant to immunotherapy. It is particularly important to study the differences in tumor microenvironment (TME) between patients with and without EGFR mutation. However, relevant research has not been reported. Our previous study showed that secreted phosphoprotein 1 (SPP1) promotes macrophage M2 polarization and PD-L1 expression in LUAD, which may influence response to immunotherapy. Here, we assessed the role of SPP1 in different populations and its effects on the TME.

Methods: We compared the expression of SPP1 in LUAD tumor and normal tissues, and in samples with wild-type and mutant EGFR. We also evaluated the influence of SPP1 on survival. The LUAD data sets were downloaded from TCGA and CPTAC databases. Clinicopathologic characteristics associated with overall survival in TCGA were assessed using Cox regression analysis. GSEA revealed that several fundamental signaling pathways were enriched in the high SPP1 expression group. We applied CIBERSORT and xCell to calculate the proportion and abundance of tumor-infiltrating immune cells (TICs) in LUAD, and compared the differences in patients with high or low SPP1 expression and wild-type or mutant EGFR. In addition, we explored the correlation between SPP1 and CD276 for different groups.

Results: SPP1 expression was higher in LUAD tumor tissues and in people with EGFR mutation. High SPP1 expression was associated with poor prognosis. Univariate and multivariate cox analysis revealed that up-regulated SPP1 expression was independent indicator of poor prognosis. GSEA showed that the SPP1 high expression group was mainly enriched in immunosuppressed pathways. In the SPP1 high expression group, the infiltration of CD8+ T cells was lower and M2-type macrophages was higher. These results were also observed in patients with EGFR mutation. Furthermore, we found that

the SPP1 expression was positively correlated with CD276, especially in patients with EGFR mutation.

Conclusion: SPP1 levels might be a useful marker of immunosuppression in patients with EGFR mutation, and could offer insight for therapeutics.

Keywords: immune checkpoint inhibitors, lung adenocarcinoma, epidermal growth factor receptor, tumor microenvironment, secreted phosphoprotein 1, tumor-infiltrating immune cells

INTRODUCTION

Lung cancer has become one of the most serious threats to human health, and its global morbidity and mortality rank first among all cancer types (1). Approximately 85% of lung cancers are non-small cell lung cancer (NSCLC), and lung adenocarcinoma (LUAD) accounts for 40%–50% of NSCLC. In China, 50%–60% of patients with LUAD also have epidermal growth factor receptor (EGFR) mutation. Epidermal growth factor receptor-tyrosine kinase inhibitor (EGFR-TKI) targeted therapy has been recommended for treating patients with EGFR sensitive mutations and such therapy has significantly improved survival in advanced NSCLC (2, 3). However, EGFR-TKI resistance has been observed in patients with NSCLC, which is challenging the prognosis of the disease (4).

Recently, immune checkpoint inhibitors (ICIs), represented by programmed cell death-1 (PD-1) and programmed cell death-ligand 1(PD-L1) monoclonal antibodies, have presented a new approach for NSCLC treatment (5, 6). ICIs achieve long-term disease control in patients who have developed an anti-tumor response, by activating the body's immune system for tumor cell recognition and removal (7). However, ICIs had poor efficacy and adverse effects in patients with EGFR mutation or secondary T790M mutation (8–10).

The IMpower 150 study found that a combination of atezolizumab, bevacizumab, and chemotherapy improved overall survival (OS) in patients with EGFR mutation (11). This study was the first randomized phase III trial of immunotherapy that showed a benefit in patients with EGFR mutation, suggesting that "primary drug resistance" could be reversed. *In-vitro* studies showed that the non-inflammatory tumor microenvironment (TME) changed in EGFR-mutated NSCLC after partial drug intervention, improving the efficacy of immunotherapy (12). Hence, there might be a connection between the EGFR-mutated NSCLC immune microenvironment and the mechanism of primary resistance to ICIs. Exploring the microenvironment characteristics may improve our knowledge of drug resistance mechanism and offer clues to reversing resistance.

Osteopontin (OPN, encoded by SPP1) is a secreted phosphorylated glycoprotein, which is produced by T, NK and other immune cells, myeloid cells, osteoblasts, bone cells, epithelial cells, etc. (13, 14). It is also a kind of multifunctional cytokine. Previously, we found that lung adenocarcinoma cells induced M2 polarization of macrophages through SPP1, and activation of T cells were observed after SPP1 silencing (15). However, the role of SPP1 mediated immunosuppression in patients with EGFR mutations remains unclear. What is more, the B7 family is important in regulating T cell immune response. PD-1 and B7-H3 (CD276) are both members of B7/CD28 family and had similar effects in TME (16). The up-regulated of CD276 expression can promote immune escaping of tumor cells, including inhibit the proliferation of T cells, reduce the secretion of IFN-γ, tumor necrosis factor-alpha (TNF-α), and other cytokines (16). As a co-inhibitory molecule of T cell, CD276 is an attractive target for cancer immunotherapy (17, 18).

In this study, we explored the TME of patients with EGFR mutation, which has been highlighted for its potential impact on the resistance of ICIs. We analyzed SPP1 expression in LUAD with or without EGFR mutation, and explored its association with clinicopathologic characteristics and patient outcomes. We further evaluated the differences in the tumor-infiltrating immune cells (TICs) in the immune microenvironment between groups with different levels of SPP1 expression, and those with or without EGFR mutation. In addition, the correlation between SPP1 and CD276 for different groups was compared. A study workflow is presented in **Figure 1**.

MATERIALS AND METHODS

Data Acquisition

LUAD patient datasets were downloaded from The Cancer Genome Atlas (TCGA, https://portal.gdc.cancer.gov/) (19, 20), including transcriptome RNA-seq gene expression profiles (Level 3), and clinical information. A total of 497 tumor tissues and 54 adjacent tissues were included. We compared SPP1 protein expression in 102 normal and 109 cancer tissues, using The Clinical Proteomic Tumor Analysis Consortium (CPTAC, https://proteomics.cancer.gov/programs/cptac) (21, 22). We collected the mutation information of TCGA cohort from UCSC Xena database (https://xenabrowser.net/datapages/) (23), in which there are 472 cases with mutation information available including 409 EGFR wild-type and 63 EGFR mutant cases. Additionally, survival of patients with LUAD was analyzed in relation to SPP1 expression in TCGA and CPTAC databases.

Cox Regression Analysis and GSEA

Univariate and multivariate cox regression analysis was performed in 435 patients (missing clinical information were excluded) to screen factors significantly associated with OS in TCGA. Gene Set Enrichment Analysis (GSEA) (http://software.broadinstitute.org/gsea/) was performed to determine the biological differences and pathways affected by differential

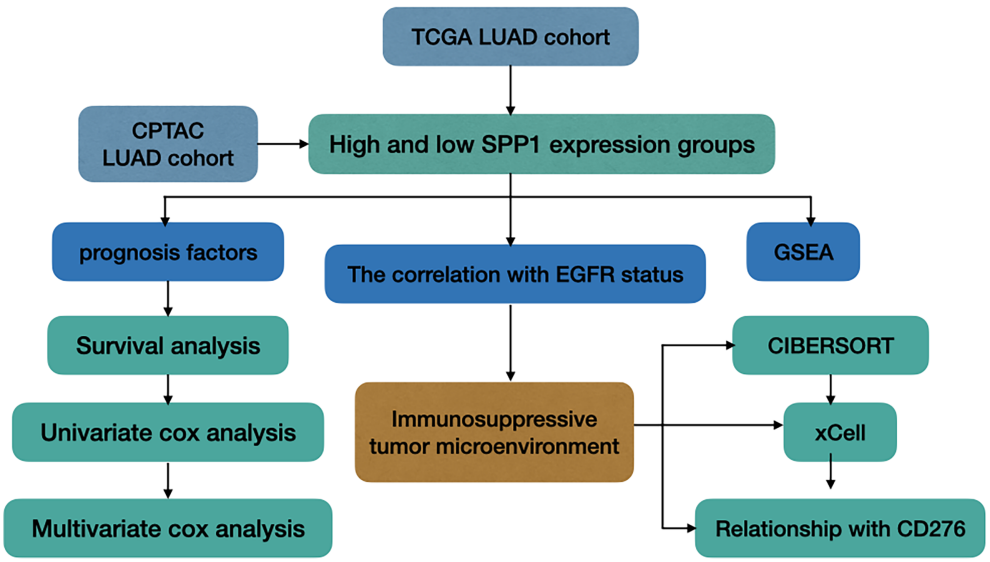

FIGURE 1 | Study workflow.

expression of SPP1 (one-fourth cutoff) in Gene Set c2(c2.cp.Kegg.v7.0.symbols) and c5(c5.all.v7.0.symbols). The number of random sample permutations was set at 1000. The significance threshold was $P < 0.05$ and false discovery rate (FDR) < 0.25.

Correlation With TICs and CD276

CIBERSORT(http://cibersort.stanford.edu/) is an immune cell infiltrating assessment analysis tool (24, 25). We assessed the influence of SPP1 expression and EGFR mutation to 22 types of immune cells by CIBERSORT. The filter criteria of each sample is set as the $P < 0.05$, which indicating that the inferred proportion of each TICs subtype are accurate and suitable for further analysis. We calculated the correlation between different immune cells, and marked those with $P < 0.05$. xCell is a gene signatures-based method, which performs cell type enrichment analysis from gene expression data for 64 immune and stroma cell types (26). To verify the results of CIBERSORT, we downloaded the results of immune cell abundance in TCGA LUAD by xCell algorithm from TIMER database (http://timer.cistrome.org/) (27). Besides, the correlation between SPP1 and CD276 for different groups was calculated using Spearman correlation coefficients.

Statistical Analysis

Statistical analysis of data from TCGA and CPTAC were performed using R-3.6.1. The independent samples t-test or Wilcoxon's rank sum-tests were used to compare continuous variables between two groups. Kruskal-Wallis one-way analysis of variance followed by a posthoc Kruskal-Dunn test with BH's method for adjusting for multiple comparisons. Prism8 software was used to plot the survival curves using the Kaplan-Meier method, and the log-rank test was used to compare the survival curves. Uni- and multi-variate analyses were performed using Cox proportional hazard models, where $P < 0.05$ was considered statistically significant. The correlation between SPP1 and CD276 was calculated using Spearman's correlation coefficient (R), with $P < 0.01$ was considered statistically significant.

RESULTS

SPP1 Expression and OS Differences

LUAD cohorts consisted of a total of 477 patients in TCGA and 109 patients in CPTAC. The clinical characteristics between low and high SPP1 expression groups were listed in **Table 1** and **Supplementary Table 1**. SPP1 expression was significantly higher in tumor tissues than in adjacent tissues, regardless of RNA or protein level (**Figures 2A, B**, $P < 0.001$). SPP1 expression was higher in EGFR-mutated tumor samples than in wild-type samples (**Figure 2C**, $P = 0.017$). The median level of SPP1 expression was used to dichotomize patients into high- or low-expression groups, and Kaplan-Meier survival analysis was performed separately for TCGA and CPTAC. Increased SPP1 expression was significantly correlated with poor OS, and the median OS of the TCGA cohort was 4.73 *vs.* 3.37 (**Figure 2D**; HR:1.48 95%CI 1.10-2.00; $P= 0.009$). Median OS was not achieved in CPTAC cohort, but differences were observed (**Figure 2E**; HR: 3.40 95%CI 1.15-10.08; $P = 0.047$). In addition, subgroup analysis of TCGA LUAD showed that patients with EGFR mutation in SPP1 high-expression group had a poor prognosis (**Supplementary Figure 1A**; HR: 1.62 95% CI 0.90-2.93; $P = 0.055$). There was no difference in survival between wild and mutant EGFR patients in SPP1 low-expression group (**Supplementary Figure 1B**; HR: 1.17 95%CI 0.56-2.44; $P = 0.662$).

TABLE 1 | The clinical characteristics of patients in TCGA.

	Total	SPP1 low expression	SPP1 high expression	P-value
Patients	477	238	239	–
Age				0.853
≤65	224 (49%)	111 (48%)	113 (50%)	
>65	234 (51%)	119 (52%)	115 (50%)	
Gender				0.967
female	260 (55%)	129 (54%)	131 (55%)	
male	217 (45%)	109 (46%)	108 (45%)	
Stage				0.291
stageI	257 (55%)	138 (59%)	119 (51%)	
stageII	109 (23%)	51 (22%)	58 (25%)	
stageIII	78 (17%)	33 (14%)	45 (19%)	
stageIV	25 (5%)	12 (5%)	13 (6%)	
T stage				0.38
T1	159 (34%)	86 (36%)	73 (31%)	
T2	255 (54%)	120 (51%)	135 (57%)	
T3+T4	60 (13%)	30 (13%)	30 (13%)	
N stage				0.005
N0	307 (66%)	169 (73%)	138 (59%)	
N1	87 (19%)	34 (15%)	53 (23%)	
N2+N3	71 (15%)	28 (12%)	43 (18%)	
M stage				0.349
M0	324 (68%)	155 (66%)	169 (71%)	
M1	24 (5%)	11 (5%)	13 (5%)	
Mx	125 (26%)	69 (29%)	56 (24%)	
EGFR				0.176
wild	409 (87%)	210 (89%)	199 (84%)	
mutation	63 (13%)	26 (11%)	37 (16%)	

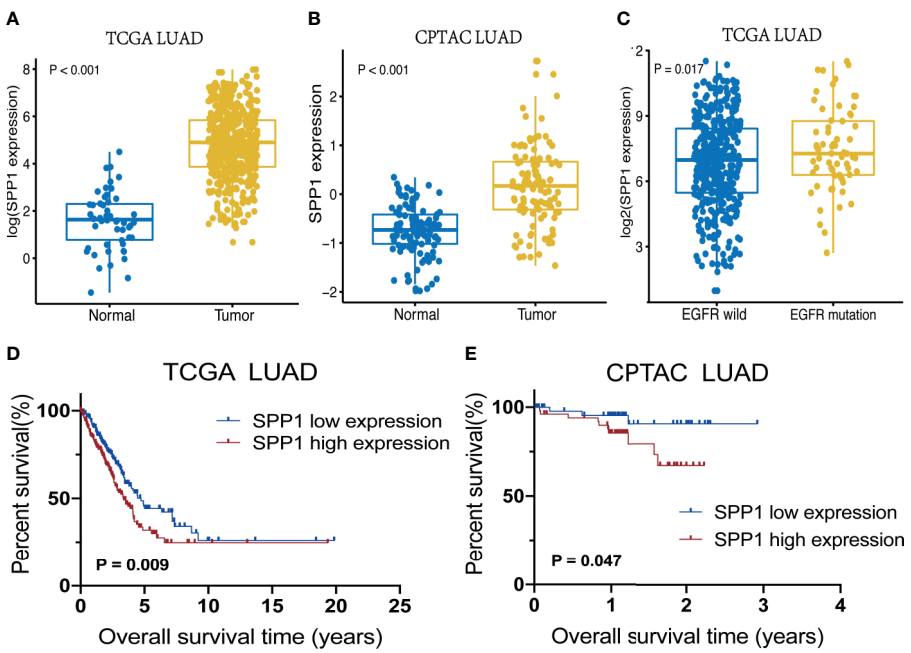

FIGURE 2 | SPP1 expression differences and survival outcomes in LUAD. **(A)** SPP1 RNA expression levels in Normal *vs*. Tumor samples. **(B)** Expression of SPP1 protein in Normal *vs*. Tumor samples. **(C)** SPP1 RNA expression in EGFR wild-type *vs*. EGFR mutant samples. **(D)** Kaplan–Meier survival curves for high and low SPP1 expression groups in TCGA. **(E)** Kaplan–Meier survival curves for high and low SPP1 expression groups in CPTAC.

Identification of Independent Prognostic Factors

A Cox proportional hazards model including differentiation age, gender, stage, T stage, N stage, EGFR status and SPP1 expression was used. The resulted of univariate and multivariate analysis revealed that different SPP1 expression in patients was significantly associated with OS. Moreover, early tumor stage, and T stage are also the independent factors of favorable prognosis (**Figures 3A, B**).

SPP1 Expression Mediates Immune Escape

To interrogate potential signaling pathways related to SPP1 gene in LUAD, we used GSEA analysis (**Figure 4**). We found that the high SPP1 expression group was significantly associated with extracellular matrix (ECM) receptor interaction (NES = 1.737, $P = 0.028$), Fc gamma r mediated phagocytosis (NES = 1.813, $P = 0.010$), glycolysis and gluconeogenesis (NES = 1.770, $P = 0.006$), and the Toll like receptor (TLR) signaling pathway (NES = 2.025, $P < 0.001$). Meanwhile, GO analysis showed that the high SPP1 expression group was positively associated with integrin-mediated cell adhesion (NES = 2.008, $P < 0.001$), interleukin 6 production (NES = 1.960, $P < 0.001$), Nik Nf-Kappa B (NF-κB) signaling (NES = 1.961, $P = 0.044$), and phagocytosis (NES = 2.043, $P < 0.001$).

Effect of SPP1 on TME

Previous analyses suggested that TICs could be markers of response to ICIs in several cancers (28). In this study, we examined how EGFR mutation and SPP1 expression are related to immune infiltration in LUAD. TCGA LUAD tumor samples (n = 477) were analyzed by CIBERSORT and 368 cases in the wild-type group and 63 cases in the mutant group met the CIBERSORT screening criteria. The results showed that EGFR mutations contribute to reducing the infiltration of CD4+ T cells, CD8+ T cells, M1 macrophages and other immune effector cells in the TME (**Figure 5A**). Taken together, these results indicate that EGFR mutations confer immunosuppressive effects. Additionally, 207 cases in the SPP1 low-expression group and 233 cases in the SPP1 high-expression group met the screening criteria. The results show that high SPP1 expression may play a role in regulating macrophage polarization to the M2 phenotype, reducing TICs such as CD8+ T cells, B cells, follicular helper T cells, NK cells, and activated dendritic cells (**Figure 5B**). These results support the contentions that SPP1 promotes host tumor immune tolerance and immune escape. The correlation heat map (**Figure 5C**) reveals that the different TIC subpopulations are weakly or moderately correlated. Subgroup analysis showed that the proportion of CD8+ T cells infiltration was the highest in patients with wild-type EGFR in SPP1 low-expression group, and the lowest in patients with EGFR mutation in SPP1 high-expression group (**Figure 5D**, P < 0.001). The infiltration of

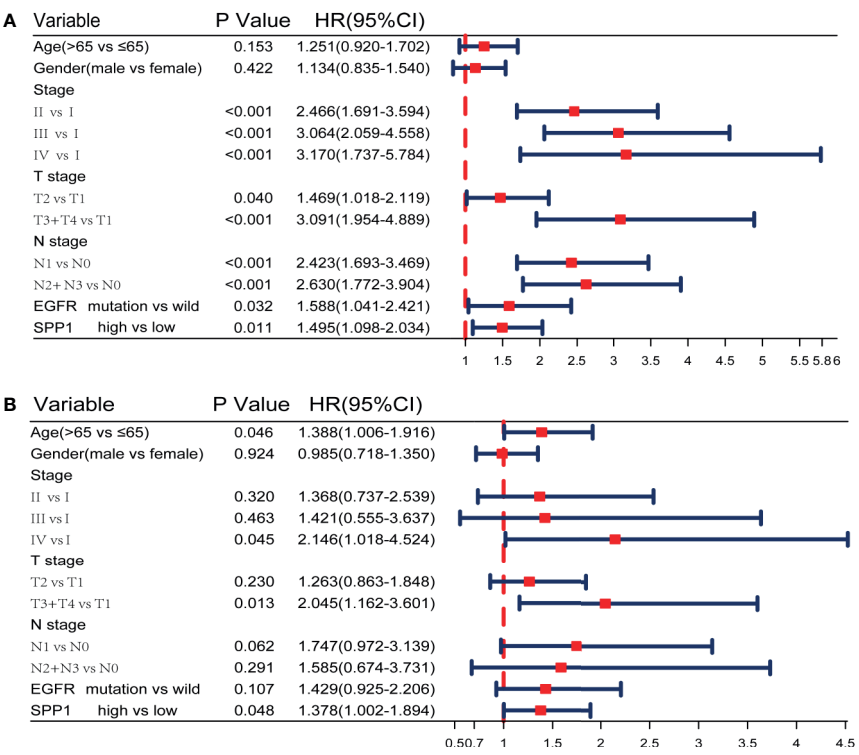

FIGURE 3 | SPP1 was an independent prognostic biomarker in TCGA. **(A, B)** Univariate and Multivariate Cox analysis of SPP1 expression and other clinicopathological factors.

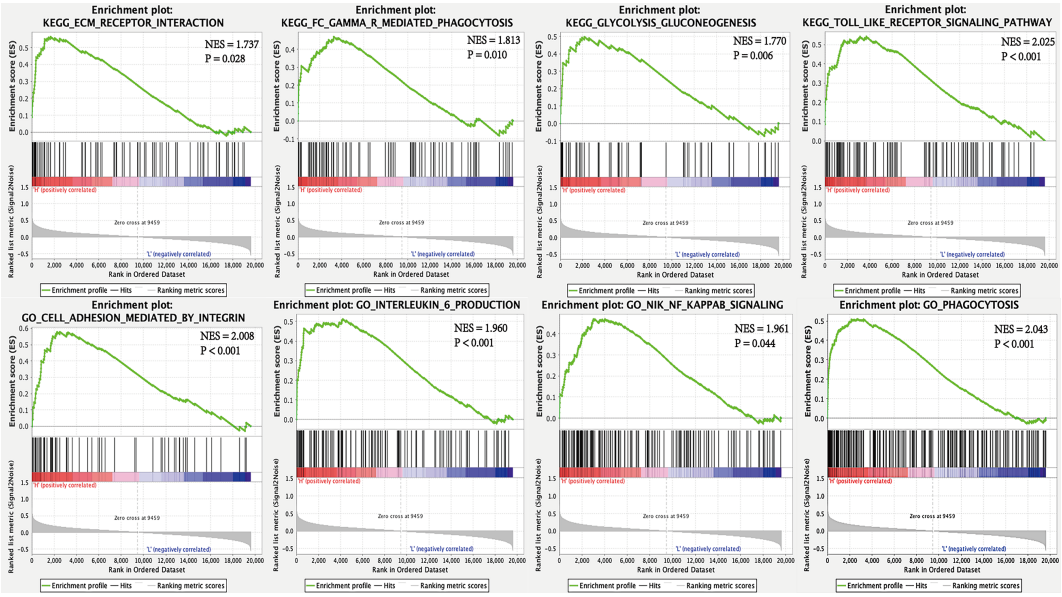

FIGURE 4 | GSEA for high and low SPP1 expression samples.

M2 macrophages was the most in patients with EGFR mutation in SPP1 high-expression group, and the least in patients with wild type EGFR in SPP1 low-expression group (**Figure 5E**, P = 0.071).

xCell results showed that the abundance of CD8+ T cells was less (P = 0.009) and M2 macrophages was more (P = 0.073) in patients with EGFR mutation (**Figure 6A**). There were more CD8+ T cells (P = 0.036) and less M2 macrophages (P = 0.018) in SPP1 low-expression group (**Figure 6B**). The abundance of CD8+ T cells was the highest in EGFR wild-type patients with SPP1 low-expression group (**Figure 6C**). M2-type macrophages in SPP1 high-expression group with EGFR mutation was higher than those of the group with SPP1 low-expression and EGFR wild type (**Figure 6D**, P = 0.073). And we compared CD8 and M2 between the group (SPP1 high and EGFR mutation) and the group (SPP1 low and EGFR wild) in supplement **Figure 2**. Moreover, we found that the SPP1 expression was positively correlated with CD276, especially in patients with EGFR mutation (**Figures 6E–G**).

DISCUSSION

Immunotherapy can eliminate tumor cells through the body's immune system and bring long-term survival benefits to patients with NSCLC, significantly ushering in a new era of antitumor therapy. EGFR mutation is a predictor of the therapeutic effects of EGFR-TKIs in patients with LUAD (2, 3). However, it was once considered as a marker of immune resistance (9, 29–31). Here, we recognized the characteristics of TICs in LUAD using bioinformatics analysis. The immune-tolerant TME is more likely to correlate with patients harboring EGFR mutation. Additionally, the observed outcomes indicate that SPP1 may be a potential indicator for patients nonresponsive to ICIs.

In this study, we showed that the SPP1 expression is significantly higher in LUAD tumor tissues and in patients with EGFR mutation. Several previous studies showed SPP1 expression is directly related to CD8+ T cell activation (32, 33), and M2 macrophage polarization (15). Consistently, we found that SPP1 expression was negatively correlated with CD8+ T cell numbers and positively correlated with M2 macrophage numbers. By applying two methods for immunocyte enrichment or proportion analysis, we can find that M2 macrophages enriched more (CD8+ T cells enriched less) in SPP1 high group or EGFR mutation group, and the phenomenon seems more obvious in the group with both SPP1 high and EGFR mutation, which indicated that tumors with both SPP1 high and EGFR mutation tend to show immune evasion phenotype. Therefore, we speculate that SPP1 might cause immune resistance in NSCLC with EGFR mutation.

OPN involved in many physiological and pathological processes, including inflammatory, angiogenesis, tumor metastasis, immune suppression in TME (34, 35). GSEA analysis results indicate the involvement of extracellular matrix (ECM) receptor interaction, Fc gamma r mediated phagocytosis, TLR signaling pathway, integrin- mediated cell adhesion, interleukin 6 production, NF-κB signaling, and phagocytosis in the high SPP1 expression group. OPN is an important component of ECM, regulating matrix interactions and cell adhesion (13). It plays a key role in tumor cell migration by interacting with integrins and CD44 (36). The interaction between OPN and CD44 transmembrane glycoprotein

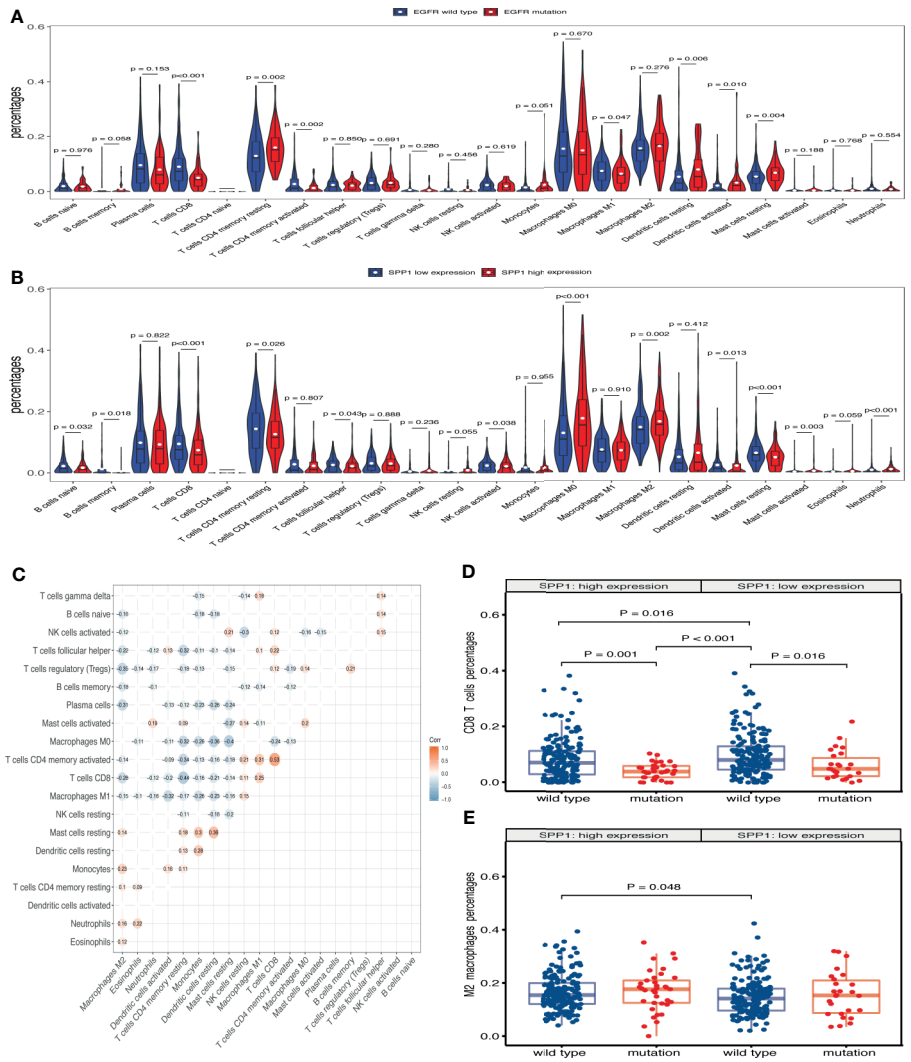

FIGURE 5 | SPP1-related immune infiltration alteration. **(A)** Violin plot showing the ratio differentiation of 22 kinds of TICs in EGFR wild-type and mutant samples. Wilcoxon rank sum was used for the significance test. **(B)** Violin plot showing the ratio differentiation of 22 kinds of TICs in low and high SPP1 expression groups. **(C)** The correlation between different TICs subpopulations. **(D)** Differences in CD8+ T cells infiltration between EGFR mutation and wild-type patients with SPP1 high- or low-expression group. **(E)** Differences in M2 macrophages infiltration between EGFR mutation and wild-type patients with SPP1 high- or low-expression group.

suppressed the CD8+ T cell activation and IFN-γ production. OPN regulation by TLR and NF-κB signaling can reshape the immune inflammatory environment (37, 38). IL-6 binds to IL-6R and activates the Janus kinase (JAK)-STAT3 pathway and the JAK-SHP-2-mitogen-activated protein (MAP) kinase pathway *via* gp130 (39). Previously, it was shown that activation of the JAK/STAT3 pathway can suppress the immune response (40) and that this pathway is activated in patients with EGFR mutation (41). However, it is not clear whether anti-OPN agents, combined with ICIs, can reverse primary resistance in EGFR mutated NSCLC. Therefore, increased SPP1 expression is consistent with a role in immunosuppression, indicating a possible mechanism through which ICIs is ineffective in EGFR-mutated NSCLC.

Pre-clinical studies, involving co-culture of tumor cells and peripheral blood mononuclear cells, show that combined EGFR-TKI and anti-PD-1 antibody therapies do not produce synergistic tumor cell killing effects (42). Multiple clinical studies of EGFR-TKIs combined with ICIs were terminated due to poor efficacy or severe toxicity (43). As a target antibody of vascular endothelial growth factor (VEGF), bevacizumab not only has the effect of anti-angiogenesis, but promotes T cell activation and invasion in tumor tissues (44). Combined with other immunoregulatory drugs, ICIs could be more efficient for the treatment of EGFR-TKI resistance in patients with EGFR mutation. OPN act as an important chemokine and contributes to immune suppression in human colon cancer and other cancers (14, 30). CIBERSORT analysis indicated a significant relationship between SPP1 expression and

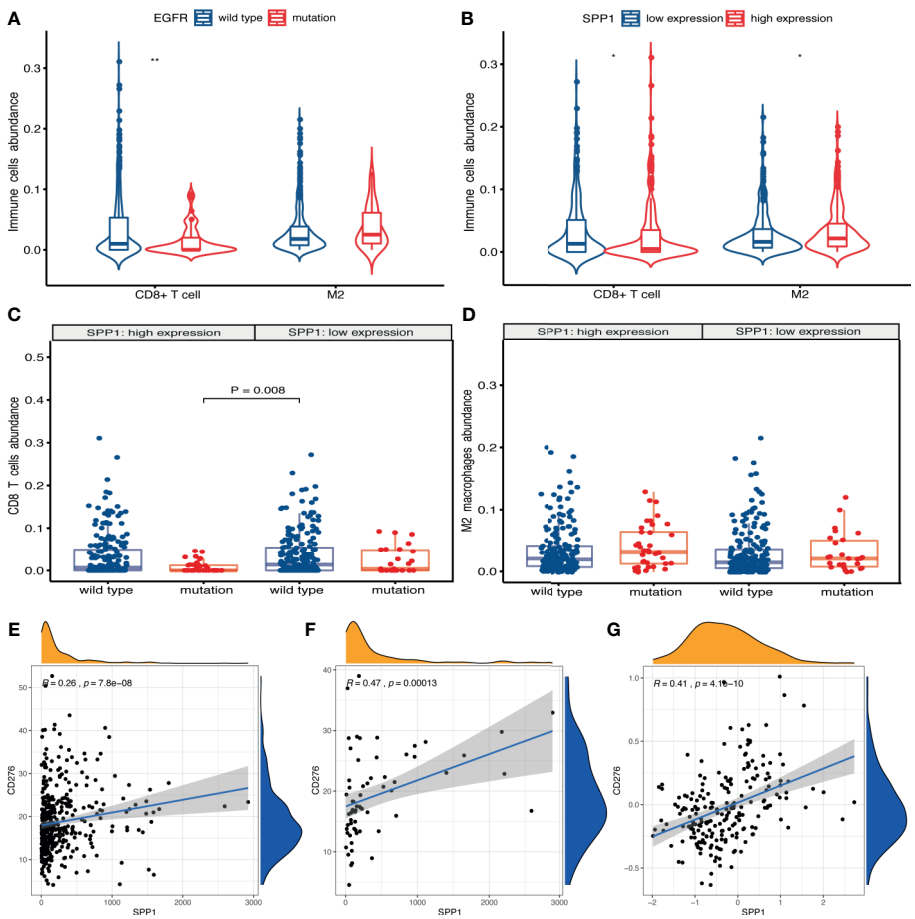

FIGURE 6 | SPP1 promotes immunosuppressive microenvironment in patients with EGFR mutation. **(A)** xCell calculated the abundance of CD8+ T cells and M2 macrophages in EGFR wild-type and mutant samples. **(B)** The abundance of CD8+ T cells and M2 macrophages in different SPP1 expression groups were evaluated by xCell. **(C)** Differences in CD8+ T cells abundance between EGFR mutation and wild-type patients with SPP1 high- or low-expression group. **(D)** Differences in M2 macrophages abundance between EGFR mutation and wild-type patients with SPP1 high- or low-expression group. **(E)** The expression of SPP1 was correlated with CD276 in EGFR wild-type patients at mRNA level. **(F)** The expression of SPP1 was correlated with CD276 in EGFR mutation patients at mRNA level. **(G)** The expression of SPP1 was correlated with CD276 at the protein level. *P < 0.05, **P < 0.01.

increased levels of M2 macrophages infiltration, and reduced CD8 + T cell, activated NK cell and activated dendritic cell infiltration. Furthermore, the similarities between CD276 and other immune checkpoints (PD-1/PD-L1, CTLA4) have led to the targeting of CD276 in novel immunotherapy strategy (16, 17). We propose that a combination regimen using anti-OPN and ICIs may be a promising treatment option for LUAD with EGFR mutation, especially with high expression of SPP1. However, further studies should be conducted.

In summary, differences in TICs in patients with EGFR mutation and those with wild-type LUAD may affect the efficacy of ICIs. We observed that LUAD with EGFR mutated have less infiltration of anti-tumor immune cells, including CD8+ T cells, activated CD4+ T cells and M1 macrophages, and increased M2 macrophages infiltration. However, SPP1 likely has an essential influence on TICs, though combined with anti-OPN therapy, has the potential to reverse immune resistance in LUAD with EGFR mutation.

DATA AVAILABILITY STATEMENT

Publicly available datasets were analyzed in this study. This data can be found here: https://portal.gdc.cancer.gov/, https://proteomics.cancer.gov/programs/cptac.

AUTHOR CONTRIBUTIONS

YaZ and SH found the clinical problem and proposed the research direction. YiZ made use of the public databases for bioinformatics analysis. CX and YH searched literatures and analyzed data results. YS and QZ contributed to the original writing of the manuscript and data consolidation. YYZ and MZ undertook the task of modifying the manuscript. All authors contributed to the article and approved the submitted version.

FUNDING

This work was supported by grants from the Natural Science Foundation of Hebei Province, China (H2019106033).

SUPPLEMENTARY MATERIAL

The Supplementary Material for this article can be found online at: https://www.frontiersin.org/articles/10.3389/fonc.2021.592854/full#supplementary-material

Supplementary Figure 1 | Effects of EGFR mutation and wild-type on prognosis of LUAD in different SPP1 expression groups in TCGA database. **(A)** Prognosis comparison of EGFR wild-type and mutant patients in SPP1 high expression group. **(B)** Prognosis comparison of EGFR wild-type and mutant patients in SPP1 low expression group.

Supplementary Figure 2 | CD8+ T cells and M2 macrophage differed between groups with high SPP1 expression and EGFR mutation and those with low SPP1 expression and wild-type EGFR. **(A)** Differences in CD8+ T cells infiltration calculated by CIBERSORT between SPP1 high-expression with EGFR mutation and SPP1 low-expression with EGFR wild type. **(B)** Differences in M2 macrophages infiltration calculated by CIBERSORT between SPP1 high-expression with EGFR mutation and SPP1 low-expression with EGFR wild type. **(C)** The difference in CD8+ T cells abundance assessed by xCell was compared between the group of SPP1 high-expression with EGFR mutation and SPP1 low-expression with EGFR wild type samples. **(D)** The difference in M2 macrophage abundance assessed by xCell was compared between the group of SPP1 high-expression with EGFR mutation and SPP1 low-expression with EGFR wild type samples.

REFERENCES

1. Bray F, Ferlay J, Soerjomataram I, Siegel RL, Torre LA, Jemal A. Global Cancer Statistics 2018: GLOBOCAN Estimates of Incidence and Mortality Worldwide for 36 Cancers in 185 Countries. *CA Cancer J Clin* (2018) 68:394–424. doi: 10.3322/caac.21492
2. Han JY, Park K, Kim SW, Lee DH, Kim HY, Kim HT, et al. First-SIGNAL: First-Line Single-Agent Iressa Versus Gemcitabine and Cisplatin Trial in Never-Smokers With Adenocarcinoma of the Lung. *J Clin Oncol* (2012) 30:1122–8. doi: 10.1200/JCO.2011.36.8456
3. Shi YK, Wang L, Han BH, Li W, Yu P, Liu YP, et al. First-Line Icotinib Versus Cisplatin/Pemetrexed Plus Pemetrexed Maintenance Therapy for Patients With Advanced EGFR Mutation-Positive Lung Adenocarcinoma (CONVINCE): A Phase 3, Open-Label, Randomized Study. *Ann Oncol* (2017) 28:2443–50. doi: 10.1093/annonc/mdx359
4. Lu X, Yu L, Zhang Z, Ren X, Smaill JB, Ding K. Targeting EGFR(L858R/T790M) and EGFR(L858R/T790M/C797S) Resistance Mutations in NSCLC: Current Developments in Medicinal Chemistry. *Med Res Rev* (2018) 38:1550–81. doi: 10.1002/med.21488
5. Reck M, Rodriguez-Abreu D, Robinson AG, Hui R, Csoszi T, Fulop A, et al. Pembrolizumab Versus Chemotherapy for PD-L1-Positive Non-Small-Cell Lung Cancer. *N Engl J Med* (2016) 375:1823–33. doi: 10.1056/NEJMoa1606774
6. Tomasini P, Greillier L, Boyer A, Jeanson A, Barlesi F. Durvalumab After Chemoradiotherapy in Stage III Non-Small Cell Lung Cancer. *J Thorac Dis* (2018) 10:S1032–S36. doi: 10.21037/jtd.2018.04.61
7. Ribas A, Wolchok JD. Cancer Immunotherapy Using Checkpoint Blockade. *Science* (2018) 359:1350–55. doi: 10.1126/science.aar4060
8. Garassino MC, Cho BC, Kim JH, Mazieres J, Vansteenkiste J, Lena H, et al. Durvalumab as Third-Line or Later Treatment for Advanced non-Small-Cell Lung Cancer (ATLANTIC): An Open-Label, Single-Arm, Phase 2 Study. *Lancet Oncol* (2018) 19:521–36. doi: 10.1016/S1470-2045(18)30144-X
9. Gainor JF, Shaw AT, Sequist LV, Fu X, Azzoli CG, Piotrowska Z, et al. Egfr Mutations and ALK Rearrangements Are Associated With Low Response Rates to PD-1 Pathway Blockade in Non-Small Cell Lung Cancer: A Retrospective Analysis. *Clin Cancer Res* (2016) 22:4585–93. doi: 10.1158/1078-0432.CCR-15-3101
10. Haratani K, Hayashi H, Tanaka T, Kaneda H, Togashi Y, Sakai K, et al. Tumor Immune Microenvironment and Nivolumab Efficacy in EGFR Mutation-Positive Non-Small-Cell Lung Cancer Based on T790M Status After Disease Progression During EGFR-TKI Treatment. *Ann Oncol* (2017) 28:1532–39. doi: 10.1093/annonc/mdx183
11. Socinski MA, Jotte RM, Cappuzzo F, Orlandi F, Stroyakovskiy D, Nogami N, et al. Atezolizumab for First-Line Treatment of Metastatic Nonsquamous Nsclc. *N Engl J Med* (2018) 378:2288–301. doi: 10.1056/NEJMoa1716948
12. Sugiyama E, Togashi Y, Takeuchi Y, Shinya S, Tada Y, Kataoka K, et al. Blockade of EGFR Improves Responsiveness to PD-1 Blockade in EGFR-mutated Non-Small Cell Lung Cancer. *Sci Immunol* (2020) 5:eaav3937. doi: 10.1126/sciimmunol.aav3937
13. Lamort AS, Giopanou I, Psallidas I, Stathopoulos GT. Osteopontin as a Link Between Inflammation and Cancer: The Thorax in the Spotlight. *Cells* (2019) 8:815. doi: 10.3390/cells8080815
14. Anborgh PH, Mutrie JC, Tuck AB, Chambers AF. Role of the Metastasis-Promoting Protein Osteopontin in the Tumour Microenvironment. *J Cell Mol Med* (2010) 14:2037–44. doi: 10.1111/j.1582-4934.2010.01115.x
15. Zhang Y, Du W, Chen Z, Xiang C. Upregulation of PD-L1 by SPP1 Mediates Macrophage Polarization and Facilitates Immune Escape in Lung Adenocarcinoma. *Exp Cell Res* (2017) 359:449–57. doi: 10.1016/j.yexcr.2017.08.028
16. Castellanos JR, Purvis IJ, Labak CM, Guda MR, Tsung AJ, Velpula KK, et al. B7-H3 Role in the Immune Landscape of Cancer. *Am J Clin Exp Immunol* (2017) 6:66–75.
17. Picarda E, Ohaegbulam KC, Zang X. Molecular Pathways: Targeting B7-H3 (CD276) for Human Cancer Immunotherapy. *Clin Cancer Res* (2016) 22:3425–31. doi: 10.1158/1078-0432.CCR-15-2428
18. Kontos F, Michelakos T, Kurokawa T, Sadagopan A, Schwab JH, Ferrone CR, et al. B7-H3: An Attractive Target for Antibody-Based Immunotherapy. *Clin Cancer Res* (2021) 27:1227–35. doi: 10.1158/1078-0432.CCR-20-2584
19. Tomczak K, Czerwinska P, Wiznerowicz M. The Cancer Genome Atlas (TCGA): An Immeasurable Source of Knowledge. *Contemp Oncol (Pozn)* (2015) 19:A68–77. doi: 10.5114/wo.2014.47136
20. Liu J, Lichtenberg T, Hoadley KA, Poisson LM, Lazar AJ, Cherniack AD, et al. An Integrated Tcga Pan-Cancer Clinical Data Resource to Drive High-Quality Survival Outcome Analytics. *Cell* (2018) 173:400–16.e11. doi: 10.1016/j.cell.2018.02.052
21. Rudnick PA, Markey SP, Roth J, Mirokhin Y, Yan X, Tchekhovskoi DV, et al. A Description of the Clinical Proteomic Tumor Analysis Consortium (CPTAC) Common Data Analysis Pipeline. *J Proteome Res* (2016) 15:1023–32. doi: 10.1021/acs.jproteome.5b01091
22. Whiteaker JR, Halusa GN, Hoofnagle AN, Sharma V, MacLean B, Yan P, et al. Cptac Assay Portal: A Repository of Targeted Proteomic Assays. *Nat Methods* (2014) 11:703–4. doi: 10.1038/nmeth.3002
23. Goldman M, Craft B, Swatloski T, Cline M, Morozova O, Diekhans M, et al. The UCSC Cancer Genomics Browser: Update 2015. *Nucleic Acids Res* (2015) 43:D812–7. doi: 10.1093/nar/gku1073
24. Petitprez F, Vano YA, Becht E, Giraldo NA, de Reynies A, Sautes-Fridman C, et al. Transcriptomic Analysis of the Tumor Microenvironment to Guide Prognosis and Immunotherapies. *Cancer Immunol Immunother* (2018) 67:981–88. doi: 10.1007/s00262-017-2058-z
25. Chen B, Khodadoust MS, Liu CL, Newman AM, Alizadeh AA. Profiling Tumor Infiltrating Immune Cells With CIBERSORT. *Methods Mol Biol* (2018) 1711:243–59. doi: 10.1007/978-1-4939-7493-1_12
26. Aran D, Hu Z, Butte AJ. xCell: Digitally Portraying the Tissue Cellular Heterogeneity Landscape. *Genome Biol* (2017) 18:220. doi: 10.1186/s13059-017-1349-1
27. Li T, Fan J, Wang B, Traugh N, Chen Q, Liu JS, et al. Timer: A Web Server for Comprehensive Analysis of Tumor-Infiltrating Immune Cells. *Cancer Res* (2017) 77:e108–e10. doi: 10.1158/0008-5472.CAN-17-0307

28. Klauschen F, Muller KR, Binder A, Bockmayr M, Hagele M, Seegerer P, et al. Scoring of Tumor-Infiltrating Lymphocytes: From Visual Estimation to Machine Learning. *Semin Cancer Biol* (2018) 52:151–57. doi: 10.1016/j.semcancer.2018.07.001
29. Dong ZY, Zhang JT, Liu SY, Su J, Zhang C, Xie Z, et al. EGFR Mutation Correlates With Uninflamed Phenotype and Weak Immunogenicity, Causing Impaired Response to PD-1 Blockade in Non-Small Cell Lung Cancer. *Oncoimmunology* (2017) 6:e1356145. doi: 10.1080/2162402X.2017.1356145
30. Li HY, McSharry M, Bullock B, Nguyen TT, Kwak J, Poczobutt JM, et al. The Tumor Microenvironment Regulates Sensitivity of Murine Lung Tumors to PD-1/PD-L1 Antibody Blockade. *Cancer Immunol Res* (2017) 5:767–77. doi: 10.1158/2326-6066.CIR-16-0365
31. Jia Y, Li X, Jiang T, Zhao S, Zhao C, Zhang L, et al. EGFR-Targeted Therapy Alters the Tumor Microenvironment in EGFR-Driven Lung Tumors: Implications for Combination Therapies. *Int J Cancer* (2019) 145:1432–44. doi: 10.1002/ijc.32191
32. Klement JD, Paschall AV, Redd PS, Ibrahim ML, Lu C, Yang D, et al. An Osteopontin/CD44 Immune Checkpoint Controls CD8+ T Cell Activation and Tumor Immune Evasion. *J Clin Invest* (2018) 128:5549–60. doi: 10.1172/JCI123360
33. Wei J, Marisetty A, Schrand B, Gabrusiewicz K, Hashimoto Y, Ott M, et al. Osteopontin Mediates Glioblastoma-Associated Macrophage Infiltration and is a Potential Therapeutic Target. *J Clin Invest* (2019) 129:137–49. doi: 10.1172/JCI121266
34. Denhardt DT, Noda M, O'Regan AW, Pavlin D, Berman JS. Osteopontin as a Means to Cope With Environmental Insults: Regulation of Inflammation, Tissue Remodeling, and Cell Survival. *J Clin Invest* (2001) 107(9):1055–61. doi: 10.1172/JCI12980
35. Pang X, Gong K, Zhang X, Wu S, Cui Y, Qian BZ. Osteopontin as a Multifaceted Driver of Bone Metastasis and Drug Resistance. *Pharmacol Res* (2019) 144:235–44. doi: 10.1016/j.phrs.2019.04.030
36. Maeda N, Maenaka K. The Roles of Matricellular Proteins in Oncogenic Virus-Induced Cancers and Their Potential Utilities as Therapeutic Targets. *Int J Mol Sci* (2017) 18:2198. doi: 10.3390/ijms18102198
37. Salvi V, Scutera S, Rossi S, Zucca M, Alessandria M, Greco D, et al. Dual Regulation of Osteopontin Production by TLR Stimulation in Dendritic Cells. *J Leukoc Biol* (2013) 94:147–58. doi: 10.1189/jlb.0412194
38. Friedmann-Morvinski D, Narasimamurthy R, Xia Y, Myskiw C, Soda Y, Verma IM. Targeting NF-kappaB in Glioblastoma: A Therapeutic Approach. *Sci Adv* (2016) 2:e1501292. doi: 10.1126/sciadv.1501292
39. Tanaka T, Narazaki M, Kishimoto T. IL-6 in Inflammation, Immunity, and Disease. *Cold Spring Harb Perspect Biol* (2014) 6:a016295. doi: 10.1101/cshperspect.a016295
40. Yu H, Pardoll D, Jove R. Stats in Cancer Inflammation and Immunity: A Leading Role for STAT3. *Nat Rev Cancer* (2009) 9:798–809. doi: 10.1038/nrc2734
41. Gao SP, Mark KG, Leslie K, Pao W, Motoi N, Gerald WL, et al. Mutations in the EGFR Kinase Domain Mediate STAT3 Activation Via IL-6 Production in Human Lung Adenocarcinomas. *J Clin Invest* (2007) 117:3846–56. doi: 10.1172/JCI31871
42. Chen N, Fang W, Zhan J, Hong S, Tang Y, Kang S, et al. Upregulation of PD-L1 by EGFR Activation Mediates the Immune Escape in EGFR-Driven NSCLC: Implication for Optional Immune Targeted Therapy for NSCLC Patients With EGFR Mutation. *J Thorac Oncol* (2015) 10:910–23. doi: 10.1097/JTO.0000000000000500
43. Ahn MJ, Sun JM, Lee SH, Ahn JS, Park K. Egfr TKI Combination With Immunotherapy in Non-Small Cell Lung Cancer. *Expert Opin Drug Saf* (2017) 16:465–69. doi: 10.1080/14740338.2017.1300656
44. Voron T, Marcheteau E, Pernot S, Colussi O, Tartour E, Taieb J, et al. Control of the Immune Response by Pro-Angiogenic Factors. *Front Oncol* (2014) 4:70. doi: 10.3389/fonc.2014.00070

Conflict of Interest: The authors declare that the research was conducted in the absence of any commercial or financial relationships that could be construed as a potential conflict of interest.

frontiers in Immunology

ORIGINAL RESEARCH
published: 23 June 2021
doi: 10.3389/fimmu.2021.606027

A 5-Genomic Mutation Signature Can Predict the Survival for Patients With NSCLC Receiving Atezolizumab

Jiamao Lin[1†], Xiaohui Wang[2†], Chenyue Zhang[3†], Shuai Bu[4], Chenglong Zhao[5] and Haiyong Wang[1]*

[1] Department of Internal Medicine Oncology, Shandong Cancer Hospital and Institute, Shandong First Medical University and Shandong Academy of Medical Sciences, Jinan, China, [2] Research Service Office, Shandong Liaocheng People's Hospital, Liaocheng, China, [3] Department of Integrated Oncology, Fudan University Shanghai Cancer Center, Shanghai, China, [4] Research Department, The Second Affiliated Hospital of Shandong University of Traditional Chinese Medicine, Jinan, China, [5] Department of Pathology, Shandong Cancer Hospital and Institute, Shandong First Medical University and Shandong Academy of Medical Sciences, Jinan, China

OPEN ACCESS

Edited by:
Meijuan Huang,
Sichuan University, China

Reviewed by:
Ashley Mark Hopkins,
Flinders University, Australia
Jian Song,
University Hospital Münster, Germany

***Correspondence:**
Haiyong Wang
wanghaiyong6688@126.com

[†]These authors have contributed equally to this work and share first authorship

Specialty section:
This article was submitted to Cancer Immunity and Immunotherapy, a section of the journal Frontiers in Immunology

Received: 14 September 2020
Accepted: 31 May 2021
Published: 23 June 2021

Citation:
Lin J, Wang X, Zhang C, Bu S, Zhao C and Wang H (2021) A 5-Genomic Mutation Signature Can Predict the Survival for Patients With NSCLC Receiving Atezolizumab. Front. Immunol. 12:606027. doi: 10.3389/fimmu.2021.606027

Background: At present, there is a lack of studies focusing on the survival prediction of patients with non-small cell lung cancer (NSCLC) receiving atezolizumab in light of gene mutation characteristic.

Methods: Patients with NSCLC receiving atezolizumab from the OAK study were defined as the training group. LASSO Cox regressions were applied to establish the gene mutation signature model to predict the overall survival (OS) rate of the training group. NSCLC patients receiving atezolizumab from the POPLAR study were defined as the testing group to validate the gene mutation signature model. In addition, we compared the OS rate between patients receiving atezolizumab and docetaxel classified according to their risk score based on our gene mutation signature model.

Results: We successfully established a 5-genomic mutation signature that included *CREBBP*, *KEAP1*, *RAF1*, *STK11* and *TP53* mutations. We found it was superior to the blood tumor mutation burden (bTMB) score and programmed death ligand 1 (PDL1) expression in the prediction of the OS rate for patients receiving atezolizumab. High-risk patients receiving atezolizumab had a worse OS rate compared with low-risk patients in the training (P = 0.0004) and testing (P = 0.0001) groups. In addition, low-risk patients using atezolizumab had a better OS rate compared with those in use of docetaxel for the training (P <0.0001) and testing groups (P = 0.0095). High-risk patients of the training group (P = 0.0265) using atezolizumab had a better OS rate compared with those using docetaxel. However, the OS difference between atezolizumab and docetaxel was not found in high-risk patients from the testing group (P = 0.6403). Multivariate Cox regression analysis showed that the risk model in light of 5-genomic mutation signature was an independent prognostic factor on OS for patients receiving atezolizumab (P <0.0001). In addition, significant OS benefit could only be found in low-risk patients receiving atezolizumab compared with docetaxel (P <0.0001).

Conclusions: The 5-genomic mutation signature could predict OS benefit for patients with NSCLC receiving atezolizumab. Therefore, the establishment of the 5-genomic

mutation panel will guide clinicians to identify optimal patients who could benefit from atezolizumab treatment.

Keywords: atezolizumab, gene mutation, non-small cell lung cancer, survival, PD-L1 inhibitor

INTRODUCTION

Atezolizumab, an immune checkpoint inhibitor, is an immunoglobulin G1 monoclonal antibody that binds to programmed death ligand 1 (PD-L1) and blocks its interactions with programmed death 1 and B7.1 receptor (1). At present, atezolizumab plays an important role in the treatment of non-small cell lung cancer (NSCLC) patients, gradually shifting from the second to the first line of treatment. Importantly, the tumor mutational burden (TMB) score and PDL1 expression have become key markers of the clinical benefits of patients receiving atezolizumab. Indeed, TMB in blood (bTMB) was identified as a biomarker for patients that improve upon atezolizumab treatment (2). The POPLAR study also found that improvements in the survival rates were associated with PDL1 expression on tumor cells and tumor-infiltrating immune cells, suggesting that PDL1 expression is can predict benefits derived from atezolizumab treatment (3). However, it is worth noting that the benefits of atezolizumab are comparable with those of chemotherapy based on these markers. In fact, increased overall survival (OS) rates were not obtained for patients receiving atezolizumab with a high bTMB score compared with those with low bTMB score from both the OAK and POPLAR studies (2, 4). A recent study even showed that advanced NSCLC patients with low TMB might have better OS than those with medium TMB (5). Therefore, it is very important to identify markers for the prediction of patients with NSCLC that could benefit from atezolizumab treatment.

Several studies have focused on the relationship between specific gene mutations and the effect of immunotherapy. A series of gene mutations such as *STK11*, *KEAP1*, *POLD1/POLE*, and *TERT* were found to influence the outcomes of patients receiving immunotherapy (6–10). Thus, we speculated that the establishment of a specific gene mutation signature could distinguish survival differences for patients receiving atezolizumab. In our study, we first established the gene mutation signature model able to predict OS rate based on the OAK study. Then, the gene mutation signature model was validated using data from the POPLAR study. Our study would be beneficial to guide the treatment of NSCLC patients receiving atezolizumab. It would also render the treatment strategy more individual-oriented.

METHODS

Patient Data

The data of our study was obtained from a previous study (2). Our study was based on POPLAR and OAK studies, the two independent clinical trials. The POPLAR study is a multicentre, open-label, phase 2 randomized controlled trial to compare atezolizumab with docetaxel for patients with previously treated NSCLC (3). The OAK study is the first randomized phase 3 study reporting results of atezolizumab treatment, which resulted in a clinically relevant improvement of OS versus docetaxel in previously treated NSCLC (11). These relevant studies and data have been published, thus informed consent and ethical committee approval were not warranted.

Study Design

This study was divided into the training group and the testing group as shown in **Figure 1**. Patients with synonymous mutations, which are that sometimes a mutation of a base pair in a DNA fragment does not change the encoded amino acid, were excluded. The synonymous mutations have been defined in published data (2). A total of 321 patients receiving atezolizumab were included from the training group (OAK study) and 105 patients were included from the testing group (POPLAR study). LASSO Cox regression model was used to predict prognosis-related markers from the training group. Then leave one out cross validation was applied to select five optimal gene mutation types to construct a risk sore evaluation model. The risk score was calculated according to the formula: $\Sigma_i\ \omega_i\ \chi_i$ where ω_i is the coefficient and χ_i is the expression value of each respective gene. The optimal cutoff to distinct high- and low-risk was estimated through time-dependent ROC curves. OS was regarded as the main endpoint of our study.

Statistical Analysis

The Kaplan–Meier curve was constructed to compare the OS difference, and the log-rank was used to perform the statistical analysis. Multivariate Cox regression analysis was applied to develop the subgroup analysis based on clinical variables. The construction of the risk score model was based on R 3.4.2. The figures were drawn using GraphPad Prism version 6.0. All *P*-values were two-tailed, and $P < 0.05$ was considered statistically significant.

RESULTS

Construction of a Genetic Mutation Signature to Predict the Survival of Patients Receiving Atezolizumab

A total of 321 NSCLC patients receiving atezolizumab from the OAK study were included in the analysis to establish the gene mutation signature. To achieve better stability and accuracy, we constructed the trend diagram of the lasso coefficient, and found a 5-genomic mutation signature obtained from 10 cross validations that could predict survival (**Figures 2A, B**). In addition, the time-dependent receiver operating characteristic (ROC) curve was

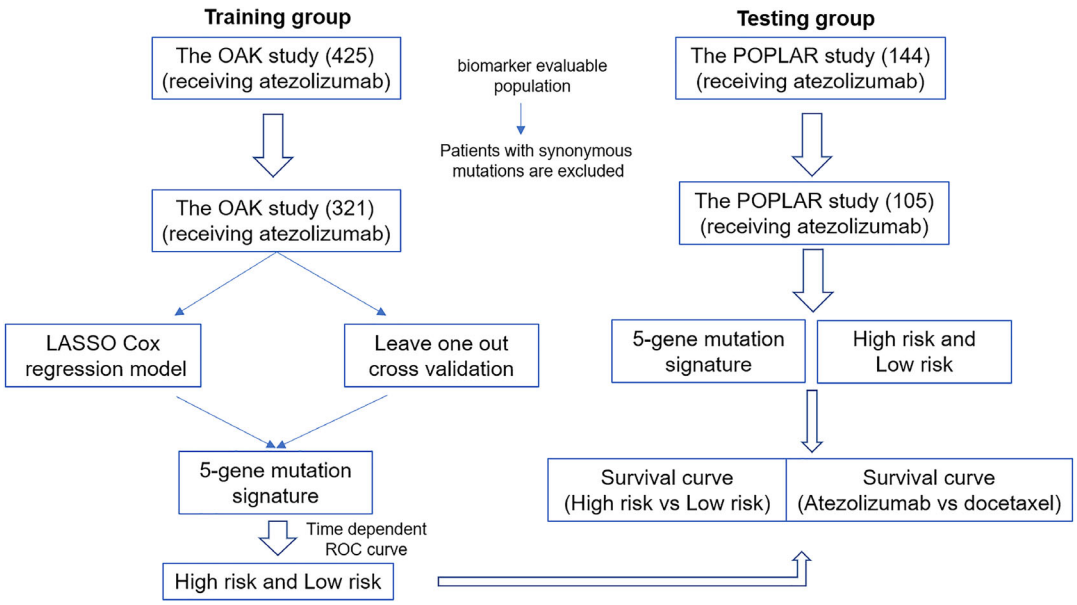

FIGURE 1 | Research and design flow chart.

applied to confirm the optimal cutoff value (0.08990467) to divide patients in high- and low-risk (**Figure 2C**). Based on the above screening, the five optimal gene mutations were: *CREBBP*, *KEAP1*, *RAF1*, *STK11* and *TP53* (**Figure 2D**). The detailed risk score is presented in **Supplementary Material 1**.

Difference in bTMB Score and PDL1 Expression High- and Low-Risk Patients Based on Our Prediction Model

Markers such as bTMB and PDL1 are vital to predict the efficacy of atezolizumab. In our study, we found that high-risk patients in the training group had a higher bTMB score compared with low-risk (high-risk 17.600 ± 1.805 *vs* low-risk 9.762 ± 0.595; P <0.0001) (**Figure 3A**). In addition, the PDL1 expression was divided into low (tumor cell (TC) <1%/immune cell (IC) <1%), medium (TC = 1–50%%/IC = 1–5%) and high (TC ≥50%/IC ≥5%) according to a previous study (3). The results showed that the PDL1 expression of high-risk patients was low in 35.29%, medium in 49.02% and high in 15.69% of patients, while for low-risk patients the PDL1 expression was low in 44.03%, medium in 36.94% and high in 19.03% of patients (**Figure 3B**).

The Survival Analysis for the Training Group Based on the Gene Mutation Signature

The survival analysis was used to compare the OS rate of high- and low-risk patients receiving atezolizumab. The results showed that low-risk patients had a better OS rate with a median survival of 15.343 months compared with high-risk patients that had a median survival of 6.308 months (P = 0.0004) (**Figure 4A**). In fact, the OS benefit of low-risk patients was demonstrated in patients receiving docetaxel from the OAK study (P <0.0001) (**Supplementary Figure 1A** and **Supplementary Material 2**). Importantly, bTMB was not a predictor of OS of patients receiving atezolizumab (P = 0.647) (**Supplementary Figure 2A**). Patients receiving atezolizumab with PDL1 ≥1% also did not present differences in OS compared with those with PDL1 <1% (P = 0.479) (**Supplementary Figure 2B**). Patients receiving atezolizumab with PDL1 ≥50% showed a 10.5 months median OS benefit compared with those with PDL1 <50% (P = 0.0058) (**Supplementary Figure 2C**). Importantly, compared with PDL1 and bTMB, our risk model had a higher Hazard Ratio (HR) and C-index to predict the OS of patients receiving atezolizumab (**Supplementary Table 1**).

Next, we analyzed the OS difference for patients receiving atezolizumab compared with those subjected to docetaxel. The results showed the high-risk patients receiving atezolizumab had a better OS benefit with a median survival of 6.308 months compared with patients receiving docetaxel that presented a 5.355 months survival (P = 0.0265) (**Figure 4B**). Importantly, the OS benefit of atezolizumab *vs* docetaxel was more obvious for low-risk patients (P <0.0001) (**Figure 4C**).

The Survival Analysis for Testing Group Patients Based on the Gene Mutation Signature

We attempted to further verify the feasibility of our prediction model using patients from the POPLAR study as our testing group. First, we screened patients receiving atezolizumab based on the same criteria (**Supplementary Material 3**). As expected, the results showed that low-risk patients receiving atezolizumab had a better OS (14.817 months) compared with high-risk

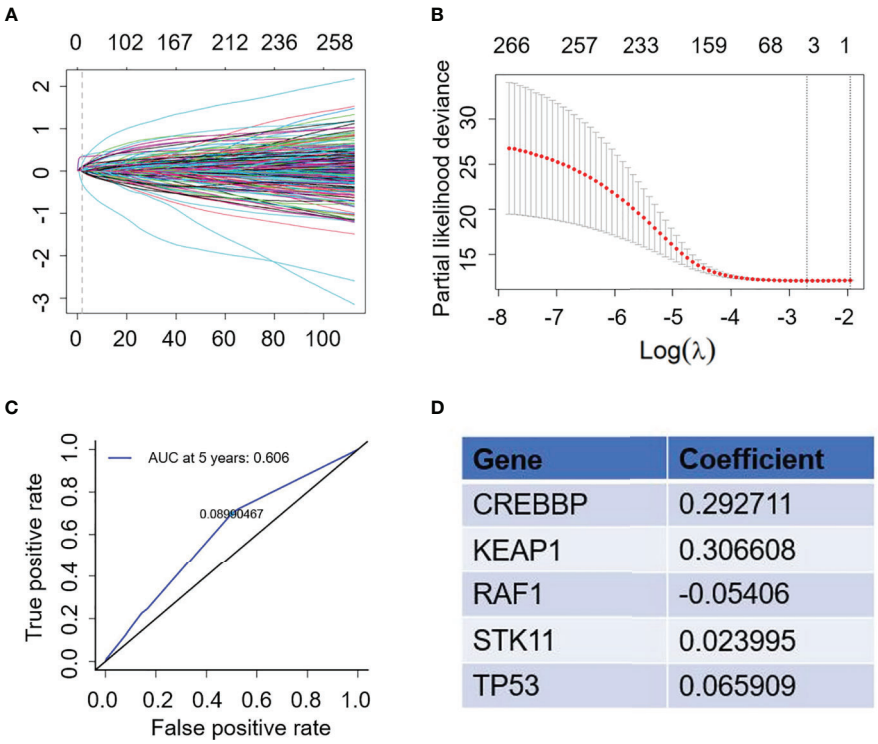

Gene	Coefficient
CREBBP	0.292711
KEAP1	0.306608
RAF1	-0.05406
STK11	0.023995
TP53	0.065909

FIGURE 2 | Construction of gene mutation signature to predict survival. **(A)** Trend graph of LASSO coefficients. **(B)** Partial likelihood deviation map. **(C)** Time dependent ROC curve. **(D)** 5 gene mutation types and matched coefficient.

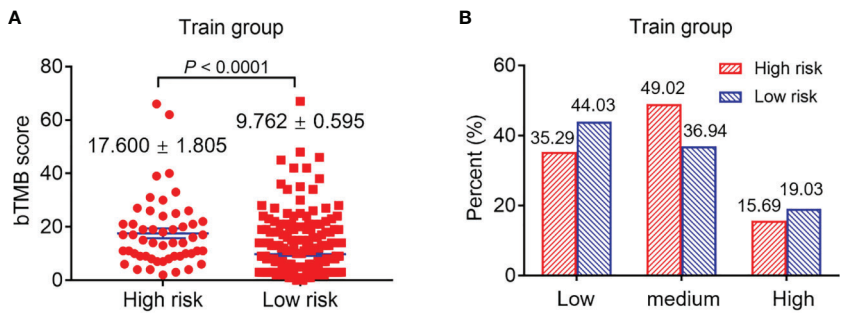

FIGURE 3 | The difference of bTMB score and PDL1 expression of patients with high and low risk. **(A)** The difference of bTMB score of patients with high and low risk ($P < 0.0001$). **(B)** The difference of PDL1 expression of patients with high and low risk.

patients (OS 6.078 months) ($P = 0.0001$) (**Figure 5A**). We also screened the patients receiving docetaxel from the POPLAR study (**Supplementary Material 4**). High-risk patients receiving docetaxel showed no OS benefits when compared to those in use of atezolizumab (median survival: 6.078 months *vs* 6.242 months, respectively) ($P = 0.6403$) (**Figure 5B**). However, low-risk patients receiving atezolizumab showed a better OS benefit with a median survival of 14.817 months compared with low-risk patients receiving docetaxel (median survival of 10.053 months) ($P = 0.0095$) (**Figure 5C**). In addition, the OS benefit of low-risk patients was also demonstrated in patients receiving docetaxel ($P = 0.0063$) (**Supplementary Figure 1B**).

Subgroup Analysis on OS After Adjusting Clinical Variables for Patients Receiving Atezolizumab Based on Training and Testing Group

Importantly, we conducted multivariate Cox analysis by adjusting clinical variables including age, race, sex, ECOG,

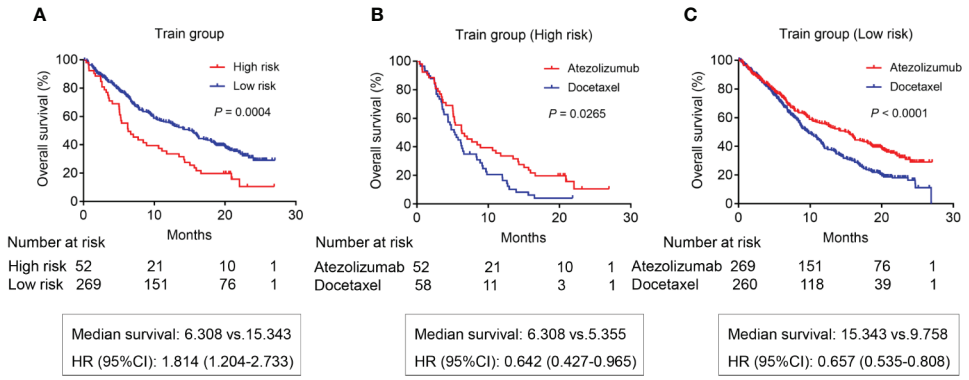

FIGURE 4 | The OS analysis for patients in the training group from OAK study. **(A)** The OS difference between the high risk and low risk patients receiving atezolizumab (P = 0.0004). **(B)** The OS difference of high-risk patients between atezolizumab and docetaxel (P = 0.0265). **(C)** The OS difference of low-risk patients between atezolizumab and docetaxel (P < 0.0001).

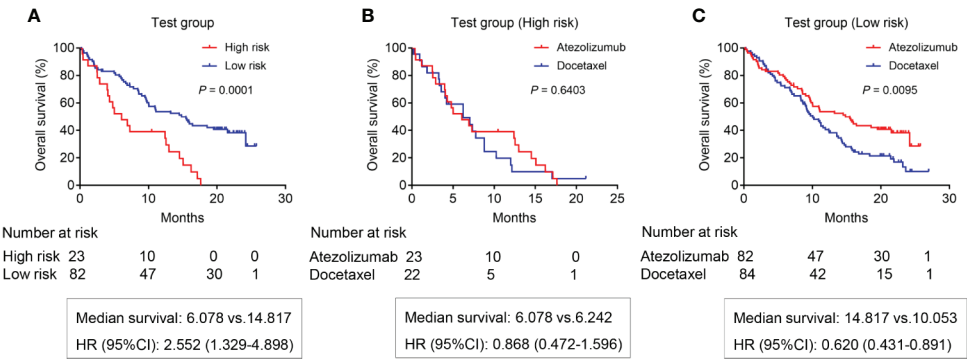

FIGURE 5 | The OS analysis for patients in the testing group from POPLAR study. **(A)** The OS difference between the high risk and low risk patients receiving atezolizumab (P = 0.0001). **(B)** The OS difference of high-risk patients between atezolizumab and docetaxel (P = 0.6403). **(C)** The OS difference of low-risk patients between atezolizumab and docetaxel (P = 0.0095).

Histopathology and smoking history based on the training and testing group. The results showed that risk model based on the 5-genomic mutation signature was an independent prognostic factor for patients receiving atezolizumab (HR: 95%CI: 2.031 (1.528–2.700; P <0.0001) (**Table 1**). Likewise, we also analyzed the prognostic factors for patients receiving docetaxel, the result also demonstrated that risk model based on the 5-genomic mutation signature was also an independent prognostic factor for these patients (HR:95%CI: 1.995 (1.528–2.604; P <0.0001) (**Supplementary Table 2**). Importantly, the results of multivariate Cox regression analysis showed that atezolizumab had better OS benefit compared with docetaxel in the low-risk patients (HR:95%CI: 1.572 (1.312–1.883; P <0.0001) (**Table 2**). However, the positive connection between treatment and OS was not found in high-risk patients in light of same analysis (HR:95%CI: 1.387 (0.980–1.962; P = 0.065) (**Table 3**). Interestingly, we found there is an obvious interaction between smoking history and treatment in low-risk patients based on training and testing group (P = 0.024) (**Table 2**).

DISCUSSION

The efficacy rate of immunotherapy is relatively low, which has made it imperative to explore markers to predict the efficacy of immunotherapy. It has been commonly acknowledged that high TMB and PD-L1 is associated with improved prognosis. However, there have been some limitations in their prediction of immunotherapy responses. Recently, a growing number of studies have focused on the role of genetic mutations in the prediction of immunotherapy. To explore the impact of genetic mutation on ICI prediction, we therefore developed a risk score model based on gene mutations to predict the OS of patients receiving atezolizumab. The clinical significance of our findings

TABLE 1 | Univariate and multivariate Cox regression analysis of clinical variables affecting OS for patients receiving atezolizumab based on training and testing group.

Variables	Univariate analysis		Multivariate analysis		Interaction*
	Wald	*P*	HR (95% CI)	*P*	*P*
Age	0.005	0.944	NI		0.692
<65					
≥65					
Race	1.656	0.198	NI		0.107
White					
Asian					
Others					
Sex	3.163	0.075	NI		0.496
Female					
Male					
Histopathology	7.668	0.006		0.005	0.806
Squamous			Reference		
Non-squamous			0.694 (0.537–0.896)	0.005	
ECOG	17.591	<0.0001		<0.0001	0.242
0			Reference		
1			1.757 (1.353–2.281)	<0.0001	
Smoking	4.242	0.039		0.180	0.098
Current			Reference		
Never			1.011 (0.649–1.576)		
Previous			1.285 (0.918–1.799)		
Risk model	25.125	<0.0001		<0.0001	
Low risk			Reference		
High risk			2.031 (1.528–2.700)	<0.0001	

*NI, not included; *Interaction between variables and risk model.*

could be seen in three aspects: First, our 5-genomic mutation signature was demonstrated to be a better predictor than PDL1 and bTMB to screen patients who would benefit from atezolizumab; It is also very convenient and economical to detect; More importantly, our 5-genomic mutation signature was able to predict OS rates of patients receiving atezolizumab, which may help clinicians select patients who could benefit more from such therapy.

The 5-genomic mutation signature of our risk score model consisted of mutations in *CREBBP*, *KEAP1*, *RAF1*, *STK11* and *TP53*. *CREBBP*, which encodes an acetyltransferase, has been frequently found to develop mutations in many tumor types (12–14). At present, there is no literature focusing on the relationship between the *CREBBP* mutation and immunotherapy outcomes. Only one previous study showed that loss of function of *CREBBP* resulted in focal depletion of enhancer *H3K27* acetylation and aberrant transcriptional silencing of genes that regulate B-cell signaling and immune responses, such as class II MHC (15). *HDAC3* inhibition represents a novel mechanism-based immune epigenetic therapy for lymphomas caused by *CREBBP* mutation (16). *KEAP1* is located at 19p13.2, and its protein has three major domains: an N-terminal broad complex, tram track, and the bric-a-brac (BTB) domain; a central intervening region (IVR); and a series of six C-terminal Kelch repeats (17). High-frequency mutations in *KEAP1* have been identified in Chinese patients with lung squamous cell carcinoma, while the somatic nonsynonymous mutation of *KEAP1* in patients with lung cancer is likely to promote tumorigenesis *via* activation of the *KEAP1/NRF2* antioxidant stress response pathway (18). Our previously study revealed that *KEAP1*-mutant NSCLC is associated with higher TMB, and also found that the OS was prolonged in NSCLC patients receiving immunotherapy with wild-type *KEAP1* compared with a mutant (6). Another study has demonstrated that *STK11/KEAP1* mutations may help identify bTMB-high patients unlikely to respond to pembrolizumab (19). Indeed, *STK11/KEAP1* mutations are prognostic, not predictive, biomarkers for anti-PD-1/anti-PDL1 therapy (20). Interestingly, we previously analyzed the relationship between *STK11* mutation and immune-related prognostic markers and immune microenvironment. The results showed that patients with the *STK11* mutation did not benefit from immune checkpoint inhibitors (6).

At present, there are a few studies focusing on *RAF1* mutation and no literature reporting the relationship between *RAF1* mutation and immunotherapy. In parallel, *BRAF* mutation was found in lung cancer even though its association with immunotherapy efficacy is controversial (21–23). *TP53* mutation is common in patients with lung cancer. Many studies focused on the relationship between *TP53* mutation and immunotherapy efficacy. Assoun et al. reported that *TP53* mutation was associated with OS benefits in NSCLC patients with advanced non-small cell lung cancer treated with immune checkpoint inhibitor (24). A study from China also demonstrated that *TP53* and *KRAS* mutations in lung adenocarcinoma might serve as a pair of potential predictive factors to guide anti-PD-1/PDL1 immunotherapy (25).

TABLE 2 | Univariate and multivariate Cox regression analysis of clinical variables affecting OS for low-risk patients based on training and testing group.

Variables	Univariate analysis		Multivariate analysis		Interaction*
	Wald	*P*	HR (95% CI)	*P*	*P*
Age	1.991	0.158	NI		0.198
<65					
≥65					
Race	2.269	0.132	NI		0.359
White					
Asian					
Others					
Sex	2.270	0.132	NI		0.826
Female					
Male					
Histopathology	15.777	<0.0001		<0.0001	0.720
Squamous			Reference		
Non-squamous			0.697 (0.577–0.842)	<0.0001	
ECOG	35.196	<0.0001		<0.0001	0.693
0			Reference		
1			1.833 (1.503–2.235)	<0.0001	
Smoking	3.367	0.067	NI		0.024
Current					
Never					
Previous					
Treatment	22.943	<0.0001		<0.0001	
Atezolizumab			Reference		
Docetaxel			1.572 (1.312–1.883)	<0.0001	

*NI, not included; *Interaction between variables and risk model.*

Altogether, the relationship between *TP53* and immunotherapy still needs further investigation.

We have successfully established a risk model based on the five genomic mutations exposed above. And the risk of death is significantly higher in high-risk cohort compared with low-risk for those receiving atezolizumab. High-risk patients were found to be those with high bTMB and PD-L1, indicating bTMB and PD-L1 were not accurate to distinguish OS for patients receiving atezolizumab. One study led by Nie also demonstrated that advanced NSCLC patients with low tumor mutation burden might derive benefit from immunotherapy (5), as consistent with our study. In fact, we compared the HR of different OS prediction models and found that our 5-genomic mutation signature had a higher HR in both the POPLAR and OAK studies when compared to other prediction models. A higher C-index was also found for our model of 5-genomic mutation signature. These results suggest that our risk score model is a better predictor of OS rate when compared to bTMB and PDL1 expression. However, more data are needed to verify our conclusions.

Another interesting finding is that our risk model could also predict the OS of patients receiving docetaxel. This may be due to the fact that these specific gene mutations are involved in the malignant biological transformation of tumors, which may not be sensitive to treatment. High-risk patients receiving atezolizumab showed a better OS compared with those treated with docetaxel from the OAK study, however, the OS benefit was not found in the POPLAR study. Maybe this is due to the smaller sample size of the POPLAR study. Moreover, there was only a one month OS benefit for high-risk patients receiving atezolizumab compared with those using docetaxel within the OAK study, which may indicate that high-risk patients have limited benefits from atezolizumab. The follow-up multivariate Cox regression analysis further proves our conjecture when combining OAK and POPLAR studies after adjusting clinical variables.

Undeniably, it has to be noted that there are some limitations of our study that need to be addressed. First, all the gene mutation types were obtained by liquid biopsies in our study, which means some gene mutations were lost. If the 5-genomic mutation signature based on liquid biopsies could be successfully verified in the future, then it could have wider clinical applications. Second, the 5-genomic mutation signature based on the OAK and POPLAR cohorts was established only to predict OS benefit for NSCLC patients receiving atezolizumab. Due to the uniqueness of PD1/PDL1 inhibitors, it is necessary to further study whether our risk score model is suitable for other immune checkpoint inhibitors. Last but not the least, we performed a data analysis based on the published OAK and POPLAR cohorts and further verification is needed in the future. And there have been several studies focusing on the role of nutritional and inflammatory indexes in the prediction of survival for patients receiving atezolizumab (26, 27). Our study distinguished from them by centering on genetic mutations. These studies are not contradictory but rather complementary to each other. Despite these limitations, our prediction model for atezolizumab still holds clinical relevance for its superiority in ICI prediction than TMB and PD-L1, as confirmed in the present study.

In conclusion, we successfully established a 5-genomic mutation signature risk score model to predict the OS rate of patients receiving atezolizumab. Importantly, low-risk patients were more

TABLE 3 | Univariate and multivariate Cox regression analysis of clinical variables affecting OS for high-risk patients based on training and testing group.

Variables	Univariate analysis		Multivariate analysis		Interaction*
	Wald	*P*	HR (95% CI)	*P*	*P*
Age	0.339	0.560	NI		0.800
<65					
≥65					
Race	2.066	0.151#		0.326	0.063
White			Reference		
Asian			0.663 (0.384–1.146)	0.141	
Others			0.868 (0.435–1.731)	0.687	
Sex	0.623	0.430	NI		0.214
Female					
Male					
Histopathology	1.540	0.215	NI		0.542
Squamous					
Non-squamous					
ECOG	1.699	0.192#		0.207	0.673
0			Reference		
1			1.270 (0.876–1.839)	0.207	
Smoking	0.297	0.586	NI		0.542
Current					
Never					
Previous					
Treatment	4.676	0.031		0.065	
Atezolizumab			Reference		
Docetaxel			1.387 (0.980–1.962)	0.065	

*NI, not included; *Interaction between variables and treatment; #P < 0.2 was included in multivariate analysis.*

likely to benefit from atezolizumab compared with those treated with docetaxel. It would be beneficial to develop a gene mutation panel to guide the treatment of NSCLC patients receiving atezolizumab in the future.

DATA AVAILABILITY STATEMENT

The original contributions presented in the study are included in the article/**Supplementary Material**. Further inquiries can be directed to the corresponding author.

AUTHOR CONTRIBUTIONS

Study design: HW. Date collection: JL and XW. Date analysis: CyZ. Writing: JL, SB and ClZ. Chart making: JL, XW, CyZ, SB and ClZ. Supervision and amendment: HW. All authors contributed to the article and approved the submitted version.

FUNDING

This study was supported jointly by special funds for Taishan Scholars Project (grant no. tsqn201812149) and Academic Promotion Programme of Shandong First Medical University (2019RC004).

SUPPLEMENTARY MATERIAL

The Supplementary Material for this article can be found online at: https://www.frontiersin.org/articles/10.3389/fimmu.2021.606027/full#supplementary-material.

Supplementary Figure 1 | The OS analysis for patients receiving docetaxel. **(A)** The OS analysis for patients receiving docetaxel from OAK study ($P < 0.0001$). **(B)** The OS analysis for patients receiving docetaxel from POPLAR study. ($P = 0.0063$).

Supplementary Figure 2 | The OS analysis for patients based on bTMB score and PDL1 expression from OAK study. **(A)** The OS difference based on different bTMB score (Cutoff=16) ($P = 0.647$). **(B)** The OS difference based on different PDL1 expression (Cutoff=1%) ($P = 0.479$). **(C)** The OS difference based on different PDL1 expression (Cutoff=50%) ($P = 0.0058$).

REFERENCES

1. Blair HA. Atezolizumab: A Review in Previously Treated Advanced Non-Small Cell Lung Cancer. *Target Oncol* (2018) 13:399–407. doi: 10.1007/s11523-018-0570-5
2. Gandara DR, Paul SM, Kowanetz M, Schleifman E, Zou W, Li Y, et al. Blood-Based Tumor Mutational Burden as a Predictor of Clinical Benefit in Non-Small-Cell Lung Cancer Patients Treated With Atezolizumab. *Nat Med* (2018) 24:1441–8. doi: 10.1038/s41591-018-0134-3
3. Fehrenbacher L, Spira A, Ballinger M, Kowanetz M, Vansteenkiste J, Mazieres J, et al. Atezolizumab Versus Docetaxel for Patients With Previously Treated Non-Small-Cell Lung Cancer (POPLAR): A Multicentre, Open-Label, Phase 2 Randomised Controlled Trial. *Lancet* (2016) 387:1837–46. doi: 10.1016/S0140-6736(16)00587-0
4. Wang Z, Duan J, Cai S, Han M, Dong H, Zhao J, et al. Assessment of Blood Tumor Mutational Burden as a Potential Biomarker for Immunotherapy in Patients With Non–Small Cell Lung Cancer With Use of a Next-Generation Sequencing Cancer Gene Panel. *JAMA Oncol* (2019) 5:696–702. doi: 10.1001/jamaoncol.2018.7098

5. Nie W, Xu MD, Gan L, Zhang Y, Qian J, Gu K, et al. Advanced Non-Small Cell Lung Cancer Patients With Low Tumor Mutation Burden Might Derive Benefit From Immunotherapy. *J Immunother* (2020) 43:189–95. doi: 10.1097/CJI.0000000000000318
6. Wang H, Guo J, Shang X, Wang Z. Less Immune Cell Infiltration and Worse Prognosis After Immunotherapy for Patients With Lung Adenocarcinoma Who Harbored STK11 Mutation. *Int Immunopharmacol* (2020) 84:106574. doi: 10.1016/j.intimp.2020.106574
7. Zhang C, Zhang C, Li J, Wang H. Keap1-Nfe2l2-Mutant NSCLC and Immune Checkpoint Inhibitors: A Large Database Analysis. *J Thorac Oncol* (2020) 15: e85–6. doi: 10.1016/j.jtho.2020.02.027
8. Li H, Li J, Zhang C, Zhang C, Wang H. TERT Mutations Correlate With Higher TMB Value and Unique Tumor Microenvironment and May Be a Potential Biomarker for Anti-CTLA4 Treatment. *Cancer Med* (2020) 15:7151–60. doi: 10.1002/cam4.3376
9. Wang F, Zhao Q, Wang YN, Jin Y, He MM, Liu ZX, et al. Evaluation of POLE and POLD1 Mutations as Biomarkers for Immunotherapy Outcomes Across Multiple Cancer Types. *JAMA Oncol* (2019) 5:1504–6. doi: 10.1001/jamaoncol.2019.2963
10. Xu X, Yang Y, Liu X, Cao N, Zhang P, Zhao S, et al. Nfe2l2/Keap1 Mutations Correlate With Higher Tumor Mutational Burden Value/PD-L1 Expression and Potentiate Improved Clinical Outcome With Immunotherapy. *Oncologist* (2020) 25:e955–63. doi: 10.1634/theoncologist.2019-0885
11. Rittmeyer A, Barlesi F, Waterkamp D, Park K, Ciardiello F, von Pawel J, et al. Atezolizumab Versus Docetaxel in Patients With Previously Treated Non-Small-Cell Lung Cancer (OAK): A Phase 3, Open-Label, Multicentre Randomised Controlled Trial. *Lancet* (2017) 389:255–65. doi: 10.1016/S0140-6736(16)32517-X
12. Vogelsberg A, Steinhilber J, Mankel B, Federmann B, Schmidt J, Montes-Mojarro IA, et al. Genetic Evolution of in Situ Follicular Neoplasia to Aggressive B-Cell Lymphoma of Germinal Center Subtype. *Haematologica* (2020). doi: 10.3324/haematol.2020.254854
13. Carazo F, Bértolo C, Castilla C, Cendoya X, Campuzano L, Serrano D, et al. DrugSniper, a Tool to Exploit Loss-of-Function Screens, Identifies CREBBP as a Predictive Biomarker of VOLASERTIB in Small Cell Lung Carcinoma (SCLC). *Cancers (Basel)* (2020) 12:1824. doi: 10.3390/cancers12071824
14. Massé J, Truntzer C, Boidot R, Khalifa E, Pérot G, Velasco V, et al. Solid-Type Adenoid Cystic Carcinoma of the Breast, a Distinct Molecular Entity Enriched in NOTCH and CREBBP Mutations. *Mod Pathol* (2020) 33:1041–55. doi: 10.1038/s41379-019-0425-3
15. Jiang Y, Ortega-Molina A, Geng H, Ying HY, Hatzi K, Parsa S, et al. Crebbp Inactivation Promotes the Development of HDAC3-Dependent Lymphomas. *Cancer Discovery* (2017) 7:38–53. doi: 10.1158/2159-8290.CD-16-0975
16. Mondello P, Tadros S, Teater M, Fontan L, Chang AY, Jain N, et al. Selective Inhibition of HDAC3 Targets Synthetic Vulnerabilities and Activates Immune Surveillance in Lymphoma. *Cancer Discov* (2020) 10:440–59. doi: 10.1158/2159-8290.CD-19-0116
17. Singh A, Misra V, Thimmulappa RK, Lee H, Ames S, Hoque MO, et al. Dysfunctional KEAP1-NRF2 Interaction in Non-Small-Cell Lung Cancer. *PloS Med* (2006) 3:e420. doi: 10.1371/journal.pmed.0030420
18. Gong M, Li Y, Ye X, Zhang L, Wang Z, Xu X, et al. Loss-of-Function Mutations in KEAP1 Drive Lung Cancer Progression Via KEAP1/NRF2 Pathway Activation. *Cell Commun Signal* (2020) 18:98. doi: 10.1186/s12964-020-00568-z
19. Aggarwal C, Thompson JC, Chien AL, Quinn KJ, Hwang WT, Black TA, et al. Baseline Plasma Tumor Mutation Burden Predicts Response to Pembrolizumab-Based Therapy in Patients With Metastatic Non-Small Cell Lung Cancer. *Clin Cancer Res* (2020) 26:2354–61. doi: 10.1158/1078-0432
20. Papillon-Cavanagh S, Doshi P, Dobrin R, Szustakowski J, Walsh AM. STK11 and KEAP1 Mutations as Prognostic Biomarkers in an Observational Real-World Lung Adenocarcinoma Cohort. *ESMO Open* (2020) 5:e000706. doi: 10.1136/esmoopen-2020-000706
21. Zhang C, Zhang C, Lin J, Li Z, Wang H. Patients With BRAF-Mutant NSCLC May Not Benefit From Immune Checkpoint Inhibitors: A Population-Based Study. *JTO Clin Res Rep* (2020) 1:100006. doi: 10.1016/j.jtocrr.2020.100006
22. Guisier F, Dubos-Arvis C, Viñas F, Doubre H, Ricordel C, Ropert S, et al. Efficacy and Safety of Anti-PD-1 Immunotherapy in Patients With Advanced NSCLC With Braf, HER2, or MET Mutations or RET Translocation: GFPC 01-2018. *J Thorac Oncol* (2020) 15:628–36. doi: 10.1016/j.jtho.2019.12.129
23. Dudnik E, Peled N, Nechushtan H, Wollner M, Onn A, Agbarya A, et al. Braf Mutant Lung Cancer: Programmed Death Ligand 1 Expression, Tumor Mutational Burden, Microsatellite Instability Status, and Response to Immune Check-Point Inhibitors. *J Thorac Oncol* (2018) 13:1128–37. doi: 10.1016/j.jtho.2018.04.024
24. Assoun S, Theou-Anton N, Nguenang M, Cazes A, Danel C, Abbar B, et al. Association of TP53 Mutations With Response and Longer Survival Under Immune Checkpoint Inhibitors in Advanced Non-Small-Cell Lung Cancer. *Lung Cancer* (2019) 132:65–71. doi: 10.1016/j.lungcan.2019.04.005
25. Dong ZY, Zhong WZ, Zhang XC, Su J, Xie Z, Liu SY, et al. Potential Predictive Value of TP53 and KRAS Mutation Status for Response to PD-1 Blockade Immunotherapy in Lung Adenocarcinoma. *Clin Cancer Res* (2017) 23:3012–24. doi: 10.1158/1078-0432.CCR-16-2554
26. Sorich MJ, Rowland A, Karapetis CS, Hopkins AM. Evaluation of the Lung Immune Prognostic Index for Prediction of Survival and Response in Patients Treated With Atezolizumab for NSCLC: Pooled Analysis of Clinical Trials. *J Thorac Oncol* (2019) 14(8):1440–6. doi: 10.1016/j.jtho.2019.04.006
27. Hopkins AM, Kichenadasse G, Garrett-Mayer E, Karapetis CS, Rowland A, Sorich MJ. Development and Validation of a Prognostic Model for Patients With Advanced Lung Cancer Treated With the Immune Checkpoint Inhibitor Atezolizumab. *Clin Cancer Res* (2020) 26(13):3280–6. doi: 10.1158/1078-0432.CCR-19-2968

Conflict of Interest: The authors declare that the research was conducted in the absence of any commercial or financial relationships that could be construed as a potential conflict of interest.

frontiers in Oncology

CASE REPORT
published: 24 June 2021
doi: 10.3389/fonc.2021.661034

Case Report: Re-Sensitization to Gefitinib in Lung Adenocarcinoma Harboring EGFR Mutation and High PD-L1 Expression After Immunotherapy Resistance, Which Finally Transform Into Small Cell Carcinoma

Xiaoqian Zhai[1†], Jiewei Liu[1†], Zuoyu Liang[2], Zhixi Li[1], Yanyang Liu[1], Lin Huang[1], Weiya Wang[2] and Feng Luo[1*]*

[1] Lung Cancer Center, West China Hospital, Sichuan University, Chengdu, China, [2] Pathology Department, West China Hospital, Sichuan University, Chengdu, China

The treatment sequence of immunotherapy (IO) and epidermal growth factor receptor (EGFR) tyrosine kinase inhibitors (TKIs) is of great importance for the survival of non-small cell lung cancer (NSCLC) patients with EGFR sensitive mutation. Here, we reported an advanced lung adenocarcinoma case concurrent with EGFR sensitive mutation and high PD-L1 expression (>50%) that was administrated with gefitinib firstly, and then became resistant to EGFR-TKI. He received the strategy of immunity-combined chemo-radiotherapy and responded significantly. However, the disease re-progressed after 10 months. Surprisingly, the tumor re-sensitized to gefitinib for 13 months. At final, following the treatment pressure of TKI-IO combination therapy-TKI strategy, tumor clone eventually transformed into small cell lung carcinoma (SCLC). For one thing, our study provided novel approach and extended the treatment spectra of overcoming immunotherapy resistance after EGFR resistance in driver oncogene-mutated NSCLC. For another thing, our case is the first time to report that SCLC transformation can be achieved after gefitinib–pembrolizumab–gefitinib resistance in EGFR sensitive mutation NSCLC, providing a new condition for SCLC transformation.

Keywords: immunotherapy resistance, targeted therapy resistance, epidermal growth factor receptor mutation, high PD-L1 expression, tyrosine kinase inhibitors, lung adenocarcinoma, small cell cancer transformation

OPEN ACCESS

Edited by:
Yanyan Lou,
Mayo Clinic, United States

Reviewed by:
Giulio Metro,
Hospital of Santa Maria della Misericordia in Perugia, Italy
Wenfeng Fang,
Sun Yat-sen University Cancer Center (SYSUCC), China

****Correspondence:***
Feng Luo
hxyyluofeng@sina.com
Weiya Wang
151422303@qq.com

†These authors have contributed equally to this work and share first authorship

Specialty section:
This article was submitted to Cancer Immunity and Immunotherapy, a section of the journal Frontiers in Oncology

Received: *30 January 2021*
Accepted: *02 June 2021*
Published: *24 June 2021*

Citation:
Zhai X, Liu J, Liang Z, Li Z, Liu Y, Huang L, Wang W and Luo F (2021) Case Report: Re-Sensitization to Gefitinib in Lung Adenocarcinoma Harboring EGFR Mutation and High PD-L1 Expression After Immunotherapy Resistance, Which Finally Transform Into Small Cell Carcinoma. Front. Oncol. 11:661034. doi: 10.3389/fonc.2021.661034

BACKGROUND

Immune checkpoint inhibitors (ICIs) and targeted therapy have revolutionized the therapy landscapes of non-small cell lung cancer (NSCLC) which is the leading cause of cancer death worldwide. The treatment sequence of immunotherapy (IO) and epidermal growth factor receptor (EGFR) tyrosine kinase inhibitors (TKIs) is of great importance for survival of NSCLC patients with

EGFR sensitive mutation. There are a few therapies having been approved in driver oncogene-mutated NSCLC after kinase inhibitor resistance. One of the study, IMpower 150, suggested the addition of atezolizumab to bevacizumab and chemotherapy (ABCP) increased PFS benefit for EGFR-TKI-resistant patients when compared with chemotherapy alone (1). However, a significant proportion of patients eventually failed to respond to ICI therapy due to the evolution of secondary resistance (2). As such, the potential treatment strategies when IO combination therapy resistance occurred sequentially after TIK resistance are still lacking. Here, we reported a lung adenocarcinoma case concurrent with EGFR sensitive mutation and high PD-L1 expression (>50%) that progressed with gefitinib, re-progressed after immune-combined chemoradiotherapy, then re-sensitized to gefitinib. Finally, following the treatment pressure of TKI-IO combination therapy-TKI strategy, tumor clone eventually transformed into small cell lung carcinoma (SCLC). For one thing, our study provided a novel approach and extended the treatment spectra of overcoming immunotherapy resistance after EGFR resistance in driver oncogene-mutated NSCLC. For another thing, our case is the first time to report that SCLC transformation can be achieved after gefitinib–embrolizumab–gefitinib resistance in EGFR sensitive mutation NSCLC, providing a new condition for SCLC transformation.

CASE PRESENTATION

A 43-year-old male Asian non-smoker underwent surgical resection of lung mass, with a diagnosis of stage IIA lung adenocarcinoma (pT2bN0M0) harboring an EGFR del-19 mutation and high PD-L1 (80.9%) expression in August 2013 (**Figure 1A**). One year later, he received a second operation for metastasis of mediastinal lymph node and left chest wall. Following that, gefitinib was given for 21 months until clinical

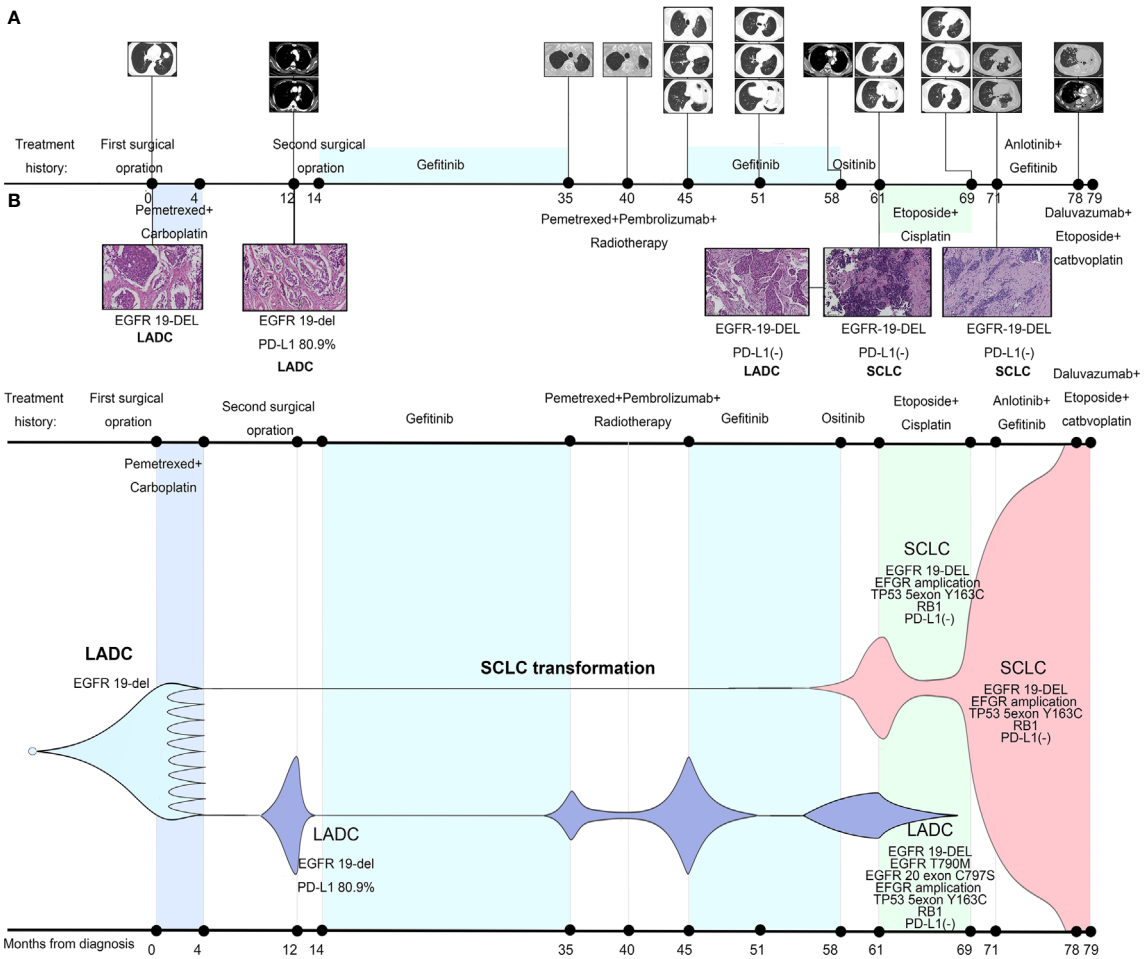

FIGURE 1 | Treatment history of our case and schematic diagram of tumor evolution. **(A)** Clinical treatment history and gene tests results of the patient. Numbers indicate time (in months) from the diagnosis of lung adenocarcinoma (LADC). Scale bar in histopathologic picture indicates 100 μm. **(B)** Presumed clonal evolution of our case which refers to Lee et al.'s study (3). The horizontal axis suggests the clinical history, and the vertical axis represents tumor volume.

resistance when a new nodule in the left residual lung appeared. But genetic testing specimens could not be obtained because it was difficult to have an operation and puncture. Thus, radiotherapy was administrated to control the local tumor. Considering highly expression of PD-L1 in this EGFR TKI resistance patient, eight cycles of pembrolizumab plus pemetrexed were offered, with best response of partial response (PR). The disease progressed again with new metastatic nodules in both lungs. But the multiple lesions were too small to perform a repeated biopsy. Meantime, the patient refused the liquid biopsy. He re-challenged gefitinib for 13 months by himself while drastic response was obtained as PR. When there was a sign of lymphadenopathy recurrence, osimertinib was taken by himself without any clear response. Three months later, the patient was hospitalized due to severe cough and dyspnea. Bronchoscopy was performed and repeated biopsy showed the left lung mass transformed into SCLC while the right remained adenocarcinoma harboring EGFR T790M and cis-C797S mutation in August 2018. Meanwhile, both sides shared the same trunk gene mutations as EGFR 19-del mutation, TP53 and RB1 mutation, with PD-L1 expression changing into negative in both sides. The patient sequentially received etoposide and cisplatin, anlotinib plus gefitinib before multiple metastasis burst out, when biopsies and gene analysis indicated pure SCLC. Finally, he died after one cycle of etoposide and carboplatin plus durvalumab treatment in March 2020.

DISCUSSION

Patients with a co-occurrence of high PD-L1 (>50%) and EGFR aberrations were disclosed less than 10% in NSCLC (4). A Japanese retrospective study found PD-1 inhibitors were more beneficial as second-line or later treatment for EGFR-TKI resistant NSCLC patients with high PD-L1 expression (TPS>50%) than patients with low PD-L1 expression (5). At the time of resistance to gefitinib, we offered the intervening treatment immunity-combined chemo-radiotherapy to our patient. Radiotherapy could better control the occurrence and development of local lung lesion. Chemotherapy and immunotherapy could diminish much further the clinical and subclinical tumor by activing anti-tumor immunity. Our patient with EGFR-TKI resistance responded well to IO combination therapy, which was consistent with the previous study (5). Thus, PD-L1 TPS 50% or higher may function a predictive role in immunotherapy efficacy after the kinase inhibitor resistance.

However, some patients evolved inevitably IO resistance due to immunosuppressive tumor microenvironment (Treg and MDSCs, VEGF) and immuno-adaption (2) after which the treatment strategies were lacking. In our case, after sequential resistance to gefitinib and pembrolizumab, the patient re-challenged geifitinib by himself. Although, Metro et al. reported that osimertinib re-challenge after chemotherapy in an EGFR T790M-positive NSCLC patient was feasible and effective (6). The safety was still uncertain because a research suggested osimertinib immediately after nivolumab increased interstitial lung disease incidence in patients with EGFR+ NSCLC (7). Fortunately, this patient did not present any serious AEs, receiving partial response and stale disease for 16 months since re-challenge of the 1st EGFR-TKI after pembrolizumab resistance. In addition, another study also described 1st or 2nd EGFR TKI immediately after nivolumab was safe and effective (8). As such, we speculated that at least for some patients, re-challenge of the 1st EGFR-TKI may be a feasible and safe way to overcome pembrolizumab resistance in EGFR-TKI resistant patients. The underlying mechanism of gefitinib re-sensitization may be that EGFR-TKI drug-resistant tumor cells were lost in the course of chemotherapy, Then in turn, the TKI-sensitive tumor cells re-grow and re-sensitize to the inhibitor (6). Meanwhile, gefitinib re-sensation may contribute to the relapse of previous EGFR+ tumor cells because of T cell exhaustion after ICI therapy resistance. There might be a synergistic effect of immunity-combined chemo-radiotherapy to get gefinitib re-sensitive. It was a process of tumor cells' evolution due to tumor heterogeneity. Different treatment methods lead to different tumor sub-clone dominant, so diversity of therapy strategies allows patients to afford durable clinical benefits. But, further investigation is warranted.

After the TKI-IO combination therapy-TKI treatment, the case eventually became fully resistant to TKI. As Dr. Robert A. Gatenby's game theory illustrated in 2018 in JAMA Oncology (9), under continuous treatment pressure, cancer cells inevitably evolved towards treatment escape and malignancy increase. In our case, on the one hand, genetic testing found p.T790M and C797S in cis mutations in the right bronchus. On the other hand, the tumor histologically transformed into SCLC in the left bronchus. In accordance to the study of Lee et al. (3), repeated biopsies of our patient and genetic tests also revealed clearly during 7 years' survival how SCLCs clone evolve dynamically early from the LADC clones under treatment pressure, eventually leading to SCLC phenotype evading anti-cancer therapy (**Figure 1B** and **Supplementary Table 1**). Furthermore, some previous studies indicated that SCLC transformation only occurred in EGFR-TKI resistant tumors or in LADC without EGFR mutation after ICI therapy resistance (10, 11). Our case is the first to report that SCLC transformation can be achieved after gefitinib–pembrolizumab–gefitinib resistance in EGFR+ NSCLC, providing a new condition for SCLC transformation.

DATA AVAILABILITY STATEMENT

The original contributions presented in the study are included in the article/**Supplementary Material**, further inquiries can be directed to the corresponding authors.

ETHICS STATEMENT

The studies involving human participants were reviewed and approved by the Institutional Review Board of West China

Hospital, Sichuan University. The patients/participants provided their written informed consent to participate in this study. Written informed consent was obtained from the individual(s) for the publication of any potentially identifiable images or data included in this article.

AUTHOR CONTRIBUTIONS

XZ and JL wrote the original draft. ZuL and ZhL collected the data and edited the manuscript. YL and LH prepared the figures and reviewed the literature. WW supervised, provided the resource, and reviewed the article. FL conceived the idea and reviewed the article. All authors contributed to the article and approved the submitted version.

FUNDING

This work was supported by the Wu Jieping Medical Foundation, China (312150082).

ACKNOWLEDGMENTS

Thanks to Burning Rock Biotech (Guangzhou, China) for support in genetic analysis technology.

SUPPLEMENTARY MATERIAL

The Supplementary Material for this article can be found online at: https://www.frontiersin.org/articles/10.3389/fonc.2021.661034/full#supplementary-material

REFERENCES

1. Reck M, Mok TSK, Nishio M, Jotte RM, Cappuzzo F, Orlandi F, et al. Atezolizumab Plus Bevacizumab and Chemotherapy in Non-Small-Cell Lung Cancer (IMpower150): Key Subgroup Analyses of Patients With EGFR Mutations or Baseline Liver Metastases in a Randomised, Open-Label Phase 3 Trial. *Lancet Respir Med* (2019) 7(5):387–401. doi: 10.1016/S2213-2600(19)30084-0
2. Horvath L, Thienpont B, Zhao L, Wolf D, Pircher A. Overcoming Immunotherapy Resistance in Non-Small Cell Lung Cancer (NSCLC) - Novel Approaches and Future Outlook. *Mol Cancer* (2020) 19(1):141. doi: 10.1186/s12943-020-01260-z
3. Lee JK, Lee J, Kim S, Kim S, Youk J, Park S, et al. Clonal History and Genetic Predictors of Transformation Into Small-Cell Carcinomas From Lung Adenocarcinomas. *J Clin Oncol* (2017) 35(26):3065–74. doi: 10.1200/JCO.2016.71.9096
4. Rangachari D, VanderLaan PA, Shea M, Le X, Huberman MS, Kobayashi SS, et al. Correlation Between Classic Driver Oncogene Mutations in EGFR, ALK, or ROS1 and 22C3-PD-L1 ≥50% Expression in Lung Adenocarcinoma. *J Thorac Oncol* (2017) 12(5):878–83. doi: 10.1016/j.jtho.2016.12.026
5. Masuda K, Horinouchi H, Tanaka M, Higashiyama R, Shinno Y, Sato J, et al. Efficacy of Anti-PD-1 Antibodies in NSCLC Patients With an EGFR Mutation and High PD-L1 Expression. *J Cancer Res Clin Oncol* (2020) 147(1):245–51. doi: 10.1007/s00432-020-03329-0
6. Metro G, Baglivo S, Siggillino A, Ludovini V, Chiari R, Rebonato A, et al. Successful Response to Osimertinib Rechallenge After Intervening Chemotherapy in an EGFR T790M-Positive Lung Cancer Patient. *Clin Drug Investig* (2018) 38(10):983–7. doi: 10.1007/s40261-018-0691-8
7. Kotake M, Murakami H, Kenmotsu H, Naito T, Takahashi T. High Incidence of Interstitial Lung Disease Following Practical Use of Osimertinib in Patients Who Had Undergone Immediate Prior Nivolumab Therapy. *Ann Oncol* (2017) 28(3):669–70. doi: 10.1093/annonc/mdw647
8. Kaira K, Kagamu H. Drastic Response of Re-Challenge of EGFR-TKIs Immediately After Nivolumab Therapy in EGFR-TKI-Resistant Patients. *J Thorac Oncol* (2019) 14(6):e135–6. doi: 10.1016/j.jtho.2019.02.011
9. Staňková K, Brown JS, Dalton WS, Gatenby RA. Optimizing Cancer Treatment Using Game Theory: A Review. *JAMA Oncol* (2019) 5(1):96–103. doi: 10.1001/jamaoncol.2018.3395
10. Arakawa S, Yoshida T, Nakayama Y, Motoi N, Ohe Y. Small Cell Cancer Transformation of Lung Adenocarcinoma During Durvalumab Treatment After Chemoradiotherapy. *J Thorac Oncol* (2020) 15(8):e145–6. doi: 10.1016/j.jtho.2019.12.117
11. Marcoux N, Gettinger SN, O'Kane G, Arbour KC, Neal JW, Husain H, et al. EGFR-Mutant Adenocarcinomas That Transform to Small-Cell Lung Cancer and Other Neuroendocrine Carcinomas: Clinical Outcomes. *J Clin Oncol* (2019) 37(4):278–85. doi: 10.1200/JCO.18.01585

Conflict of Interest: The authors declare that the research was conducted in the absence of any commercial or financial relationships that could be construed as a potential conflict of interest.

frontiers in Oncology

ORIGINAL RESEARCH
published: 20 September 2021
doi: 10.3389/fonc.2021.700023

Immune Checkpoint Inhibitors Plus Single-Agent Chemotherapy for Advanced Non-Small-Cell Lung Cancer After Resistance to EGFR-TKI

*Haiyi Deng†, Xinqing Lin†, Xiaohong Xie†, Yilin Yang, Liqiang Wang, Jianhui Wu, Ming Liu, Zhanhong Xie, Yinyin Qin and Chengzhi Zhou**

State Key Laboratory of Respiratory Disease, National Clinical Research Centre for Respiratory Disease, Guangzhou Institute of Respiratory Health, First Affiliated Hospital, Guangzhou Medical University, Guangzhou, China

OPEN ACCESS

Edited by:
Meijuan Huang, Sichuan University, China

Reviewed by:
Peng Luo, The University of Hong Kong, Hong Kong, SAR China
Xuchao Zhang, Guangdong Provincial People's Hospital, China

***Correspondence:**
Chengzhi Zhou
doctorzcz@163.com

†*These authors have contributed equally to this work*

Specialty section:
This article was submitted to Cancer Immunity and Immunotherapy, a section of the journal Frontiers in Oncology

Received: *25 April 2021*
Accepted: *02 September 2021*
Published: *20 September 2021*

Citation:
Deng H, Lin X, Xie X, Yang Y, Wang L, Wu J, Liu M, Xie Z, Qin Y and Zhou C (2021) Immune Checkpoint Inhibitors Plus Single-Agent Chemotherapy for Advanced Non-Small-Cell Lung Cancer After Resistance to EGFR-TKI. Front. Oncol. 11:700023. doi: 10.3389/fonc.2021.700023

Purpose: Platinum-based chemotherapy remains the classic treatment option for patients with advanced non-small-cell lung cancer (NSCLC) who progress while receiving treatment with epidermal growth factor receptor-tyrosine kinase inhibitors (EGFR-TKIs). In this study, we analyzed real-world outcomes of treatment with immune checkpoint inhibitors (ICIs) combined with platinum-free chemotherapy in patients with NSCLC after developing resistance to EGFR-TKIs.

Methods: This retrospective study included patients with mutation-positive NSCLC after developing resistance to EGFR-TKIs. Patients who received chemotherapy alone plus ICIs with or without anti-angiogenic drugs (cohort A) or platinum-based chemotherapy (cohort B) between February 2019 and August 2020 were enrolled. Clinical characteristics, EGFR mutation status, response to therapy, and adverse events (AEs) were retrospectively analyzed.

Results: Seventeen patients were eligible and included in the analysis, including 8 in cohort A and 9 in cohort B. After a median follow-up of 7.6 months, the median progression-free survival was 6.5 months [95% confidence interval (CI), 6.1 to 7.0] in cohort A and 3.6 months (95% CI, 1.3–5.8) in cohort B (hazard ratios, 0.22; 95% CI, 0.05–0.93; P = 0.039). The overall response and disease control rates were 50% and 100% in cohort A, and 22% and 89% in cohort B, respectively. Adverse events of grade 3 or higher occurred in 25% of the patients in cohort A and in 33.3% of the patients in cohort B.

Conclusion: ICIs plus platinum-free, single-agent chemotherapy provides promising progression-free survival and overall response rate benefit, along with a low rate of severe AEs in patients with EGFR-TKI-resistant advanced NSCLC.

Keywords: epidermal growth factor receptor gene (EGFR), immune checkpoint inhibitor, immunotherapy, non-small-cell lung cancer, single-agent chemotherapy

INTRODUCTION

Lung cancer is the first-leading cause of cancer-related death worldwide (1). The vast majority (85%) of lung cancer cases are non-small-cell lung cancer (NSCLC), and approximately 50% of them harbor epidermal growth factor receptor gene (EGFR) mutations in Asia (2). Multiple clinical studies have confirmed the significant response of patients with EGFR mutation to EGFR-tyrosine kinase inhibitors (EGFR-TKIs) (3). According to the current guidelines, the use of EGFR-TKIs has been recommended for the first-line treatment of advanced NSCLC with EGFR mutation. However, these patients develop resistance to EGFR-TKIs after 9–14 months. Approximately 50% of the patients with resistance to first- and second-generation TKIs have T790M mutations, which can be treated with third-generation TKIs (4). Unfortunately, these patients also develop resistance to third-generation EGFR-TKIs after approximately 1 year. According to the guidelines, chemotherapy is generally selected for follow-up treatment of T790M-negative or T790M-positive patients with resistance to third-generation TKIs; however, the efficacy of this regimen is unsatisfactory.

Immune checkpoint inhibitors (ICIs) offer a survival benefit to NSCLC patients without EGFR mutation, but not to those with EGFR mutations (5). The potential benefits of ICIs to patients with resistance to EGFR-TKIs are currently being explored. A meta-analysis showed that ICI alone does not exert a better effect than chemotherapy for patients who have progressed after treatment with TKIs (6). A phase II study (CT18, NCT03513666) of toripalimab combined with pemetrexed and carboplatin showed favorable efficacy (7). IMpower 150, which enrolled patients with EGFR mutation, demonstrated that ICI combined with chemotherapy and an anti-angiogenic drug prolonged progression-free survival (PFS) *versus* chemotherapy plus an anti-angiogenic drug (8). However, these two clinical studies also showed higher proportion of grades 3–5 adverse events (AEs).

A study showed that the immunomodulatory effects of pemetrexed or paclitaxel appeared to be reduced when combined with platinum (9). In addition, CheckMate 9LA confirmed that dual immunotherapy combined with limited chemotherapy exerts a good effect (10). The addition of chemotherapy to immunotherapy should not be restricted to the regimen of four courses of platinum-based chemotherapy. Our previous study proposed the concept of "chemo-reform": the addition of post-reform chemotherapy to immunotherapy, including single-drug chemotherapy (without platinum), platinum alone, low-dose chemotherapy, chemotherapy with adjusted course, or cycle interval–adjusted chemotherapy (11). This retrospective study was designed to assess the efficacy and safety of ICIs combined with single-drug chemotherapy without platinum in patients with EGFR-TKI-resistant advanced NSCLC in a real-world setting.

PATIENTS AND METHODS

Patients

Eligible patients with incurable NSCLC were treated with ICIs combined with single-drug chemotherapy without platinum, with or without anti-angiogenic treatment (cohort A) or platinum-containing chemotherapy (cohort B) at the First Affiliated Hospital of Guangzhou Medical University (Guangzhou, China) between February 2019 and August 2020. All patients had incurable advanced or metastatic NSCLC [unresectable stage III or IV according to the 8th edition TNM classification (12)]. Patients had to have sensitizing EGFR mutations [exon 19 deletions (Del19); exon 21 L858R mutation (L858R)] detected at the initial biopsy, clinical or radiological progression after at least one treatment with EGFR-TKIs, and no mutations that can be targeted for treatment. There was no upper limit regarding the number of prior treatments with EGFR-TKIs or systemic therapies. This study was approved by the local Ethics Committee of the First Affiliated Hospital of Guangzhou Medical University.

Data Collection and Outcome Assessment

The following information was retrospectively collected from the medical records of the patients: patient demographics, prior treatments with EGFR-TKIs or systemic therapies, lines of immunotherapy, Eastern Cooperative Oncology Group (ECOG) performance status (PS), EGFR mutation type, programmed death-ligand 1 (PD-L1) tumor proportion score (TPS), tumor imaging, tumor response to therapy, and AEs. The ECOG PS was evaluated prior to treatment. PD-L1 expression was tested by anti-human PD-L1 (Dako 22C3) according to the manufacturer's recommendations, using 4–5 μm formalin-fixed and paraffin-embedded (FFPE) sections. The cutoff value was 1% for PD-L1 positivity or negativity (PD-L1+/−). Tumor response was assessed in accordance with the Response Evaluation Criteria in Solid Tumors (RECIST version 1.1) (13). The objective response rate (ORR) was defined as the percentage of patients who exhibited response (complete or partial). The disease control rate (DCR) corresponds to all cases with complete response (CR), partial response (PR), and stable disease (SD). PFS was defined as the time from therapy initiation to disease progression or death. AEs were graded

according to the National Cancer Institute Common Terminology Criteria for Adverse Events, version 4.0.

Statistical Analysis

Continuous and categorical data were summarized as medians (ranges) and frequencies (percentages), respectively. An independent-samples t-test or the Mann-Whitney U test was used to analyze continuous variables. Differences in categorical variables were assessed using either Chi-square ($\chi 2$) or Fisher's exact test. We used the binomial exact method to evaluate the ORR and DCR with 95% confidence intervals (CIs). The Kaplan–Meier method was used to evaluate PFS with 95% CI. Statistical tests were two-sided, and a P-value <0.05 denoted statistically significant difference. Statistical analyses were performed using the IBM SPSS Statistics version 25.0 (Armonk, NY, USA) software.

RESULTS

Patients

In total, 17 patients were eligible and enrolled in the study. Patients' demographics are summarized in **Tables 1** and **2**. The median age of all patients was 59 (range: 42–73)years; nine patients (52.9%) were males and 82.4% had never smoked. All patients were adenocarcinoma. EGFR mutation status in the initial biopsy was Del19 and L858R in 11 and 6 patients, respectively. Nine patients were positive for the T790M mutation. Third or later lines were reported in 76.5% of patients, and 11 patients were treated with at least two EGFR-TKIs. For the 14 participants with available PD-L1 TPS values, 6 (42.8%), 4 (28.6%), and 4 (28.6%) patients had TPS values less than 1%, 1–49%, and ≥50%.

Cohort A included 8 (47.1%) patients and cohort B had 9 (52.9%) patients. In the cohort A, 2 patients received ICI combined with single agent chemotherapy and 6 patients received ICI

TABLE 1 | Characteristics of patients at baseline.

Characteristics	Cohort A (N = 8)	Cohort B (N = 9)	P value
Age,y; median (Range)	66 (53-73)	58 (42-71)	0.18
Sex (male/ female)	4/4	5/4	1
Smoking status			0.58
Current/former	2 (25)	1 (11.1)	
Never	6 (75)	8 (88.9)	
ECOG PS (at initiation of ICI/chemotherapy)			0.58
0	2 (25)	1 (11.1)	
1	6 (75)	8 (88.9)	
Disease status			0.47
III B	1 (12.5)	0	
IV	7 (87.5)	9 (100)	
Site of metastasis (at initiation of ICI/ chemotherapy)			
Brain	3 (37.5)	4 (44.4)	1
Liver	3 (37.5)	2 (22.2)	0.62
EGFR mutation status (initial biopsy/pre-TKI)			1
Del19	5 (62.5)	6 (66.7)	
L858R	3 (37.5)	3 (33.3)	
T790M status (rebiopsy/ post-TKI)			0.64
Positive	5 (62.5)	4 (44.4)	
Negative	3 (37.5)	5 (55.6)	
Prior treatment lines			0.57
1	2 (25)	2 (22.2)	
2	3 (37.5)	6 (66.7)	
3	3 (37.5)	1 (11.1)	
PD-L1 TPS			0.11
<1%	3 (37.5)	3 (33.3)	
1-49%	4 (50)	0	
≥50%	1 (12.5)	3 (33.3)	
Unknown	0	3 (33.3)	

ECOG PS, Eastern Cooperative Oncology Group performance status; EGFR, epidermal growth factor receptor gene; ICI, immune checkpoint inhibitor; TKI, tyrosine kinase inhibitor; Del19, exon 19 deletions; PD-L1 TPS, programmed death-ligand 1 tumor proportion score.

TABLE 2 | Characteristics of patients with EGFR-TKIs resistance who received immunotherapy or chemotherapy.

Patients	Gender	Age	Smoking status	EGFR mutation	T790M status (post-TKI)	Prior treatment lines	PFS on first TKI (months)	PD-L1 Expression level (%)	Response to ICI or chemotherapy
A-1	Female	54	Never	Del19	Negative	3	6.0	50	SD
A-2	Female	58	Never	L858R	Negative	1	10.3	2	SD
A-3	Female	68	Never	L858R	Positive	2	6.7	2	SD
A-4	Male	53	Former	Del19	Positive	3	9.7	<1	PR
A-5	Male	70	Former	L858R	Negative	1	4.6	<1	PR
A-6	Male	66	Never	Del19	Positive	2	11.9	10	PR
A-7	Male	66	Never	Del19	Positive	3	10.3	<1	SD
A-8	Female	73	Never	Del19	Positive	2	7.4	5	PR
B-1	Female	70	Never	L858R	Negative	2	3.7	<1	SD
B-2	Female	55	Never	Del19	Positive	2	8.1	<1	SD
B-3	Female	42	Never	Del19	Negative	1	4.6	80	PR
B-4	Male	59	Never	L858R	Negative	1	4.9	80	PR
B-5	Female	59	Never	Del19	Negative	2	6.1	<1	PD
B-6	Male	57	Never	Del19	Negative	2	9.5	NA	SD
B-7	Male	58	Never	Del19	Positive	2	10.9	NA	SD
B-8	Male	71	Former	L858R	Positive	2	12.2	NA	SD
B-9	Male	48	Never	Del19	Positive	3	7.6	50	SD

EGFR, epidermal growth factor receptor gene; Del19, exon 19 deletions; TKI, tyrosine kinase inhibitor; PFS, progression-free survival; PD-L1 , programmed death-ligand 1; ICI, immune checkpoint inhibitor, A-, cohort A; B-, cohort B; NA, unknown.

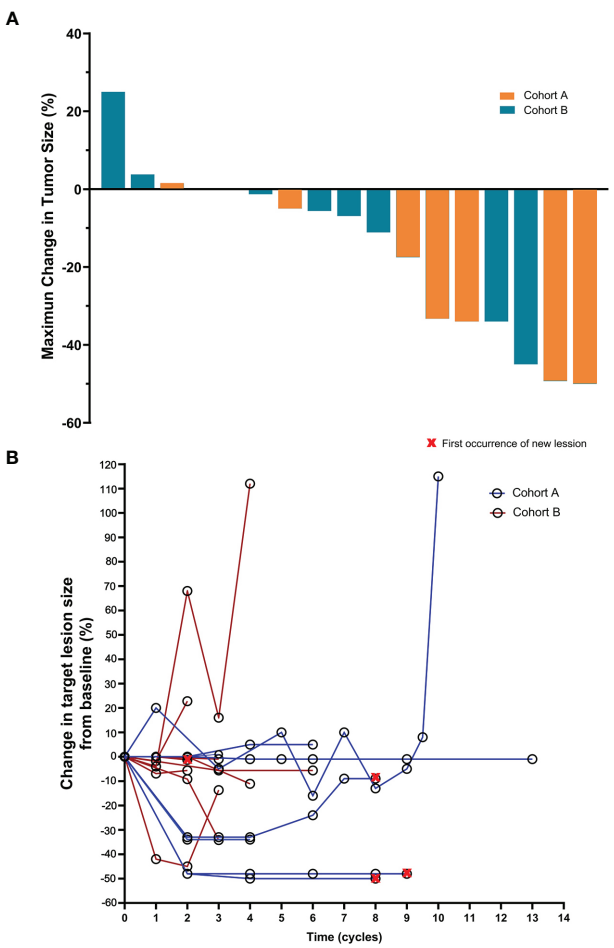

FIGURE 1 | Maximum percent change from baseline in the sum of the diameter of the longest target lesion according to the Response Evaluation Criteria in Solid Tumors (RECIST) version 1.1 in patients with measurable disease at baseline **(A)**. Positive and negative change in tumor size indicates tumor growth and reduction, respectively. Percent change in target lesion tumor burden from baseline and throughout the course of immunotherapy **(B)**.

combined with single-agent chemotherapy and anti-angiogenesis therapy. Baseline demographic and disease characteristics were no significant difference between groups (**Table 1**).

Efficacy

A total of 17 patients were evaluable for response. Partial responses were observed in 4 of 8 patients in cohort A and in 2 of 9 patients in cohort B. None of the patients had CR as their best reponse. The confirmed ORR was 50% (95% CI, 16–84) in cohort A and 22% (95% CI, 3–60) in cohort B (P = 0.34; **Table 2** and **Figure 1**). The DCR was 100% in cohort A and 88.9% in cohort B. The overall median follow-up for this analysis was 7.6 months. With 10 events of progression or death, the median PFS was 6.5 months (95% CI, 6.1 to 7.0) in cohort A and 3.6 months (95% CI, 1.3–5.8) in cohort B [hazard ratios (HR) for PFS, 0.22; 95% CI, 0.05–0.93; P = 0.039; **Figure 2**]. The 6-month PFS rate was 60.0% in cohort A and 16.7%

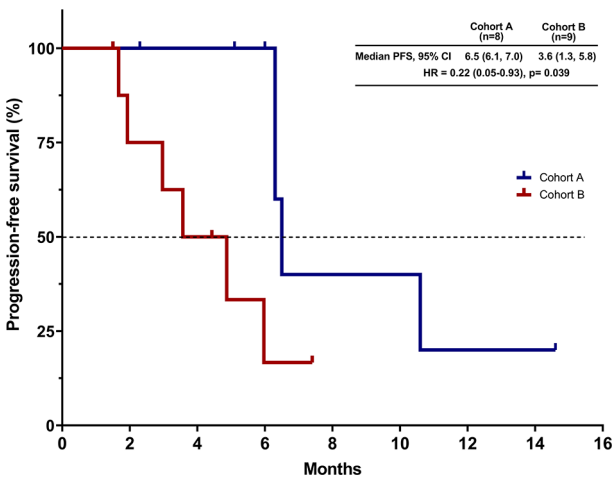

FIGURE 2 | Kaplan–Meier curve for progression-free survival (PFS). CI, confidence interval; HR, hazard ratio.

in cohort B. During the follow-up, the median overall survival was not reached.

Safety

A summary of the safety data of all treated patients is shown in **Table 3**. During treatment, AEs of any grade, regardless of attribution to treatment by the investigator, occurred in all patients. AEs of grade 3 or higher occurred in 25% of the patients in cohort A and in 33.3% of the patients in cohort B. There was no occurrence of toxicity-related deaths. None of the AEs led to discontinuation of treatment with ICIs in cohort A. The most common AEs in cohort A were anemia (75%), constipation (75%), and fatigue (50%), and the most common AEs in cohort B were anemia (77.8%) and decreased neutrophil count (33.3%).

DISCUSSION

The results of this study involving patients with advanced NSCLC patients after TKI acquired resistance showed that ICIs plus platinum-free chemotherapy, as compared with platinum-containing chemotherapy, prolonged median progression-free survival by 2.9 months (6.5 *vs.* 3.6 months).The risk of disease progression or death was 22% lower in cohort A than in cohort B. The ORR was higher in the in cohort A than in cohort B (50% *vs.* 22%). To our knowledge, this is the first study to demonstrate the efficacy and safety of immunotherapy combined with platinum-free chemotherapy in such patients.

The subsequent therapy of EGFR positive patients after TKI resistance is a conundrum. *In vitro*, PD-1 inhibitor prolonged the survival of mice with EGFR-mutant lung cancer by enhancing effector T cell function and reducing the level of tumor-promoting cytokines (14). However, previous studies showed ICI monotherapy has no survival benefit than docetaxel in the

TABLE 3 | Adverse Events of Any Cause.

Event	Cohort A (N = 8)		Cohort B (N = 9)	
	Any Grade	Grade 3 or 4	Any Grade	Grade 3 or 4
Any event	8 (100)	2 (25)	9 (100)	3 (33.3)
Anemia	6 (75)	2 (25)	7 (77.8)	1 (11.1)
Constipation	6 (75)	0	0	0
Fatigue	4 (50)	0	1 (11.1)	0
Decreased appetite	3 (37.5)	0	2 (22.2)	0
Skin reactions	3 (37.5)	0	2 (22.2)	0
Peripheral edema	3 (37.5)	0	1 (11.1)	0
Mucosal inflammation	3 (37.5)	0	1 (11.1)	0
Hyperthyroidism	2 (25)	0	1 (11.1)	0
Diabetes	2 (25)	0	0	0
Hepatitis	2 (25)	0	2 (22.2)	1 (11.1)
Dizziness	2 (25)	0	0	0
Neutrophil count decreased	1 (12.5)	0	3 (33.3)	1 (11.1)
Pneumonitis	1 (12.5)	0	0	0
Vomiting	1 (12.5)	0	0	0
Hypothyroidism	1 (12.5)	0	0	0
Nephritis	1 (12.5)	0	0	0

treatment of TKI resistant NSCLC patients (6), which may be associated with low rates of concurrent PD-L1 expression and CD8(+) TILs within the tumor microenvironment (15). Chemotherapy and immunotherapy had synergistic effects by upregulating PD-L1 expression (16).

Platinum-based chemotherapy is regarded as the standard treatment for EGFR-TKI resistant patients and is an appropriate comparator for this study. Although there were confounding effects compared with historical data, the outcomes of cohort B were consistent with the expectations based on previous studies (17, 18). Also, the outcomes of cohort A were consistent with that reported in the CT18 study (ORR: 50%; median PFS: 7 months) in advanced NSCLC patients received toripalimab combined with chemotherapy after resistance to prior EGFR TKIs (7). Nevertheless, 75% of patients enrolled in our study had received third or later lines of therapy, including four patients with T790M positive and resistance to third-generation TKIs. In the cohort A, 6/8 patients received received ICI plus chemotherapy and anti-angiogenesis therapy, of which 4 cases (66.7%) achieved PR. IMpower150 (8) included patients with EGFR mutation treated with ACP (atezolizumab + carboplatin + paclitaxel) or BCP (carboplatin + paclitaxel + bevacizumab) or ABCP (atezolizumab + carboplatin + paclitaxel +bevacizumab). Our ORR appeared to be numerically higher than those reported in these three subgroups (16% *vs.* 18% *vs.* 24%, respectively). The numerically lower PFS in cohort A, compared with that of ABCP group in IMpower150 study, may be explained in part by the inclusion of 2 patients who received ICI-chemotherapy without anti-angiogenic drugs.

The adverse-event profile observed in our study was as expected on the basis of the known events, and no new safety signals were found. The present results reveal that the proportion of grade ≥3 AEs (25%) in cohort A was numerically lower than those reported in the CT18 (55%) (7) and IMpower150 (ACP *vs.* BCP *vs.* ABCP, 57% *vs.* 57% *vs.* 64%, respectively) studies (8). Additionally, there were no grade 3–5 immune-related AEs recorded in our study. The majority of AEs were resolved or improved and were manageable.

This study had some limitations. Firstly, it was a retrospective study performed in a real-world setting, with potential for bias. We did not perform subgroup analysis due to a small sample size. We are currently conducting relevant prospective clinical studies (NCT04316351, NCT04310943). Secondly, the present findings provide only a narrow time window with limited follow-up of some patients. As a result, we did not calculate OS, and were able to analyze ORR and PFS as measures of short-term efficacy. The follow-up results will provide a more comprehensive analysis.

In conclusion, we showed a clinically meaningful survival benefit and a lower rate of severe AEs in patients treated with ICIs plus "chemo-reform". These clinically relevant data support the use of immunotherapy combined with single-drug chemotherapy may be a new treatment option for patients with advanced NSCLC after developing resistance to EGFR-TKIs. Prospective clinical studies are needed for further validation.

DATA AVAILABILITY STATEMENT

The raw data supporting the conclusions of this article will be made available by the authors, without undue reservation.

ETHICS STATEMENT

The studies involving human participants were reviewed and approved by the Institutional Review Board of the First Affiliated Hospital of Guangzhou Medical University (Guangzhou, Guangdong, China). The patients/participants provided their written informed consent to participate in this study.

AUTHOR CONTRIBUTIONS

HD, XL, XX, and CZ designed the study. HD, YY, LW, and JW collected the patients' data. HD, XL, ZX, ML, and YQ analyzed the data. HD, XL, XX, and CZ drafted and revised the

manuscript. All authors contributed to the article and approved the submitted version.

FUNDING

This study was supported by State Key Laboratory of Respiratory Disease-The open project (SKLRD-OP-202111), Beijing Xisike Clinical Oncology Research Foundation (Y-2019Genecast-076), and Beijing Bethune Charitable Foundation (BQE-TY-SSPC(5)-S-03).

ACKNOWLEDGMENTS

We sincerely thank the participating patients and all medical staff members.

SUPPLEMENTARY MATERIAL

The Supplementary Material for this article can be found online at: https://www.frontiersin.org/articles/10.3389/fonc.2021.700023/full#supplementary-material

REFERENCES

1. Sung H, Ferlay J, Siegel RL, Laversanne M, Soerjomataram I, Jemal A, et al. Global Cancer Statistics 2020: GLOBOCAN Estimates of Incidence and Mortality Worldwide for 36 Cancers in 185 Countries. *CA: Cancer J Clin* (2021) 71(3):209–249. doi: 10.3322/caac.21660
2. Midha A, Dearden S, McCormack R. EGFR Mutation Incidence in non-Small-Cell Lung Cancer of Adenocarcinoma Histology: A Systematic Review and Global Map by Ethnicity (Mutmapii). *Am J Cancer Res* (2015) 5(9):2892–911.
3. Zhang Y, Sheng J, Yang Y, Fang W, Kang S, He Y, et al. Optimized Selection of Three Major EGFR-TKIs in Advanced EGFR-Positive non-Small Cell Lung Cancer: A Network Meta-Analysis. *Oncotarget* (2016) 7(15):20093–108. doi: 10.18632/oncotarget.7713
4. Wang ZF, Ren SX, Li W, Gao GH. Frequency of the Acquired Resistant Mutation T790 M in non-Small Cell Lung Cancer Patients With Active Exon 19Del and Exon 21 L858R: A Systematic Review and Meta-Analysis. *BMC Cancer* (2018) 18(1):148. doi: 10.1186/s12885-018-4075-5
5. Lee CK, Man J, Lord S, Links M, Gebski V, Mok T, et al. Checkpoint Inhibitors in Metastatic EGFR-Mutated Non-Small Cell Lung Cancer-A Meta-Analysis. *J Thorac Oncol* (2017) 12(2):403–7. doi: 10.1016/j.jtho.2016.10.007
6. Cavanna L, Citterio C, Orlandi E. Immune Checkpoint Inhibitors in EGFR-Mutation Positive TKI-Treated Patients With Advanced non-Small-Cell Lung Cancer Network Meta-Analysis. *Oncotarget* (2019) 10(2):209–15. doi: 10.18632/oncotarget.26541
7. Zhang J, Zhou C, Zhao Y, Mu X, Zhou J, Bao Z, et al. A PII Study of Toripalimab, a PD-1 mAb, in Combination With Chemotherapy in EGFR Plus Advanced NSCLC Patients Failed to Prior EGFR TKI Therapies. *J Thorac Oncol* (2019) 14(10):S292–S. doi: 10.1016/j.jtho.2019.08.587
8. Reck M, Mok TSK, Nishio M, Jotte RM, Cappuzzo F, Orlandi F, et al. Atezolizumab Plus Bevacizumab and Chemotherapy in non-Small-Cell Lung Cancer (IMpower150): Key Subgroup Analyses of Patients With EGFR Mutations or Baseline Liver Metastases in a Randomised, Open-Label Phase 3 Trial. *Lancet Respir Med* (2019) 7(5):387–401. doi: 10.1016/s2213-2600(19)30084-0
9. Schaer DA, Geeganage S, Amaladas N, Lu ZH, Rasmussen ER, Sonyi A, et al. The Folate Pathway Inhibitor Pemetrexed Pleiotropically Enhances Effects of Cancer Immunotherapy. *Clin Cancer Res* (2019) 25(23):7175–88. doi: 10.1158/1078-0432.Ccr-19-0433
10. Paz-Ares L, Ciuleanu TE, Cobo M, Schenker M, Zurawski B, Menezes J, et al. First-Line Nivolumab Plus Ipilimumab Combined With Two Cycles of Chemotherapy in Patients With non-Small-Cell Lung Cancer (CheckMate 9LA): An International, Randomised, Open-Label, Phase 3 Trial. *Lancet Oncol* (2021) 22(2):198–211. doi: 10.1016/s1470-2045(20)30641-0
11. Deng H, Zhou C. From CheckMate 227 to CheckMate 9LA: Rethinking the Status of Chemotherapy in the Immunotherapy Era-Chemo-Free or Chemo-Reform? *Transl Lung Cancer Res* (2021) 10(4):1924–7. doi: 10.21037/tlcr-21-179
12. Goldstraw P, Chansky K, Crowley J, Rami-Porta R, Asamura H, Eberhardt WE, et al. The IASLC Lung Cancer Staging Project: Proposals for Revision of the TNM Stage Groupings in the Forthcoming (Eighth) Edition of the TNM Classification for Lung Cancer. *J Thorac Oncol* (2016) 11(1):39–51. doi: 10.1016/j.jtho.2015.09.009
13. Eisenhauer EA, Therasse P, Bogaerts J, Schwartz LH, Sargent D, Ford R, et al. New Response Evaluation Criteria in Solid Tumours: Revised RECIST Guideline (Version 1.1). *Eur J Cancer (Oxford England: 1990)* (2009) 45 (2):228–47. doi: 10.1016/j.ejca.2008.10.026
14. Akbay EA, Koyama S, Carretero J, Altabef A, Tchaicha JH, Christensen CL, et al. Activation of the PD-1 Pathway Contributes to Immune Escape in EGFR-Driven Lung Tumors. *Cancer Discovery* (2013) 3(12):1355–63. doi: 10.1158/2159-8290.CD-13-0310
15. Gainor JF, Shaw AT, Sequist LV, Fu X, Azzoli CG, Piotrowska Z, et al. EGFR Mutations and ALK Rearrangements Are Associated With Low Response Rates to PD-1 Pathway Blockade in Non-Small Cell Lung Cancer: A Retrospective Analysis. *Clin Cancer Res* (2016) 22(18):4585–93. doi: 10.1158/1078-0432.CCR-15-3101
16. Xue Y, Gao S, Gou J, Yin T, He H, Wang Y, et al. Platinum-Based Chemotherapy in Combination With PD-1/PD-L1 Inhibitors: Preclinical and Clinical Studies and Mechanism of Action. *Expert Opin Drug Delivery* (2021) 18(2):187–203. doi: 10.1080/17425247.2021.1825376
17. Soria JC, Wu YL, Nakagawa K, Kim SW, Yang JJ, Ahn MJ, et al. Gefitinib Plus Chemotherapy *Versus* Placebo Plus Chemotherapy in EGFR-Mutation-Positive non-Small-Cell Lung Cancer After Progression on First-Line Gefitinib (IMPRESS): A Phase 3 Randomised Trial. *Lancet Oncol* (2015) 16 (8):990–8. doi: 10.1016/s1470-2045(15)00121-7
18. Goldberg SB, Oxnard GR, Digumarthy S, Muzikansky A, Jackman DM, Lennes IT, et al. Chemotherapy With Erlotinib or Chemotherapy Alone in Advanced non-Small Cell Lung Cancer With Acquired Resistance to EGFR Tyrosine Kinase Inhibitors. *Oncologist* (2013) 18(11):1214–20. doi: 10.1634/theoncologist.2013-0168

Conflict of Interest: The authors declare that the research was conducted in the absence of any commercial or financial relationships that could be construed as a potential conflict of interest.

Publisher's Note: All claims expressed in this article are solely those of the authors and do not necessarily represent those of their affiliated organizations, or those of the publisher, the editors and the reviewers. Any product that may be evaluated in this article, or claim that may be made by its manufacturer, is not guaranteed or endorsed by the publisher.

frontiers in Oncology

CASE REPORT
published: 23 September 2021
doi: 10.3389/fonc.2021.731429

Case Report: Long Progression-Free Survival of Immunotherapy for Lung Adenocarcinoma With Epidermal Growth Factor Receptor Mutation

Jianfeng Peng[1], *Xianguang Zhao*[2], *Kaikai Zhao*[3,4] *and Xiangjiao Meng*[2]*

[1] Department of Radiation Oncology, Shandong Cancer Hospital Affiliated to Shandong First Medical University, Jinan, China, [2] Department of Radiation Oncology, Shandong Cancer Hospital, Jinan, China, [3] Department of Radiation Oncology, The First Affiliated Hospital of China Medical University, Shenyang, China, [4] Department of Radiation Oncology, Yantai Affiliated Hospital of Binzhou Medical University, Yantai, China

OPEN ACCESS

Edited by:
Yanyan Lou,
Mayo Clinic, United States

Reviewed by:
Minglei Zhuo,
Peking University Cancer Hospital, China
Xuefei Li,
Shanghai Pulmonary Hospital, China
Chunxia Su,
Shanghai Pulmonary Hospital, China

***Correspondence:**
Xiangjiao Meng
mengxiangjiao@126.com

Specialty section:
This article was submitted to Cancer Immunity and Immunotherapy, a section of the journal Frontiers in Oncology

Received: 27 June 2021
Accepted: 02 September 2021
Published: 23 September 2021

Citation:
Peng J, Zhao X, Zhao K and Meng X (2021) Case Report: Long Progression-Free Survival of Immunotherapy for Lung Adenocarcinoma With Epidermal Growth Factor Receptor Mutation. Front. Oncol. 11:731429. doi: 10.3389/fonc.2021.731429

Background: Immune checkpoint inhibitors (ICIs) have been clinically proven to be efficient in non-small cell lung cancer (NSCLC). However, it has also been found that immunotherapy is not effective for all patients. For instance, some patients with epidermal growth factor receptor (EGFR) mutation tumors have a low overall response rate to ICIs. As a result, we retrospectively analyzed the efficacy of anti-programmed death-ligand 1 (anti-PD-L1) blockade (atezolizumab) treatment for a patient with EGFR mutation, and we explored the interaction between immunotherapy and EGFR mutations in NSCLC.

Case Presentation: A patient, 62-year-old non-smoking female, with lung adenocarcinoma was initially misdiagnosed as EGFR wild type and received a third-line treatment with atezolizumab, experiencing partial response (PR) and progression-free survival (PFS) for 23 months. She had later been confirmed with EGFR L858R mutation prior to taking atezolizumab. On top of that, the patient developed T790M mutation after being administered with atezolizumab instead of EGFR tyrosine kinase inhibitors (TKIs). She started with osimertinib, although the lesion continued to progress. Tumor mutational burden (TMB), PD-L1 expression, and tumor-infiltrating lymphocytes (TILs) had been tested for further analysis.

Conclusion: The case report and literature review indicate that ICIs might be more effective for L858R mutation than for other EGFR mutant subtypes, which correlates with certain potential predictors such as TMB and concurrent PD-L1 plus $CD8^+$ TIL expression. However, there is no report on progression from non-primary EGFR T790M mutation to T790M mutation of patients who neither previously suffered from EGFR-TKIs nor responded to osimertinib. This case report will offer some information to guide the investigation on how to identify those who can benefit from immunotherapy and those who do not respond to EGFR-TKIs among the patients with EGFR mutations.

Keywords: non-small cell lung cancer (NSCLC), immunotherapy, EGFR mutation, EGFR-TKIs, biomarkers

INTRODUCTION

Immunotherapy using monoclonal antibodies directed at checkpoint proteins has become the newest treatment modality in lung cancer, including PD-1, programmed death-ligand 1 (PD-L1), and CTLA4 (1). Previous studies have shown better overall survival (OS) with immune checkpoint inhibitors (ICIs) compared with second- or third-line docetaxel (2). Compared with traditional cytotoxic chemotherapy, ICI monotherapy or combination therapy has shown to be a reliable and safe first- and second-line therapy for non-small cell lung cancer (NSCLC) without driver gene mutations (3–6). Thus, National Comprehensive Cancer Network (NCCN) guidelines recommends them as first-line and second-line treatments for NSCLC patients.

However, single-agent ICIs do not appear to have a striking advantage over cytotoxic agents in NSCLC harboring epidermal growth factor receptor (EGFR) mutations (2). As a major molecular subtype in Asian lung cancer patients, EGFR mutation accounts for 40% of lung adenocarcinoma, of which the two most common mutations are exon 19 deletion (60%) and L858R missense replacement (35%) (7). The specific criteria of the choice of EGFR tyrosine kinase inhibitors (TKIs) and ICIs for NSCLC patients with EGFR mutation appear to be the focus and challenge of the current research.

This case report describes a lung adenocarcinoma patient who achieved long progression-free survival (PFS) with an EGFR mutation treated with atezolizumab.

CASE PRESENTATION

A 62-year-old non-smoking woman with cough and chest tightness was initially found to have space-occupying lesions in her lungs in a physical examination at another hospital. Then she came to our hospital for further treatment. At this time, she had an Eastern Cooperative Oncology Group (ECOG) performance status of 1. And she had no relevant medical or surgical history. Enhanced CT showed a 3.0 × 3.0 cm mass in the left lower lung with diffuse miliary metastases in both lungs and no distant lymph node metastasis. The clinical stage was T1cN0M1a, and the pathological puncture diagnosis was lung adenocarcinoma in December 2016. She refused the gene test and received first-line treatment: pemetrexed 0.5 mg/m^2 d1 + cisplatin 75 mg/m^2 d1, q3w, for six cycles from January 2017 to June 2017. From July 2017 to April 2018, pemetrexed was given 0.8 d1, q3w, for nine cycles, and the best response was stable disease (SD) (**Figure 1**). In May 2018, CT reexamination revealed multiple vertebral metastases in the spine, and the efficacy was evaluated as progressive disease (PD). Therefore, second-line treatment regimen was used: docetaxel 120 mg d1, q21d, five cycles, from May 2018 to September 2018. Then CT reexamination after the end of treatment showed that the response was PD.

This time, the patient expressed a strong desire for treatment, and we had full discussions with the patient and her family to determine the next step of treatment. On October 22, 2018, we performed genetic testing on the patient using PCR, and the results showed that EGFR, ALK, and ROS1 were all wild types (**Figure 2A**). Atezolizumab treatment was initiated on November 2, 2018, based on the results of the OAK clinical trial (6) and the guidelines. After two cycles, CT showed partial response (PR) (**Figure 3**).

At cycle 18 of atezolizumab, free triiodothyronine (FT3) decreased to 3.62 pmol/L, and the patient was treated with the addition of levothyroxine sodium tablet 50 μg qd po. Liver metastasis occurred, and lung disease progressed on October 13, 2020 (**Figure 2C**). PFS was as long as 23 months. The clinical stage at this time was T2aN0M1c. After discussion of the multidisciplinary team (MDT), pathological puncture and genetic testing were conducted again for the patient, and the results showed EGFR L858R and T790M mutations (**Figure 2B**). Research by Hsu et al. suggested that mutations in EGFR are associated with a higher

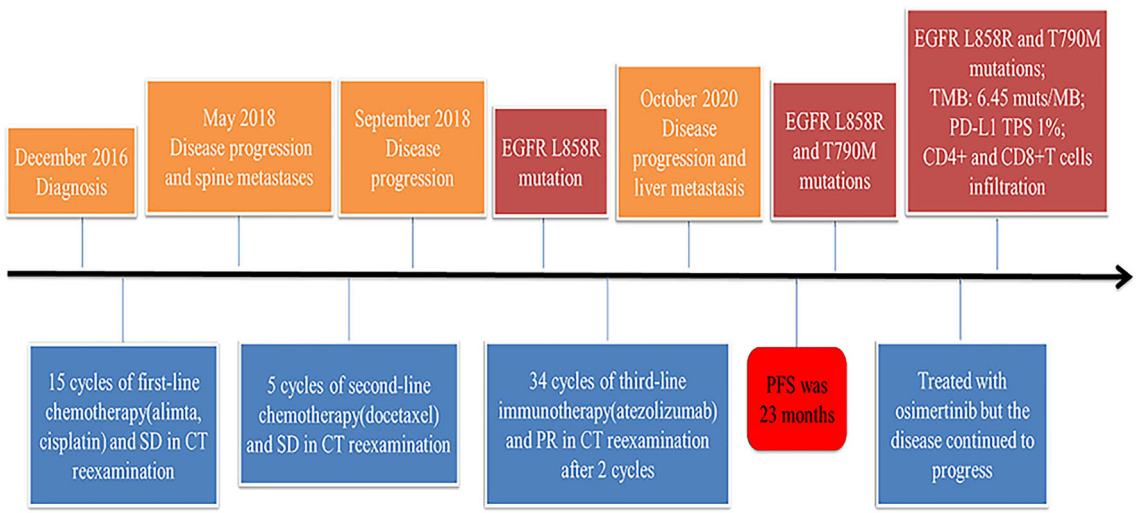

FIGURE 1 | Timeline of disease status and corresponding treatment regimens.

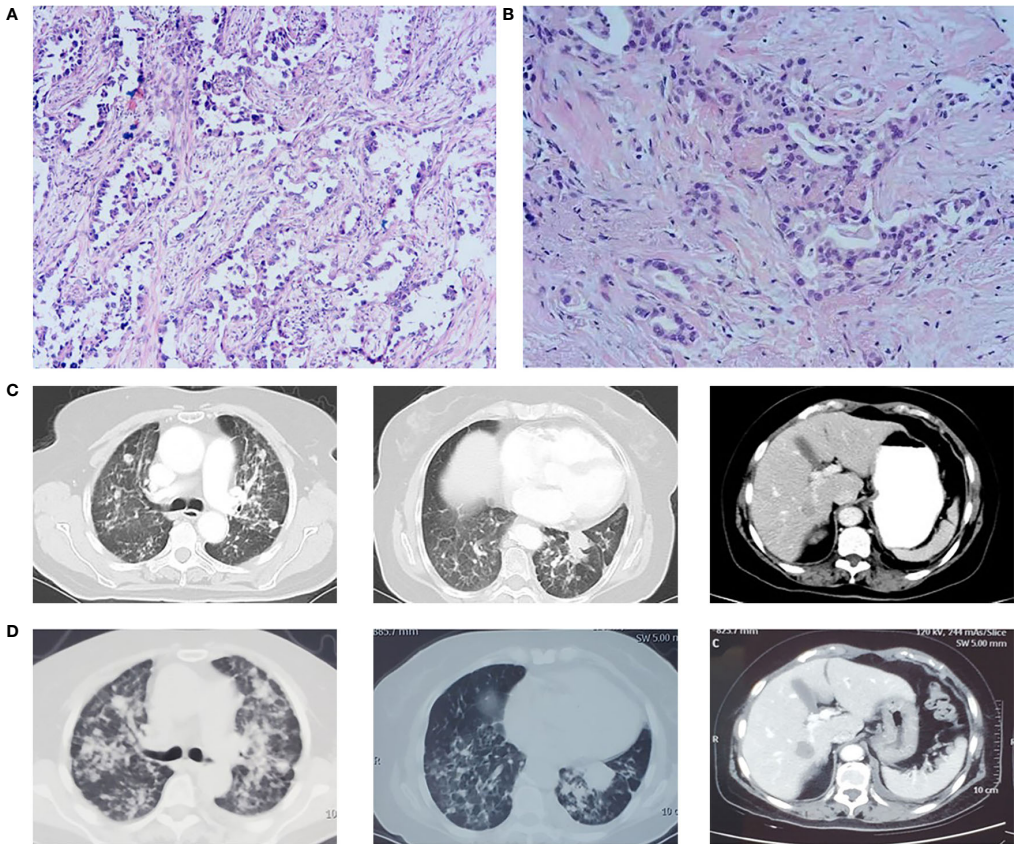

FIGURE 2 | **(A)** Pathological biopsy on October 22, 2018. **(B)** Pathological biopsy on November 11, 2020. **(C)** Lung lesion progression and liver metastasis on October 13, 2020. **(D)** Lesion progression in March 2021 after osimertinib treatment.

rate of miliary lung metastases (8); for the sake of precision, we redid genetic testing on the patient's 2018 pathological specimen using a more accurate next-generation sequencing (NGS) (9), and we found that the patient had the EGFR L858R mutation prior to the use of atezolizumab. Then the patient was treated with osimertinib in view of $EGFR^{T790M}$, but the follow-up CT until March 2021 showed that the lesion continued to progress (**Figure 2D**).

In order to explore why the patient responded well to atezolizumab but not to osimertinib, we performed the whole gene test (825 gene) by NGS and immunohistochemistry (IHC). At this time, the patient carried EGFR L858R, T790M, and TP53 R282W mutations; and her plasma sample had a low tumor mutational burden (TMB) of 6.45 muts/Mb. IHC showed PD-L1 tumor proportion score (TPS) <1% (antibody was 22C3), but the expression of PD-L1 in immune cells was 5%. In addition, $CD4^+$ and $CD8^+$ T cells were highly infiltrated (**Figure 4**).

DISCUSSION

Atezolizumab, a kind of ICIs, is a humanized monoclonal antibody that can specifically bind to PD-L1 to alter the immune escape mechanism of tumors and plays a role in anti-tumor activity (10). Several clinical trials have shown that ICIs can significantly prolong PFS and OS in tumors, whereas the benefit is limited to patients with EGFR wild type and ALK wild type. The OAK study subgroup showed that the patients with EGFR mutation received similar OS benefit with atezolizumab and docetaxel (6), which is consistent with the results of the CheckMate 057 and Keynote 010 trials (5, 11).

In this case, the patient with EGFR L858R mutation who was not pretreated with EGFR-TKIs was treated with atezolizumab. She obtained an extremely long PFS, although previous studies show different results. Some clinical trials have shown that certain EGFR mutant subtypes of tumors do respond to ICIs; for example, Hastings et al. observed that patients with EGFR L858R mutation receiving immunotherapy showed similar response rates and OS as patients with EGFR wild-type lung cancer, but they had much worse PFS (12). Her longer PFS may be related to some biomarkers. The predictive biomarkers such as PD-L1 TPS in cancer cells and microsatellite instability (13) have been approved by the U.S. Food and Drug Administration (FDA) for determining suitable advanced NSCLC patients that can benefit from ICIs (13). Moreover, other markers, including TMB, tumor-infiltrating lymphocytes (TILs), and other components of tumor microenvironment (TME), are being

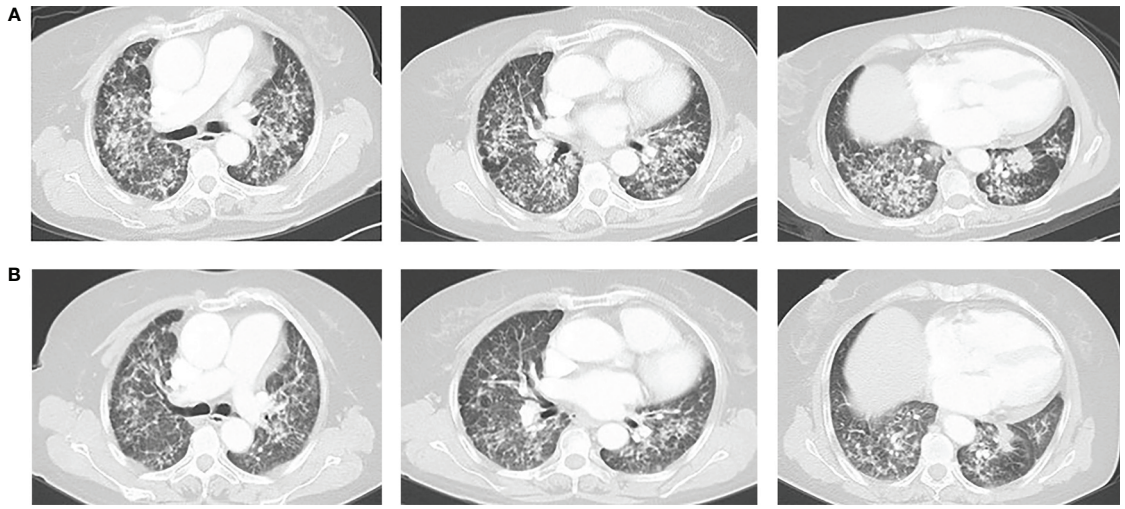

FIGURE 3 | **(A)** Chest CT on October 25, 2018. **(B)** Chest CT on December 21, 2018. The response was partial response (PR).

actively investigated (13). High level of PD-L1 expression, TMB, and $CD8^+$ TIL is associated with benefits of blocking PD-L1 and may lead to better PFS, OS, and response rates (13, 14). In this case, genetic testing and IHC of this patient showed low TMB level and low PD-L1 expression but a high level of $CD8^+$ TILs, which is a beneficial advantage for patient receiving immunotherapy. $CD8^+$ T cell can specifically recognize tumor antigens to kill tumors directly or target cells indirectly by secreting cytokines (15). In addition, previous studies have concluded that the expression of PD-L1 on both dendritic cells and macrophages is in relation to the efficacy of ICIs (16, 17). This patient's PD-L1 expression in immune cells takes 5%, which might be one of the reasons for the response to atezolizumab. Furthermore, this patient was pretreated with multiline chemotherapeutic agents before receiving atezolizumab. Results from the ATLANTIC showed that when durvalumab is used as a third-line treatment or above, NSCLC patients who are with EGFR mutations and have at least 25% of tumor cells with PD-L1

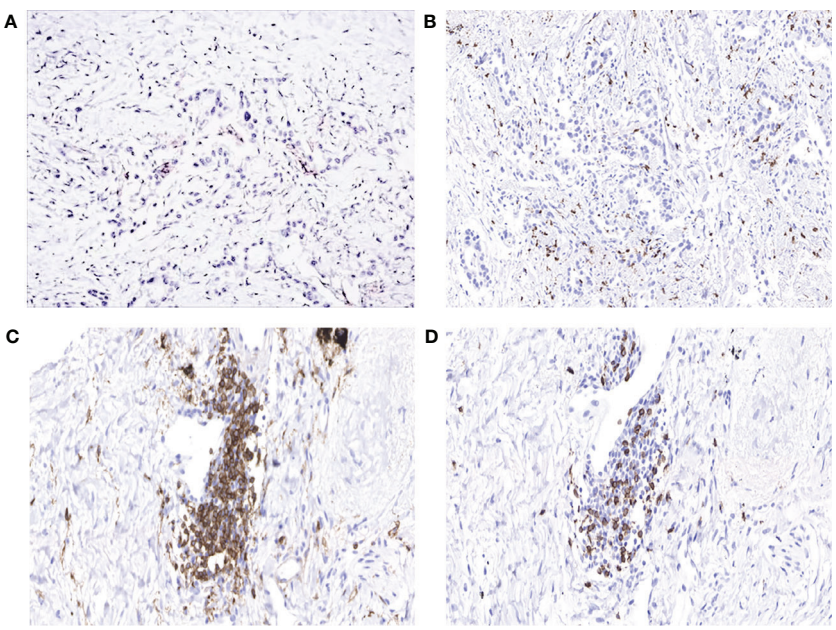

FIGURE 4 | **(A)** Programmed death-ligand 1 (PD-L1) tumor proportion score (TPS) <1%. **(B)** High infiltration of $CD8^+$ tumor-infiltrating lymphocytes (TILs). **(C)** Presence of large numbers of $CD4^+$ T cells in the stroma of the tumor. **(D)** Presence of large numbers of $CD8^+$ T cells in the stroma of the tumor.

expression could benefit from durvalumab with an objective response rate of 12.2% (9/74 patients, 95% CI 5.7–21.8). The objective response rate in patients accounting for less than 25% of tumor cells with PD-L1 expression is only 3.6% (1/28 patients, 95% CI 0.1–18.3) (18). Therefore, for this patient, further studies are needed to confirm whether NSCLC harboring EGFR L858R mutations with a high degree of $CD8^+$ TILs might benefit from atezolizumab or even obtain longer PFS after having multiline chemotherapy. In addition, the whole gene testing of the patient revealed that she also carried the TP53 R282W mutation, which is considered to be a positive gene (19). Previous studies have found that TP53 mutation increases the expression of PD-L1, thus making patients more likely to benefit from immunotherapy (20). Wu and his team found that TP53 mutations not only triggered these changes but also increased the proportion of $CD8^+$ T cells (21), which is consistent with this case. However, a clinical retrospective study has shown a contrasting result, suggesting that TP53 mutation is negatively correlated with immunotherapy efficacy (22). Therefore, subsequent studies are needed to confirm the correlation between TP53 mutation and immunotherapy and to clarify the relevant mechanisms.

Moreover, T790M mutations are a common resistance mutation, causing about 60% resistance to EGFR-TKIs (23). T790M mutations can be divided into two types—primary or acquired. Acquired T790M mutation is usually the resistant gene after the first or second generation of EGFR-TKIs, and both primary and secondary mutations have shown good responses to osimertinib (a type of third-generation EGFR-TKIs) therapy (24, 25). The patient presented in this report with non-primary EGFR T790M mutation who developed T790M mutation after ICIs rather than EGFR-TKIs, and she had a complete failure to respond to osimertinib. It has not been previously reported whether immunotherapy will induce new EGFR mutations or affect the efficacy of osimertinib. In addition, it is also worth exploring if high $CD8^+$ TILs cause the above effect. A retrospective study conducted by Su et al. reports a high proportion of $PD\text{-}L1^+$/$CD8^+$ cases in advanced NSCLC patients who were *de novo* resistant to first-line EGFR-TKIs. These patients, despite their poor response to EGFR-TKIs, exhibited higher immunogenicity, which, as a result, may benefit from immunotherapy (26). Another retrospective study performed by Yoshiya et al. also found that EGFR-TKIs as first-line treatment may have less benefit in EGFR-mutated tumors with both high expression of PD-L1 and $CD8^+$ TILs (27). However, in their study, high $CD8^+$ TIL (cohort 4) had longer PFS than low $CD8^+$ TILs (cohort 2) under the same low expression level of PD-L1 can be observed (27). Due to the small sample sizes of these two groups, further studies are needed to be conducted to confirm the relationship between $CD8^+$ TILs and the efficacy of EGFR-TKIs. In addition, it has been reported that the relative EGFR mutation abundance also could affect the therapeutic effect of using EGFR-TKI (28, 29). NGS of plasma performed prior to the application of osimertinib showed a mutation frequency of only 0.9% for EGFR T790M. The results of the study of Wang et al. showed that patients with low T790M mutation frequency are more likely to develop resistance and thus fail to benefit from osimertinib treatment (30).

However, there is one limitation to this case. Due to the insufficient pathological samples of patients saved before immunotherapy, we only performed genetic tests and could not perform IHC, so we did not know the levels of TMB, PD-L1 expression, and TILs before immunotherapy. For our subsequent studies, it is necessary to pay attention to the dynamic changes of biomarkers.

CONCLUSION

At present, how to select immunotherapy regimens for NSCLC patients with EGFR mutations is still controversial, but it is undeniable that some mutant subtypes do respond to ICIs, which may be due to the different effects of EGFR mutation subtypes on PD-L1 expression, TMB, and TME, thus affecting the efficacy of ICIs. However, we do not know much about whether ICIs or $CD8^+$ TILs affect the EGFR pathway and the efficacy of EGFR-TKIs. We need to further study this, so as to provide reference value for the selection of drug regimens for NSCLC with EGFR mutations in the future.

DATA AVAILABILITY STATEMENT

The datasets presented in this study can be found in online repositories. The names of the repository/repositories and accession number(s) can be found below: NCBI [accession: PRJNA752895].

ETHICS STATEMENT

The studies involving human participants were reviewed and approved by Shan Dong Cancer Hospital and Institute. The patient provided her written informed consent to participate in this study. Written informed consent was obtained from the individual for the publication of any potentially identifiable images or data included in this article.

AUTHOR CONTRIBUTIONS

XM designed the study, edited, and approved the final manuscript. KZ and XZ collected clinical data and performed histological analysis. JP collected and analyzed the data and drafted the manuscript. All authors contributed to the article and approved the submitted version.

FUNDING

This work was supported by the National Natural Science Foundation of China (grant numbers 81972796) and Natural Science Foundation of Shandong Province (grant numbers ZR2019MH010 and ZR2019MH289).

REFERENCES

1. Bunn PAJr. Karnofsky Award 2016: A Lung Cancer Journey, 1973 to 2016. *J Clin Oncol* (2017) 35(2):243–52. doi: 10.1200/JCO.2016.70.4064
2. Soo RA, Lim SM, Syn NL, Teng R, Soong R, Mok TSK, et al. Immune Checkpoint Inhibitors in Epidermal Growth Factor Receptor Mutant non-Small Cell Lung Cancer: Current Controversies and Future Directions. *Lung Cancer* (2018) 115:12–20. doi: 10.1016/j.lungcan.2017.11.009
3. Bylicki O, Barazzutti H, Paleiron N, Margery J, Assie JB, Chouaid C. First-Line Treatment of Non-Small-Cell Lung Cancer (NSCLC) With Immune Checkpoint Inhibitors. *BioDrugs* (2019) 33(2):159–71. doi: 10.1007/s40259-019-00339-4
4. Lee CK, Man J, Lord S, Cooper W, Links M, Gebski V, et al. Clinical and Molecular Characteristics Associated With Survival Among Patients Treated With Checkpoint Inhibitors for Advanced Non-Small Cell Lung Carcinoma: A Systematic Review and Meta-Analysis. *JAMA Oncol* (2018) 4(2):210–6. doi: 10.1001/jamaoncol.2017.4427
5. Borghaei H, Paz-Ares L, Horn L, Spigel DR, Steins M, Ready NE, et al. Nivolumab Versus Docetaxel in Advanced Nonsquamous Non-Small-Cell Lung Cancer. *N Engl J Med* (2015) 373(17):1627–39. doi: 10.1056/NEJMoa1507643
6. Rittmeyer A, Barlesi F, Waterkamp D, Park K, Ciardiello F, von Pawel J, et al. Atezolizumab Versus Docetaxel in Patients With Previously Treated non-Small-Cell Lung Cancer (OAK): A Phase 3, Open-Label, Multicentre Randomised Controlled Trial. *Lancet* (2017) 389(10066):255–65. doi: 10.1016/s0140-6736(16)32517-x
7. Chan BA, Hughes BG. Targeted Therapy for non-Small Cell Lung Cancer: Current Standards and the Promise of the Future. *Transl Lung Cancer Res* (2015) 4(1):36–54. doi: 10.3978/j.issn.2218-6751.2014.05.01
8. Hsu F, Nichol A, Toriumi T, De Caluwe A. Miliary Metastases are Associated With Epidermal Growth Factor Receptor Mutations in Non-Small Cell Lung Cancer: A Population-Based Study. *Acta Oncol* (2017) 56(9):1175–80. doi: 10.1080/0284186X.2017.1328128
9. Xuan J, Yu Y, Qing T, Guo L, Shi L. Next-Generation Sequencing in the Clinic: Promises and Challenges. *Cancer Lett* (2013) 340(2):284–95. doi: 10.1016/j.canlet.2012.11.025
10. Dhillon S, Syed YY. Atezolizumab First-Line Combination Therapy: A Review in Metastatic Nonsquamous NSCLC. *Target Oncol* (2019) 14(6):759–68. doi: 10.1007/s11523-019-00686-w
11. Herbst RS, Baas P, Kim DW, Felip E, JL P-G, Han JY, et al. Pembrolizumab Versus Docetaxel for Previously Treated, PD-L1-Positive, Advanced non-Small-Cell Lung Cancer (KEYNOTE-010): A Randomised Controlled Trial. *Ann Oncol* (2015) 387: (10027):1540–50. doi: 10.1016/S0140-6736(15)01281-7
12. Hastings K, Yu HA, Wei W, Sanchez-Vega F, DeVeaux M, Choi J, et al. EGFR Mutation Subtypes and Response to Immune Checkpoint Blockade Treatment in non-Small-Cell Lung Cancer. *Ann Oncol* (2019) 30(8):1311–20. doi: 10.1093/annonc/mdz141
13. Bustamante-Alvarez JG, Owen DH. Biomarkers for Immunotherapy. *Thorac Surg Clin* (2020) 30(2):207–14. doi: 10.1016/j.thorsurg.2020.01.010
14. Yu Y, Zeng D, Ou Q, Liu S, Li A, Chen Y, et al. Association of Survival and Immune-Related Biomarkers With Immunotherapy in Patients With non-Small Cell Lung Cancer: A Meta-Analysis and Individual Patient-Level Analysis. *JAMA Netw Open* (2019) 2(7):e196879. doi: 10.1001/jamanetworkopen.2019.6879
15. Simoni Y, Becht E, Fehlings M, Loh CY, Koo SL, Teng KWW, et al. Bystander CD8(+) T Cells are Abundant and Phenotypically Distinct in Human Tumour Infiltrates. *Nature* (2018) 557(7706):575–9. doi: 10.1038/s41586-018-0130-2
16. Lin H, Wei S, Hurt EM, Green MD, Zhao L, Vatan L, et al. Host Expression of PD-L1 Determines Efficacy of PD-L1 Pathway Blockade-Mediated Tumor Regression. *J Clin Invest* (2018) 128(2):805–15. doi: 10.1172/JCI96113
17. Tang H, Liang Y, Anders RA, Taube JM, Qiu X, Mulgaonkar A, et al. PD-L1 on Host Cells is Essential for PD-L1 Blockade-Mediated Tumor Regression. *J Clin Invest* (2018) 128(2):580–8. doi: 10.1172/JCI96061
18. Garassino MC, Cho B-C, Kim J-H, Mazières J, Vansteenkiste J, Lena H, et al. Durvalumab as Third-Line or Later Treatment for Advanced Non-Small-Cell Lung Cancer (ATLANTIC): An Open-Label, Single-Arm, Phase 2 Study. *Lancet Oncol* (2018) 19(4):521–36. doi: 10.1016/s1470-2045(18)30144-x
19. Assoun S, Theou-Anton N, Nguenang M, Cazes A, Danel C, Abbar B, et al. Association of TP53 Mutations With Response and Longer Survival Under Immune Checkpoint Inhibitors in Advanced Non-Small-Cell Lung Cancer. *Lung Cancer* (2019) 132:65–71. doi: 10.1016/j.lungcan.2019.04.005
20. Serra P, Petat A, Maury JM, Thivolet-Bejui F, Chalabreysse L, Barritault M, et al. Programmed Cell Death-Ligand 1 (PD-L1) Expression Is Associated With RAS/TP53 Mutations in Lung Adenocarcinoma. *Lung Cancer* (2018) 118:62–8. doi: 10.1016/j.lungcan.2018.02.005
21. Dong ZY, Zhong WZ, Zhang XC, Su J, Xie Z, Liu SY, et al. Potential Predictive Value of TP53 and KRAS Mutation Status for Response to PD-1 Blockade Immunotherapy in Lung Adenocarcinoma. *Clin Cancer Res* (2017) 23(12):3012–24. doi: 10.1158/1078-0432.CCR-16-2554
22. Carlisle JW, Nho NT, Kim C, Chen Z, Li S, Hill C, et al. Impact of TP53 Mutations on Efficacy of PD-1 Targeted Immunotherapy in Non-Small Cell Lung Cancer (NSCLC). *J Clin Oncol* (2018) 36(15_suppl):e21090–0. doi: 10.1200/JCO.2018.36.15_suppl.e21090
23. Li X, Lian Z, Wang S, Xing L, Yu J. Interactions Between EGFR and PD-1/PD-L1 Pathway: Implications for Treatment of NSCLC. *Cancer Lett* (2018) 418:1–9. doi: 10.1016/j.canlet.2018.01.005
24. Wang S, Yan B, Zhang Y, Xu J, Qiao R, Dong Y, et al. Different Characteristics and Survival in non-Small Cell Lung Cancer Patients With Primary and Acquired EGFR T790M Mutation. *Int J Cancer* (2019) 144(11):2880–6. doi: 10.1002/ijc.32015
25. Li H, Zhang S, Cheng Y. Advanced Research on T790M Mutation in non-Small Cell Lung Cancer. *Zhongguo Fei Ai Za Zhi* (2013) 16(6):314–20. doi: 10.3779/j.issn.1009-3419.2013.06.08
26. Su S, Dong ZY, Xie Z, Yan LX, Li YF, Su J, et al. Strong Programmed Death Ligand 1 Expression Predicts Poor Response and De Novo Resistance to EGFR Tyrosine Kinase Inhibitors Among NSCLC Patients With EGFR Mutation. *J Thorac Oncol* (2018) 13(11):1668–75. doi: 10.1016/j.jtho.2018.07.016
27. Matsumoto Y, Sawa K, Fukui M, Oyanagi J, Izumi M, Ogawa K, et al. Impact of Tumor Microenvironment on the Efficacy of Epidermal Growth Factor Receptor-Tyrosine Kinase Inhibitors in Patients With EGFR-Mutant non-Small Cell Lung Cancer. *Cancer Sci* (2019) 110(10):3244–54. doi: 10.1111/cas.14156
28. Zhou Q, Zhang XC, Chen ZH, Yin XL, Yang JJ, Xu CR, et al. Relative Abundance of EGFR Mutations Predicts Benefit From Gefitinib Treatment for Advanced Non-Small-Cell Lung Cancer. *J Clin Oncol* (2011) 29(24):3316–21. doi: 10.1200/JCO.2010.33.3757
29. Li X, Cai W, Yang G, Su C, Ren S, Zhao C, et al. Comprehensive Analysis of EGFR-Mutant Abundance and its Effect on Efficacy of EGFR Tkis in Advanced NSCLC With EGFR Mutations. *J Thorac Oncol* (2017) 12(9):1388–97. doi: 10.1016/j.jtho.2017.06.006
30. Wang Y, He Y, Tian P, Wang W, Wang K, Chuai S, et al. Low T790M Relative Allele Frequency Indicates Concurrent Resistance Mechanisms and Poor Responsiveness to Osimertinib. *Transl Lung Cancer Res* (2020) 9(5):1952–62. doi: 10.21037/tlcr-20-915

Conflict of Interest: The authors declare that the research was conducted in the absence of any commercial or financial relationships that could be construed as a potential conflict of interest.

frontiers in Oncology

ORIGINAL RESEARCH
published: 01 October 2021
doi: 10.3389/fonc.2021.680402

Expression of Microtubule-Associated Proteins in Relation to Prognosis and Efficacy of Immunotherapy in Non-Small Cell Lung Cancer

Jieyan Luo[1†], Qipeng Hu[1†], Maling Gou[2], Xiaoke Liu[1], Yi Qin[1], Jiao Zhu[1], Chengzhi Cai[1], Tian Tian[1], Zegui Tu[1], Yijia Du[1] and Hongxin Deng[3]*

[1] Department of Thoracic Oncology, West China Hospital, Sichuan University, Chengdu, China, [2] State Key Laboratory of Biotherapy, West China Hospital, Sichuan University, Chengdu, China, [3] State Key Laboratory of Biotherapy and Cancer Center, West China Hospital, Sichuan University and Collaborative Innovation Center for Biotherapy, Chengdu, China

OPEN ACCESS

Edited by:
Yanyan Lou,
Mayo Clinic, United States

Reviewed by:
Gong Zhang,
Shanxi Medical University, China
Zhengxiang Han,
Xuzhou Medical University, China

***Correspondence:**
Hongxin Deng
denghongx@scu.edu.cn

[†]These authors have contributed equally to this work

Specialty section:
This article was submitted to Cancer Immunity and Immunotherapy, a section of the journal Frontiers in Oncology

Received: *14 March 2021*
Accepted: *06 September 2021*
Published: *01 October 2021*

Citation:
Luo J, Hu Q, Gou M, Liu X, Qin Y, Zhu J, Cai C, Tian T, Tu Z, Du Y and Deng H (2021) Expression of Microtubule-Associated Proteins in Relation to Prognosis and Efficacy of Immunotherapy in Non-Small Cell Lung Cancer. Front. Oncol. 11:680402. doi: 10.3389/fonc.2021.680402

Background: Microtubule-associated proteins (MAPs) have been considered to play significant roles in the tumor evolution of non-small cell lung cancer (NSCLC). Nevertheless, mRNA transcription levels and prognostic value of distinct MAPs in patients with NSCLC remain to be clarified.

Methods: In this study, the Oncomine database, Gene Expression Profiling Interactive Analysis (GEPIA) database, and Human Protein Atlas were utilized to analyze the relationship between mRNA/protein expression of different MAPs and clinical characteristics in NSCLC patients, including tumor type and pathological stage. The correlation between the transcription level of MAPs and overall survival (OS) of NSCLC patients was analyzed by Kaplan–Meier plotter. Besides, 50 frequently altered neighbor genes of the MAPs were screened out, and a network has been constructed *via* the cBioPortal and Search Tool for the Retrieval of Interacting Genes/Proteins (STRING) dataset. Meanwhile, we performed Gene Ontology (GO) and Kyoto Encyclopedia of Genes and Genomes (KEGG) pathway analysis on the expression data of MAPs and their 50 frequently altered neighbor genes in NSCLC tissues. Furthermore, The Cancer Immunome Atlas (TCIA) was utilized to analyze the relationship between MAP expression and the response to immunotherapy. Finally, we used reverse transcription-quantitative polymerase chain reaction (RT-qPCR) to verify the expression of MAPs in 20 patients with NSCLC.

Results: The present study discovered that the mRNA transcription levels of MAP7/7D2 were enriched in NSCLC tissues, while those of the MAP2/4/6/7D3 were lower in NSCLC specimens than those in control specimens. The mRNA transcription level of MAP6 was significantly associated with the advanced stage of NSCLC. Besides, survival analysis indicated that higher mRNA expressions of MAP2/4/6/7/7D3 were correlated

considerably with favorable OS of NSCLC patients, whereas increased mRNA expression levels of MAP1A/1S were associated with poor OS. Moreover, the expression of MAP1A/1B/1S/4/6/7D1/7D3 was significantly correlated with immunophenoscore (IPS) in NSCLC patients.

Conclusions: Our analysis indicated that MAP1A/1S could serve as potential personalized therapeutic targets for patients with NSCLC, and the enriched MAP2/4/6/7/7D3 expression could serve as a biomarker for favorable prognosis in NSCLC. Besides, the expression of MAP1A/1B/1S/4/6/7D1/7D3 was closely related to the response to immunotherapy. Taken together, MAP expression has potential application value in the clinical treatment and prognosis assessment of NSCLC patients, and further verifiable experiments can be conducted to verify our results.

Keywords: MAP, non-small cell lung cancer, prognosis, immunotherapy, The Cancer Genome Atlas (TCGA)

INTRODUCTION

Non-small cell lung cancer (NSCLC), a common pathological type of lung cancer (LC), is one of the leading causes of cancer-related death worldwide (1, 2). NSCLC includes lung squamous cell carcinoma (LUSC), lung adenocarcinoma (LUAD), and large cell carcinoma. Meanwhile, patients with NSCLC account for approximately 85% of all LC patients (2). Although there has been substantial advancement in early screening and personalized treatment, the 5-year overall survival (OS) rate of LC remained at 21.2% in the United States (3). Hence, the underlying pathogenesis, prognostic markers, and equivalent targets of NSCLC should be understood and identified to enhance individualized therapeutic methods and associated prognosis. The changes in specific protein-related genes, such as mutations, translocations, deletions, and insertions, may assist in cancer development and tumor genetic regulation. In reality, some studies have demonstrated that microtubule-associated proteins (MAPs) are abnormally expressed in a variety of tumors, such as glioma (4), leukemia (5), and NSCLC (6).

MAP family, a series of proteins that were initially discovered to bind and stabilize microtubules, is generally classified into five groups based on their mode of function: (a) motile MAPs (7, 8), (b) depolymerase MAPs (9), (c) microtubule nucleated MAPs (10), (d) microtubule terminal-binding MAPs (11), and (e) structural MAPs. These MAP family members enhance the stability of microtubules, regulate the relationship between microtubules and other cellular components, and play pivotal roles in a variety of physiological processes, such as the spindle assembly and neuron formation (12, 13).

To date, more than 13 subtypes of MAPs have been recognized in mammalian cells. These proteins have been sequentially numbered, including MAP1A, MAP1B, MAP1S, MAP2, MAP4, MAP6, MAP7, MAP7D1, MAP7D2, MAP7D3 (14). Previous studies have found aberrant expressions and their prognostic value in some members of the MAP family. For instance, MAP4 was considerably overexpressed in LUAD clinical tissues and multiple cell lines (15). High expression of MAP4 was significantly associated with clinical and pathological stages of LUAD. At the same time, MAP2 is expressed explicitly in neuroendocrine carcinoma and relevant tumor cell lines, such as small cell lung cancer and neuroblastoma (15–17). Another study revealed that knockdown of MAP 1B-LC1 can decrease cell migration and invasion during epithelial–mesenchymal transition (EMT) in A549 cells (18). Nonetheless, the underlying mechanism by which MAP-related genes are regulated and the unique functions of MAP members in the development of NSCLC remain to be elucidated.

The relationship between abnormal expression levels of MAP family members and clinicopathologic staging and prognosis of NSCLC patients has been partially reported. Nevertheless, the roles of MAP members in the progression of NSCLC have not been analyzed using bioinformatics techniques. Hence, this study attempted to address this problem by analyzing the mRNA expression and mutations of different MAPs *via* microarray technology (19) and to identify the therapeutic potential personalized targets and prognostic value of MAPs for NSCLC patients. Meanwhile, the present study also determined the expected signaling pathways and corresponding functions of the MAP mutations as well as their 50 frequently altered neighbor genes.

Abbreviations: BP, biological process; CC, cell component; CIs, confidence intervals; DAVID, Database for Annotation, Visualization, and Integrated Discovery; EMT, epithelial–mesenchymal transition; GEPIA, Gene Expression Profiling Interactive Analysis; GO, Gene Ontology; HR, hazard ratio; KEGG, Kyoto Encyclopedia of Genes and Genomes; LC, lung carcinoma; LUAD, lung adenocarcinoma; LUSC, lung squamous cell carcinoma; MAPs, microtubule-associated proteins; MF, molecular function; NSCLC, non-small cell lung cancer; OS, overall survival; STRING, Search Tool for the Retrieval of Interacting Genes/Proteins; TCGA, The Cancer Genome Atlas; TCIA, The Cancer Immunome Atlas.

MATERIALS AND METHODS

Oncomine Analysis

Oncomine network station (http://www.oncomine.org/) is a tumor bioinformatics database that can provide services to DNA or RNA sequence analyses (20). In this study,

transcriptional expressions of 10 different MAPs in diverse cancer tissues were analyzed *via* the Oncomine datasets. The MAP mRNA transcription levels of different cancer specimens were compared with those in corresponding control specimens. And the differences in the expression levels of MAP mRNA were compared by Student's t-test. Cutoffs of p-value and fold change of expression levels were as follows: p-value: 0.01, fold change: 1.5, gene rank: 10%.

Gene Expression Profiling Interactive Analysis Dataset

The GEPIA website (http://gepia.cancer-pku.cn/) is a network database which can provide analytical services for the mRNA transcriptional expressions of tumor or normal tissues derived from TCGA and other projects (21). The relationships between mRNA expression of different MAPs family members and the clinical data of NSCLC patients, which involve the tumor types and pathological stages, were analyzed in this GEPIA dataset. The mRNA expression plots in GEPIA were consistent with the Log2(TPM + 1) scale.

Human Protein Atlas

The Human Protein Atlas website (https://www.proteinatlas.org) is a dataset that includes the various protein immunohistochemical patterns for common kinds of tumors and the corresponding different pathological types of these tumors (22). This network database can be utilized to identify specific mRNA/protein expression patterns in given tumors. In this study, the protein expression of different MAP members between human NSCLC and normal tissue specimens was compared directly by immunohistochemistry image.

The Kaplan–Meier Plotter

The potential prognostic value of different MAP members' transcription levels for patients with NSCLC was evaluated by an online database, Kaplan–Meier Plotter (http://kmplot.com/analysis/) (23). To analyze the correlation between the transcription levels of MAPs with OS of NSCLC patients, cancer specimens were split into two sets on account of median values of MAP mRNA expression (enriched and poor expression groups) and evaluated by Kaplan–Meier survival curves. In this study, the Kaplan–Meier survival plots include information on the hazard ratio (HR), 95% confidence intervals (CIs), and log-rank p-value that can be found in the Kaplan–Meier Plotter webpage. Additionally, the number-at-risk is revealed underneath the Kaplan–Meier survival patterns.

The Cancer Genome Atlas and cBioPortal

The Cancer Genome Atlas (TCGA) (24), a comprehensive project aimed at the prevention of cancer ultimately, included gene sequencing data of diverse human tumors. By selecting Pan-Lung Cancer (TCGA, Nat Genet 2016) dataset containing genetic data from 1,144 case reports, the online tool cBioportal (25) (http://www.cbioportal.org/) was employed to analyze the mutation status of all MAPs in the Pan-Lung Cancer. Genomic profiles in the Pan-Lung Cancer (TCGA, Nat Genet 2016) dataset included somatic mutations and putative copy number alterations from genomic identification of significant targets in cancer (GISTIC).

Extraction and Construction of Neighbor Gene Network

The Search Tool for the Retrieval of Interacting Genes/Proteins (STRING, https://string-db.org/) dataset, an interactive web server, is applicable to visualize, explore, and analyze the interrelationship between different proteins and equivalent genes (26). In this study, 50 frequently altered neighbor genes of the MAP family members were screened out, and a network has been constructed *via* the STRING dataset. This network of MAPs and neighbor genes provides valuable clues for analyzing the progress of NSCLC. This network pattern of MAPs and neighbor genes was constructed *via* the STRING website with the following setting: meaning of network edges: confidence; active interaction sources: text mining, experiments, databases, neighborhood; minimum required interaction score: 0.400; maximum number of interactors to show: 2nd shell–no more than 50 interactors.

The Gene Ontology and Kyoto Encyclopedia of Genes and Genomes Analysis

Gene Ontology (GO) and Kyoto Encyclopedia of Genes and Genomes (KEGG) were utilized to analyze the expected signaling pathways and corresponding functions of MAP mutations and their 50 frequently altered neighbor genes *via* the Database for Annotation, Visualization, and Integrated Discovery (DAVID) dataset (27) (https://david.ncifcrf.gov/summary.jsp). Starting from the three directions of biological process (BP), cell component (CC), and molecular function (MF), the expected functions of target gene mutation can be predicted and analyzed by GO analysis. Meanwhile, KEGG tool was exploited to analyze MAP mutations and their 50 frequently altered neighbor genes and to identify the MAP-associated predictive pathways.

The Cancer Immunome Atlas

The Cancer Immunome Atlas (TCIA; https://tcia.at/) is a dataset that contains TCGA data for 20 solid cancers with >8,000 tumor samples and can detect the immunophenoscore (IPS) of tumor samples, which can predict the response to cytotoxic T lymphocyte antigen-4 (CTLA-4) and programmed cell death protein 1 (PD-1) blockers (28). In this study, we got 1,037 IPSs of NSCLC samples *via* TCIA dataset. Meanwhile, NSCLC samples were divided into high and low expression groups according to the median value of MAPs/IPSs, respectively. In this way, we can analyze the relationships between MAPs and IPSs by the chi-square test and further clarify the correlations between MAPs and the response to immunotherapy.

Tissue Collection

NSCLC tissues and adjacent non-tumor lung tissues were obtained from 20 patients (10 LUAD and 10 LUSC) who had undergone surgical resection of NSCLC during 2010–2013 in

West China Hospital (WCH), Sichuan University, China. The patients were diagnosed with NSCLC based on histopathological evaluation. No treatment was performed preoperatively. All tissue samples were immediately snap-frozen in liquid nitrogen and then stored at −80°C until RNA extraction. The non-tumor tissue was located 5 cm from the edge of the tumor. According to the pathologist, no significant tumor cells were found in these areas. The study was approved by the Research Ethics Committee of WCH, Sichuan University, China.

RNA Extraction and Reverse Transcription-Quantitative Polymerase Chain Reaction Analyses

Total RNA was extracted from tissues with the TRIzol reagent (Invitrogen, USA) according to the instructions. A reverse transcription kit (Takara, China) was used for cDNA synthesis. The reverse transcription-quantitative polymerase chain reaction (RT-qPCR) analysis was performed using a standard protocol from Power SYBR Green (Takara, China). The expression of MAPs was normalized using glyceraldehyde-3-phosphate dehydrogenase (GAPDH) as reference. The primers were synthesized by Tsingke (Chengdu, China). The primer sequences used in the studies are shown in **Supplementary Table S1**. The relative expression level of MAPs was calculated using $2^{-\Delta\Delta Ct}$ method and normalized by log2.

RESULTS

Transcriptional Levels of Diverse Family Members of Microtubule-Associated Proteins in Non-Small Cell Lung Cancer

In order to compare the mRNA transcriptional levels of different MAP members in tumors with those in control specimens, mRNA expression data were accessed and analyzed using the Oncomine database (www.oncomine.org). As shown in **Figure 1**, mRNA transcription levels of 10 members of MAPs in 20 types of tumors were retrieved and compared with those in normal tissues. Significantly higher mRNA expressions of MAP1A/1B/1S/2/7/7D2 were found in lung cancer specimens in numerous datasets (**Figure 1**). In this study, mRNA transcription levels of MAPs in NSCLC patients were our main observation object. In the Garber Lung dataset (29), MAP1B overexpression was found in LUSC specimens compared to control specimens with a fold change of 4.108 (p = 3.95E-4). Meanwhile, a 2.384-fold increase in MAP1B mRNA expression was observed in large cell lung carcinoma samples (p = 4E-3). Besides, the Hou Lung dataset (30) revealed a 3.136-fold increase in MAP1B mRNA expression in large cell lung carcinoma tissues (p = 9.06E-6) (**Table 1**). In the Selamat Lung dataset (31), MAP1S was enriched in LUAD with a 1.786-fold increase (p = 6.09E-17) (**Table 1**). Similarly, the Su Lung dataset (32) showed another mRNA expression with a boost; that is, MAP2 has a 1.620-fold increase in LUAD specimens compared with control specimens (p = 7.13E-4) (**Table 1**).

Moreover, the Su Lung dataset (32) showed a 1.706-fold increase in MAP7 mRNA expression in LUAD tissues (p = 1.25E-4) (**Table 1**). Significant upregulation of MAP7D2 was also found in NSCLC specimens compared to normal tissues. The result from the Hou Lung dataset (30) showed that there were 5.453-fold (p = 1.33E-6) in MAP7D2 mRNA expression in large cell lung carcinoma. In contrast, the Okayama Lung dataset (33) revealed a 6.785-fold increase in MAP7D2 mRNA expression in LUAD tissues (p = 4.31E-11) (**Table 1**).

The Transcriptional Pattern of Microtubule-Associated Proteins in The Cancer Genome Atlas

GEPIA is a newly developed interactive web server for analyzing the RNA sequencing expression data of 9,736 tumors and 8,587 normal samples from TCGA and the GTEx projects using a standard processing pipeline. In order to explore potential personalized therapeutic targets and prognostic value of different MAP members in NSCLC tissues with those in normal specimens, mRNA and protein expression data were accessed and analyzed by Gene Expression Profiling Interactive Analysis (GEPIA) dataset and Human Protein Atlas (https://www.proteinatlas.org). Firstly, utilizing the GEPIA, transcription levels of different MAPs between LUAD, LUSC, and normal lung specimens were compared. The results indicated that the transcription levels of MAP7/7D2 were higher in LUAD and LUSC specimens than those in normal lung specimens, while those of MAP2/4/6/7D3 were just the opposite (**Figure 2**). MAP2/4/6/7/7D2/7D3 groups significantly varied, whereas MAP1A/1B/1S/7D1 groups did not significantly differ (**Supplementary Figure S1**). Furthermore, the transcription levels of the MAP4 group in LUAD tissues and the MAP7D3 group in LUSC tissues were not significantly different from those in normal lung specimens (**Figure 2**). Besides, transcription levels of different MAPs with clinical cancer stage were also analyzed for LUSC and LUAD. The results indicated that the transcription level of MAP6 in NSCLC was significantly varied and correlated with advanced tumor stage (**Figure 3**).

After comparing the transcription levels of MAPs in LUAD, LUSC, and normal lung specimens, in the present study, Human Protein Atlas was implemented to examine and measure the protein expression levels of MAPs in LUAD, LUSC tissues, and normal lung specimens. MAP1A protein was not expressed in LUAD, LUSC, and normal lung specimens, as diagrammed in **Figure 4**. Meanwhile, MAP1B/7D2 proteins were not observed to be expressed in normal lung specimens, while medium expression was shown in LUSC specimens (**Figure 4**). Similarly, low protein expression of MAP7 was observed in normal lung specimens, while high protein expression was demonstrated in LUAD and LUSC specimens (**Figure 4**). Furthermore, higher protein expression of MAP1S/2/4/6/7D1/7D3 was expressed in normal lung specimens, while lower protein expression was observed in LUAD or/and LUSC tissues (**Figure 4**). Taken together, the results derived from the Human Protein Atlas dataset showed

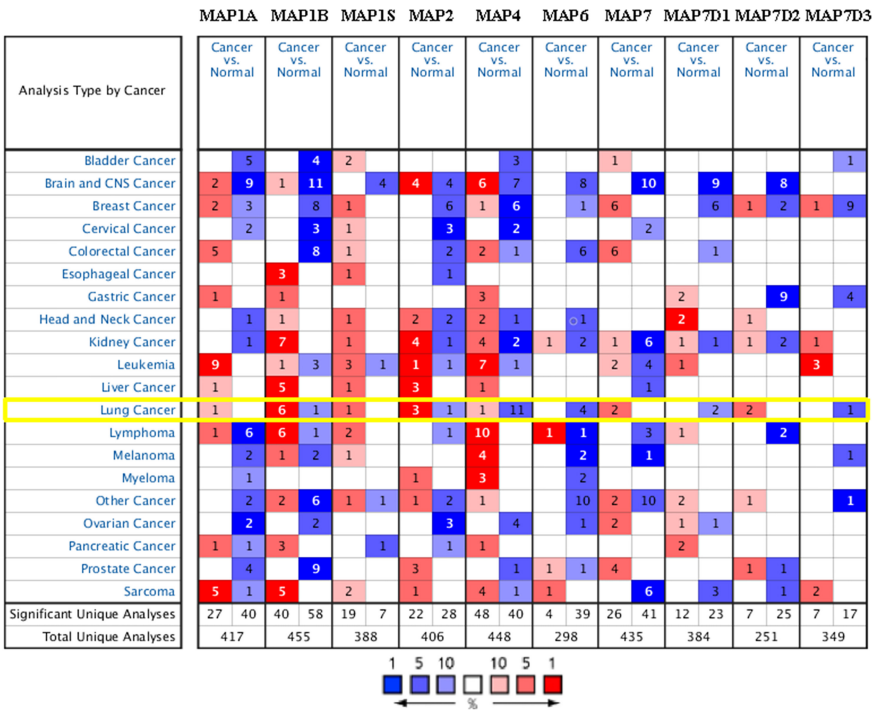

FIGURE 1 | Transcriptional expression of MAPs in 20 types of tumors (Oncomine database). Differences in mRNA levels of MAPs were compared by Student's t-test. Cutoffs of p-value and fold change of expression levels were as follows: p-value: 0.01, fold change: 1.5, gene rank: 10%. MAP, microtubule-associated protein.

TABLE 1 | Differences in transcriptional expression of diverse MAPs between NSCLC and normal lung specimens (Oncomine Database).

	Types of NSCLC *vs.* Lung	Fold Change	p-Value	Source and/or Reference
MAP1B				
	Squamous cell lung carcinoma	4.108	3.95E-4	Garber Lung (29)
	Large cell lung carcinoma	2.384	4E-3	Garber Lung (29)
	Large cell lung carcinoma	3.136	9.06E-6	Hou Lung (30)
MAP1S				
	Lung adenocarcinoma	1.786	6.09E-17	Selamat Lung (31)
MAP2				
	Lung adenocarcinoma	1.620	7.13E-4	Su Lung (32)
MAP7				
	Lung adenocarcinoma	1.706	1.25E-4	Su Lung (32)
MAP7D2				
	Large cell lung carcinoma	5.453	1.33E-6	Hou Lung (30)
	Lung adenocarcinoma	6.785	4.31E-11	Okayama Lung (33)

NSCLC, non-small cell lung cancer; MAP, microtubule-associated protein.

that transcriptional and proteinic expression levels of MAP1B/7/7D2 were more enriched in LUAD or/and LUSC specimens than those in normal lung specimens, while those of MAP1S/2/4/6/7D1/7D3 were just the opposite.

Prognostic Value of Diverse Microtubule-Associated Proteins in Non-Small Cell Lung Cancer

Furthermore, the Kaplan–Meier plotter was applicable to analyze the correlation between mRNA transcription levels of MAPs and patient prognosis in NSCLC. As **Figure 5** shows, most MAPs were significantly correlated with the prognosis of NSCLC. The analysis plots revealed that higher mRNA expression of MAP1A/1S was significantly correlated with shorter OS of NSCLC patients, while that of MAP2/4/6/7/7D3 was just the opposite (**Figure 5**). Besides, MAP1B/7D1/7D2 mRNA expression levels showed no significant correlation with prognosis of NSCLC patients (**Supplementary Figure S2**). The above results revealed that the mRNA expression levels of MAP1A/1S/2/4/6/7/7D3 were significantly associated with the prognosis of NSCLC patients, and they might be utilized as possible prognostic markers in NSCLC patients.

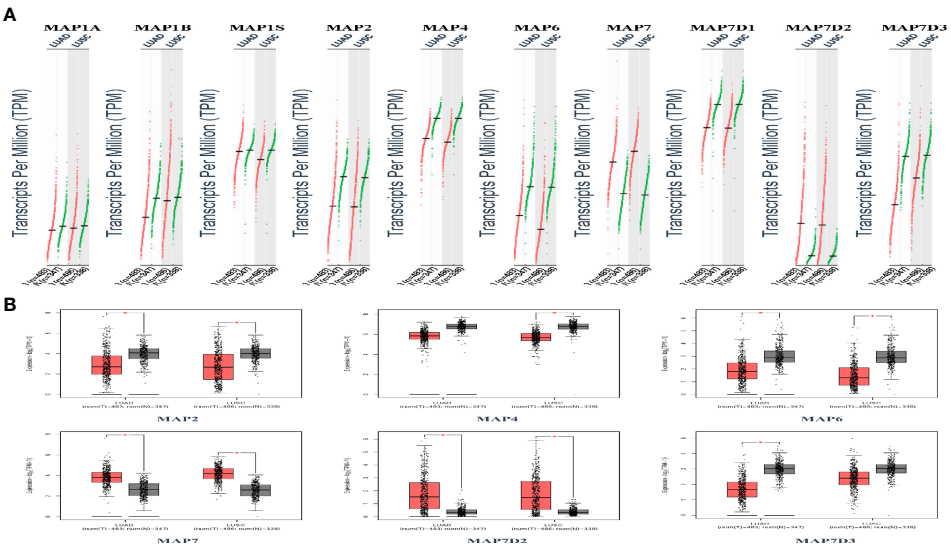

FIGURE 2 | Transcription levels of distinct MAPs in LUAD, LUSC, and normal lung specimens (GEPIA). **(A)** Scatter diagram. **(B)** Box plot. *p < 0.05. GEPIA, Gene Expression Profiling Interactive Analysis; LUAD, lung adenocarcinoma; LUSC, lung squamous cell carcinoma; MAP, microtubule-associated protein.

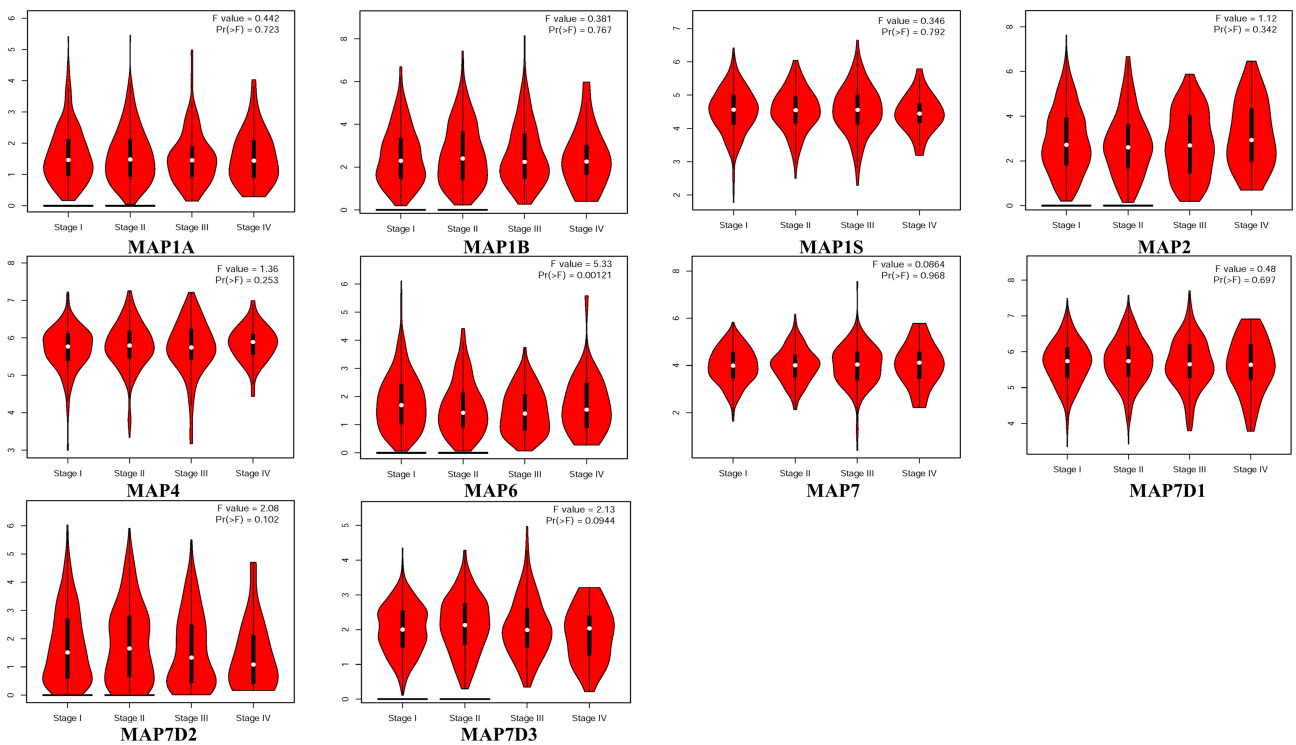

FIGURE 3 | Correlation between MAP expression and cancer stage in NSCLC (GEPIA). GEPIA, Gene Expression Profiling Interactive Analysis; MAP, microtubule-associated protein; NSCLC, non-small cell lung cancer.

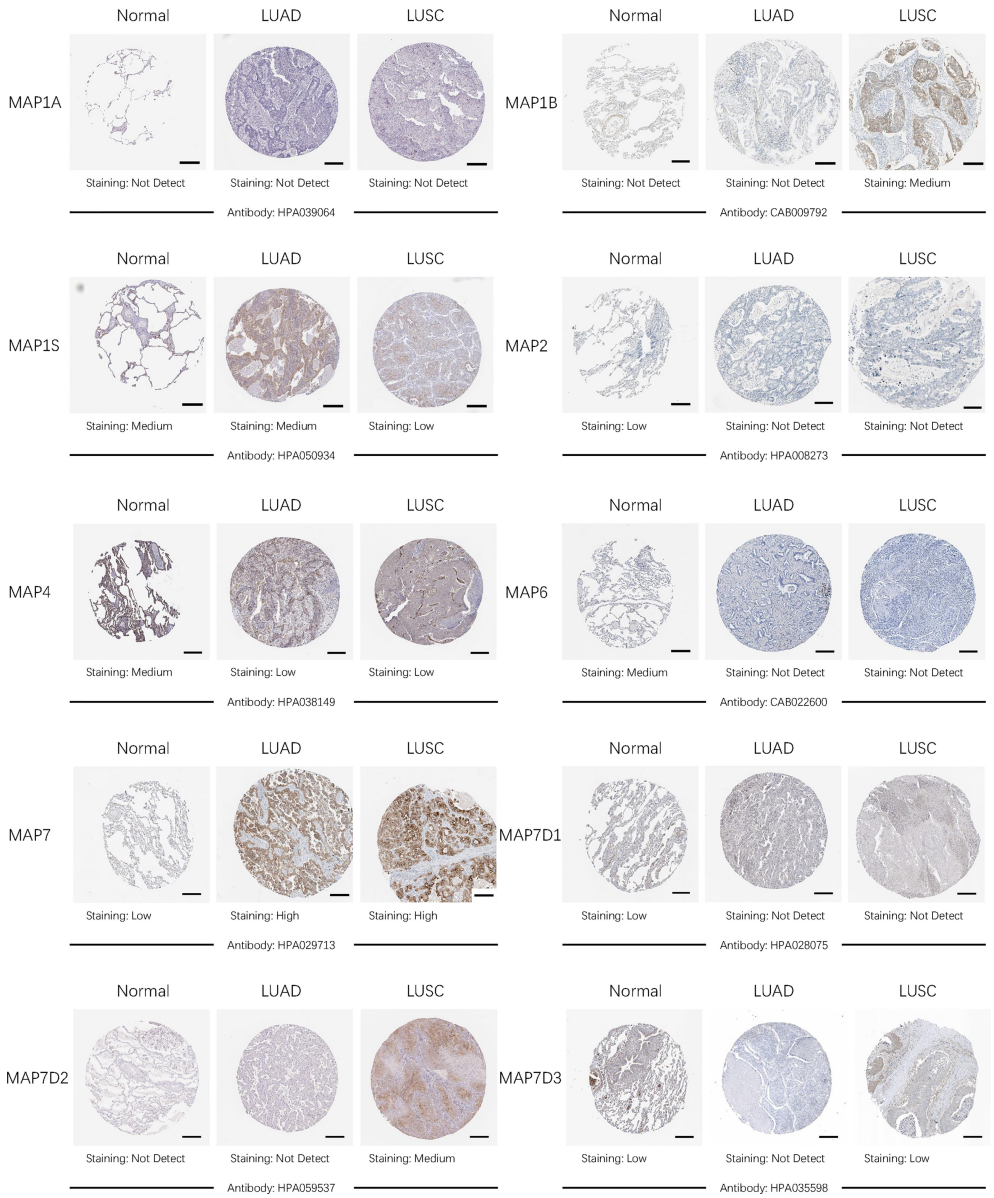

FIGURE 4 | Representative immunohistochemistry images of distinct MAPs in cancer and paratumor tissues (Human Protein Atlas). MAP, microtubule-associated protein.

Expected Signaling Pathways and Corresponding Functions of the Microtubule-Associated Protein Mutations and Their Frequently Altered Neighbor Genes in Non-Small Cell Lung Cancer

After analyzing the prognostic value of different MAPs in NSCLC, the MAP alterations were analyzed by utilizing the cBioPortal dataset (www.cbioportal.org) for NSCLC (**Figure 6**). The results showed that MAP alterations were present in 324/1144 NSCLC patients (28%) (**Figure 6**). Next, 50 frequently altered neighbor genes, which were significantly correlated with MAP mutations, and associated networks were further analyzed and constructed *via* the STRING dataset (**Figure 7**). The results showed that the Hippo signaling pathway-related genes, including DLG1, DLG2, DLG3, DLG4, RASSF1, and GSK-3β, were significantly associated with MAP alterations (**Figure 7**).

Moreover, in the present study, GO and KEGG were utilized to analyze the expected signaling pathways and corresponding functions of MAP mutations and their 50 frequently altered neighbor genes *via* the DAVID dataset. Proceeding from the three directions of BP, CC, and MF, the expected functions of target gene mutation can be predicted and analyzed by GO analysis (**Figure 8**). The BPs such as GO: 0022604 (regulation of cell morphogenesis),

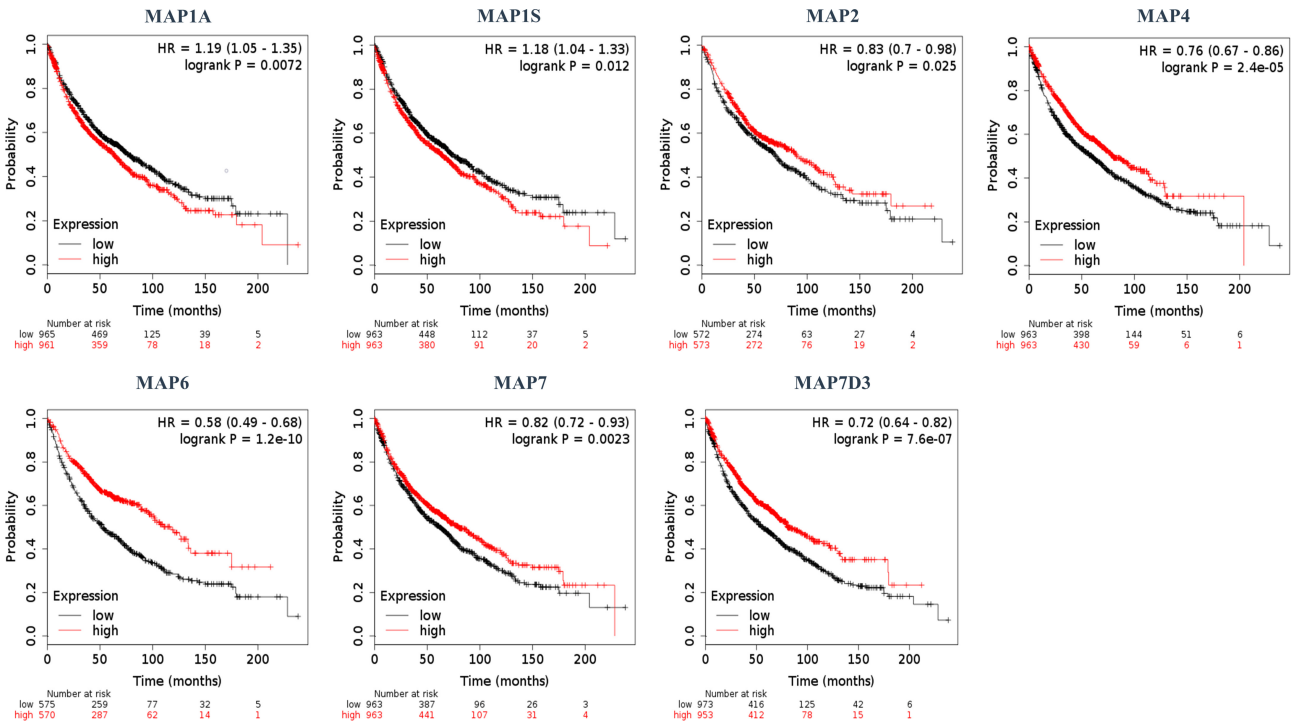

FIGURE 5 | Kaplan–Meier survival curves stratified by seven MAPs, respectively. MAP, microtubule-associated protein.

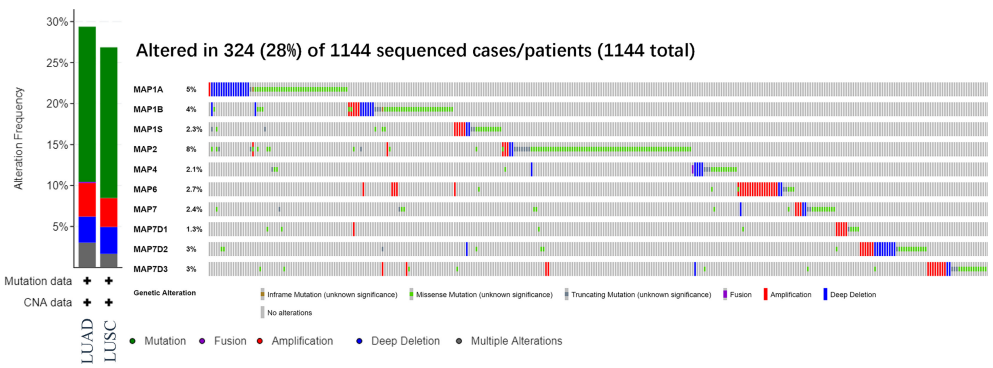

FIGURE 6 | MAP gene alterations analysis in LUAD and LUSC (cBioPortal). LUAD, lung adenocarcinoma; LUSC, lung squamous cell carcinoma; MAP, microtubule-associated protein.

GO: 0010975 (regulation of neuron projection development), GO: 0007409 (axonogenesis), GO: 0016358 (dendrite development), and GO: 0010769 (regulation of cell morphogenesis involved in differentiation) were remarkably regulated by the MAP mutations in NSCLC (**Figure 8**). The CCs, including GO: 0005874 (microtubule), GO: 0033267 (axon part), GO: 0043025 (neuronal cell body), and GO: 0150034 (distal axon) were likewise significantly associated with the MAP alterations (**Figure 8**). Also, MAP mutations prominently affected the MFs, such as GO: 0015631 (tubulin binding), GO: 0008017 (microtubule binding), and GO: 0003779 (actin binding) (**Figure 8**).

Furthermore, in this study, we exploited the KEGG tool to analyze MAP mutations and their 50 frequently altered neighbor genes and to identify the MAP-related predictive pathways (**Figure 9**). The analysis result indicated that three pathways including has: 04390 (Hippo signaling pathway), has: 05017 (Spinocerebellar ataxia), and has: 05165 (Human papillomavirus infection) were associated with the functions of MAP mutations in NSCLC (**Figure 9**). As shown in **Figure 10**, the human papillomavirus infection signal pathway regulated by MAP mutations of NSCLC patients can be predicted using KEGG analysis.

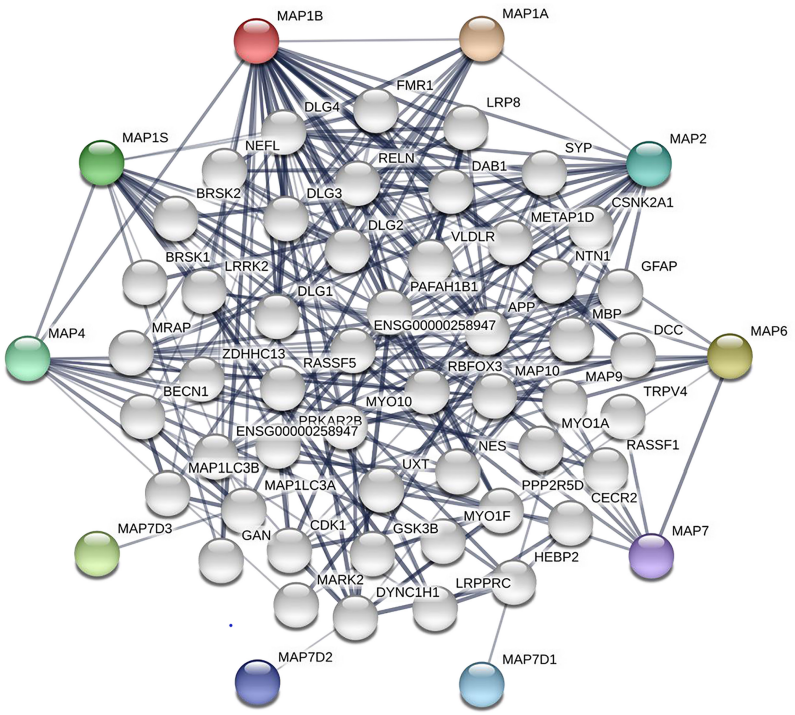

FIGURE 7 | Network of MAP mutations and their 50 frequently altered neighbor genes in NSCLC (STRING). MAP, microtubule-associated protein; NSCLC, non-small cell lung cancer; STRING, Search Tool for the Retrieval of Interacting Genes/Proteins.

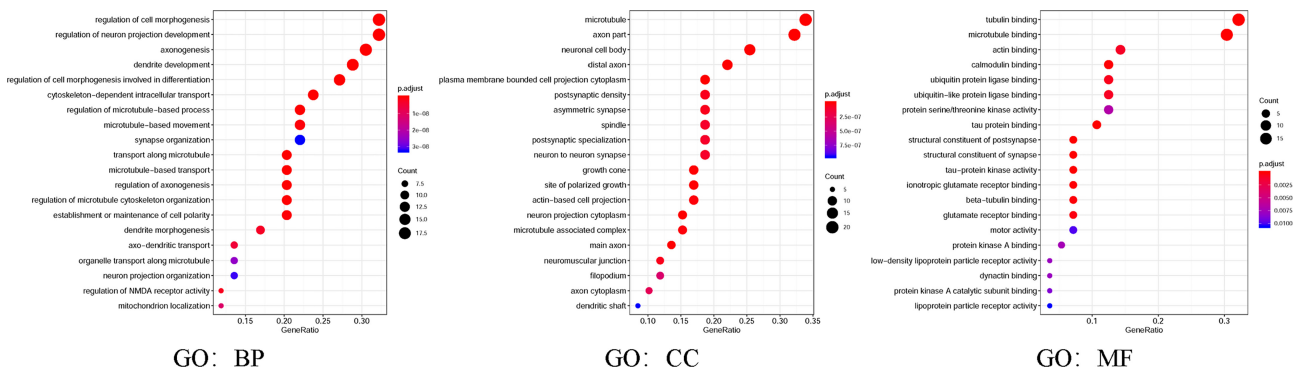

FIGURE 8 | Gene Ontology (GO) was utilized to analyze the expected functions of MAP mutations and their 50 frequently altered neighbor genes *via* the DAVID dataset. Starting from the three directions of biological processes (GO: BP), cell components (GO: CC), and molecular functions (GO: MF), the expected functions of target gene mutation can be predicted and analyzed. DAVID, Database for Annotation, Visualization, and Integrated Discovery; MAP, microtubule-associated protein.

Microtubule-Associated Protein Expression Was Significantly Correlated With Response to Immunotherapy in Non-Small Cell Lung Cancer

Tumor-infiltrating lymphocytes were different in the high and low expression groups of MAPs (**Supplementary Figure S3**). In order to determine the relationship between MAPs and the response to CTLA-4 and PD-1 blockers, firstly, we calculated the IPS of 1,037 NSCLC samples exported from TCGA database by TCIA (https://tcia.at/) database (**Supplementary Material S1** and **Supplementary Table S2**). Then, the 1,037 NSCLC samples were divided into high and low expression groups according to the median value of MAPs/IPS (**Supplementary Tables S2, S3**), respectively. Next, the relationships between MAPs and IPS were analyzed by the chi-square test. As **Table 2** shows, the expression levels of MAP1A/1B/1S/4/6/7D1/7D3 were significantly correlated with IPS in NSCLC patients. The higher the IPS, the better the response to CTLA-4 and PD-1 blockers (28). Thus, we can conclude

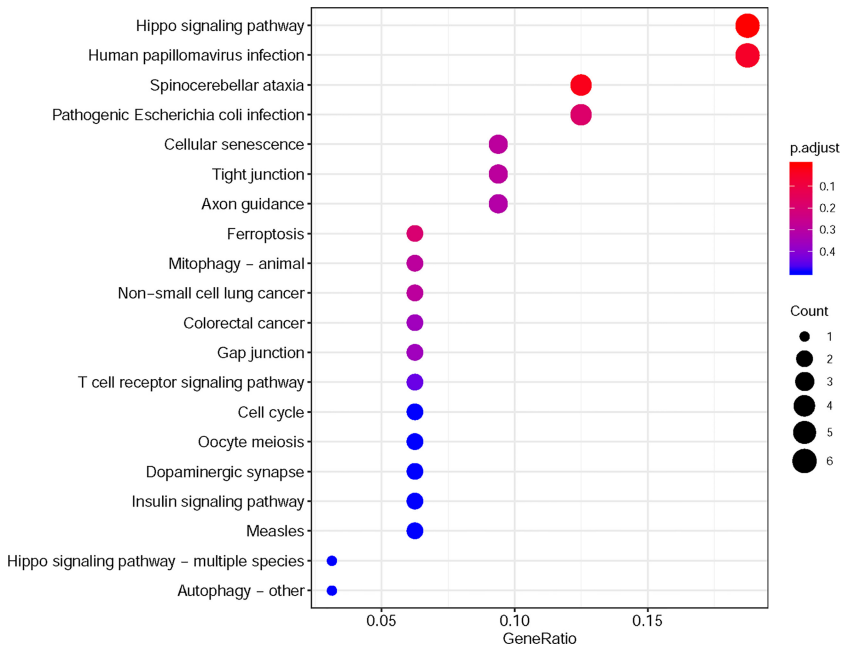

FIGURE 9 | KEGG pathway analysis tool was utilized to analyze the predicted pathways of MAP mutations and their 50 frequently altered neighbor genes *via* the DAVID dataset. DAVID, Database for Annotation, Visualization, and Integrated Discovery; KEGG, Kyoto Encyclopedia of Genes and Genomes; MAP, microtubule-associated protein.

that the expression levels of MAP1A/1B/1S/4/6/7D1/7D3 were closely related to the response to immunotherapy.

Reverse Transcription-Quantitative Polymerase Chain Reaction Results Agreed With Gene Expression Profiling Interactive Analysis: MAP7/7D2 Expression Was Higher in Non-Small Cell Lung Cancer Samples Than That in Paratumor Tissues, but MAP2/4/6/7D3 Expression Was the Opposite

Expression profiles of MAPs in 20 pairs of NSCLC samples and paratumor tissues were evaluated using RT-qPCR that was performed by ourselves. Results are given below: MAP7/7D2 expression was higher in NSCLC samples than that in paratumor tissues, but MAP2/4 expression was the opposite. Besides, MAP1A/1B/1S/7D1 expression was similar between NSCLC samples and paratumor tissues (**Figure 11**; * $p < 0.05$). Similarly, MAP6/7D3 expression was also lower in NSCLC samples than in paratumor tissues, albeit with no statistical significance achieved (**Supplementary Figure S4**). All the above results are consistent with the analysis results of GEPIA.

DISCUSSION

Being important components to bind and stabilize microtubules in a variety of physiologies, such as the assembly of spindles during cell division in mammalian cells, MAP family members are implicated in the development of multiple cancers, including NSCLC. Although the MAP family has been ascertained to play critical roles in tumorigenesis and prognosis of a variety of tumors, further bioinformatics analysis of distinct roles of MAP family members in NSCLC remains to be performed. The present study explored the mRNA transcription levels, protein expression levels, and associated prognosis (OS) of diverse members of MAPs in NSCLC patients. Moreover, it is supposed that the findings of the present research might contribute to broadening current knowledge, improving the design of cancer treatments, and improving the accuracy of prognosis in patients with NSCLC.

Results from this research indicated that enriched mRNA transcription and protein expression levels were observed in fractional members of MAP relevant genes, and mRNA expression of MAP members was associated with cancer stages in NSCLC patients. Higher transcription levels of MAP1/1S were significantly correlated with shorter OS in NSCLC, while higher mRNA expression levels of MAP2/4/6/7/7D3 exhibited superiority in OS of NSCLC patients. Besides, the 50 frequently altered neighbor genes, which were significantly correlated with MAP mutations, and associated network were further analyzed and constructed. This study revealed that the Hippo signaling pathway relevant genes, such as DLG1, DLG2, DLG3, DLG4, RASSF1, and GSK-3β, were significantly associated with MAP alterations. Moreover, the results from GO enrichment analysis and KEGG analysis revealed that the

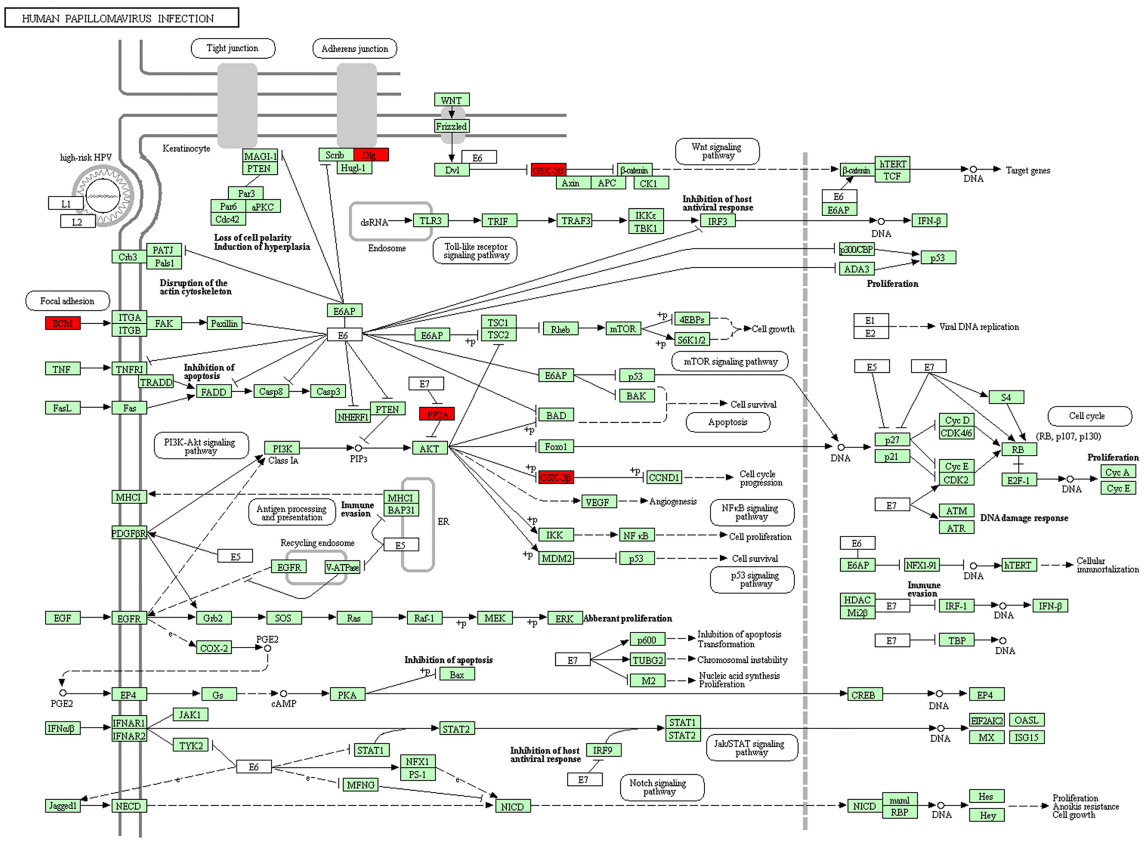

FIGURE 10 | Human papillomavirus infection signal pathway regulated by MAP mutations of NSCLC patients (DAVID). DAVID, Database for Annotation, Visualization, and Integrated Discovery; MAP, microtubule-associated protein; NSCLC, non-small cell lung cancer.

TABLE 2 | Correlations between MAPs and IPS (chi-square test).

	Gene expression	Cases	IPS-High	IPS-Low	p-Value
MAP1A	High	518	320	198	0.004480 *
	Low	519	365	154	
MAP1B	High	518	310	208	0.000033 *
	Low	519	375	144	
MAP1S	High	518	364	154	0.005147 *
	Low	519	321	198	
MAP2	High	518	349	169	0.406379
	Low	519	336	183	
MAP4	High	518	317	201	0.001213 *
	Low	519	368	151	
MAP6	High	518	373	145	0.000069 *
	Low	519	312	207	
MAP7	High	518	342	176	0.965447
	Low	519	343	176	
MAP7D1	High	518	323	195	0.014336 *
	Low	519	362	157	
MAP7D2	High	518	342	176	0.965447
	Low	519	343	176	
MAP7D3	High	518	295	223	<0.000001*
	Low	519	390	129	

*MAP, microtubule-associated protein; IPS, immunophenoscore. *p < 0.05.*

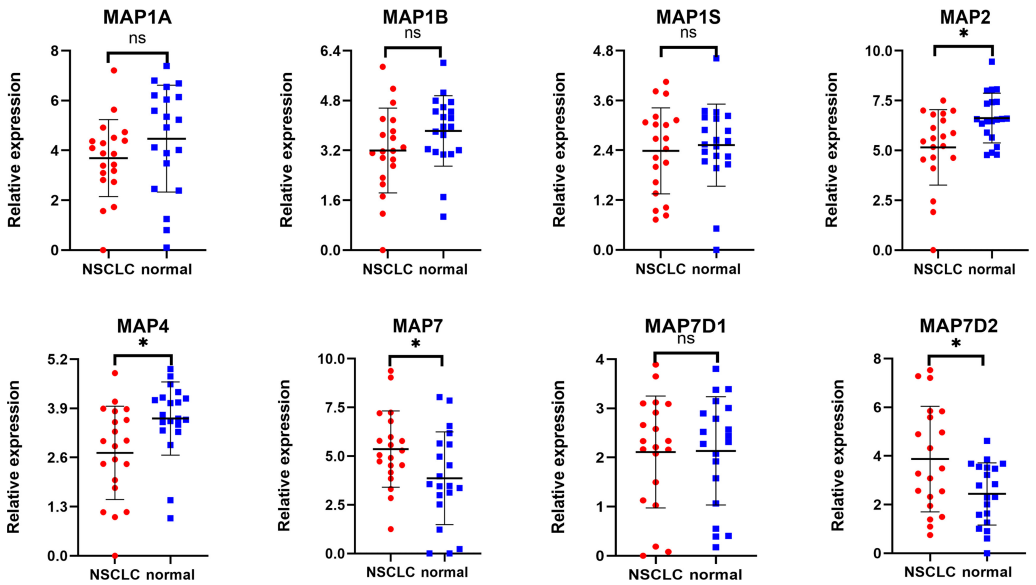

FIGURE 11 | RT-qPCR analysis of MAP expression in 20 pairs of NSCLC samples and paratumor tissues. *p < 0.05. MAP, microtubule-associated protein; NSCLC, non-small cell lung cancer; RT-qPCR, reverse transcription-quantitative polymerase chain reaction. ns, not significant.

BPs such as GO: 0022604 (regulation of cell morphogenesis), CCs such as GO: 0005874 (microtubule), MFs such as GO: 0015631 (tubulin binding), and pathways such as has: 04390 (Hippo signaling pathway) were remarkably regulated by the MAP mutations in NSCLC. Further analysis of TCIA showed that the expression levels of MAP1A/1B/1S/4/6/7D1/7D3 were closely related to the response to immunotherapy. Finally, this study verified MAP7/7D2 expression was higher in NSCLC samples than in paratumor tissues of 20 NSCLC patients, but MAP2/4/6/7D3 expression was the opposite by RT-qPCR.

Among the MAPs, the MAP1 family is the first group of microtubule lattice-binding structural proteins discovered in the body that can interact with actin and microtubules (34). In the human genome, the MAP1 family typically consists of three members, namely, the MAP1A, MAP1B, and MAP1S (35). Recent studies have revealed that when exposed to cisplatin, increased autophagy level of LUAD cells was detected by Western blot analysis of the autophagosome-associated light chain 3 of MAP1A/1B (36). Moreover, the MAP1B has been reported to be a new target in paraneoplastic neuropathy and has a high predictive value for small cell lung cancer (5). In fact, knockdown of MAP1B-LC1 can also decrease cell migration and invasion during EMT in A549 cells (19). And similarly, MAP1S can bridge autophagic components with microtubules and mitochondria in both autophagosomal biogenesis and degradation (37). Another related article shows that the increased expression level of MAP1S could trigger autophagy, thereby inhibiting genomic instability to inhibit tumors (38). The present report indicated that the mRNA transcription level of MAP1A/1B/1S in NSCLC specimens was lower than the transcription level of normal specimens. Furthermore, through GEPIA, the results revealed that there was no significant correlation between mRNA transcription levels of MAP1A/1B/1S and the clinical stage of NSCLC patients. Furthermore, the MAP1 family relevant prognostic prediction of NSCLC patients was determined utilizing the Kaplan–Meier plotter. In NSCLC patients followed for 200 months, higher MAP1A and MAP1S expressions were significantly associated with poorer OS. But to our surprise, there was no significant correlation between the mRNA transcription level of MAP1B and the OS of NSCLC patients.

MAP2 is widely found in neurons and neurogenic tumor cells (39), and its ability to interact with microtubules plays a critical role in neuronal morphogenesis, such as neurite initiation (40). MAP2 is one of the neuronal MAPs that controls the cargo transport in the pre-axonal filtering zone of neurons (41). It has been shown that MAP2 is a valuable diagnostic tool to recognize and diagnose low-grade neuroepithelial neoplasms (17). In fact, MAP2 has been shown to be specifically expressed in neuroendocrine carcinoma and relevant tumor cell lines, such as small cell lung cancer and neuroblastoma (17, 18). In the present study, the results indicated that the mRNA transcription level of MAP2 in NSCLC specimens was lower than the transcription level of normal specimens, and this mRNA transcription level was not associated with the clinical stage of NSCLC patients. Besides, the lower MAP2 mRNA transcription level in NSCLC was significantly associated with a shorter OS.

The expression of MAP4 is ubiquitously observed in non-neural specimens and plays a critical role in microtubule assembly processes in human cells. The researchers found a higher proportion of MAP4 to stathmin mRNA in NSCLC tissues than the above proportion in normal specimens, demonstrating that this proportion might be a potential prognostic marker in NSCLC patients (42). Furthermore, *in vitro* studies have shown that MAP4 knockdown can effectively

prevent cancer cell migration and tumor invasion during tumor development in LUAD (16). Clinical statistical analysis also showed that MAP4 protein could accelerate tumor invasion and cancer cell migration, which are closely related to the progression of LUAD and poor prognosis (16). Another study showed that MAP4 had been identified as a potential prognostic marker for predicting the clinical efficacy of platinum-based chemotherapy in patients with NSCLC through proteomics analysis (7). In the present study, the results indicated that the mRNA transcription level of MAP4 in NSCLC specimens was lower than the transcription level of normal specimens, and this mRNA transcription level was not associated with the clinical stage of NSCLC patients. In addition, in all of the patients with NSCLC, a lower MAP4 mRNA transcription level was significantly associated with a shorter OS.

MAP6 is found highly expressed in several cells, such as neuron and skeletal muscle cells (43, 44). The deletion or abnormal expression of MAP6 gene can lead to a variety of diseases, such as schizophrenia and skeletal muscle dysfunction (44, 45). But, until now, there are still few studies on the correlation between the mRNA transcription level of MAP6 and the corresponding prognosis of NSCLC patients. In the present study, the results indicated that the mRNA transcription level of MAP6 was lower in NSCLC specimens than in normal specimens, but this mRNA transcription level was significantly correlated with the clinical stage of NSCLC patients. The lower mRNA transcription level of MAP6 was significantly correlated with shorter OS in all of the NSCLC patients. The RT-qPCR results verified that the expression level of MAP6 in NSCLC samples was relatively low compared with that in paratumor tissues, although it was not statistically significant, possibly because the sample size was not large enough.

Up to now, four different MAP7 subtypes have been discovered in the human genome, namely, MAP7, MAP7D1, MAP7D2, and MAP7D3 genes (46). Indeed, some studies indicate that MAP7 family proteins can directly or indirectly promote the binding process of Kalinin-1 with microtubules and contribute to the microtubule transport of cellular cargoes (46). Besides, other studies have shown that in cytogenetically normal patients with acute myeloid leukemia (AML), patients with high mRNA transcription levels of MAP7 are correlated with adverse OS compared to those with low MAP7 expression (6). At the same time, MAP7 has also been reported to promote the EMT process of human cervical cancer cells by regulating the autophagy pathway and accelerate the tumor progression of cervical cancer (47). But the correlation between the mRNA transcription level of MAP7 family and the corresponding prognosis of NSCLC patients has not been reported. The results demonstrated that mRNA transcription levels of MAP7 and MAP7D2 were obviously increased in NSCLC tissues, while the mRNA transcription levels of MAP7D1 and MAP7D3 were reversed. Next, more enriched mRNA transcription levels of MAP7/7D3 were significantly associated with favorable OS of NSCLC patients. The RT-qPCR results verified that the expression level of MAP7D3 in NSCLC samples was relatively low compared with that in paratumor tissues, although it was not statistically significant, possibly because the sample size was not large enough.

Although this study explored the relationship between mRNA transcription levels and protein expression levels of different MAPs and associated prognosis in NSCLC patients, it should be noted that there are some limitations in this study. Firstly, there are a large number of MAP family members, but not all of them are included in each database, so this study only discusses MAP members that exist in each database. Secondly, the expression data of MAPs in this study are derived from diverse literature and databases, so the research results may be affected by selection or information bias. Therefore, we need further verification in more clinical and basic studies.

CONCLUSIONS

In conclusion, this research systematically analyzed the correlation between the mRNA transcription level of MAP members and the corresponding prognosis/response to immunotherapy of NSCLC patients. The results of the present study revealed that more enriched mRNA transcription levels of MAP2/4/6/7/7D3 were observed to be prominently associated with favorable OS of NSCLC patients, while more enriched mRNA transcription levels of MAP1A/1S were associated with shorter OS. These results implied the high MAP1A/1S expression could serve as potential personalized therapeutic targets for patients with NSCLC, and the high MAP2/4/6/7/7D3 expression could serve as biomarkers for favorable prognosis in NSCLC. Moreover, the expression levels of MAP1A/1B/1S/4/6/7D1/7D3 were significantly correlated with IPS in NSCLC patients. Finally, the expression levels of MAP1A/1B/1S/4/6/7D1/7D3 were closely related to the response to immunotherapy.

DATA AVAILABILITY STATEMENT

The original contributions presented in the study are included in the article/**Supplementary Material**. Further inquiries can be directed to the corresponding author.

ETHICS STATEMENT

The present research was ratified *via* the West China Hospital of Sichuan University Biomedical Research Ethics Committee and was carried out in accordance with the principles of the Declaration of Helsinki. Besides, all data in this study were derived from databases and published literature to ensure that all written informed consent had already been signed.

AUTHOR CONTRIBUTIONS

JL and QH are co-first authors, who contributed equally to this work. Study design: JL, QH, and HD. Data collection: JL, TT, ZT,

YD, CC, and MG. Data reduction: JL, QH, HD, YQ, JZ, and XL. Results discussion and analysis: All authors. Article writing: JL. Manuscript modification: HD, MG, and XL. All authors contributed to the drafting and critical revision of the manuscript. All authors contributed to the article and approved the submitted version.

FUNDING

This study was supported by the National Natural Science Foundation of China Program grant (81972607) and 1.3.5 project for disciplines of excellence, West China Hospital, Sichuan University (ZYGD20003).

ACKNOWLEDGMENTS

We appreciate all the genetic and tumor databases mentioned in this article for providing sufficient data support for this study. We also thank all the individuals who contributed to this article for their extensive support in analyzing the data, writing the article, and facilitating communication.

SUPPLEMENTARY MATERIAL

The Supplementary Material for this article can be found online at: https://www.frontiersin.org/articles/10.3389/fonc.2021.680402/full#supplementary-material

REFERENCES

1. Arbour KC, Riely GJ. Systemic Therapy for Locally Advanced and Metastatic Non–Small Cell Lung Cancer: A Review. *JAMA* (2019) 322:764–74. doi: 10.1001/jama.2019.11058
2. Govindan R, Page N, Morgensztern D, Read W, Tierney R, Vlahiotis A, et al. Changing Epidemiology of Small-Cell Lung Cancer in the United States Over the Last 30 Years: Analysis of the Surveillance, Epidemiologic, and End Results Database. *J Clin Oncol* (2006) 24:4539–44. doi: 10.1200/JCO.2005.04.4859
3. Allemani C, Matsuda T, Carlo VD, Harewood R, Matz M, Niksic M, et al. Global Surveillance of Trends in Cancer Survival 2000-14 (CONCORD-3) Analysis of Individual Records for 37 513 025 Patients Diagnosed With One of 18 Cancers From 322 Population-Based Registries in 71 Countries. *Lancet* (2018) 391:1023–75. doi: 10.1016/S0140-6736(17)33326-3
4. Gadoth A, Kryzer TJ, Fryer J, Mckeon A, Lennon VA, Pittock SJ. Microtubule-Associated Protein 1B: Novel Paraneoplastic Biomarker. *Ann Neurol* (2017) 81:266–77. doi: 10.1002/ana.24872
5. Fu L, Fu H, Zhou L, Xu K, Pang Y, Hu K, et al. High Expression of MAP7 Predicts Adverse Prognosis in Young Patients With Cytogenetically Normal Acute Myeloid Leukemia. *Sci Rep* (2016) 6:34546. doi: 10.1038/srep34546
6. Bottger F, Schaaij-Visser TB, de Reus I, Piersma SR, Pham TV, Nagel R, et al. Proteome Analysis of Non-Small Cell Lung Cancer Cell Line Secretomes and Patient Sputum Reveals Biofluid Biomarker Candidates for Cisplatin Response Prediction. *J Proteomics* (2019) 196:106–19. doi: 10.1016/j.jprot.2019.01.018
7. Hirokawa N, Noda Y, Tanaka Y, Niwa S. Kinesin Superfamily Motor Proteins and Intracellular Transport. *Nat Rev Mol Cell Biol* (2009) 10:682–96. doi: 10.1038/nrm2774
8. Bhabha G, Johnson GT, Schroeder CM, Vale RD. How Dynein Moves Along Microtubules. *Trends Biochem Sci* (2016) 41:94–105. doi: 10.1016/j.tibs.2015.11.004
9. Mcnally FJ, Roll-Mecak A. Microtubule-Severing Enzymes: From Cellular Functions to Molecular Mechanism. *J Cell Biol* (2018) 217:4057–69. doi: 10.1083/jcb.201612104
10. Roostalu J, Surrey T. Microtubule Nucleation: Beyond the Template. *Nat Rev Mol Cell Biol* (2017) 18:702–10. doi: 10.1038/nrm.2017.75
11. Akhmanova A, Steinmetz MO. Control of Microtubule Organization and Dynamics: Two Ends in the Limelight. *Nat Rev Mol Cell Biol* (2015) 16:711–26. doi: 10.1038/nrm4084
12. Prosser SL, Pelletier L. Mitotic Spindle Assembly in Animal Cells: A Fine Balancing Act. *Nat Rev Mol Cell Biol* (2017) 18:187–201. doi: 10.1038/nrm.2016.162
13. Deloulme JC, Gory-Faure S, Mauconduit F, Chauvet S, Jonckheere J, Boulan B, et al. Microtubule-Associated Protein 6 Mediates Neuronal Connectivity Through Semaphorin 3E-Dependent Signalling for Axonal Growth. *Nat Commun* (2015) 6:7246. doi: 10.1038/ncomms8246
14. Bodakuntla S, Jijumon AS, Villablanca C, Gonzalezbillault C, Janke C. Microtubule-Associated Proteins: Structuring the Cytoskeleton. *Trends Cell Biol* (2019) 29:804–19. doi: 10.1016/j.tcb.2019.07.004
15. Xia X, He C, Wu A, Zhou J, Wu J. Microtubule-Associated Protein 4 Is a Prognostic Factor and Promotes Tumor Progression in Lung Adenocarcinoma. *Dis Markers* (2018) 2018:1–8. doi: 10.1155/2018/8956072
16. Blumcke I, Muller S, Buslei R, Riederer BM, Wiestler OD. Microtubule-Associated Protein-2 Immunoreactivity: A Useful Tool in the Differential Diagnosis of Low-Grade Neuroepithelial Tumors. *Acta Neuropathol* (2004) 108:89–96. doi: 10.1007/s00401-004-0873-8
17. Molenaar WM, Baker DL, Pleasure D, Lee VM, Trojanowski JQ. The Neuroendocrine and Neural Profiles of Neuroblastomas, Ganglioneuroblastomas, and Ganglioneuromas. *Am J Pathol* (1990) 136:375–82.
18. Li L, Yan S, Zhang H, Zhang M, Huang G, Chen M. Interaction of hnRNP K With MAP 1b-LC1 Promotes TGF-Beta1-Mediated Epithelial to Mesenchymal Transition in Lung Cancer Cells. *BMC Cancer* (2019) 19:894. doi: 10.1186/s12885-019-6119-x
19. Zhang W, Yu Y, Hertwig F, Thierry-Mieg J, Zhang W, Thierry-Mieg D, et al. Comparison of RNA-Seq and Microarray-Based Models for Clinical Endpoint Prediction. *Genome Biol* (2015) 16:133. doi: 10.1186/s13059-015-0694-1
20. Cheng G, Fan X, Hao M, Wang J, Zhou X, Sun X. Higher Levels of TIMP-1 Expression Are Associated With a Poor Prognosis in Triple-Negative Breast Cancer. *Mol Cancer* (2016) 15:30. doi: 10.1186/s12943-016-0515-5
21. Tang Z, Li C, Kang B, Gao G, Li C, Zhang Z. GEPIA: A Web Server for Cancer and Normal Gene Expression Profiling and Interactive Analyses. *Nucleic Acids Res* (2017) 45:W98–W102. doi: 10.1093/nar/gkx247
22. Thul PJ, Lindskog C. The Human Protein Atlas: A Spatial Map of the Human Proteome. *Protein Sci* (2018) 27:233–44. doi: 10.1002/pro.3307
23. Gyorffy B, Surowiak P, Budczies J, Lanczky A. Online Survival Analysis Software to Assess the Prognostic Value of Biomarkers Using Transcriptomic Data in Non-Small-Cell Lung Cancer. *PloS One* (2013) 8:e82241. doi: 10.1371/journal.pone.0082241
24. Sanchez-Vega F, Mina M, Armenia J, Chatila WK, Luna A, La KC, et al. Oncogenic Signaling Pathways in The Cancer Genome Atlas. *Cell* (2018) 173:321–37. doi: 10.1016/j.cell.2018.03.035
25. Soh KP, Szczurek E, Sakoparnig T, Beerenwinkel N. Predicting Cancer Type From Tumour DNA Signatures. *Genome Med* (2017) 9:104. doi: 10.1186/s13073-017-0493-2
26. Szklarczyk D, Morris JH, Cook H, Kuhn M, Wyder S, Simonovic M, et al. The STRING Database in 2017: Quality-Controlled Protein-Protein Association Networks, Made Broadly Accessible. *Nucleic Acids Res* (2017) 45:D362–8. doi: 10.1093/nar/gkw937
27. Kumar SU, Kumar DT, Siva R, Doss C, Zayed H. Integrative Bioinformatics Approaches to Map Potential Novel Genes and Pathways Involved in Ovarian Cancer. *Front Bioeng Biotechnol* (2019) 7:391. doi: 10.3389/fbioe.2019.00391
28. Charoentong P, Finotello F, Angelova M, Mayer C, Efremova M, Rieder D, et al. Pan-Cancer Immunogenomic Analyses Reveal Genotype-

Immunophenotype Relationships and Predictors of Response to Checkpoint Blockade. *Cell Rep* (2017) 18(1):248–62. doi: 10.1016/j.celrep.2016.12.019
29. Garber ME, Troyanskaya OG, Schluens K, Petersen S, Thaesler Z, Pacyna-Gengelbach M, et al. Diversity of Gene Expression in Adenocarcinoma of the Lung. *Proc Natl Acad Sci USA* (2001) 98:13784–9. doi: 10.1073/pnas.241500798
30. Hou J, Aerts J, den Hamer B, van Ijcken W, den Bakker M, Riegman P, et al. Gene Expression-Based Classification of non-Small Cell Lung Carcinomas and Survival Prediction. *PloS One* (2010) 5:e10312. doi: 10.1371/journal.pone.0010312
31. Selamat SA, Chung BS, Girard L, Zhang W, Zhang Y, Campan M, et al. Genome-Scale Analysis of DNA Methylation in Lung Adenocarcinoma and Integration With mRNA Expression. *Genome Res* (2012) 22:1197–211. doi: 10.1101/gr.132662.111
32. Su LJ, Chang CW, Wu YC, Chen KC, Lin CJ, Liang SC, et al. Selection of DDX5 as a Novel Internal Control for Q-RT-PCR From Microarray Data Using a Block Bootstrap Re-Sampling Scheme. *BMC Genomics* (2007) 8:140. doi: 10.1186/1471-2164-8-140
33. Okayama H, Kohno T, Ishii Y, Shimada Y, Shiraishi K, Iwakawa R, et al. Identification of Genes Upregulated in ALK-Positive and EGFR/KRAS/ALK-Negative Lung Adenocarcinomas. *Cancer Res* (2012) 72:100–11. doi: 10.1158/0008-5472.CAN-11-1403
34. Mohan R, John A. Microtubule-Associated Proteins as Direct Crosslinkers of Actin Filaments and Microtubules. *IUBMB Life* (2015) 67:395–403. doi: 10.1002/iub.1384
35. Halpain S, Dehmelt L. The MAP1 Family of Microtubule-Associated Proteins. *Genome Biol* (2006) 7:224. doi: 10.1186/gb-2006-7-6-224
36. Wu T, Wang MC, Jing L, Liu ZY, Guo H, Liu Y, et al. Autophagy Facilitates Lung Adenocarcinoma Resistance to Cisplatin Treatment by Activation of AMPK/mTOR Signaling Pathway. *Drug Des Devel Ther* (2015) 9:6421–31. doi: 10.2147/DDDT.S95606
37. Xie R, Nguyen S, Mckeehan K, Wang F, Mckeehan WL, Liu L. Microtubule-Associated Protein 1S (MAP1S) Bridges Autophagic Components With Microtubules and Mitochondria to Affect Autophagosomal Biogenesis and Degradation. *J Biol Chem* (2011) 286:10367–77. doi: 10.1074/jbc.M110.206532
38. Liu L, Mckeehan WL, Wang F, Xie R. MAP1S Enhances Autophagy to Suppress Tumorigenesis. *Autophagy* (2012) 8:278–80. doi: 10.4161/auto.8.2.18939
39. Zhou Y, Wu S, Liang C, Lin Y, Zou Y, Li K, et al. Transcriptional Upregulation of Microtubule-Associated Protein 2 Is Involved in the Protein Kinase A-Induced Decrease in the Invasiveness of Glioma Cells. *Neuro Oncol* (2015) 17:1578–88. doi: 10.1093/neuonc/nov060
40. Dehmelt L, Halpain S. The MAP2/Tau Family of Microtubule-Associated Proteins. *Genome Biol* (2005) 6:204. doi: 10.1186/gb-2004-6-1-204
41. Gumy LF, Katrukha EA, Grigoriev I, Jaarsma D, Kapitein LC, Akhmanova A, et al. MAP2 Defines a Pre-Axonal Filtering Zone to Regulate KIF1- Versus KIF5-Dependent Cargo Transport in Sensory Neurons. *Neuron* (2017) 94:347–62. doi: 10.1016/j.neuron.2017.03.046
42. Cucchiarelli V, Hiser L, Smith H, Frankfurter A, Spano A, Correia JJ, et al. Beta-Tubulin Isotype Classes II and V Expression Patterns in Nonsmall Cell Lung Carcinomas. *Cell Motil Cytoskeleton* (2008) 65:675–85. doi: 10.1002/cm.20297
43. Tortosa E, Adolfs Y, Fukata M, Pasterkamp RJ, Kapitein LC, Hoogenraad CC. Dynamic Palmitoylation Targets MAP6 to the Axon to Promote Microtubule Stabilization During Neuronal Polarization. *Neuron* (2017) 94:809–25. doi: 10.1016/j.neuron.2017.04.042
44. Sebastien M, Giannesini B, Aubin P, Brocard J, Chivet M, Pietrangelo L, et al. Deletion of the Microtubule-Associated Protein 6 (MAP6) Results in Skeletal Muscle Dysfunction. *Skelet Muscle* (2018) 8:30. doi: 10.1186/s13395-018-0176-8
45. Merenlender-Wagner A, Shemer Z, Touloumi O, Lagoudaki R, Giladi E, Andrieux A, et al. New Horizons in Schizophrenia Treatment: Autophagy Protection Is Coupled With Behavioral Improvements in a Mouse Model of Schizophrenia. *Autophagy* (2014) 10:2324–32. doi: 10.4161/15548627.2014.984274
46. Hooikaas PJ, Martin M, Mühlethaler T, Kuijntjes GJ, Peeters C, Katrukha EA, et al. MAP7 Family Proteins Regulate Kinesin-1 Recruitment and Activation. *J Cell Biol* (2019) 218:1298–318. doi: 10.1083/jcb.201808065
47. Zhang L, Liu X, Song L, Zhai H, Chang C. MAP7 Promotes Migration and Invasion and Progression of Human Cervical Cancer Through Modulating the Autophagy. *Cancer Cell Int* (2020) 20:17. doi: 10.1186/s12935-020-1095-4

Conflict of Interest: The authors declare that the research was conducted in the absence of any commercial or financial relationships that could be construed as a potential conflict of interest.

Publisher's Note: All claims expressed in this article are solely those of the authors and do not necessarily represent those of their affiliated organizations, or those of the publisher, the editors and the reviewers. Any product that may be evaluated in this article, or claim that may be made by its manufacturer, is not guaranteed or endorsed by the publisher.

frontiers in Immunology

CASE REPORT
published: 04 November 2021
doi: 10.3389/fimmu.2021.686057

Case Report: Complete Response to Nivolumab in a Patient With Programmed Cell Death 1 Ligand 1-Positive and Multiple Gene-Driven Anaplastic Lymphoma Kinase Tyrosine Kinase Inhibitor-Resistant Lung Adenocarcinoma

Wen Dong[1†], *Pengfei Lei*[2†], *Xin Liu*[3], *Qin Li*[3] *and Xiangyang Cheng*[4*]

[1] Department of Respiratory Medicine, Hainan Cancer Hospital, Haikou, China, [2] Department of Cardiothoracic Surgery, Yueyang Second People's Hospital, Yueyang, China, [3] Department of Medical Center, Geneplus-Beijing Institution, Beijing, China, [4] State Key Laboratory of Respiratory Disease, National Clinical Research Center for Respiratory Disease, Guangzhou Institute of Respiratory Health, The First Affiliated Hospital of Guangzhou Medical University, Guangzhou, China

OPEN ACCESS

Edited by:
Hongbo Hu,
Sichuan University, China

Reviewed by:
Devikala Gurusamy,
National Institutes of Health (NIH), United States
Xuchao Zhang,
Guangdong Provincial People's Hospital, China

***Correspondence:**
Xiangyang Cheng
xuewu1901@sina.com

[†]These authors have contributed equally to this work

Specialty section:
This article was submitted to Cancer Immunity and Immunotherapy, a section of the journal Frontiers in Immunology

Received: 26 March 2021
Accepted: 22 October 2021
Published: 04 November 2021

Citation:
Dong W, Lei P, Liu X, Li Q and Cheng X (2021) Case Report: Complete Response to Nivolumab in a Patient With Programmed Cell Death 1 Ligand 1-Positive and Multiple Gene-Driven Anaplastic Lymphoma Kinase Tyrosine Kinase Inhibitor-Resistant Lung Adenocarcinoma. Front. Immunol. 12:686057. doi: 10.3389/fimmu.2021.686057

Multiple gene-driven programmed cell death 1 ligand 1 (PD-L1)-expressing non-small-cell lung cancer (NSCLC) is very rare. Previous studies have shown that patients with NSCLC with anaplastic lymphoma kinase (*ALK*) gene rearrangement rarely benefit from PD-L1 inhibitors. Besides the secondary mutations in *ALK* gene, other mechanisms might contribute to tumor resistance to ALK tyrosine kinase inhibitors (ALK-TKIs). Herein, we present a case of PD-L1-overexpressing lung adenocarcinoma that harbors both *EML4-ALK* gene rearrangement and *BRAF* mutation. In particular, a second molecular analysis after resistance to first- and second-generation ALK-TKIs revealed a high PD-L1 expression and tumor mutation burden. Therefore, treatment with nivolumab monotherapy, an anti-PD-1 inhibitor, was started and the patient achieved complete remission. This case report suggested that PD-1 inhibitors might be an effective treatment option for patients with multiple gene-driven PD-L1-expressing NSCLC harboring *ALK* gene rearrangement.

Keywords: lung cancer, EML4-ALK, nivolumab, complete remission, PD-L1

INTRODUCTION

Next-generation sequencing has revealed new mechanisms that might contribute to drug resistance to anaplastic lymphoma kinase tyrosine kinase inhibitors (ALK-TKIs) in patients with non-small-cell lung cancer (NSCLC) with *ALK* gene rearrangement. These mechanisms include secondary *ALK* mutations and activation of bypass and downstream signaling pathways (1). Different strategies have been applied to overcome crizotinib resistance, including the use of second and third-generation ALK-TKIs for tumors with secondary *ALK* mutations, and corresponding targeted drugs to address drug resistance caused by activation of bypass or downstream signaling (1). However, additional complex drug

resistance mechanisms have not been reported on a large scale; therefore, no standard treatment strategies exist for patients with such resistance mechanisms. Herein, we present a 37-year-old patient with NSCLC with both *ALK* gene rearrangement and *BRAF* mutation detected at the time of diagnosis. Programmed cell death 1 ligand 1 (PD-L1) overexpression and bypass and downstream pathway-activating mutations were acquired after disease progression with crizotinib and ceritinib treatments. The patient was switched to nivolumab monotherapy and finally achieved complete remission.

CASE DESCRIPTION

A 37-year-old non-smoker patient presented to our department with cough, sputum, and shortness of breath in December 2018. Computed tomography (CT) revealed a mass in the anterior inner basal segment of the left lower lobe with obstructive pneumonia. Lymph node metastasis was also found in the left hilar and mediastinal regions, and pericardial infiltration could not be excluded. Biopsy of the left lower lobe mass suggested a diagnosis of poorly differentiated adenocarcinoma (**Figure 1A**), and immunohistochemistry (IHC) showed positive expression of ALK (by VENTANA D5F3, Ventana Medical Systems, Inc., Oro Valley, AZ) and PD-L1 (Tumor Proportion Score, TPS=60%, by 22C3 pharmDx assay, Dako, Carpinteria, CA, USA) (**Figures 1B, C**). The initial DNA-based next-generation sequencing revealed echinoderm microtubule-associated protein-like 4 (*EML4*)-*ALK* fusion (v3), *BRAF* G466A, *PIK3CA* V344M mutation, and high tumor mutation burden (TMB, 13 Muts/Mb) in the plasma. The patient was finally diagnosed with left lung adenocarcinoma with multiple lymph node metastases (T2N3M0, Stage IIIb) and was treated with crizotinib, the first-generation ALK-TKI, 250 mg twice daily from December 2018. Treatment efficacy was evaluated as a partial remission in June 2019, while CT re-examination in July 2019 indicated an enlarged left lung mass, suggesting disease progression. Therefore, the patient was switched from crizotinib to a second-generation ALK-TKI ceritinib. However, 3 months later, CT showed a continued growth of the primary tumor as well as pericardial infiltration. In addition, simultaneous brain magnetic resonance imaging (MRI) suggested a right frontal lobe metastasis. A needle rebiopsy was performed on the patient's left lower lung lesion, along with a molecular analysis, ALK and PD-L1 detection. Results revealed a new *KRAS* G12D mutation, the EML4-ALK fusion was not detected in DNA analysis, but ALK positive expression was seen in IHC. The mutation frequencies of all gene mutations were less than 5% and close to each other (**Supplementary Table 1**). Additionally, the TMB was still high (14.4 Muts/Mb), and PD-L1 expression increased compared to the pre-treatment values (TPS=90%). IHC assay of CD4 (clone: B468A1, diluted at 1:200, Santa Cruz, Texas, USA) and CD8 (clone 144B, diluted at 1:100, Abcam, Cambridge, UK) expression

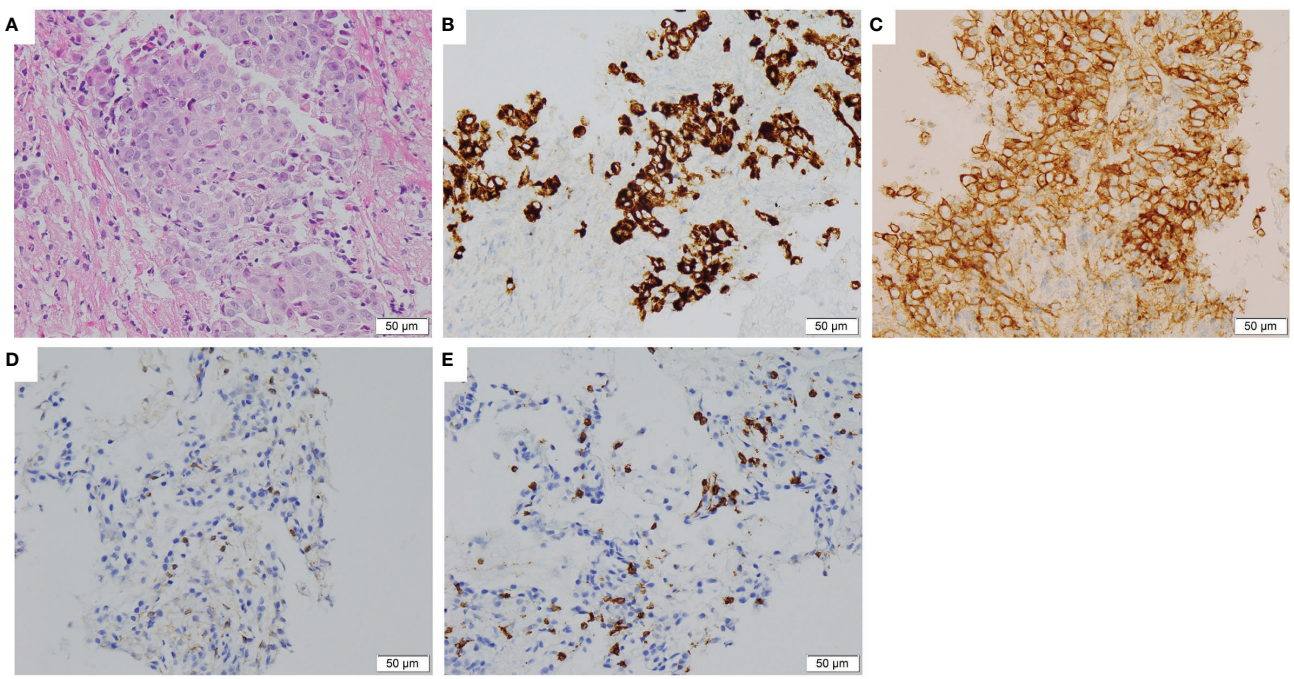

FIGURE 1 | Histopathological and immunohistochemical staining of the lung tumor tissue sample. **(A)** Hematoxylin and eosin staining showing a poorly differentiated adenocarcinoma of primary biopsy (400×). **(B)** IHC staining showed ALK overexpression in 95% tumor cells of primary biopsy (400×). **(C)** IHC staining showed PD-L1 expression with Tumor Proportion Score 60% of primary biopsy (400×). **(D, E)** IHC staining CD4 and CD8 expression on T cells of rebiopsy showed that CD8 was positive (about 10%), and CD4 was only infiltrated individually (400×). IHC, immunohistochemical; ALK, anaplastic lymphoma kinase; PD-L1, Programmed cell death 1 ligand 1.

on T cells showed that CD8 was positive (about 10%), and CD4 was only infiltrated individually (**Figures 1D, E**). Finally, the patient was switched to PD-1 inhibitor nivolumab monotherapy because he declined chemotherapy. In December 2019, after four cycles of nivolumab treatment, the primary lung lesion and metastatic lymph nodes almost disappeared, and the intracranial lesion decreased in size. Positron emission tomography-CT (PET-CT) showed that all target lesions disappeared in September 2020. Therefore, treatment efficacy was evaluated as complete remission (CR), according to the Response Evaluation Criteria in Solid Tumors version 1.1 (RECIST 1.1). The latest follow-up was in April 2021, suggesting that the patient remained in CR for 7 months and was under continuous treatment with nivolumab. No obvious toxic and side effects were observed during the treatment. The treatment process and radiological evaluation were summarized in **Figure 2**.

DISCUSSION

Acquired resistance to crizotinib, a first-generation ALK inhibitor, usually emerges one year after treatment onset (2). Previous studies have shown that secondary *ALK* mutations and bypass or downstream pathway mutations in *EGFR*, *KRAS*, *ErbB*, *PIK3CA*, and *MET* contribute to acquired ALK-TKI resistance (1, 3). Second- and third-generation ALK-TKIs have been developed to overcome drug resistance conferred by ALK kinase domain mutations (4, 5). This patient received crizotinib and ceritinib treatments sequentially; however, his progression-free survival (PFS) was less than one year. Although EML4-ALK fusion existed before and after ALK-TKIs treatment, it is worth noting that there were many other bypass and downstream pathway activation mutations at the same time. *BRAF* mutations exist in 1–3% of patients with lung cancer. The *BRAF* G466A mutation in the protein kinase domain has been reported in colorectal, lung, and skin cancers. Studies have shown that this mutation can lead to impaired kinase activity; however, it can activate the mitogen-activated protein kinase kinase-extracellular signal-regulated kinase (MEK/ERK) signaling *via* RAF1 (2, 6). We speculated that *BRAF* and *PIK3CA* mutations might lead to the continuous activation of downstream signaling pathways, which could explain the short PFS. Moreover, after disease progression, along with acquiring a new *KRAS* mutation might lead to continuous activation of the downstream signaling pathways, which might explain the disease progression after switching to ceritinib. In addition, activation of the phosphoinositide 3-kinase (PI3K) signaling pathway can lead to PD-L1 upregulation (7), which has been shown as a major contributor to tumor immune escape (8) and might also explain tumor progression in this patient after ALK-TKI treatment.

Previous studies have shown that *ALK* rearranged NSCLC patients had low PD-L1 expression and low CD8+ tumor

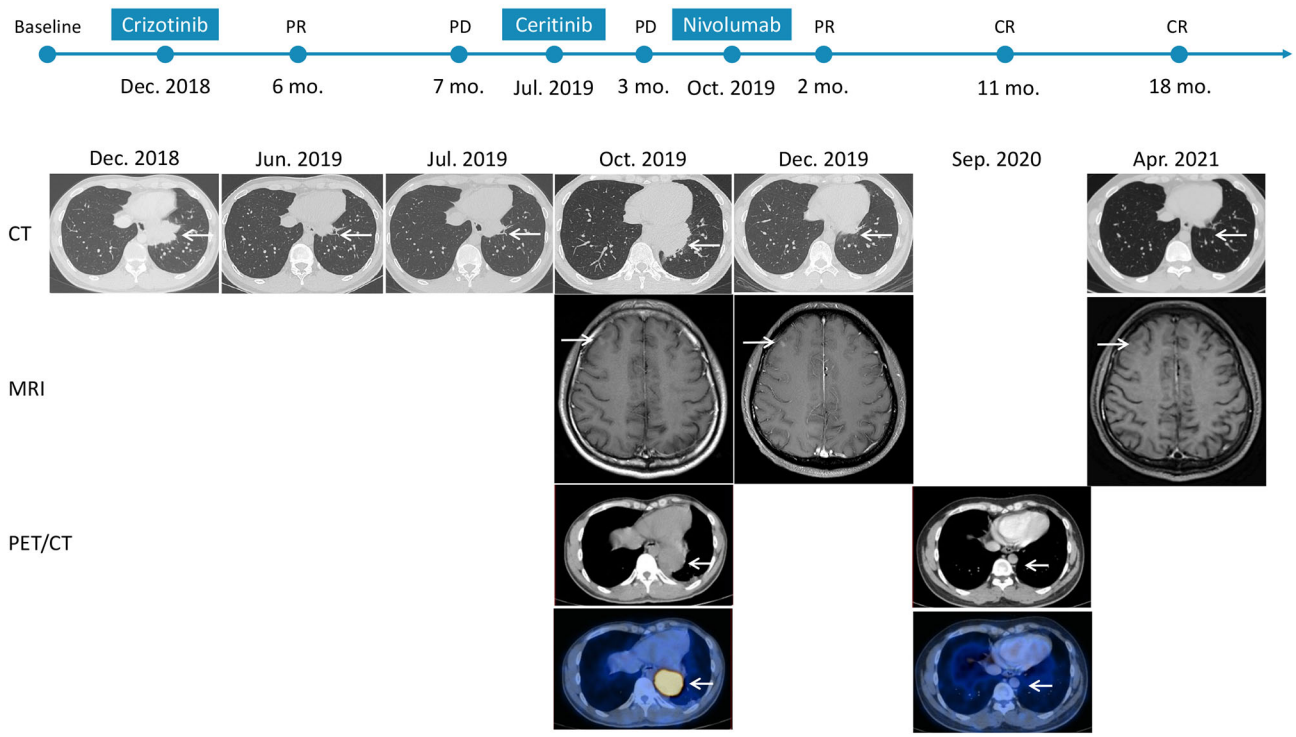

FIGURE 2 | Time course depicting treatment process and radiological evaluation from 2018 to 2021. The PFS of crizotinib and ceritinib were 7 months and 3 months, respectively. And the duration of nivolumab was 18 months at the time of this report, and the patient is at present still on treatment and is receiving the drug. PR, partial response; PD, progressive disease; CR, complete response; CT, computed tomography; MRI, magnetic resonance imaging; PET/CT, positron emission tomography/computed tomography.

infiltrating lymphocytes (7–9), and TMB is low with fewer non-synonymous mutations (10). In addition, retrospective studies have shown lack of efficacy with single-agent PD-1/PD-L1 inhibitor in *ALK* rearranged NSCLC (7, 11–13). However, immunotherapy has shown considerable efficacy in patients with *KRAS* or *BRAF* non-V600 mutations (11, 14). Since the mutation frequencies of all gene mutations were less than 5% and close to each other, it is difficult to analyze the clonal and subclone distribution of these gene alterations, including ALK. The patient in this report successful benefited from nivolumab may be due to multiple factors rarely co-occurring with *ALK* rearrangement, including high expression of PD-L1, positive CD8+ tumor infiltrating lymphocytes, high TMB, and co-mutation with *KRAS* and *BRAF*.

In conclusion, ALK positive NSCLC with multiple driving mutations, high TMB, PD-L1 overexpression, and CD8+ tumor infiltrating lymphocytes is very rare. The selection of an appropriate therapeutic strategy is very important for this group of patients. The case presented here showed that tumor gene mutations changed with disease progression, suggesting the necessity of large-panel genetic tests in the process of targeted therapy for patients with NSCLC, especially those with disease progression. Moreover, the high efficacy of nivolumab suggested that PD-L1 inhibitors might be a good treatment option for these patients.

DATA AVAILABILITY STATEMENT

The datasets presented in this study can be found in online repositories. The names of the repository/repositories and accession number(s) can be found in the article/**Supplementary Material**.

ETHICS STATEMENT

The studies involving human participants were reviewed and approved by Institutional Review Board of the First Affiliated Hospital of Guangzhou Medical University (Guangzhou, Guangdong, China). The patients/participants provided their written informed consent to participate in this study.

AUTHOR CONTRIBUTIONS

XC conceptualized and designed the study. WD and PL collected, processed, and analyzed the data. XL and QL drafted the manuscript and figures. All authors contributed to the article and approved the submitted version.

ACKNOWLEDGMENTS

We thank the patient for voluntarily providing valuable medical and genetic data for scientific analysis.

SUPPLEMENTARY MATERIAL

The Supplementary Material for this article can be found online at: https://www.frontiersin.org/articles/10.3389/fimmu.2021.686057/full#supplementary-material

REFERENCES

1. Kang J, Chen HJ, Zhang XC, Su J, Zhou Q, Tu HY, et al. Heterogeneous Responses and Resistant Mechanisms to Crizotinib in ALK-Positive Advanced Non-Small Cell Lung Cancer. *Thorac Cancer* (2018) 9:1093–103. doi: 10.1111/1759-7714.12791
2. Schrank Z, Chhabra G, Lin L, Iderzorig T, Osude C, Khan N, et al. Current Molecular-Targeted Therapies in NSCLC and Their Mechanism of Resistance. *Cancers (Basel)* (2018) 10:224. doi: 10.3390/cancers10070224
3. Doebele RC, Pilling AB, Aisner DL, Kutateladze TG, Le AT, Weickhardt AJ, et al. Mechanisms of Resistance to Crizotinib in Patients With ALK Gene Rearranged Non-Small Cell Lung Cancer. *Clin Cancer Res* (2012) 18:1472–82. doi: 10.1158/1078-0432.CCR-11-2906
4. Shaw AT, Engelman JA. Ceritinib in ALK-Rearranged Non-Small-Cell Lung Cancer. *N Engl J Med* (2014) 370:2537–9. doi: 10.1056/NEJMc1404894
5. Awad MM, Shaw AT. ALK Inhibitors in Non-Small Cell Lung Cancer: Crizotinib and Beyond. *Clin Adv Hematol Oncol* (2014) 12:429–39.
6. Wan PT, Garnett MJ, Roe SM, Lee S, Niculescu-Duvaz D, Good VM, et al. Mechanism of Activation of the RAF-ERK Signaling Pathway by Oncogenic Mutations of B-RAF. *Cell* (2004) 116:855–67. doi: 10.1016/s0092-8674(04)00215-6
7. Gainor JF, Shaw AT, Sequist LV, Fu X, Azzoli CG, Piotrowska Z, et al. EGFR Mutations and ALK Rearrangements Are Associated With Low Response Rates to PD-1 Pathway Blockade in Non-Small Cell Lung Cancer: A Retrospective Analysis. *Clin Cancer Res* (2016) 22:4585–93. doi: 10.1158/1078-0432.CCR-15-3101
8. Jiang X, Wang J, Deng X, Xiong F, Ge J, Xiang B, et al. Role of the Tumor Microenvironment in PD-L1/PD-1-Mediated Tumor Immune Escape. *Mol Cancer* (2019) 18:10. doi: 10.1186/s12943-018-0928-4
9. Rangachari D, Vanderlaan PA, Shea M, Le X, Huberman MS, Kobayashi SS, et al. Correlation Between Classic Driver Oncogene Mutations in EGFR, ALK, or ROS1 and 22C3-PD-L1 >/=50% Expression in Lung Adenocarcinoma. *J Thorac Oncol* (2017) 12:878–83. doi: 10.1016/j.jtho.2016.12.026
10. Singal G, Miller PG, Agarwala V, Li G, Kaushik G, Backenroth D, et al. Association of Patient Characteristics and Tumor Genomics With Clinical Outcomes Among Patients With Non-Small Cell Lung Cancer Using a Clinicogenomic Database. *JAMA* (2019) 321:1391–9. doi: 10.1001/jama.2019.3241
11. Mazieres J, Drilon A, Lusque A, Mhanna L, Cortot AB, Mezquita L, et al. Immune Checkpoint Inhibitors for Patients With Advanced Lung Cancer and Oncogenic Driver Alterations: Results From the IMMUNOTARGET Registry. *Ann Oncol* (2019) 30:1321–8. doi: 10.1093/annonc/mdz167
12. Oya Y, Kuroda H, Nakada T, Takahashi Y, Sakakura N, Hida T. Efficacy of Immune Checkpoint Inhibitor Monotherapy for Advanced Non-Small-Cell Lung Cancer With ALK Rearrangement. *Int J Mol Sci* (2020) 21:2623. doi: 10.3390/ijms21072623
13. Jahanzeb M, Lin HM, Pan X, Yin Y, Baumann P, Langer CJ. Immunotherapy Treatment Patterns and Outcomes Among ALK-Positive Patients With Non-Small-Cell Lung Cancer. *Clin Lung Cancer* (2021) 22:49–57. doi: 10.1016/j.cllc.2020.08.003
14. Calles A, Riess JW, Brahmer JR. Checkpoint Blockade in Lung Cancer With Driver Mutation: Choose the Road Wisely. *Am Soc Clin Oncol Educ Book* (2020) 40:372–84. doi: 10.1200/EDBK_280795

Conflict of Interest: The authors declare that the research was conducted in the absence of any commercial or financial relationships that could be construed as a potential conflict of interest.

this article, or claim that may be made by its manufacturer, is not guaranteed or endorsed by the publisher.

frontiers in Oncology

ORIGINAL RESEARCH
published: 05 November 2021
doi: 10.3389/fonc.2021.755341

Pan-Cancer Analysis of IGF-1 and IGF-1R as Potential Prognostic Biomarkers and Immunotherapy Targets

Yinqi Zhang[1,2†], Chengqi Gao[3†], Fei Cao[2,3†], Ying Wu[2,3†], Shuanggang Chen[4], Xue Han[2,3], Jingqin Mo[1], Zhiyu Qiu[2,3], Weijun Fan[2,3], Penghui Zhou[3] and Lujun Shen[2,3*]*

[1] Zhongshan School of Medicine, Sun Yat-Sen University, Guangzhou, China, [2] Department of Minimally Invasive Interventional Therapy, Sun Yat-Sen University Cancer Center, Guangzhou, China, [3] State Key Laboratory of Oncology in South China, Collaborative Innovation Center of Cancer Medicine, Sun Yat-Sen University, Guangzhou, China, [4] Department of Oncology, Yuebei People's Hospital, Shantou University Medical College, Shaoguan, China

Aim: Insulin-like growth factor-1 receptor (IGF-1R) is one of the main members of the tyrosine protein kinase receptor family. This receptor binds insulin-like growth factor-1 (IGF-1) with a high affinity. IGF-1 is a member of a family of proteins involved in mediating growth and development. However, the correlations of IGF-1 and IGF-1R to prognosis and tumor-infiltrating lymphocytes in different cancers remain unclear.

Method: This research comprehensively analyzed the expression pattern of IGF-1 and IGF-1R and the influence of IGF-1 and IGF-1R on clinical significance in prognosis prediction among 33 types of malignancies using The Cancer Genome Atlas (TCGA) and the Cancer Cell Line Encyclopedia (CCLE) databases. The correlation between IGF-1, IGF-1R, and cancer immunity was explored.

Results: IGF-1 and IGF-1R displayed inconsistent gene expression levels among diverse cancer cell lines. Typically, high expression level of IGF-1 and IGF-1R was detected in most malignant tumors. High expression of IGF-1 was closely bound up with the unfavorable overall survival (OS) for patients in BLCA, CHOL, and LAML upon Cox and Kaplan-Meier analyses. While high expression of IGF-1R was closely bound up with the unfavorable overall survival (OS) for patients in BLCA, LIHC, and LUAD. Furthermore, high expression level of IGF-1 and IGF-1R were closely connected with high degrees of tumor infiltrates, including CD4+ T cell, dendritic cells, and macrophages. In addition, we found that IGF-1 was commonly positively correlated with the expression of gene markers including LAIR1, ICOS, CD40LG, CTLA4, CD48, CD28, CD200R1, HAVCR2, and CD86.

OPEN ACCESS

Edited by:
Hongbo Hu,
Sichuan University, China

Reviewed by:
Alessandro Rizzo,
Sant'Orsola-Malpighi Polyclinic, Italy
Xindong Liu,
Army Medical University, China

***Correspondence:**
Lujun Shen
shenlj@sysucc.org.cn
Penghui Zhou
zhouph@sysucc.org.cn

†These authors have contributed equally to this work

Specialty section:
This article was submitted to Cancer Immunity and Immunotherapy, a section of the journal Frontiers in Oncology

Received: 08 August 2021
Accepted: 14 October 2021
Published: 05 November 2021

Citation:
Zhang Y, Gao C, Cao F, Wu Y, Chen S, Han X, Mo J, Qiu Z, Fan W, Zhou P and Shen L (2021) Pan-Cancer Analysis of IGF-1 and IGF-1R as Potential Prognostic Biomarkers and Immunotherapy Targets. Front. Oncol. 11:755341. doi: 10.3389/fonc.2021.755341

Whereas, IGF-1R was commonly positively correlated with the expression of gene markers including NRP1 and CD276. More importantly, IGF-1 and IGF-1R expression were correlated with tumor mutation burden (TMB), microsatellite instability (MSI), mismatch repair (MMR), and DNA methyltransferase (DNMT) of different types of cancers.

Conclusions: The impact of high IGF-1 and IGF-1R on prognosis and immune infiltrates differs across cancer types. Anti-IGF-1R therapy may inhibit tumor growth and contribute to immunotherapy in LIHC and KIRC.

Keywords: pan-cancer, IGF-1, IGF-1R, prognostic biomarker, immunity

INTRODUCTION

Insulin-like growth factor 1 receptor (IGF-1R), one of the main members of tyrosine protein kinase receptor family, plays an important role in maintaining the malignant phenotype and tumor anti-apoptosis. Insulin-like growth factor-1 (IGF-1), ligand of IGF-1R, is a kind of growth hormone mainly synthesized in liver. Population studies provide substantial direct and circumstantial evidence that cancer risk and cancer prognosis are influenced by IGF-1 and insulin levels (1). The overexpression of IGF-1 and its receptor IGF-1R have been implicated in carcinogenesis and are also considered risk factors for the progression of diverse human cancers (2–4). On the other hand, studies have proved that anti-IGF-1R monoclonal antibody has potential therapeutic value in diverse cancers (5–7). Researchers have also found that the differentiation of *ex vivo*-expanded CD34+ cells through manipulation of RAS/MAPK, IGF-1R, and TGF-β signaling pathways is an efficient approach for generating functional NK cells that can be used for cancer immunotherapy (8). However, the correlations of IGF-1 and IGF-1R to prognosis and tumor-infiltrating lymphocytes in different cancers remain unclear. Since cancer is a leading cause of death worldwide, and the low efficacy of many existing therapies is a major clinical challenge, it is essential to understand the prognostic and immunological impact of IGF-1 and IGF-1R among cancer types comprehensively in order to develop novel immunotherapies.

Molecular-level pan-cancer analyses have provided insights into the common features and heterogeneity of various human malignancies. Since the establishment of The Cancer Genome Atlas based on various human cancer samples and normal tissues at epigenomic, genomic, proteomic, and transcriptomic levels, diverse cancer samples are offered so that deeper pan-cancer analysis could be conducted (9). Therefore, we conducted a pan-cancer analysis taking advantage of its large datasets. The analysis aimed to (a) describe the expression of IGF-1 and IGF-1R among different cancer types; (b) assess the prognostic values of IGF-1 and IGF-1R among varied tumors; and (c) evaluate the associations between IGF-1/IGF-1R and tumor immunity features including intratumoral immune infiltrates, checkpoint markers, tumor mutation burden (TMB), and microsatellite instability (MSI), which have been identified as biomarkers for predicting response to immune checkpoint inhibitor treatment (10).

METHODS

Patient Datasets and Processing

The Cancer Genome Atlas (TCGA), a milestone of the cancer genomics project, characterizes thousands of primary cancer samples and matched adjacent noncarcinoma samples from 33 types of cancers. In this study, the TCGA level 3 RNA sequencing processed data and the corresponding clinical annotations were acquired using the UCSC cancer genome browser (https://tcga.xenahubs.net, accessed May 2020). The Cancer Cell Line Encyclopedia (CCLE) public project is established through the comprehensive characterization of tremendous human tumor models at both genetic and pharmacological levels (https://portals.broadinstitute.org/ccle). To examine the differential gene expression in cancers at a larger a scale, the CCLE database containing the RNA-sequencing datasets for over 1,000 cell lines (https://portals.broadinstitute.org/ccle) was used in this study. The approval from the Ethics Committee was exempted as only the open-access data were used.

IGF-1/IGF-1R Differential Expression and Survival-Associated Cancers

To compare the gene expression levels between cancer and adjacent noncarcinoma samples, data regarding the gene expression profiles of IGF-1/IGF-1R were extracted from the 33 cancer types in TCGA to from an expression matrix. It is thereafter merged with corresponding clinical information by patient ID. Univariate Cox model was applied in calculating the associations between gene expression levels and patient survival among 33 cancer types, and a difference of $p < 0.05$ for IGF-1 and IGF-1R in a specific cancer indicated statistical significance. The survival-associated forest plot is also made. Moreover, the Kaplan-Meier (KM) analysis by log-rank test was conducted to compare the overall survival (OS) and disease-specific survival (DSS) for TCGA cancer patients stratified based on the median gene expression level of IGF-1/IGF-1R.

IGF-1/IGF-1R and Tumor Immune Microenvironment

The tumor-infiltrating immunocyte levels among different types of cancers were estimated by Tumor Immune Estimation Resource (TIMER, https://cistrome.shinyapps.io/timer/) (11) and CIBERSORT (12) based on related gene expression data, through deconvolution statistical method. The relationships

between each immune infiltrate among 33 cancer types and IGF-1/IGF-1R expression were analyzed.

Estimation of STromal and Immune cells in MAlignant Tumor tissues using Expression data (ESTIMATE) is used to predict tumor purity and the infiltrating stromal cells/immunocytes in tumor tissue based on gene expression profiles (13). The ESTIMATE algorithm produces three scores based on the gene set enrichment analysis (GSEA) of single samples, including stromal score, which determines stromal cells in tumor tissues and immune score, which stands for the immunocyte infiltration level in tumor tissues. In this study, ESTIMATE algorithm is used to estimate the stromal and immune scores in tumor tissues according to corresponding transcriptional data and calculated the correlations of these scores with the expression of IGF-1/IGF-1R.

The relationships between the expression level of IGF-1/IGF-1R and the gene markers in tumor infiltrating immunocytes selected with reference to previous research were further conducted (14, 15). Correlation analysis was conducted to generate the estimated statistical significance and Spearman's correlation coefficient. The somatic mutation data of all TCGA patients were downloaded (https://tcga.xenahubs.net) in order to calculate TMB scores and MSI scores and explore the correlation of IGF1/IGF-1R with MMR genes and DNMT.

Gene Set Enrichment Analysis

GSEA were performed on IGF-1 and IGF-1R to understand the interrelated biological functions and pathways of IGF-1/IGF-1R. The molecular signature Database (MSigDB) H (hallmark gene sets) collection of chemical and genetic perturbations and KEGG subsets of canonical pathways and cancer modules were employed, and the analysis was completed on Sangerbox (http://sangerbox.com/). Normalized enrichment scores (NES) were used to show GSEA results, accounting for the size and degree to which a gene set is overrepresented at the top or bottom of the ranked list of genes (nominal p-value <0.05 and FDR ≤ 0.25). Bioconductor (http://bioconductor.org/) and R software (http:///www.r-project.org/) were used to visualize the enrichment maps of results.

Statistical Analysis

In the present work, the clinical survival types, including OS and disease-specific survival (DSS), were selected for analysis. Generally, OS is deemed as the duration from the date of diagnosis to the date of death due to any course, DSS is considered disease progression or death due to the disease.

Wilcox log rank test was adopted to determine the presence or absence of a markedly increased sum of gene expression z-scores in cancer tissues compared with adjacent normal tissues. Meanwhile, Kruskal-Wallis test was employed to compare the difference in the expression of IGF-1 and IGF-1R. Survival was analyzed by the KM curves, log-rank test, and the Cox proportional hazard regression model. Spearman' test was utilized for correlation analysis. The R language (version 3.6.0; R Foundation) was used for all analyses. A two-sided difference of $p < 0.05$ indicated statistical significance.

RESULTS

Pan-Cancer Expression Landscape of IGF-1 and IGF-1R

Comparison of expression of IGF-1/IGF-1R between normal and tumor samples across TCGA cancer types and the combined datasets based on integrated database of GTEx and TCGA datasets were conducted and shown in **Figure 1**. Consistent high expression level of IGF-1 could be seen in normal tissues than most types of tumor based on both comparisons, and significant decreased expression of IGF-1 could be seen in tumor samples including ACC, BLCA, BRCA, CESC, CHOL, COAD, ESCA, LAML. LGG, LIHC, LUAD, OV, PRAD, READ, SKCM, STAD, TGCT, THCA, UCEC, and UCS based on the integrated database. Whereas, high expression level of IGF-1R could be seen in most types of tumors than normal tissue based on both comparisons, and significant increased expression of IGF-1R could be seen in tumor samples including BRCA, CHOL, COAD, ESCA, GBM, HNSC, LAML, LGG, LIHC, LUAD, LUSC, PAAD, PRAD, SKCM, STAD, TGCT, and THCA based on the integrated database. Patients with different tumor stage and gender did not differ in the expression of IGF-1/IGF-1R in tumor samples.

Correlation of IGF-1/IGF-1R Expression Level and Overall Survival of Cancer Patients

Figures 2 and **3** summarized the results of OS analyses of IGF-1 and IGF-1R expression across the 33 cancer types. In univariate analysis, high expression of IGF-1 in tumor samples correlates with unfavorable prognosis in BLCA (HR = 1.09, p = 0.0012), CHOL (HR = 1.27, p = 0.0011) and LAML (HR = 3.88, p = 0.018); whereas, high expression of IGF-1 correlates with favorable prognosis in SARC (HR = 0.93, p = 0.00063) (**Figures 2A–D**). Cox regression model confirmed the prognostic impact of IGF-1 in BLCA (p = 4.4e−0.6), CHOL (p = 3.8e−0.2), LAML (p = 7.8e−0.3), and SARC (p = 4.2e−0.2) with the same trend (**Figure 2E**). On the other hand, high expression of IGF-1R in tumor samples correlates with unfavorable prognosis in BLCA (HR = 1.01, p = 0.045), LIHC (HR = 1.06, p = 0.013), and LUAD (HR = 1.01, p = 0.024); whereas, high expression of IGF-1R correlates with favorable prognosis in KIRC (HR = 0.97, $p < 0.0001$) and LAML (HR = 0.98, p = 0.0011) (**Figures 3A–E**). Cox regression model confirmed the prognostic impact of IGF-1R in BLCA (p = 4.0e−0.2), LIHC (p = 1.3e−0.2), LUAD (p = 2.7e−0.2), KIRC (p = 9.3e−0.8), and LAML (p = 3.2e−0.2) with the same trend (**Figure 3F**).

Correlation of IGF-1/IGF-1R Expression Level and Immune Infiltrates

Systemic analysis of immune infiltrates in different cancer types could be conducted by using a deconvolution statistical approach to infer tumor-infiltrating lymphocyte (TIL) counts based on gene expression data thanks to TIMER (https://cistrome.shinyapps.io/timer/). In this study, we analyzed the impact of IGF-1 and IGF-1R on the abundance of six immune infiltrates in cancers that harbor prognostic value, which are B cells, CD4+

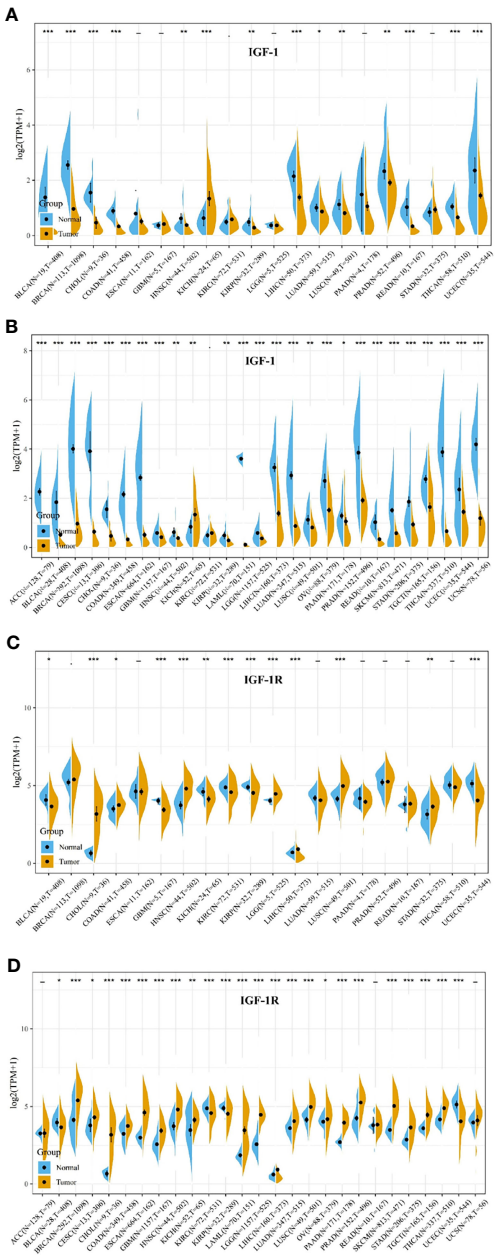

FIGURE 1 | IGF-1/IGF-1R expression levels in different types of human cancers. The expression levels of IGF-1 between tumor and normal tissues were compared in 20 cancer types based on the TCGA database **(A)** and 27 cancer types based on the integrated database from TCGA and GTEx datasets **(B)**. The expression levels of IGF-1R between tumor and normal tissues were compared in 20 cancer types based on the TCGA database **(C)** and 27 cancer types based on the integrated database from TCGA and GTEx datasets **(D)**. Consistent high expression level of IGF-1 could be seen in normal tissues than most types of tumor based on both comparisons, and significant decreased expression of IGF-1 could be seen in tumor samples including ACC, BLCA, BRCA, CESC, CHOL, COAD, ESCA, LAML, LGG, LIHC, LUAD, OV, PRAD, READ, SKCM, STAD, TGCT, THCA, UCEC, and UCS based on the integrated database. Consistent high expression level of IGF-1R could be seen in most types of tumor than normal tissue based on the both comparisons, and significant increased expression of IGF-1R could be seen in tumor samples including BRCA, CHOL, COAD, ESCA, GBM, HNSC, LAML, LGG, LIHC, LUAD, LUSC, PAAD, PRAD, SKCM, STAD, TGCT, and THCA based on the integrated database. "*, **, ***" means $p < 0.05$, $p < 0.01$ and $p < 0.001$, respectively.

cells, CD8+ cells, dendritic cells, macrophages, and neutrophils. The correlation between the expression of IGF-1/IGF-1R and the immune infiltration levels across diverse cancer types is derived from TIMER. As for IGF-1, three of the most significant associations were BLCA (**Figure 4A**), BRCA (**Figure 4B**), and CHOL (**Figure 4C**). While for IGF-1R, three of the most significant associations were BLCA (**Figure 4D**), LIHC (**Figure 4E**), and PRAD (**Figure 4F**). TIMER showed that both

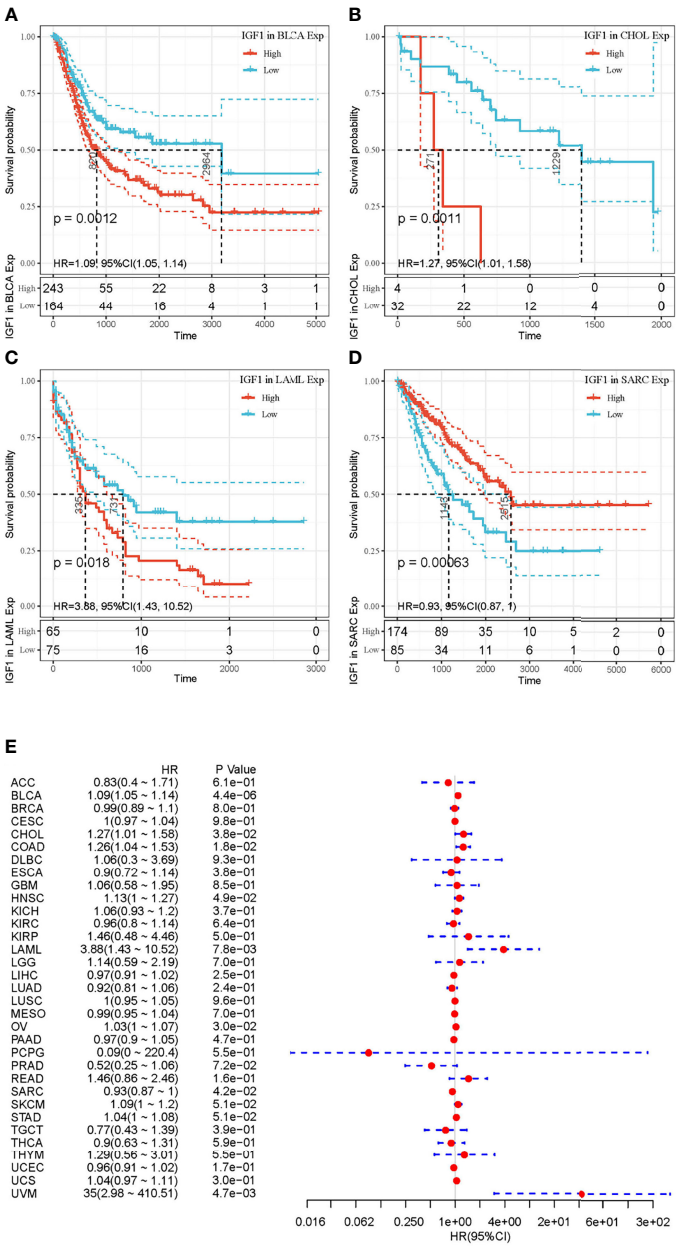

FIGURE 2 | Selected Kaplan-Meier plots and forest plot comparing the high and low expressions of IGF-1 on overall survival across different cancers. **(A–C)** Kaplan-Meier method showed high expression of IGF-1 correlated with unfavorable prognosis in BLCA, CHOL, and LAML. **(D)** Kaplan-Meier method showed high expression of IGF-1 correlated with favorable prognosis in SARC. **(E)** Forest plot displaying the impact of high expression of IGF-1 on OS across 33 cancer types using Cox regression model. Confidence level is shown in dashed lines.

IGF-1 and IGF-1R are positively correlated with the abundance of CD4+ T cell, dendritic cells, and macrophages.

The ESTIMATE method is developed to calculate the immune and stromal scores of cancer tissues. By adopting the ESTIMATE method, we calculated the immune, stromal scores, respectively. As for IGF-1, three of the most significant correlation according to stromal scores were found in ESCA, GBM, and LGG (**Figures 5A–C**), while three of the most significant correlation according to immune scores were found in GBM, LGG, and LUSC (**Figures 5D–F**). As for IGF-1R, three of the most significant correlation according to stromal scores were found in LIHC, LGG, and COAD (**Figures 5G–I**), while three of the most significant correlation according to immune scores were found in BRCA, KIRC, and LUAD (**Figures 5J–L**).

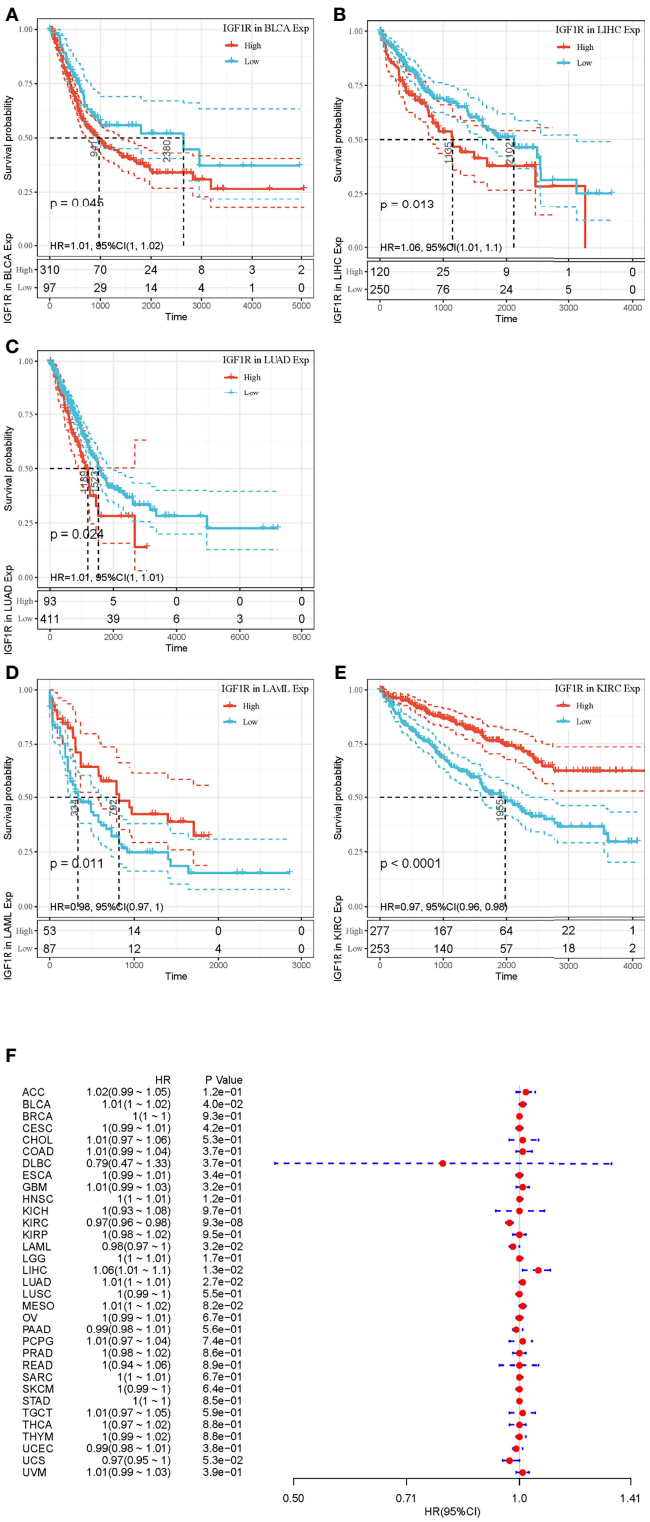

FIGURE 3 | Selected Kaplan-Meier plots and forest plot comparing the high and low expressions of IGF-1R on overall survival across different cancers. **(A–C)** Kaplan-Meier method showed high expression of IGF-1R correlated with unfavorable prognosis in BLCA, LIHC, and LUAD. **(D, E)** Kaplan-Meier method showed high expression of IGF-1R correlated with favorable prognosis in LAML and KIRC. **(F)** Forest plot displaying the impact of high expression of IGF-1R on OS across 33 cancer types using Cox regression model.

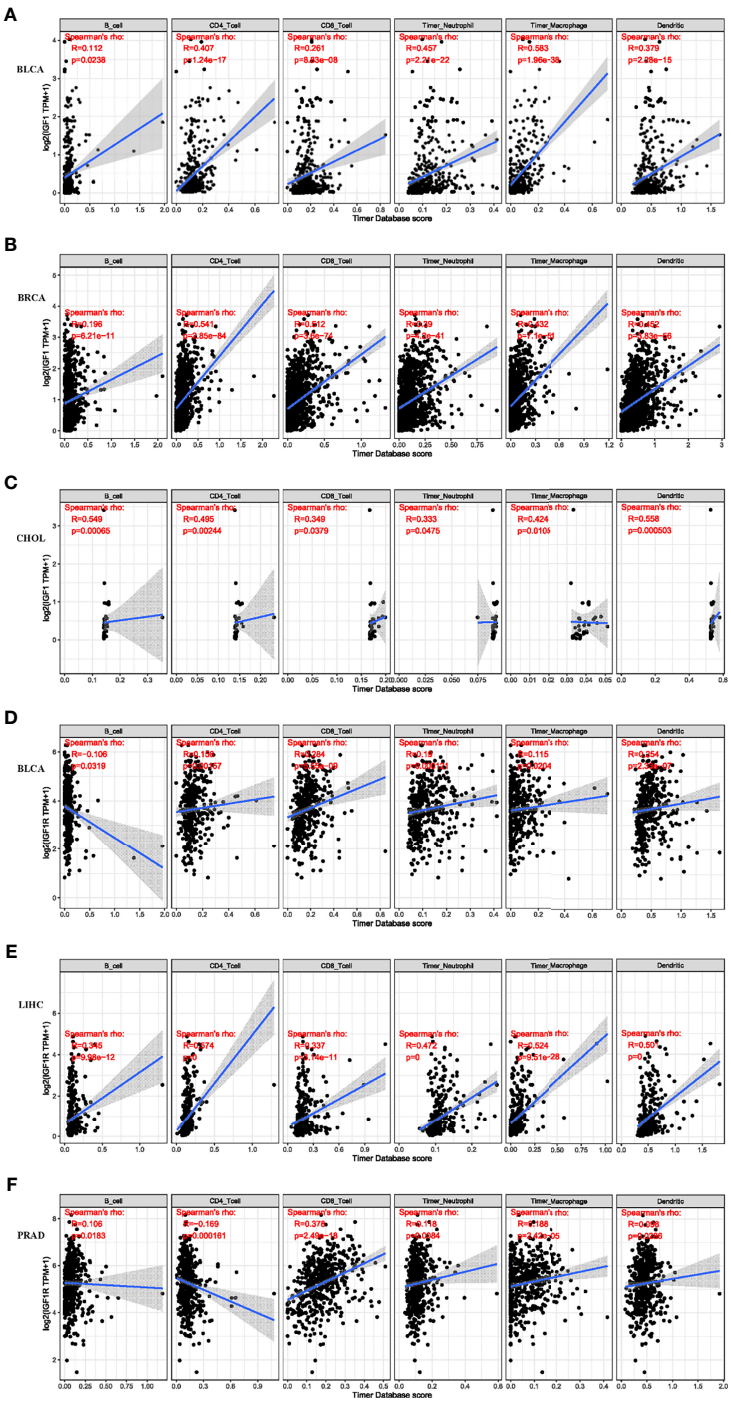

FIGURE 4 | Correlation of IGF-1 expression level with immune infiltration level in BLCA, BRCA, and CHOL. Correlation of IGF-1R expression level with immune infiltration level in BLCA, LIHC, and PRAD. **(A–C)** IGF-1 expression is significantly positively correlated with CD4+ T cell, dendritic cell, and macrophage infiltration in BLCA, BRCA, and CHOL. **(D–F)** IGF-1R expression is significantly positively correlated with CD4+ T cell, dendritic cell, and macrophage infiltration in BLCA, LIHC, and PRAD.

Correlation Analysis on Checkpoint Gene Markers

To further explored the potential mechanism of immune inhibition of IGF-1/IGF-1R signaling, the associations of IGF-1/IGF-1R expressions with multiple checkpoint markers were compared across different cancer types (**Figure 6**). Generally, IGF-1 expression positively correlates with the expression of LAIR1, ICOS, CD40LG, CTLA4, CD48, CD28, CD200R1,

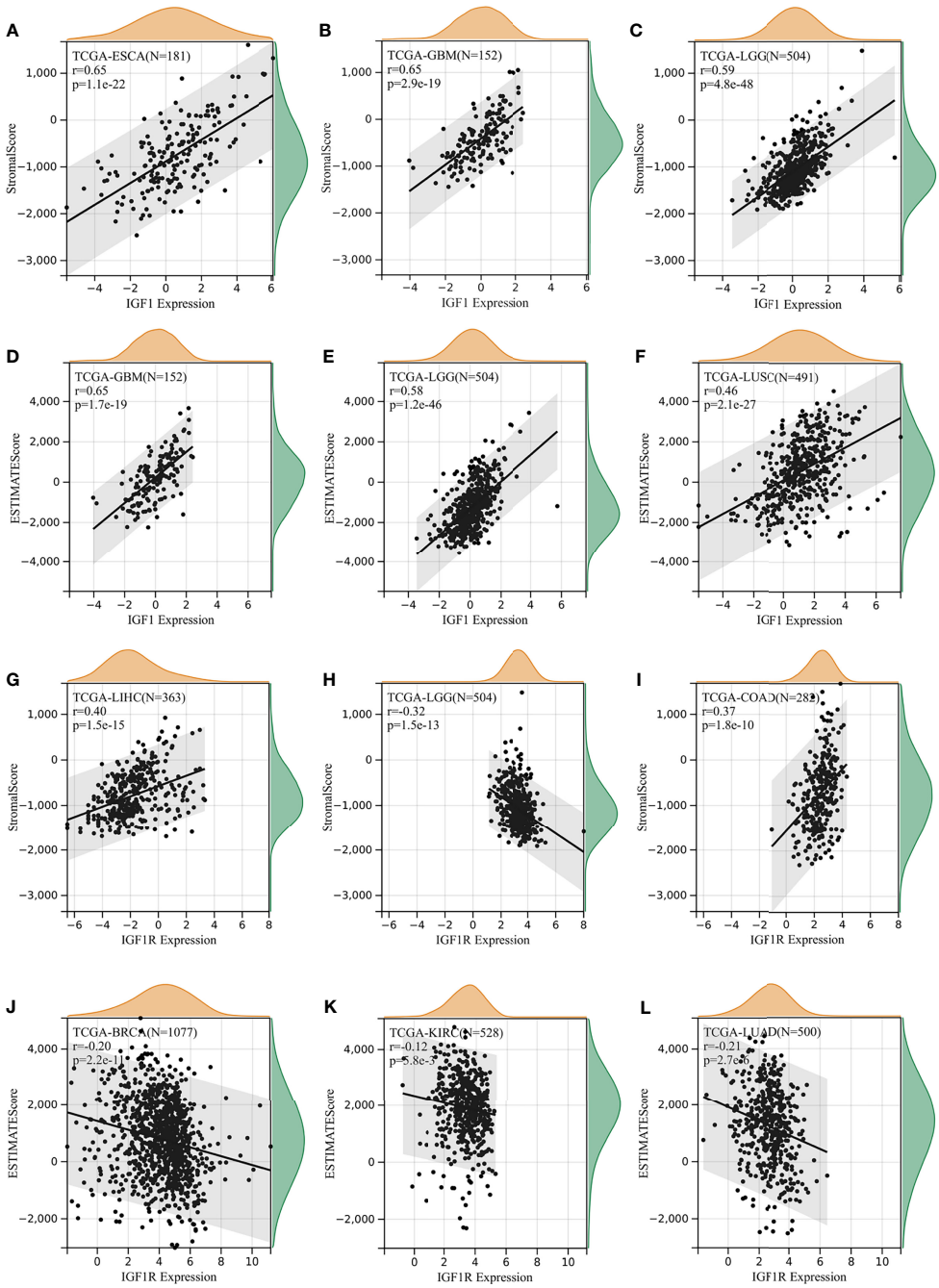

FIGURE 5 | Correlation of IGF-1/IGF-1R expression with estimate score. **(A–C)** IGF-1 expression significantly correlated with stromal scores in esophageal carcinoma (ESCA), glioblastoma multiforme (GBM), and lower-grade glioma (LGG). **(D–F)** IGF-1 expression significantly correlated with immune scores in glioblastoma multiforme (GBM), lower-grade glioma (LGG), and lung squamous cell carcinoma (LUSC). **(G–I)** IGF-1R expression significantly correlated with stromal scores in liver hepatocellular carcinoma (LIHC), lower-grade glioma (LGG), and lung squamous cell carcinoma (LUSC). **(J–L)** IGF-1R expression significantly correlated with immune scores in breast invasive carcinoma (BRCA), kidney renal clear cell carcinoma (KIRC), and lung adenocarcinoma (LUAD).

HAVCR2, and CD86 in the majority of 33 cancer types (**Figure 6A**). On the other hand, IGF-1R expression positively correlates with the expression of NRP1 and CD276 in the majority of 33 cancer types (**Figure 6B**).

Correlation Analysis on TMB, MSI, MMR, and DNMT

Tumor mutational burden (TMB) is a quantifiable biomarker which is used to reflect the number of mutations contained in malignancies.

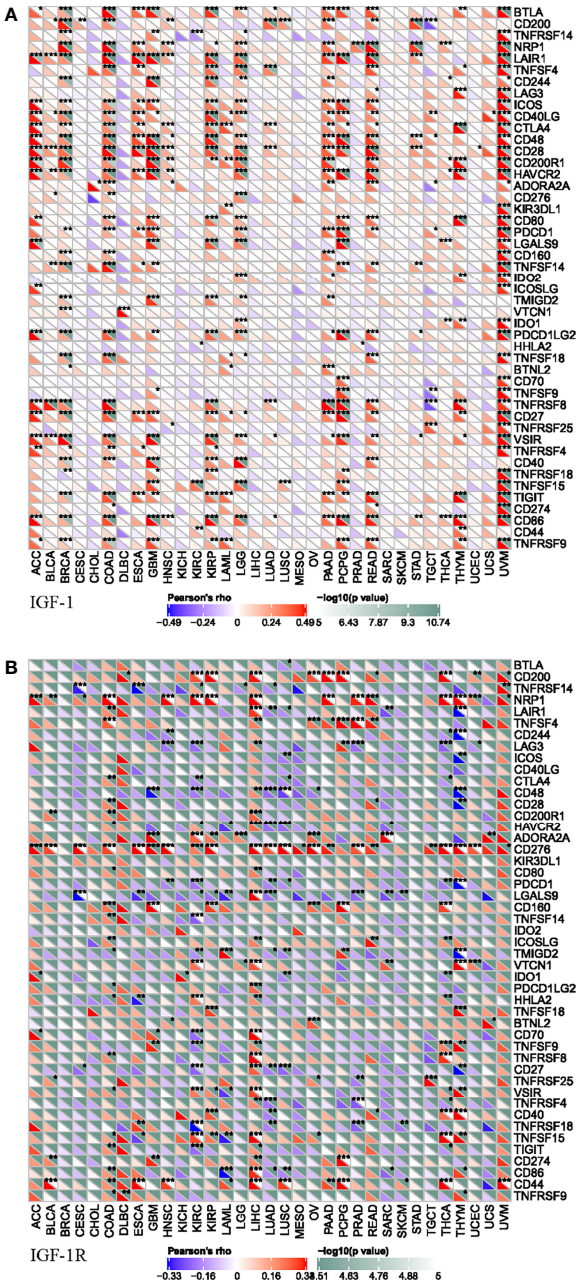

FIGURE 6 | Correlation of IGF-1 **(A)** and IGF-1R **(B)** expressions with expression of immune checkpoint genes across 33 cancer types. "*, **, ***" means significant correlation $p < 0.05$, $p < 0.01$ and $p < 0.001$, respectively.

Microsatellite instability (MSI) refers to the occurrence of new microsatellite alleles due to the insertion or deletion of duplicate units and cause changes in the length of a microsatellite compared with normal tissue. The association of TMB/MSI with IGF-1/IGF-1R expression was evaluated. Expression of IGF-1 positively correlated with TMB in THYM, CHOL, LAML, LIHC, and OV while negatively correlated with the TMB in BLCA, BRCA, CESC, COAD, DLBC, ESCA, GBM, HNSC, KICH, KIRC, KIRP, LGG, LUAD, LUSC, MESO, PAAD, PCPG, PRAD, READ, SARC, STAD, TGCT, THCA, UCEC, UCS, and UVMP (**Figure 7A**). Expression of IGF-1R positively correlated with TMB in GBM, HNSC, KICH, LAML, LGG, MESO, SKCM, and THYM while negatively correlated with TMB in BLCA, BRCA, CESC, COAD, ESCA, KIRC, KIRP, LIHC, OV, PAAD, PRAD, READ, STAD, TGCT, THCA, UCEC, UCS, and UVM (**Figure 7B**). The correlations of IGF-1/IGF-1R with MSI are shown in **Figures 7C, D**.

The correlation analysis between MMR genes (MLH1, MSH2, MSH6, PMS2, EPCAM) and IGF-1/IGF-1R expression was further

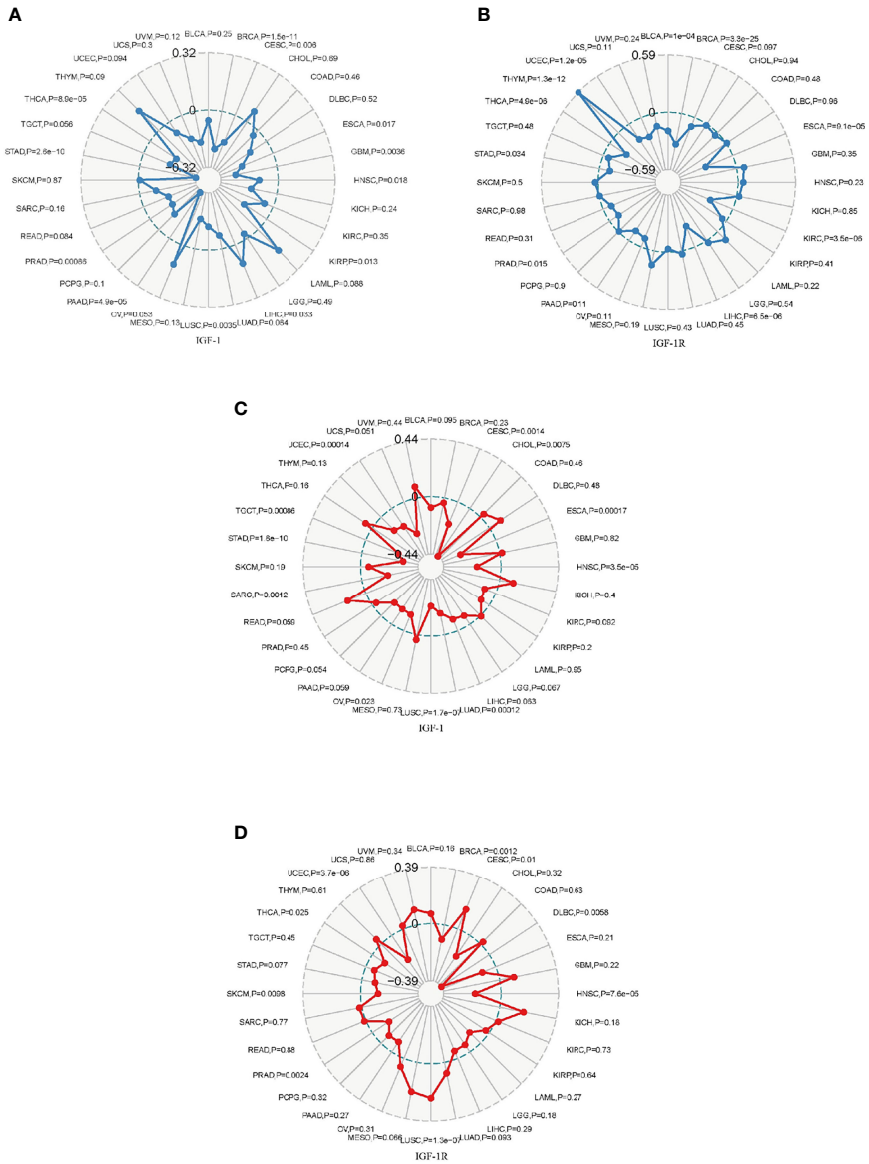

FIGURE 7 | Radar map plotting the correlation of tumor mutation burden (TMB) **(A)** and microsatellite instability (MSI) **(B)** with IGF-1 expression across 33 cancer types. Radar map plotting the correlation of tumor mutation burden (TMB) **(C)** and microsatellite instability (MSI) **(D)** with IGF-1R expression across 33 cancer types.

performed. IGF-1 expression was correlated with at least one MMR genes in BRCA, COAD, HNSC, LIHC, PAAD, STAD, and TGCT (**Supplementary Figure S1**). IGF-1R expression was correlated with at least one MMR genes in almost all of the 33 cancer types except for BRCA, STAD, and UCS (**Supplementary Figure S2**). Moreover, the correlation analysis between DNMT (DNMT1, DNMT2, DNMT3A, and DNMT3B) and IGF-1/IGF-1R expression was also conducted. The result is as shown in **Supplementary Figures S3** and **S4**.

Functional Analysis by Gene Set Enrichment Analysis

The biological role of IGF-1 and IGF-1R were illustrated through GSEA. The pan-cancer functional KEGG and HALLMARK terms of IGF-1/IGF-1R are shown in **Figure 8**, respectively. Generally, the top 3 negatively enriched KEGG terms in high IGF-1 subgroups were hematopoietic cell lineage, cytokine cytokine receptor interaction, and B-cell receptor signaling pathway (**Figure 8A**), and the top positively enriched KEGG terms were glutathione metabolism, pentose phosphate pathway, fructose and mannose metabolism, and base excision repair (**Figure 8B**). The top 3 negatively enriched HALLMARK terms in high IGF-1 subgroups were epithelial mesenchymal transition, KRAS upsignaling, and allograft rejection (**Figure 8C**), and the top positively enriched HALLMARK terms were MYC targets V2, reactive oxygen species pathway, oxidative phosphorylation, and DNA repair (**Figure 8D**). As for IGF-1R, the top 3 negatively enriched KEGG terms were WNT signaling pathway,

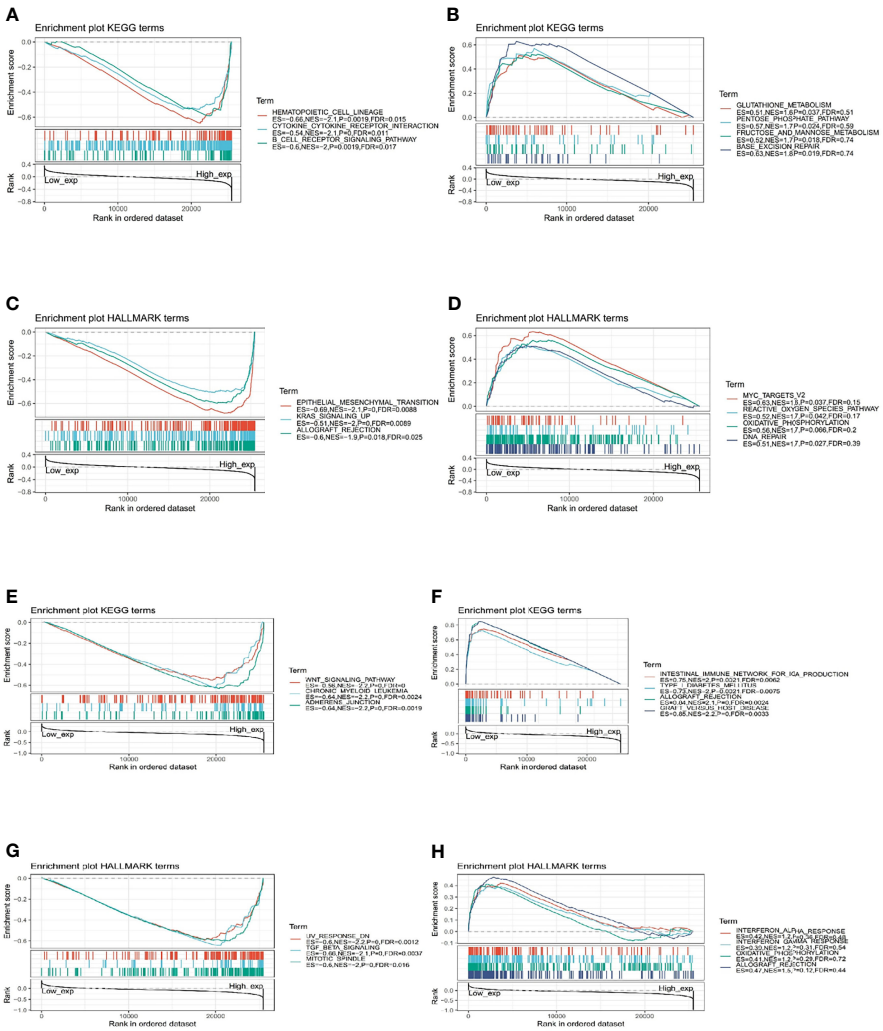

FIGURE 8 | Functional Enrichment of KEGG and HALLMARK terms on IGF-1 and IGF-1R through GSEA. The top 3 negatively and positively enriched KEGG terms on IGF-1 are displayed in **(A, B)**, respectively. The top 3 negatively and positively enriched KEGG terms on IGF-1 are displayed in **(C, D)**, respectively. The top 3 negatively and positively enriched KEGG terms on IGF-1R are displayed in **(E, F)**, respectively. The top 3 negatively and positively enriched KEGG terms on IGF-1R are displayed in **(G, H)**, respectively.

chronic myeloid leukemia, and adherens junction (**Figure 8E**), and the top positively enriched KEGG terms were intestinal immune network for IgA production, type I diabetes mellitus, allograft rejection, and graft-versus-host disease (**Figure 8F**). The top 3 negatively enriched HALLMARK terms in high IGF-1R subgroups were UV response DN, TGF beta signaling, and mitotic spindle (**Figure 8G**), and the top positively enriched HALLMARK terms were interferon alpha response, interferon gamma response, oxidative phosphorylation, and allograft rejection (**Figure 8H**).

DISCUSSION

The present work illustrated a comprehensive workflow for pan-cancer analysis and thoroughly investigated the role of IGF-1 and IGF-1R in cancers. The prognostic impact of IGF-1 and IGF-1R expression among different cancer types was reported. It was found that most cancer types showed a higher IGF-1/IGF-1R alteration frequency and the expression of IGF-1 and IGF-1R served as the prognostic factor in some cancer types, including BLCA and LAML upon both Cox and KM survival analyses. However, the relationship between IGF-1/IGF-1R overexpression and tumor immunity was still unclear. Secondly, though IGF-1 and IGF-1R share the same signaling pathway, whether they have different prognostic and immunologic values in different types of cancer needs further investigation. Moreover, the relationship between IGF1/IGF1R expression and tumor prognoses, such as TMB, MSI, MMR, and DNMT, which can predict the efficacy of immunotherapy, remains unclear. Base on this, our bioinformatics analysis

studied the IGF-1/IGF-1R expression-associated KEGG terms and HALLMARK pathways.

Our study showed that IGF-1 and IGF-1R harbor distinct prognostic values among different cancer types. The low expression of IGF-1 served as a favorable prognostic factor in some cancer types, including BLCA, CHOL, LAML, and UVM; whereas in SARC, high expression of IGF-1 served as a favorable prognostic factor. On the other hand, high expression of IGF-1R served as a significant prognostic factor in such cancer types including KIRC and LAML; whereas in BLCA, LIHC, and LUAD, low expression of IGF-1R served as a favorable prognostic factor. Previous study has proven that the epithelial-mesenchymal transition (EMT) process of gastric cancer cells could be induced by IGF-1 through the IGF-1R/STAT3 signaling pathway so that cancer cells would achieve metastasis (16). It has also been found that in liver cancer, IGF-1 promotes the invasion and metastasis of liver cancer cells by inhibiting the degradation of cathepsin B (17). Wu et al. proved that the increasing secretion of IGF-1 and CCL20 promotes brain metastasis of lung cancer cells by polarizing microglia and suppressing innate immune function (18). Studies done by Somri-Gannam et al. provide evidence that IGF-1R axis inhibition could be a therapeutic strategy for ovarian cancer by restoring dendritic cell (DC)-mediated antitumor immunity (19). Therefore, the distinct prognostic value of changeable IGF-1/IGF-1R expression across different cancers may result from its synthetic effect of immune suppressive activity and tumor suppressive activity in each cancer type. The distinct prognostic value of IGF-1 and IGF-1R expression may give rise to some new researches and questions for discussion. Both IGF-1 and IGF-1R are positively correlated with the abundance of CD4+ T cell, dendritic cells, and macrophages. Cellular infiltration of CD4+ T cell, dendritic cells, and macrophages would lead to immunosuppressive tumor microenvironment and cause unfavorable prognosis. The expression of IGF-1 is positively correlated with the expression of most immune checkpoint genes in UVM. The expression of IGF-1R is positively correlated with the expression of CD276 in most cancer types, and since CD276 is related to immunosuppression, this may explain why the increased expression of IGF-1R in tumor has an impact on the prognosis.

The expressions of IGF-1 and IGF-1R were correlated with TMB and MSI in some cancer types. TMB could impact the patient response to immune checkpoint inhibitors through affecting the generation possibility of immunogenic peptide (20). MSI is a vital index to predict tumor genesis and development (21). The NCCN guidelines have recommended MSI testing for all rectum adenocarcinoma (READ) subtypes, and the READ mortality can be reduced by the early detection of MSI (22). FDA has approved the use of Keytruda for the treatment of MSI-H solid tumors. As a result, TMB and MSI can serve as the predicting factors for efficacy. The expressions of IGF-1/IGF-1R share negative correlation with TMB and MSI in most cancer types, which means high expression of IGF-1/IGF-1R indicates immunosuppression. Our findings provide clues on the correlation between IGF-1/IGF-1R expression and cancer immunity and suggest that it could be a potential predictive maker of the efficacy of immunotherapy. Our study systematically compared the immune effects of IGF-1 and IGF1-R, which is conducive to localize the target molecules more accurately. A series of drugs targeting IGF-1/IGF1-R in the treatment of cancer are in clinical trials. The associated results may be released in the next 5 years.

Our study has several limitations. First, the result of our study should be interpreted with caution since checkpoint inhibitor treatment has not been analyzed in our study. Second, the result of our study lacks external validation in other public datasets. We need clinical specimens from our center for further verification. Only the gene expression level was analyzed in this study; we may conduct a more comprehensive analysis from the perspective of single and multiple omics. More efforts are needed to undermine the value of IGF-1/IGF-1R as a potential target of immunotherapy.

To conclude, our comprehensive pan-cancer analysis has characterized IGF-1/IGF-1R expression in different cancer cell lines and tissues. According to our results, IGF-1 and IGF-1R can serve as a valuable prognostic biomarker in some cancer types. They are also related to cancer immunity and could be potential predictive maker of the efficacy of immunotherapy, which may help develop the new targeted treatment.

DATA AVAILABILITY STATEMENT

The original contributions presented in the study are included in the article/**Supplementary Material**. Further inquiries can be directed to the corresponding authors.

AUTHOR CONTRIBUTIONS

LS and PZ designed and implemented the study design. YZ, CG, FC, YW, and SC participated in data analysis. XH, JM, ZQ, and WF managed and advised on the project. YZ, CG, FC, and YW wrote the paper. All authors contributed to the article and approved the submitted version.

FUNDING

This study was supported by the National Outstanding Youth Science Fund Project of Natural Science Foundation of China (81801804).

SUPPLEMENTARY MATERIAL

The Supplementary Material for this article can be found online at: https://www.frontiersin.org/articles/10.3389/fonc.2021.755341/full#supplementary-material

Supplementary Figure 1 | Correlations of IGF-1 expression with MMR genes.

Supplementary Figure 2 | Correlations of IGF-1R expression with MMR genes.

Supplementary Figure 3 | Correlations of IGF-1 expression with DNMT.

Supplementary Figure 4 | Correlations of IGF-1R expression with DNMT.

REFERENCES

1. Pollak M. Insulin and Insulin-Like Growth Factor Signalling in Neoplasia. *Nat Rev Cancer* (2008) 8(12):915–28. doi: 10.1038/nrc2536
2. Majchrzak-Baczmańska D, Malinowski A. Does IGF-1 Play a Role in the Biology of Endometrial Cancer? *Ginekologia Polska* (2016) 87(8):598–604. doi: 10.5603/gp.2016.0052
3. Majchrzak-Baczmańska D, Malinowski A, Głowacka E, Wilczyński M. Does IGF-1 Play a Role in the Biology of Ovarian Cancer? *Ginekologia Polska* (2018) 89(1):13–9. doi: 10.5603/GP.a2018.0003
4. Li Y, Liu Q, He H, Luo W. The Possible Role of Insulin-Like Growth Factor-1 in Osteosarcoma. *Curr Problems Cancer* (2019) 43(3):228–35. doi: 10.1016/j.currproblcancer.2018.08.008
5. Ma H, Zhang T, Shen H, Cao H, Du J. The Adverse Events Profile of Anti-IGF-1R Monoclonal Antibodies in Cancer Therapy. *Br J Clin Pharmacol* (2014) 77(6):917–28. doi: 10.1111/bcp.12228
6. Wang W, Zhang Y, Lv M, Feng J, Peng H, Geng J, et al. Anti-IGF-1R Monoclonal Antibody Inhibits the Carcinogenicity Activity of Acquired Trastuzumab-Resistant SKOV3. *J Ovarian Res* (2014) 7:103. doi: 10.1186/s13048-014-0103-5
7. Lu H, Jiang Z. Advances in Antibody Therapeutics Targeting Small-Cell Lung Cancer. *Adv Clin Exp Med Off Organ Wroclaw Med Univ* (2018) 27(9):1317–23. doi: 10.17219/acem/70159
8. Shokouhifar A, Anani Sarab G, Yazdanifar M, Fereidouni M, Nouri M, Ebrahimi M. Overcoming the UCB HSCs -Derived NK Cells Dysfunction Through Harnessing RAS/MAPK, IGF-1R and TGF-β Signaling Pathways. *Cancer Cell Int* (2021) 21(1):298. doi: 10.1186/s12935-021-01983-z
9. Tomczak K, Czerwińska P, Wiznerowicz M. The Cancer Genome Atlas (TCGA): An Immeasurable Source of Knowledge. *Contemp Oncol (Poznan Poland)* (2015) 19:A68–77. doi: 10.5114/wo.2014.47136
10. Rizzo A, Ricci A, Brandi G. PD-L1, TMB, MSI, and Other Predictors of Response to Immune Checkpoint Inhibitors in Biliary Tract Cancer. *Cancers* (2021) 13(3). doi: 10.3390/cancers13030558
11. Li T, Fan J, Wang B, Traugh N, Chen Q, Liu J, et al. TIMER: A Web Server for Comprehensive Analysis of Tumor-Infiltrating Immune Cells. *Cancer Res* (2017) 77(21):e108–e10. doi: 10.1158/0008-5472.can-17-0307
12. Newman A, Steen C, Liu C, Gentles A, Chaudhuri A, Scherer F, et al. Determining Cell Type Abundance and Expression From Bulk Tissues With Digital Cytometry. *Nat Biotechnol* (2019) 37(7):773–82. doi: 10.1038/s41587-019-0114-2
13. Becht E, Giraldo N, Lacroix L, Buttard B, Elarouci N, Petitprez F, et al. Estimating the Population Abundance of Tissue-Infiltrating Immune and Stromal Cell Populations Using Gene Expression. *Genome Biol* (2016) 17(1):218. doi: 10.1186/s13059-016-1070-5
14. Cristescu R, Mogg R, Ayers M, Albright A, Murphy E, Yearley J, et al. Pan-Tumor Genomic Biomarkers for PD-1 Checkpoint Blockade-Based Immunotherapy. *Sci (New York NY)* (2018) 362(6411). doi: 10.1126/science.aar3593
15. Pan J, Zhou H, Cooper L, Huang J, Zhu S, Zhao X, et al. LAYN Is a Prognostic Biomarker and Correlated With Immune Infiltrates in Gastric and Colon Cancers. *Front Immunol* (2019) 10:6. doi: 10.3389/fimmu.2019.00006
16. Xu L, Zhou R, Yuan L, Wang S, Li X, Ma H, et al. IGF1/IGF1R/STAT3 Signaling-Inducible IFITM2 Promotes Gastric Cancer Growth and Metastasis. *Cancer Lett* (2017) 393:76–85. doi: 10.1016/j.canlet.2017.02.014
17. Lei T, Ling X. IGF-1 Promotes the Growth and Metastasis of Hepatocellular Carcinoma *via* the Inhibition of Proteasome-Mediated Cathepsin B Degradation. *World J Gastroenterol* (2015) 21(35):10137–49. doi: 10.3748/wjg.v21.i35.10137
18. Wu S, Xing F, Sharma S, Wu K, Tyagi A, Liu Y, et al. Nicotine Promotes Brain Metastasis by Polarizing Microglia and Suppressing Innate Immune Function. *J Exp Med* (2020) 217(8). doi: 10.1084/jem.20191131
19. Somri-Gannam L, Meisel-Sharon S, Hantisteanu S, Groisman G, Limonad O, Hallak M, et al. IGF1R Axis Inhibition Restores Dendritic Cell Antitumor Response in Ovarian Cancer. *Trans Oncol* (2020) 13(8):100790. doi: 10.1016/j.tranon.2020.100790
20. Chan T, Yarchoan M, Jaffee E, Swanton C, Quezada S, Stenzinger A, et al. Development of Tumor Mutation Burden as an Immunotherapy Biomarker: Utility for the Oncology Clinic. *Ann Oncol Off J Eur Soc Med Oncol* (2019) 30(1):44–56. doi: 10.1093/annonc/mdy495
21. Chang L, Chang M, Chang H, Chang F. Microsatellite Instability: A Predictive Biomarker for Cancer Immunotherapy. *Appl Immunohistochem Mol Morphol AIMM* (2018) 26(2):e15–21. doi: 10.1097/pai.0000000000000575
22. Ganesh K, Stadler Z, Cercek A, Mendelsohn R, Shia J, Segal N, et al. Immunotherapy in Colorectal Cancer: Rationale, Challenges and Potential. *Nat Rev Gastroenterol Hepatol* (2019) 16(6):361–75. doi: 10.1038/s41575-019-0126-x

Conflict of Interest: The authors declare that the research was conducted in the absence of any commercial or financial relationships that could be construed as a potential conflict of interest.

frontiers in Oncology

ORIGINAL RESEARCH
published: 23 November 2021
doi: 10.3389/fonc.2021.739090

Front-Line ICI-Based Combination Therapy Post-TKI Resistance May Improve Survival in NSCLC Patients With EGFR Mutation

Tian Tian[1†], Min Yu[1†], Juan Li[2], Maoqiong Jiang[3], Daiyuan Ma[4], Shubin Tang[5], Zhiyu Lin[6], Lin Chen[1], Youling Gong[1], Jiang Zhu[1], Qiang Zhou[7], Meijuan Huang[1] and You Lu[1]*

[1] Department of Thoracic Oncology, Cancer Center, West China Hospital, Sichuan University, Chengdu, China, [2] Department of Thoracic Cancer, Medical Oncology Center, Sichuan Cancer Hospital & Institute, Sichuan Cancer Center, School of Medicine, University of Electronic Science and Technology of China, Chengdu, China, [3] Department of Thoracic Oncology, The Second People's Hospital of Yibin, Yibin, China, [4] Department of Oncology, Cancer Center, Affiliated Hospital of North Sichuan Medical College, Nan Chong, China, [5] Department of Oncology, The First People's Hospital of Neijiang, Neijiang, China, [6] Department of Oncology and Hematology, Leshan People's Hospital, Leshan, China, [7] Cancer Center, Suining Central Hospital, Suining, China

OPEN ACCESS

Edited by:
Taichi Matsubara, Kitakyushu Municipal Medical Center, Japan

Reviewed by:
Tao Jiang, Shanghai Pulmonary Hospital, China
Qian Chu, Huazhong University of Science and Technology, China
Chunxia Su, Shanghai Pulmonary Hospital, China
Shengxiang Ren, Tongji University, China

***Correspondence:**
Meijuan Huang
hmj107@163.com

[†]These authors share first authorship

Specialty section:
This article was submitted to Cancer Immunity and Immunotherapy, a section of the journal Frontiers in Oncology

Received: *10 July 2021*
Accepted: *04 November 2021*
Published: *23 November 2021*

Citation:
Tian T, Yu M, Li J, Jiang M, Ma D, Tang S, Lin Z, Chen L, Gong Y, Zhu J, Zhou Q, Huang M and Lu Y (2021) Front-Line ICI-Based Combination Therapy Post-TKI Resistance May Improve Survival in NSCLC Patients With EGFR Mutation. Front. Oncol. 11:739090. doi: 10.3389/fonc.2021.739090

Background: Data on the use of immune checkpoint inhibitors (ICIs) in advanced non-small cell lung cancer (NSCLC) patients with epidermal growth factor receptor (EGFR) mutation are limited. The current study aimed to assess the efficacy of ICIs in EGFR-mutant advanced NSCLC and explore the relevant influential factors.

Materials and Methods: Relevant clinical data of EGFR-mutant NSCLC patients who had received ICIs were collected from multiple hospitals. The primary endpoint was progression-free survival (PFS), and the secondary endpoints were overall survival (OS), objective response rate (ORR), and relevant influential factors.

Results: A total of 122 advanced EGFR-mutant NSCLC patients were included in the final analysis. The total cohort had an objective response rate (ORR) of 32.0%, a median progression-free survival (mPFS) of 5.0 months, and a median overall survival (mOS) of 14.4 months. Among 96 patients with common EGFR mutations (19Del, 52 patients; L858R, 44 patients), those who were administered front-line ICI exhibited better survival benefits than those who received later-line ICI after disease progression on tyrosine kinase inhibitors (TKIs) treatment (mPFS: 7.2 months *vs.* 3.4 months, respectively, $P < 0.0001$; mOS: 15.1 months *vs.* 8.4 months, respectively, $P < 0.0001$). Moreover, the efficacy of ICI-based combination therapy was better than that of ICI monotherapy (mPFS: 5.0 months *vs.* 2.2 months, respectively, $P = 0.002$; mOS: 14.4 months *vs.* 7.0 months, respectively, $P = 0.001$). Multivariate analysis showed that ICI-based combination therapy and front-line ICI administration after progression on EGFR-TKI were associated with significant improvements in both PFS and OS ($P < 0.05$). A high PD-L1 expression (tumor proportion score, TPS≥50%) and the EGFR L858R mutation were only significantly

associated with a better PFS (P <0.05). A better Eastern Cooperative Oncology Group (ECOG) status was independently associated with a favorable OS (P <0.05).

Conclusions: Taken together, combination immunotherapy in front-line was associated with improvement of survival in EGFR-mutant NSCLC patients post-TKI resistance. Further prospective studies with large sample sizes are required to identify the optimal combinatorial treatment strategy.

Keywords: non–small cell lung cancer, immune checkpoint inhibitor, tyrosine kinase inhibitor, epidermal growth factor receptor, resistance

INTRODUCTION

Epidermal growth factor receptor tyrosine kinase inhibitors (EGFR-TKIs) as a standard first-line treatment for advanced non-small-cell lung cancer harboring EGFR mutation yield great efficacy but acquired resistance and disease progression are inevitable (1–3). Salvage treatment options following available TKI failure are limited; chemotherapy serves as the primary modality with unsatisfactory efficacy (4–7). Immune checkpoint inhibitors (ICIs), such as anti-programmed cell death 1 (PD-1) and programmed cell death-ligand 1 (PD-L1) agents, have considerably improved the survival of driver gene wild-type advanced NSCLC (8–10). Although a few reports have been published recently, the role of ICI in EGFR-mutant NSCLC after EGFR-TKI failure is still controversial. Disappointing results have been demonstrated with ICI monotherapy in IMMUNOTARGET (11) and other studies (12–14), while some physicians advocate that ICI-based combination therapy may be an option (15). Subgroup analysis in the IMpower 150 study showed that the combination of paclitaxel, carboplatin, bevacizumab, and atezolizumab improved PFS but not significant OS benefit as compared to that with bevacizumab plus chemotherapy. This four-drug regimen owned an incidence of grade 3 to 4 treatment-related adverse events of 57% (16). Two studies with a combination approach have reported promising results on response rate (RR) and survival (17, 18), while flaws exist due to the small sample size and insufficient information on patients with T790M. Another study with ICI combination treatment got a worse outcome with an objective response rate (ORR) of 18.6% and a median progression-free survival (mPFS) of 2.8 months (19). Moreover, a few studies with small samples have retrospectively analyzed the data of EGFR 20 insertion mutation (EGFR 20Ins) to evaluate the efficacy of ICI (20–22). Therefore, more studies are urgent to explore the role of ICI in EGFR-mutant NSCLC patients.

This retrospective study aimed to summarize the efficacy of ICI in EGFR-mutant NSCLC after progression on TKI treatment and explore issues, such as the administration timing of ICI, whether ICI monotherapy or ICI-based combination therapy is better, and the efficacy of ICI for EGFR 20Ins.

Abbreviations: EGFR, epidermal growth factor receptor; TKI, tyrosine kinase inhibitors; ICI, immune checkpoint inhibitors; NSCLC, non-small-cell lung cancer; TMN stages, tumor size, lymph node, and metastasis; PFS, progression-free survival; OS, overall survival; ORR, objective response rate; DCR, disease control rate; EGFR 20Ins, EGFR Exon 20 insertion; EGFR19 Del, EGFR exon 19 deletion; EGFR 21 L858R, EGFR exon 21 L858R mutation; T790M, T790M mutation.

MATERIALS AND METHODS

Patients' Clinical Data

The clinical data of eligible patients were extracted from the electronic medical records of seven different institutions in China (including West China Hospital of Sichuan University, Sichuan Cancer Hospital & Institute, The Second People's Hospital of Yibin, Affiliated Hospital of North Sichuan Medical College, The First People's Hospital of Neijiang, Leshan people's Hospital, Suining Central Hospital) from September 2016 to May 2020. The inclusion criteria were as follows: treatment with ICI (anti-PD-1/PD-L1 inhibitor); a pathological diagnosis of NSCLC and at stage IV according to tumor size, lymph node, and metastasis (TNM) stages; exhibition the activation of EGFR mutations on exons 18 to 21. Patients who had participated in clinical trials or had other cancers were excluded. Related baseline demographic variables, including sex, age, Eastern Cooperative Oncology Group (ECOG) performance status, immunotherapy strategy, smoking history, sites of metastasis, histological type, and prior treatment information, were collected. This study adhered to the tenets of the Declaration of Helsinki and was performed following the principles of good clinical practice and approved by the institutional ethical review board. As only anonymous medical records of patients were used, the requirement for informed consent was waived by the ethical committee.

EGFR Mutation and PD-L1 Analysis

Tumor tissue samples obtained from biopsy, resection, and cytology were used for immunohistochemical detection. PD-L1 status was determined by immunohistochemistry analyses (23), and EGFR mutations were evaluated by polymerase chain reaction or next-generation sequencing (24), which was used according to standard protocols of the respective centers. The PD-L1 tumor proportion score (TPS) refers to the percentage of tumor cells showing partial or complete membrane staining (25). PD-L1 expression≥50% was classified as a strong positive result (26). All gene alterations and PD-L1 expression status were part of the patients' clinical information at baseline.

Statistical Analysis

Categorical variables are presented as numbers and percentiles, whereas continuous variables are presented as medians and ranges. Each patient's response to ICI treatment was assessed using the Response Evaluation Criteria in Solid Tumors (RECIST) v.1.1. PFS was defined as the time from treatment initiation to disease

progression or death from any cause. The patients still alive at the date of last follow-up visit (April 1, 2021) were censored. Kaplan–Meier survival curves were constructed for PFS and OS, and the differences between groups were identified using the log-rank test. The Cox proportional hazards regression model was used for univariate and multivariate analyses. The follow–up time was calculated using the reverse Kaplan–Meier method. Two-tailed P values were calculated for all analyses and statistical significance was set at P<0.05. All statistical analyses were performed using SPSS 25.0 and GraphPad 8.0 statistical software.

RESULTS

Patient Characteristics

A total of 122 eligible patients with EGFR-mutant NSCLC were finally included. The median follow-up time was 15.4 months (range: 0.6–28.8 months) and median age was 56 years (range: 30–85 years). The majority of the patients had a good performance status (ECOG = 0–1; 105/122, 86.1%) and were diagnosed with adenocarcinoma (112/122, 91.8%). EGFR mutation subtypes consisted of EGFR exon 19 deletion (19Del) (N = 52, 42.6%), EGFR exon 21 L858R mutation (EGFR 21 L858R) (N = 44, 36.1%), EGFR 20Ins (N = 23, 18.9%), and three other patients had uncommon mutations (G719X, N = 2; L861Q, N = 1). 69 of patients carrying EGFR common mutation (19Del, 21 L858R) underwent gene re-test after first or second-generation TKI treatment, with 31 cases acquired T790M mutation. 43 cases with common EGFR mutation were treated with osimertinib after progression on first and second-generation TKI. Most patients received an anti-PD-1 agent (116/122, 95.1%). The PD-L1 expression status was known in 86 patients (86/122, 70.5%). Further details of patients' characteristics are shown in **Table 1**.

Survival of EGFR-Mutant Patients

The ORR of the total 122 patients was 32.0% (39/122), and the disease control rate was 70.0% (85/122). The median PFS (mPFS) and OS (mOS) were 5.0 months (95% CI = 4.1–5.8 months) and 14.4 months (95% CI = 12.5–16.4 months), respectively (**Figure 1** and **Table 2**).

The group with common EGFR mutations (19Del and L858R) had an ORR, mPFS and mOS of 31.3% (30/96), 4.4 months (95%CI = 3.7–5.1 months) and 13.4 months (95%CI = 11.7–15.1 months), respectively (**Table 2**).

ICI for patients carrying EGFR 20Ins displayed an ORR of 34.8% (8/23) and a median PFS of 6.4 months (95%CI = 4.8–8 months); the median OS was not reached. Among another three patients with uncommon EGFR mutations [L861Q (1patient), G719X (2 patients)], the median PFS and OS were 7.7 months and 18.4months, respectively (**Table 2**).

Clinical Features Associated With Outcomes in Patients With Common EGFR Mutations

All 96 patients with common EGFR mutations (19Del and L858R) had previously been treated with EGFR-TKIs. All patients with prior TKI treatment failure who carried the acquired T790M mutation have received osimertinib. Further analyses of clinical features were subsequently performed to identify the benefitting population.

46 patients were immediately administered ICI after progression on TKI, which was defined as front-line ICI post-TKI progression, whereas the remaining 50 patients received later-line ICI because they received other systemic therapy regimens in the interval between TKIs and ICI treatment. The patients who received front-line ICI showed enhanced survival benefits compared to those who received ICI as a later line post-TKIs progression (mPFS, 7.2 months [95% CI = 5.4–9 months], *vs.* 3.4 months [95% CI = 2.2– 4.5 months], respectively, P <0.0001; mOS, 15.1 months [95% CI = 13.5–16.7 months], *vs.* 8.4m [95% CI = 6.2–10.6 months], respectively, P<0.0001; **Figure 2**). The group treated with front-line ICI had a better ECOG performance score and higher PD-L1 expression than the group treated with later-line ICI.

A total of 72 patients were treated with ICI-based combination therapy: 50 received a combination of ICI with chemotherapy, 8 received a combination of ICI with chemotherapy and radiotherapy, 12 received a combination of ICI with chemotherapy plus an anti-angiogenic agent, and 2 received dual ICIs (an anti-PD-1 agent combined with an anti-cytotoxic-T-lymphocyte-associated protein 4 inhibitor). The efficacy of ICI-based combination therapy was better than that of ICI monotherapy (mPFS, 5.0 months [95% CI 3.2–6.8 months) *vs.* 2.2 months [95% CI = 0.9–3.5 months], respectively, P = 0.002; mOS, 14.4 months [95% CI = 12.8–16 months] *vs.* 7.0 months [95% CI = 5.6–8.3 months], respectively, P=0.001; **Figure 3**).

In patients with available PD-L1 expression data (n = 69/96, 71.9%), 31 patients exhibited strongly positive PD-L1 expression (TPS≥50%), whereas 38 patients presented PD-L1 expression less than 50%. A significant PFS benefit was observed in patients with strongly positive PD-L1 expressions (TPS≥50%) compared with the cohort with a lower PD-L1 expression (TPS<50%) (7.5 *vs.* 3.0 months, respectively, P = 0.001). However, the difference in OS was not statistically significant (**Figure 4**).

A multivariate analysis was performed by including factors that were found to be significant in the univariate analysis (P<0.05) and those considered to be clinically significant (**Table 3**). The results indicated that strongly positive PD-L1 expression (TPS≥50%), ICI-based combination therapy, front-line ICI treatment after EGFR TKI progression, and the EGFR L858R genotype were all significantly associated with improved PFS (P <0.05) (**Figure 5**). A good ECOG status, ICI-based combination therapy, and front-line ICI treatment after EGFR TKI progression were found to be independently associated with a favorable OS, after adjusting for other clinical factors (P <0.05; **Table 3**).

DISCUSSION

Chemotherapy, as the most common subsequent treatment regimen after the discontinuation of EGFR-TKI therapy, has limited benefits for EGFR-mutant NSCLC patients (4–7). A retrospective study indicated that 27% of patients received chemotherapy combined with ICI after the failure of osimertinib

TABLE 1 | Characteristics of NSCLC patients with EGFR mutation treated with the immune checkpoint inhibitors.

Clinical Characteristic	All EGFR (*N* = 122)	$EGFR^{19Del}$ (*N* = 52)	$EGFR^{L858R}$ (*N* = 44)	$EGFR^{20Ins}$ (*N* = 23)	$EGFR^{Other*}$ (*N* = 3)
Age, median (range)	56 (30~85)	55 (39~71)	56.5 (30~82)	58 (35~85)	49 (43~70)
Age					
>65	24 (19.7%)	11 (21.2%)	9 (20.5%)	3 (13.0%)	1 (33.3%)
≦65	98 (80.3%)	41 (78.8%)	35 (79.5%)	20 (87.0%)	2 (66.7%)
ECOG					
0	44 (36.1%)	15 (29.0%)	18 (40.9%)	9 (39.1%)	2 (66.7%)
1	61 (50.0%)	28 (54.0%)	20 (45.5%)	12 (52.2%)	1 (33.3%)
≧2	17 (13.9%)	9 (17.0%)	6 (13.6%)	2 (8.7%)	0 (0.0%)
Gender					
Male	59 (48.4%)	29 (55.8%)	15 (34.1%)	12 (52.2%)	3 (100%)
Female	63 (51.6%)	23 (44.2%)	29 (65.9%)	11 (47.8%)	0 (0.0%)
Smoking					
Current/Former	33 (27.0%)	16 (30.8%)	8 (18.2%)	7 (30.4%)	2 (66.7%)
Never	89 (73.0%)	36 (69.2%)	36 (81.8%)	16 (69.6%)	1 (33.3%)
Histology					
Adenocarcinoma	112 (91.8%)	48 (92.3%)	42 (95.5%)	19 (82.6%)	3 (100%)
Squamous cell carcinoma	10 (8.2%)	4 (7.7%)	2 (4.5%)	4 (17.4%)	0 (0.0%)
Metastasis Site					
brain	49 (40.2%)	22 (42.3%)	20 (45.5%)	7 (30.4%)	0 (0.0%)
bone	61 (50.0%)	26 (50.0%)	21 (47.7%)	13 (56.5%)	1 (33.3%)
liver	23 (18.9%)	11 (21.2%)	6 (13.6%)	6 (26.1%)	0 (0.0%)
The line of ICI					
1	9 (7.4%)	0 (0.0%)	0 (0.0%)	9 (39.1%)	0 (0.0%)
2	31 (25.4%)	11 (21.2%)	12 (27.3%)	6 (26.1%)	2 (66.7%)
3	42 (34.4%)	21 (40.4%)	15 (34.1%)	5 (21.7%)	1 (33.3%)
≧4	40 (32.8%)	20 (38.4%)	17 (38.6%)	3 (13.0%)	0 (0.0%)
ICI Treatment					
ICI Monotherapy	32 (26.2%)	12 (23.1%)	12 (27.3%)	8 (34.8%)	0 (0.0%)
ICI-based combination therapy	90 (73.8%)	40 (76.9%)	32 (72.7%)	15 (65.2%)	3 (100%)
ICI Drug					
PD-1	116 (95.1%)	50 (96%)	40 (90.9%)	23 (100%)	3 (100%)
PD-L1	6 (4.9%)	2 (4.0%)	4 (9.1%)	0 (0.0%)	0 (0.0%)
PD-L1 expression					
<1%	24 (19.7%)	12 (23.1%)	6 (13.6%)	5 (21.7%)	1 (33.3%)
1-49%	28 (23.0%)	14 (26.9%)	6 (13.6%)	8 (34.8%)	0 (0.0%)
≧50%	34 (27.8%)	14 (26.9%)	17 (38.6%)	2 (8.7%)	1 (33.3%)
unknown	36 (29.5%)	12 (23.1%)	15 (34.1%)	8 (34.8%)	1 (33.3%)

**G719X 2, L861Q 1.*

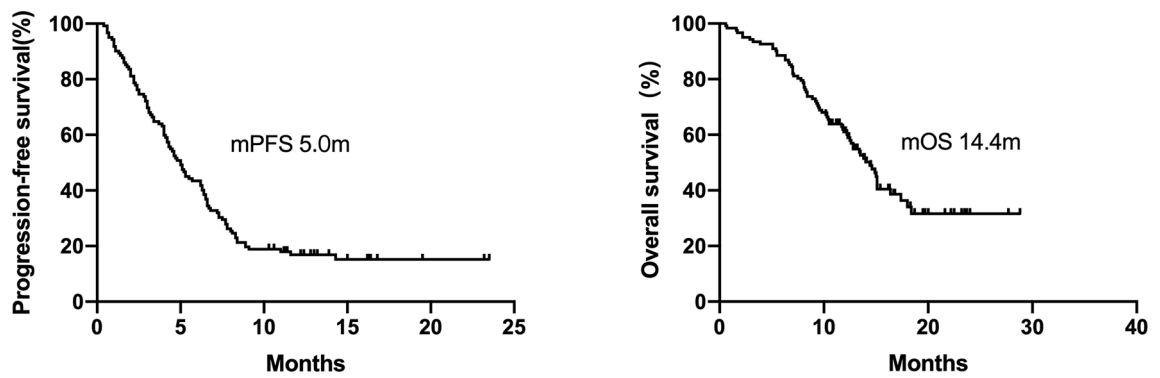

FIGURE 1 | Kaplan–Meier curves for progression-free survival and overall survival of patients with EGFR-mutant NSCLC (n = 122). The median PFS and OS were 5.0 months and 14.4 months, respectively.

(27), suggesting that the efficacy of salvage chemotherapy alone was unsatisfactory, and thus physicians were enthusiastic to explore ICI in EGFR-mutant NSCLC. Although the role of ICI monotherapy uses in EGFR-mutant NSCLC is debatable (11–14), our study indicated that ICI treatment for EGFR-mutant NSCLC obtained a mPFS of 5 months and a mOS of 14.4 months. In detail, ICI-based combination therapy outperformed ICI monotherapy, with a mPFS of 5 months versus 2.2 months and mOS of 14.4

TABLE 2 | The treatment responses of different EGFR mutation types.

RECISTResponse	All patients (n = 122)	Common mutations (n = 96)	19Del (n = 52)	L858R (n = 44)	Uncommon mutations (n = 26)	20Ins (n = 23)	Other* (n = 3)
Complete response	0	0	0	0	0	0	0
Partial response	39 (32%)	30 (31.3%)	16 (30.8%)	14 (31.8%)	9 (34.6%)	8 (34.8%)	1 (33.3%)
Stable disease	46 (37.7%)	37 (38.5%)	16 (30.8%)	21 (47.7%)	9 (34.6%)	8 (34.8%)	1 (33.3%)
Progressive disease	37 (30.3%)	29 (30.2%)	20 (38.5%)	9 (20.5%)	8 (30.8%)	7 (30.4%)	1 (33.3%)
Overall response rate	32.0%	31.3%	30.8%	31.8%	34.6%	34.8%	33.3%
Disease control rate	70.0%	70.0%	61.5%	79.5%	69.2%	69.6%	66.7%
Median progression-free survival, months	5.0	4.4	3.8	6.1	6.4	6.4	7.7
Median overall survival, months	14.4	13.4	12.8	13.5	NR	NR	18.4

**G719X 2, L861Q 1.*
NR, not reached.

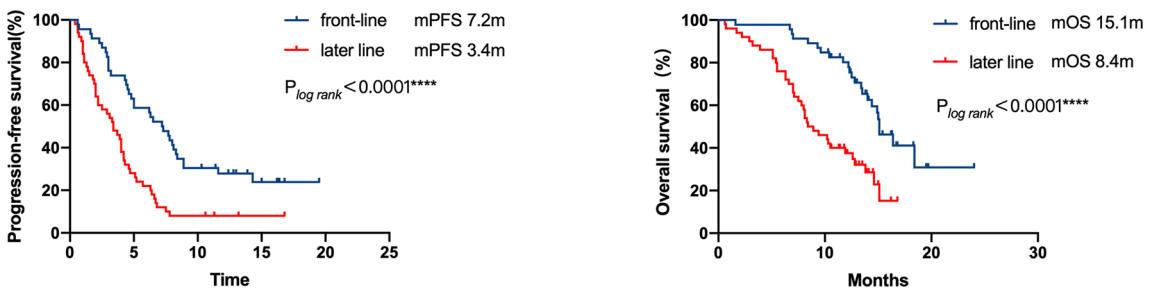

FIGURE 2 | Kaplan–Meier curves of progression-free survival and overall survival of patients who received ICI therapy at different lines of treatment. The patients who were administered front-line ICI exhibited superior survival benefits than those who received ICI as later line after progression on TKI (mPFS 7.2 months *vs.* 3.4 months, respectively, P < 0.0001; mOS 15.1 months *vs.* 8.4 months, respectively, P < 0.0001).

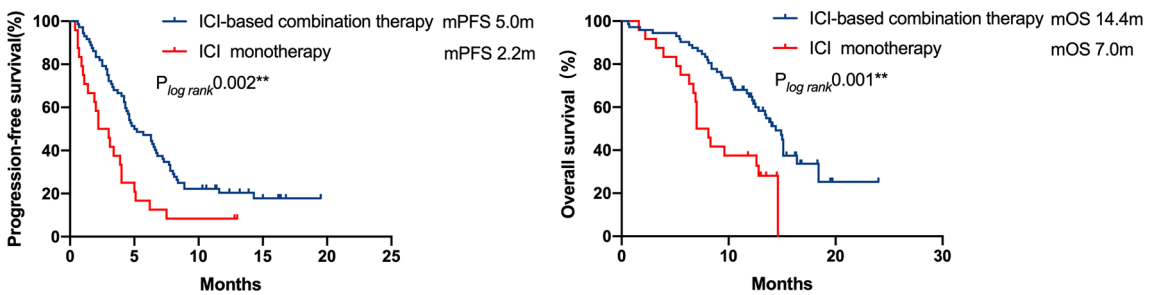

FIGURE 3 | Kaplan–Meier curves of progression-free survival and overall survival of patients who received ICI-based combination therapy *versus* ICI monotherapy. The efficacy of ICI-based combination therapy was better than that of ICI monotherapy (mPFS 5.0months *vs.* 2.2 months, P = 0.002, mOS 14.4 months *vs.* 7.0 months, P = 0.001).

months versus 7 months, respectively. These results were somewhat interesting.

Previous single-arm studies on ICI-based combination regimens in EGFR-mutant NSCLC patients after EGFR TKI failure have reported inconsistent results (17–19). The CT 18 study (18) and other studies using a combination approach of ICI with chemotherapy have exhibited survival benefits (16, 17), which was also observed in our study, whereas a study with camrelizumab plus apatinib achieved inferior outcome (19). Basic studies support that chemotherapy, antiangiogenic drugs, and radiotherapy exert synergistic effects with ICI *via* positive regulation of the immune system, changing the tumor immune microenvironment, and releasing tumor neoantigens (28–32). Besides the role of ICI, the optimal combination strategy is still unclear. Our study including patients who received first–, second–, third-generation EGFR TKI in the first-line or after acquired T790M mutation reflected the real-world situation, and the majority of cases received ICI combined with chemotherapy. The current study evaluated the efficacy of ICI combination regimen versus monotherapy and observed improved survival from ICI-based combination therapy. Considering the toxicities of ICI combined with chemotherapy (16), an alternative combined

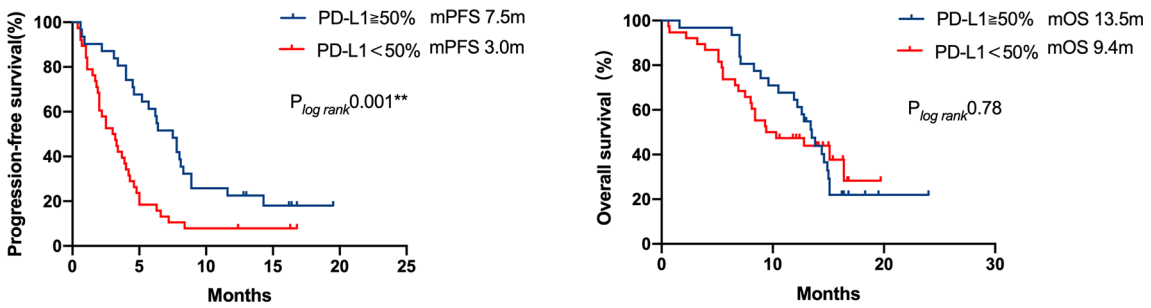

FIGURE 4 | Kaplan–Meier curves of progression-free survival and overall survival of patients with differential PD-L1 expression. A significant PFS benefit was observed in patients with strong positive PD-L1 expression (TPS ≥ 50%) compared with that in patients with a lower PD-L1 expression (TPS < 50%) (7.5 months *vs* 3.0 months, respectively, P = 0.001), but the difference in OS was not statistically significant.

TABLE 3 | The univariable and multivariable analyses of PFS and OS among the EGFR common mutation population.

	Univariable analysis				Multivariable analysis			
	PFS		OS		PFS		OS	
	HR (95%CI)	*P*	HR (95%CI)	*P*	HR (95%CI)	*P*	HR (95%CI)	*P*
Age ≦65 *vs* >65	1.01 (0.58~1.78)	0.969	0.89 (0.66~1.22)	0.47	1.08 (0.56~2.083)	0.819	0.57 (0.27~1.17)	0.123
Smoking status Yes *vs* No	1.22 (0.74~2.01)	0.437	1.02 (0.56~1.86)	0.953	0.93 (0.56~1.57)	0.792	1.03 (0.55~1.93)	0.916
ECOG score 0>1 *vs* ≧2	0.74 (0.56~1.00)	0.048	0.54 (0.39~0.75)	<0.0001	0.62 (0.32~1.21)	0.161	0.33 (0.16~0.71)	0.004
PD-L1 expression ≧50% *vs* <50%	0.42 (0.25~0.71)	0.001	0.92 (0.52~1.65)	0.782	0.49 (0.28~0.88)	0.017	1.45 (0.75~2.78)	0.271
Treatment strategy Combined *vs* Mono	0.46 (0.28~0.75)	0.002	0.39 (0.22~0.70)	0.002	0.38 (0.21~0.68)	0.001	0.47 (0.25~0.91)	0.024
Time of ICI treatment front-line *vs* later line	0.64 (0.51~0.80)	<0.0001	0.58 (0.44~0.77)	<0.0001	0.53 (0.31~0.92)	0.024	0.35 (0.17~0.69)	0.003
EGFR mutation subtype L858R *vs* 19Del	0.49 (0.31~0.77)	0.002	0.81 (0.48~1.36)	0.422	0.49 (0.30~0.79)	0.004	0.70 (0.40~1.23)	0.219

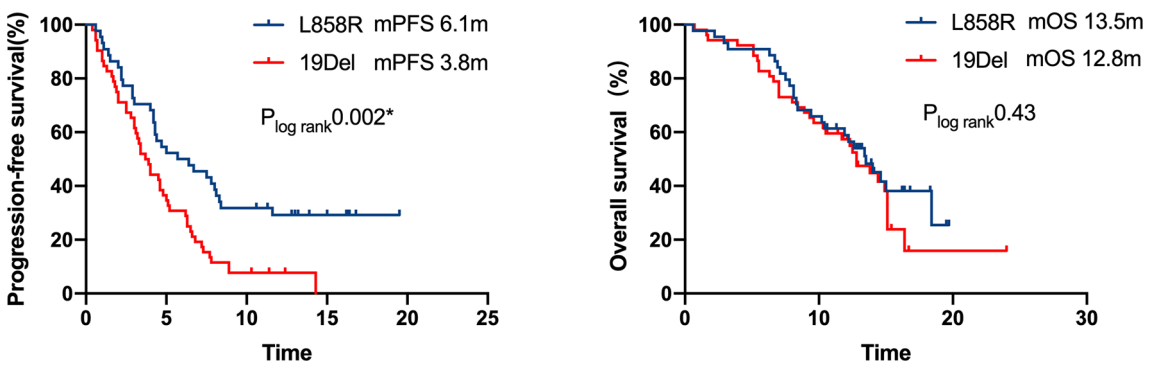

FIGURE 5 | Kaplan–Meier curves of progression-free survival and overall survival of patients with differential mutation type. A significant PFS benefit was observed in patients with L858R compared with that in patients with 19Del (6.1 months *vs*. 3.8 months, respectively, P = 0.002), but the difference in OS was not statistically significant.

partner from chemotherapy to antiangiogenic drugs seems reasonable (19), but the efficacy of the chemotherapy-free combined strategy needed to be further explored.

Several studies concerning gene wild-type NSCLC have indicated that the earlier the use of ICIs, the better the outcome maybe (33, 34). Some studies on EGFR-mutant NSCLC after EGFR TKI failure recruited patients without prior palliative chemotherapy (17, 18), whereas a study of camrelizumab plus apatinib (19) including patients in the later setting exhibited lower RR and shorter PFS. Our study showed that front-line administration of ICI after EGFR-TKI resistance was more beneficial in terms of PFS and OS. This phenomenon is consistent with that observed in patients with wild-type driver gene. Although the tumor microenvironment (TME) of EGFR-mutant NSCLC is immunosuppressive (28), EGFR-TKI may activate the TME by increasing dendritic cells and CD8+ cells, reducing Tregs, and inhibiting M2-like macrophages polarization at an early stage (35). EGFR-TKI could also affect the expression of PD-L1 (36) and the distribution of the CD4+, and Foxp3+ cells within the TME (37–39). We speculate that the insertion of other treatments before ICI may possibly perturb the favorable immune microenvironment that may exist after TKI treatment. Therefore, the administration timing of ICI treatment for this population may be also important.

The predictive effect of PD-L1 status on the efficacy of ICI treatment among EGFR-mutant NSCLC patients is inadequate and debatable. It is thought that the PD-L1 expression in EGFR-mutant NSCLC patients is mainly mediated by carcinogenic signaling pathways rather than an adaptive immune process, resulting in a lowered capacity to predict the efficacy of immunotherapy (40, 41). Some studies have found that the status of PD-L1 expression could not be used to screen out ICI responders in EGFR-mutant NSCLC patients (42). On the contrary, other studies demonstrated that ICIs can also be used for EGFR-mutant NSCLC patients who have high PD-L1 expression (43). In cohort 1 (n=111) of the ALTLANTIC study (44), durvalumab was used as the third or later line treatment for advanced EGFR/ALK-positive NSCLC patients. Patients with PD-L1 expression ≥ 25% had an ORR of 12%, and better median PFS and 2-year OS rates than patients with PD-L1 expression < 25% (13.3 months *vs.* 9.9 months, 40.7% *vs.* 14.7%, respectively). Similarly, the results of our study indicated that PD-L1 expression ≥50% at baseline was related to better PFS of ICI treatment. EGFR L858R was found to be associated with favorable PFS in our study, which is consistent with the finding of a previous study (45).

It must be noted that this study has certain limitations. First, the results should be interpreted with caution because of the retrospective nature of the study. Second, PD-L1 expression data were not available for every individual. Finally, we could not obtain the PD-L1 expression status data after EGFR-TKI discontinuation, which may be more accurate to predict the efficacy of ICI treatment. Despite these limitations, this retrospective study was performed rigorously and ethically to provide a certain reference value for clinical practice.

In conclusion, ICI therapy, especially front-line ICI therapy and ICI-based combination therapy, may be beneficial for improving the prognosis of advanced EGFR-mutant NSCLC patients after EGFR-TKI therapy discontinuation. These findings need to be verified by prospective randomized controlled phase III clinical studies.

DATA AVAILABILITY STATEMENT

The raw data supporting the conclusions of this article will be made available by the authors, without undue reservation.

ETHICS STATEMENT

The studies involving human participants were reviewed and approved by the institutional ethical review board. Written informed consent for participation was not required for this study in accordance with the national legislation and the institutional requirements.

AUTHOR CONTRIBUTIONS

Study design and data analysis: TT, MY, and MH. Data collection: TT, MY, MH, JL, MJ, DM, ST, ZL, LC, YG, JZ, QZ, and YL. Paper writing: TT. Manuscript modification: MY, and MH. All authors contributed to the article and approved the submitted version.

ACKNOWLEDGMENTS

We thank all participating centers for supporting this study.

REFERENCES

1. Kobayashi S, Boggon TJ, Dayaram T, Jänne PA, Kocher O, Meyerson M, et al. EGFR Mutation and Resistance of Non- Small- Cell Lung Cancer to Gefitinib. *N Engl J Med* (2005) 352(8):786–92. doi: 10.1056/NEJMoa 044238
2. Zhou C, Wu YL, Chen G, Feng J, Liu XQ, Wang C, et al. Erlotinib Versus Chemotherapy as First-Line Treatment for Patients With Advanced EGFR Mutation-Positive Non-Small-Cell Lung Cancer (OPTIMAL, CTONG-0802): A Multicentre, Open- Label, Randomised, Phase 3 Study. *Lancet Oncol* (2011) 12:735–42. doi: 10.1016/S1470-2045(11)70184-X
3. Ohashi K, Maruvka YE, Michor F, Pao W. Epidermal Growth Factor Receptor Tyrosine Kinase Inhibitor- Resistant Disease. *J Clin Oncol* (2013) 31:1070–80. doi: 10.1200/JCO.2012.43.3912
4. Mok TS, Wu Y-L, Ahn M-J, Garassino MC, Kim HR, Ramalingam SS, et al. Osimertinib or Platinum-Pemetrexed in EGFR T790M-Positive Lung Cancer. *N Engl J Med* (2017) 376(7):629–40. doi: 10.1056/NEJMoa1612674
5. Soria JC, Wu YL, Nakagawa K, Kim SW, Yang JJ, Ahn MJ, et al. Gefitinib Plus Chemotherapy Versus Placebo Plus Chemotherapy in EGFR-Mutation-Positive Non-Small-Cell Lung Cancer After Progression on First-Line Gefitinib (IMPRESS): A Phase 3 Randomised Trial. *Lancet Oncol* (2015) 16 (8):990–8. doi: 10.1016/S1470-2045(15)00121-7

6. Yoshida T, Kuroda H, Oya Y, Shimizu J, Horio Y, Sakao Y, et al. Clinical Outcomes of Platinum-Based Chemotherapy According to T790M Mutation Status in EGFR-Positive non-Small Cell Lung Cancer Patients After Initial EGFR-TKI Failure. *Lung Cancer* (2017) 109:89–91. doi: 10.1016/j.lungcan.2017.05.001
7. Han B, Yang L, Wang X, Yao L. Efficacy of Pemetrexed-Based Regimens in Advanced non-Small Cell Lung Cancer Patients With Activating Epidermal Growth Factor Receptor Mutations After Tyrosine Kinase Inhibitor Failure: A Systematic Review. *Onco Targets Ther* (2018) 11:2121–9. doi: 10.2147/OTT.S157370
8. Yang Y, Yu Y, Lu S. Effectiveness of PD-1/PD-L1 Inhibitors in the Treatment of Lung Cancer: Brightness and Challenge. *Sci China Life Sci* (2020) 63 (10):1499–514. doi: 10.1007/s11427-019-1622-5
9. Doroshow DB, Sanmamed MF, Hastings K, Politi K, Rimm DL, Chen L, et al. Immunotherapy in Non-Small Cell Lung Cancer: Facts and Hopes. *Clin Cancer Res* (2019) 25(15):4592–602. doi: 10.1158/1078-0432.CCR-18-1538
10. Rittmeyer A, Barlesi F, Waterkamp D, Park K, Ciardiello F, von Pawel J, et al. Atezolizumab Versus Docetaxel in Patients With Previously Treated non-Small-Cell Lung Cancer (OAK): A Phase 3, Open-Label, Mul- Ticentre Randomised Controlled Trial. *Lancet* (2017) 389(10066):255–65. doi: 10.1016/S0140-6736(16)32517-X
11. Mazieres J, Drilon A, Lusque A, Mhanna L, Cortot AB, Mezquita L, et al. Immune Checkpoint Inhibitors for Patients With Advanced Lung Cancer and Oncogenic Driver Alterations: Results From the IMMUNOTARGET Registry. *Ann Oncol* (2019) 30(8):1321–8. doi: 10.1093/annonc/mdz167
12. Lisberg A, Cummings A, Goldman JW, Bornazyan K, Reese N, Wang T, et al. A Phase II Study of Pembrolizumab in EGFR-Mutant, PD-L1+, Tyrosine Kinase Inhibitor Naïve Patients With Advanced NSCLC. *J Thorac Oncol* (2018) 13(8):1138–45. doi: 10.1016/j.jtho.2018.03.035
13. Lee CK, Man J, Lord S, Cooper W, Links M, Gebski V, et al. Clinical and Molecular Characteristics Associated With Survival Among Patients Treated With Checkpoint Inhibitors for Advanced non- Small Cell Lung Carcinoma: A Systematic Review and Meta-Analysis. *JAMA Oncol* (2018) 4(2):210–6. doi: 10.1001/jamaoncol.2017.4427
14. Ng TL, Liu Y, Dimou A, Patil T, Aisner DL, Dong Z, et al. Predictive Value of Oncogenic Driver Subtype, Programmed Death-1 Ligand (PD-L1) Score, and Smoking Status on the Efficacy of PD-1/PD-L1 Inhibitors in Patients With Oncogene-Driven non–Small Cell Lung Cancer. *Cancer* (2019) 125(7):1038–49. doi: 10.1002/cncr.31871
15. Qiao M, Jiang T, Liu X, Mao S, Zhou F, Li X, et al. Immune Checkpoint Inhibitors in EGFR-Mutated NSCLC: Dusk or Dawn? *J Thorac Oncol* (2021) 16(8):1267–88. doi: 10.1016/j.jtho.2021.04.003
16. Reck M, Mok TSK, Nishio M, Jotte RM, Cappuzzo F, Orlandi F, et al. Atezolizumab Plus Bevacizumab and Chemotherapy in non-Small-Cell Lung Cancer (IMpower150): Key Subgroup Analyses of Patients With EGFR Mutations or Baseline Liver Metastases in a Randomised, Open-Label Phase 3 Trial. *Lancet Respir Med* (2019) 7(5):387–401. doi: 10.1016/S2213-2600(19)30084-0
17. Lam TC, Tsang KC, Choi HC, Lee VH, Lam KO, Chiang CL, et al. Combination Atezolizumab, Bevacizumab, Pemetrexed and Carboplatin for Metastatic EGFR Mutated NSCLC After TKI Failure. *Lung Cancer* (2021) 159:18–26. doi: 10.1016/j.lungcan.2021.07.004
18. Jiang T, Wang P, Zhang J, Zhao Y, Zhou J, Fan Y, et al. Toripalimab Plus Chemotherapy as Second-Line Treatment in Previously EGFR-TKI Treated Patients With EGFR-Mutant-Advanced NSCLC: A Multicenter Phase-II Trial. *Signal Transduct Target Ther* (2021) 6(1):355. doi: 10.1038/s41392-021-00751-9
19. Gao G, Wang Y, Ren S, Liu Z, Chen G, Gu K, et al. Efficacy of Camrelizumab (SHR-1210) Plus Apatinib in Advanced NSCLC With EGFR Mutation. *J Thorac Oncol* (2021) 16(3):S654–4. doi: 10.1016/j.jtho.2021.01.1198
20. Choudhury NJ, Schoenfeld AJ, Flynn J, Falcon CJ, Rizvi H, Rudin CM, et al. Response to Standard Therapies and Comprehensive Genomic Analysis for Patients With Lung Adenocarcinoma With EGFR Exon 20 Insertions. *Clin Cancer Res* (2021) 27(10):2920–7. doi: 10.1158/1078-0432.CCR-20-4650
21. Chen K, Pan G, Cheng G, Zhang F, Xu Y, Huang Z, et al. Immune Microenvironment Features and Efficacy of PD-1/PD-L1 Blockade in non-Small Cell Lung Cancer Patients With EGFR or HER2 Exon 20 Insertions. *Thorac Cancer* (2021) 12(2):218–26. doi: 10.1111/1759-7714.13748
22. Metro G, Baglivo S, Bellezza G, Mandarano M, Gili A, Marchetti G, et al. Sensitivity to Immune Checkpoint Blockade in Advanced Non-Small Cell Lung Cancer Patients With EGFR Exon 20 Insertion Mutations. *Genes (Basel)* (2021) 12(5):679. doi: 10.3390/genes12050679
23. Büttner R, Gosney JR, Skov BG, Adam J, Motoi N, Bloom KJ, et al. Programmed Death-Ligand 1 Immunohistochemistry Testing: A Review of Analytical Assays and Clinical Implementation in Non-Small-Cell Lung Cancer. *J Clin Oncol* (2017) 35(34):3867–76. doi: 10.1200/JCO.2017.74.7642
24. Seo JS, Ju YS, Lee WC, Shin JY, Lee JK, Bleazard T, et al. The Transcriptional Landscape and Mutational Profile of Lung Adenocarcinoma. *Genome Res* (2012) 22(11):2109–19. doi: 10.1101/gr.145144.112
25. Garon EB, Rizvi NA, Hui R, Leighl N, Balmanoukian AS, Eder JP, et al. Pembrolizumab for the Treatment of non-Small-Cell Lung Cancer. *N Engl J Med* (2015) ;372(21):2018–28. doi: 10.1056/NEJMoa1501824
26. Reck M, Rodríguez-Abreu D, Robinson AG, Hui R, Csőszi T, Fülöp A, et al. Five-Year Outcomes With Pembrolizumab Versus Chemotherapy for Metastatic Non-Small-Cell Lung Cancer With PD-L1 Tumor Proportion Score ≥ 50. *J Clin Oncol* (2021) 39(21):2339–49. doi: 10.1200/JCO.21.00174
27. Janne PA, Lee JK, Madison R, Venstrom JM. Incidence and Heterogeneity of C797S and Other EGFR Resistance Mutations on Routine Comprehensive Genomic Profiling (CGP). *J Clin Oncol* (2021) 39(suppl 15):9101–1. doi: 10.1200/JCO.2021.39.15_suppl.9101
28. Zhou F, Zhou C. Chemotherapy Should Be Combined With Checkpoint Inhibitors in the Treatment of Patients With Stage IV EGFR-Mutant NSCLC Whose Disease Has Progressed on All Available Tyrosine Kinase Inhibitors. *J Thorac Oncol* (2021) 16(10):1622–6. doi: 10.1016/j.jtho.2021.07.011
29. McLaughlin M, Patin EC, Pedersen M, Wilkins A, Dillon MT, Melcher AA, et al. Inflammatory Microenvironment Remodelling by Tumour Cells After Radiotherapy. *Nat Rev Cancer* (2020) 20(4):203–17. doi: 10.1038/s41568-020-0246-1
30. Yin Z, Li C, Wang J, Xue L. Myeloid-Derived Suppressor Cells: Roles in the Tumor Microenvironment and Tumor Radiotherapy. *Int J Cancer* (2019) 144 (5):933–46. doi: 10.1002/ijc.31744
31. Vacchelli E, Ma Y, Baracco EE, Sistigu A, Enot DP, Pietrocola F, et al. Chemotherapy-Induced Antitumor Immunity Requires Formyl Peptide Receptor 1. *Science* (2015) 350(6263):972–8. doi: 10.1126/science.aad0779
32. Fukumura D, Kloepper J, Amoozgar Z, Duda DG, Jain RK. Enhancing Cancer Immunotherapy Using Antiangiogenics: Opportunities and Challenges. *Nat Rev Clin Oncol* (2018) 15(5):325–40. doi: 10.1038/nrclinonc.2018.29
33. Blumenthal GM, Zhang L, Zhang H, Kazandjian D, Khozin S, Tang S, et al. Milestone Analyses of Immune Checkpoint Inhibitors, Targeted Therapy, and Conventional Therapy in Metastatic Non-Small Cell Lung Cancer Trials: A Meta-Analysis. *JAMA Oncol* (2017) 3(8):e171029. doi: 10.1001/jamaoncol.2017.1029
34. Park SE, Lee SH, Ahn JS, Ahn MJ, Park K, Sun JM. Increased Response Rates to Salvage Chemotherapy Administered After PD-1/PD-L1 Inhibitors in Patients With Non-Small Cell Lung Cancer. *J Thorac Oncol* (2018) 13 (1):106–11. doi: 10.1016/j.jtho.2017.10.011
35. Jia Y, Li X, Jiang T, Zhao S, Zhao C, Zhang L, et al. EGFR-Targeted Therapy Alters the Tumor Microenvironment in EGFR-Driven Lung Tumors: Implications for Combination Therapies. *Int J Cancer* (2019) 145(5):1432–44. doi: 10.1002/ijc.32191
36. Ichihara E, Harada D, Inoue K, Shibayama T, Hosokawa S, Kishino D, et al. Characteristics of Patients With EGFR-Mutant non-Small-Cell Lung Cancer Who Benefited From Immune Checkpoint Inhibitors. *Cancer Immunol Immunother.* (2021) 70(1):101–6. doi: 10.1007/s00262-020-02662-0
37. Isomoto K, Haratani K, Hayashi H, Shimizu S, Tomida S, Niwa T, et al. Impact of EGFR-TKI Treatment on the Tumor Immune Microenvironment in EGFR Mutation-Positive Non-Small Cell Lung Cancer. *Clin Cancer Res* (2020) 26(8):2037–46. doi: 10.1158/1078-0432.CCR-19-2027
38. Yang CY, Liao WY, Ho CC, Chen KY, Tsai TH, Hsu CL, et al. Association Between Programmed Death-Ligand 1 Expression, Immune Microenvironments, and Clinical Outcomes in Epidermal Growth Factor Receptor Mutant Lung Adenocarcinoma Patients Treated With Tyrosine Kinase Inhibitors. *Eur J Cancer* (2020) 124:110–22. doi: 10.1016/j.ejca.2019.10.019
39. Lin A, Wei T, Meng H, Luo P, Zhang J. Role of the Dynamic Tumor Microenvironment in Controversies Regarding Immune Checkpoint Inhibitors for the Treatment of non-Small Cell Lung Cancer (NSCLC)

With EGFR Mutations. *Mol Cancer* (2019) 18(1):139. doi: 10.1186/s12943-019-1062-7
40. Toki MI, Mani N, Smithy JW, Liu Y, Altan M, Wasserman B, et al. Immune Marker Profiling and Programmed Death Ligand 1 Expression Across NSCLC Mutations. *J Thorac Oncol* (2018) 13(12):1884–96. doi: 10.1016/j.jtho.2018.09.012
41. Akbay EA, Koyama S, Carretero J, Altabef A, Tchaicha JH, Christensen CL, et al. Activation of the PD-1 Pathway Contributes to Immune Escape in EGFR-Driven Lung Tumors. *Cancer Discov* (2013) 3(12):1355–63. doi: 10.1158/2159-8290.CD-13-0310
42. Yamada T, Hirai S, Katayama Y, Yoshimura A, Shiotsu S, Watanabe S, et al. Retrospective Efficacy Analysis of Immune Checkpoint Inhibitors in Patients With EGFR-Mutated non-Small Cell Lung Cancer. *Cancer Med* (2019) 8(4):1521–9. doi: 10.1002/cam4.2037
43. Masuda K, Horinouchi H, Tanaka M, Higashiyama R, Shinno Y, Sato J, et al. Efficacy of Anti-PD-1 Antibodies in NSCLC Patients With an EGFR Mutation and High PD-L1 Expression. *J Cancer Res Clin Oncol* (2021) 147(1):245–51. doi: 10.1007/s00432-020-03329-0
44. Garassino MC, Cho BC, Kim JH, Mazières J, Vansteenkiste J, Lena H, et al. Final Overall Survival and Safety Update for Durvalumab in Third- or Later-Line Advanced NSCLC: The Phase II ATLANTIC Study. *Lung Cancer* (2020) 147:137–42. doi: 10.1016/j.lungcan.2020.06.032
45. Hastings K, Yu HA, Wei W, Sanchez-Vega F, DeVeaux M, Choi J, et al. EGFR Mutation Subtypes and Response to Immune Checkpoint Blockade Treatment in Non-Small-Cell Lung Cancer. *Ann Oncol* (2019) 30(8):1311–20. doi: 10.1093/annonc/mdz141

Conflict of Interest: The authors declare that the research was conducted in the absence of any commercial or financial relationships that could be construed as a potential conflict of interest.

Publisher's Note: All claims expressed in this article are solely those of the authors and do not necessarily represent those of their affiliated organizations, or those of the publisher, the editors and the reviewers. Any product that may be evaluated in this article, or claim that may be made by its manufacturer, is not guaranteed or endorsed by the publisher.

frontiers in Immunology

ORIGINAL RESEARCH
published: 21 December 2021
doi: 10.3389/fimmu.2021.788985

ERAP2 Is Associated With Immune Infiltration and Predicts Favorable Prognosis in SqCLC

Zhenlin Yang[1†], He Tian[1†], Fenglong Bie[1†], Jiachen Xu[2], Zheng Zhou[1], Junhui Yang[3], Renda Li[1], Yue Peng[1], Guangyu Bai[1], Yanhua Tian[4], Ying Chen[5], Lei Liu[1], Tao Fan[1], Chu Xiao[1], Yujia Zheng[1], Bo Zheng[6], Jie Wang[2], Chunxiang Li[1], Shugeng Gao[1*] and Jie He[1*]*

[1] Department of Thoracic Surgery, National Cancer Center/National Clinical Research Center for Cancer/Cancer Hospital, Chinese Academy of Medical Sciences, Peking Union Medical College, Beijing, China, [2] Department of Medical Oncology, National Cancer Center/National Clinical Research Center for Cancer/Cancer Hospital, Chinese Academy of Medical Sciences, Peking Union Medical College, Beijing, China, [3] Genetron Health (Beijing) Co. Ltd., Beijing, China, [4] Department of Thoracic Surgery/Head & Neck Medical Oncology, The University of Texas (UT) MD Anderson Cancer Center, Houston, TX, United States, [5] Department of Thoracic Surgery I, The Third Affiliated Hospital of Kunming Medical University (Yunnan Cancer Hospital, Yunnan Cancer Center), Kunming, China, [6] Department of Pathology, National Cancer Center/National Clinical Research Center for Cancer/Cancer Hospital, Chinese Academy of Medical Sciences, Peking Union Medical College, Beijing, China

OPEN ACCESS

Edited by:
Qian Chu,
Huazhong University of Science and Technology, China

Reviewed by:
Anastasia Mpakali,
National Centre of Scientific Research Demokritos, Greece
Wenjun Mou,
Capital Medical University, China

***Correspondence:**
Jie He
prof.jiehe@gmail.com
Shugeng Gao
gaoshugeng@cicams.ac.cn
Chunxiang Li
lichunxiang@cicams.ac.cn

[†]These authors have contributed equally to this work and share the first authorship

Specialty section:
This article was submitted to Cancer Immunity and Immunotherapy, a section of the journal Frontiers in Immunology

Received: *04 October 2021*
Accepted: *06 December 2021*
Published: *21 December 2021*

Citation:
Yang Z, Tian H, Bie F, Xu J, Zhou Z, Yang J, Li R, Peng Y, Bai G, Tian Y, Chen Y, Liu L, Fan T, Xiao C, Zheng Y, Zheng B, Wang J, Li C, Gao S and He J (2021) ERAP2 Is Associated With Immune Infiltration and Predicts Favorable Prognosis in SqCLC. Front. Immunol. 12:788985. doi: 10.3389/fimmu.2021.788985

Background: Immunotherapy has been proven effective among several human cancer types, including Squamous cell lung carcinoma (SqCLC). ERAP2 plays a pivotal role in peptide trimming of many immunological processes. However, the prognostic role of ERAP2 and its relationship with immune cell infiltration in SqCLC remains unclear.

Methods: The differential expression of ERAP2 was identified *via* GEO and TCGA databases. We calculated the impact of ERAP2 on clinical prognosis using the Kaplan-Meier plotter. TIMER was applied to evaluate the abundance of immune cells infiltration and immune markers. SqCLC tissue microarrays containing 190 patients were constructed, and we performed immunohistochemical staining for ERAP2, CD8, CD47, CD68, and PD-L1 to validate our findings in public data.

Results: In the GEO SqCLC database, ERAP2 was upregulated in patients with better survival (p=0.001). ERAP2 expression in SqCLC was significantly lower than that of matched normal samples (p<0.05) based on TCGA SqCLC data. Higher expression of ERAP2 was significantly associated with better survival in SqCLC patients from TCGA (p=0.007), KM-plotter (p=0.017), and our tissue microarrays (TMAs) (p=0.026). In univariate and multivariate Cox analysis of SqCLC TMAs, high ERAP2 expression was identified as an independent protective factor for SqCLC patients (Univariate Cox, HR=0.659, range 0.454-0.956, p<0.05. Multivariate Cox, HR=0.578, range 0.385-0.866, p<0.05). In TIMER, ERAP2 was positively correlated with several immune markers (CD274, p=1.27E-04; CD68, p=5.88E-08) and immune infiltrating cells ($CD8^+$ T cell, p=4.09E-03; NK cell, p=1.00E-04). In our cohort, ERAP2 was significantly correlated with $CD8^+$ tumor-infiltrating lymphocytes (TILs) (p=0.0029), and patients with

higher ERAP2 expression had a higher percentage of PD-L1 positive patients (p=0.049) and a higher $CD8^+$ TILs level (p=0.036).

Conclusions: For the first time, our study demonstrates that higher expression of ERAP2 is tightly associated with the immuno-supportive microenvironment and can predict a favorable prognosis in SqCLC. Meanwhile, ERAP2 may be a promising immunotherapeutic target for patients with SqCLC.

Keywords: ERAP2, squamous cell lung cancer (SqCLC), prognosis, immune microenvironment, biomarker

INTRODUCTION

According to the newest data published in 2021, lung cancer has the highest mortality rate among all cancer types and is a significant health care concern throughout the world (1). Approximately 85% of lung cancer can be classified into a histological subtype generally known as non-small cell lung cancer (NSCLC), 25% to 30% of which is squamous cell lung cancer (SqCLC) (2). SqCLC had specific clinicopathologic characteristics, including male gender, older age, smoker preference, comorbidities, and centrally located tumors (3). Patients with SqCLC are usually diagnosed at an advanced stage, and the 5-year overall survival rate of advanced SqCLC was less than 20%.

Even though standard platinum-based chemotherapy is the mainstay of first-line treatment for most SqCLC patients (4), there are still many patients who cannot receive satisfying outcomes (5). Additionally, different from lung adenocarcinoma (LUAD), which has greatly benefited from targeted therapies against driver mutations such as epidermal growth factor receptor (EGFR) mutations, etc., inroads in targeted therapy are rare in SqCLC (6, 7). Over the past few decades, the limited therapeutic options rendered SqCLC a challenging-to-treat disease. The introduction of immunotherapy, particularly blockers of the PD-1 axis, into the treatment of NSCLC has revolutionized the therapeutic stand-care of this recalcitrant disease, yielding significant survival benefits (8). However, only a minority of SqCLC patients have achieved sustained benefits. Primary and acquired resistances are common phenomena in SqCLC immunotherapy (9). The immunotherapy of SqCLC is still in its infancy, and more immune-related treatments are warranted.

ERAP2 (Endoplasmic Reticulum Aminopeptidase 2), located on chromosome 5q15, belongs to the oxytocinase subfamily of M1 aminopeptidases and is closely related to ERAP1 (endoplasmic Reticulum Aminopeptidase 1), a homologous enzyme of it (10). Both ERAP2 and ERAP1 mainly participate in the final trimming of peptides that will be loaded on MHC-I (Major Histocompatibility Complex class I) molecules at the cell surface for $CD8^+$ T cells/Natural Killer (NK) cells recognition (11, 12). The length of some peptides entering ER is not suitable for being loaded onto MHC I molecule and thus will be trimmed by ERAP1/2 (13). In the immune-evading tumor, malfunction ERAP2 can undermine tumor-associated antigenic episodes while the immune checkpoints are over-expressed, thus anti-tumor T cell response is suspended (14). Previous studies have highlighted that ERAPs are potential targets for enhancing T/NK cell-mediated immunogenicity of malignant cells for developing anti-tumor immunotherapy (15, 16). In addition, Lim et al. has proved that in bladder cancer patients receiving anti-PD-L1 therapy, ERAP2 expression can stratify overall survival (17). The deficiencies in the expression and function of ERAPs have been demonstrated in multiple tumor types, including lung cancer (18–20). So far, the biological roles of ERAP2 in SqCLC have remained unclear.

This study explored the predictive value and immune-related roles of ERAP2 in SqCLC using public databases. We validated our conclusions in a large-scale SqCLC tissue-microarray with long-term follow-up data. We aimed to illustrate the biological functions of ERAP2 in SqCLC and provide novel clues for administering immunotherapy in SqCLC.

MATERIALS AND METHODS

Bioinformatic Mining of ERAP2

Using R software, we obtained differentially expressed genes (DEGs) from patients with distinct survival in the GEO dataset (GSE30219). GSE30219 dataset contained 61 SqCLC patients, whose median survival time (59 months) was used to stratify groups with better and worse survival. Totally 11 DEGs ($p<0.05$) of the two groups were extracted using the R package limma. The list of DEGs and corresponding logFC values were shown in **Figure 1A**. Using GEPIA (http://gepia2.cancer-pku.cn/#index), an online analysis website containing pan-cancer transcriptome data from TCGA (https://portal.gdc.cancer.gov/), we explored the ERAP2 expression level among multiple cancer types and paired normal samples (**Figure 1B**), in which the SqCLC dataset included 486 tumor samples and 338 normal samples (Red Arrow in **Figure 1B**).Using patients with follow-up data from the GEO dataset (GSE30219), we performed survival analysis in SqCLC stratified by ERAP2 expression. KM-plotter (http://www.kmplot.com/lung/) was used to validate the prognostic effect of ERAP2 in SqCLC that we found in the GEO dataset.

Tissue Microarray Construction and IHC Staining

Following the IRB (Institutional Review Board) approval, formalin-fixed, paraffin-embedded tissue microarrays (TMAs) were created using SqCLC samples collected from patients who underwent surgery from April 2010 to August 2011 in the

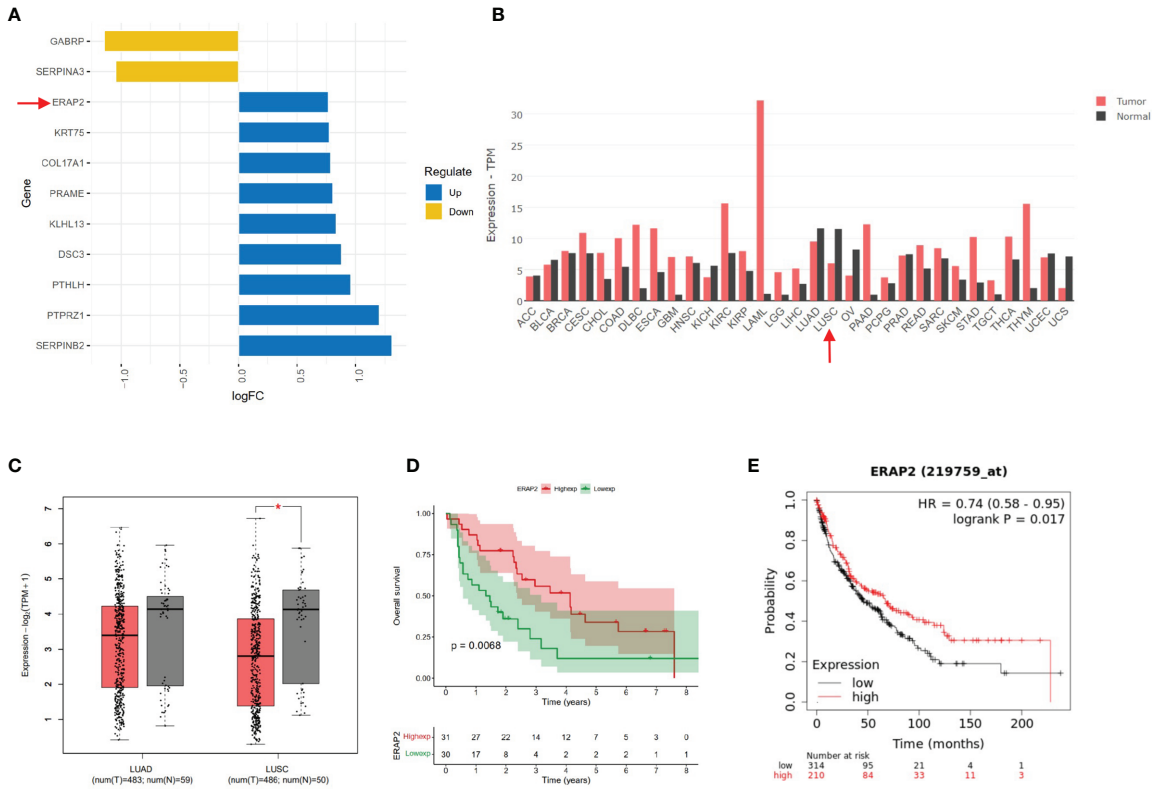

FIGURE 1 | Bioinformatic mining of ERAP2. **(A)** High and low expression genes of SqCLC patients with better survival based on GEO dataset GSE30219. The length of the bar represents the log (fold change) of gene expression between patients with different survival. Orange, low expression genes in patients with better survival. Blue, high expression genes in patients with longer survival. **(B)** ERAP2 expression profiles across all 31 tumor types and paired normal tissues based on TCGA data. The height of the bar represents the median expression of certain tumor types or normal samples. Red, tumor; Black, normal tissue. Arrow, ERAP2 expression in SqCLC. ACC, Adrenocortical carcinoma; BLCA, Bladder Urothelial Carcinoma; BRCA, Breast invasive carcinoma; CESC, Cervical squamous cell carcinoma and endocervical adenocarcinoma; CHOL, Cholangiocarcinoma; COAD, Colon adenocarcinoma; DLBC, Lymphoid Neoplasm Diffuse Large B-cell Lymphoma; ESCA, Esophageal carcinoma; GBM, Glioblastoma multiforme; HNSC, Head and Neck squamous cell carcinoma; KICH, Kidney Chromophobe; KIRC, Kidney renal clear cell carcinoma; KIRP, Kidney renal papillary cell carcinoma; LAML, Acute Myeloid Leukemia; LGG, Brain Lower Grade Glioma; LIHC, Liver hepatocellular carcinoma; LUAD, Lung adenocarcinoma; LUSC, Lung squamous cell carcinoma; OV, Ovarian serous cystadenocarcinoma; PAAD, Pancreatic adenocarcinoma; PCPG, Pheochromocytoma and Paraganglioma; PRAD, Prostate adenocarcinoma; READ, Rectum adenocarcinoma; SARC, Sarcoma; SKCM, Skin Cutaneous Melanoma; STAD, Stomach adenocarcinoma; TGCT, Testicular Germ Cell Tumors; THCA, Thyroid carcinoma; THYM, Thymoma; UCEC, Uterine Corpus Endometrial Carcinoma; USC, Uterine Carcinosarcoma. **(C)** ERAP2 expression in LUAD and LUSC based on data in GEPIA. Left, LUAD. Right, LUSC. Red, tumor sample. Grey, normal sample. Asterisk, p value<0.05; Centerline, median; box limits, upper and lower quartiles; points, outliers. **(D)** K-M curve showing the overall survival of SqCLC patients stratified by ERAP2 expression in the GEO dataset. Red, ERAP2 high expression group. Green, ERAP2 low expression group. **(E)** K-M curve showing the overall survival of SqCLC patients stratified by ERAP2 expression in the KM-Plotter dataset. Red, ERAP2 high expression group. Black, ERAP2 low expression group.

Department of Thoracic Surgery, Cancer Hospital, Chinese Academy of Medical Sciences and Peking Union Medical College. The TMAs contained 190 SqCLC tumor samples. The tumor tissues were fixed by formalin and embedded in paraffin. We took two 2-mm cores from each sample to constitute the TMAs, and then 4-μm thick TMA sections were manufactured. All manual process was conducted by professional pathological technicians from the Department of Pathology of our hospital. All specimens in the 3 TMAS were diagnosed, selected, and confirmed by two certified pathological clinicians.

We performed immunohistochemistry (IHC) of several markers on the TMA, including ERAP2, PD-L1, CD47, CD8, and CD68. We incubated the TMAs with the primary antibodies against ERAP2 (Sigma, HPA034498), PD-L1 (Abcam, 28-8), CD47 (Abcam, EPR21794), CD8 (CST, D8A8Y), and CD68 (Abcam, KP1), and then with the secondary antibodies and 3, 3'-diaminobenzidine (DAB).

Two independent pathologists without prior knowledge of our research evaluated the IHC staining results. ERAP2 expression was scored using a combined method (21). Negative, weak, moderate, and strong intensities were scored as 0, 1, 2, and 3, respectively. The percentage of cells that stained at each intensity score was estimated visually. The ultimate score for each specimen was calculated as the sum of the percentage of stained cells multiplied by the intensity scores. For instance, a sample with 10% negative staining, 40% moderate staining, and

50% strong staining would be assessed a score of 2.3 (0.1×0 + 0.4×2 + 0.5×3 = 2.3). All samples were scored twice independently by two pathologists who were blinded to our study. For PD-L1 and CD47, membranous tumor proportion score (TPS) was applied, during which TPS ≥ 1% and TPS ≥ 5% were set as the positive standard for the two markers, respectively. Co-expression of PD-L1 and CD47 was defined as samples positive in both PD-L1 and CD47. For CD8 and CD68, we calculated the number of CD8-positive TILs and CD68-positive macrophages under six high-power fields and took the average for each specimen.

Survival Analysis

Overall survival (OS) was used to evaluate the prognosis in both public data and our SqCLC cohort. OS was determined as the time from the diagnosis of SqCLC to the patient's death, independent from the cause of death. For OS of our cohort, patients who were alive on September 20, 2018, were defined as censored data. The K-M curve was applied to analyze the survival data of patients. We used the R software package "RMS" to portray the Nomogram for patients based on several clinicopathological factors and immune biomarkers, including ERAP2 expression level. In our model, the total point of a patient was generated based on facts from each element and had corresponding 1-year, 2-year, and 3-year survival rates.

Gene Function Analysis

Based on TCGA (502 samples) and GEO dataset GSE30219 (61 samples) SqCLC transcription data, we used gene enrichment analysis to explore the function of ERAP2-related differentially expressed genes. The enrichment analysis method was described in the previous research (22). The gene enrichment analysis was performed using the following database and gene set: Gene Ontology (GO, c5.all.v7.4.symbols.gmt [Gene ontology]), Kyoto Encyclopedia of Genes and Genomes (KEGG, c2.cp.kegg.v7.4.symbols.gmt [Curated]), Immunologic signatures (c7.all.v7.4.symbols.gmt [Immunologic signatures]). R software was used to visualize the results of gene function enrichment analysis. Based on the above-mentioned TCGA and GEO transcriptome dataset, we classified patients into ERAP2 high and low expression groups using the median ERAP2 expression value and performed differentially expressed genes (DEGs)analysis between them ($p<0.05$, R package "edgeR" and "limma" were for TCGA data and GEO data, respectively). Then we conducted GO and KEGG enrichment analysis based on the DEGs and drew the bubble charts.

Immune-Associated Exploration of ERAP2

To identify the potential connection between each two factors of the TMAs, we performed pairwise association analysis. For ERAP2, we classified all SqCLC TMAs patients into high and low expression groups according to the median staining score. The expression of other immune markers was evaluated based on their cut-off values (CD8, CD68: median. PD-L1: 1% and 10%. CD47: 5% and 20%).

We also explored the immune-associated function of ERAP2 in public data using TIMER (http://timer.comp-genomics.org). With this tool, we study the associations between the expression of ERAP2 and several immune markers in SqCLC, including CD68, CD8A, CTLA4, FOXP3, CD274, and CD4. We also explored the relationship between ERAP2 expression and immune cell infiltration levels in SqCLC, including $CD8^+$T cell, M0 macrophage, regulatory T cell, M1 macrophage, activated NK cell, and M2 macrophage. CIBERSORT (23) algorithm was applied by TIMER for analysis.

Statistical Analysis

All data were managed using R software (R x64 4.0.2 Version) and GraphPad Prism 8. An independent-sample was used to make comparisons of continuous and categorical variables between groups. The univariate/multivariate Cox proportional hazard models were used to assess the prognosis. The Kaplan–Meier method was applied to evaluate survival, and the log-rank test was used to determine significance. We used Spearman correlation to explore the associations between variables. We regarded a two-tailed p-value <0.05 as statistically significant.

RESULTS

Bioinformatic Mining of ERAP2

We used the GEO dataset GSE30219 (containing SqCLC patients) and classified the patients into better and worse survival groups. DEGs were acquired based on the two groups. According to the p-value and fold-change (FC), we showed 11 DEGs in **Figure 1A**. ERAP2 upregulated in patients with better survival (p-value=0.001, logFC=0.767). According to previous studies, ERAP2 was closely related with CD8 T cell, NK cell, and several immune process (13), indicating it may play important roles in cancer immunology. We then profiled the expression of ERAP2 in multiple cancer types and matched normal tissues by GEPIA2, as shown in **Figure 1B**. We then drew boxplots to show more details on the expression of ERAP2 for NSCLC. We found that ERAP2 expression in SqCLC was statistically lower than that in paired normal tissues (**Figure 1C**), suggesting that the deficiency of ERAP2 might participate in the carcinogenesis of SqCLC. Further, using the GEO dataset GSE30219 (**Figure 1D**) and KM-plotter (http://kmplot.com/analysis/index.php?p=service&cancer=lung) (**Figure 1E**), we drew K-M curves stratified by ERAP2 expression, exhibiting that patients with high ERAP2 expression had longer overall survival in SqCLC ($p<0.05$).

Prognostic Roles of ERAP2 in Our Cohort

To validate the prognostic impact of ERAP2 on SqCLC, we established an independent SqCLC cohort, including a total of 190 SqCLC patients, and the tumor samples were retrospectively collected to constitute TMAs. The clinicopathological information of our cohort is shown in **Table 1**. Most patients were males (183, 96.32%) and smokers (176, 92, 63%). According to the 8^{th} AJCC (American Joint Committee on Cancer) Staging Manual (24), there were 34 (17.89%) stage I patients, 70 (36.84%) stage II patients, and 86 (45.26%) stage III patients at diagnosis. At the last follow-up, 112 (58.95%) patients were dead, while the

TABLE 1 | Clinicopathological characteristics of SqCLC patients in tissue microarrays.

Characteristics	Groups	Number of patients (%)
Gender	Male	183 (96.32%)
	Female	7 (3.68%)
Age	≤60 years old	88 (46.32%)
	>60 years old	102 (53.68%)
Smoking	Yes	176 (92.63%)
	No	14 (7.37%)
T stage	T1	25 (13.16%)
	T2	99 (52.11%)
	T3	45 (23.68%)
	T4	21 (11.05%)
N stage	N0	64 (33.68%)
	N1	67 (35.26%)
	N2	59 (31.05%)
TNM stage	I	34 (17.89%)
	II	70 (36.84%)
	III	86 (45.26%)
Tumor diameter*	≤4.5mm	98 (51.58%)
	>4.5mm	92 (48.42%)

*The median of tumor diameter is 4.5mm.

left 78 (41.05%) patients were alive or censored. The median follow-up time was 66.5 months.

IHC of ERAP2 on our TMAs was conducted, and we calculated an IHC score for each specimen as the sum of the percentage of stained cells multiplied by the staining intensity. The standard of staining intensity was displayed in **Figure 2A**. The median IHC score of ERAP2 is 1.375, and we classified the samples into high and low ERAP2 expression subgroups using the median score as the cut-off value. Representative images of high expression and low expression of ERAP2 were shown in **Figure 2B**. We profiled the demographic information for each patient annotated for the expression level of ERAP2, and the distributions of characteristic features did not show a noticeable difference between ERAP2 high and low expression subgroups (**Figure 2C**). K-M curve exhibited that in our cohort, patients with ERAP2 high expression had significantly longer overall survival than the ERAP2 low expression subgroup (**Figure 2D**).

To further explore the prognostic marker of SqCLC, firstly we performed a univariate analysis in our cohort (**Figure 2E** and **Table 2**). Then we conducted the multivariate analysis using the variables that were proved to be statistically significant in univariate analysis (**Figure 2F** and **Table 3**). ERAP2 was identified as an independent protective factor for SqCLC (Univariate, HR =0.659, 95% CI, 0.454-0.956, p-value=0.028; Multivariate, HR =0.523, 95% CI, 0.353-0.775, p value=0.001). The ERAP2 score and clinical information of each sample in our cohort was recorded in **Supplementary Data 1**.

Construction of Nomogram

The 190 SqCLC patients with complete clinical information and follow-up survival time from our cohort were used to establish a prognostic nomograph using R software with the RMS package (**Figure 3**). All clinicopathological factors and immune markers expression status were included in the nomogram model. In the nomogram, the ERAP2 expression was a decisive parameter among all immune markers, for which score 0 represented 100 points and scored three indicated 0 points. The T stage behaved like a very effective indicator among clinicopathological factors, and T3 represented 100 points. The weight of gender, tumor diameter, PD-L1, and CD68+ macrophages were relatively low compared to other indicators. Total points over 700 could predict a survival rate <50% in 1-year survival, a survival rate <20% in 2-year survival, and a survival rate <10% in 3-year survival.

Exploration of ERAP2-Related Function by Pathway Enrichment

Based on SqCLC data from TCGA (**Figures 4A–C**) and GEO (**Figures 4D–F**), we analyzed signaling pathway enrichment for patients with ERAP2 expression levels. We revealed that high ERAP2 expression was synergistic with several immune-promoting biological processes. In both TCGA and GEO databases, high ERAP2 expression was enriched in the natural killer cell-mediated cytotoxicity pathway and T cell receptor signaling pathway, consistent with previous studies. In the TCGA database, high ERAP2 expression was also enriched in the positive regulation of lymphocyte differentiation, T cell activation terms, and positive regulation of innate immune response, suggesting that high ERAP2 expression was correlated with the immune active environment. In the GEO database, high ERAP2 expression was enriched in the PI3K-Akt signaling pathway, JAK-STAT pathway, and the Toll-like receptor pathway, arousing our interest in the molecular network about ERAP2.

Immune-Related Exploration of ERAP2 in Public Data

Inspired by the pathway enrichment analysis results, we further explored the correlations between the expression of ERAP2 and several immune markers in public data using TIMER (an online tool). In **Figure 5A**, we showed the association between the expression level of ERAP2 and CD68, CD8A, CTLA4, FOXP3, CD274 (PD-L1), and CD4, in which ERAP2 was positively correlated with these markers and all the correlations were statistically significant (p=5.88e-08 for CD68, p=4.35e-14 for CD8A, p=1.28e-15 for CTLA4, p=1.65e-14 for FOXP3, p=1.27e-04 for CD274, p=9.98e-14 for CD4), indicating that ERAP2 may enhance the antitumor immune response.

We then characterized the interactions between ERAP2 expression and immune cell infiltration levels in SqCLC samples (**Figure 5B**). Several immune cells were selected, including $CD8^+$ T cells, M0 macrophages, regulatory T cells, M1 macrophages, activated NK cells, and M2 macrophages. ERAP2 expression was significantly positively correlated to the infiltration levels ($CD8^+$ T cells, p=4.09e-03; M0 macrophages, p=1.93e-02; regulatory T cells, p=2.29e-02; M1 macrophages, p=2.16e-08; activated NK cells, p=1.00e-04; M2 macrophages, p=1.24e-06), consistent with previous findings in our study, further suggesting that ERAP2 may act as a tumor suppressor in SqCLC in an immune-promoting manner.

Immune-Related Exploration of ERAP2 in Our Cohort

We evaluated the IHC expression level of PD-L1, CD47, CD8, and CD68 in our cohort, and as shown in **Figure 6A**, pairwise

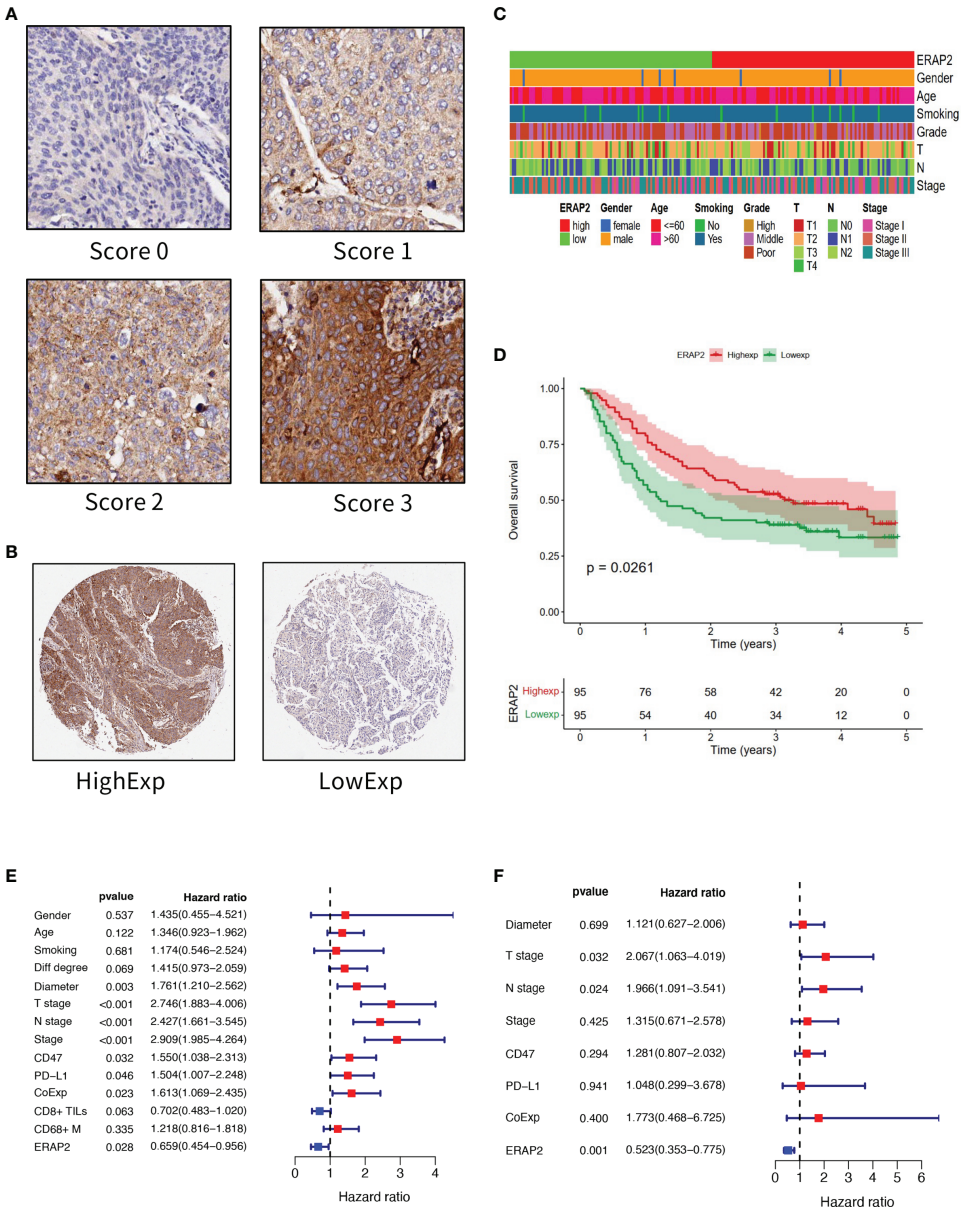

FIGURE 2 | ERAP2 expression in SqCLC tumor microarray (TMA). **(A)** ERAP2 staining intensity scoring standard. ERAP2 expression was graded into 4 categories: 0, 1, 2, and 3 according to the staining intensity. The larger number represented higher ERAP2 staining intensity (100×). The final score of samples is evaluated by multiplying the grade and corresponding area percentages. **(B)** Example of high and low ERAP2 expression in TMA. Left, high expression sample. Right, low expression sample (20×). **(C)** Clinicopathological information related heatmap of SqCLC TMA. **(D)** K-M curve showing the overall survival in SqCLC TMA stratified by ERAP2 expression. Red, ERAP2 high expression group. Green, low expression group. **(E)** Univariate analysis forest plot of clinicopathological factors, ERAP2 expression, and other immune markers' expression in SqCLC TMA. CoExp, PD-L1, and CD47 co-expression. CD8+ TILs, CD8+ tumor infiltration lymphocytes. CD68+ M, CD68+ infiltration macrophages infiltration level. The red square represents risk factors for prognosis, while the blue square represents protective factors for patients. **(F)** Multivariate analysis forest plot of factors, which could predict the overall survival in the univariate analysis. CoExp, PD-L1, and CD47 co-expression. CD8+ TILs, CD8+ tumor infiltration lymphocytes. The red square represents risk factors for prognosis, while the blue square represents protective factors for patients.

correlation analysis was performed for all clinicopathological factors and molecular markers. We found that ERAP2 expression was significantly correlated with $CD8^+$ TILs (Spearman r=0.22, p=0.0029, **Figure 6B**). Applying the median staining score of ERAP2 expression as the cut-off value (median=1.375), we classified all 190 SqCLC patients of our cohort into two groups and compared the expression levels CD47 and PD-L1 and the infiltrating density of $CD8^+$ TILs

TABLE 2 | Univariate Cox Regression of Prognostic Factors in SqCLC.

	OS	
	HR (95% CI)	**p**
Age		0.122
≤60y	1.000	
>60y	1.346 (0.923-1.962)	
Gender		0.537
Female	1.000	
Male	1.435 (0.455-4.521)	
Smoking		0.681
No	1.000	
Yes	1.174 (0.546-2.524)	
Tumor Diameter		0.003
≤median	1.000	
>median	1.761 (1.210-2.562)	
T stage		1.56E-07
T1+T2	1.000	
T3+T4	2.746 (1.883-4.006)	
N stage		0.000
N0+N1	1.000	
N2	2.427 (1.661-3.545)	
TNM Stage		0.000
I+II	1.000	
III	2.090 (1.985-4.264)	
CD47 expression		0.032
Low	1.000	
High	1.55 (1.038-2.313)	
PD-L1 expression		0.046
Negative	1.000	
Positive	1.504 (1.007-2.248)	
PD-L1 and CD47 co-expression		0.023
No	1.000	
Yes	1.163 (1.069-2.435)	
CD8+ TILs level		0.063
Low	1.000	
High	0.702 (0.483-1.02)	
CD68+Macrophage infiltration level		0.335
Low	1.000	
High	1.218 (0.816-1.818)	
ERAP2 expression		0.028
Low	1.000	
High	0.659 (0.454-0.956)	

All p values were two sides and less than 0.05 were considered significant.
SqCLC, Squamous cell lung cancer; OS, overall survival; HR, hazard ratio; CI, confidence interval.
Low and high expression was classified as the median except for CD47 (1% as cut-off value).

TABLE 3 | Multivariate Cox Regression of Prognostic Factors in SqCLC.

	OS	
	HR (95% CI)	**p**
Diameter		0.699
≤60y	1.000	
>60y	1.121 (0.627-2.006)	
T stage		0.032
T1+T2	1.000	
T3+T4	2.067 (1.063-4.019)	
N stage		0.024
N0+N1	1.000	
N2	1.966 (1.091-3.541)	
TNM stage		0.425
I+II	1.000	
III	1.315 (0.671-2.578)	
CD47 expression		0.294
Negative	1.000	
Positive	1.281 (0.807-2.032)	
PD-L1 expression		0.941
Negative	1.000	
Positive	1.048 (0.299-3.678)	
PD-L1 and CD47 co-expression		0.400
No	1.000	
Yes	1.773 (0.468-6.725)	
ERAP2 expression		0.001
Low	1.000	
High	0.523 (0.353-0.775)	

All p values were two sides and less than 0.05 were considered significant.
SqCLC, Squamous cell lung cancer; OS, overall survival; HR, hazard ratio; CI, confidence interval.
Low and high expression was classified as the median except for CD47 (1% as cut-off value).

and $CD68^+$ Macrophages of them (**Figure 6C**). In the ERAP2 high expression group, the expression level of PD-L1 was significantly higher ($p<0.05$), meanwhile, the infiltrating density of $CD8^+$ TILs were also considerably higher in the ERAP2 high expression group ($p<0.05$). ERAP2 expression in positive groups was significantly higher than in negative groups for all three immune markers, implying ERAP2 may exert significant functions in anti-tumor immunity. The representative images of each one patient from the ERAP2 high and low expression group (**Figure 6D**). In addition, we distributed all the patients of our cohort into positive and negative groups according to the status of PD-L1 (10% TPS as cutoff value), the status of PD-L1/CD47 co-expression (co-expression criteria: 1% for PD-L1 and 5% for CD47) and infiltrating density of $CD8^+$ TILs (median as cutoff value). We compared the ERAP2 expression levels between the groups (**Figure 6E**).

DISCUSSION

SqCLC has been a refractory disease for decades, with few inroads in targeted therapy, and only a minority of SqCLC patients have achieved sustained benefits from immunotherapy (5, 25). Based on public databases and our SqCLC cohort (190 patients), our study identified ERAP2 as a favorable prognostic indicator and potential enhancer for ICIs in SqCLC.

It is reasonable for us to believe that ERAP2 may exert a significant role in SqCLC. Using GEO and TCGA data, we found ERAP2 was lowly expressed in SqCLC and was significantly associated with longer survival. As an endoplasmic reticulum-settled enzyme, ERAP2 is responsible for the final trimming of peptides represented by the major histocompatibility complex (MHC) class I molecules (13). Previous researcher has demonstrated that ERAP2 enzyme function could affect T cell and NK cell responses towards normal and cancer cells as well as the synthesis of inflammatory cytokines (26). Since ERAP2 is deeply involved in the generation and destruction of immunopeptidome, its deficiency can lead to disorders in anti-

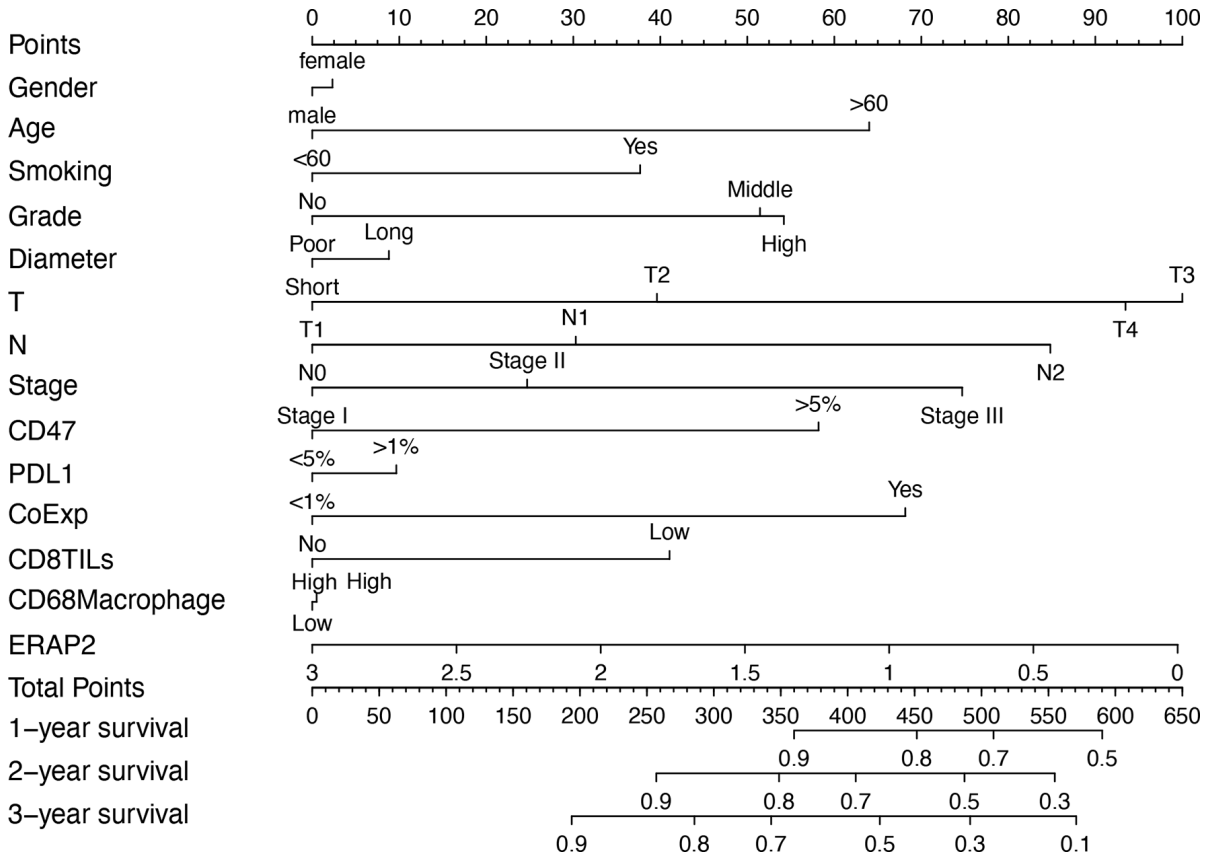

FIGURE 3 | Prognostic nomogram based on the clinicopathological factors, ERAP2 expression, and other immune markers predicting the 1-year, 2-year, and 3-year overall survival rate in our SqCLC cohort. T, T stage. N, N stage. CoExp, PD-L1and CD47 co-expression. CD8TILs, CD8+ tumor infiltration lymphocytes. CD68 Macrophage, CD68+ infiltration macrophages.

tumor immunity activation. Considering our findings in the public database, we speculated that ERAP2 is of great worth in SqCLC.

We are the first to illustrate the predictive value of ERAP2 in SqCLC. The predictive value of ERAP2 was validated in SqCLC TMAs with high quality. All patients in our cohort accepted no pre-surgery treatments, and the most recent patient was diagnosed in 2011, offering a long enough follow-up period. In our cohort, ERAP2 expression was positively related to overall survival, consistent with what we found in the public database, providing further evidence for the definition of ERAP2 as a prognostic indicator in SqCLC. Moreover, using multivariate analysis, we confirmed that ERAP2 expression was an independent prognostic factor for SqCLC individuals based on our cohort.

Based on previous research, we hypothesized that the positive predictive function of ERAP2 in SqCLC derived from its ability to prevent immune evasion by modulating immune recognition (27) because improper trimming of peptides in ER is one of the strategies that cancer cells avoid the attack from the immune system (28). In 2021, Mpakali et al. (14) reported that ERAP2 can trim the peptides that enter the ER and are too long to fit into MHC I molecule. However, while trimming peptides, ERAP2 can also destroy tumor-associated antigenic peptides destined for loading on MHC I, thus affecting avoiding T cell response.

Little was known about how ERAP2 behaves in lung cancer. In 2014, Zhou et al. (29) reported that ERAP2 rs2248374/rs2549782-AG haplotype was significantly associated with increased NSCLC risk, while ERAP2 rs2248374/rs2549782-GT haplotype individuals tended to indicate a reduced risk. In 2021, Wis´niewski et al. (30) asserted that the extent of ERAP2 presence could affect the anti-cancer response of ERAP1 in NSCLC. To our knowledge, there has been no study focusing on the ERAP2 expression in lung cancer so far, and the area of ERAP2 in SqCLC has never been set foot in.

One of the highlight conclusions of our study is that in both public data and our cohort, high expression of ERAP2 is correlated with the immunoreactive tumor microenvironment, which is favorable for administering immunotherapy in SqCLC. Due to its malignant nature and intricate genomic architecture, many SqCLC patients are marginalized in the prosperity of immunotherapy, failing to obtain sustained benefits from ICIs

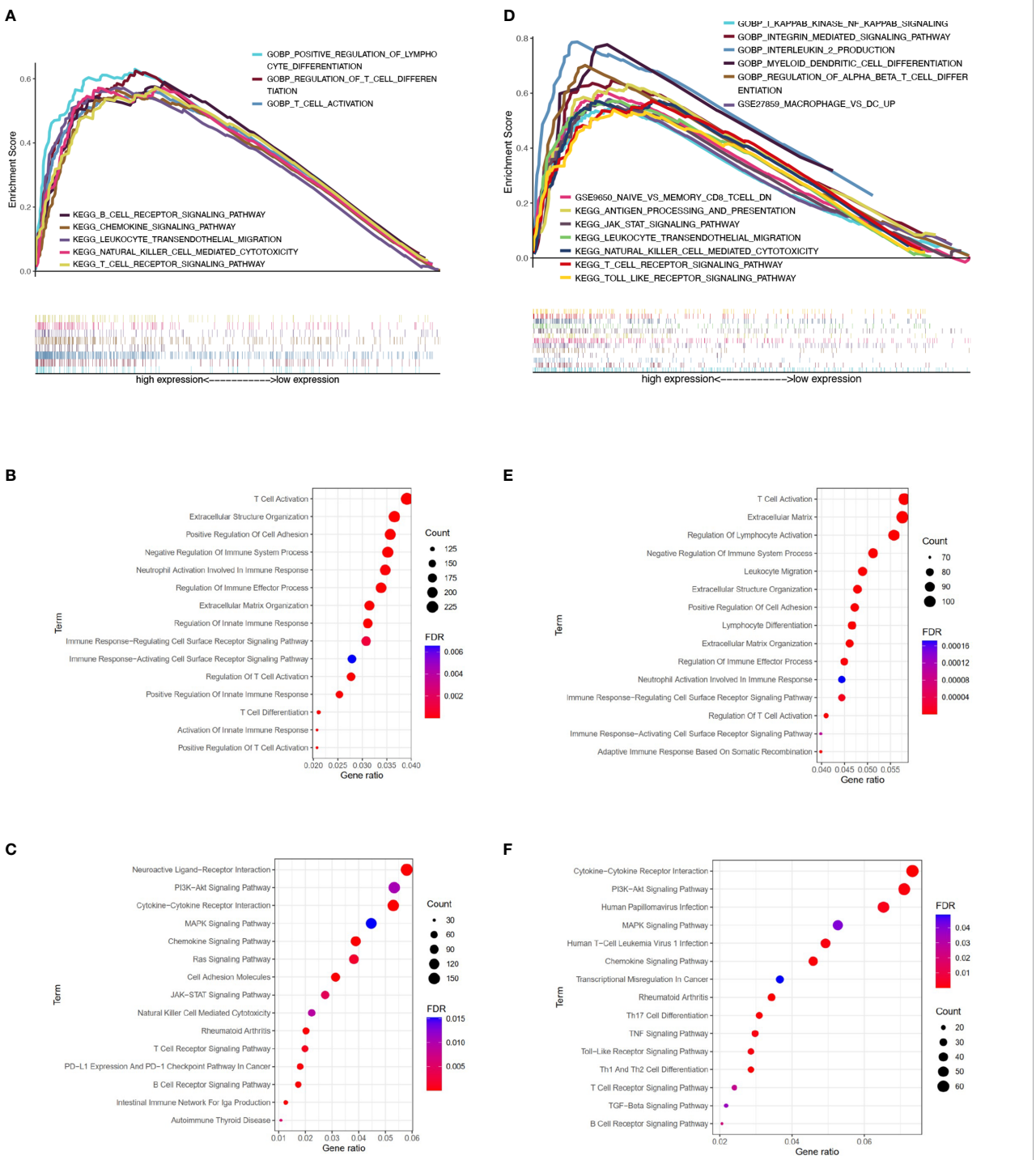

FIGURE 4 | Pathway enrichment analysis of patients with different ERAP2 expression level in SqCLC public data. **(A)** Enrichment analysis based on TCGA SqCLC data. Upper: pathways, terms, or gene sets enriched in ERAP2 high expression group. **(B)** Representative GO terms and pathways enriched in DEGs between high and low ERAP2 expression groups based on TCGA SqCLC data. **(C)** Representative KEGG terms and pathways enriched in DEGs between high and low ERAP2 expression groups based on TCGA SqCLC data. **(D)** Enrichment analysis based on GEO SqCLC data. Upper: pathways, terms, or gene sets enriched in ERAP2 high expression group. **(E)** Representative GO terms and pathways enriched in DEGs between high and low ERAP2 expression groups based on GEO SqCLC data. **(F)** Representative KEGG terms and pathways enriched in DEGs between high and low ERAP2 expression groups based on GEO SqCLC data.

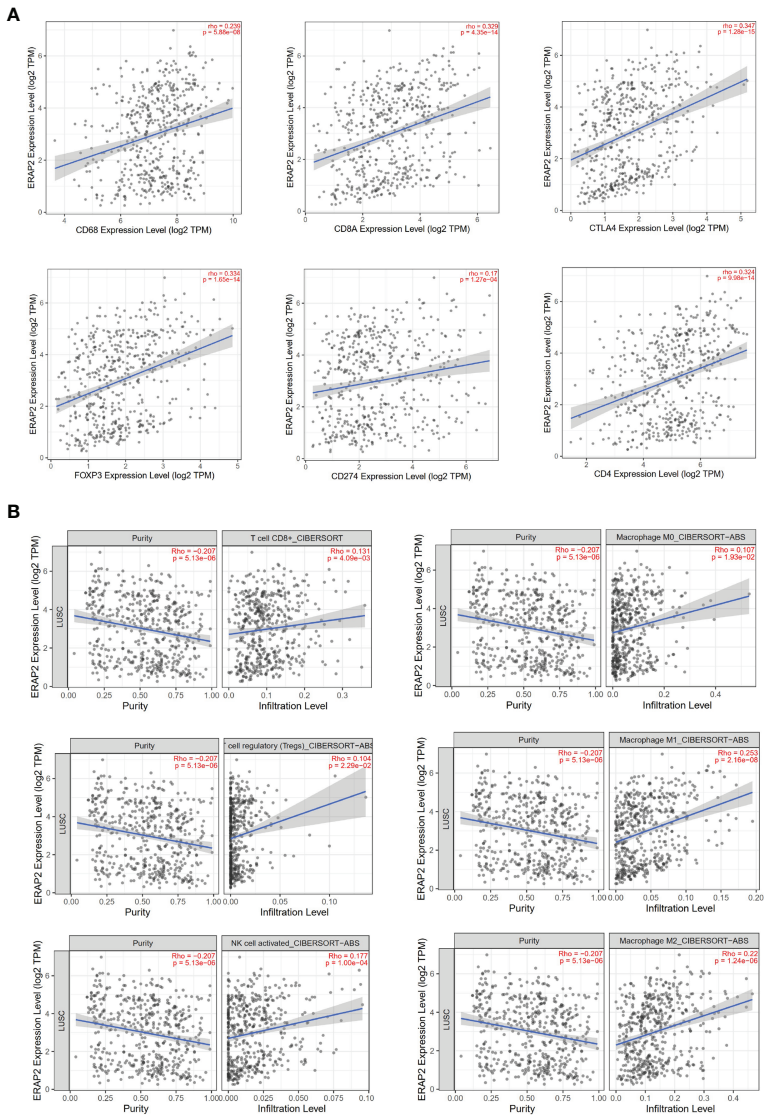

FIGURE 5 | Immune associations about ERAP2 expression using public data (TIMER). **(A)** Correlations between the expression of ERAP2 and immune markers in SqCLC. Top: CD68, CD8A, CTLA4. Bottom: FOXP3, CD274, CD4. The correlation coefficient and p-value are in the top right corner of each picture. **(B)** Correlations between ERAP2 expression and immune cell infiltration level in SqCLC. Top CD8+ T cell, M0 macrophage. Middle: regulatory T cell regulatory, M1 macrophage. Bottom: Activated NK cell, M2 macrophage.

(31). In the realm of SqCLC, methods that can boost immunotherapy efficacy are demanding. The tumor microenvironment (TME) is an integral component of cancer, composed of various cell types crucial to tumor immunology (32). The TME infrastructure and the interactions between cancer cells and TME during cancer initiation and progression could dictate the response to immunotherapy (33). In our study, high ERAP2 expression was associated with high levels of multiple immune markers and cells, including PD-L1, CD47, $CD8^+$ TILs, $CD68^+$ Macrophages, and NK cells which were positive indicators for immunotherapy. Our findings of ERAP2 and NK cells were consistent with previous studies (13, 15), while we are the first to illustrate the associations between ERAP2 and other immune cells and markers. The positive association between ERAP2 and FOXP3 aroused our interest. Although FOXP3 was previously reported to promote tumor growth and metastasis in NSCLC (34), there were also researches asserting that tumoral FOXP3 had the potential to suppress tumor function in SqCLC (35). The involvements between FOXP3 and tumor immunity have not been clearly illustrated, and current results of tumor FOXP3 are inconsistent and inconclusive (36). The ERAP2 high expression group harbored an immune-active TME, suggesting the feasibility of immune-related treatments among SqCLC with ERAP2 high expression

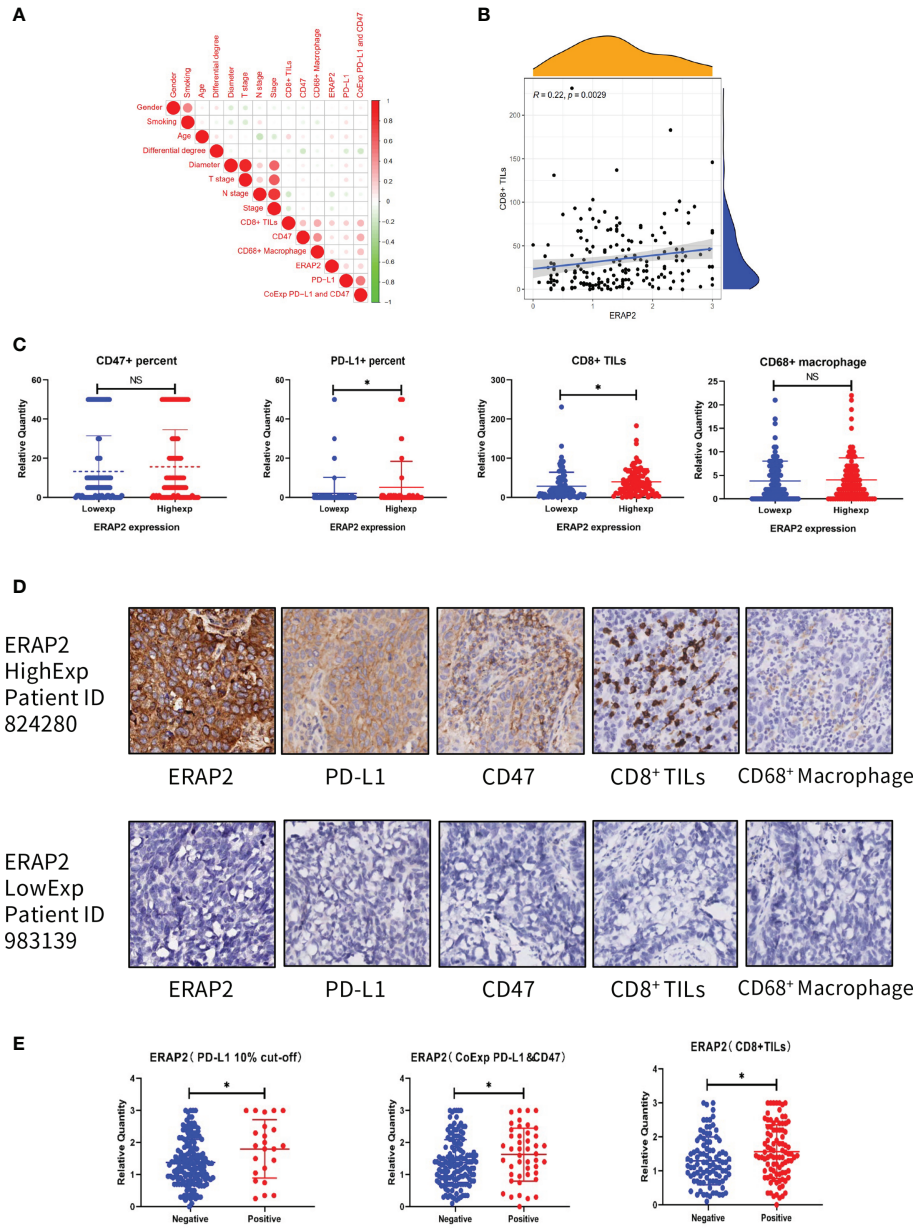

FIGURE 6 | Association between ERAP2 expression and multiple immune markers in our SqCLC TMA. **(A)** Associations among all clinicopathological and immune markers in SqCLC TMAs. The circle color represents the correlational tendency. The circle size represents the statistical significance. Red, positive correlation. Green, negative correlation. Larger circle represents the lower p-value. **(B)** Correlation between ERAP2 expression and CD8+ TILs. Spearman relevant coefficient = 0.22, p-value=0.0029. **(C)** The relative quantity of immune markers in ERAP2 high and low expression patients of SqCLC TMAs. From left to right: CD47, PD-L1, CD8, and CD68. Blue, ERAP2 low expression group. Red, ERAP2 high expression group. Asterisk, p-value<0.05. **(D)** IHC images of representative patients in the ERAP2 high and low expression group (100×). Upper: representative patient with high ERAP2 expression. Lower: representative patient with low ERAP2 expression. From left to right: ERAP2, PD-L1, CD47, $CD8^+$ TILs and $CD68^+$ Macrophages. **(E)** The relative quantity of ERAP2 among patients with different immune marker statuses. From left to right: PD-L1, PD-L1 and CD47 co-expression, CD8+ TILs. Asterisk, p-value < 0.05.

and the potentiality of ERAP2 as a biomarker for SqCLC immunotherapy. ERAP2 was also involved in autoimmune diseases, such as ankylosing spondylitis (34), whose etiology is unclear. The immune activation process during pre-eclampsia was also reported to be engaged with the differential expression of ERAP1/2 (37), suggesting the importance of ERAP2 in the immune system (38).

Under the pandemic of SARS-CoV-2, ERAP2 abnormity is related to the unfavorable clinical outcomes of COVID-19 infected patients, while ERAP2 may also inspire the development of the

vaccine. Recently, ERAP2 was reported to participate in the virus antigen presentation process of COVID-19 (39, 40). ERAP2 and its homolog ERAP1 constituted an efficient filter to epitope presentation by greatly limiting the diversity of virus antigenic peptides sequences produced, suggesting the promising value of ERAP2 in SARS-CoV-2 immunogenicity studies and vaccine design (41). The rs150892504 mutations in the ERAP2 gene were believed to be a genetic factor related to severe life-threatening complications in individuals infected with coronavirus (42). Since ERAP2 was involved in the renin-angiotensin system (RAS), ERAP2 dysfunction was hypothesized to exacerbate the symptomatology and prognosis of the SARS-CoV-2.

Several limitations existed in our study. First, our TMAs only contained tumor tissue of each patient, lacking the data of matched normal samples. Secondly, we only performed IHC to a limited number of immune markers, which were far from enough to represent the whole ecosystem of TME. Third, we did not validate our findings at the transcriptional level because there were no fresh or fresh frozen samples.

In conclusion, our study is the first to intensively illustrate the role of ERAP2 in lung cancer. We identified ERAP2 as a positive prognostic biomarker for SqCLC and revealed its potentiality in predicting immunotherapy response, offering novel ideas for the administration of ICIs in SqCLC.

FOOTNOTE

The authors are accountable for all aspects of the work in ensuring that questions related to the accuracy or integrity of any part of the word are approximately investigated and resolved.

Written informed consents for the publication of details relating to any participant were obtained from that person.

DATA AVAILABILITY STATEMENT

The raw data supporting the conclusions of this article will be made available by the authors, without undue reservation.

ETHICS STATEMENT

The studies involving human participants were reviewed and approved by the Ethics Committee of National Cancer Center/ Cancer Hospital, Chinese Academy of Medical Sciences, and Peking Union Medical College. The patients/participants provided their written informed consent to participate in this study.

AUTHOR CONTRIBUTIONS

JH, SG, and CL were responsible for conception and design. JH, SG, JW, CL, and BZ offered administrative support. HT and ZY provided study materials and clinical resources. HT, FB, and ZZ were responsible for the collection and assembly of data. HT, ZY, FB, and JY were responsible for data analysis. JX, RL, YP, GB, YT, YC, LL, TF, CX, and YZ were responsible for data interpretation. All authors were contributed to the writing and final approval of the manuscript.

FUNDING

This work was supported by the National Natural Science Foundation of China (No: 81972196, 8210103136, 82060426, 81702274); the National Key R&D Program of China (2020AAA0109505); the Beijing Municipal Science & Technology Commission (Z191100006619119); the Special Research Fund for Central Universities, Peking Union Medical College (3332021028, 3332021029); Beijing Hope Run Special Fund of Cancer Foundation of China (LC2018B14, LC2020B09).

ACKNOWLEDGMENTS

We appreciate the technical support of Cunming Hu from Outdo Biotech Co., LTD., Shanghai, and we appreciated the TCGA and GEO organization for providing us with solid public data.

SUPPLEMENTARY MATERIAL

The Supplementary Material for this article can be found online at: https://www.frontiersin.org/articles/10.3389/fimmu.2021.788985/full#supplementary-material

Supplementary Data Sheet 1 | The clinicopathological data of Tissue Microarrays.

REFERENCES

1. Siegel RL, Miller KD, Fuchs HE, Jemal A. Cancer Statistics, 2021. *CA Cancer J Clin* (2021) 71(1):7–33. doi: 10.3322/caac.21654
2. Herbst RS, Morgensztern D, Boshoff C. The Biology and Management of non-Small Cell Lung Cancer. *Nature* (2018) 553(7689):446–54. doi: 10.1038/nature25183
3. Friedlaender A, Banna G, Malapelle U, Pisapia P, Addeo A. Next Generation Sequencing and Genetic Alterations in Squamous Cell Lung Carcinoma: Where Are We Today? *Front Oncol* (2019) 9:166. doi: 10.3389/fonc.2019.00166
4. Hanna N, Johnson D, Temin S, Baker S Jr, Brahmer J, Ellis PM, et al. Systemic Therapy for Stage IV Non-Small-Cell Lung Cancer: American Society of Clinical Oncology Clinical Practice Guideline Update. *J Clin Oncol* (2017) 35 (30):3484–515. doi: 10.1200/JCO.2017.74.6065
5. Yang CY, Yang JC, Yang PC. Precision Management of Advanced Non-Small Cell Lung Cancer. *Annu Rev Med* (2020) 71:117–36. doi: 10.1146/annurev-med-051718-013524
6. Reck M, Rabe KF. Precision Diagnosis and Treatment for Advanced Non-Small-Cell Lung Cancer. *N Engl J Med* (2017) 377(9):849–61. doi: 10.1056/NEJMra1703413
7. Stewart PA, Welsh EA, Slebos RJC, Fang B, Izumi V, Chambers M, et al. Proteogenomic Landscape of Squamous Cell Lung Cancer. *Nat Commun* (2019) 10(1):3578. doi: 10.1038/s41467-019-11452-x
8. Doroshow DB, Sanmamed MF, Hastings K, Politi K, Rimm DL, Chen L, et al. Immunotherapy in Non-Small Cell Lung Cancer: Facts and

Hopes. *Clin Cancer Res* (2019) 25(15):4592–602. doi: 10.1158/1078-0432.CCR-18-1538
9. Somasundaram A, Burns TF. The Next Generation of Immunotherapy: Keeping Lung Cancer in Check. *J Hematol Oncol* (2017) 10(1):87. doi: 10.1186/s13045-017-0456-5
10. Fierabracci A, Milillo A, Locatelli F, Fruci D. The Putative Role of Endoplasmic Reticulum Aminopeptidases in Autoimmunity: Insights From Genomic-Wide Association Studies. *Autoimmun Rev* (2012) 12(2):281–8. doi: 10.1016/j.autrev.2012.04.007
11. Saveanu L, Carroll O, Lindo V, Del Val M, Lopez D, Lepelletier Y, et al. Concerted Peptide Trimming by Human ERAP1 and ERAP2 Aminopeptidase Complexes in the Endoplasmic Reticulum. *Nat Immunol* (2005) 6(7):689–97. doi: 10.1038/ni1208
12. López de Castro JA. How ERAP1 and ERAP2 Shape the Peptidomes of Disease-Associated MHC-I Proteins. *Front Immunol* (2018) 9:2463. doi: 10.3389/fimmu.2018.02463
13. Haroon N, Inman RD. Endoplasmic Reticulum Aminopeptidases: Biology and Pathogenic Potential. *Nat Rev Rheumatol* (2010) 6(8):461–7. doi: 10.1038/nrrheum.2010.85
14. Mpakali A, Stratikos E. The Role of Antigen Processing and Presentation in Cancer and the Efficacy of Immune Checkpoint Inhibitor Immunotherapy. *Cancers (Basel)* (2021) 13(1):6–7. doi: 10.3390/cancers13010134
15. Cifaldi L, Lo Monaco E, Forloni M, Giorda E, Lorenzi S, Petrini S, et al. Natural Killer Cells Efficiently Reject Lymphoma Silenced for the Endoplasmic Reticulum Aminopeptidase Associated With Antigen Processing. *Cancer Res* (2011) 71(5):1597–606. doi: 10.1158/0008-5472.CAN-10-3326
16. Cifaldi L, Romania P, Falco M, Lorenzi S, Meazza R, Petrini S, et al. ERAP1 Regulates Natural Killer Cell Function by Controlling the Engagement of Inhibitory Receptors. *Cancer Res* (2015) 75(5):824–34. doi: 10.1158/0008-5472.CAN-14-1643
17. Lim YW, Chen-Harris H, Mayba O, Lianoglou S, Wuster A, Bhangale T, et al. Germline Genetic Polymorphisms Influence Tumor Gene Expression and Immune Cell Infiltration. *Proc Natl Acad Sci USA* (2018) 115(50):E11701–e11710. doi: 10.1073/pnas.1804506115
18. Babaie F, Hosseinzadeh R, Ebrazeh M, Seyfizadeh N, Aslani S, Salimi S, et al. The Roles of ERAP1 and ERAP2 in Autoimmunity and Cancer Immunity: New Insights and Perspective. *Mol Immunol* (2020) 121:7–19. doi: 10.1016/j.molimm.2020.02.020
19. Compagnone M, Cifaldi L, Fruci D. Regulation of ERAP1 and ERAP2 Genes and Their Disfunction in Human Cancer. *Hum Immunol* (2019) 80(5):318–24. doi: 10.1016/j.humimm.2019.02.014
20. Fruci D, Giacomini P, Nicotra MR, Forloni M, Fraioli R, Saveanu L, et al. Altered Expression of Endoplasmic Reticulum Aminopeptidases ERAP1 and ERAP2 in Transformed non-Lymphoid Human Tissues. *J Cell Physiol* (2008) 216(3):742–9. doi: 10.1002/jcp.21454
21. Chang KP, Hao S-P, Chang J-H, Wu C-C, Tsang N-M, Lee Y-S, et al. Macrophage Inflammatory Protein-3alpha is a Novel Serum Marker for Nasopharyngeal Carcinoma Detection and Prediction of Treatment Outcomes. *Clin Cancer Res* (2008) 14(21):6979–87. doi: 10.1158/1078-0432.CCR-08-0090
22. Ma S, Sun S, Geng L, Song M, Wang W, Ye Y, et al. Caloric Restriction Reprograms the Single-Cell Transcriptional Landscape of Rattus Norvegicus Aging. *Cell* (2020) 180(5):984–1001.e22. doi: 10.1016/j.cell.2020.02.008
23. Newman AM, Steen CB, Liu CL, Gentles AJ, Chaudhuri AA, Scherer F, et al. Determining Cell Type Abundance and Expression From Bulk Tissues With Digital Cytometry. *Nat Biotechnol* (2019) 37(7):773–82. doi: 10.1038/s41587-019-0114-2
24. Chansky K, Detterbeck FC, Nicholson AG, Rusch VW, Vallières E, Groome P, et al. The IASLC Lung Cancer Staging Project: External Validation of the Revision of the TNM Stage Groupings in the Eighth Edition of the TNM Classification of Lung Cancer. *J Thorac Oncol* (2017) 12(7):1109–21. doi: 10.1016/j.jtho.2017.04.011
25. Socinski MA, Obasaju C, Gandara D, Hirsch FR, Bonomi P, Bunn PA Jr, et al. Current and Emergent Therapy Options for Advanced Squamous Cell Lung Cancer. *J Thorac Oncol* (2018) 13(2):165–83. doi: 10.1016/j.jtho.2017.11.111
26. Stratikos E, Stamogiannos A, Zervoudi E, Fruci D. A Role for Naturally Occurring Alleles of Endoplasmic Reticulum Aminopeptidases in Tumor Immunity and Cancer Pre-Disposition. *Front Oncol* (2014) 4:363. doi: 10.3389/fonc.2014.00363
27. Lee ED. Endoplasmic Reticulum Aminopeptidase 2, a Common Immunological Link to Adverse Pregnancy Outcomes and Cancer Clearance? *Placenta* (2017) 56:40–3. doi: 10.1016/j.placenta.2017.03.012
28. Jhunjhunwala S, Hammer C, Delamarre L. Antigen Presentation in Cancer: Insights Into Tumour Immunogenicity and Immune Evasion. *Nat Rev Cancer* (2021) 21(5):298–312. doi: 10.1038/s41568-021-00339-z
29. Zhou J, Ma Q, Guo C, Shi L, Yao Y, Yu J, et al. A Study on the Relationship Between Endoplasmic Reticulum Aminopeptidase2 Genetic Polymorphisms and non-Small Cell Lung Cancer in Yunnan Han Population. *Zhonghua Jie He He Hu Xi Za Zhi* (2014) 37(12):909–14. doi: 10.1016/s0169-5002(96)90254-8
30. Wiśniewski A, Sobczyński M, Pawełczyk K, Porębska I, Jasek M, Wagner M, et al. Polymorphisms of Antigen-Presenting Machinery Genes in Non-Small Cell Lung Cancer: Different Impact on Disease Risk and Clinical Parameters in Smokers and Never-Smokers. *Front Immunol* (2021) 12:664474. doi: 10.3389/fimmu.2021.664474
31. Hai J, Zhang H, Zhou J, Wu Z, Chen T, Papadopoulos E, et al. Generation of Genetically Engineered Mouse Lung Organoid Models for Squamous Cell Lung Cancers Allows for the Study of Combinatorial Immunotherapy. *Clin Cancer Res* (2020) 26(13):3431–42. doi: 10.1158/1078-0432.CCR-19-1627
32. Pitt JM, Marabelle A, Eggermont A, Soria J-C, Kroemer G, Zitvogel L. Targeting the Tumor Microenvironment: Removing Obstruction to Anticancer Immune Responses and Immunotherapy. *Ann Oncol* (2016) 27 (8):1482–92. doi: 10.1093/annonc/mdw168
33. Murciano-Goroff YR, Warner AB, Wolchok JD. The Future of Cancer Immunotherapy: Microenvironment-Targeting Combinations. *Cell Res* (2020) 30(6):507–19. doi: 10.1038/s41422-020-0337-2
34. Yang S, Liu Y, Li M-Y, Ng CSH, Yang S-L, Wang S, et al. FOXP3 Promotes Tumor Growth and Metastasis by Activating Wnt/β+-Catenin Signaling Pathway and EMT in non-Small Cell Lung Cancer. *Mol Cancer* (2017) 16 (1):124. doi: 10.1186/s12943-017-0700-1
35. Won KY, Kim HK, Kim GY, Min Song J, Lim S-J. Hippo Pathway and Tumoral FOXP3 Expression Correlate With Tumor Growth in Squamous Cell Carcinoma of the Lung. *Pathol Res Pract* (2020) 216(7):153003. doi: 10.1016/j.prp.2020.153003
36. Jia H, Qi H, Gong Z, Yang S, Ren J, Liu Y, et al. The Expression of FOXP3 and its Role in Human Cancers. *Biochim Biophys Acta Rev Cancer* (2019) 1871 (1):170–8. doi: 10.1016/j.bbcan.2018.12.004
37. Seamon K, Kurlak LO, Warthan M, Stratikos E, Strauss JF 3rd, Mistry HD, et al. The Differential Expression of ERAP1/ERAP2 and Immune Cell Activation in Pre-Eclampsia. *Front Immunol* (2020) 11:396. doi: 10.3389/fimmu.2020.00396
38. Paladini F, Fiorillo MT, Tedeschi V, Mattorre B, Sorrentino R. The Multifaceted Nature of Aminopeptidases ERAP1, ERAP2, and LNPEP: From Evolution to Disease. *Front Immunol* (2020) 11:1576. doi: 10.3389/fimmu.2020.01576
39. Saulle I, Vanetti C, Goglia S, Vicentini C, Tombetti E, Garziano M, et al. A New ERAP2/Iso3 Isoform Expression Is Triggered by Different Microbial Stimuli in Human Cells. Could It Play a Role in the Modulation of SARS-CoV-2 Infection? *Cells* (2020) 9(9):5–9. doi: 10.3390/cells9091951
40. Saulle I, Vicentini C, Clerici M, Biasin M. Antigen Presentation in SARS-CoV-2 Infection: The Role of Class I HLA and ERAP Polymorphisms. *Hum Immunol* (2021) 82(8):551–60. doi: 10.1016/j.humimm.2021.05.003
41. Stamatakis G, Samiotaki M, Mpakali A, Panayotou G, Stratikos E. Generation of SARS-CoV-2 S1 Spike Glycoprotein Putative Antigenic Epitopes *in Vitro* by Intracellular Aminopeptidases. *J Proteome Res* (2020) 19(11):4398–406. doi: 10.1021/acs.jproteome.0c00457
42. Malkova A, Kudlay D, Kudryavtsev I, Starshinova A, Yablonskiy P, Shoenfeld Y. Immunogenetic Predictors of Severe COVID-19. *Vaccines (Basel)* (2021) 9 (3):5. doi: 10.3390/vaccines9030211

Conflict of Interest: Author JY was employed by company Genetron Health (Beijing) Co. Ltd.

The remaining authors declare that the research was conducted in the absence of any commercial or financial relationships that could be construed as a potential conflict of interest.

the publisher, the editors and the reviewers. Any product that may be evaluated in this article, or claim that may be made by its manufacturer, is not guaranteed or endorsed by the publisher.

frontiers in Immunology

ORIGINAL RESEARCH
published: 18 February 2022
doi: 10.3389/fimmu.2022.813072

Predicting EGFR and PD-L1 Status in NSCLC Patients Using Multitask AI System Based on CT Images

Chengdi Wang[1], Jiechao Ma[2], Jun Shao[1], Shu Zhang[2], Zhongnan Liu[2], Yizhou Yu[2,3] and Weimin Li[1]**

[1] Department of Respiratory and Critical Care Medicine, Med-X Center for Manufacturing, National Clinical Research Center for Geriatrics, Frontiers Science Center for Disease-related Molecular Network, West China Hospital, West China School of Medicine, Sichuan University, Chengdu, China, [2] AI Lab, Deepwise Healthcare, Beijing, China, [3] Faculty of Engineering, The University of Hong Kong, Hong Kong, Hong Kong SAR, China

OPEN ACCESS

Edited by:
Qian Chu,
Huazhong University of Science and Technology, China

Reviewed by:
Yongsheng Li,
Chongqing University, China
Zhaocai Zhou,
Fudan University, China

***Correspondence:**
Weimin Li
weimi003@scu.edu.cn
Yizhou Yu
yizhouy@acm.org

Specialty section:
This article was submitted to Cancer Immunity and Immunotherapy, a section of the journal Frontiers in Immunology

Received: *11 November 2021*
Accepted: *17 January 2022*
Published: *18 February 2022*

Citation:
Wang C, Ma J, Shao J, Zhang S, Liu Z, Yu Y and Li W (2022) Predicting EGFR and PD-L1 Status in NSCLC Patients Using Multitask AI System Based on CT Images. Front. Immunol. 13:813072. doi: 10.3389/fimmu.2022.813072

Background: Epidermal growth factor receptor (EGFR) genotyping and programmed death ligand-1 (PD-L1) expressions are of paramount importance for treatment guidelines such as the use of tyrosine kinase inhibitors (TKIs) and immune checkpoint inhibitors (ICIs) in lung cancer. Conventional identification of EGFR or PD-L1 status requires surgical or biopsied tumor specimens, which are obtained through invasive procedures associated with risk of morbidities and may be unavailable to access tissue samples. Here, we developed an artificial intelligence (AI) system that can predict EGFR and PD-L1 status in using non-invasive computed tomography (CT) images.

Methods: A multitask AI system including deep learning (DL) module, radiomics (RA) module, and joint (JO) module combining the DL, RA, and clinical features was developed, trained, and optimized with CT images to predict the EGFR and PD-L1 status. We used feature selectors and feature fusion methods to find the best model among combinations of module types. The models were evaluated using the areas under the receiver operating characteristic curves (AUCs).

Results: Our multitask AI system yielded promising performance for gene expression status, subtype classification, and joint prediction. The AUCs of DL module achieved 0.842 (95% CI, 0.825–0.855) in the EGFR mutated status and 0.805 (95% CI, 0.779–0.829) in the mutated-EGFR subtypes discrimination (19Del, L858R, other mutations). DL module also demonstrated the AUCs of 0.799 (95% CI, 0.762–0.854) in the PD-L1 expression status and 0.837 (95% CI, 0.775–0.911) in the positive-PD-L1 subtypes (PD-L1 tumor proportion score, 1%–49% and ≥50%). Furthermore, the JO module of our AI system performed well in the EGFR and PD-L1 joint cohort, with an AUC of 0.928 (95% CI, 0.909–0.946) for distinguishing EGFR mutated status and 0.905 (95% CI, 0.886–0.930) for discriminating PD-L1 expression status.

Conclusion: Our AI system has demonstrated the encouraging results for identifying gene status and further assessing the genotypes. Both clinical indicators and radiomics features showed a complementary role in prediction and provided accurate estimates to

predict EGFR and PD-L1 status. Furthermore, this non-invasive, high-throughput, and interpretable AI system can be used as an assistive tool in conjunction with or in lieu of ancillary tests and extensive diagnostic workups to facilitate early intervention.

Keywords: EGFR, PD-L1, NSCLC, deep learning, computed tomography

INTRODUCTION

Lung cancer is the second most commonly diagnosed cancer and the leading cause of mortality tumor throughout the world (1, 2). In China, there are around 733,000 new cases of lung cancer annually, and with over 610,000 deaths due to lung cancer (3), accounting for 37% new cases and 39.2% death cases of the world, respectively (4). Approximately 85% of lung cancer patients were histologically identified as non-small cell lung cancer (NSCLC), of which comprises the most common subtype such as lung adenocarcinoma (LUAD) and lung squamous cell carcinoma (LUSC) (5). Targeted therapies, as represented by epidermal growth factor receptor (EGFR) tyrosine kinase inhibitors (TKIs), and immune checkpoint inhibitor (ICI) treatments targeted the programmed death-1 (PD-1) receptor on T cells, or the programmed death ligand-1 (PD-L1) expressed by tumor cells; these two treatment paradigms have significantly revolutionized cancer treatment and improved survival outcome for lung cancer. Identifying predictive biomarkers is therefore crucial for choosing individuals who are potentially suitable to therapy.

In the era of precision medicine, lung cancer treatment depended on the genetics. Patients with EGFR mutated lung adenocarcinoma could achieve a longer progression-free survival (PFS) from EGFR-TKIs than conventional chemotherapy (6–8). However, the medication and efficacy varied among NSCLC patients with EGFR 19Del, L858R, or other types of mutations (9, 10). Meanwhile, ICIs targeting PD-1 or PD-L1 offer promising paradigm to treatment in NSCLC with high PD-L1 expression. The first-line pembrolizumab monotherapy can enhance overall survival (OS) and PFS in lung cancer patients with PD-L1 tumor proportion score (TPS) ≥50% (11, 12). However, gene detection is determined by surgical or biopsied tissue-based assays at present, which has many limitations: difficulties in accessing suitable tumor tissues due to their extensive genetic heterogeneity; associated morbidities or tumor metastasis during the invasive biopsies; and different antibodies, multiple scoring criteria, and poor DNA quality resulting in high heterogeneity of results (13). What is more, gene mutations could change over the course and progression during whole therapy, making it impractical and challenging to obtain tumor biopsy during multiple times. However, molecular profiling of relative high costs is not routinely performed for every patient, especially in low-resource settings. Therefore, a non-invasive method for identifying the mutation status is urgently needed.

Radiological images reflect abundant information on the entire tumor in non-invasive way (14). Recent advances in machine learning have promoted the disease diagnosis based on computed tomography (CT) images. Conventional radiomics methods, which are tedious and time consuming, include image segmentation, feature extraction and selection, model building, and data analysis. The radiological characteristics are affected by manual segmentation and CT scan parameters, and repeated professional analysis by doctors is necessary (14). Advances in deep learning could overcome these problems and have demonstrated accurate, reliable, and reproducible performance on triage tasks for detecting the abnormalities and diagnosing the disease (15, 16). These proposed deep learning models and techniques have achieved a predictive performance in estimating malignancy risk in pulmonary nodules and diagnosing pneumonia quickly during the COVID-19 pandemic. Recent new and exciting developments in artificial intelligence (AI) have provided new potential opportunities to predict the EGFR mutation or PD-L1 expression status on the basis of CT images (17, 18). However, the small datasets and binary task limit its applicability in the routine clinical work. There still exists a considerable challenge to objectively evaluate the ability of the model to predict the gene mutation status and gene subtypes.

In the present study, we proposed an AI system to mine CT image information to predict EGFR mutation status and mutated subtype (i.e., 19Del and L858R) and investigate the PD-L1 expression level and positive PD-L1 subtypes (PD-L1 TPS, 1%–49% and ≥50%) and further simultaneously identify both EGFR and PD-L1 status, aiming to provide support for clinical decision-making.

MATERIALS AND METHODS

Patients Cohort and Data Collection

This study retrospectively included consecutive patients with NSCLC who visited West China Hospital of Sichuan University (Sichuan, China) from June 2019 and June 2021. The current study was performed in compliance with the Declaration of Helsinki and approved by the Institutional Review Board (IRB)/ Ethics Committee. Written informed consent was waived because the data used for system development were de-identified by removing personal information. Patients who meet the following inclusion criteria were collected into this study: (1) histologically verified primary NSCLC, (2) pathological analysis of tumor tissues with thorough EGFR or PD-L1 testing results, and (3) preoperative CT images. Patients were excluded if (1) clinical data such as age, sex, and stage were missing; (2) preoperative treatment was received; (3) the duration between CT examination and subsequent surgery exceeded 1 month; or (4) tumors <1cm in size and CT imaging artifact were found. Following the screening of

exclusion criteria, we selected our primary cohort (n = 3,816) for model development. Furthermore, we created a subset of EGFR cohort (n = 3,629), PD-L1 cohort (n=873), and EGFR and PD-L1 joint cohort (n = 818) who underwent staining based on surgery or biopsy specimens and gene testing (EGFR, PD-L1 or both), with the goal of evaluating the performance of our models for three prediction tasks: gene mutation status, gene subtypes, and joint prediction.

EGFR gene status was determined to be mutated (including 19Del, L858R, and Others) and wild by amplification refractory mutation system-polymerase chain reaction (ARMS-PCR) or next-generation sequencing (NGS). PD-L1 expression status was identified as positive and negative according to PD-L1 TPS (≥1% vs. <1%; TPS is the percentage of tumor cells with membranous PD-L1 staining, with TPS ≥1% indicating positivity; TPS 1%–49% and ≥50% indicating low PD-L1+ and high PD-L1+, respectively) using SP142 antibody in immunohistochemical (IHC) assays performed on the Ventana Benchmark platform. After being reviewed by senior pathologists, these gene testing results were regarded as the gold criteria in the current study. The CT data utilized in this study came from a variety of suppliers (GE, Philips, Siemens United Imaging Health) to assess the resilience of our AI system in multiple clinical contexts. All CT scans had a resolution of 512 × 512, with slice spacing ranging from 0.625 to 5 mm in the axial direction. For the electronic health records (EHRs) data collection in our study, ideally, for a unique patient, his/her EHRs data should at least include basic information, i.e., age, sex, tumor stage, and smoking status, and radiology reports in line with international standards.

For multitask AI system, we collected multimodal data that comprised (a) deep learning features based on CT images, which consisted of a global texture feature and a tumor local texture feature; (b) radiomics features that extracted and analyzed a large number of advanced quantitative image features with high throughput; and (c) clinical features that included demographics, comorbidities, and clinical symptoms.

Data Pre-Processing

In this experiment, we obtained the training and testing cohorts from the EGFR/PD-L1 dataset by stratified and random sampling of patients at a ratio of 4:1. For the CT images, two groups of doctors were asked to delineate of the specific mask of the entire tumor. The tumor–mask pair was then fed into the radiomics model, which extracted radiomic characteristics, and the deep learning model, which extracted deep learning features. For deep learning feature analysis, a cubic region of interest (ROI) containing the entire tumor with surrounding information was supplied and retrieved local deep learning features by the local DL model, and the global DL model took the corresponding origin CT volume as input. Finally, as deep learning features, local deep feature and global deep feature were combined. Using pre-computed windowing information, all cubic ROI and origin CT volume pixels were normalized to 0–255, and all CT volumes were resized to the same size of 36 × 36 × 36 using third-order spline interpolation. To reduce overfitting, data augmentations such as horizontal flip, random resizing cropping, random rotation, and random color jittering were used throughout the training phase. For the final model training and inference, a random crop of 32 × 32 × 32 would be employed.

Construction of AI System

We developed a deep-learning-based AI system for scalable gene prediction in patients. To summarize, our proposed AI system employed a modular pipeline method with four key components (**Figure 1**): deep learning module, radiomics module, clinical module, and feature fusion module. The following was a full description of the AI system.

For the deep learning module (**Figure 1B**), in order to pay more attention to contextual features (different lesion signs usually appear at the same time) and use these correlation lesion signs to improve the model's representation learning ability, this study proposed a novel dual-pathway deep learning network architecture that performs CT volume and tumor volume feature as local and global information, using the weighted-share backbone to capture the dependence between tumor detail information and the whole CT information in a large range. To be more specific, both the encoders of the framework (local and global) were composed of several 3D convolution and residual blocks, and the continuous multislice (tumor and full CT images) were used to form trainable 3D data patches, which were then fed as two branch inputs to realize multiscale local and global information extraction through progressive fusion, making full use of context texture information of 3D image space. In addition, due to the different roles of global feature and local feature in specific prediction, it was necessary to conduct corresponding modeling for different extracted features; therefore, we adopted an asymmetric non-local fusion layer to implicitly modeled the attentional mechanism. For each weight-sharing branch of the backbone, for 3D volumes, we applied a 3D ResNet-18 feature extractor and fine-tuned the parameters by the pre-trained model. As a consequence, transfer learning was employed to address the issue of insufficient training data by first learning the neural network's unique weights on the source data set. Because several gene mutations might co-exist or overlap on the same patient, a multilabel triage loss function with sigmoid active function was used instead of the standard multiclass classification loss.

The radiomics module (**Figure 1C**) retrieved and quantified a large number of characteristic data from tumor images and processed genetic and tumor information from more high-dimensional features that cannot be observed by the human naked eye to construct clinical features. The following pipeline steps were used to extract image radiomics features: (1) precise segmentation of suspected tumors, (2) extraction of large high-dimensional characteristics from suspected tumor area, and (3) filtered and reduced correlation features to prevent overfitting. To begin, 1,247 radiomics characteristics were extracted from each tumor–mask pair volume (segmented by the doctors). These characteristics included first-order (HU stats), shape, and texture properties.

The first-order feature depicted the intensity distribution of CT values in the volume of interest by common basic measures,

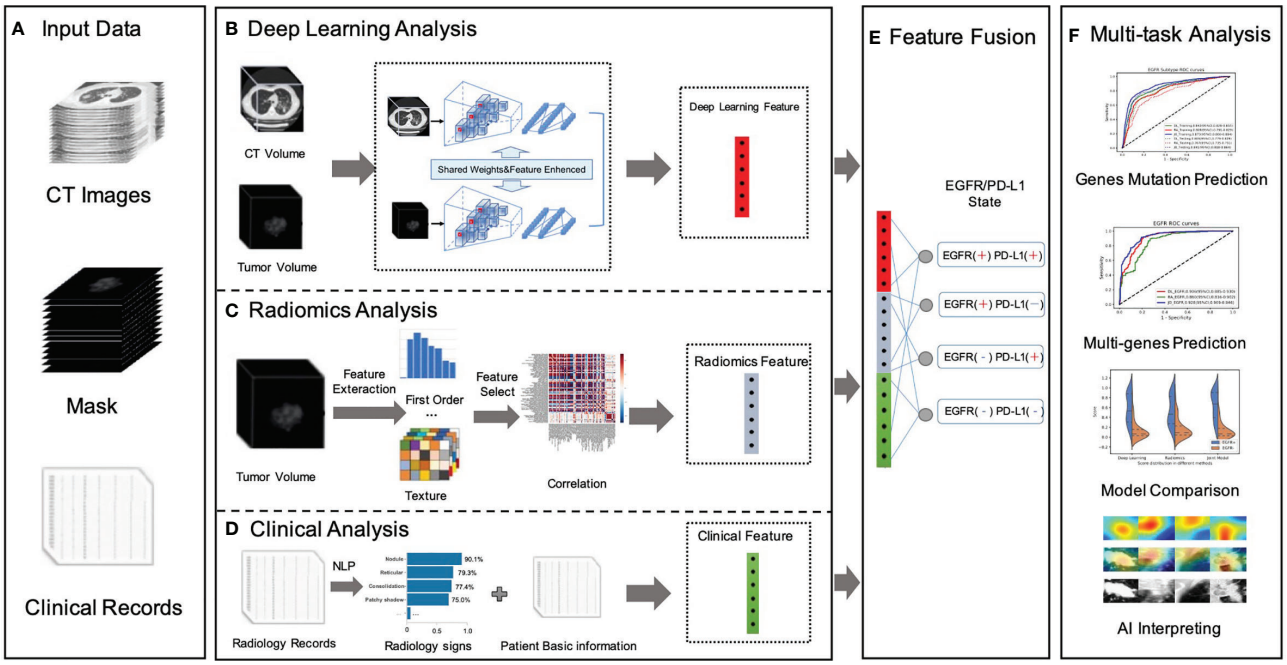

FIGURE 1 | Overall workflow in our study. **(A)** Data preparation stage included original CT image data, with manually labeled tumor images, NGS testing gene mutation status, gene mutation subtypes, radiology records, and patients' fundamental clinical indications. **(B)** A novel dual-pathway deep learning network architecture that performed CT volume and tumor volume feature extraction, named DL feature, using the trained backbone for gene prediction and further to fuse the extracted feature with another learnable pathway using an asymmetric non-local fusion module. **(C)** The pipeline of radiomics analysis model extracted radiomics features based on manually segmented contour of the tumor. **(D)** The clinical feature considered a full coverage of clinical information, including radiology signs that applied NLP techniques to extract structured labels from radiology reports. **(E)** The feature fusion utilized full connection to provide self-adaptation on the combination of deep learning features, radiomics features, and clinical features. **(F)** Validation of the proposed AI system.

such as mean, range, and standard deviation. The texture features were classified into five categories: (1) the gray-level co-occurrence matrix, (2) the gray-level difference matrix, (3) the gray-level run-length matrix, (4) the gray-level size-zone matrix, and (5) the gray-tone difference matrix in the neighborhood. Following that, for each feature in a specific tumor, we summarized and examined the distribution of the feature's values across nine filters and eight wavelet transformations in high dimensions. Then, the least absolute shrinkage and selection operator (LASSO) method was used on the feature set to eliminate the correlation radiomics characteristics with low variance (<0.8). Finally, around 100-dimensional features were selected as the most useful radiomics features in LASSO model.

The clinical module (**Figure 1D**) acquired structured abnormality symptoms and the patients' basic clinical information. Although CT imaging can provide some insight into the effectiveness of cancer immunotherapy, the clinical information of patients including age, sex, tumor staging, number, size, past recurrence, and medication status had all been linked to the efficacy of cancer immunotherapy. How to effectively combine imaging and clinical information to construct an individual prediction model remained another key problem. For the structured information, such as sex, we mainly used the one-hot strategy to convert category variables into a sparse vector space that machine learning algorithms can easily use. For the free-text reports, such as radiology record, we used the natural language processing (NLP) algorithm to perform free-text record analysis to predict patients' radiological abnormalities into a structured label vector format (binary vector of labels for the targeting abnormality). To create uniform length vectors, the raw free texts were first vectorized using a data vectorization process. The text classifier was then trained using supervised learning, which may be used to generate labels (e.g., radiological abnormalities) automatically. The text classifier was trained using pre-annotated text–label pairs. Then, these structured symptoms label vectors and structured patients' basic clinical information were merged into the combined vector as our clinical features.

The fusion module made use of the fully connectivity layer to provide self-adaptation based on a combination of deep learning (DL), radiomics (RA), and clinical (CL) features. Prior to the fusion action, both features were followed by a new conversion layer, specifically, a 512D-output full connection layer, which bridged the dimensional gap between the types of features and boosts the convergence of our feature fusion module. As a consequence, our model could jointly project these diverse features to an embedding feature space, allowing us to make better use of individual feature strength.

Statistical Analysis

The following measures were used to assess the performance of our classifiers: area under the receiver operating characteristic curve (AUC), accuracy, sensitivity, and specificity. The 95% confidence intervals (CIs) for the AUC were calculated through DeLong technique. The median and interquartile range (IQR) with a 95% CI were used to represent continuous variables. Independent sample t-test was used to assess the significance of mean age of EGFR mutant and EGFR genotyping patients. The same statistical analysis was performed for scores in the PD-L1 mutant group and the PPD-L1 negative (PD-L1-) and positive (low PD-L1+; high PD-L1+) groups. χ^2 test was used to evaluate the differences in sex and other symptoms in each cohort. The ANOVA test was used to determine whether there was a difference between the joint categories of genes mutant patients. All statistical tests were two-tailed, with statistical significance set at $P < 0.05$ considered as significant. Our implementation of the deep learning model used the Pytorch toolkit and Python 3.7.

RESULTS

Patient Characteristics of Enrolled Datasets

A total of 4,404 patients were initially identified who had been pathologically diagnosed with lung cancer and had undergone the molecular (EGFR or PD-L1) test (**Figure 2**). Following eligibility screening, this study included three cohorts of 3,816 eligible patients with consecutive chest CT images. The EGFR cohort (n = 3,629), PD-L1 cohort (n = 873), and EGFR and PD-L1 cohort (n = 818) were enrolled, divided into 80% training/internal validation and 20% testing sets, to develop and optimize our AI systems for differentiating positive EGFR mutation or PD-L1 expression status from negative ones. The sum of three cohorts were not equal to the number of total cohorts due to that molecular profiling of EGFR or PD-L1 was not routinely performed for every patient. Among the whole patients, the mean age was 59 years, and 2,067 (54.17%) patients were male. There were 2,067 (54.17%) never-smokers, 3,353 (87.87%) with no family history of cancer, and 2,937 (76.97%) LUAD patients. For tumor stage, patients with stages I, II, III, and IV were 1,136 (29.77%), 284 (7.44%), 742 (19.44%), and 1,475 (38.65%), respectively. There was no significant difference for age (p = 0.508), sex (p = 0.143), smoking status (p = 0.759), family history of cancer (p = 0.503), histopathology (p = 0.324), tumor stage (p = 0.497) among these three cohorts. Demographic and clinical characteristics of included dataset are depicted in **Table 1**.

Evaluation of Model Performance in Predicting EGFR Mutation Status

In this step, three models including deep learning (DL) model, radiomics (RA) model, and joint (JO) model combining the DL, RA, and CL features were trained and developed to distinguish the mutated EGFR from the wild EGFR patients and subsequently discriminate the mutated EGFR subtypes (19Del, L858R, and others). On the binary task of distinguishing mutated EGFR from wild ones, the AUCs of DL, RA, and JO models were 0.880 (95% CI, 0.871–0.892) and 0.842 (95% CI, 0.825–0.855), 0.838 (95% CI, 0.827–0.850) and 0.805 (95% CI, 0.789–0.827), and 0.919 (95% CI, 0.914-0.924) and 0.895 (95% CI, 0.883–0.907) in training and testing sets, separately (**Figure 3** and **Table 2**). Pertaining to three-way triage task discriminating the mutated EGFR subtypes, DL, RA, and JO models achieved the mean AUCs of 0.842 (95% CI, 0.828–0.855) and 0.805 (95% CI, 0.779–0.829), 0.809 (95% CI, 0.791–0.829) and 0.767 (95% CI, 0.735–0.791), and 0.873 (95% CI, 0.860–0.884) and 0.841 (95% CI, 0.818–0.864) in predicting 19Del, L858R, and other mutation status on the training and testing sets, respectively (**Figure 3** and **Table 2**). No matter which task, the proposed binary task and subtype classification, the performance of the joint model showed the best performance, and the combination of radiomics and clinical features contributed most to the EGFR prediction, which implied the associations and the complementarity of deep learning, radiomics, and clinical features.

Evaluation of Model Performance in Predicting PD-L1 Expression Status

The trained AI system was also evaluated on the PD-L1 cohort to distinguish the positive PD-L1-positive (PD-L1 TPS ≥1%) from the PD-L1-nagetive (PD-L1 TPS <1%) patients and subsequently discriminate the PD-L1-positive subtypes (low positive PD-L1, 1%–49%; high positive PD-L1, TPS ≥50%). On the binary task of distinguishing positive PD-L1 from negative PD-L1 ones, the AUCs of DL, RA, and JO models were 0.851 (95% CI, 0.833–0.872) and 0.799 (95% CI, 0.762–0.854), 0.819 (95% CI, 0.800–0.845) and 0.795 (95% CI, 0.748–0.843), 0.885 (95% CI, 0.867–0.905) and 0.867 (95% CI, 0.817–0.897) in training and testing sets, separately (**Figure 3** and **Table 2**). Pertaining to binary task classifying the positive-PD-L1 subtypes into low positive and high positive groups, DL, RA, and JO models achieved predictive performance with the AUCs of 0.911 (95% CI, 0.875–0.941) and 0.837 (95% CI, 0.775–0.911), 0.884 (95% CI, 0.841–0.917) and 0.836 (95% CI, 0.775–0.892), and 0.919 (95% CI, 0.889–0.942) and 0.864 (95% CI, 0.802–0.924) in the training and testing sets, respectively (**Figure 3** and **Table 3**). The performance of DL model outperformed RA models in both training and testing cohorts. What is more, JO model also performed superior than both DL and RA models. Both results confirmed that the JO model was sensitive to radiomics and clinical information and differentiating positive PD-L1 from negative PD-L1 with reasonable accuracy as a diagnostic tool.

Evaluation of Model Performance in Predicting Both EGFR and PD-L1 Expression Status

We next investigated the feasibility of assessing the multigenes mutation status. Three models also demonstrated the robust performance in the co-existing immunity cohort. In the multiple task in terms of four-way classification (multitask classifier) into EGFR(+)PD-L1(+), EGFR(+)PD-L1(−), EGFR(−)PD-L1(+), and EGFR(−)PD-L1(−) groups, DL, RA, and JO model achieved the

TABLE 1 | Clinical characteristics of patients used to measure EGFR mutation and PD-L1 expression status.

	Total (N = 3,816, %)	EGFR (N = 3,629, %)	PD-L1 (N = 873, %)	EGFR&PD-L1 (N = 818, %)	*p*-value
Age (years)	59.32	59.29	58.72	58.77	0.508
Sex, N(%)					0.143
Male	2,067(54.17)	1,955(53.87)	471(53.95)	449(54.89)	
Female	1,749(45.83)	1,674(46.13)	402(46.05)	369(45.11)	
Smoking status					0.759
Current or former	1,500(39.30)	1,413(38.94)	281(32.19)	257(31.42)	
Never	2,067(54.17)	1,981(54.59)	566(64.83)	543(66.38)	
Unknown	249(6.52)	235(6.47)	26(2.98)	18(2.2)	
Family history of cancer					0.503
Yes	248(6.50)	236(6.50)	69(7.90)	67(8.19)	
No	3,353(87.87)	3,188(87.85)	791(90.61)	745(91.08)	
Unknown	215(5.63)	205(5.65)	13(1.49)	6(0.73)	
Histopathology					0.324
LUAD	2,937(76.97)	2,787(76.80)	789(90.38)	743(90.83)	
LUSC	607(15.90)	592(16.31)	47(5.38)	42(5.13)	
Other	272(7.12)	250(6.89)	37(4.24)	33(4.03)	
Stage					0.497
I	1,136(29.77)	1,092(30.09)	354(40.55)	347(42.42)	
II	284(7.44)	272(7.50)	68(7.79)	63(7.7)	
III	742(19.44)	700(19.29)	160(18.33)	150(18.34)	
IV	1,475(38.65)	1,402(38.63)	260(29.78)	236(28.85)	
Unknown	179(4.69)	163(4.49)	31(3.55)	22(2.69)	
EGFR Mutation (%)					0.934
EGFR Wild	1,436(37.63)	1,436(39.57)	–	183(22.37)	
EGFR Mutant	2,193(57.47)	2,193(60.43)	–	635(77.63)	
PD-L1 Expression (%)					0.639
PD-L1-	562(64.38)	–	562(64.38)	539(65.89)	
PD-L1 +	311(35.62)	–	311(35.62)	279(34.11)	
Mutated EGFR Subtype (%)					0.367
19Del	919(24.08)	919(24.08)	–	–	
L858R	1,090(28.56)	1,090(30.04)	–	–	
Others	184(4.82)	184(5.07)	–	–	
Positive PD-L1 Expression (%)					0.215
≥50%	268(7.02)	–	268(30.70)	–	
1-49%	43(1.13)	–	43(4.93)	–	

EGFR, epidermal growth factor receptor; PD-L1, programmed death ligand-1; LUAD, lung adenocarcinoma; LUSC, lung squamous cell carcinoma.

AUCs of 0.906 (95% CI, 0.885–0.930) and 0.879 (95% CI, 0.854–0.906), 0.860 (95% CI, 0.816–0.902) and 0.856 (95% CI, 0.815–0.897), and 0.928 (95% CI, 0.909–0.946) and 0.905 (95% CI, 0.886–0.930) in the training and testing sets, respectively (**Figure 4**; **Table 4**). These results proved the potential of our joint model' ability to predict multigene events that may occur in at least two mutants on a single patient.

Deep Learning Model Interpretability

For each image, the attention of the model can be visualized for human interpretability and validation. High-resolution feature visualization provides an intuitive manner to understand the distribution of features used in this investigation. The aim of this section was to evaluate and validate the potential clinical application of the joint model of heatmaps as saliency models through CT volumes. In the attention map of the deep learning model through CAM, the dark color areas might be the tumor center, visualizing the attention regions located at the border of the lesion of a network to capture the discriminative information pertaining to the prediction results of distinct mutant categories (**Figure 5**). When the deep learning model predicts gene mutation status, it could simultaneously tell human experts which area draws the attention of the model. Additionally, the deep learning framework was based on pixel-level models, with the shallow layers of the model focused on textural information between pixels in CT images, such as horizontal and diagonal edges, while ignoring some general information about the tumor. On the contrary, as the network becomes deeper, more complicated characteristics, such as tumor semantics, were learned at the deep convolutional layer. Furthermore, the radiomics model concentrates primarily on some general tumor properties rather than on specific local low-dimensional tumor aspects. As a result, for a better understanding of the joint deep learning feature, we compared the model based only on deep learning feature and the joint model feature incorporating radiomics and clinical factors on the convolution filter.

DISCUSSION

Accurate and rapid quantification of EGFR mutation and PD-L1 expression status is of paramount importance in identifying of NSCLC patients more suitable for EGFR-TKI or ICI therapies,

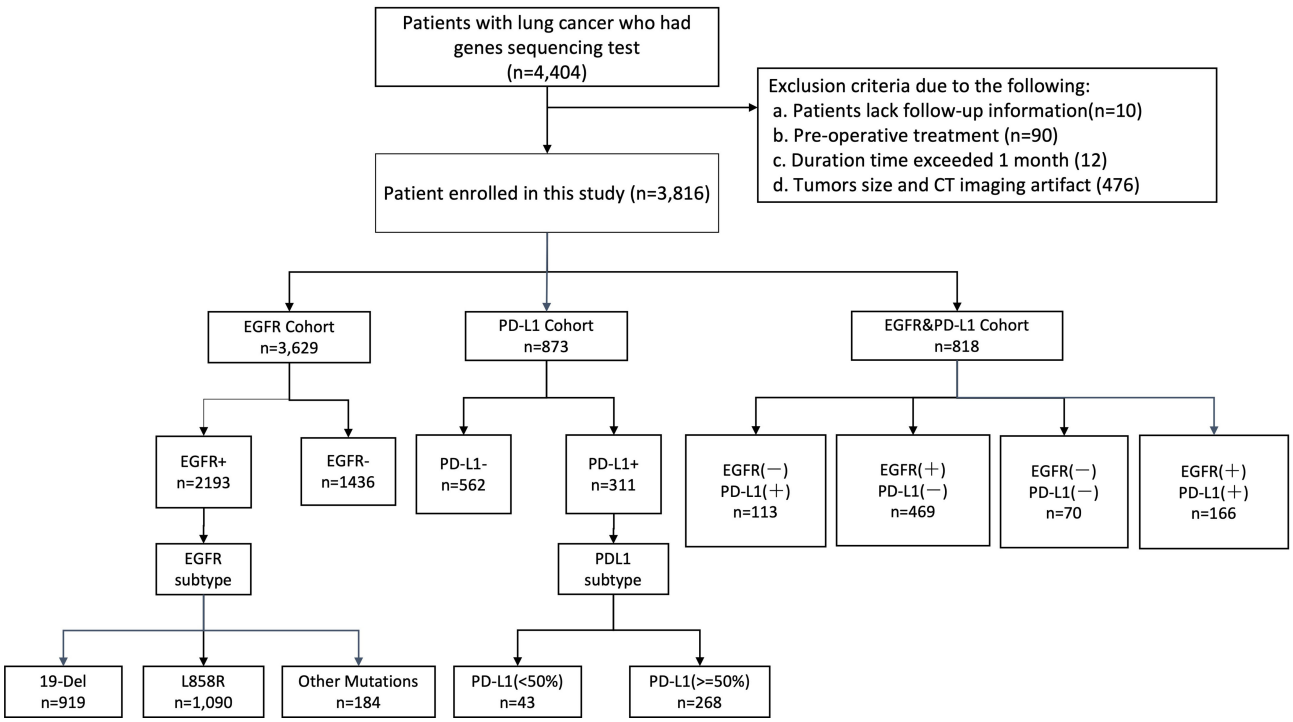

FIGURE 2 | Illustration of workflow in this study. Between June 2019 and June 2021, this study included primary cohort 3,816 consecutive patients with NSCLC who visited West China Hospital (Sichuan, China) for model development and validation. Additionally, we built a subset (EGFR cohort and PD-L1 cohort) for patients who underwent staining based on histological specimens and molecular test (EGFR, PD-L1), aiming to evaluate the performance of our models on predicting events gene mutation status and gene subtype. Cohort EGFR and PD-L1 was used to evaluate model performance in joint immunity prediction.

further guiding clinical decision-making. However, the dynamic change in proportion of cells expressing EGFR mutation or PD-L1 level and the invasive tissue/biopsy-based nature limit the applicability of EGFR or PD-L1 testing compared to image-based assays. Thus, there is a need for a non-invasive, accurate, reliable, and reproducible method to assess EGFR/PD-L1 status. In this study, we proposed a deep learning model using non-invasive chest CT images, which demonstrated the favorable performance to predict EGFR mutation/PD-L1 expression status and their subtypes for NSCLC patients.

According to the National Comprehensive Cancer Network (NCCN) Guidelines, multiple gene status especially EGFR and PD-L1 TPS should be known before deciding whether to use either targeted therapy or immunotherapy (19). However, gene detection posed a challenge, as suitable specimens were obtained through invasive procedure. These assessments were affected by heterogeneity of antibodies, platforms, and different clinicians. For example, the current study utilized SP142 antibody to score membrane-localized PD-L1 staining in tumor cells and tumor-infiltrating immune cells, which ignored cytoplasmic- or nuclei-located PD-L1. In addition, although the treatment strategy for NSCLC has rapidly evolved with the emergence of targeted therapy and immunotherapy, persistent drug responses remain limited to a subset of patients, such as the response rates of ICIs ranged from 14% to 20% in unselected patients (20, 21). Patients with PD-L1 level ≥50% would benefit from chemoimmunotherapy than single-agent immunotherapy (response rates of 60% and 40%, respectively) (11, 22, 23). The median PFS in patients with EGFR 19Del was longer than in patients with EGFR L858R treated with EGFR-TKI (10, 24). It was worth exploring the comprehensive method to assess precise gene status.

In clinical practice, CT scans are routinely available. Frontier studies combined radiological images and deep learning technology and have become trend in screening, diagnosis, gene prediction, and prognosis of lung cancer (15, 25, 26). Previous studies proposed deep learning models trained on CT images to predict high PD-L1 expression or EGFR mutated status of NSCLC (17, 18). Meanwhile, a deep-learning model based on radiology text reports was performed to estimate objective response of PD-1 blockade in NSCLC patients (27). However, these models only focused on binary tasks of gene status constructed on single-omics data, which were unsuitable for routine clinical work. Herein, we explored an approach with promising performance to predict gene mutation and further specific type based on large sample CT images and clinical features. This detailed molecular information including EGFR mutated (19Del, L858R, other) or wild; PD-L1 (≥50%) assists physician in accurate treatment. Additionally, several studies using deep learning inferred therapeutic effects of TKIs or ICIs in NSCLS patients (18, 28, 29). We would further update this

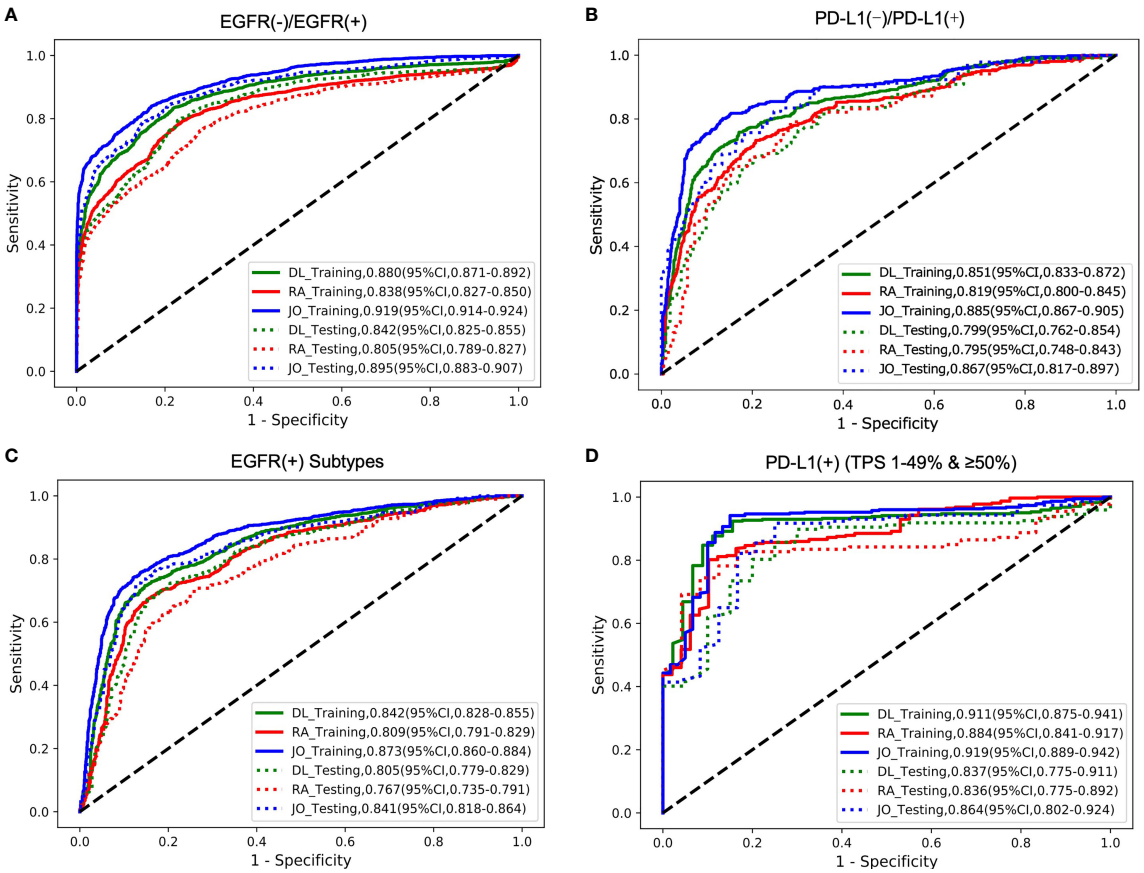

FIGURE 3 | The model performances in the prediction of two outcomes (EGFR cohort and PD-L1 cohort). The ROC curves for predicting **(A)** EGFR gene mutation status (mutant or wild); **(B)** PD-L1 status (positive or negative); **(C)** EGFR gene subtype mutations (19Del; L858R or Other); **(D)** PD-L1expression status (PD-L1 TPS 1%–49% or ≥50%). DL indicated that our image-based DL system used local tumor volume and global CT volume. RA indicated that our image-based radiomics model and the JO indicated that the joint model combined with the DL feature, radiomics feature, and clinical features. The solid line represents the performances on the training set, and the dotted line represents the effect on the test set.

TABLE 2 | Predictive performance of EGFR status and EGFR mutated subtypes using three methods in the training and testing cohorts.

Methods	Cohorts	AUC(95%CI)	Accuracy(%)	Sensitivity(%)	Specificity(%)
		EGDFR Mutation Status			
DL	Training	0.880(0.871-0.892)	0.805(0.797-0.815)	0.832(0.820-0.845)	0.783(0.769-0.798)
	Testing	0.842(0.825-0.855)	0.763(0.750-0.777)	0.797(0.777-0.818)	0.769(0.746-0.789)
Radiomics	Training	0.838(0.827-0.850)	0.769(0.758-0.779)	0.794(0.780-0.812)	0.760(0.743-0.771)
	Testing	0.805(0.789-0.827)	0.735(0.720-0.755)	0.768(0.748-0.793)	0.716(0.696-0.734)
Joint	Training	0.919(0.914-0.924)	0.840(0.831-0.850)	0.839(0.829-0.852)	0.831(0.820-0.844)
	Testing	0.895(0.883-0.907)	0.819(0.803-0.835)	0.791(0.765-0.816)	0.850(0.834-0.870)
		EGFR Subtypes			
DL	Training	0.842(0.828-0.855)	0.753(0.740-0.769)	0.716(0.696-0.739)	0.853(0.836-0.873)
	Testing	0.805(0.779-0.829)	0.732(0.707-0.755)	0.707(0.676-0.742)	0.815(0.787-0.849)
Radiomics	Training	0.809(0.791-0.829)	0.725(0.708-0.743)	0.672(0.647-0.702)	0.848(0.830-0.870)
	Testing	0.767(0.735-0.791)	0.697(0.663-0.728)	0.705(0.670-0.745)	0.742(0.712-0.773)
Joint	Training	0.873(0.860-0.884)	0.790(0.776-0.804)	0.758(0.739-0.778)	0.862(0.844-0.881)
	Testing	0.841(0.818-0.864)	0.767(0.746-0.790)	0.767(0.732-0.798)	0.827(0.803-0.858)

EGFR, epidermal growth factor receptor; PD-L1, programmed death ligand-1; DL model, deep learning model.

TABLE 3 | Predictive performance of PD-L1 status and PD-L1 expression using three methods in the training and testing cohorts.

Methods	Cohorts	AUC (95%CI)	Accuracy (%)	Sensitivity (%)	Specificity (%)
			PD-L1 Status		
DL	Training	0.851(0.833-0.872)	0.824(0.809-0.840)	0.758(0.729-0.791)	0.829(0.807-0.852)
	Testing	0.799(0.762-0.854)	0.770(0.727-0.800)	0.680(0.604-0.756)	0.793(0.746-0.839)
Radiomics	Training	0.819(0.800-0.845)	0.797(0.777-0.816)	0.732(0.688-0.775)	0.791(0.764-0.810)
	Testing	0.795(0.748-0.843)	0.759(0.717-0.797)	0.790(0.707-0.851)	0.716(0.659-0.769)
Joint	Training	0.885(0.867-0.905)	0.869(0.850-0.884)	0.801(0.768-0.842)	0.865(0.847-0.881)
	Testing	0.867(0.817-0.897)	0.808(0.771-0.846)	0.822(0.758-0.884)	0.752(0.714-0.810)
			Positive PD-L1 Expression with low and high PD-L1(+)		
DL	Training	0.911(0.875-0.941)	0.899(0.868-0.925)	0.924(0.894-0.943)	0.844(0.750-0.940)
	Testing	0.837(0.775-0.911)	0.868(0.820-0.910)	0.857(0.816-0.905)	0.750(0.611-0.933)
Radiomics	Training	0.884(0.841-0.917)	0.831(0.798-0.865)	0.802(0.764-0.837)	0.898(0.811-0.963)
	Testing	0.836(0.775-0.892)	0.796(0.745-0.854)	0.744(0.672-0.809)	0.917(0.810-1.000)
Joint	Training	0.919(0.889-0.942)	0.917(0.894-0.938)	0.941(0.918-0.960)	0.850(0.773-0.922)
	Testing	0.864(0.802-0.924)	0.884(0.845-0.934)	0.917(0.877-0.955)	0.750(0.636-0.875)

EGFR, epidermal growth factor receptor; PD-L1, programmed death ligand-1; DL model, deep learning model.

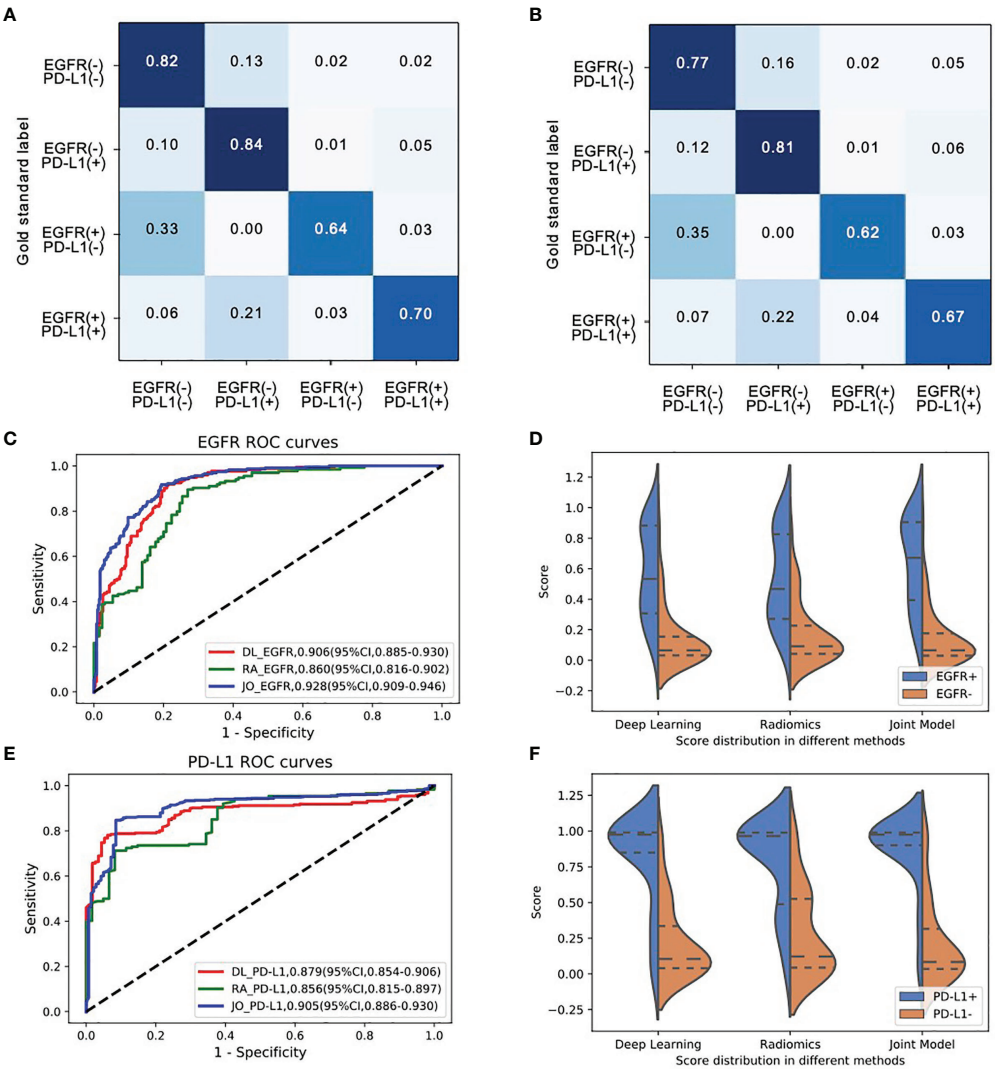

FIGURE 4 | The model performances in the prediction of joint-mutant genes (EGFR and PD-L1 cohort). Confusion matrix of **(A)** training set and **(B)** testing set indicated most errors occurred in the adjacent groups. **(C)** The ROC curves and **(D)** three model scores predicting EGFR mutation; **(E)** the ROC curves and **(F)** three model scores predicting PD-L1 expression status.

TABLE 4 | Predictive performance of EGFR and PD-L1 status performance using three methods in the joint cohort.

Methods	Categories	AUC (95% CI)	Accuracy (%)	Sensitivity (%)	Specificity (&)
			EGFR&PD-L1 Status		
DL	EGFR	0.906(0.885-0.930)	0.767(0.735-0.798)	0.920(0.884-0.954)	0.787(0.748-0.827)
	PD-L1	0.879(0.854-0.906)	0.793(0.762-0.819)	0.781(0.742-0.819)	0.939(0.904-0.969)
Radiomics	EGFR	0.860(0.816-0.902)	0.659(0.617-0.705)	0.896(0.856-0.944)	0.731(0.664-0.801)
	PD-L1	0.856(0.815-0.897)	0.719(0.677-0.766)	0.713(0.661-0.763)	0.918(0.864-0.972)
Joint	EGFR	0.928(0.909-0.946)	0.831(0.807-0.856)	0.917(0.883-0.941)	0.807(0.771-0.846)
	PD-L1	0.905(0.886-0.930)	0.848(0.825-0.874)	0.847(0.818-0.879)	0.915(0.876-0.951)

EGFR, epidermal growth factor receptor; PD-L1, programmed death ligand-1; DL model, deep learning model.

multitask AI system to predict the clinical outcomes of treatment more accurately.

In terms of algorithm, radiomics and deep learning features were integrated to mine CT image features. In addition, clinical features were integrated to try to build a prediction model with superior performance, which was more in line with routine clinical work. Not surprisingly, the performance of the integrated model was better than the deep learning model and radiomics model. This also reflected the trend of characteristic fusion. Although our AI system performed well in this aspect, it failed well short of the gold standard set by laboratory studies. To increase prediction accuracy, our AI system, for example, would benefit from other source data kinds. For example, clinical or laboratory information (such as blood biochemical analysis) might be incorporated as an additional information source to our joint AI system.

Our study has some limitations. First, this was a single-center study, and the predictive value of our model still needs to be validated in other medical centers. Second, this was a retrospective study. NSCLC patients may take multiple genes detection during treatment, which may cause some selection biases. Finally, this research only focused on EGFR and PD-L1. More extensive data would be collected to support additional mutation of NSCLC, such as ALK, ROS1, and KRAS mutation in the future.

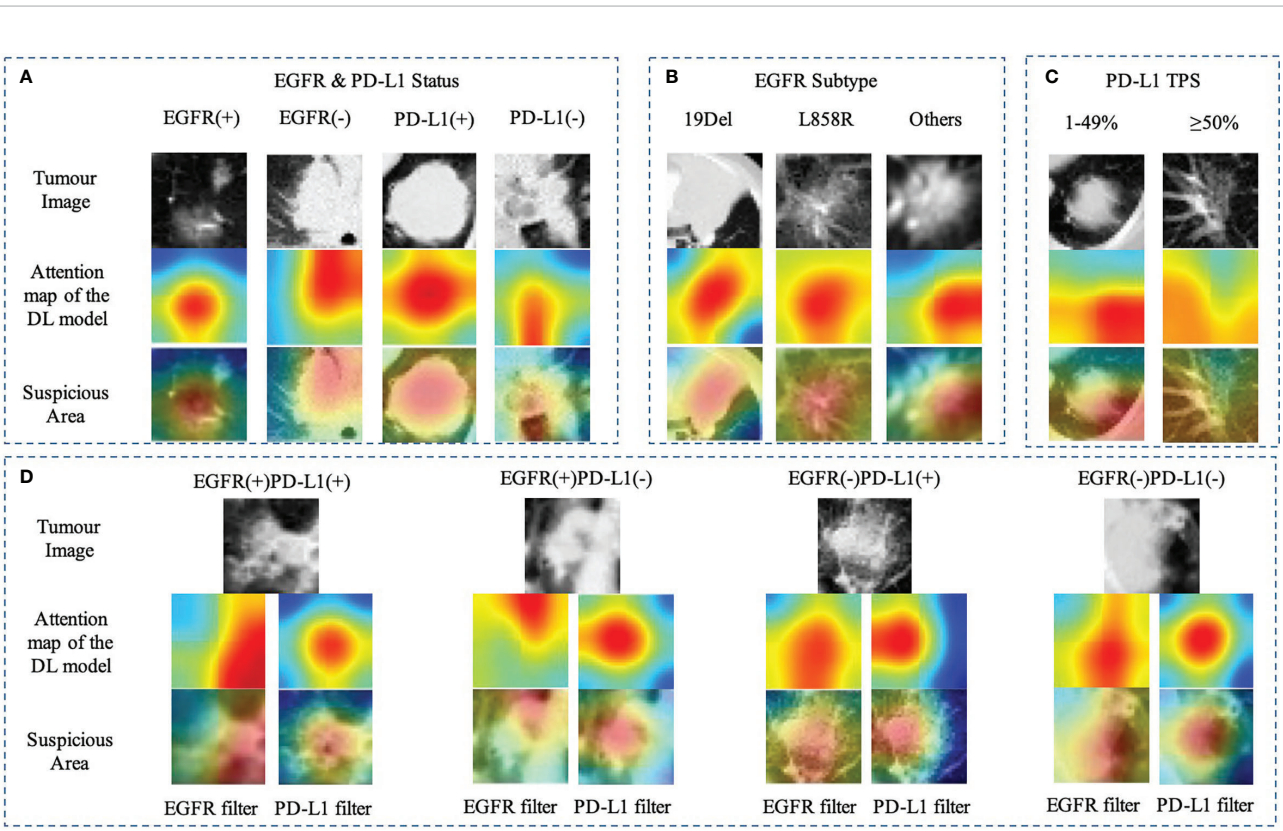

FIGURE 5 | Heatmap of characteristics that contributed to the prediction of gene mutation **(A)** EGFR and PD-L1 status; **(B)** EGFR subtype (19Del, L858R, or other); **(C)** PD-L1expression status (PD-L1 TPS, 1%–49% or ≥50%); **(D)** EGFR mutation combined with PD-L1 status using different filters. The first row showed the origin tumor image in the 3D volume; the second and third rows visualize the attention regions of a network for distinct mutant categories.

In conclusion, this study demonstrated an AI system's value in assisting medical professionals provide a non-invasive and easy-to-use method to identify the expression status of common genes EGFR and PD-L1 through CT images, which may serve as a predictive biomarker for guiding the target therapy and immunotherapy in NSCLC patients. Future refinement and improvement will expand its use into predicting other common genes mutation in larger and prospective trials.

DATA AVAILABILITY STATEMENT

The raw data supporting the conclusions of this article will be made available by the authors, without undue reservation.

ETHICS STATEMENT

The studies involving human participants were reviewed and approved by the Institutional Review Board (IRB)/Ethics Committee of West China Hospital. The patients/participants provided their written informed consent to participate in this study.

AUTHOR CONTRIBUTIONS

WL and YY were involved in the study design. CW, JM, and JS were involved in the organization of the entire project, data analysis with a clinical perspective, and manuscript writing. CW and JS collected the imaging and clinical data. JM, SZ, and ZL were involved in the establishment of the algorithm. All authors contributed to the article and approved the submitted version.

FUNDING

The study was supported by National Natural Science Foundation of China (82100119, 91859203, and 81871890), the Science and Technology Project of Sichuan (2020YFG0473), Chinese Postdoctoral Science Foundation (2021M692309), Postdoctoral Program of Sichuan University (2021SCU12018), and the Science and Technology Achievements Transformation Foundation and Postdoctoral Program of West China Hospital, Sichuan University (CGZH21009 and 2020HXBH084).

REFERENCES

1. Sung H, Ferlay J, Siegel RL, Laversanne M, Soerjomataram I, Jemal A, et al. Global Cancer Statistics 2020: Globocan Estimates of Incidence and Mortality Worldwide for 36 Cancers in 185 Countries. *CA Cancer J Clin* (2021) 71 (3):209–49. doi: 10.3322/caac.21660
2. Wang C, Wu Y, Shao J, Liu D, Li W. Clinicopathological Variables Influencing Overall Survival, Recurrence and Post-Recurrence Survival in Resected Stage I Non-Small-Cell Lung Cancer. *BMC Cancer* (2020) 20(1):150. doi: 10.1186/s12885-020-6621-1
3. Chen W, Zheng R, Baade PD, Zhang S, Zeng H, Bray F, et al. Cancer Statistics in China, 2015. *CA Cancer J Clin* (2016) 66(2):115–32. doi: 10.3322/caac.21338
4. Shi JF, Wang L, Wu N, Li JL, Hui ZG, Liu SM, et al. Clinical Characteristics and Medical Service Utilization of Lung Cancer in China, 2005-2014: Overall Design and Results From a Multicenter Retrospective Epidemiologic Survey. *Lung Cancer* (2019) 128:91–100. doi: 10.1016/j.lungcan.2018.11.031
5. Herbst RS, Morgensztern D, Boshoff C. The Biology and Management of Non-Small Cell Lung Cancer. *Nature* (2018) 553(7689):446–54. doi: 10.1038/nature25183
6. Ramalingam SS, Vansteenkiste J, Planchard D, Cho BC, Gray JE, Ohe Y, et al. Overall Survival With Osimertinib in Untreated, EGFR-Mutated Advanced NSCLC. *N Engl J Med* (2020) 382(1):41–50. doi: 10.1056/NEJMoa1913662
7. Tang W, Li X, Xie X, Sun X, Liu J, Zhang J, et al. EGFR Inhibitors as Adjuvant Therapy for Resected Non-Small Cell Lung Cancer Harboring EGFR Mutations. *Lung Cancer* (2019) 136:6–14. doi: 10.1016/j.lungcan.2019.08.001
8. Mitsudomi T, Morita S, Yatabe Y, Negoro S, Okamoto I, Tsurutani J, et al. Gefitinib Versus Cisplatin Plus Docetaxel in Patients With Non-Small-Cell Lung Cancer Harbouring Mutations of the Epidermal Growth Factor Receptor (Wjtog3405): An Open Label, Randomised Phase 3 Trial. *Lancet Oncol* (2010) 11(2):121–8. doi: 10.1016/s1470-2045(09)70364-x
9. Gieszer B, Megyesfalvi Z, Dulai V, Papay J, Kovalszky I, Timar J, et al. EGFR Variant Allele Frequency Predicts EGFR-TKI Efficacy in Lung Adenocarcinoma: A Multicenter Study. *Transl Lung Cancer Res* (2021) 10 (2):662–74. doi: 10.21037/tlcr-20-814
10. Liu X, Hong L, Nilsson M, Hubert SM, Wu S, Rinsurongkawong W, et al. Concurrent Use of Aspirin With Osimertinib Is Associated With Improved Survival in Advanced EGFR-Mutant Non-Small Cell Lung Cancer. *Lung Cancer* (2020) 149:33–40. doi: 10.1016/j.lungcan.2020.08.023
11. Mok TSK, Wu YL, Kudaba I, Kowalski DM, Cho BC, Turna HZ, et al. Pembrolizumab Versus Chemotherapy for Previously Untreated, PD-L1-Expressing, Locally Advanced or Metastatic Non-Small-Cell Lung Cancer (Keynote-042): A Randomised, Open-Label, Controlled, Phase 3 Trial. *Lancet* (2019) 393(10183):1819–30. doi: 10.1016/s0140-6736(18)32409-7
12. Brody R, Zhang Y, Ballas M, Siddiqui MK, Gupta P, Barker C, et al. PD-L1 Expression in Advanced NSCLC: Insights Into Risk Stratification and Treatment Selection From a Systematic Literature Review. *Lung Cancer* (2017) 112:200–15. doi: 10.1016/j.lungcan.2017.08.005
13. Büttner R, Gosney JR, Skov BG, Adam J, Motoi N, Bloom KJ, et al. Programmed Death-Ligand 1 Immunohistochemistry Testing: A Review of Analytical Assays and Clinical Implementation in Non-Small-Cell Lung Cancer. *J Clin Oncol* (2017) 35(34):3867–76. doi: 10.1200/jco.2017.74.7642
14. Zhou Y, Xu X, Song L, Wang C, Guo J, Yi Z, et al. The Application of Artificial Intelligence and Radiomics in Lung Cancer. *Precis Clin Med* (2020) 3(3):214–27. doi: 10.1093/pcmedi/pbaa028
15. Ardila D, Kiraly AP, Bharadwaj S, Choi B, Reicher JJ, Peng L, et al. End-To-End Lung Cancer Screening With Three-Dimensional Deep Learning on Low-Dose Chest Computed Tomography. *Nat Med* (2019) 25(6):954–61. doi: 10.1038/s41591-019-0447-x
16. Zhang K, Liu X, Shen J, Li Z, Sang Y, Wu X, et al. Clinically Applicable Ai System for Accurate Diagnosis, Quantitative Measurements, and Prognosis of Covid-19 Pneumonia Using Computed Tomography. *Cell* (2020) 181 (6):1423–33.e11. doi: 10.1016/j.cell.2020.04.045
17. Wang S, Shi J, Ye Z, Dong D, Yu D, Zhou M, et al. Predicting EGFR Mutation Status in Lung Adenocarcinoma on Computed Tomography Image Using Deep Learning. *Eur Respir J* (2019) 53(3):1800986. doi: 10.1183/13993003.00986-2018
18. Tian P, He B, Mu W, Liu K, Liu L, Zeng H, et al. Assessing PD-L1 Expression in Non-Small Cell Lung Cancer and Predicting Responses to Immune Checkpoint Inhibitors Using Deep Learning on Computed Tomography Images. *Theranostics* (2021) 11(5):2098–107. doi: 10.7150/thno.48027
19. Ettinger DS, Wood DE, Aisner DL, Akerley W, Bauman JR, Bharat A, et al. NCCN Guidelines Insights: Non-Small Cell Lung Cancer, Version 2.2021. *J Natl Compr Canc Netw* (2021) 19(3):254–66. doi: 10.6004/jnccn.2021.0013
20. Chen DS, Mellman I. Elements of Cancer Immunity and the Cancer-Immune Set Point. *Nature* (2017) 541(7637):321–30. doi: 10.1038/nature21349
21. Xia L, Liu Y, Wang Y. PD-1/PD-L1 Blockade Therapy in Advanced Non-Small-Cell Lung Cancer: Current Status and Future Directions. *Oncologist* (2019) 24(Suppl 1):s31–s41. doi: 10.1634/theoncologist.2019-IO-S1-s05
22. Reck M, Rodríguez-Abreu D, Robinson AG, Hui R, Csőszi T, Fülöp A, et al. Pembrolizumab Versus Chemotherapy for PD-L1-Positive Non-Small-Cell Lung Cancer. *N Engl J Med* (2016) 375(19):1823–33. doi: 10.1056/NEJMoa1606774

23. Herbst RS, Giaccone G, de Marinis F, Reinmuth N, Vergnenegre A, Barrios CH, et al. Atezolizumab for First-Line Treatment of PD-L1-Selected. *N Engl J Med* (2020) 383(14):1328–39. doi: 10.1056/NEJMoa1917346
24. Wu YL, Cheng Y, Zhou X, Lee KH, Nakagawa K, Niho S, et al. Dacomitinib Versus Gefitinib as First-Line Treatment for Patients With EGFR-Mutation-Positive Non-Small-Cell Lung Cancer (ARCHER 1050): A Randomised, Open-Label, Phase 3 Trial. *Lancet Oncol* (2017) 18(11):1454–66. doi: 10.1016/s1470-2045(17)30608-3
25. Lu MT, Raghu VK, Mayrhofer T, Aerts H, Hoffmann U. Deep Learning Using Chest Radiographs to Identify High-Risk Smokers for Lung Cancer Screening Computed Tomography: Development and Validation of a Prediction Model. *Ann Intern Med* (2020) 173(9):704–13. doi: 10.7326/m20-1868
26. Wang C, Shao J, Lv J, Cao Y, Zhu C, Li J, et al. Deep Learning for Predicting Subtype Classification and Survival of Lung Adenocarcinoma on Computed Tomography. *Transl Oncol* (2021) 14(8):101141. doi: 10.1016/j.tranon.2021.101141
27. Arbour KC, Luu AT, Luo J, Rizvi H, Plodkowski AJ, Sakhi M, et al. Deep Learning to Estimate RECIST in Patients With NSCLC Treated With PD-1 Blockade. *Cancer Discov* (2021) 11(1):59–67. doi: 10.1158/2159-8290.Cd-20-0419
28. Mu W, Jiang L, Zhang J, Shi Y, Gray JE, Tunali I, et al. Non-Invasive Decision Support for NSCLC Treatment Using PET/CT Radiomics. *Nat Commun* (2020) 11(1):5228. doi: 10.1038/s41467-020-19116-x
29. Mu W, Jiang L, Shi Y, Tunali I, Gray JE, Katsoulakis E, et al. Non-Invasive Measurement of PD-L1 Status and Prediction of Immunotherapy Response Using Deep Learning of PET/CT Images. *J Immunother Cancer* (2021) 9(6): e002118. doi: 10.1136/jitc-2020-002118

Conflict of Interest: The authors declare that the research was conducted in the absence of any commercial or financial relationships that could be construed as a potential conflict of interest.

Publisher's Note: All claims expressed in this article are solely those of the authors and do not necessarily represent those of their affiliated organizations, or those of the publisher, the editors and the reviewers. Any product that may be evaluated in this article, or claim that may be made by its manufacturer, is not guaranteed or endorsed by the publisher.

frontiers in Immunology

ORIGINAL RESEARCH
published: 21 February 2022
doi: 10.3389/fimmu.2022.811601

Various Subtypes of EGFR Mutations in Patients With NSCLC Define Genetic, Immunologic Diversity and Possess Different Prognostic Biomarkers

Youming Lei[1†], Kun Wang[2†], Yinqiang Liu[1†], Xuming Wang[3†], Xudong Xiang[4], Xiangu Ning[5], Wanbao Ding[6], Jin Duan[1], Dingbiao Li[7], Wei Zhao[1], Yi Li[8], Fujun Zhang[1], Xiaoyu Luo[1], Yunfei Shi[1], Ying Wang[7], Depei Huang[9], Yuezong Bai[9] and Hushan Zhang[9]*

[1] Department of Geriatric Thoracic Surgery, The First Affiliated Hospital of Kunming Medical University, Kunming, China, [2] Department of Thoracic Surgery, Anning First Peoples Hospital affiliate to Kunming University of Science and Technology (Kunming Forth People's Hospital), Kunming, China, [3] Department of Pulmonary and Critical Care Medicine, The First Affiliated Hospital of Kunming Medical University, Kunming, China, [4] Department of Thoracic Surgery, The Third Affiliated Hospital of Kunming Medical University, Kunming, China, [5] Department of Thoracic Surgery, The First Peoples Hospital of Yunnan Province, Kunming, China, [6] Department of Oncology, Yan'an Hospital Affiliated to Kunming Medical University, Kunming, China, [7] Department of Thoracic Surgery, Yan'an Hospital Affiliated to Kunming Medical University, Kunming, China, [8] Department of Oncology, Yunnan Provincial Hospital of Traditional Chinese Medicine, Kunming, China, [9] The Medical Department, 3D Medicines Inc., Shanghai, China

OPEN ACCESS

Edited by:
Hongbo Hu,
Sichuan University, China

Reviewed by:
Khaled Murshed,
Hamad Medical Corporation, Qatar
Peng Luo,
The University of Hong Kong, Hong Kong SAR, China

***Correspondence:**
Hushan Zhang
15111010041@fudan.edu.cn

†These authors have contributed equally for this work

Specialty section:
This article was submitted to Cancer Immunity and Immunotherapy, a section of the journal Frontiers in Immunology

Received: *09 November 2021*
Accepted: *24 January 2022*
Published: *21 February 2022*

Citation:
Lei Y, Wang K, Liu Y, Wang X, Xiang X, Ning X, Ding W, Duan J, Li D, Zhao W, Zhang F, Luo X, Shi Y, Wang Y, Huang D, Bai Y and Zhang H (2022) Various Subtypes of EGFR Mutations in Patients With NSCLC Define Genetic, Immunologic Diversity and Possess Different Prognostic Biomarkers. Front. Immunol. 13:811601. doi: 10.3389/fimmu.2022.811601

Based on data analysis of 9649 Chinese primary NSCLC patients, we calculated the exact proportion of EGFR subtypes in NSCLC and evaluated the TMB level, PD-L1 expression level and tumor immune microenvironment among different EGFR mutation subtypes. Postoperative follow-up data for 98 patients were collected and analyzed. The results showed that several uncommon EGFR mutation subtypes have a higher proportion of TMB-high or strong positive PD-L1 expression than the total EGFR mutation group. In addition, different subtypes have different characteristics related to the immune microenvironment, such as G719 mutations being associated with more $CD8^+$ T cell infiltration into tumors; except for EGFR 19del, $CD8^+$ T cell infiltration into tumors of other EGFR mutation subtypes were similar to that of wildtype EGFR. Moreover, follow-up results revealed that components of the immune microenvironment have prognostic value for NSCLC patients, with different prognostic biomarkers for NSCLC patients with and without EGFR mutations. These results suggest that patients with different EGFR mutations need to be treated differently. The prognosis of NSCLC patients may be assessed through components of tumor immune microenvironment, and ICIs treatment may be considered for those with some uncommon EGFR mutation subtypes.

Keywords: NSCLC, EGFR - epidermal growth factor receptor, immune microenviroment, prognosis, biomarkers

Abbreviations: CAP, College of American Pathologists; CLIA, Clinical Laboratory Improvement Amendment; EGFR, Epidermal growth factor receptor; FFPE, Formalin-fixed paraffin-embedded; ICI, Immune checkpoint inhibitors; IHC, Immunocytochemistry; NGS, Next generation sequencing; NSCLC, Non-small cell lung cancer; PFS, Progression-free survival; PD-1(L1), Programmed cell death protein 1/programmed cell death ligand 1; TILs, Tumor-infiltrating lymphocytes; TIME, Tumor immune microenvironment; TKI, Tyrosine kinase inhibitor; TMB, Tumor mutation burden; WES, Whole exome sequencing; 19del, EGFR exon 19 deletion.

INTRODUCTION

Lung cancer is a complex disease consisting of a variety of molecular and histological types of clinical relevance. The incidence of lung cancer is rising globally. GLOBOCAN estimated 2.09 million new cases in 2018, which is higher than the 1.8 million new cases reported in 2012. The 5-year survival of lung cancer was reported in 2019 to be 19.4% (1). Clinical diagnosis of lung cancer is divided according to pathology into small cell lung cancer (SCLC) and non-small-cell lung cancer (NSCLC). NSCLC can be further classified into squamous cell carcinoma (SCC), adenocarcinoma (ADC), large-cell lung carcinoma (LCLC), and other types, including salivary gland-type tumors and sarcomatoid carcinomas, etc. (2). EGFR mutations are detected in 15% of lung adenocarcinomas in the United States, and the most common mutations occur in exon 19 and exon 21 (3, 4); in China, however, the proportion of EGFR mutations in lung cancer is very different from that in other regions. In this study, we used data for 9649 Chinese primary NSCLC patients to calculate the exact ratio of different EGFR mutation subtypes reported to be associated with the efficacy of tyrosine kinase inhibitors (TKIs) and immune checkpoint inhibitors (ICIs). Large-scale molecular profiling helps to identify potential molecular targets that can be applied in treating patients with specific lung cancers and facilitates a more refined molecular classification of lung cancer.

Programmed cell death protein 1/programmed cell death ligand 1 (PD-1/PD-L1) act to suppress activation of T lymphocytes, and anti-PD-1/PD-L1 therapy has gained great success in the treatment of several solid tumors, such as lung cancer. In addition, biomarkers that can be used to predict response to immunotherapy, to optimize patient benefit and to minimize negative effects have been widely explored and utilized, including PD-L1, TMB, MSI/dMMR (5, 6), and components of the tumor immune microenvironment. PD-1/PD-L1 immunotherapy strategies have recently been explored for NSCLC treatment. Before examining the potential of immunotherapy for each EGFR mutation subtypes of NSCLC, we attempted to unveil the genetic and immunologic landscape of NSCLC harboring different EGFR mutations.

Heterogeneity is an important feature of tumors, and in addition to cancer cells, a wide range of immune cells can infiltrate into human tumor tissues, including both innate and adaptive immune cells. Immune cells within the tumor microenvironment, termed the tumor immune microenvironment (TIME), play important roles in tumor evolution. It is now increasingly accepted that cancer cells interact closely with the components of the TIME, and in turn, the characteristics of the TIME can affect tumor response to immunotherapy. Moreover, the prognostic significance of components in the TIME, such as $CD8^+$ T cells, has been revealed for several cancers (7, 8). Among adaptive immune cells, tumor-infiltrating lymphocytes (TILs) have been explored widely (9). By definition, TILs include several immune cells, such as T-cells, B-cells, and NK cells (10). The components and characteristics of a specific tumor microenvironment can be considered predictive biomarkers and, to some extent, provide clues regarding the potential application of ICIs.

MATERIAL AND METHODS

Clinical Specimens

The Formalin-Fixed Paraffin-Embedded (FFPE) tissues samples from 9649 primary NSCLC patients who have underwent next-generation sequencing (NGS) in a laboratory accredited by the Clinical Laboratory Improvement Amendment (CLIA) and College of American Pathologists (CAP) (3D Medicines Inc., Shanghai, China) from June 2015 to October 2020 were analyzed. Formalin-Hematoxylin and eosin (H&E) staining was used to evaluated tumor cell content of FFPE tissue sections using. Only samples with a tumor content of 20% and above were allowed for subsequent analyses. The written informed consent was obtained from all included patients. The postoperative follow-up data of 98 NSCLC patients were collected, the median follow-up is 27.3 months., as of now, three of these patients have died. Characteristics of these patients have been listed in the table (**Table 1**).

Tissue Processing and Genomic DNA Extraction

FFPE tissue sections were placed in a 1.5 microcentrifuge tube and deparaffinized with mineral oil. Then incubated the samples with proteinase and lysis buffer K overnight at 56° C t until the tissue was fully digested. Subsequently, the lysate was incubated at 80°C for 4 hours to reverse formaldehyde crosslinks. Then followed the manufacturer's protocol, isolated genomic DNA from tissue samples using the ReliaPrep™ FFPE gDNA Miniprep System (Promega) and quantified using the Qubit™ dsDNA HS Assay Kit (Thermo Fisher Scientific).

Library Preparation and Targeted Capture (for WES)

Samples of 70 patients were underwent whole exome sequencing (WES). An S220 focused ultrasonicator (Covaris) was used to spear DNA extracts (30-200 ng) to 250 bp fragments using a. Libraries were subsequently prepared using the KAPA Hyper Prep Kit (KAPA Biosystems) according to the manufacturer's introduction. The fragment size distribution and concentration of each library were determined using a LabChip GX Touch HT Analyzer (PerkinElmer) and a Qubit 3.0 fluorometer (Thermo Fisher Scientific), respectively. Briefly, 500 ng of indexed DNA libraries were pooled to obtain 2 μg of DNA, which was then mixed with Human Cot-1 DNA and xGen Universal Blockers-TS Mix and dried down in a SpeedVac system. The Hybridization Master Mix was added, followed by incubation at 95°C for 10 min. Four microliters of the exGen Exome Research Panel v1.0 (IDT) were then added and the mixture was incubated at 65°C overnight. Target regions were captured following the manufacturer's instructions. The size distribution and concentration of the final library were determined using a LabChip GX Touch HT Analyzer (PerkinElmer) and a Qubit 3.0 fluorometer (Thermo Fisher Scientific), respectively.

Library Preparation and Targeted Capture (for Tissue-Based Targeted Panel Sequencing)

An S220 focused ultrasonicator (Covaris) was used to spear DNA extracts (30-200 ng) to 250 bp fragments using an. Then KAPA

TABLE 1 | Patient characteristics in the follow-up cohort.

Characteristics	N	%
Total	98	
Gender		
Male	53	54.08
Female	45	45.92
Age		
>60	42	42.86
<60	56	57.15
Histology		
Squamous-cell carcinoma	5	5.10
Adenocarcinoma	89	90.82
Adeno-squamous carcinoma	2	2.04
Large cell carcinoma	2	2.04
Stage		
1	46	46.94
2	30	30.61
3	22	22.45
EGFR mutation		
Without (EGFR-)	41	41.84
With (EGFR+)	57	58.16
Subtypes of EGFR mutation		
EGFR exon 19 deletion (19del)	17	17.35
EGFR L858R	14	14.29
G719A\C\S	12	12.24
S768I	13	13.27
Others (N468K, E709A, N771delinsGY, H870R, P772_H773dup, I740_K745dup, V774M, A767_V769dup, R451H, D761Y and amplification)	15	15.31
At least two EGFR mutation subtypes	14	14.29
Available TIME analysis	39	39.80
Available TMB analysis	32	32.65
Postoperative therapy		
Targeted therapy	13	13.27
Chemotherapy	34	34.69

Hyper Prep Kit (KAPA Biosystems) was used to prepare libraries were prepared. The fragment size distribution and concentration of each library were determined using a LabChip GX Touch HT Analyzer (PerkinElmer) a Qubit 3.0 fluorometer (Thermo Fisher Scientific), respectively. For targeted capture, indexed libraries were subjected to probe-based hybridization with a customized NGS panel targeting whole exons of 733 cancer-related genes (**Supplementary Table 1**), where the probe baits were individually synthesized 5′ biotinylated 120 bp DNA oligonucleotides (IDT). According to the annotation of UCSC Genome RepeatMasker, repetitive elements were filtered out from intronic baits. The xGen® Hybridization and Wash Kit (IDT) was used for hybridization enrichment. Briefly, 500 ng indexed DNA libraries were pooled to obtain a total amount of 2 μg of DNA. The pooled DNA sample was then mixed with human cot DNA and xGen Universal Blockers-TS Mix and dried down in a SpeedVac system. The Hybridization Master Mix was added to the samples and incubated in a thermal cycler at 95°C for 10 min, before being mixed and incubated with 4 μl of probes at 65°C overnight. The target regions were captured following the manufacturer's instructions. The size distribution and concentration of the final library were determined using a LabChip GX Touch HT Analyzer (PerkinElmer) and a Qubit 3.0 fluorometer (Thermo Fisher Scientific), respectively.

DNA Sequencing, Data Processing, and Variant Calling (for Tissue-Based Testing)

The captured libraries were loaded onto a NovaSeq 6000 platform (Illumina) for 100 bp paired-end sequencing with a mean sequencing depth of 35000X. Using the Burrows-Wheeler Aligner (v0.7.12) to map the raw data of paired samples (an FFPE sample and its normal tissue control) to the reference human genome hg19. Deleted PCR duplicate reads and used Picard (v1.130) and SAMtools (v1.1.19) to collect sequence metrics, respectively. Using an in-house developed R package to detect Somatic single nucleotide variants (SNVs) to execute a variant detection model based on binomial test. Local realignment was performed to detect indels. Filtered variants though their unique supporting read depth, base quality and strand bias, as described before (11). Then filtered all variants using an automated false positive filtering pipeline to ensure specificity and sensitivity at an allele frequency (AF) of ≥ 5%. Indels and single-nucleotide polymorphism (SNPs) were annotated by ANNOVAR against the following databases: 1000Genome, dbSNP (v138) and ESP6500 (population frequency > 0.015). Only stopgain, missense, frameshift and non-frameshift indel mutations were retained. Gene rearrangements and copy number variations (CNVs) were detected as described earlier (11).

PD-L1 Expression by Immunohistochemistry (IHC) 22C3 Antibody

FFPE tissue sections were subjected to assessment of PD-L1 expression using the PDL1 IHC 22C3 pharmDx assay (Agilent Technologies). In brief, FFPE tissue sections were dried, and fixed on positively charged slides at 56 to 60°C for 1 hour. With antigen repaired, then placed the slides in the Autostainer Link 48 platform (Dako) to incubate with the anti-human PD-L1 monoclonal antibody, clone 22C3 pharmDx, then incubated with the secondary antibody, and subsequent a substrate-chromogen solution (DAB). Tumor Proportion Score (TPS), as described previously (12, 13), was calculated to evaluate PD-L1 expression level.,

Tumor Microenvironment (TME) by Multiplex Immunofluorescence (mIF)

Multiplex immunofluorescence staining was conducted using the PANO 7-plex IHC kit (Panovue). Primary antibodies targeting CD8 (clone C8/144B), CD56 (clone 123C3), HLA-DR (clone EPR3692), CD68 (clone BP6036) and PanCK (Cocktail) were sequentially applied to FFPE tissue slides, subsequently, incubated with horseradish peroxidase-conjugated secondary antibody and tyramide signal amplification. The slides were heat-treated in a microwave after each round of tyramide signal amplification. Cell nuclei acids were stained with 4′-6′-diamidino-2-phenylindole (DAPI, SIGMA-ALDRICH) once all immune cells had been labelled. A Mantra workstation, capture fluorescent spectra at 20 nm wavelength intervals from 420 nm to 720 nm with an absolute magnification of ×200 and ×100 and fixed exposure time, was used to scan multiplex stained slides. Then superimposed all scans for each slide to obtain a single image.

Images of monoplex stained and unstained slides were applied to subtract the spectrum of each tissue autofluorescence and fluorophore, respectively. The inForm Image Analysis Software (PerkinElmer) was applied to create a spectral library required for multispectral unmixing. This spectral library was used to re-constructure slide images without autofluorescence. The quantity of immune cells including macrophages, $CD8^+$ T cells, and NK cells were calculated as the number of positively stained cells per square millimeter and percentage of positively stained cells in all nucleated cells.

TMB

For data processing and reads mapping, please refer to "DNA sequencing, data processing, and variant calling (for tissue-based testing)". TMB was defined as the count of synonymous and nonsynonymous somatic SNVs and indels in detected coding regions, excluding driver mutations. All indels and SNVs in the coding region were considered, including missense, silent, stop gain, stop loss, in-frame and frameshift mutations.

MSS/MSI

100 microsatellite loci were selected for determination of MSI and for each assay, the top 30 loci with the best coverage were included for evaluation of final MSI score. An in-house developed R script was applied to assess the distribution of read counts among different repeat length of each microsatellite locus. A MSI score was defined as the percentage of unstable loci. The sample of MSI-H was the one with MSI score ≥ 0.4, otherwise it was MSS.

Statistical Analysis

Data were analyzed using the GraphPad Prism software (version 7.01). Data were presented as the mean ± standard error of the mean (SEM). Differences between two groups were analyzed using the student unpaired t test or an unpaired t test with Welch's correction. analysis of variance was used to investigate more than two groups. Univariate Cox proportional hazards models of survival and biological baseline variables were built to estimate hazard ratios (HRs) with a 95% CI. Survival curve was assessed using Kaplan-Meier and log-rank test, and p-value of less than 0.05 (two- tailed) was considered as significant difference.

RESULTS

Frequencies of Different Subtypes of EGFR Mutations in Chinese Primary NSCLC

Different histologic types of NSCLC in China were calculated based on data for 9649 primary NSCLC patients (**Figure 1A**). EGFR mutations were detected in 51.3% of Chinese NSCLC patients, as illustrated in the pie chart in **Figure 1B**. Different subtypes of EGFR mutations in primary NSCLC patients were evaluated (**Figure 1C**), and more EGFR mutations were found in adenocarcinoma than in squamous cell carcinoma and large cell carcinoma (**Figure 1D**), and. Furthermore, we compared the frequency of several of EGFR mutations in our research to that in the prospective MSKCC cohort (14). (**Figure 1E**). A total of 9649 samples of NSCLC patients were used to analyze EGFR mutations, and then some of them were subjected to subsequent genetic and immunological analysis (**Figure 1F**).

Some EGFR Mutation Subtypes Displayed Higher TMB Levels, With a Higher Proportion of TMB-High Patients

Both the results of WES and panel sequencing that covered the whole exome of 733 cancer-related genes showed lower TMB levels in NSCLC patients with than in those without EGFR mutations (**Figures 2A, B**). Based on WES, TMB≥10 mutations/Mb was defined as TMB-High, and otherwise TMB-Low. The proportion of TMB-Low detected by WES in those without EGFR mutation was 69.4%. We hypothesize that if the panel is sensitive enough to detect the TMB, then the proportion of this part detected by this panel should be similar to the WES detection result; that is, the proportion of TMB-Low detected by the panel in group without EGFR mutation should be 69.4%. The same ratio of TMB-Low was set as the EGFR wildtype group as counted by WES, and the cutoff of TMB-High and TMB-Low by the panel was 14.5 mutations/Mb. Based on these results, subsequent analysis showed that TMB levels differed among EGFR mutation subtypes. NSCLC patients without EGFR mutation showed higher TMB-levels than in 19del, L858R and T790M groups. However, no significant difference between the group without EGFR mutation and the other EGFR mutation group, except for 19del, L858R and T790M, was found. Moreover, the 768I and "Others" groups showed a higher TMB than the 19del or L858R group. In summary, the results indicated that NSCLC patients with uncommon mutations have TMB levels similar to those of EGFR wildtype patients (**Figure 2C**). The results of both WES and panel sequencing revealed lower proportion of TMB-High in NSCLC patients with EGFR mutation. The descending order in TMB-High proportion was L858R, other uncommon mutations, 19del, S768I, T790M, G718A, LL861Q, G719C and 20ins (**Figure 2D**). In the group of other uncommon mutations, S768I, L861Q and G719A mutation groups, TMB-High was observed in more than 15% of patients (**Figure 2E**).

The Level of Tumor PD-L1 Expression Was Different Among EGFR Mutation Subtypes, and Differences in Immune Cell Infiltration Were Associated With Different Levels of PD-L1 Expression

PD-L1 expression was detected in 1674 tumor samples *via* IHC. Among available tumor samples, a higher proportion of tumors without EGFR mutations had positive PD-L1 expression (TPS≥1) and strong positive PD-L1 expression (TPS≥50). Tumors without EGFR mutations, with EGFR G719S, S768I and other uncommon EGFR mutations, had a higher proportion of positive PD-L1 expression than the left subtypes (**Figures 3A, B**).

Furthermore, we evaluated the TIME among different TPS groups. Although no difference in $CD8^+$ T cells infiltrating into tumors was found in different TPS groups, in the stroma and in tumor+stroma, more $CD8^+$ T cells were found in the group with strong PD-L1 expression (TPS≥50). More M1 macrophages

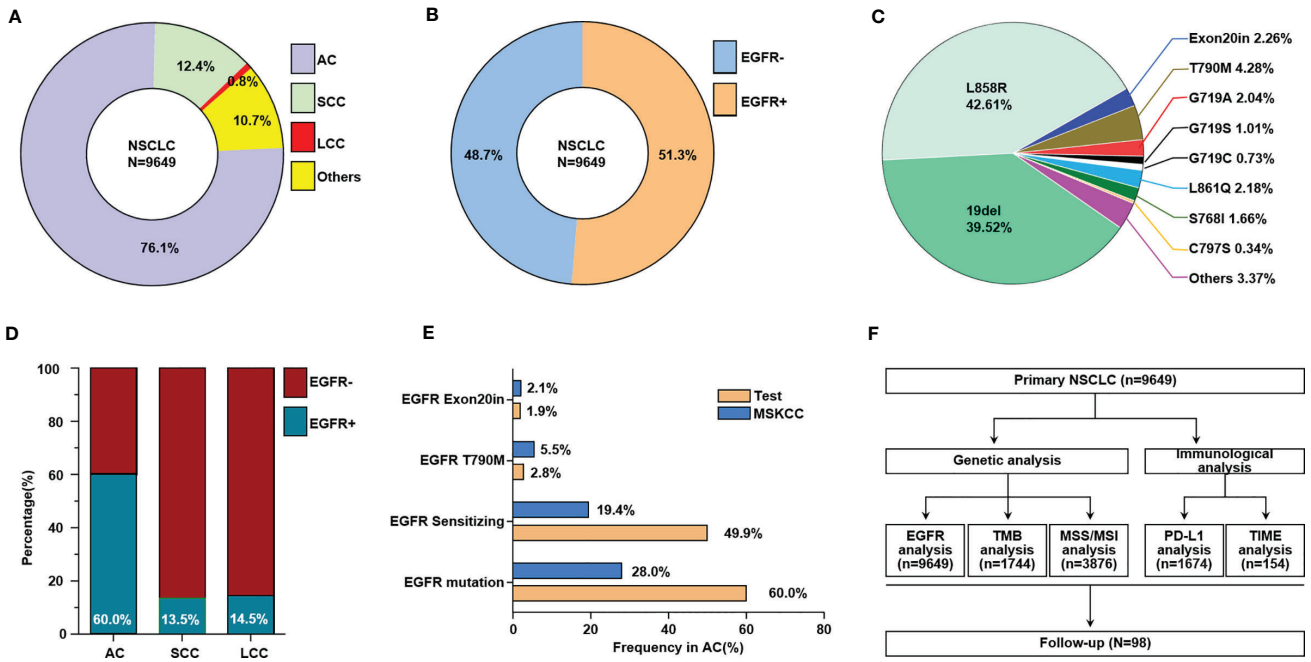

FIGURE 1 | The frequencies of different subtypes of EGFR mutations in Chinese primary NSCLC. **(A)** The proportion of different histologic types of NSCLC, others including adenosquamous carcinoma, sarcomatoid carcinoma, typical carcinoid, atypical carcinoid, lyphoepithelionma-like carcinoma, etc. **(B)** The ratio of NSCLC patients with EGFR mutation and without EGFR mutation. **(C)** The ratio of different EGFR mutation subtypes in NSCLC patients. **(D)** The ratio of patients with EGFR mutation and without EGFR mutation in different histologic types of NSCLC. **(E)** Comparison of selected gene alteration frequencies in this research and MSKCC cohort. **(F)** Flow charts for data analysis in this research. AC, adenocarcinoma; SCC, squamous cell carcinoma; LCC, large cell carcinoma.

infiltrated into the tumor in the PD-L1-negative group than in the PD-L1-positive group; in the stroma, more M1 macrophages were found in the group with strong PD-L1 expression. No differences in other immune cells were found in the tumor, stroma, or tumor +stroma (**Figures 3C–F**).

Differences in Infiltration of Various Immune Cells Were Found Among Tumors With Different EGFR Mutation Subtypes

We evaluated the difference in immune cell infiltration between tumors with and without EGFR mutations. Among $CD8^+$ T cells, M1 ($CD68^+HLA\text{-}DR^+$) tumor-associated macrophages (TAMs), M2 TAMs ($CD68^+HLA\text{-}DR^-$), $CD56^{bright}$ NK cells and $CD56^{dim}$ NK cells, less $CD8^+$ T cell infiltration was found in the EGFR mutation group than in the group without EGFR mutation ($p<0.05$). In addition, more M1 TAMs infiltrated in the tumor and in tumor+stroma were found in the EGFR mutation group than in the EGFR wildtype group ($p<0.05$) (**Figures 4A–C**).

The main differences among $CD8^+$ T cells, M1 TMAs, M2 TAMs, $CD56^{bright}$ NK cells and $CD56^{dim}$ NK cells were regarding counts of $CD8^+$ T cells and TAMs for different EGFR mutation subtypes (**Figures 4D–H**). In detail, compared with the group without EGFR mutations, only the 19del group showed fewer infiltrated $CD8^+$ T cells ($p<0.05$) (**Figure 4D**). Comparing different EGFR mutation subtypes with the EGFR wildtype group, no significant differences were found in the numbers of $CD8^+$ T cells in either the stroma or in tumor+stroma. However, differences in the numbers of $CD8^+$ T cells in the tumor, stroma, and tumor+stroma were found for some EGFR mutation subtypes; for example, more $CD8^+$ T cell infiltration in the tumor was found in the EGFR G719A/C/S mutation group than in the 19del and S768I groups (**Figure 4D**). Except for more M1 infiltration in the S768I mutation group, there were no differences in the number of M1 macrophages in the other EGFR mutation subtype groups compared with the EGFR wildtype group (**Figure 4E**). Despite no significant differences in M2 infiltration, more M2 infiltration was present in stroma in the EGFR G719A/C/S group than in the EGFR wildtype ($p<0.05$) and 19del ($p<0.05$), L858R mutation groups ($p<0.01$) (**Figure 4F**).

Different Prognostic Biomarkers Were Found for Patients With and Without EGFR Mutations

To explore prognostic biomarkers for NSCLC, we followed up 98 postoperative NSCLC patients. These patients were stratified according to without and with EGFR mutation (EGFR-/+), TMB level, immune cells, including $CD8^+$ T cells, M1/M2 macrophages, $CD56^{bright}$ and $CD56^{dim}$ NK cells. Log-rank progression-free survival (PFS) analysis was performed by using cutoff values of the top ½ density of tumor-infiltrating immune cells, such as $CD8^+$ T cells ($CD8^+$ T-high defined as patients with the top ½ $CD8^+$ T cell density in the tumor; others defined as

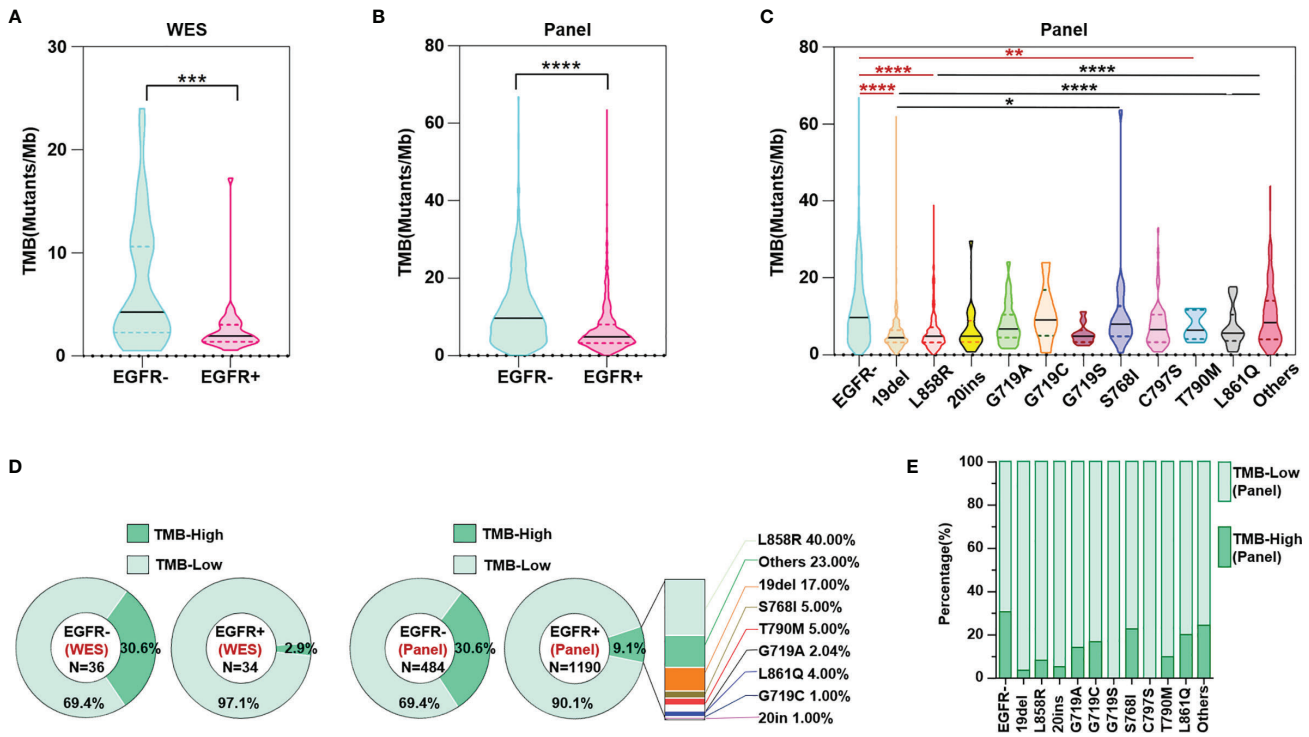

FIGURE 2 | TMB level evaluated both through WES and panel sequencing. **(A)** WES calculated TMB level in NSCLC patients with and without EGFR mutation. **(B)** Panel sequencing calculated TMB level in NSCLC patients with and without EGFR mutation. **(C)** Panel sequencing calculated TMB level in NSCLC patients of different EGFR mutation subtypes. **(D)** Ratio of TMB high or low evaluated by WES and panel sequencing. **(E)** Ratio of TMB high or low evaluated by panel sequencing in different subtypes of EGFR mutation. *means $p < 0.05$, **means $p < 0.01$, ***means $p < 0.001$, ****means $p < 0.0001$.

$CD8^+$ T-low), M1/M2 macrophages and $CD56^{bright}$, $CD56^{dim}$ NK cells, in NSCLC tissues (**Figures 5A–H**). According to the results, EGFR mutation (**Figures 5A, B**), TMB level (**Figure 5C**), and components of the TIME (**Figures 5D–H**), $CD8^+$ T cells were associated with different prognoses; in detail, a longer PFS was associated with $CD8^+$ T cell-high ($p<0.01$) (**Figure 5D**). We further analyzed the potential prognostic significance of the TIME in NSCLC patients with and without EGFR mutations, and identified different prognostic biomarkers (**Figures 6A–J**). The prognostic significance of $CD8^+$ T cells was only observed for patients without EGFR mutations ($p<0.05$) (**Figure 6A**); for patients with EGFR mutations, a longer PFS was found for the $CD56^{dim}$ NK cell-high cohort than the $CD56^{dim}$ NK cell-low cohort ($p<0.05$) (**Figure 6J**). Thus, NSCLC patients with and without EGFR mutations have different prognostic biomarkers.

DISCUSSION

Although EGFR is reported to be a major driver oncogene in lung cancer in Asia, especially adenocarcinoma, the exact proportion of Chinese NSCLC patients with EGFR mutations varies by report, and the difference may be related to the limited number of patients previously evaluated (3, 15). We recalculated the precise proportion of EGFR mutation and different EGFR mutation subtypes based on data for 9649 Chinese primary NSCLC patients. We compared the frequency of several of EGFR mutation types in lung adenocarcinoma in our research, including total EGFR mutations, EGFR sensitizing mutations, T790M mutation and exon 20 insertion, to that in the prospective MSKCC cohort (14). This result confirmed that the mutation frequency of the Chinese population is significantly different from that of populations in other regions previously reported. This suggests that for the Chinese population, clinical trials, treatments and clinical management strategies that are different from other populations should be given in the future practice.

ICIs have poor activity in NSCLC with driver alterations, and they have been excluded from the NCCN Guide for System Therapy of NSCLC. However, in ATLANTIC, a phase 2, open-label, single-arm trial, the effect of durvalumab treatment was assessed in patients with NSCLC; cohort 1 comprised EGFR+/ALK+ NSCLC patients, and the results for this cohort showed that $EGFR^+$ NSCLC patients with ≥25% of tumor cells expressing PD-L1 benefit from ICIs (16). Responses to ICIs in NSCLC patients with EGFR 19del, L858R, T790 M and EGFR ex20ins have also been evaluated, including patients with the common EGFR exon del 19 or L858R mutation who exhibited ORRs to ICI <20% and PFS less than 3.5 months (17). However, another study showed that compared 212 lung cancers without EGFR mutation, outcomes of ICI treatment

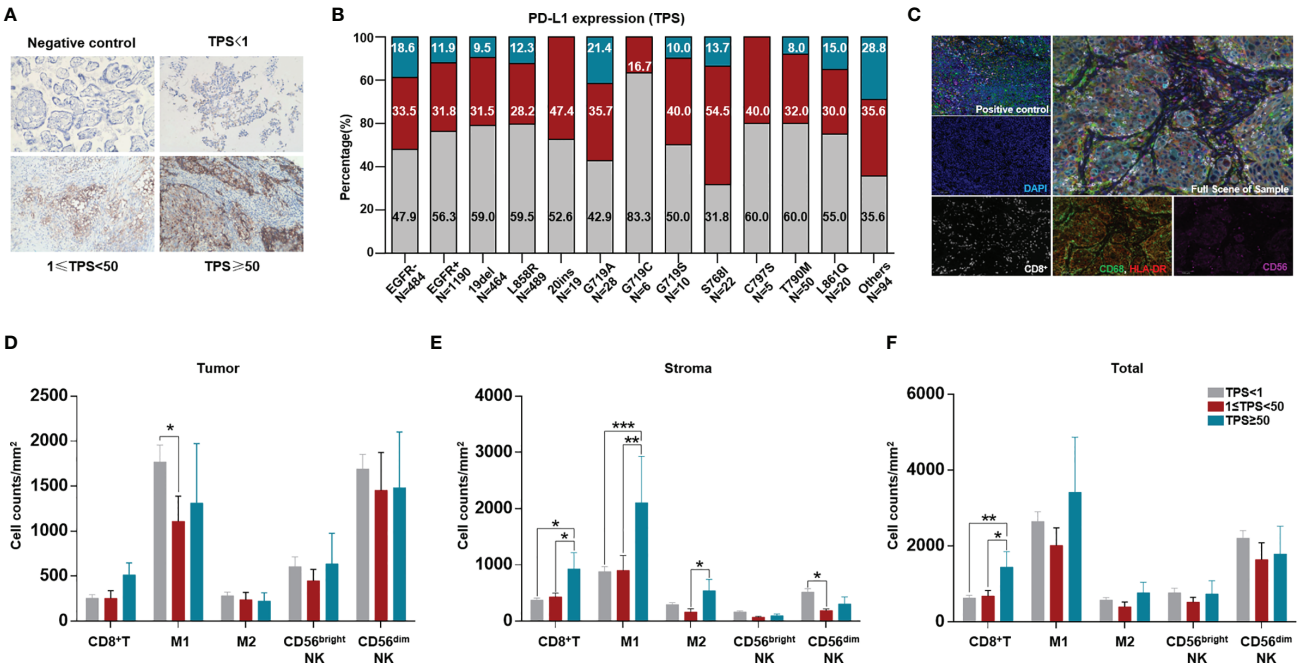

FIGURE 3 | Comparation of tumor PD-L1 expression and ratio among different EGFR mutation subtypes and difference of TIME among different TPS groups. PD-L1 expression was quantified as negative (TPS<1%), intermediate positive (1%≤TPS<49%), and strong positive (TPS≥50%) for available cases and tabulated across different EGFR mutation subtypes. **(A)** Representative staining of PD-L1 expression through IHC (200X). **(B)** Comparation of PD-L1 expression between tumors with and without EGFR mutation, and among different EGFR mutation subtypes. **(C)** Ratio of patients with MSI-H in Chinese NSCLC. A total of 3876 were available for count the ratio of MSI-H. A total of 141 NSCLC patients were available for analysis of both PD-L1 expression and TIME. **(D)** Representative staining for $CD8^+$T cells, $CD56^{bright}$ and $CD56^{dim}$ NK cells, $CD68^+HLA\text{-}DR^+$ M1, $CD68^+HLA\text{-}DR^-$ M2 TAM. CD8 (white), CD56 (purple), CD68 (green), HLA-DR (red), panCK/S100(cyan), DAPI (blue). **(E, F)** different immune cell counts in intra-tumoral region, stroma, and sum of both. *means $p < 0.05$, **means $p < 0.01$, ***means $p < 0.001$.

were worse in patients with EGFR19del but similar in those with EGFR L858R; in contrast, EGFRT790M status did not affect response to ICI treatment (18). The results of a cohort of 58 patients treated with PD-1/PD-L1 inhibitors revealed that NSCLCs harboring EGFR mutations are associated with poor response, and such mutations were speculated to be associated with low rates of concurrent PD-L1 expression and $CD8^+$ T cells within the tumor microenvironment (19). Furthermore, patients with EGFR exon 20 insertions (20ins) benefit less from ICIs than those without 20ins (20). Compared with NSCLC patients without targetable oncogenes, patients with EGFR 20ins NSCLC have better outcomes with platinum chemotherapy but derive less benefit from ICIs, as explained by lower levels of TMB and PD-L1 expression (20). These studies may indicate that not all patients with EGFR mutations show a lack of response to ICI treatment. Overall, comprehensive analysis of PD-L1 expression, TMB and even $CD8^+$ T cell infiltration would help to better evaluate response to ICI therapy. Indeed, we should distinguish the genetic, immunologic and even clinical heterogeneity of each EGFR mutation subtype, as different subtypes may have different responses to ICIs. MSI-H is another important biomarker approved for ICI treatment in solid tumors (21), and we analyzed MSI-H in Chinese patients with NSCLC. Although more patients with MSI-H were found in the group with than in the group without EGFR mutations, similar with previous report (21, 22), only a very small portion of NSCLC cases were MSI-H (<1%) (**Supplementary Figure 1**). Therefore, other factors and mechanisms should be considered, and we should identify the specific characteristics of each subtype and analyze more TIME factors. We assessed both genomic and immunophenotypic characteristics of almost all EGFR subtypes that are reported to be related to different responses to TKIs and ICIs therapy, and based on our results, different strategies should be recommended for NSCLC patients with different EGFR mutation subtypes.

PD-L1 expression and MSI-H/dMMR have been recognized by the FDA as predictive biomarkers of immunotherapy response, furthermore, based on efficacy data from KEYNOTE-158 (NCT02628067) (23), the FDA granted accelerated approval to pembrolizumab for the treatment of patients with solid tumors of TMB-High (TMB≥10 Mutants/Mb) (23). In addition, a meta-analysis revealed TMB≥10 mutations/Mb to be significantly associated with enhanced objective response rates for immunotherapy (24). Therefore, we also defined WES-detected TMB≥10 mutations/Mb as TMB-high and WES-detected TMB<10 mutations/Mb as TMB-low. Following the principle that the proportion of TMB-Low in the Chinese population detected and calculated by WES and the panel should be consistent, we calculated that our 733-gene panel TMB cutoff equivalent to the WES TMB cutoff of 10 mutations/Mb should be 14.5 mutations/Mb (**Figure 2D**). In

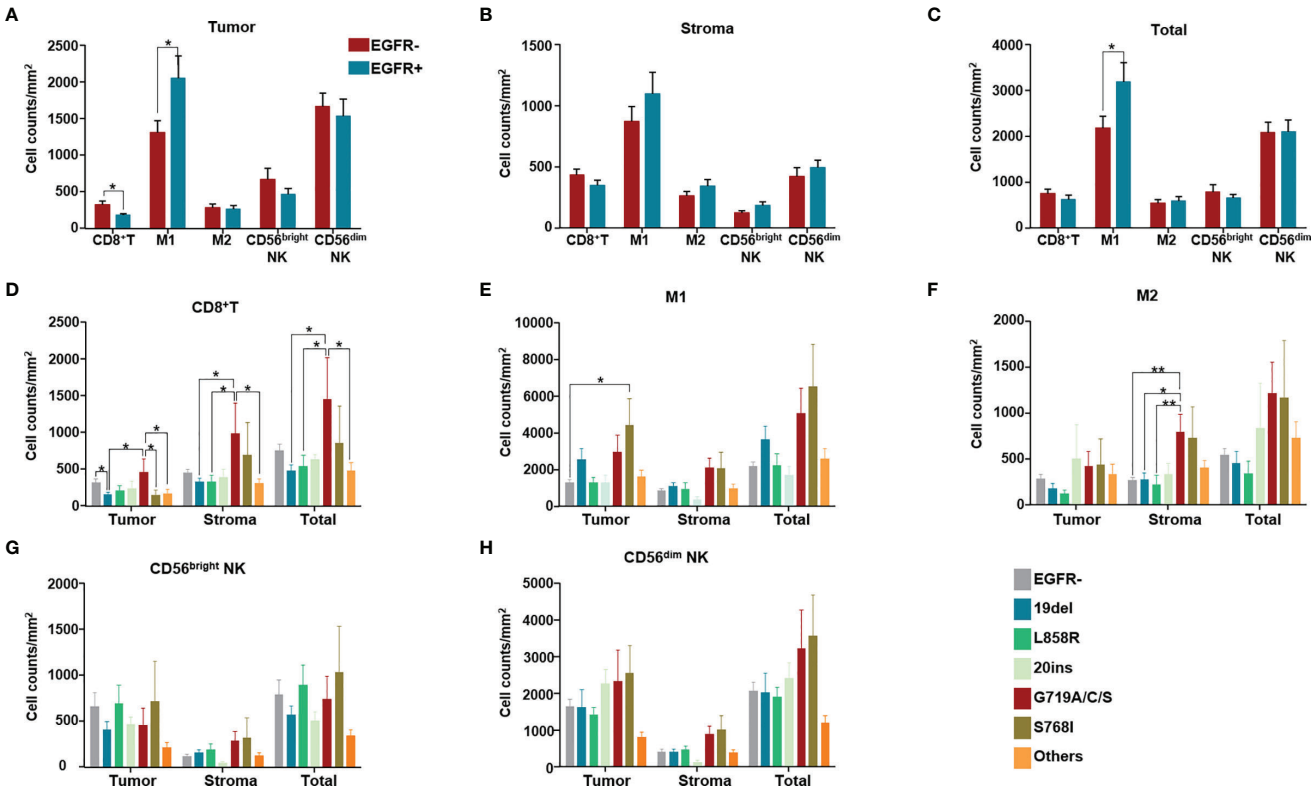

FIGURE 4 | Immune cell counts both in tumor (intra-tumoral region) and stroma of 154 NSCLC patients. Immune cell counts both in tumor (intra-tumoral region) and stroma of 154 NSCLC patients of EGFR wild type and with different EGFR mutation subgroups. **(A)** Numbers of different immune cells in tumor were compared between without and with EGFR mutation groups. **(B)** Numbers of different immune cells in stroma were compared between without and with EGFR mutation groups. **(C)** Numbers of different immune cells in total (stroma and tumor) were compared between without and with EGFR mutation groups. **(D–H)** Numbers of $CD8^+$ T cells, M1, M2 TAM, CD56bright NK cells, CD56dim NK cells in tumor, stroma, in total (tumor and stroma) were compared among patients of different EGFR mutation subgroups. (in the group termed as "other uncommon mutations", contained EGFR amplification, EGFR p.E709A, EGFR p.E709K, EGFR p.E709V, EGFR p.F254L, EGFR p.H773dup, EGFR p.H870R, EGFR p.I740_K745dup, EGFR p.L747P, EGFR p.N468K, EGFR p.R451H, EGFR p.R776C, EGFR p.R776L and EGFR p.S768_D770dup). *means $p < 0.05$, **means $p < 0.01$.

the ensuing analysis, we used 14.5 mutations/Mb as the TMB cutoff of our 733-gene panel; that is, we considered TMB≥14.5 mutations/Mb as TMB-High and others as TMB-Low. Although previous evidence has shown that EGFR 19del and L858R are common mutations in NSCLC patients carrying EGFR mutations, our results indicates that 19del and L858R account for 39.52% and 42.61% of NSCLC cases with EGFR mutations, respectively (**Figure 1D**). ICIs have no/limited activity in $EGFR^+$ NSCLC, and almost all clinical trials exclude $EGFR^+/ALK^+$ patients, which may be because previous trials mainly enrolled these common mutations (accounting for at least 80% of EGFR mutations), which have lower TMB levels. As our results demonstrated, at least some cases of uncommon EGFR mutations, such as S768I and G719, should be considered for ICIs treatment because the TMB levels with these mutations were similar to those of the EGFR wildtype group.

The poor response to ICIs was previously partially explained as a lower TMB or PD-L1 expression level (25). Nevertheless, some recent evidence suggests that the predictive power of PD-L1 or TMB with regard to response to ICIs is limited in NSCLC patients with EGFR common mutations (26).Chen et al. proposed a classification system of human cancer based on both PD-L1 expression and TIME to search for potential situations suitable for immunotherapy (27). Therefore, identifying the type of TIME is necessary for guiding immunotherapy. We detected infiltration of $CD8^+$ T cells, NK cells, and M1 and M2 TAMs, as based on some recent evidence. For example, changes in immune subpopulations between pretherapy and on-therapy samples from 68 patients with advanced melanoma revealed numerous changes in the immune response. In detail, an increase in the number of $CD8^+$ T and NK cells and a decrease in M1 macrophages were associated with response to therapy (28). The density of T-cells infiltrating the tumor microenvironment has also been associated with clinical benefit from ICIs. Tumeh and colleagues (29) analyzed the relationship between TILs and response to pembrolizumab in patients with melanoma; the results showed higher $CD8^+$ T cell densities at the invasive margin and within the tumor parenchyma in responding patients than in patients with disease progression. TILs and

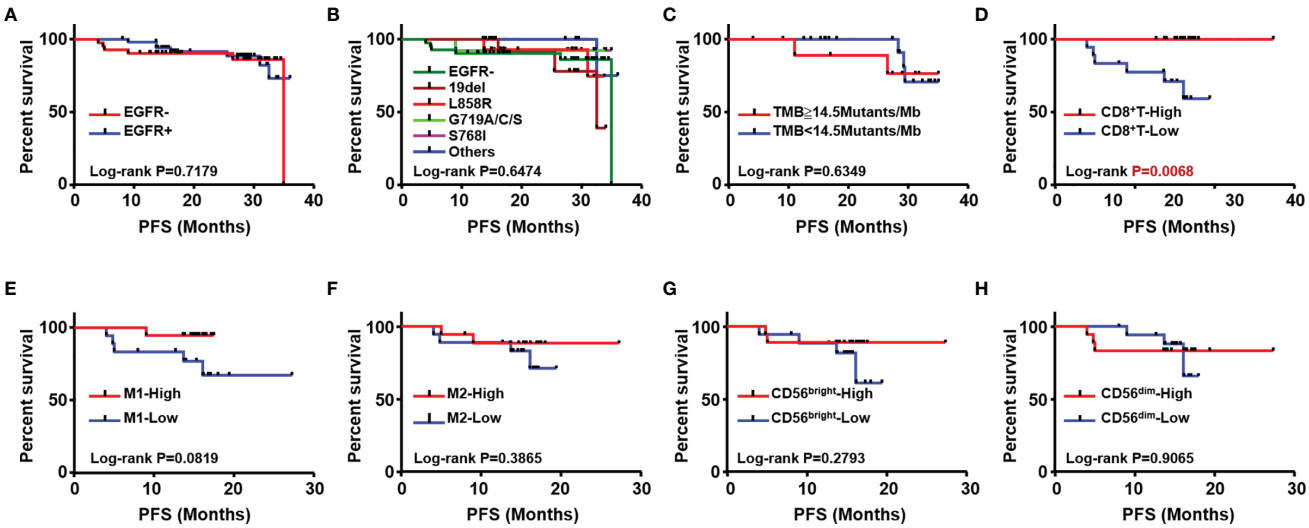

FIGURE 5 | Analysis of association with patients' outcome. Kaplan Meier estimates for progression-free survival (PFS); patients were stratified according to with (EGFR+) and without EGFR mutation (EGFR-) **(A)** different subtypes of EGFR mutation **(B)** TMB **(C)** CD8+T **(D)** M1 **(E)** M2 macrophages **(F)**, CD56bright NK **(G)** and CD56dim NK cells **(H)**.

components associated with TILs as prognostic biomarkers and their potential value in predicting response to ICIs in sarcoma have been explored (30). Therefore, other factors such as TIME should also be considered when evaluating response to ICIs in NSCLC patients with different EGFR mutation subtypes. Although some of theoretical conditions suitable for ICIs therapy were showed in several of EGFR mutation subtypes in this research, however, no clinical cohort of ICIs treatment was established in this manuscript. Obviously, further studies need to be carried out for clinical verification.

In addition to genetic and immunologic differences, differences in prognosis should be considered for each subtype of EGFR mutation. The prognostic significance of TILs has been confirmed in several solid tumors, but less is known about whether components of the TIME have prognostic value in NSCLC, especially in each EGFR-mutated subtype. Only 98 patients were available for follow-up, and among them, data for analysis of TIME in each EGFR mutation subtype were not available. Therefore, we only analyzed the TIME as a prognostic biomarker in patients without and with EGFR mutation (EGFR-/+) and found different

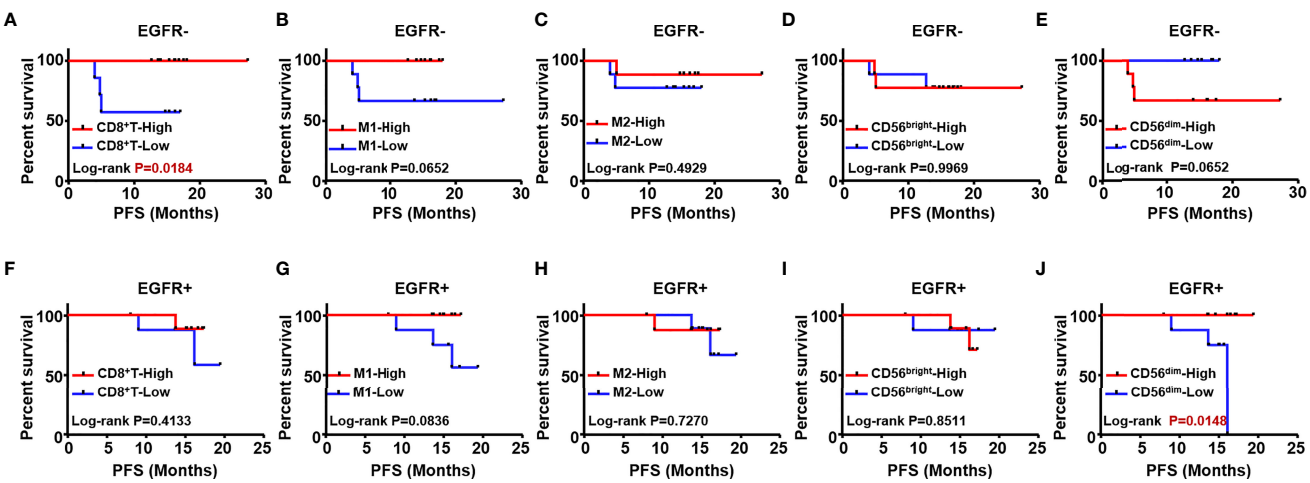

FIGURE 6 | The prognostic value of different immune cells was evaluated in NSCLC patients with and without EGFR mutation. Kaplan Meier estimates for PFS; Patients without EGFR mutation (EGFR-) were stratified according to CD8+T **(A)**, M1 macrophages **(B)** M2 **(C)** CD56bright NK **(D)** and CD56dim NK **(E)** Patients with EGFR mutation (EGFR+) were stratified according to CD8+T **(F)** M1 macrophages **(G)** M2 **(H)** CD56bright NK cells **(I)** and CD56dim NK cells **(J)**.

prognostic biomarkers (**Figure 6**). Hence, based on the above results of genetic and immunologic differences, we infer that the difference in prognostic biomarkers is not limited to EGFR mutation. In general, each subtype may have different prognostic factors, but a larger sample may be needed for confirmation.

In conclusion, EGFR positive NSCLC is one kind of complex disease, this research demonstrated genetic and immunological heterogeneity, and the differences in prognosis. These results suggested that NSCLC patients with various EGFR mutation should be treated and managed differently in clinical practice. ICIs may not be excluded for total EGFR positive NSCLC. Of course, more studies are needed, especially interventional studies are needed for further confirmation.

DATA AVAILABILITY STATEMENT

The datasets presented in this article are not readily available because sequencing data contains sequencing algorithm and other core trade information of 3D Medicines Inc. Requests to access the datasets should be directed to the corresponding author Hushan Zhang (E-mail address: 15111010041@fudan.edu.cn/hush111@126.com).

ETHICS STATEMENT

The studies involving human participants were reviewed and approved by Ethics Committee of the First Affiliated Hospital of Kunming Medical University, Ethics Committee of the First People's Hospital of Anning, Yunnan province. The patients/participants provided their written informed consent to participate in this study.

AUTHOR CONTRIBUTIONS

HZ, YML, KW, YQL, and XW put forward the content of the paper. HZ wrote the manuscript. The others literature and clinical data were collected and reviewed. All authors read and approved the final manuscript.

FUNDING

This research was supported by the following funding: Scientific Research Foundation of Education Department of Yunnan Province, item number: 2021J0361 and 2021J0362.

SUPPLEMENTARY MATERIAL

The Supplementary Material for this article can be found online at: https://www.frontiersin.org/articles/10.3389/fimmu.2022.811601/full#supplementary-material

Supplementary Figure 1 | Proportion of MSI-H in NSCLC patients with and without EGFR mutation.

REFERENCES

1. Bade BC, Dela Cruz CS. Lung Cancer 2020: Epidemiology, Etiology, and Prevention. *Clin Chest Med* (2020) 41(1):1–24. doi: 10.1016/j.ccm.2019.10.001
2. Langer CJ, Besse B, Gualberto A, Brambilla E, Soria JC, et al. The Evolving Role of Histology in the Management of Advanced non-Small-Cell Lung Cancer. *J Clin Oncol* (2010) 28(36):5311–20. doi: 10.1200/JCO.2010.28.8126
3. Saito M, Shiraishi K, Kunitoh H, Takenoshita S, Yokota J, Kohno T, et al. Gene Aberrations for Precision Medicine Against Lung Adenocarcinoma. *Cancer Sci* (2016) 107(6):713–20. doi: 10.1111/cas.12941
4. Riess JW, Gandara DR, Frampton GM, Madison R, Peled N, Bufill JA, et al. Diverse EGFR Exon 20 Insertions and Co-Occurring Molecular Alterations Identified by Comprehensive Genomic Profiling of NSCLC. *J Thorac Oncol* (2018) 13(10):1560–8. doi: 10.1016/j.jtho.2018.06.019
5. Boumber Y. Tumor Mutational Burden (TMB) as a Biomarker of Response to Immunotherapy in Small Cell Lung Cancer. *J Thorac Dis* (2018) 10(8):4689–93. doi: 10.21037/jtd.2018.07.120
6. Wojas-Krawczyk K, Kalinka E, Grenda A, Krawczyk P, Milanowski J. Beyond PD-L1 Markers for Lung Cancer Immunotherapy. *Int J Mol Sci* (2019) 20(8):1915. doi: 10.3390/ijms20081915
7. Althobiti M, Aleskandarany MA, Joseph C, Toss M, Mongan N, Diez-Rodriguez M, et al. Heterogeneity of Tumour-Infiltrating Lymphocytes in Breast Cancer and its Prognostic Significance. *Histopathology* (2018) 73(6):887–96. doi: 10.1111/his.13695
8. Yang Y, Attwood K, Bshara W, Mohler JL, Guru K, Xu B, et al. High Intratumoral CD8(+) T-Cell Infiltration is Associated With Improved Survival in Prostate Cancer Patients Undergoing Radical Prostatectomy. *Prostate* (2021) 81(1):20–8. doi: 10.1002/pros.24068
9. Binnewies M, Roberts EW, Kersten K, Chan V, Fearon DF, Merad M, et al. Understanding the Tumor Immune Microenvironment (TIME) for Effective Therapy. *Nat Med* (2018) 24(5):541–50. doi: 10.1038/s41591-018-0014-x
10. Santoiemma PP, Powell DJJr. Tumor Infiltrating Lymphocytes in Ovarian Cancer. *Cancer Biol Ther* (2015) 16(6):807–20. doi: 10.1080/15384047.2015.1040960
11. Su D, Zhang D, Chen K, Lu J, Wu J, Cao X, et al. High Performance of Targeted Next Generation Sequencing on Variance Detection in Clinical Tumor Specimens in Comparison With Current Conventional Methods. *J Exp Clin Cancer Res* (2017) 36(1):121. doi: 10.1186/s13046-017-0591-4
12. Boyer M, Sendur MAN, Rodriguez-Abreu D, Park K, Lee DH, Cicin I, et al. Pembrolizumab Plus Ipilimumab or Placebo for Metastatic Non-Small-Cell Lung Cancer With PD-L1 Tumor Proportion Score >/= 50%: Randomized, Double-Blind Phase III KEYNOTE-598 Study. *J Clin Oncol* (2021) 39(21):2327–38. doi: 10.1200/JCO.20.03579
13. Chen H, Molberg K, Strickland AL, Castrillon DH, Carrick K, Jiang Q, et al. PD-L1 Expression and CD8+ Tumor-Infiltrating Lymphocytes in Different Types of Tubo-Ovarian Carcinoma and Their Prognostic Value in High-Grade Serous Carcinoma. *Am J Surg Pathol* (2020) 44(8):1050–60. doi: 10.1097/PAS.0000000000001503
14. Jordan EJ, Kim HR, Arcila ME, Barron D, Chakravarty D, Gao J, et al. Prospective Comprehensive Molecular Characterization of Lung Adenocarcinomas for Efficient Patient Matching to Approved and Emerging Therapies. *Cancer Discov* (2017) 7(6):596–609. doi: 10.1158/2159-8290.CD-16-1337
15. Zhuang X, Zhao C, Li J, Su C, Chen X, Ren S, et al. Clinical Features and Therapeutic Options in non-Small Cell Lung Cancer Patients With Concomitant Mutations of EGFR, ALK, ROS1, KRAS or BRAF. *Cancer Med* (2019) 8(6):2858–66. doi: 10.1002/cam4.2183
16. Garassino MC, Cho BC, Kim JH, Mazieres J, Vansteenkiste J, Lena H, et al. Durvalumab as Third-Line or Later Treatment for Advanced Non-Small-Cell

Lung Cancer (ATLANTIC): An Open-Label, Single-Arm, Phase 2 Study. *Lancet Oncol* (2018) 19(4):521–36. doi: 10.1016/S1470-2045(18)30144-X
17. Mazieres J, Drilon A, Lusque A, Mhanna L, Cortot AB, Mezquita L, et al. Immune Checkpoint Inhibitors for Patients With Advanced Lung Cancer and Oncogenic Driver Alterations: Results From the IMMUNOTARGET Registry. *Ann Oncol* (2019) 30(8):1321–8. doi: 10.1093/annonc/mdz167
18. Hastings K, Yu HA, Wei W, Sanchez-Vega F, DeVeaux M, Choi J, et al. EGFR Mutation Subtypes and Response to Immune Checkpoint Blockade Treatment in non-Small-Cell Lung Cancer. *Ann Oncol* (2019) 30(8):1311–20. doi: 10.1093/annonc/mdz141
19. Gainor JF, Shaw AT, Sequist LV, Fu X, Azzoli CG, Piotrowska Z, et al. EGFR Mutations and ALK Rearrangements Are Associated With Low Response Rates to PD-1 Pathway Blockade in Non-Small Cell Lung Cancer: A Retrospective Analysis. *Clin Cancer Res* (2016) 22(18):4585–93. doi: 10.1158/1078-0432.CCR-15-3101
20. Choudhury NJ, Schoenfeld AJ, Flynn J, Falcon CJ, Rizvi H, Rudin CM, et al. Response to Standard Therapies and Comprehensive Genomic Analysis for Patients With Lung Adenocarcinoma With EGFR Exon 20 Insertions. *Clin Cancer Res* (2021) 27(10):2920–7. doi: 10.1158/1078-0432.CCR-20-4650
21. Le DT, Durham JN, Smith KN, Wang H, Bartlett BR, Aulakh LK, et al. Mismatch Repair Deficiency Predicts Response of Solid Tumors to PD-1 Blockade. *Science* (2017) 357(6349):409–13. doi: 10.1126/science.aan6733
22. Zang YS, Dai C, Xu X, Cai X, Wang G, Wei J, et al. Comprehensive Analysis of Potential Immunotherapy Genomic Biomarkers in 1000 Chinese Patients With Cancer. *Cancer Med* (2019) 8(10):4699–708. doi: 10.1002/cam4.2381
23. Subbiah V, Solit DB, Chan TA, Kurzrock R. The FDA Approval of Pembrolizumab for Adult and Pediatric Patients With Tumor Mutational Burden (TMB) >/=10: A Decision Centered on Empowering Patients and Their Physicians. *Ann Oncol* (2020) 31(9):1115–8. doi: 10.1016/j.annonc.2020.07.002
24. Osipov A, Lim SJ, Popovic A, Azad NS, Laheru DA, Zheng L, et al. Tumor Mutational Burden, Toxicity, and Response of Immune Checkpoint Inhibitors Targeting PD(L)1, CTLA-4, and Combination: A Meta-Regression Analysis. *Clin Cancer Res* (2020) 26(18):4842–51. doi: 10.1158/1078-0432.CCR-20-0458
25. Lan B, Ma C, Zhang C, Chai S, Wang P, Ding L, et al. Association Between PD-L1 Expression and Driver Gene Status in non-Small-Cell Lung Cancer: A Meta-Analysis. *Oncotarget* (2018) 9(7):7684–99. doi: 10.18632/oncotarget.23969
26. Schoenfeld AJ, Rizvi H, Bandlamudi C, Sauter LJ, Travis WD, Rekhtman N, et al. Clinical and Molecular Correlates of PD-L1 Expression in Patients With Lung Adenocarcinomas. *Ann Oncol* (2020) 31(5):599–608. doi: 10.1016/j.annonc.2020.01.065
27. Sanmamed MF, Chen L. A Paradigm Shift in Cancer Immunotherapy: From Enhancement to Normalization. *Cell* (2018) 175(2):313–26. doi: 10.1016/j.cell.2018.09.035
28. Riaz N, Havel JJ, Makarov V, Desrichard A, Urba WJ, Sims JS, et al. Tumor and Microenvironment Evolution During Immunotherapy With Nivolumab. *Cell* (2017) 171(4):934–49.e16. doi: 10.1016/j.cell.2017.09.028
29. Tumeh PC, Harview CL, Yearley JH, Shintaku IP, Taylor EJ, Robert L, et al. PD-1 Blockade Induces Responses by Inhibiting Adaptive Immune Resistance. *Nature* (2014) 515(7528):568–71. doi: 10.1038/nature13954
30. Liang J, Chen D, Chen L, She X, Zhang H, Xiao Y. The Potentiality of Immunotherapy for Sarcomas: A Summary of Potential Predictive Biomarkers. *Future Oncol* (2020) 16(17):1211–23. doi: 10.2217/fon-2020-0118

Conflict of Interest: Author DH, YB, HZ was employed by 3D Medicines Inc.

The remaining authors declare that the research was conducted in the absence of any commercial or financial relationships that could be construed as a potential conflict of interest.

Publisher's Note: All claims expressed in this article are solely those of the authors and do not necessarily represent those of their affiliated organizations, or those of the publisher, the editors and the reviewers. Any product that may be evaluated in this article, or claim that may be made by its manufacturer, is not guaranteed or endorsed by the publisher.

frontiers in Oncology

CASE REPORT
published: 22 February 2022
doi: 10.3389/fonc.2022.765997

Case Report: An "Immune-Cold" EGFR Mutant NSCLC With Strong PD-L1 Expression Shows Resistance to Chemo-Immunotherapy

Qian Zhao[1†], Xue Zhang[1†], Qiang Ma[2†], Nuo Luo[1], Zhulin Liu[1], Renyuan Wang[1], Yong He[1] and Li Li[1*]*

[1] Department of Respiratory Disease, Daping Hospital, Third Military Medical University (Army Medical University), Chongqing, China, [2] Department of Pathology, Daping Hospital, Third Military Medical University (Army Medical University), Chongqing, China

OPEN ACCESS

Edited by:
Cara Haymaker, University of Texas MD Anderson Cancer Center, United States

Reviewed by:
Fang Wu, Central South University, China
Diego Signorelli, Niguarda Ca 'Granda Hospital, Italy

***Correspondence:**
Li Li
dpyyhxlili@tmmu.edu.cn
Yong He
heyong@tmmu.edu.cn

[†]These authors have contributed equally to this work

Specialty section:
This article was submitted to Cancer Immunity and Immunotherapy, a section of the journal Frontiers in Oncology

Received: *28 August 2021*
Accepted: *31 January 2022*
Published: *22 February 2022*

Citation:
Zhao Q, Zhang X, Ma Q, Luo N, Liu Z, Wang R, He Y and Li L (2022) Case Report: An "Immune-Cold" EGFR Mutant NSCLC With Strong PD-L1 Expression Shows Resistance to Chemo-Immunotherapy. Front. Oncol. 12:765997. doi: 10.3389/fonc.2022.765997

Long-term survival benefit has been noticed in non-small-cell lung cancer (NSCLC) patients treated with immune checkpoint inhibitors (ICIs), such as PD-1 inhibitors. However, it is still controversial whether patients with EGFR-activating mutations may benefit from ICIs. Recently, in stage IIIA NSCLC, chemo-immunotherapy has led to significant pathological response, yet patients with the presence of known EGFR mutations were excluded from some randomized trials of neoadjuvant therapy. Herein, we report a case of a 50-year-old female patient, who was initially diagnosed as stage IIIA lung squamous cell carcinoma. Immunohistochemistry analysis showed that the patient presented with high PD-L1 expression. Then, chemo-immunotherapy was given to the patient but the disease progressed quickly with distant metastasis. A re-biopsy revealed a poorly differentiated lung adenocarcinoma together with EGFR p.L858R mutation. Then the patient received gefitinib, which resulted in significant regression of primary lung lesion. A detailed examination of pre-treatment tumor sections demonstrated rare infiltration of $CD8^+$ T cells, indicating that the current patient presented with an "immune-cold" microenvironment, which might explain the primary resistance to chemo-immunotherapy. Taken together, our case indicated that comprehensive detection of PD-L1 expression, driver gene status, together with tumor immune microenvironment, may offer a better prediction of treatment efficacy.

Keywords: chemo-immunotherapy, EGFR, case report, tumor microenvironment, resistance

INTRODUCTION

Immune checkpoint inhibitors (ICIs), such as anti-PD-1 and anti-PD-L1 antibodies, have become a standard option for the management of locally advanced and metastatic lung cancer (1). Approximately 20% of patients with non-small-cell lung cancer (NSCLC) are in stage IIIA (2), with a 3-year overall survival of 30% and no major treatment advances in the past 25 years (3). Recently, chemo-immunotherapy in stage IIIA NSCLC has led to significant pathological responses

and downstaging, together with favorable progression-free survival (PFS) and overall survival (OS) at 24 months (4). Also, in the NADIM study, PD-L1 expression was strongly associated with pathologic complete response (pCR), while no significant association was found between PD-L1 tumor proportion score (TPS) and PFS or OS. Besides, in a randomized phase III study, neoadjuvant chemo-immunotherapy has showed significant improvement in pCR rate compared to chemotherapy for resectable (IIIB–IIIA) NSCLC (5). Of note, epidermal growth factor receptor (EGFR) mutations have been generally exclusion criteria in above-mentioned trials and also the IMpower 030 study (6), although patients with EGFR mutations have been allowed in the KEYNOTE-671 study, another neoadjuvant chemo-immunotherapy trial which is still going on (7). Therefore, it is not clear whether a stage IIIA EGFR mutant NSCLC patient with strong PD-L1 expression may benefit from chemo-immunotherapy. Here, we report a case of a stage IIIA EGFR mutant NSCLC with high PD-L1 TPS of 80% yet presented with primary resistance to chemo-immunotherapy, which might be due to rare infiltration of $CD8^+$ T cells in the tumor microenvironment.

CASE DESCRIPTION

A 57-year-old nonsmoking female patient was admitted to the Daping Hospital of Army Medical University on May 6, 2020, with cough since 10+ days ago. The physical examination showed no abnormalities. Computed tomography (CT) revealed a mass in the lower lobe of the right lung (3.9 × 3.1 cm) (**Figure 1A**). CT-guided biopsy of the mass followed by the histopathological diagnosis confirmed squamous cell lung carcinoma (**Figures 2A**–**D**). A brain magnetic resonance imaging and a bone single photon emission computed tomography showed no distant metastasis. The patient was therefore diagnosed as T2aN2M0, stage IIIA squamous cell lung carcinoma according to the VIII TNM edition. PD-L1 was found positive (TPS = 80%) using immunohistochemistry (Ventana SP263; **Figure 2E**). After a multidisciplinary team panel discussion, from a "neoadjuvant" perspective, the patient received one cycle of chemo-immunotherapy (albumin-bound paclitaxel + carboplatin + nivolumab 240 mg). There were no severe adverse events after initial treatment. However, the patient suffered from symptoms related to disease progression such as cough, hemoptysis and fever after 3 weeks of treatment. Chest CT illustrated an enlargement of the right lung lesion (4.3×3.1cm) with the obstruction of the right middle bronchus (**Figure 1B**), lung atelectasis and spinal metastases. A re-biopsy through electronic bronchoscopy was performed and a poorly differentiated lung adenocarcinoma was reported in the right middle bronchus tissue by pathologic analysis (**Figures 2F**–**H**). The patient was finally diagnosed as adenosquamous carcinoma. Thereafter, a tissue-based next generation sequencing (NGS, 733 genes, 4.53 Mb, 3D Medicines Inc., China) revealed EGFR p.L858R mutation and TP53 p.R248G mutation. Afterwards, gefitinib was given to the patient (250 mg, once daily) which was well tolerated with slight skin rash that did not require any medical intervention. After one month of treatment, the symptoms of the patient were obviously relieved, and the primary tumor was significantly regressed (**Figure 1C**). Nevertheless, an enlargement of spinal metastases was found and then local radiotherapy combined systemic chemotherapy (albumin-bound paclitaxel + carboplatin; for two cycles) was implemented in addition to gefitinib without any adverse events. Then the spinal lesion was under control and gefitinib alone was still ongoing with persistent regression of primary lung lesion up to Mar 28, 2021 (**Figures 1D**–**F**). We further performed another tissue-based NGS in the baseline sample of squamous cell carcinoma and found the same genetic mutations of EGFR and TP53. Furthermore, a multi-color immunofluorescent staining of pre-treatment tumor sections demonstrated spare infiltration of $CD8^+$ T cells (91/mm^2) and $CD68^+HLA^-DR^+$ M1 macrophages (21/mm^2) in the tumor parenchyma, while the infiltration of $CD56^{dim}$ NK cells was high (1,271/mm^2) (**Figures 3A**–**D**). Further examination of CD8 immunohistochemistry staining on tumor tissue at disease progression on immunotherapy found intense $CD8^+$ T cell infiltration (**Figure 3E**), as compared to that of baseline. However, very few of these cells expressed Granzyme B (**Figure 3F**), indicating little cytotoxicity of T cells.

DISCUSSION

In the current case, we have reported a stage IIIA EGFR mutant NSCLC patient with high PD-L1 expression who showed primary resistance to nivolumab with platinum-based chemotherapy. Further detection of pre-treatment tumor microenvironment revealed rare infiltration of $CD8^+$ T cells. Therefore, the case indicated that a comprehensive detection of PD-L1 expression, driver gene status, and tumor immune microenvironment might be helpful for the treatment options.

Several studies have reported that EGFR mutant NSCLC patients benefit little from ICIs, especially in the setting of immuno-monotherapy. A meta-analysis indicated that an ICI as second-line therapy did not improve OS over that with docetaxel therapy in EGFR-mutated advanced NSCLC (8). In a prospective study, among ten EGFR mutant NSCLC patients, first-line pembrolizumab showed no response (seven cases with strong PD-L1 expression) (9). In another study, genomic alterations in EGFR were even suggested to be associated with hyper-progressive disease to ICIs (10). However, the use of ICIs for EGFR mutant NSCLC should not be completely ruled out, since dramatic response to PD-1/PD-L1 inhibitors have been reported in some EGFR mutant cases with strong PD-L1 expression (11). Meanwhile, the combination of chemo-immunotherapy in those patients has been tested in several randomized trials. The IMpower 130 trial failed to improve OS of the outcome of EGFR-mutant NSCLC patients when treated with atezolizumab plus carboplatin and nab-paclitaxel versus chemotherapy alone (12). By contrast, according to the IMpower 150 study, patients with EGFR mutations benefitted from atezolizumab plus bevacizumab, carboplatin, and paclitaxel (ABCP) regimen compared with BCP

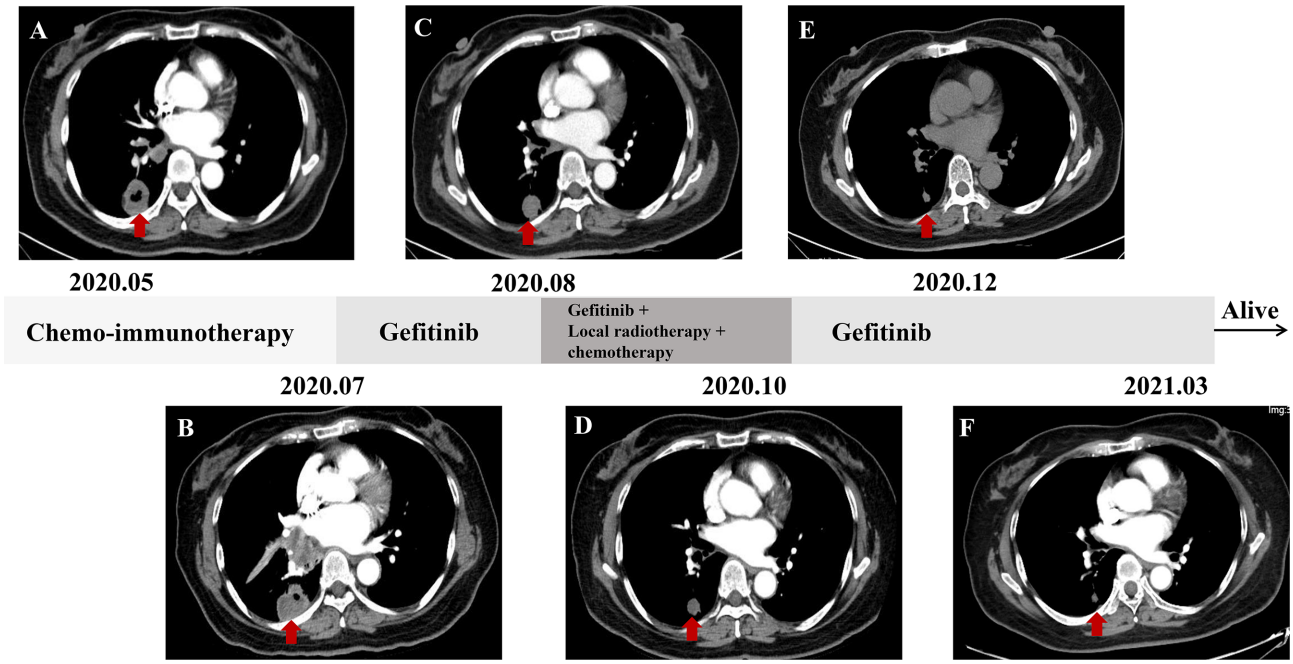

FIGURE 1 | Chest CT scanning of the patient. **(A)** baseline; **(B)** after one cycle of neoadjuvant immuno-chemotherapy (albumin-bound paclitaxel + carboplatin + nivolumab 240 mg); **(C–F)** chest images at indicated time points.

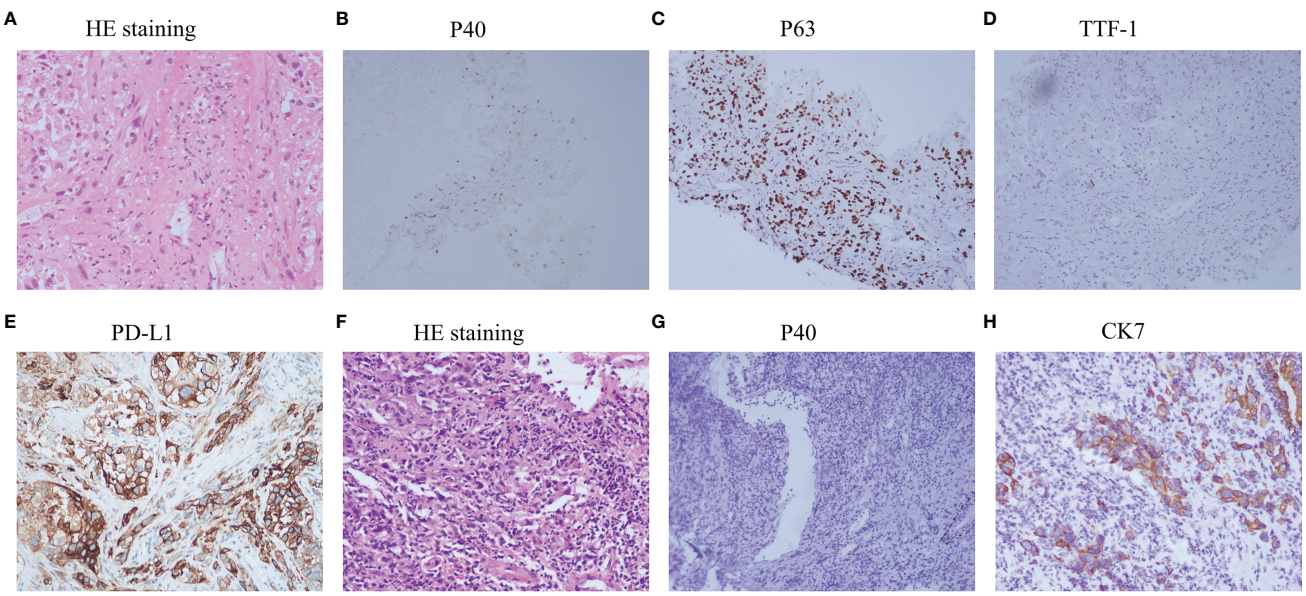

FIGURE 2 | Examinations of pathology and immunohistochemistry. **(A–E)**, Histology of primary lung lesion (CT guided biopsy) and immunohistochemistry analysis, PD-L1 expression; **(F–H)** histology of enlarged lung lesion (re-biopsy through electronic bronchoscopy) and immunohistochemistry analysis.

regimen (13), which suggested that the addition of bevacizumab to chemo-immunotherapy might confer activity to PD-L1 inhibition in EGFR-mutant NSCLC. One possible reason might be that bevacizumab could regulate tumor microenvironment such as promoting T-cell tumor infiltration by normalizing tumor vasculature (14). Other prospective clinical trials such as the KEYNOTE-789 and the CheckMate-722 which evaluate the role of chemo-immunotherapy combination in EGFR-mutant

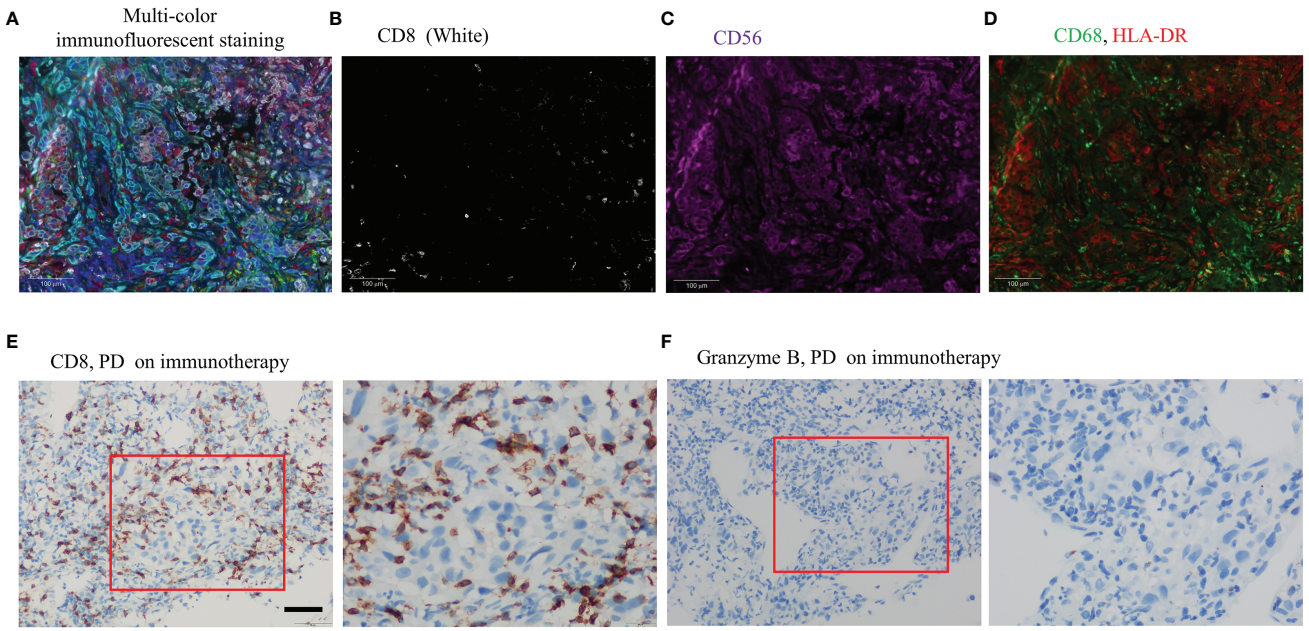

FIGURE 3 | Examinations of tumor microenvironment on tumor tissue sample as indicated. **(A)** Multi-color immunofluorescent staining of tumor microenvironment (white: CD8, purple: CD56, green: CD68, red: HLA-DR, cyan: panCK/S100, blue: DAPI) (magnification ×200); **(B)** CD8 (white) (magnification ×200); **(C)** CD56 (purple) (magnification ×200); **(D)** CD68 (green), HLA-DR (red) (magnification ×200); **(E)** Immunohistochemistry staining of CD8 with tumor tissue on disease progression of albumin-bound paclitaxel + carboplatin + nivolumab, Scale bar 50 um; **(F)** Immunohistochemistry staining of Granzyme B with tumor tissue on disease progression of albumin-bound paclitaxel + carboplatin + nivolumab, Scale bar 50 um.

advanced NSCLC patients are in expectation (15, 16). However, in a neoadjuvant setting, it is still not clear whether EGFR-TKIs or immunotherapy should be given in the first place to those with EGFR mutations. The Phase III NeoADAURA study will evaluate the efficacy and safety of neoadjuvant osimertinib in patients with resectable EGFR-mutant NSCLC (17). In the current study, we have reported a stage IIIA EGFR mutant NSCLC with high PD-L1 expression, for whom nivolumab plus chemotherapy brought little benefit. Taken together, our case indicated that PD-L1 expression alone might not be enough to predict immunotherapy efficacy. Other aspects, such as tumor microenvironment, may also need to be considered.

Tumor immune microenvironment (TIME), comprising multiple immune cells, has important roles in predicting efficacy of ICIs. For example, infiltration of $CD8^+$ T cells can predict benefit from PD-1 inhibitors in lung cancer patients (18). However, mutational activation of EGFR might downregulate MHC-I expression, which could result in a decreased number of infiltrating $CD8^+$ T cells, then contributing to the poor response to ICIs (19). Furthermore, high levels of $HLA\text{-}DR^+/CD68^+M1$ macrophages are independent prognostic factors of prolonged survival in NSCLC (20). Nevertheless, an analysis demonstrated that a high proportion of $CD56^+CD3^-$ cells was associated with a reduction in the proportion of $CD4^+$ tumor-infiltrating lymphocytes (TILs) and, to a greater degree, proportion of $CD8^+$ TILs (21). There out, the presence of M1 macrophages or NK cells also play important roles in predicting response cancer immunotherapy (20, 21). In our study, there is a baseline infiltration of CD56 dim NK cells and low $CD8^+$ T cells from tumor cells. In addition, the increase of $CD8^+$ T cells with low Granzyme B staining on post treatment samples suggests that these $CD8^+$ T cells are bystanders rather than tumor specific. Those facts may explain primary resistance of the patient to nivolumab plus chemotherapy even with high PD-L1 expression. Taken together, comprehensive analysis of PD-L1 expression, driver gene status, and TIME may better predict the efficacy of immunotherapy.

Our study has the following limitations. First, the genetic testing was not performed at baseline, which was important for a female patient with no smoking history and small sample tissue. Secondly, the PD-L1 and multi-color immunofluorescent of the re-biopsy tissues after disease progression were not implemented on comparison with that of the baseline tissues due to shortage of samples.

In conclusion, our case suggests a possible biological rationale which could explain the resistance to chemo-immunotherapy, indicating that comprehensive detection of PD-L1 expression, driver gene status, together with tumor immune microenvironment may offer a better prediction of treatment efficacy for EGFR mutant NSCLC patients, even in the case of high PD-L1 expression.

DATA AVAILABILITY STATEMENT

The original contributions presented in the study are included in the article/supplementary material. Further inquiries can be directed to the corresponding authors.

ETHICS STATEMENT

The studies involving human participants were reviewed and approved by the Daping Hospital, Army Medical University. The patients/participants provided their written informed consent to participate in this study.

AUTHOR CONTRIBUTIONS

Concept and design: LL, HY. Acquisition, analysis, or interpretation of data: ZQ, ZX, MQ, LN, WR, and LZ. Drafting of the manuscript: ZQ, ZX, and LL. Critical revision of the manuscript for important intellectual content: All authors. Obtained funding: LL, HY. Supervision: HY. All authors listed have made a substantial, direct, and intellectual contribution to the work and approved it for publication.

FUNDING

This work was supported by the Daping Hospital of Army Medical University (2019CXLCA003, 2019CXLCB011) and a Science Foundation for Outstanding Young People of the Army Medical University. The funders of the current study had no role in study design, data collection and analysis, decision to publish, or preparation of the manuscript.

REFERENCES

1. Lim SM, Hong MH, Kim HR. Immunotherapy for Non-Small Cell Lung Cancer: Current Landscape and Future Perspectives. *Immune Netw* (2020) 20: e10. doi: 10.4110/in.2020.20.e10
2. Siegel RL, Miller KD, Jemal A. Cancer Statistics, 2020. *CA Cancer J Clin* (2020) 70:7–30. doi: 10.3322/caac.21590
3. Ramnath N, Dilling TJ, Harris LJ, Kim AW, Michaud GC, Balekian AA, et al. Treatment of Stage III Non-Small Cell Lung Cancer: Diagnosis and Management of Lung Cancer, 3rd Ed: American College of Chest Physicians Evidence-Based Clinical Practice Guidelines. *Chest* (2013) 143(5 Suppl):e314S–40S. doi: 10.1378/chest.12-2360
4. Provencio M, Nadal E, Insa A, García-Campelo MR, Casal-Rubio J, Dómine M, et al. Neoadjuvant Chemotherapy and Nivolumab in Resectable Non-Small-Cell Lung Cancer (NADIM): An Open-Label, Multicentre, Single-Arm, Phase 2 Trial. *Lancet Oncol* (2020) 21:1413–22. doi: 10.1016/S1470-2045(20)30453-8
5. Forde PM, Spicer J, Lu S, Provencio M, Mitsudomi T, Awad MM, et al. Nivolumab + Platinum-Doublet Chemotherapy vs Chemotherapy as Neoadjuvant Treatment for Resectable (IB–IIIA) Non-Small Cell Lung Cancer in the Phase 3 CheckMate 816 Trial. *Oral presentation at: American Association for Cancer Research*; April 10–15, 2021; virtual. Abstract CT003.
6. Peters S, Kim AW, Solomon B, Gandara DR, Dziadziuszko R, Brunelli A, et al. 82tip - Impower030: Phase III Study Evaluating Neoadjuvant Treatment of Resectable Stage II-IIIB Non-Small Cell Lung Cancer (NSCLC) With Atezolizumab (Atezo) + Chemotherapy. Abstract Book of the European Lung Cancer Congress (ELCC) (2019) Apr 10-13, Geneva, Switzerland. *Ann Oncol* (2019) 30:ii30–. doi: 10.1093/annonc/mdz064.014
7. Tsuboi M, Luft A, Ursol G, Kato T, Levchenko E, Eigendorff E, et al. 1235tip Perioperative Pembrolizumab + Platinum-Based Chemotherapy for Resectable Locally Advanced Non-Small Cell Lung Cancer: The Phase III KEYNOTE-671 Study. *Ann Oncol* (2020) 31:S801–2. doi: 10.1016/j.annonc.2020.08.1437
8. Lee CK, Man J, Lord S, Links M, Gebski V, Mok T, et al. Checkpoint Inhibitors in Metastatic EGFR-Mutated Non-Small Cell Lung Cancer-a Meta-Analysis. *J Thorac Oncol* (2017) 12:403–7. doi: 10.1016/j.jtho.2016.10.007
9. Lisberg A, Cummings A, Goldman JW, Bornazyan K, Reese N, Wang T, et al. A Phase II Study of Pembrolizumab in EGFR-Mutant, PD-L1+, Tyrosine Kinase Inhibitor Naïve Patients With Advanced NSCLC. *J Thorac Oncol* (2018) 13:1138–45. doi: 10.1016/j.jtho.2018.03.035
10. Kato S, Goodman A, Walavalkar V, Barkauskas DA, Sharabi A, Kurzrock R. Hyperprogressors After Immunotherapy: Analysis of Genomic Alterations Associated With Accelerated Growth Rate. *Clin Cancer Res* (2017) 23:4242–50. doi: 10.1158/1078-0432.CCR-16-3133
11. Cho JH, Jung HA, Lee SH, Ahn JS, Ahn MJ, Park K, et al. Impact of EGFR Mutation on the Clinical Efficacy of PD-1 Inhibitors in Patients With Pulmonary Adenocarcinoma. *J Cancer Res Clin Oncol* (2019) 145:1341–9. doi: 10.1007/s00432-019-02889-0
12. West H, McCleod M, Hussein M, Morabito A, Rittmeyer A, Conter HJ, et al. Atezolizumab in Combination With Carboplatin Plus Nab-Paclitaxel Chemotherapy Compared With Chemotherapy Alone as First-Line Treatment for Metastatic Non-Squamous Non-Small-Cell Lung Cancer (Impower130): A Multicentre, Randomised, Open-Label, Phase 3 Trial. *Lancet Oncol* (2019) 20:924–37. doi: 10.1016/S1470-2045(19)30167-6
13. Reck M, Mok TSK, Nishio M, Jotte RM, Cappuzzo F, Orlandi F, et al. Atezolizumab Plus Bevacizumab and Chemotherapy in Non-Small-Cell Lung Cancer (Impower150): Key Subgroup Analyses of Patients With EGFR Mutations or Baseline Liver Metastases in a Randomised, Open-Label Phase 3 Trial. *Lancet Respir Med* (2019) 7:387–401. doi: 10.1016/S2213-2600(19)30084-0
14. Hegde PS, Wallin JJ, Mancao C. Predictive Markers of Anti-VEGF and Emerging Role of Angiogenesis Inhibitors as Immunotherapeutics. *Semin Cancer Biol* (2018) 52(Pt 2):117–24. doi: 10.1016/j.semcancer.2017.12.002
15. Riely G, Hui R, Carbone D, Park K, Carrigan M, Xu X, et al. P1.01-81 Phase 3 Study of Pemetrexed-Platinum With or Without Pembrolizumab for TKI-Resistant/EGFR-Mutated Advanced NSCLC: KEYNOTE-789. *J Thorac Oncol* (2018) 13:S494–. doi: 10.1016/j.jtho.2018.08.637
16. Park K, Yang JC, Girard N, Mok T, Gainor J, Nakagawa K, et al. P1-182 - Nivolumab + Chemotherapy vs Chemotherapy in EGFR-Mutated NSCLC After 1L or 2L EGFR-Tkis (Checkmate 722. *Ann Oncol* (2019) 30:vi126–. doi: 10.1093/annonc/mdz343.039. 2019 the Japanese Society of Medical Oncology Annual Meeting; 2019 Jul 18–20; Kyoto, Japan.
17. Tsuboi M, Weder W, Escriu C, Blakely C, He J, Dacic S, et al. Neoadjuvant Osimertinib With/Without Chemotherapy Versus Chemotherapy Alone for EGFR-Mutated Resectable Non-Small-Cell Lung Cancer: Neoadaura. *Future Oncol* (2021) 17:4045–55. doi: 10.2217/fon-2021-0549
18. Fumet JD, Richard C, Ledys F, Klopfenstein Q, Joubert P, Routy B, et al. Prognostic and Predictive Role of CD8 and PD-L1 Determination in Lung Tumor Tissue of Patients Under Anti-PD-1 Therapy. *Br J Cancer* (2018) 119:950–60. doi: 10.1038/s41416-018-0220-9
19. Watanabe S, Hayashi H, Haratani K, Shimizu S, Tanizaki J, Sakai K, et al. Mutational Activation of the Epidermal Growth Factor Receptor Down-Regulates Major Histocompatibility Complex Class I Expression *via* the Extracellular Signal-Regulated Kinase in Non-Small Cell Lung Cancer. *Cancer Sci* (2019) 110:52–60. doi: 10.1111/cas.13860
20. Rakaee M, Busund LR, Jamaly S, Paulsen EE, Richardsen E, Andersen S, et al. Prognostic Value of Macrophage Phenotypes in Resectable Non-Small Cell Lung Cancer Assessed by Multiplex Immunohistochemistry. *Neoplasia* (2019) 21:282–93. doi: 10.1016/j.neo.2019.01.005
21. Crome SQ, Nguyen LT, Lopez-Verges S, Yang SY, Martin B, Yam JY, et al. A Distinct Innate Lymphoid Cell Population Regulates Tumor-Associated T Cells. *Nat Med* (2017) 23:368–75. doi: 10.1038/nm.4278

Conflict of Interest: The authors declare that the research was conducted in the absence of any commercial or financial relationships that could be construed as a potential conflict of interest.

this article, or claim that may be made by its manufacturer, is not guaranteed or endorsed by the publisher.

frontiers in Immunology

ORIGINAL RESEARCH
published: 09 March 2022
doi: 10.3389/fimmu.2021.749461

Characterization of Somatic Mutations That Affect Neoantigens in Non-Small Cell Lung Cancer

*Hongge Liang[1,2], Yan Xu[1], Minjiang Chen[1], Jing Zhao[1], Wei Zhong[1], Xiaoyan Liu[1], Xiaoxing Gao[1], Shanqing Li[3], Ji Li[4], Chao Guo[3], He Jia[5] and Mengzhao Wang[1]**

[1] Department of Respiratory and Critical Care Medicine, Peking Union Medical College Hospital, Chinese Academy of Medical Sciences and Peking Union Medical College, Beijing, China, [2] Department of Respiratory and Critical Care Medicine, Peking University People's Hospital, Beijing, China, [3] Department of Thoracic Surgery, Peking Union Medical College Hospital, Chinese Academy of Medical Sciences and Peking Union Medical College, Beijing, China, [4] Department of Pathology, Peking Union Medical College Hospital, Chinese Academy of Medical Sciences and Peking Union Medical College, Beijing, China, [5] Department of Biological Information, Beijing Neoantigen Biotechnology Co., Ltd., Beijing, China

OPEN ACCESS

Edited by:
Hongbo Hu,
Sichuan University, China

Reviewed by:
Chengzhi Zhou,
Clinical Management Department of National Respiratory Medical Center, China
Chengdi Wang,
Independent researcher, Chengdu, China

***Correspondence:**
Mengzhao Wang
mengzhaowang@sina.com

Specialty section:
This article was submitted to Cancer Immunity and Immunotherapy, a section of the journal Frontiers in Immunology

Received: *29 July 2021*
Accepted: *27 December 2021*
Published: *09 March 2022*

Citation:
Liang H, Xu Y, Chen M, Zhao J, Zhong W, Liu X, Gao X, Li S, Li J, Guo C, Jia H and Wang M (2022) Characterization of Somatic Mutations That Affect Neoantigens in Non-Small Cell Lung Cancer. Front. Immunol. 12:749461. doi: 10.3389/fimmu.2021.749461

Purpose: Immune checkpoint inhibitors (ICIs) have recently emerged as an important option for treating patients with advanced non-small cell lung cancer (NSCLC). Neoantigens are important biomarkers and potential immunotherapy targets that play important roles in the prognosis and treatment of patients with NSCLC. This study aimed to evaluate and characterize the relationships between somatic mutations and potential neoantigens in specimens from patients who underwent surgical treatment for NSCLC.

Patients and Methods: This prospective study evaluated specimens from patients with NSCLC who underwent surgical treatment at the Peking Union Medical College, China, from June 2019 to September 2019. Whole-exome sequencing was performed for tumor tissues and corresponding normal tissues. Candidate neoantigens were predicted using generative software, and the relationships between various mutation characteristics and number of neoantigens were evaluated.

Results: Neoantigen-related gene mutations were less frequent than mutations affecting the whole genome. Genes with high neoantigen burden had more types and higher frequencies of mutations. The number of candidate neoantigens was positively correlated with missense mutations, code shift insertions/deletions, split-site variations, and nonsense mutations. However, in the multiple linear regression analysis, only missense mutations were positively correlated with the number of neoantigens. The number of neoantigens was also positively correlated with base transversions (A>C/C>A, T>G/G>T, and C>G/G>C) and negatively correlated with base transitions (A>G/G>A and C>T/T>C).

Conclusion: The number of candidate neoantigens in NSCLC specimens was associated with mutation frequency, type of mutation, and type of base substitution.

Keywords: non-small cell lung cancer, whole exome sequencing, neoantigens, tumor neoantigen burden, genetic mutation characteristics

INTRODUCTION

Despite advances in treatment strategies during the last 20 years, lung cancer remains the leading cause of cancer-related deaths worldwide. Immune checkpoint inhibitors (ICIs) are antibody-derived molecules that have recently emerged as treatment options for many types of cancers. They target regulatory receptors such as cytotoxic T-lymphocyte associated protein 4, programmed cell death 1 (PD-1), and programmed cell death-ligand 1 (PD-L1). These treatments have provided significant clinical benefits and changed the treatment landscape for patients with advanced non-small cell lung cancer (NSCLC). Although ICIs used in first-line and second-line treatments provide survival advantages compared with chemotherapy, the objective response rate is only approximately 20% among unselected patients (1–11). Thus, it is important to effectively select patients who are expected to benefit from ICI treatment.

Currently, the only approved biomarker for predicting response to ICI treatment is PD-L1 expression. However, patients with low tumor expression of PD-L1 can still experience a treatment response, suggesting that PD-L1 is not entirely effective for selecting patients to receive immunotherapy (12). Other potential biomarkers for guiding ICI treatment include major histocompatibility complex (MHC) expression, lymphocyte count, tumor T-cell marker expression, tumor burden (TMB), and the neoantigen expression (13). Among the potential biomarkers, mutation-derived neoantigens have attracted considerable attention. These tumor cell-specific mutant peptides can be presented by MHC molecules (14, 15) and recognized by T cells. Thus, neoantigens can mediate the immune response to tumor cells (14, 15) and allow the host immune system to recognize and destroy them.

Recent advances in genomics and bioinformatics have laid the foundation for the effective selection of the strongest immunogenic neoantigens based on the tumor's spectrum of somatic mutations. However, there are few reports regarding neoantigen-associated gene mutations in NSCLC. This information could be useful in identifying patients who might benefit from ICI treatment. Therefore, this study aimed to evaluate and characterize the relationship between somatic mutations and potential neoantigens in specimens from patients who underwent surgical treatment for NSCLC.

PATIENTS AND METHODS

Patients

We prospectively collected patients with NSCLC who underwent surgical treatment at the thoracic surgery department of Peking Union Medical College Hospital between June 2019 and September 2019. The inclusion criteria were histopathologically confirmed NSCLC, complete clinical and pathological data, sufficient tumor and corresponding normal tissue for whole-exome sequencing, and provision of informed consent by the patient for the research use of their specimens for research purposes. Data such as sex, age, smoking history, histological type, TNM stage, and clinical stage were collected. The study protocol was approved by our institutional review board.

Neoantigen Prediction

Whole-exome sequencing results were obtained for tumor tissues and corresponding normal tissues. Neopipe software was then used to predict candidate neoantigens by combining gene expression with the molecule's predicted affinity for class I MHC (**Figure 1**). Data on RNA expression were not obtained because of financial constraints. However, gene expressions were referenced from the TCGA database for NSCLC (**Figure 2**). For lung adenocarcinoma and lung squamous cell carcinoma, the mean values for transcriptional and genetic quantification were

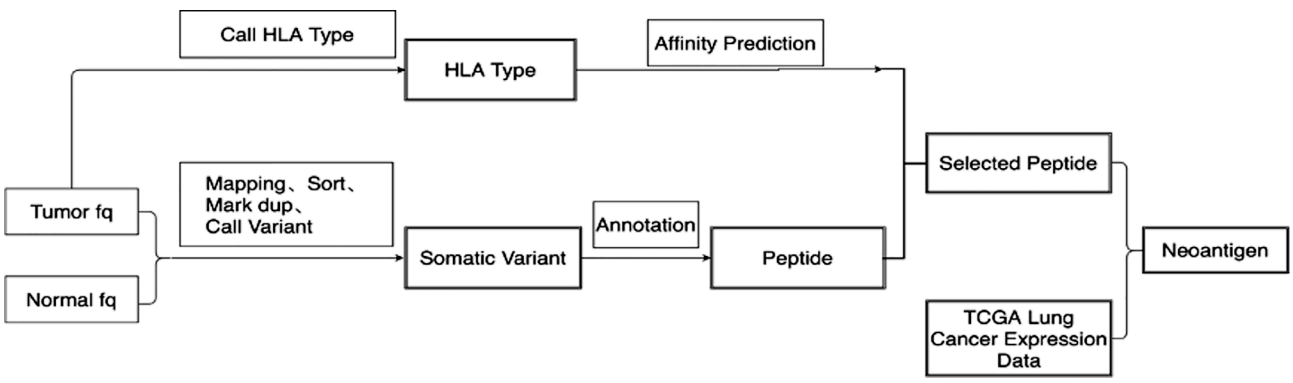

FIGURE 1 | Flow chart of candidate neoantigen design. 1) Quality control and statistical analysis were performed on original tumor and normal FASTQ data. 2)Bwa was used to compare FASTQ data to human reference genome HG19. Samblaster was used to mark duplication on reads. 3)SamTools was used to convert the Sam file into BAM file and build index. 4)GATK Mutect2 was used to call and filter somatic mutation, and then obtain mutation information. 5)The original FASTQ information was used for HLA typing using Optitype. 6) Netmhcpan4 was used to predict peptide affinity according to HLA type. 7) The expression data of lung cancer patients in TCGA were downloaded, and the mean values of expression data of lung adenocarcinoma and lung squamous cell carcinoma patients were calculated respectively. 8) Neoantigen was scored according to the sequencing data, mutation frequency, expression of HLA, expression of transcript, expression of immune-related gene to obtain the final neoantigen results.

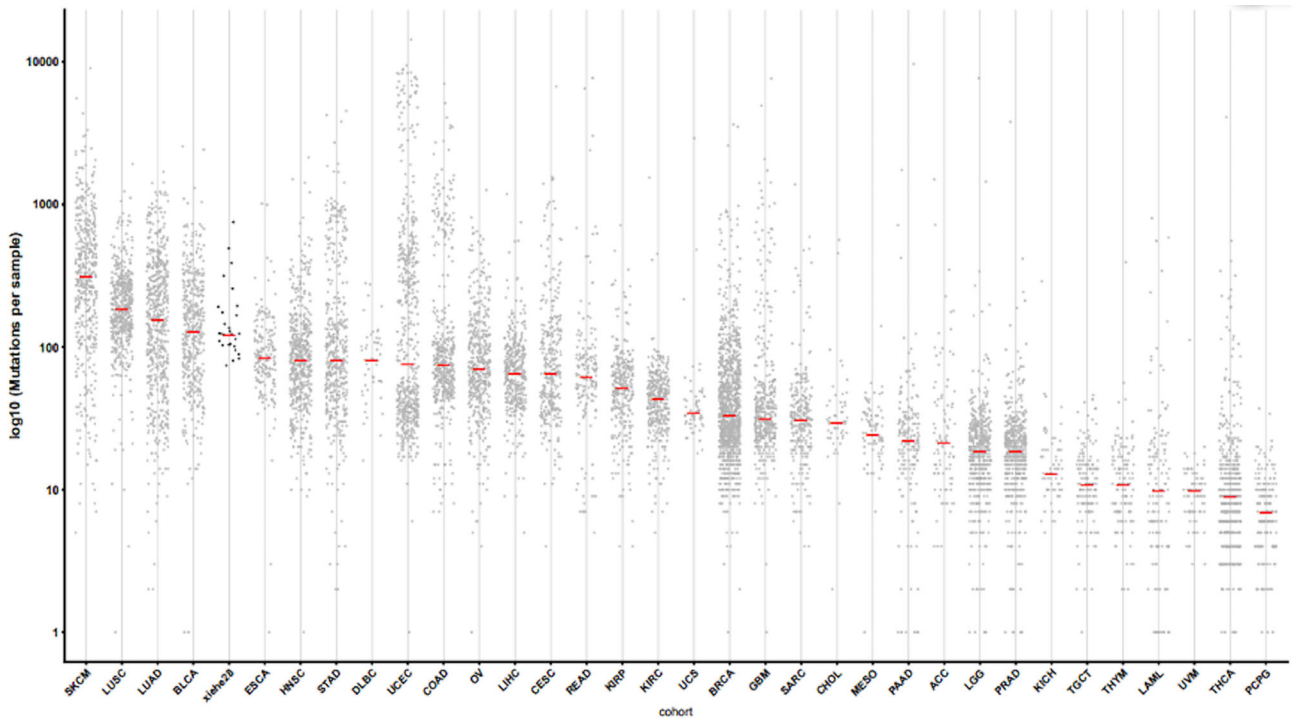

FIGURE 2 | Gene disturbance map. The X-axis represents the sample type, and "xiehe28" is our 28 samples, and the other samples are tumors in TCGA database. The Y-axis represents log 10 (mutations per sample). The red line in the figure represents the mean value. Note, SKCM, skin cutaneous melanoma. LUSC, lung squamous cell carcinoma. LUAD, lung adenocarcinoma. BLCA, bladder cancer; ESCA, esophageal cancer; HNSC, head and neck squamous cell carcinoma; STAD, stomach adenocarcinoma; DLBC, Diffuse large B-cell lymphoma; UCEC, Uterine corpus endometrial carcinoma; COAD, colon adenocarcinoma; OV, Ovarian cancer; LIHC, liver hepatocellular carcinoma; CESC, cervical squamous cell carcinoma; READ, rectal adenocarcinoma; KIPP, Kidney renal papillary cell carcinoma; KIRC, kidney renal clear cell carcinoma; UCS, uterine carcinosarcoma; BRCA, breast cancer; GBM, glioblastoma; SARC, sarcoma; CHOL, cholangiocarcinoma; MESO, mesothelioma; PAAD, pancreatic adenocarcinoma; ACC, adrenocortical carcinoma; LGG, lower grade glioma; PRAD, Prostate adenocarcinoma; KICH, kidney chromophobe; TGCT, tenosynovial giant cell tumor; THYM, thymoma; LAML, acute myeloid leukemia; UVM, uveal melanoma; THCA, thyroid carcinoma; PCPG, pheochromocytoma and paraganglioma.

collected from 574 lung adenocarcinoma cases and 548 lung squamous cell carcinoma cases. For all other pathological types, the mean values for transcriptional and genetic quantification were collected from all NSCLC cases.

To facilitate future research regarding *in vitro* synthesis and administration, neoantigens were designed as 25-mer peptides. Mutated 8–11-mer peptides that could bind to MHC were defined as neoepitopes. Given the difference in neoantigen epitopes and MHC affinities, the accuracy of predicting immune stimulation would be low if it was based only on the number of neoantigen epitopes. Therefore, the main results included the neoantigen-related gene mutation characteristics without considering neoepitopes.

Statistical Analysis

All analyses were performed using SPSS software (version 21.0; IBM Corp., Armonk, NY, USA). Results are reported as median, number, frequency, and composition ratio, as appropriate. Nonparametric tests were used to analyze clinicopathological features associated with the number of neoantigens. Spearman's test was used to analyze the correlation between neoantigens and gene mutation characteristics. Multiple linear regression analysis was conducted for the various neoantigen-related gene mutation types. Heat maps were created, and related cluster analyses were performed using Rstudio software. Using a bilateral test, results were considered statistically significant at $P < 0.05$.

RESULTS

Clinicopathological Features and Prediction of Candidate Neoantigens

Between June and September 2019, 34 patients underwent surgery for NSCLC at our center. We excluded 6 patients because of insufficient tissue samples or incomplete clinical data. Therefore, 28 patients were ultimately included in the study. The median age was 60.5 years (range: 38–76 years); 17 patients (60.7%) were men, and 15 patients (53.6%) had a history of smoking. The pathological types were adenocarcinoma (24 cases, 85.7%), squamous cell carcinoma (3 cases, 10.7%), and large-cell neuroendocrine carcinoma (1 case, 3.6%). The tumors were classified as stage I (19 patients, 67.9%), stage II (6 patients, 21.4%), and stage III (3 patients, 10.7%). Six patients (21.4%) had a family history of tumors (**Table 1**).

TABLE 1 | Clinicopathological characteristics of 28 patients.

No.	Gender	Age	Smoking history (pack years)	Pathology	TNM stage	Clinical stage	Tumor size	Tumor history
1	Male	38	No	A	T1bN0M0	Ia2	14mm	No
2	Male	61	20	A	T1bN0M0	Ia2	23mm	No
3	Male	59	No	A	T1aN0M0	Ia1	10mm	No
4	Male	58	30	A	T1aN0M0	Ia1	8mm	No
5	Female	70	No	A	T1bN0M0	Ia2	20mm	No
6	Female	76	No	A	T1bN0M0	Ia2	20mm	Yes
7	Male	56	30	A	T1bN1M0	IIb	20mm	No
8	Male	70	10	A	T2aN0M0	Ib	40mm	No
9	Male	59	No	A	T1cN0M0	Ia3	25mm	No
10	Male	47	30	A	T2bN2M0	IIIa	20mm	No
11	Female	52	No	A	T1aN0M0	Ia1	10mm	No
12	Female	41	2	A	T3N2M0	IIIb	20mm	No
13	Female	60	No	A	T1cN0M0	Ia3	18mm	No
14	Female	68	No	A	T1bN0M0	Ia2	15mm	No
15	Male	73	No	A	T1cN0M0	Ia3	30mm	Yes
16	Female	60	No	A	T1bN0M0	Ia2	13mm	No
17	Female	54	3	A	T1cN0M0	Ia3	27mm	Yes
18	Female	71	No	A	T1bN0M0	Ia2	15mm	No
19	Female	58	No	A	T3N0M0	IIb	60mm	No
20	Female	63	No	A	T1bN0M0	Ia2	20mm	No
21	Male	49	30	S	T2aN1M0	IIb	32mm	No
22	Male	61	40	A	T1bN0M0	Ia2	15mm	Yes
23	Male	61	35	A	T2bN1M0	IIb	40mm	No
24	Male	56	30	A	T2bN2M0	IIIa	28mm	No
25	Male	63	40	A	T2aN0M0	Ib	36mm	Yes
26	Male	64	50	S	T1cN1M0	IIb	30mm	No
27	Male	64	3	S	T2bN1M0	IIb	60mm	Yes
28	Male	64	40	LCNEC	T2aN0M0	Ib	40mm	No

A, adenocarcinoma; S, squamous carcinoma; LCNEC, large-cell-neuroendocrine carcinoma.

Whole-exome sequencing was performed for 28 NSCLC specimens, which identified 5,017 non-synonymous mutations, including 4,037 missense mutations, 419 frame-shift insertions/deletions, 313 in-frame insertions/deletions, 229 nonsense mutations, 10 non-stop mutations, and 9 splice site mutations. A total of 7,452 single-nucleotide variants, including A>T/T>A (n=539), A>C/C>A (n=966), A>G/G>A (n=2,006), T>C/C>T (n=1,990), T>G/G>T (n=1,025), and C>G/G>C (n=926), were identified. Using results from the 28 specimens, the Neopipe software predicted a total of 2,942 neoantigens (median: 78, range: 28–510) and 7,912 neoepitopes (median: 200, range: 48–1,300) (**Figure 3**). Spearman's correlation analysis revealed a positive correlation between the tumor's longest diameter and the number of predicted neoantigens (correlation coefficient=0.575, P=0.001). Additionally, the number of candidate neoantigens was higher among patients with a family tumor history (rank mean: 20.42 *vs*. 12.89, P=0.046) and patients with squamous cell carcinoma (rank mean: 26.47 *vs*. 13.28, P=0.019) (**Table S1**).

Nine of the twenty-eight patients had EGFR-sensitive mutations, including six cases with 21L858R, two cases with 19DEL, and one with 20INS. Nonparametric testing revealed that the number of candidate neoantigens was not correlated with EGFR mutations (P =0.087) (**Table S1**). One patient had EML4-ALK fusion (85 candidate neoantigens) and one patient had ROS1 fusion (36 candidate neoantigens). Three patients had KRAS mutations, including KRAS G12D mutation (87 neoantigens), KRAS G12D mutation combined with CDKN2A D108H mutation (28 neoantigens), and KRAS G12V mutation combined with TP53 K132E mutation and STK11 N181Y mutation (85 neoantigens).

Gene Mutation Characteristics Associated With Candidate Neoantigens

We analyzed whole genome mutations and neoantigen-related gene mutations and found revealed that the ten most commonly mutated genes were MUC17 (57%), AHNAK (54%), ANKRD36C (54%), HERC2 (50%), ZNF208 (50%), ZNF729 (50%), AHNAK2 (43%), MUC16 (43%), CDC27 (39%), and MUC12 (39%) (**Figure 4A**). The ten most commonly mutated neoantigen-related genes were CDC27 (29%), HERC2 (25%), MUC16 (21%), ANKRD36C (21%), BCLAF1 (18%), GPR32 (18%), MUC12 (18%), MUC17 (18%), PBMX (18%), and TTN (18%) (**Figure 4B**). Among the whole genome mutations, higher frequencies and more types of mutations were observed, including missense mutations, nonsense mutations, in-frame deletions, frame-shift deletions, in-frame insertions, frame-shift insertions, and mixed mutations. Conversely, the most common type of neoantigen-related gene mutations only involved missense mutations, nonsense mutations, in-frame insertions, frame-shift insertions, and mixed mutations.

Comparing Mutation Characteristics According to Neoantigen Load

We defined tumor neoantigen burden (TNB) as the total number of neoantigens per million bases (Mbs) in a tumor sample. Using the median value (n=14), patients were assigned to a high TNB

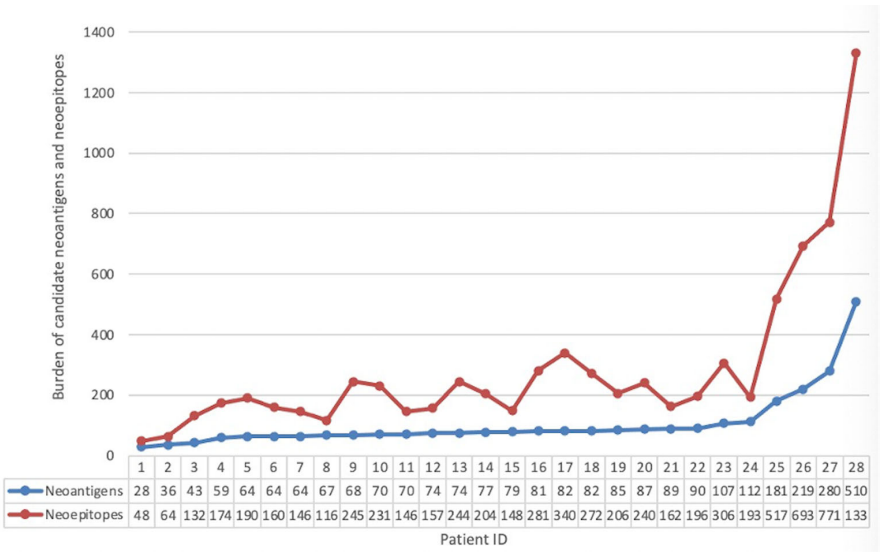

FIGURE 3 | Neoepitope and neoantigen maps of the patients included in our study.

group (n>14) and a low TNB group (n ≤ 14), and the gene mutation characteristics were compared. In the high TNB group, the ten most commonly mutated genes were MUC17 (17%), AHNAK (57%), ANKRD36C (57%), HERC2 (57%), ZNF729 (57%), AHNAK2 (50%), CDC27 (50%), MUC12 (50%), TTN (50%), and CACNA1A (43%) (**Figure 4C**). In the low TNB group, the ten most commonly mutated genes were MUC16 (57%), ZNF208 (57%), AHNAK (50%), ANKRD36C (50%), EGFR (43%), FLG (43%), HERC2 (43%), MUC17 (43%), ZNF729 (43%), and ZNF91 (43%) (**Figure 4D**). Patients with high TNB had a higher frequency of gene mutations and more mutation types, including missense mutations, nonsense mutations, in-frame deletions, frame-shift deletions, in-frame insertions, frame-shift insertions, and mixed mutations. Furthermore, patients with high TNB had significantly more frequent mixed mutations, insertion mutations, and deletion mutations than patients with low TNB. Patients with low TNB had missense mutations, nonsense mutations, in-frame deletions, frame-shift deletions, in-frame insertions, and mixed mutations.

Therefore, neoantigen-related mutations had fewer mutation types than whole genome mutations, indicating that tumor neoantigen burden (TNB) is related to both the number and type of gene mutations. Patients with a high TNB also had more types of gene mutations than those with low TNB, which indicates that some mutation types may create a higher neoantigen load.

Effects of Different Gene Mutation Types on Candidate Neoantigens

Spearman's correlation analysis was performed to access the features of neoantigen-related gene mutations (**Table 2**). The number of neoantigens was positively correlated with the number of non-synonymous mutations (correlation coefficient=0.641, P <0.001). All non-synonymous mutation types were subsequently annotated and analyzed, and the number of neoantigens was positively correlated with missense mutations (correlation coefficient= 0.603, P <0.001), frame-shift insertions/deletions (correlation coefficient=0.755, P <0.001), nonsense mutations (correlation coefficient=0.501, P =0.007), and splice site mutations (correlation coefficient= 0.546, P =0.003) (**Table 2**). These four mutation types were included in a multiple linear regression analysis, and the neoantigen number was only positively correlated with missense mutations (beta=0.674, P <0.001) (**Table 3**). This may be related to the high frequency of these mutations. Moreover, the lack of statistical significance between the number of candidate neoantigens and other mutation types might be related to their rarity, although they may produce a greater neoantigen load. The correlation between base substitution and number of neoantigens was also analyzed using Spearman's correlation analysis. The number of neoantigens was positivity correlated with the following base transversions: A>C/C>A (correlation coefficient= 0.641, P <0.001), T>G/G>T (correlation coefficient=0.388, P=0.041), and G>C/C>G (correlation coefficient=0.418, P=0.027). The number of neoantigens was negatively correlated with base transitions: A>G/G>A (correlation coefficient=-0.690, P<0.001) and T>C/C>T (correlation coefficient=-0.535, P=0.003) (**Table 2**).

Therefore, the number of candidate neoantigens was related to both the number and type of mutations present in tumors and was also positively correlated with base transversions and negatively correlated with base transitions.

Gene Mutations Associated With Multiple Candidate Neoantigens

There were 1,922 genes alterations that were associated with neoantigens, with each alternation creating 1–28 neoantigens. Among them, there were 21 genes that were associated with ≥7 neoantigens. Cluster analysis was performed for those 21 genes (**Figure 5**), and no significant correlation was observed between

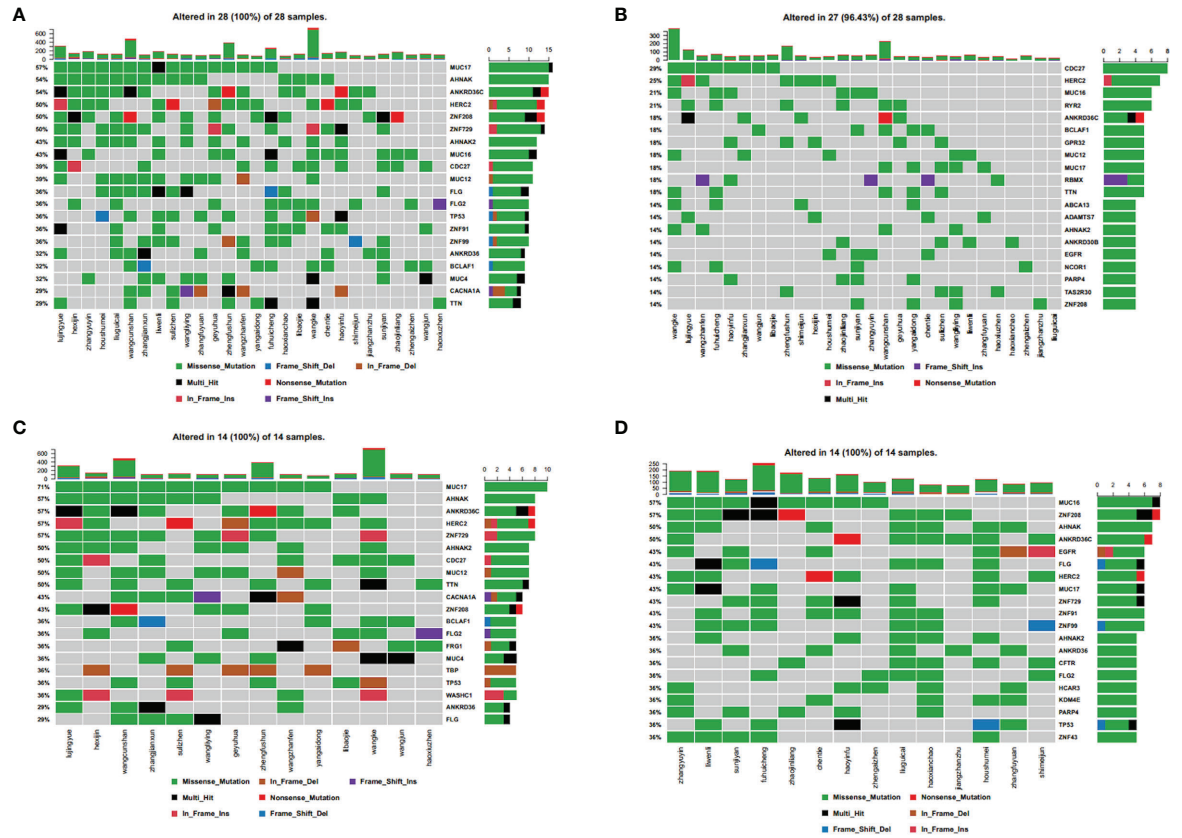

FIGURE 4 | Spectral heat map of common gene mutations. **(A)** all mutations; **(B)** neoantigen-associated mutations. Spectrum heat map of common gene mutations in patients. **(C)** with high tumor neoantigen burden; **(D)** with low tumor neoantigen burden.

the number of neoantigens and the expression of those genes in each patient.

DISCUSSION

ICIs are more effective in patients with NSCLC with a high TMB. This has led to the suggestion that TMB might be a biomarker for predicting response to ICI treatment (16). Moreover, preclinical and clinical studies have indicated that tumor-specific missense mutations may produce particular neoantigens that mediate response to ICIs (14, 17). Accordingly, this suggests that a high TMB could lead to the production of a higher number of neoantigens and thus increase immunogenicity and result in better response to ICI treatment (18). This is further supported by our findings, which showed that non-synonymous mutations

TABLE 2 | Spearman correlation analysis of candidate neoantigens.

Neoantigens	N	Correlation coefficient	P-value
nonsynonymous mutation	28	0664	<0.001
Frame shift indel	28	0.755	<0.001
In frame indel	28	0.071	0.718
Missense mutation	28	0.603	0.001
Nonsense mutation	28	0.501	0.007
Nonstop mutation	28	0.211	0.282
Splice site	28	0.546	0.003
A>T/T>A mutation frequency	28	0.279	0.151
A>C/C>A mutation frequency	28	0.641	<0.001
A>G/G>A mutation frequency	28	-0.690	<0.001
T>C/C>T mutation frequency	28	-0.535	0.003
T>G/G>T mutation frequency	28	0.388	0.041
C>G/G>C mutation frequency	28	0.418	0.027

TABLE 3 | Multiple linear regression of candidate neoantigens.

Variants	Unstandardized coefficients		Unstandardized coefficients Beta	t-value	P-value	95.0% confidence interval of B	
	B	Standard error				Lower limit	Higher limit
(Constant)	-2.811	10.84		-0.259	0.798	-25.235	19.614
Frameshift indel	1.612	1.139	0.154	1.415	0.17	-0.744	3.968
Missense mutation	0.5	0.115	0.674	4.342	0	0.262	0.739
Nonsense mutation	0.782	1.418	0.08	0.552	0.587	-2.152	3.716
Splice site	16.209	12.101	0.104	1.339	0.194	-8.825	41.243

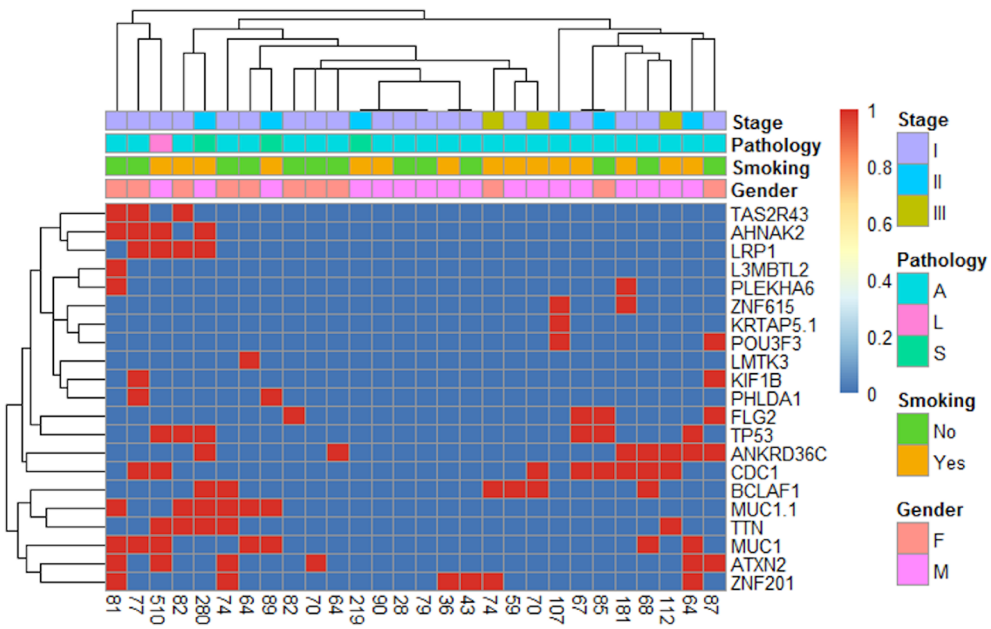

FIGURE 5 | Gene heat map of different numbers of neoantigens in 28 patients.

were positively correlated with the number of neoantigens. We performed additional classifications and analyses and found that the number of neoantigens was positively correlated with the presence of missense mutations (the most common mutation) and less common mutation types such as frame-shift insertions/deletions, nonsense mutations, and split-site mutations. There is evidence that frame-shift insertions or deletion are less frequent than non-synonymous single nucleotide mutations. However, they can be highly immunogenic mutations that can increase the neoantigen load and provide greater affinity for MHCs (19, 20).

Numerous studies have indicated that tumor-specific splicing is an important source of neoantigens (21–23), and although splicing frequency is relatively low, the neoantigens obtained from splicing sites are more frequent than those obtained from single-nucleotide mutations (24). We found that the frequency of nonsense mutations was lower. Nonetheless, it was also positively correlated with the number of neoantigens, indicating that nonsense mutations may produce a greater abundance of neoantigens. To the best of our knowledge, studies regarding the correlation between nonsense mutations and neoantigens have not yet been reported; therefore, further studies are needed to address this issue.

We also observed that the neoantigen load was positively correlated with base transversions and negatively correlated with base transitions. A previous study (25) of patients who received pembrolizumab revealed that patients with a durable clinical benefit were more likely to have C>A transversions and less likely to have C>T transitions (Mann-Whitney test; P=0.01). These findings are in concordance with our results.

Previous studies have used the TSNAD software to predict potential neoantigens from somatic mutations in 9,155 tumor samples from the International Cancer Genome Consortium database. They revealed that the most common potential neoantigens were encoded by KRAS, PIK3CA, and TP53. For instance, the ten most common potential neoantigens included six neoantigens derived from KRAS, which involved the G12D and G12V mutations (26). Another study of genomic, transcriptomic, and proteomic data from KRAS-mutated lung adenocarcinoma (27) identified three biological subgroups: STK11/LKB1 (KL subtype), TP53 (KP subtype), and CDKN2A/B (KC subtype). In this context, lung adenocarcinoma with the KP subtype showed a strong inflammatory response and enhanced expression of multiple co-stimulators and co-suppressors. In contrast, lung

adenocarcinoma with the KL subtype expressed lower levels of immune markers. Despite similar exposures to smoking, the KP subtype had a higher mutation rate than the KL subtype, which may explain the differences in their immunogenicity (27). In our study, only three of twenty-eight patients had KRAS mutations, including one with a KRAS G12V mutation (a KP and KL mixed type) that had 85 candidate neoantigens. Another patient with a KRAS G12D mutation (the KC subtype) had 28 candidate neoantigens, and a third patient with only a KRAS G12D mutation (no combined mutations) had 87 candidate neoantigens. The number of candidate neoantigens was noticeably below the median value only in the patient with the KC subtype, while the number in the other two patients was slightly above the median value. Thus, our findings are not consistent with results reported previously regarding the correlation between KRAS mutations and neoantigens. This could be explained by the very small sample size for our analyses (only three patients with KRAS mutations).

Our study has two important limitations. First, because of financial constraints, we could not retrieve RNA-related data to guide the neoantigen prediction. Instead, this was based on the expressions of lung cancer-related genes from the TCGA database. Second, the sample size was small; therefore, a larger study will be needed to validate our findings.

In conclusion, we found that the number of candidate neoantigens was related to both the number and type of mutations. Among the mutational types, missense mutations had the highest frequency. Although less frequent, frame-shift insertions/deletions, splice site variations, and nonsense mutations were also associated with the number of candidate neoantigens, possibly because they can produce a greater abundance of neoantigens. Nevertheless, only missense mutations were positively correlated with the number of neoantigens in the multiple linear regression analysis. The number of neoantigens was positively correlated with base transversions and negatively correlated with base transitions.

DATA AVAILABILITY STATEMENT

The original contributions presented in the study are publicly available. This data can be found here: https://ngdc.cncb.ac.cn/gsa/, accession number HRA002055.

ETHICS STATEMENT

The studies involving human participants were reviewed and approved by Ethics Committee at the Peking Union Medical College Hospital. The patients/participants provided their written informed consent to participate in this study.

AUTHOR CONTRIBUTIONS

HL: conceptualization, methodology, formal analysis, investigation, and writing – original draft. YX: conceptualization, investigation, writing – review and editing. MC: conceptualization, investigation, resources. JZ: conceptualization, investigation, and resources. WZ: conceptualization, investigation, and resources. XL: conceptualization, investigation, and resources. XG: conceptualization, investigation, and resources. SL: investigation and resources. JL: investigation and resources. CG: investigation and resources. HJ: software, formal analysis, and data curation. MW: conceptualization and methodology, writing – review and editing, supervision, and funding acquisition. All authors contributed to the article and approved the submitted version.

FUNDING

This study was supported by the '13th Five-Year' National Science and Technology Major Project for New Drugs (No: 2019ZX09734001-002), CAMS Innovation Fund for Medical Sciences (CIFMS) (to MW) (Grant No. 2018-I2M-1-003), and National Science and Technology Major Project (Grant No. 2019ZX09201-002). The funder was not involved in the study design, collection, analysis, and interpretation of data, the writing of this article or the decision to submit it for publication.

SUPPLEMENTARY MATERIAL

The Supplementary Material for this article can be found online at: https://www.frontiersin.org/articles/10.3389/fimmu.2021.749461/full#supplementary-material

REFERENCES

1. Spigel DR, Reckamp KL, Rizvi NA, Poddubskaya E, West HJ, Eberhardt WEE, et al. A Phase III Study (CheckMate 017) of Nivolumab (NIVO; Anti-Programmed Death-1 [PD-1]) vs Docetaxel (DOC) in Previously Treated Advanced or Metastatic Squamous (SQ) Cell Non-Small Cell Lung Cancer (NSCLC). *J Clin Oncol* (2015) 33:8009. doi: 10.1200/jco.2015.33.15_suppl.8009
2. Borghaei H, Paz-Ares L, Horn L, Spigel DR, Steins M, Ready NE, et al. Nivolumab Versus Docetaxel in Advanced Nonsquamous Non-Small-Cell Lung Cancer. *N Engl J Med* (2015) 373:1627–39. doi: 10.1056/NEJMoa1507643
3. Wu YL, Lu S, Cheng Y, Zhou C, Wang J, Mok T, et al. Nivolumab Versus Docetaxel in a Predominantly Chinese Patient Population With Previously Treated Advanced NSCLC: CheckMate 078 Randomized Phase III Clinical Trial. *J Thorac Oncol: Off Publ Int Assoc Study Lung Cancer* (2019). doi: 10.1158/1538-7445.AM2018-CT114
4. Horn L, Spigel DR, Vokes EE, Holgado E, Ready EN, Steins M, et al. Nivolumab Versus Docetaxel in Previously Treated Patients With Advanced Non-Small-Cell Lung Cancer: Two-Year Outcomes From Two Randomized, Open-Label, Phase III Trials (CheckMate 017 and CheckMate 057). *J Clin Oncol* (2017) 35:3924–33. doi: 10.1200/JCO.2017.74.3062
5. Herbst RS, Baas P, Kim DW, Felip E, Perez-Gracia JL, Han JY, et al. Pembrolizumab Versus Docetaxel for Previously Treated, PD-L1-Positive, Advanced Non-Small-Cell Lung Cancer (KEYNOTE-010): A Randomised Controlled Trial. *Lancet (Lond Engl)* (2016) 387:1540–50. doi: 10.1016/S0140-6736(15)01281-7
6. Reck M, Rodriguez-Abreu D, Robinson AG, Hui R, Csoszi T, Fulop A, et al. Pembrolizumab Versus Chemotherapy for PD-L1-Positive Non-Small-Cell Lung Cancer. *N Engl J Med* (2016) 375:1823–33. doi: 10.1056/NEJMoa1606774
7. Gandhi L, Rodriguez-Abreu D, Gadgeel S, Esteban E, Felip E, De Angelis F, et al. Pembrolizumab Plus Chemotherapy in Metastatic Non-Small-Cell

Lung Cancer. *N Engl J Med* (2018) 378:2078–92. doi: 10.1056/NEJMoa1801005
8. Paz-Ares L, Luft A, Vicente D, Tafreshi A, Gumus M, Mazieres J, et al. Pembrolizumab Plus Chemotherapy for Squamous Non-Small-Cell Lung Cancer. *N Engl J Med* (2018) 379:2040–51. doi: 10.1056/NEJMoa1810865
9. Rittmeyer A, Barlesi F, Waterkamp D, Park K, Ciardiello F, von Pawel J, et al. Atezolizumab Versus Docetaxel in Patients With Previously Treated Non-Small-Cell Lung Cancer (OAK): A Phase 3, Open-Label, Multicentre Randomised Controlled Trial. *Lancet (Lond Engl)* (2017) 389:255–65. doi: 10.1016/S0140-6736(16)32517-X
10. Socinski MA, Jotte RM, Cappuzzo F, Orlandi F, Stroyakovskiy D, Nogami N, et al. Atezolizumab for First-Line Treatment of Metastatic Nonsquamous NSCLC. *N Engl J Med* (2018) 378:2288–301. doi: 10.1056/NEJMoa1716948
11. Antonia SJ, Villegas A, Daniel D, Vicente D, Murakami S, Hui R, et al. Overall Survival With Durvalumab After Chemoradiotherapy in Stage III NSCLC. *N Engl J Med* (2018) 379:2342–50. doi: 10.1056/NEJMoa1809697
12. Topalian SL, Taube JM, Anders RA, Pardoll DM. Mechanism-Driven Biomarkers to Guide Immune Checkpoint Blockade in Cancer Therapy. *Nat Rev Cancer* (2016) 16:275–87. doi: 10.1038/nrc.2016.36
13. Penault-Llorca F, Radosevic-Robin N. Tumor Mutational Burden in Non-Small Cell Lung Cancer-the Pathologist's Point of View. *Trans Lung Cancer Res* (2018) 7:716–21. doi: 10.21037/tlcr.2018.09.26
14. Schumacher TN, Schreiber RD. Neoantigens in Cancer Immunotherapy. *Science* (2015) 348:69–74. doi: 10.1126/science.aaa4971
15. Gubin MM, Artyomov MN, Mardis ER, Schreiber RD. Tumor Neoantigens: Building a Framework for Personalized Cancer Immunotherapy. *J Clin Invest* (2015) 125:3413–21. doi: 10.1172/JCI80008
16. Alexandrov LB, Nik-Zainal S, Wedge DC, Aparicio SAJR, Behjati S, Biankin AV, et al. Signatures of Mutational Processes in Human Cancer. *Nature* (2013) 500:415. doi: 10.1038/nature12477
17. Gubin MM, Zhang XL, Schuster H, Caron E, Ward JP, Noguchi T, et al. Checkpoint Blockade Cancer Immunotherapy Targets Tumour-Specific Mutant Antigens. *Nature* (2014) 515:577. doi: 10.1038/nature13988
18. McGranahan N, Furness AJS, Rosenthal R, Ramskov S, Lyngaa R, Saini SK, et al. Clonal Neoantigens Elicit T Cell Immunoreactivity and Sensitivity to Immune Checkpoint Blockade. *Science* (2016) 351:1463–9. doi: 10.1126/science.aaf1490
19. Turajlic S, Litchfield K, Xu H, Rosenthal R, McGranahan N, Reading JL, et al. Insertion-And-Deletion-Derived Tumour-Specific Neoantigens and the Immunogenic Phenotype: A Pan-Cancer Analysis. *Lancet Oncol* (2017) 18:1009–21. doi: 10.1016/S1470-2045(17)30516-8
20. Linnebacher M, Gebert J, Rudy W, Woerner S, Yuan YP, Bork P, et al. Frameshift Peptide-Derived T-Cell Epitopes: A Source of Novel Tumor-Specific Antigens. *Int J Cancer* (2001) 93:6–11. doi: 10.1002/ijc.1298
21. Hoyos LE, Abdel-Wahab O. Cancer-Specific Splicing Changes and the Potential for Splicing-Derived Neoantigens. *Cancer Cell* (2018) 34:181–3. doi: 10.1016/j.ccell.2018.07.008
22. Jayasinghe RG, Cao S, Gao QS, Wendl MC, Vo NS, Reynolds SM, et al. Systematic Analysis of Splice-Site-Creating Mutations in Cancer. *Cell Rep* (2018) 23:270. doi: 10.1016/j.celrep.2018.03.052
23. Park J, Chung Y-J. Identification of Neoantigens Derived From Alternative Splicing and RNA Modification. *Genomics Inf* (2019) 17:e23–3. doi: 10.5808/GI.2019.17.3.e23
24. Kahles A, Ong CS, Zhong Y, Ratsch G. SplAdder: Identification, Quantification and Testing of Alternative Splicing Events From RNA-Seq Data. *Bioinformatics* (2016) 32:1840–7. doi: 10.1093/bioinformatics/btw076
25. Rizvi NA, Hellmann MD, Snyder A, Kvistborg P, Makarov V, Havel JJ, et al. Mutational Landscape Determines Sensitivity to PD-1 Blockade in Non-Small Cell Lung Cancer. *Science* (2015) 348:124–8. doi: 10.1126/science.aaa1348
26. Zhou Z, Lyu XZ, Wu JC, Yang XY, Wu SS, Zhou J, et al. TSNAD: An Integrated Software for Cancer Somatic Mutation and Tumour-Specific Neoantigen Detection. *Roy Soc Open Sci* (2017) 4:170050. doi: 10.1098/rsos.170050
27. Skoulidis F, Byers LA, Diao LX, Papadimitrakopoulou VA, Tong P, Izzo J, et al. Co-Occurring Genomic Alterations Define Major Subsets of KRAS-Mutant Lung Adenocarcinoma With Distinct Biology, Immune Profiles, and Therapeutic Vulnerabilities. *Cancer Discov* (2015) 5:860–77. doi: 10.1158/2159-8290.CD-14-1236

Conflict of Interest: Author HJ was employed by company Beijing Neoantigen Biotechnology Co., Ltd.

The remaining authors declare that the research was conducted in the absence of any commercial or financial relationships that could be construed as a potential conflict of interest.

Advantages of publishing in Frontiers

OPEN ACCESS
Articles are free to read for greatest visibility and readership

FAST PUBLICATION
Around 90 days from submission to decision

HIGH QUALITY PEER-REVIEW
Rigorous, collaborative, and constructive peer-review

TRANSPARENT PEER-REVIEW
Editors and reviewers acknowledged by name on published articles

Frontiers
Avenue du Tribunal-Fédéral 34
1005 Lausanne | Switzerland

Visit us: www.frontiersin.org
Contact us: frontiersin.org/about/contact

REPRODUCIBILITY OF RESEARCH
Support open data and methods to enhance research reproducibility

DIGITAL PUBLISHING
Articles designed for optimal readership across devices

FOLLOW US
@frontiersin

IMPACT METRICS
Advanced article metrics track visibility across digital media

EXTENSIVE PROMOTION
Marketing and promotion of impactful research

LOOP RESEARCH NETWORK
Our network increases your article's readership